THE FRASER LAKES ZONE B U-TH-REE DEPOSIT AND ITS HOST ROCKS: IMPLICATIONS FOR PEGMATITE- AND LEUCOGRANITE-HOSTED U-TH-REE DEPOSITS IN NORTHERN SASKATCHEWAN, CANADA

A Thesis Submitted to the College of
Graduate Studies and Research
In Partial Fulfillment of the Requirements
For the Degree of Master of Science
In the Department of Geological Sciences
University of Saskatchewan
Saskatoon

By

CHRISTINE LOUISE MCKECHNIE

PERMISSION TO USE

In presenting this thesis in partial fulfilment of the requirements for a Postgraduate degree from the University of Saskatchewan, I agree that the Libraries of this University may make it freely available for inspection. I further agree that permission for copying of this thesis in any manner, in whole or in part, for scholarly purposes may be granted by the professor or professors who supervised my thesis work or, in their absence, by the Head of the Department or the Dean of the College in which my thesis work was done. It is understood that any copying or publication or use of this thesis or parts thereof for financial gain shall not be allowed without my written permission. It is also understood that due recognition shall be given to me and to the University of Saskatchewan in any scholarly use which may be made of any material in my thesis.

Requests for permission to copy or to make other use of material in this thesis in whole or part should be addressed to:

Head of the Department of Geological Sciences
University of Saskatchewan
Saskatoon, Saskatchewan S7N 5E2

OR

Dean
College of Graduate Studies and Research
University of Saskatchewan
107 Administration Place
Saskatoon, Saskatchewan S7N 5A2
Canada

ABSTRACT

The Fraser Lakes Zone B U-Th-LREE deposit is located approximately 50 km SE of the Key Lake uranium mine in the Wollaston Domain of Northern Saskatchewan, Canada. Here, a number of variably radioactive pegmatites and leucogranites intruded the highly sheared, unconformable contact between Paleoproterozoic Wollaston Group metasedimentary rocks and the underlying Archean orthogneisses, in a NNE-plunging antiformal fold nose.

The U-Th-LREE mineralized pegmatites were subdivided into two groups based on their mineralogical and spatial differences. Both groups contain variable amounts of quartz, k-feldspar, plagioclase, biotite, magnetite, and ilmenite. The Group A pegmatites, in the eastern part of the fold nose, contain small amounts of uraninite, uranoan thorite, zircon, and rare coffinite and allanite, and are typically U- ±Th-enriched (Th/U ~1). The Group B pegmatites, in the central part of the fold nose, are Th- and LREE- enriched (Th/U up to ~20) and contain small amounts of monazite, uranoan thorite, and zircon, with rare allanite and pyrochlore-group minerals. The Group A pegmatites are interpreted to represent slightly more evolved crust melts that underwent higher degrees of restite unmixing, whereas the Group B pegmatites are postulated to have resulted from partial melting and incorporation of more restitic and peritectic material.

Field relationships and chemical age dating of the pegmatites suggests that they formed between 1.85 to 1.80 Ga, during peak thermal metamorphism and ensuing decompression related to the ca. 1.9 to 1.8 Ga Trans-Hudson Orogen (THO). Examination of the pelitic gneiss host rocks at Fraser Lakes Zone B revealed that the area underwent high temperature (up to ~780°-800° C), low to medium pressure (max pressures of ~7-8 kbar), upper amphibolite to granulite facies metamorphism (accompanied by partial melting), followed by isothermal decompression (down to ~3 kbar) at approximately 1.81-1.80 Ga. After this, the rocks began to cool and retrograde metamorphism took place at amphibolite to greenschist facies. Later faulting and hydrothermal fluid flow served to alter the pegmatites and led to local remobilization of U and other metals in fractures and faults.

The pegmatite-forming melts are interpreted to have formed by partial melting (*via* biotite-dehydration reactions) of U-, Th- and REE-enriched rocks similar to the Wollaston Group at depth. The melts migrated upwards to the emplacement level within and along major structural zones, including sheared fold limbs, metamorphic foliations, and the deformed Archean/Paleoproterozoic contact. The melt was concentrated in antiformal fold noses and other dilational zones, where it crystallized to form the pegmatite and leucogranite bodies. The style of mineralization and the structural control is similar to other pegmatite-hosted uranium deposits, including the Rössing alaskite-hosted deposit in Namibia. The knowledge gained from this study can be applied to exploration for similar deposits in northern Saskatchewan and other areas with similar geology.

ACKNOWLEDGMENTS

First off, I would like to acknowledge the patience, support, and guidance of my graduate supervisors Dr. Irvine Annesley and Dr. Kevin Ansdell. In particular, I want to thank Irvine for acting as a liaison with JNR Resources Inc., and for his friendship, mentoring, and abundant advice. Big thanks also go out to Kevin for taking care of all university matters related to my thesis, and for the excellent introduction to igneous petrology and mineral deposits he gave me when I was an undergraduate student at the U of S. I also greatly benefitted from the contributions of my advisory committee, additional co-authors, and manuscript reviewers: Dr. Yuanming Pan, Dr. Jim Merriam, Dr. Guoxiang Chi, Dr. Julien Mercadier, Dr. Eric Potter, Dr. Steven McCutcheon, Dr. Bob Martin, Colin Card, Dr. Dave Lentz, Dr. Miguel Galliski, and an anonymous reviewer. Discussions with Dr. Michel Cuney, Michelle McKeough, Robert Millar, Kyle Reid, Marjolaine Pascal, and others whose names I omit for brevity all helped to improve this work.

I am very grateful to JNR Resources Inc. for giving me the opportunity to work on this thesis, and for their financial and logistical support. Thanks go out to their staff for their sharing of ideas and discussion of the Fraser Lakes geology, in particular the Fraser Lakes Zone B deposit. Additional funds for this research from the University of Saskatchewan (Kevin Ansdell's Department Heads Research Grant and my Graduate Scholarship) and NSERC (Kevin Ansdell's Discovery Grant), and travel grants from the Mineralogical Association of Canada and the Society of Economic Geologists, were also greatly appreciated.

I also want to thank the Saskatchewan Research Council (SRC), and in particular Robert Millar, for the geochemical analyses, as well as Steven Creighton and Tom Bonli for their help with the electron microprobe analyses, Blaine Novakovski for preparing my thin sections, and Kimberly Bradley for her petrography assistance.

I appreciate the camaraderie and knowledge that the students and professors in the Department of Geological Sciences shared with me during my time as a student. Special thanks go out to Dr. Yuanming Pan for giving me my first taste of research as an undergraduate student. I am forever grateful for my family and numerous friends, whose support made the completion of this thesis possible. I especially want to thank my parents, Jeffrey and Marlene Austman, for supporting my studies, including helping pay for field gear and field schools. Last but certainly not least, I acknowledge my husband, Michael McKechnie, for his enduring love, patience, and understanding, and our dog Buddy, for making me smile whenever I had a bad day.

I would like to dedicate this thesis to my dearly departed grandfather, Stanley Joseph Austman, who always encouraged me to live my dreams and never give up even when times were rough. You were proof that no matter how hard you fall, you can always pick yourself back up. Your positivity and caring concern greatly enhanced the lives of everyone around you, and you will be forever missed.

TABLE OF CONTENTS

LIST OF TABLES

LIST OF FIGURES

CHAPTER 1
INTRODUCTION

The Fraser Lakes granitic pegmatite- and leucogranite-hosted uranium, thorium, and rare earth element (REE) mineralized granitic pegmatites are located in northern Saskatchewan, Canada, 55 km southeast of the Key Lake uranium mine, and 25 km from the southeastern edge of the Athabasca Basin. The mineralization at Fraser Lakes Zone B is just one of the many known occurrences of granitoid-hosted U, Th, and REE mineralization within the Wollaston Domain of northern Saskatchewan, but prior to this study had only been described in limited detail by Foster (1970) and Ko (1971). Similar mineralized pegmatites within the Wollaston Domain were examined by Mawdsley (1952, 1953, and 1955), Thomas (1983), Parslow and Thomas (1982), and Parslow *et al.* (1985) and references therein. However, these studies were regional in nature and did not examine the pegmatites in sufficient detail to fully understand the controls on their genesis and mineralization. More recent studies by Annesley *et al.* (2000, 2005, 2009, 2010 a, b, c), Annesley and Madore (1999), and Madore *et al.* (2000) focused more on their relationship (U- protore?) to the Athabasca Basin uranium deposits and thus are not as useful in exploration for pegmatite-hosted uranium deposits. The current study was initiated to examine the Fraser Lakes Zone B U-Th-LREE-mineralized granitic pegmatites and leucogranites in more detail than previous studies, in order to update the model for this type of mineralization in northern Saskatchewan, Canada.

Research Objectives

The main goal of this research was to develop a detailed model to explain the origin of the Fraser Lakes Zone B U-Th-LREE-mineralized granitic pegmatites and leucogranites, and establish the controls on the mineralization in order to aid in exploration for this type of U-Th-LREE deposit in northern Saskatchewan, Canada.

The specific objectives of the research were:

- Determine how these granitic pegmatites formed, including their relationship to their host rocks and regional metamorphism and deformation in the Fraser Lakes area.
- Determine the mineralogy of the granitic pegmatites and leucogranites, and in particular, the uranium, thorium, and rare-earth mineralization within them.
- Explain the apparent change in composition (in particular, the U, Th, and REE contents) of the granitic pegmatites at Zone B from U +/- Th enriched in the western part of the fold nose to highly Th and REE enriched in the northern part of the fold nose.
- Obtain additional information on metamorphism that took place during the ca. 1.8 Ga Trans-Hudson Orogeny.
- Develop a metallogenetic model for the Fraser Lakes U, Th, and REE mineralization that can be used in exploring for similar mineralization within the Wollaston Domain.
- Discuss the role these U-Th-REE-mineralized intrusives may have played in the formation of unconformity-related uranium deposits in the nearby Athabasca Basin.

Methodology

The author logged drill core from the Fraser Lakes Zone B pegmatite at JNR Resources Inc.'s Way Lake camp. Over a dozen drill holes were examined in order to document the macroscopic features of the granitic pegmatites and their host rocks and to obtain samples for petrographic study and geochemical analysis. Additionally, the outcrop previously mapped by Ko (1971 – see Figure 2-3b) was examined and additional samples were collected from the historical trenches and selected outcrop locations. Attempts were made to collect macroscopically fresh, unweathered samples that were representative of the pegmatites and their host rocks, as well as a number of their altered equivalents. Eighty-seven samples, mostly from drill core, were sent to the Saskatchewan Research Council Geoanalytical Laboratories for geochemical analysis by inductively coupled plasma-optical emission spectrometer (ICP-OES) after lithium metaborate fusion (whole rock major element oxides and selected trace elements), by ICP-OES or ICP-MS following acid digestion of the whole-rock powder (additional trace elements), $NaO_2/NaCO_3$ fusion prior to analysis by ICP-OES (boron), by combusting pulverized sample material in a LECO induction furnace supplied with oxygen (carbon and sulfur), by titration (FeO_{total}) and by

X-ray Fluorescence (XRF) using pressed pellets (major elements and selected trace elements). The full set of geochemical results is compiled in Appendix B (Table B-1).

All of the polished thin sections used in this study were prepared in the Thin Section Laboratory in the Department of Geological Sciences at the University of Saskatchewan. Transmitted and reflected light petrography was done at the University of Saskatchewan and JNR Resources Inc. in order to describe the mineral assemblages, textures, and paragenesis in the thin sections prior to microprobe analysis. Appendix A contains a summary table of the modal mineralogy of the thin sections examined in this study.

From this larger group of samples, four pegmatite (two Group A and two Group B) and three pelitic gneiss samples were selected for additional study using an electron microprobe. Care was taken to select relatively unaltered samples with numerous crystals of interest for chemical age dating and geothermobarometry. However many samples that appeared macroscopically fresh were in fact altered when examined using the petrographic microscope, thus making sample selection difficult. The automated wavelength-dispersive electron-microprobe analyses for this study utilized either a Cameca SX–100 Ultra electron-microprobe analyzer (EMPA) at the Saskatchewan Research Council (SRC, see SRC 2012) or a JEOL 8600 Superprobe EMPA at the University of Saskatchewan. Prior to analysis, the phases of interest were examined and identified using SEM back-scattered electron imagery (SEM–BSE) and SEM energy–dispersive electron-microprobe spectrometry (SEM–EDS). Further discussion of the microprobe methods is provided in Chapter 3. One of the specific goals of the microprobe work was to do chemical age dating of the pegmatites and inclusions in metamorphic minerals in the pelitic gneisses using the CHIME approach (cf. Bowles 1990, Montel *et al.* 1996, Förster 1999, Annesley *et al.* 2000, and Kempe 2003). This was followed by thermobarometry of both the pegmatites and the pelitic gneisses, using the geothermometers of Luhr *et al.* (1984), Holdaway (2000), Lepage (2003), and Henry *et al.* (2005) and the geobarometer of Wu *et al.* (2004). The full suite of microprobe data, including the results of thermobarometry utilizing this data, can be found in appendices C through K.

All of the previously collected information was used in further defining the model for the Fraser Lakes Zone B U-Th-LREE-mineralization, which is discussed in detail in Chapters 2, 3 and 4. As part of an agreement with JNR Resources Inc., a short implications for uranium exploration section was written up and is included in Chapter 5.

Thesis Structure

The subsequent three chapters of this thesis were written as manuscripts intended for publication. The author was responsible for all of the fieldwork, data analysis, and manuscript preparation for this thesis. Dr. Irvine Annesley and Dr. Kevin Ansdell edited all manuscripts prior to submission. Dr. Eric Potter, Colin Card, and Dr. Laura Lauri reviewed Chapter 2, and Dr. Robert Martin, Dr. Dave Lentz, Dr. Miguel Galliski, and an anonymous reviewer reviewed portions of Chapters 3 and 4 (which were initially submitted as one paper and subsequently split into two). Each chapter can be considered as a stand-alone document, and accordingly has its introduction, methodology, results, discussion, conclusions, and references. The references for all chapters were integrated into a reference list at the end of the thesis due to the amount of repetition between chapters.

Chapter 2 “Geological setting, petrology and geochemistry of granitic pegmatites and leucogranites hosting the Fraser Lakes Zone B U-Th-REE mineralization, Wollaston Domain, northern Saskatchewan, Canada”, discusses the mineralogy and chemistry of the Fraser Lakes Zone B U-Th-LREE-mineralized intrusives and their host rocks, and presents a model for the origin of the mineralization. Two spatially, mineralogically, and geochemically distinct groups (titled A and B) of mineralized, variably radioactive intrusions were delineated in this paper based on their geochemistry and mineralogical assemblages. After describing the pegmatites and their host rocks, the model for the origin of the Fraser Lakes Zone B mineralization is introduced. Partial melting of a metasedimentary rock-dominated source at ca. 850°C and 9 kbar, entrainment of accessory minerals in the melt, and assimilation-fractional crystallization processes during transport and crystallization, are postulated to have led to U, Th, and REE enrichment of the granitic pegmatites. This model expands upon the model previously developed for uranium-mineralized pegmatites and leucogranites in the Wollaston Domain (Parslow & Thomas 1982, Thomas 1983, and Parslow *et al.* 1985), and is similar to the models developed for the origin of the Rössing alaskites (Berning *et al.* 1976, Basson & Greenway 2004, and Cuney & Kyser 2008) and the Grenville Province U-mineralized granitic pegmatites (Fowler & Doig 1983, Goad, 1990, and Lentz 1991, 1996). Additionally, the implications of these mineralized pegmatites for the origin of unconformity-related uranium deposits in the Athabasca Basin are briefly discussed. This paper has been accepted for publication in a special issue of Exploration and Mining Geology on "Geological Environments hosting Uranium Deposits".

Chapter 3 "Radioactive abyssal granitic pegmatites and leucogranites in the Wollaston Domain, Northern Saskatchewan, Canada: mineral compositions and conditions of emplacement in the Fraser Lakes area" builds upon the previous paper, by describing the U-Th-REE-rich accessory minerals and their chemistry, determining the timing of crystallization of the pegmatites using CHIMA dating of uraninite (Group A) and monazite (Group B) as well as providing constraints on the temperatures at which the Fraser Lakes Zone B pegmatites intruded. As well, a discussion of the processes (restite unmixing, amount of restite in the source, assimilation, transport distance, etc.) that led to the different mineralogy and chemistry of the Groups A and B pegmatites is also introduced in this chapter. This paper has been accepted for publication in the second special issue (December 2012) of Canadian Mineralogist dedicated to Petr Černý for his extensive work on granitic pegmatites.

Chapter 4 "Medium to low pressure pelitic gneisses of Fraser Lakes Zone B, northern Saskatchewan, Canada: Mineral chemistry, metamorphic P-T-t path, and implications for the genesis of radioactive abyssal granitic pegmatites" provides more detail on the metamorphism that took place during the ca. 1.9 - 1.8 Ga Trans-Hudson Orogeny in the Fraser Lakes area. Geothermobarometry and mineral assemblages were used to deduce the P-T path for the pelitic gneisses, which shows similarities to previous work done in the Wollaston Domain (in particular, that of Tran 2001, Tran *et al.* 1998, 2008, Annesley *et al.* 2005, Card et al 2007, and Yeo & Delaney 2007). The upper amphibolite to lower granulite facies conditions recorded by the pelitic gneisses are well within the range of partial melting conditions (cf. Le Breton & Thompson 1988, Bucher & Frey 1994, Patiño Douce 1999, Spear & Kohn 1999, Brown 2007, 2010, Sawyer 2008, Vernon & Clarke 2008, and Sawyer et al 2011 and references therein); this provides further evidence for the model developed in Chapters 2 and 3. Additionally, this work shows that while there was significant partial melting at the level of the intrusion of the pegmatites at around the same time, the pegmatite-forming melts more likely formed from partial melting of similar lithologies at depth. This paper has also been accepted for publication in the second special issue (December 2012) of Canadian Mineralogist.

A short summary of the three papers and conclusions follows in Chapter 5. A number of appendices were also included at the end of the thesis after the reference list; these include a number of supplementary data tables for Chapters 2, 3, and 4, and additionally, the final Appendix (Appendix L) contains a manuscript “Magmatic and metamorphic uraninite mineralization in the western margin of the Trans-Hudson Orogen (Saskatchewan, Canada): a uranium source for unconformity-related uranium deposits?” which has been accepted for publication in Economic Geology. The paper was authored by Julien Mercadier, Irvine Annesley, Christine McKechnie, Terrance Bogdan, and Steven Creighton. The author contributed to this paper by supplying some of the figures and data for the study, and also edited the manuscript prior to submission. Julien Mercadier has given permission for this to be included as an appendix in this thesis.

CHAPTER 2

GEOLOGICAL SETTING, PETROLOGY AND GEOCHEMISTRY OF GRANITIC PEGMATITES AND LEUCOGRANITES HOSTING THE FRASER LAKES ZONE B U-TH-REE MINERALIZATION, WOLLASTON DOMAIN, NORTHERN SASKATCHEWAN, CANADA

Abstract

The U-Th-REE mineralization at Fraser Lakes Zone B is hosted by granitic pegmatites and leucogranites, which lie along the deformed contact between Paleoproterozoic metasedimentary gneiss of the Wollaston Group and Archean orthogneiss, approximately 25 km from the southeastern edge of the Athabasca Basin. The pegmatites/leucogranites are subcordant to concordant with the regional foliation and are concentrated within a northeast-plunging antiformal fold nose, the study area, which lies west of Fraser Lakes. The mineralized pegmatites/leucogranites in the western part of the study area (Group A) are typically enriched in U (± Th) with Th/U ~1, and contain uraninite, thorite, zircon, and allanite. Those intruding the central part of the study area (Group B) are generally enriched in Th and LREE, with Th/U >2, and contain monazite, thorite (commonly U-enriched), and zircon. The pegmatites and leucogranites in Group A tend to be slightly enriched in SiO_2 and depleted in TiO_2 relative to those in Group B and are interpreted to represent more evolved crustal melts. Both groups are peraluminous and show varied chemistry. Partial melting (~850ºC and 9 kbar) of a metasedimentary rock-dominated source, entrainment of accessory minerals as xenocrysts, and assimilation–fractional crystallization processes combined to enrich the granitic pegmatites/leucogranites in U, Th, and REE elements. Transfer of melt from the source region to the crystallization sites was assisted by deformation within and along major structural zones, such as the folded Archean–Paleoproterozoic discontinuity. The character of mineralization and structural control in the study area is reminiscent of the alaskite-hosted deposits at Rössing, Namibia.

Sommaire

La minéralisation en U-Th-ÉTR de la Zone B de Fraser Lake est contenue dans des pegmatites granitiques et des leucogranites localisés le long du contact déformé entre des gneiss métasédimentaires d'âge Paléoprotérozoïque du Groupe de Wollaston et des orthogneiss d'âge archéen, à environ 25 km de l'extrémité sud-est du bassin d'Athabasca. Les pegmatites / leucogranites sont subcordants à concordants avec la foliation régionale et se concentrent dans la charnière d'un antiforme plongeant vers le nord-est dans la zone d'étude, laquelle est située à l'ouest de Fraser Lake. Les pegmatites minéralisées / leucogranites de la partie ouest de la zone d'étude (Groupe A) sont généralement enrichis en U (Th ±), présentent un rapport Th / U ~ 1, et contiennent de l'uraninite, de la thorite, du zircon et de l'allanite. Celles faisant intrusion dans la partie centrale de la zone d'étude (groupe B) sont généralement enrichies en Th et en terres rares légères, avec un rapport Th / U > 2, et contiennent de la monazite, de la thorite (communément enrichie en U), et du zircon. Les pegmatites et les leucogranites du groupe A tendent à être légèrement enrichis en SiO_2 et appauvris en TiO_2 par rapport à ceux du groupe B et proviendraient de liquides plus évolués d'origine crustale. Les deux groupes sont hyperalumineux et présentent des compositions chimiques variées. La fusion partielle (à ~ 850 ° C et à 9 kbar) d'une source dominée par des roches métasédimentaires s'est combinée à l'entraînement de minéraux accessoires en tant que xénocristaux, ainsi qu'aux processus d'assimilation et de cristallisation fractionnée expliquerait l'enrichissement des pegmatites granitiques / leucogranites en U, Th, et en éléments des terres rares. La déformation à l'intérieur et en périphérie de zones structurales majeures, tel la discordance plissée entre l'Archéen et le Paléoprotérozoïque, a contribué à la migration des liquides de fusion partielle de la région source aux sites de cristallisation. La nature de la minéralisation et le contrôle structural dans la zone d'étude rappellent les gîtes contenus dans des alaskites à Rössing, en Namibie.

Introduction

Economic concentrations of uranium can be found in a wide variety of geological environments, although the highest average grades, up to 18.3% U_3O_8 (Cigar Lake

Deposit; Cameco, 2012), are typically found in the unconformity-related deposits of the Athabasca Basin, northern Saskatchewan, Canada (Fig. 2-1a, 2-1b; e.g., Kyser and Cuney, 2008). In contrast, some of the lowest grade uranium deposits (as low as 0.01% U) are hosted in granitic pegmatite and/or leucogranite, although they can be economically significant if of large enough tonnage. For example, the largest of this type currently being mined is the Rössing deposit in Namibia (Berning *et al.*, 1976; Basson and Greenway, 2004); in 2010 it produced 3077 tU (~6% of the global uranium production for that year) and was the world's third largest uranium producer (World Nuclear Association, 2011).

In Canada, some of the best understood mineralized pegmatite bodies occur within the Grenville Province (Fowler and Doig, 1983; Lentz, 1991, 1996). Uranium-enriched granitic pegmatites (from 100 ppm up to %-level enrichment are known from numerous locations in northern Saskatchewan, including the Charlebois Lake pegmatite (Mudjatik Domain), and many occurrences within the Wollaston Domain (e.g., Mawdsley, 1952, 1953, 1955; Parslow and Thomas, 1982; Parslow *et al.*, 1985; Annesley and Madore, 1999; Annesley *et al.*, 2000; Madore *et al.*, 2000). These latter occurrences are assigned to the Paleoproterozoic Wollaston Group and underlying Archean rocks that form the basement to the eastern Athabasca Basin.

Uranium-enriched granitic pegmatites are associated with many unconformity-related uranium deposits, such as Moore Lakes (Annesley *et al.*, 2000), McLean Lake, and P-Patch (Key Lake: see Madore *et al.*, 2000). Uranium-enriched granitic pegmatites are considered to be an important source of uranium for unconformity-related uranium deposits, although the debate continues over the method by which U was transported from pegmatites to deposit site (Kotzer and Kyser, 1995; Hecht and Cuney, 2000; Madore *et al.*, 2000; Alexandre *et al.*, 2005; Derome *et al.*, 2005; Jefferson *et al.*, 2007; Cloutier *et al.*, 2009; Boiron *et al.*, 2010; Mercadier *et al.*, 2010; and Richard *et al.*, 2010).

This paper presents the results of a petrological and geochemical study of granitic pegmatites hosting uranium, thorium, and rare-earth-element (REE) mineralization at Fraser Lakes Zone B in the Wollaston Domain of northern Saskatchewan. Forster (1970) and KO (1971) initially described the uranium mineralization at Fraser Lakes Zone B; however, a more comprehensive delineation of the mineralization at Fraser Lakes Zone A and Zone B occurred during recent prospecting and drilling by JNR Resources (Annesley *et al.*, 2009; JNR Resources Inc., 2012). Both outcrop and drill core samples were collected during this study, followed by petrographic and major- and trace-element geochemical analyses of the samples. The analytical work permitted better characterization of the geological relationships, complexity, and evolution of the U-Th-REE mineralization. The high-grade metamorphic rocks in the Fraser Lakes area are overprinted by late faults that could represent conduits for fluids and heat, which may have altered the pegmatites and remobilized uranium and associated metals (Annesley *et al.*, 2010a).

The ultimate aim of this research is to develop a metallogenic model for granitic pegmatite-hosted uranium deposits in the Wollaston Domain, and to determine whether there is a direct or indirect relationship with unconformity-related uranium deposits in the region.

Regional and Local Geological Setting

The Fraser Lakes area (Fig. 2-2) is underlain by rocks of the eastern Wollaston Domain, and is located approximately 55 km from the Key Lake uranium mine and 25 km from the southeastern edge of the Athabasca Basin (Fig. 2-1b). The Wollaston, Mudjatik, Virgin River, and Peter Lake domains comprise the Hearne Province (Fig. 2-1b; Tran, 2001; Annesley *et al.*, 2005; Tran *et al.*, 2008, and references within), formerly known as the Cree Lake Zone (Lewry and Sibbald, 1977, 1980; Tran, 2001). The Wollaston Domain is a northeast-trending, highly metamorphosed fold-thrust belt comprising Paleoproterozoic metasedimentary rocks overlying Archean felsic gneisses. In contrast, the northwesterly adjacent Mudjatik Domain (Fig. 2-1b) is dominated by

Archean gneisses exhibiting a ‘dome and basin’ structural style (Lewry and Sibbald, 1977).

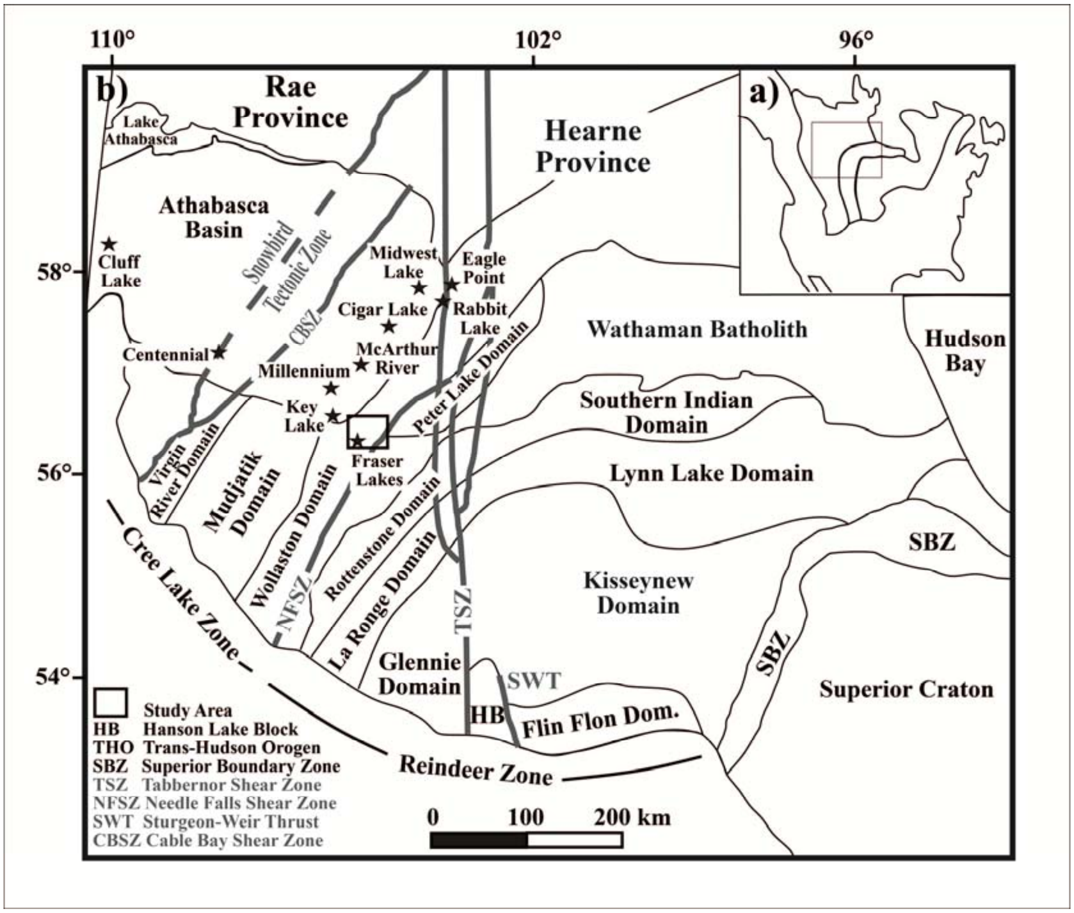

Figure 2-1. a) Map of North America, showing the Archean Hearne-Rae and Superior cratons, welded by the Paleoproterozoic Trans-Hudson Orogeny. Grey box shows the location of Figure 1b. b) Lithotectonic domains in northern Saskatchewan and Manitoba, showing the location of several unconformity-type uranium deposits within the Athabasca Basin. Black box shows the location of Figure 2-2. Figure after Annesley et al. (2005).

Lewry and Sibbald (1980) and Tran (2001) initially considered the boundary between the Wollaston and Mudjatik domains to be gradational, although Annesley and Madore (1989, 1994) postulated that a significant crustal-scale shear zone lies along this boundary. The Needle Falls Shear Zone (Fig. 2-1b) marks the southeastern boundary of the Wollaston Domain, separating it from the 1.865 Ga Wathaman Batholith and the Peter Lake Domain (Tran, 2001; Annesley *et al.*, 2005; Tran *et al.*, 2008, and references within). The Hearne Province and the Reindeer Zone to the southeast underwent multiphase deformation and metamorphism during the collisional stages of the ca. 1.9–1.8 Ga Trans-Hudson Orogeny, which produced a Himalayan-scale mountain belt that welded Archean cratons together to form the core of Laurentia (Hoffman, 1990; Lewry and Collerson, 1990; Ansdell, 2005; Corrigan *et al.*, 2009).

The Wollaston Domain has been the subject of numerous studies focusing on its stratigraphy, structure, metamorphism, geochronology, and mineral potential (cf. Tran, 2001; Tran *et al.*, 2003, 2008, and references therein; Annesley *et al.*, 2005; Yeo and Delaney, 2007). Overall, the domain contains Archean orthogneisses (predominantly granitic gneiss) that are unconformably overlain by metasedimentary rocks of the Paleoproterozoic Wollaston Group, which was deposited in rift, passive margin, and foreland basin environments. Hudsonian granites, amphibolites, leucogranites, migmatites, and granitic pegmatites are also locally abundant. The area of Figure 2-2 was originally mapped by Ray (1980) and is representative of the eastern Wollaston Domain (Annesley *et al.*, 2005). It contains the Fraser Lakes Zones A and B and is described in detail below.

The Fraser Lakes Inlier and Johnson River Inlier (Fig. 2-2) of the Wollaston Domain consist of granitic orthogneisses and are dated by U-Pb zircon geochronology at 2593 ± 13 Ma and 2574 ± 3 Ma, respectively (Hamilton and Delaney, 2000). The inliers are overlain by metasedimentary rocks of the Wollaston Group; in the eastern Wollaston Domain, these metasedimentary rocks comprise two subgroups: an upper calc-silicate-rich subgroup, and a lower pelitic to psammitic subgroup (Tran *et al.*, 1998, 2008; Tran, 2001).

The upper subgroup (Geikie River Group of Yeo and Delaney, 2007), consisting of calcareous and calc-silicate gneisses, is interpreted to be particularly thick in the Fraser Lakes area (Delaney *et al.*, 1996), although the thickest sections lie to the east of the study area. The lower subgroup contains six units as described by Annesley *et al.* (2005); these are 1) graphitic pelitic gneiss, 2) partly calcareous, pelitic gneiss interlayered with garnetite-metaquartzite and tourmalinite, 3) psammopelitic gneiss, 4) metasedimentary calc-silicate gneiss, 5) psammitic gneiss, and 6) sillimanite-bearing metaquartzite. In the Fraser Lakes area, the lower subgroup (Daly Lake Group of Yeo and Delaney, 2007) consists of pelitic and quartzo-feldspathic psammitic gneisses (Table 2-1). Graphite-bearing pelitic gneiss occurs immediately adjacent to the Archean inliers and is delineated by electromagnetic (EM) conductors (Fig. 2-2, 2-3a).

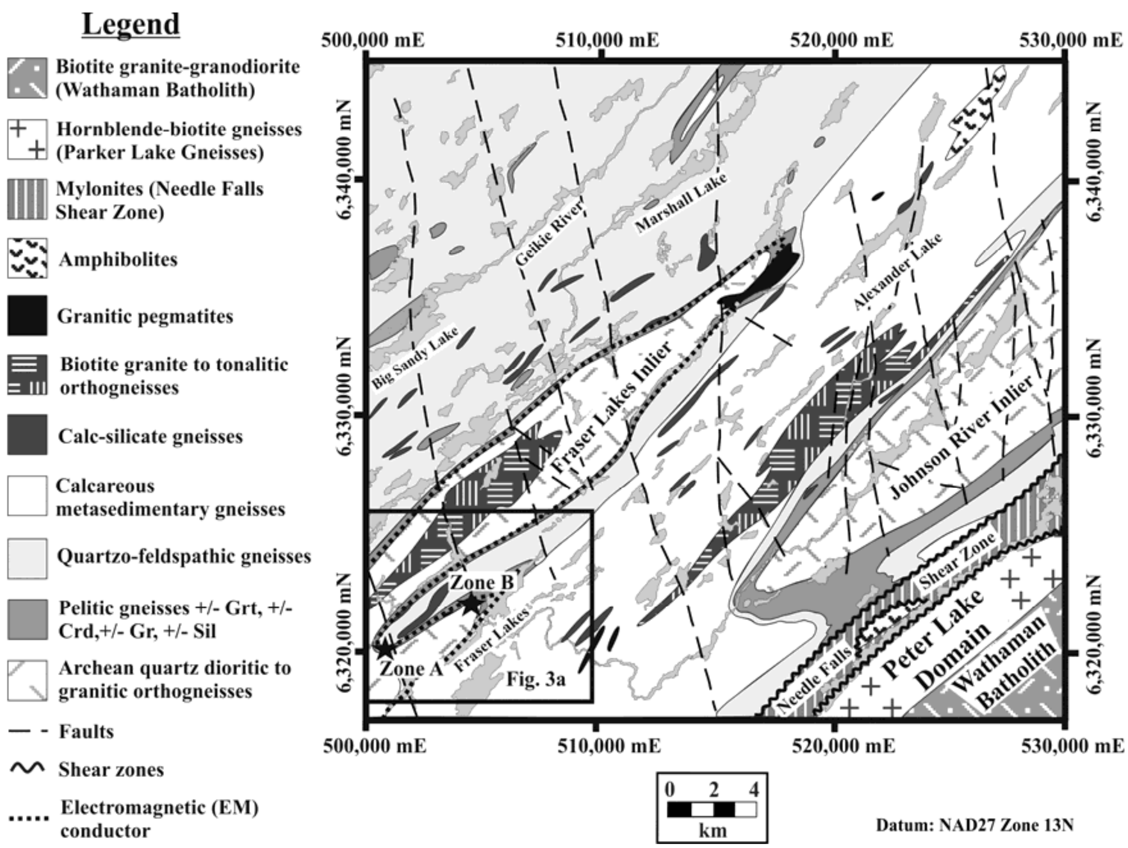

Figure 2-2. Regional geological map of the Fraser Lakes and surrounding area, modified from Ray (1980). Box shows the location of Figure 2-3a.

The Wollaston Group was intruded in various places by biotite-bearing monzogranite, granodiorite, and tonalite that range in age from 1840 Ma to 1810 Ma; rare metagabbros and amphibolites that range from 1830 Ma to 1820 Ma; and granitic pegmatites that range from 1820 Ma to 1800 Ma (Annesley *et al.*, 2005). These intrusions document two main phases of melting at 1835 Ma and 1815 Ma, the latter being more voluminous, as observed elsewhere in the western margin of the Trans-Hudson Orogen (Clarke *et al.*, 2005; Schneider *et al.*, 2007; van Breeman *et al.*, 2007; Tran *et al.*, 2008). The rocks were metamorphosed under upper amphibolite to granulite facies conditions and were strongly deformed ca. 1.86–1.78 Ga (Annesley *et al.*, 2005; Yeo and Delaney, 2007). Annesley *et al.* (1997, 2005) and Tran (2001) have introduced P-T-t paths for this metamorphism, which show that the gneissose fabric developed before or at peak pressure and before peak temperature in the western Trans-Hudson Orogen.

The dominant, generally northeast-trending structural fabric in the Fraser Lakes area formed by tight folding of this gneissose fabric; for example, a mapped EM conductor bordering the Fraser Lakes Inlier delineates northeast-plunging isoclinal folds (Fig. 2-2). North- to north-northwest-trending brittle faults offset lithological units in the area, which may be associated with the Tabbernor Shear Zone (Fig. 2-1b).

The area in the immediate vicinity of the Fraser Lakes A and B mineralized zones is underlain by metasedimentary gneiss (including graphitic and non-graphitic pelitic gneisses, psammopelitic gneiss, and calc-silicate gneiss) of the Wollaston Group and underlying Archean orthogneiss of the Fraser Lakes Inlier (Fig. 2-2; Ray, 1980; Delaney and Tisdale, 1996). The contact between the Wollaston Group and Archean orthogneiss is marked by a 65 km long, folded EM conductor that defines northeast-plunging regional folds with shallow to moderately plunging fold axes and highly sheared and transposed fold limbs (Fig. 2-2, 2-3a; Annesley *et al.*, 2009). An aeromagnetic map (Fig. 2-3a) emphasizes the northeast-trending regional structural trend but also shows the location of younger brittle faults.

The granitic pegmatites hosting the U-Th-REE mineralization are located in a ~500 m by 1500 m area west-northwest of the Fraser Lakes within an antiformal fold nose cross-cut by a number of east–west-trending ductile-brittle structures, and north-northwest- and north-northeast- trending brittle faults (Fig. 2-3a, 2-3b). The granitic pegmatites intrude the highly deformed, folded, northeast-plunging, unconformable contact zone between pelitic gneiss of the basal Wollaston Group, which is graphitic in places, and Archean granitic and tonalitic gneisses of the Fraser Lakes Inlier (Fig. 2-3b, 2-3c).

Table 2-1 - Comparison of lithostratigraphic units in the Wollaston Domain, Hearne Province, Saskatchewan.

This paper	Wollaston supergroup (Yeo and Delaney, 2007)	Western Wollaston Domain (Yeo and Delaney, 2007)		Eastern Wollaston Domain (Coombe, 1994)	Annesley et al. (1997, 2005)
Calcareous metasedimentary & calc-silicate gneisses	Calc-silicate rocks & marble	Geike River Group	Hidden Bay Assemblage		
	Calc-silicate-bearing arkose		Fraser Lakes Formation	Causier Creek Formation	
	Arkose, conglomerate, wacke, & calc-silicate breccia		Rafuse Lake Formation		
	Conglomerate & arkose		Janice Lake Formation		
Psammopelitic gneiss	Arkose & quartzite	Daly Lake Group	Burbridge Lake Formation		Metaquartzite
	Arkose & psammopelite		Roper Bay Formation		Psammopelitic gneiss–psammitic gneiss
	Psammopelite & pelite		Thomson Bay Formation		Calc-pelitic gneiss
Pelitic gneiss ± Sil ± Grt ± Crd	Cordierite-sillimanite psammopelite & pelite		Bole Bay Formation		
	Garnet pelite & psammopelite ± iron formation		Karin Lake Formation	Spence Lake Formation	Garnetite, thin metaquartzite
	Pelite & psammopelite			George Lake Formation	Pelitic gneiss with amphibolite or quartzite
Graphitic pelitic gneiss ± Sil ± Grt ± Crd	Garnet-Graphite pelite & psammopelite ± quartzite				Garnetite, thin metaquartzite
	Garnet-Orthopyroxene-Graphite-Amphibolite gneiss				Graphitic pelitic gneiss
	Quartzite & psammopelite			Souter Lake Group	
	Conglomerate & arkose ± volcanic rocks			Courtney Lake Group	
					Marginal rocks including skarn, amphibolite, pegmatite
Archean granitic to granodioritic orthogneisses	Granitoid rocks				Undivided granitoids (Archean)
					Granite to granodiorite, foliated–gneissic (Archean)
Archean tonalitic to quartz dioritic orthogneisses					Tonalite–Trondhjemite–Granodiorite Suite (Archean)

Notes: 1. Granitic pegmatites/leucogranites and leucosomes of this study are age-equivalent to inlier marginal rocks of Hudsonian age of Annesley et al. (2005).
2. The position of lithological units in this table is based on their relative stratigraphic position, not their relative ages.

The area in the immediate vicinity of the Fraser Lakes A and B mineralized zones consists of Wollaston Group metasedimentary gneisses (including graphitic- and non-graphitic pelitic gneisses, psammopelitic gneisses, and calc-silicate gneisses) overlying Archean orthogneisses of the Fraser Lakes inlier (Figure 2-2; Ray, 1980; Delaney and Tisdale, 1996). The contact between the Wollaston Group and Archean orthogneisses is defined by a 65 km long folded EM conductor that defines NE-plunging regional folds with shallow to moderately plunging fold axes and highly sheared and transposed fold limbs (Figures 2-2 and 2-3a; Annesley *et al.* 2009). The regional aeromagnetic signature emphasizes the NE-trending regional structural trend, but also shows the location of younger brittle structures (Figure 2-3a).

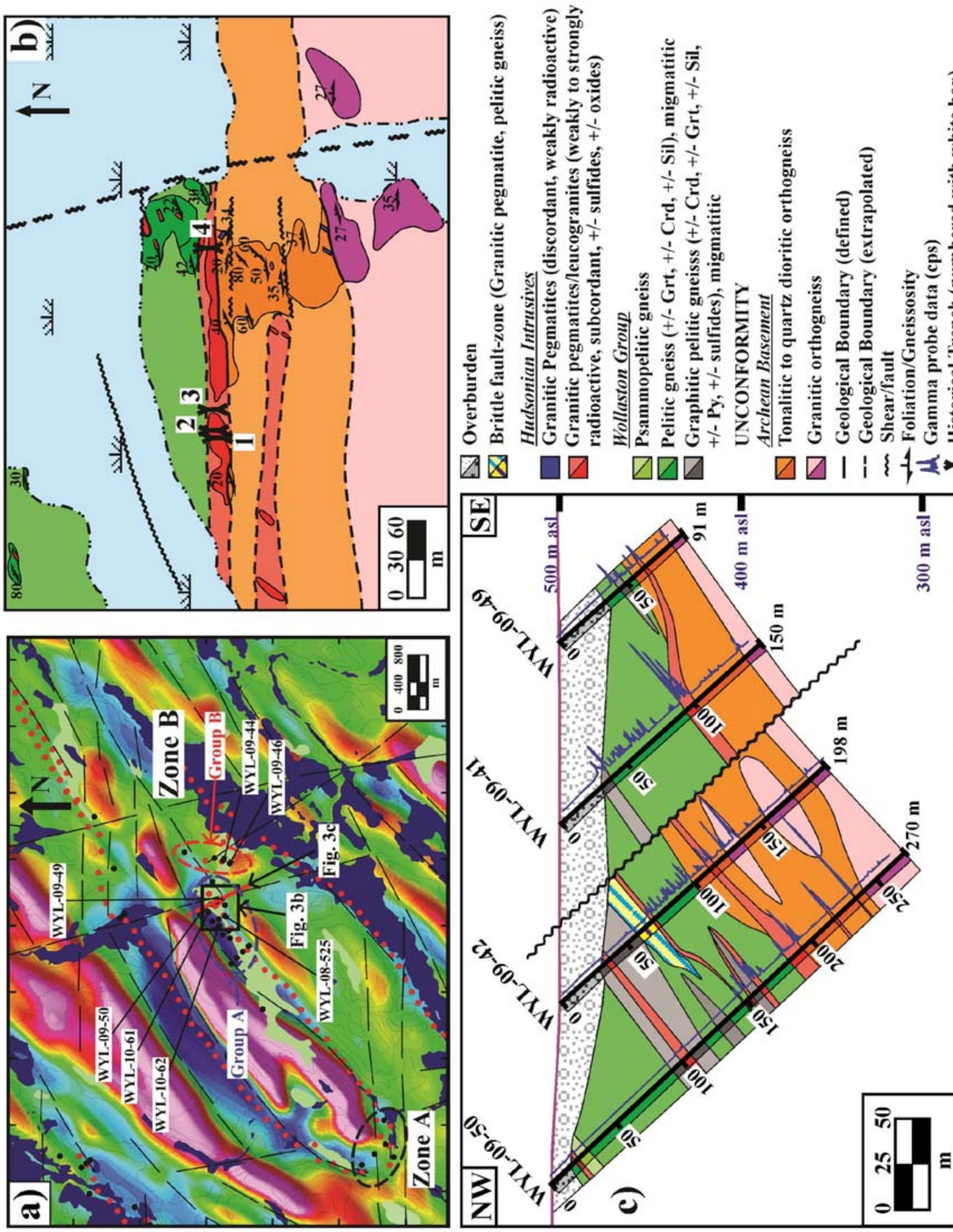

Figure 2-3. Geophysical and geological characteristics of the Fraser Lakes Zone B area. a) First vertical derivative aeromagnetic map of the Fraser Lakes area. Pink/red = areas of high magnetic potential; blue/green = low magnetic potential. Black dots = drill holes (study samples are labeled). Red dots = regional-scale electromagnetic conductor. Figure also shows the location of Groups A and B pegmatites/intrusives, Figure 3b, and Figure 3c. b) Geological map of the Fraser Lakes Zone B outcrop, showing Trenches 1 to 4. The uraniferous granitic pegmatites (in red) intruded at or near the contact zone between

Archean orthogneiss and metasedimentary rocks of the Wollaston Group. Modified from Ko (1971). c) Geological cross-section showing drill holes WYL-09-41, -42, -49, and -50. Many pegmatites intrude both pelitic gneiss and orthogneiss. Blue lines represent the downhole gamma probe results, and the largest peaks coincide with the location of pegmatites. The largest peak (in WYL-09-50) corresponds to ~5800 counts per second (cps) of radioactivity.

The granitic pegmatites that host the U, Th and REE mineralization at Fraser Lakes Zone B are located in a ~500 m x 1500 m area WNW of the Fraser Lakes within an antiformal fold nose cross-cut by a number of E-W ductile-brittle and NNW- and NNE-trending brittle structures (Figures 2-3a and b). The granitic pegmatites intrude the highly deformed, folded, NE-plunging, unconformable contact zone between pelitic gneisses of the basal Wollaston Group, which is graphitic in places, and Archean granitic and tonalitic gneisses of the Fraser Lakes Inlier (Figures 2-3b and c).

Field Relationships and Petrography

Archean orthogneisses

The orthogneiss in the Fraser Lakes area is grayish to reddish pink in drill core, and typically is fine to medium grained, with local coarse-grained and pegmatitic leucosome sections (Fig. 2-4a). It is relatively equigranular and tends to approach granoblastic polygonal texture in biotite-poor rocks. The orthogneiss ranges in composition from granodiorite to syenogranite and locally is gradational into tonalitic to quartz dioritic gneiss at its margins. Because the tonalitic orthogneiss and the basal pelitic gneiss of the Wollaston Group are both dark gray in color, it can be difficult to distinguish the two rocks in drill core, especially where they have a protomylonitic to mylonitic fabric.

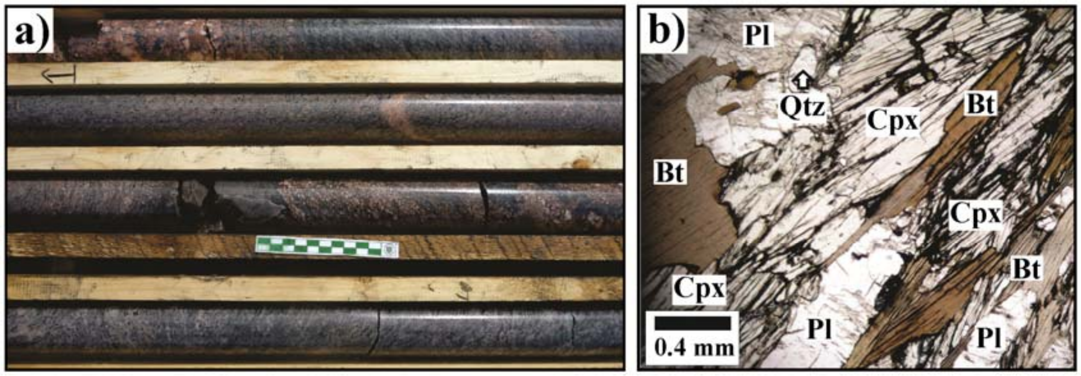

Figure 2-4. Archean orthogneissic rocks of the Fraser Lakes Inlier. a) Layered granitic and tonalitic orthogneisses intruded by granitic pegmatite (drill core from WYL-09-46). Scale bar in cm. b) Photomicrograph of clinopyroxene- and biotite-bearing tonalitic orthogneiss (WYL-09-49- 53.9). Bt = biotite, Cpx = clinopyroxene, Pl = plagioclase, Qtz = quartz. Abbreviations for all mineral names after Kretz (1983).

In the granitic orthogneiss, quartz, plagioclase, and K-feldspar are the dominant minerals (>75%), with biotite being the most common mafic mineral; perthitic feldspar intergrowths occur locally. Hornblende, magnetite, ilmenite, and pyrite are minor minerals, and accessory minerals include zircon, apatite, and rare allanite and uraninite. The granitic orthogneiss has undergone weak retrograde alteration, comprising chlorite and fluorite alteration of biotite (typically along cleavage planes), and sericite and saussurite alteration of feldspar. Ductile deformation has led to the development of a moderately intense foliation, plagioclase deformation twins, and undulose extinction in quartz.

The tonalitic orthogneiss is dominated by plagioclase and quartz, with significant amounts of hornblende, biotite, ilmenite, and magnetite, and varied amounts of clinopyroxene and orthopyroxene (Fig. 2-4b). Accessory minerals include zircon, apatite, and rare epidote and spinel. Most thin sections show evidence of weak retrograde metamorphism or alteration, indicated by the presence of chlorite, clay, and sericite. Locally, a weak, fracture-controlled carbonate and hematite alteration is present. Textures exhibited by the tonalitic to quartz dioritic orthogneiss include myrmekitic intergrowths, plagioclase deformation twinning, undulose extinction in quartz, and symplectite textures formed by quartz and hornblende on the edge of hornblende crystals. This gneiss is moderately foliated with the foliation defined primarily by biotite and/or pyroxene and hornblende (Fig. 2-4b).

Wollaston Group gneisses

In the larger Fraser Lakes area, the Wollaston Group consists of a number of units (Table 2-1), but in the study area, it is composed mainly of pelitic gneiss that can be subdivided into graphitic and non-graphitic varieties.

The graphitic gneiss is commonly porphyroblastic (garnet and/or cordierite), and the grain size ranges from very fine to medium grained, with an average size of <2 mm (Fig. 2-5a). This gneiss consists mostly of quartz, plagioclase, K-feldspar, biotite, and graphite (up to a maximum of 10–15% in thin section). It also contains varied amounts of cordierite, sillimanite, garnet, pyrite, chalcopyrite, and ilmenite; accessory minerals include apatite, monazite, and zircon (Fig. 2-5b). The graphitic gneiss tends to be quite heterogeneous in composition and is generally interlayered (Fig. 2-5c) with the non-graphitic pelitic gneiss, especially near the contact with Archean orthogneiss, which is the locus of most of the mineralized pegmatites (Fig. 2-3b, 2-3c).

Non-graphitic gneiss is common in the Fraser Lakes area, where it forms extensive layers of varied thicknesses (up to tens of meters). It is fairly heterogeneous in composition, commonly exhibits layering, and is gradational into other units of the Wollaston Group (see Table 2-1). The non-graphitic gneiss is typically dark gray, fine to medium (and, locally, coarse) grained, and is generally inequigranular. Porphyroblasts are common within this gneiss and typically are composed of inclusion-rich cordierite and/or garnet (Fig. 2-5d, 2-5e). The gneiss is composed of quartz, plagioclase, K-feldspar (generally subordinate), biotite, ± garnet, ± cordierite, ± sillimanite, ± ilmenite, ± rutile, ± pyrite, and ± chalcopyrite. Accessory minerals include zircon, monazite, apatite, titanite, uraninite, and allanite. The two main alteration assemblages are an early, retrograde chlorite, muscovite, leucoxene, clay, and epidote alteration; and a late, fracture-associated hematite, chlorite, and clay mineral alteration.

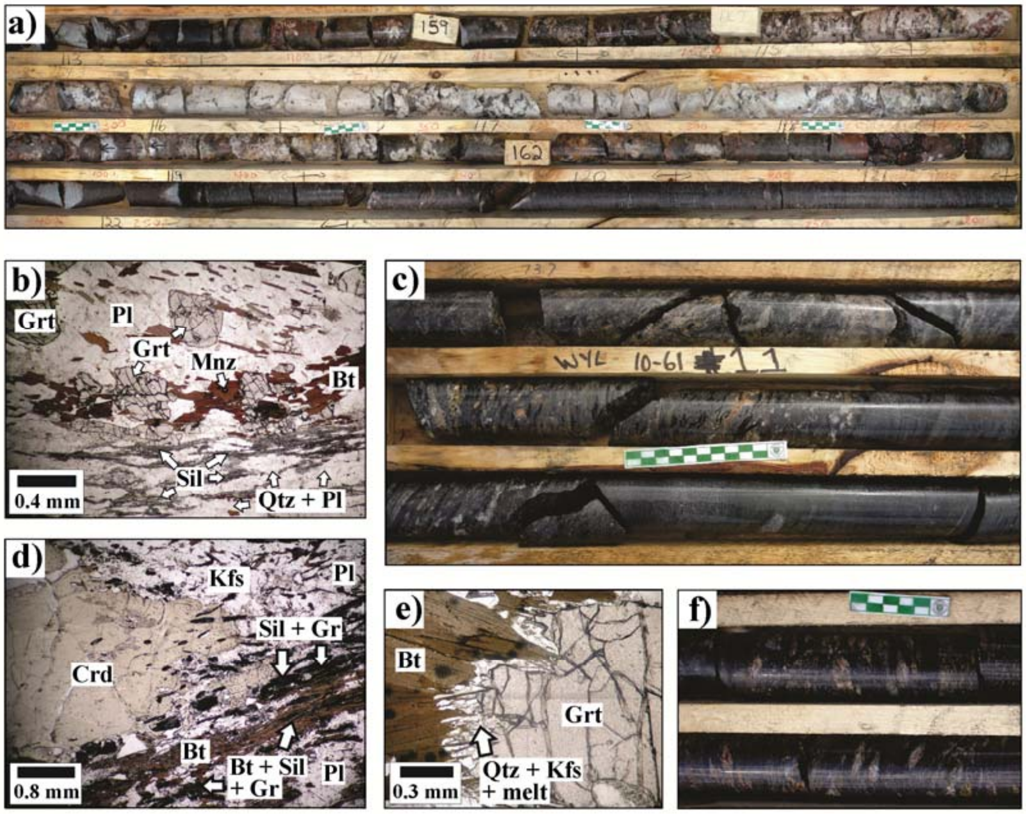

Figure 2-5. Pelitic gneisses hosting the Fraser Lakes Zone B pegmatite. a) Graphitic pelitic gneiss intruded by zoned quartz and K-feldspar-rich, weakly mineralized granitic pegmatite parallel to gneissosity (WYL-09-50). b) Pelitic gneiss containing biotite, garnet, sillimanite, monazite, quartz, and feldspars (WYL-09-49-36.1). c) Pelitic gneiss showing its compositional variation, including graphite-cordierite-sillimanite-rich layers (WYL-10-61). d) Pelitic gneiss with altered cordierite, biotite, sillimanite, feldspar, and quartz (WYL-10-61-78.1). e) Garnetiferous pelitic gneiss with melt microtextures at the contact between garnet and biotite (WYL-09-44-61.4). Biotite was consumed in the melt-generating reaction. f) Boudinaged, lighter colored leucosomes (K-feldspar + quartz-dominated) accentuating the dominant gneissosity and foliation shown by the darker pelitic gneisses (WYL-09-37). Scale bar in cm. Bt = biotite, Crd = cordierite, Fsp = feldspar, Grt = garnet, Kfs = K-feldspar, Mnz = monazite, Pl = plagioclase, Qtz = quartz, Sil = sillimanite.

Both the graphitic and non-graphitic gneisses are generally tightly folded and are typically well banded with a gneissic to mylonitic fabric. Migmatitic textures are common. They include evidence of small-scale melt reactions (Fig. 2-5e); deformed, boudinaged felsic leucosome bands (Fig. 2-5f); and dikelets of remobilized felsic leucosome that lie parallel to, and cross-cut the gneissosity. Stromatic and diatexite migmatite are present. The fabric is defined by the preferred orientation of biotite, sillimanite, and graphite, where present (Fig. 2-5b, 2-5d). Porphyroblasts of cordierite tend to be flattened, stretched, and elongated parallel to the fabric. Garnet porphyroblasts rarely are slightly flattened, but more typically are round to irregular in shape (Fig. 2-5b).

Other rocks of the Wollaston Group in the Fraser Lakes area include garnetite, quartzo-feldspathic gneiss, calcareous metasedimentary rocks, and calc-silicate gneiss. These units were rarely intersected in drill core and are gradational into each other and the more voluminous graphitic and non-graphitic pelitic gneisses. The psammopelitic gneiss and calc-silicate gneiss are concentrated near the top of several drill holes (e.g., WYL-09-50: Fig. 2-3c) and generally overlie the pelitic ± graphite gneiss that lies closer to the contact with the Archean orthogneiss. However, due to their subordinate presence in the Fraser Lakes drill core, the psammopelitic gneiss and calc-silicate gneiss were not examined in detail for this study.

Granitic pegmatites and leucogranites

The two types of granitic (sensu lato) pegmatites/leucogranites in the Fraser Lakes area can be distinguished on the basis of their cross-cutting relationships. For brevity, the rocks are herein termed ‘pegmatites’ and ‘intrusions,’ although they are properly classified as granitic pegmatites and leucogranites.

The first type of pegmatites is weakly radioactive, typically showing less than two times background radioactivity as measured by a Radiation Solutions RS-125 handheld scintillometer. It features a simple mineralogy of quartz, K-feldspar, plagioclase, and rarely biotite. These intrusions are inequigranular, typically pink, and coarse grained to pegmatitic; they commonly show graphic textures and perthitic intergrowths in quartz and feldspars. They occur sporadically in drill core and outcrop as discordant dikes and sheets, which significantly post-date the main phase of ductile deformation in the Fraser Lakes area. These intrusions were not examined in detail during the present study.

The second type of pegmatites is weakly to strongly radioactive, typically showing greater than two to three times background radioactivity. These radioactive pegmatites have a varied primary mineralogy, including quartz, plagioclase, K-feldspar, biotite, ± magnetite, ± ilmenite, ± zircon, ± U-Th-REE-bearing accessory minerals, ± fluorite, ± titanite, ± apatite, ± graphite, ± garnet (Table 2-1, Fig. 2-6a to 2-6f, 2-7a to 2-7d). The pegmatites range in width from a few centimeters to a decameter or more in both outcrop and drill core; the thicker bodies are concentrated close to fold noses, and the thinner bodies are on the limbs. The rocks are inequigranular, with grain size ranging from coarse grained to pegmatitic (Fig. 2-5a, 2-6a).

The majority of the radioactive accessory minerals in this second type of pegmatites tend to be associated with biotite, quartz, and magnetite (Fig. 2-6b to 2-6d, 2-7a to 2-7d). Quartz, feldspar, biotite, and magnetite grains tend to be much larger and form crystals up to a few centimeters in size (Fig. 2-5a, 2-6a). The individual pegmatite bodies are subcordant to concordant with the dominant gneissosity/foliation of the host rocks (Fig. 2-7a) and thus are interpreted to have been intruded syn-tectonically with respect to the Trans-Hudson Orogeny.

The highly radioactive intrusions can be further subdivided into two subgroups on the basis of their general location, geochemistry, and mineral assemblages:

- a U-enriched group, the 'Group A pegmatites/leucogranites,' hereafter referred to as the Group A intrusions, and
- a Th- and LREE-enriched group, the 'Group B pegmatites/ leucogranites,' hereafter referred to as the Group B intrusions.

The composition of the host rocks also influences the mineral assemblages of both groups, as magnetite is found only in pegmatites that intruded the Archean orthogneiss, whereas graphite and garnet occur sporadically in pegmatites hosted by rocks of the Wollaston Group.

The U-Th-REE accessory minerals in Group A intrusions include uraninite, U-enriched thorite, zircon, allanite, and apatite (Fig. 2-6b to 2-6f; Table 2-2), with rare monazite. These intrusions occur within the western part of the study area (Fig. 2-3a) and crop out at the original showing (Fig. 2-3b) that was initially described by Foster (1970) and later mapped by Ko (1971). Biotite grains in these pegmatites exhibit strong red-brown pleochroism (Fig. 2-6b, 2-6c). Low-Ca plagioclase (albite to oligoclase) is common. Zircons are typically zoned with distinct cores and rims that generally have different colors and birefringence (Fig. 2-6c). Uraninite (Fig. 2-6b, 2-6d) is typically present as small, altered cubic grains containing small galena (radiogenic?) and pyrite inclusions. Thorite and allanite are generally strongly altered, making them difficult to recognize in thin section.

The Group B intrusions are located mainly in the central part of the study area (Fig. 2-3a). The U-Th-REE accessory minerals include monazite and U-enriched thorite (commonly with pyrite inclusions), as well as thorite; and zircon, with rare allanite, xenotime (surrounding monazite), and apatite (Fig. 2-7a to d; Table 2-2). A single grain of an unusual Nb-rich mineral was also observed in one thin section from drill hole WYL-09-46. Monazite grains are commonly altered to hematite and partly rimmed by a mixture of chlorite ± clay (Fig. 2-7a to c). Allanite is also strongly altered and difficult to recognize in thin section. The monazite crystals are up to 1–2 mm in size and are typically associated with thorite, biotite, and zircon. The biotite exhibits slightly brownish to greenish pleochroism and commonly contains inclusions of rutile.

Zoning is common in most of the intrusions and varies among different bodies. Typical zoning patterns include plagioclase or quartz-rich cores with K-feldspar more predominant at the margins, but a consistent pattern has not been established. However, the highest radioactivity (as determined by a handheld scintillation counter) in both groups of intrusions is associated with biotite-rich zones. Quartz-rich zones in some intrusions also tend to contain significant concentrations of uranium and thorium.

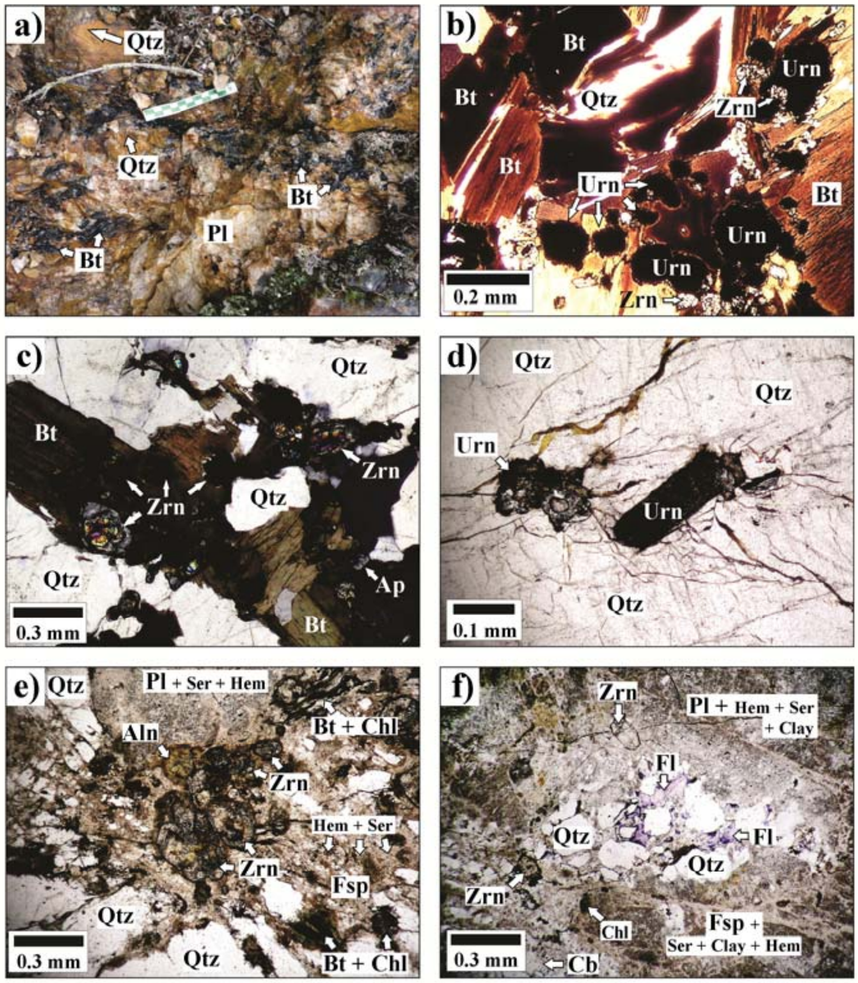

Figure 2-6. Field photograph and photomicrographs of Group A granitic pegmatites and leucogranites from Fraser Lakes Zone B. a) Typical U-rich granitic pegmatite showing coarse grain size of plagioclase-, biotite-, and quartz-rich mineralogy; from outcrop at Trench 2 (see Fig. 3b). Scale bar in cm. b) Granitic pegmatite, rich in biotite, zircon, and uraninite (sample Trench 2-2). c) Granitic pegmatite with abundant zoned zircon, and apatite in a cluster of biotite (WYL-09-50 at ~191.6 m). d) Quartz-rich granitic pegmatite sample containing partially altered uraninite (Sample QTZPEG 0004-2). e) Moderate to strongly altered (hematite, chlorite, and sericite) quartz-plagioclase pegmatite containing zircon and a strongly altered mineral that is possibly allanite (WYL-09-50-215.8). f) Altered pegmatite showing fluorite, carbonate, and strong clay mineral (Clay) + sericite + hematite + chlorite alteration of feldspar (WYL-09-50-215.8). Aln = allanite, Ap = apatite, Bt = biotite, Cb = carbonate, Chl = chlorite, Fl = fluorite, Fsp = feldspar, Hem = hematite, Pl = plagioclase, Qtz = quartz, Ser = sericite, Urn = uraninite, Zrn = zircon.

Table 2-2. Pegmatite mineralogy, with minerals listed in order of abundance. Yellow = major minerals. Green = U-Th-REE-bearing accessory minerals.

U-rich pegmatites	Th-REE-rich pegmatites
Quartz	Quartz
K-feldspar	K-feldspar
Plagioclase	Plagioclase
Biotite	Biotite
Magnetite	Magnetite
Ilmenite	Ilmenite
Pyrite	Pyrite
Fluorite	Fluorite
Zircon	Monazite
Rutile	Zircon
Uraninite	Rutile
Thorite	U-enriched thorite
Allanite	Thorite
Titanite	Allanite
Molybdenite	Xenotime
Garnet	Molybdenite
Apatite	Titanite
Sphalerite	Apatite
Chalcopyrite	Sphalerite
Pyrrhotite	Garnet
Graphite	Chalcopyrite
	Pyrrhotite
	Graphite
	Nb-oxide

The radioactive pegmatites show a variety of igneous textures, including occasional granophyric, graphic, perthitic, and myrmekitic intergrowths. They also tend to show a hypidiomorphic granular texture overall, with euhedral to subhedral grains, especially in early-formed accessory minerals. Radial cracks are accompanied by the development of reaction rims and pleochroic damage haloes in the surrounding minerals (Fig. 2-6c, 2-6d, 2-7c). These features are interpreted to be the result of metamictization and associated crystal volume changes of radioactive minerals.

Ductile deformation of the radioactive intrusions is strongly dependent on their size, with the largest bodies showing only weak ductile deformation in their cores. Small intrusions and the margins of larger bodies exhibit signs of ductile deformation, including folding and the development of a weak foliation (defined by the alignment of biotite). Quartz and K-feldspar typically show undulose extinction due to strain, and deformation twins are common within plagioclase. Brittle deformation in the radioactive intrusions is common and consists of cross-cutting fractures and fault zones. Brittle deformation is highly varied in intensity and is likely related to large-scale ductile-brittle and brittle faulting that took place in the Wollaston Domain at 1760–1700 Ma (Annesley *et al.*, 2005). The most prominent fault in the Fraser Lakes area is the north-northwest- striking Tabbernor Shear Zone (Fig. 2-1), a major fault that extends for many kilometers.

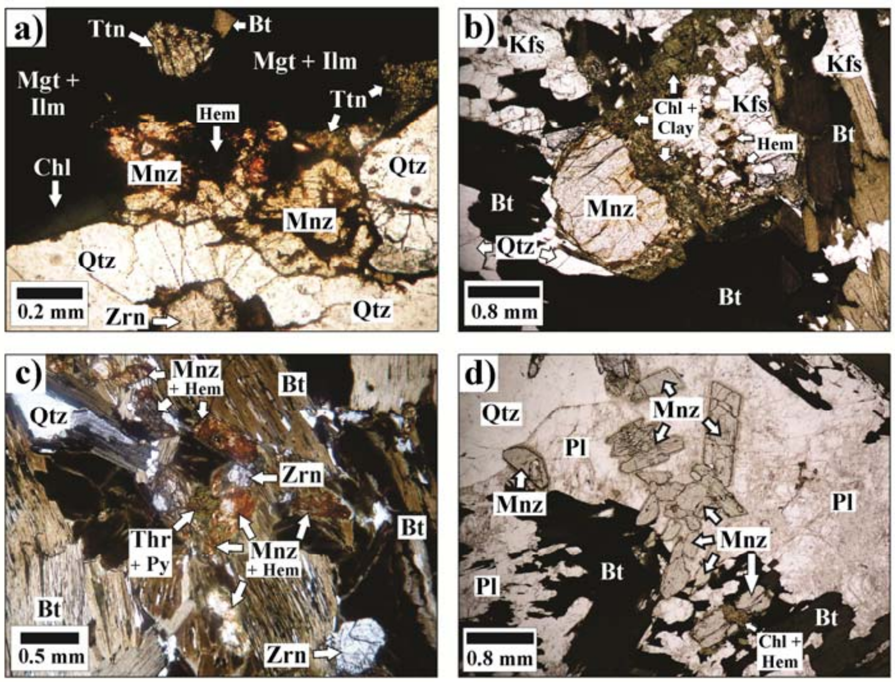

Figure 2-7. Photomicrographs of Group B pegmatites and leucogranites from Fraser Lakes Zone B. a) WYL-09-46-83.0, and b) WYL-09-46-42.8, both of which show monazite, zircon, ilmenite, magnetite, and titanite mineralization. c) Biotite-rich section of a granitic pegmatite (WYL-09-46-36.1) with hematite-altered monazite, U-enriched thorite with pyrite inclusions, and zoned zircon. Note weakly chloritized biotite. Monazite typically is weakly (a) to strongly (c) altered to hematite, chlorite, and clay minerals (Clay). d) Monazite-rich granitic pegmatite (WYL-09-46-32.6). Bt = biotite, Chl = chlorite, Hem = hematite, Ilm = ilmenite, Kfs = K-feldspar, Mgt = magnetite, Mnz = monazite, Py = pyrite, Qtz = quartz, Thr = thorite, Ttn = titanite, Zrn = zircon.

All of the pegmatites commonly show weak sericite, saussurite, and clay mineral alteration of feldspar and rare chloritization of biotite (Fig. 2-6e, 2-6f, 2-7a to 2-7c). Carbonate and hematite alteration of the intrusions is typically very late and is generally related to brittle fractures running through the pegmatites and their host rocks. The carbonate and hematite alteration is locally associated with fluorite, clay minerals, and chlorite (Fig. 2-6e, 2-6f). It affects not only the major minerals in the pegmatites and their host rocks, but also the U-Th-REE-bearing accessory minerals—in particular monazite, uraninite, and U-enriched thorite, which show weak to locally strong alteration (Fig. 2-7a to c). In some drill holes in the Fraser Lakes Zone B area, this alteration is strong and resembles hydrothermal alteration typical of unconformity-related uranium deposits of the nearby Athabasca Basin (Annesley *et al.*, 2010b; JNR Resources Inc., 2012).

Rarely, the pegmatites cut calc-silicate rocks, which resulted in the development of skarns along the margins of these intrusive bodies, a phenomenon common elsewhere in the Wollaston Domain (Annesley *et al.*, 2005).

Sampling and Analytical Techniques

Diamond drill cores from more than one dozen holes were logged to determine the macroscopic features of the granitic pegmatites and their host rocks, and to focus sampling for the petrographic study and geochemical analysis. In addition, one outcrop previously mapped by Ko (1971; Fig. 2-3b) was examined; representative samples of relatively unweathered pegmatite and pelitic gneiss were taken from this outcrop and from trenches dug by JNR Resources Inc. Polished thin sections were prepared in the Thin Section Laboratory in the Department of Geological Sciences at the University of Saskatchewan. Transmitted and reflected light petrography were performed at the University of Saskatchewan and JNR Resources Inc.

The definitions of rock types, rock classification, nomenclature, and other terms used in this study follow those of the International Union of Geological Sciences (IUGS) Subcommission on the Systematics of Igneous Rocks (Le Maître, 2002) and the Subcommission on Metamorphic Rocks (Fettes and Desmons, 2007). In addition, this study used the definitions, textural terminology, and genetic models of pegmatites, migmatites, and metamorphic rocks put forth by London (2008), Sawyer (2008), and Vernon and Clarke (2008), respectively.

Sample preparation and geochemical analysis were performed at the Saskatchewan Research Council (SRC) Geoanalytical Laboratories. Detailed descriptions of procedures at SRC Geoanalytical Laboratories can be found on their website (SRC, 2012). A total of 87 samples, most of which were from drill core, were analyzed for major- and trace-element chemistry.

Whole-rock major-element oxides, loss on ignition (LOI), and selected trace elements (Ba, Cr, Sc, Sr, Y, and Zr) were analyzed by a Perkin Elmer inductively coupled plasma-optical emission spectrometer (ICP-OES) after lithium metaborate fusion. Detection limits were ~0.01% for the major elements (except SiO_2), 0.1% for LOI and SiO_2, and 2 ppm for the trace elements. The remaining trace elements, with the exception of B, were analyzed by ICP-OES or ICP-MS following acid digestion of the rock powder; the detection limit was ~1 ppm. Samples for B analysis underwent NaO_2/$NaCO_3$ fusion prior to analysis by ICP-OES; the detection limit was ~2 ppm. Carbon and sulfur concentrations were determined by combusting pulverized sample material in a LECO induction furnace supplied with oxygen. Instrument calibrations were used to determine the weight percent concentrations of both elements in the sample. Detection limits for both carbon and sulphur were ~0.01%. As part of the quality control and assurance procedures at the SRC, in-house standards and the United States Geological Survey GSP-2 standard (Wilson, 2009) were routinely analyzed, along with duplicate sample pulps and blanks.

Representative samples of pelitic gneiss, orthogneiss, and granitic pegmatite were also analyzed by X-ray Fluorescence (XRF) to determine fluorine, chlorine, and sulphur contents, as well as major- and trace-element concentrations. The sample preparation involved the formation of pressed pellets, which were analyzed in a vacuum using a Bruker S8 TIGER XRF spectrometer. Detection limits varied depending on the element; they ranged from 0.005% to 0.10% for the major elements; were 0.01% for F, S, and Cl; and ranged from 1 ppm to 10 ppm for the remaining elements.

Reanalysis of samples previously done by ICP-OES provided constraints on analytical accuracy, and the results from both techniques were very similar (see Supplementary Data Table (SDT) (Appendix B). Readers interested in this full geochemical data set (the SDT) may e-mail the corresponding author for a copy of the Excel file. Titration analysis was performed on selected samples to obtain a value for FeO_{total} in the rocks. The amounts of ferrous and ferric iron in the samples were calculated from the values obtained using ICP-OES, XRF, and titration.

Geochemical Results

Gneissic host rocks

The three analyzed samples of Archean granitic orthogneiss show consistent major-element compositions, as typified by Sample WYL-09-50-252.7 (Table 2-3, Fig. 2-8a to e, SDT). The samples are also enriched in U (av. 7 ppm), Th (av. 29 ppm), and Zr (av. 444 ppm) relative to average continental crustal values of 1.3 ppm, 5.7 ppm, and 210 ppm, respectively (Weaver and Tarney, 1984). The less abundant tonalitic to dioritic orthogneiss shows a more varied chemical composition, due to its more diverse primary mineralogy; it tends to have higher concentrations of V, Cr, Co, Ni, and Zn, and lower total REE than the granitic orthogneiss (Table 2-3, SDT), reflecting its more mafic composition. All of the Archean orthogneiss samples have major- and trace-element characteristics that indicate they are calc-alkaline, similar to other Archean inliers in the Wollaston Domain (e.g. Tran, 2001).

Pelitic gneiss samples show considerable variation in chemical composition, with SiO_2 ranging from 37.3 wt. % to 64 wt. %, and Al_2O_3 from 10.5 wt. % to 21.2 wt. % (Table 2-3, Fig. 2-8b, SDT); the compositional variation reflects their mineralogical variation. The two samples with the lowest SiO_2 content (<40 wt. %) also have the highest $Fe_2O_{3\ tot}$ (23.1–25.1 wt. %) and high K_2O (5.5–6.2 wt. %), indicating they are biotite-rich. The range in major-element compositions is similar to that presented by Tran *et al.* (2003) in their study of metasedimentary rocks from other parts of the Wollaston Domain.

Table 2-3. Representative whole-rock, major- and trace-element geochemical analysis of pegmatites and gneissic host rocks.

Sample #	WYL-09-50-237	WYL-09-50-252.7	WA-08-0-0046	WYL-10-62-68.9	WYL-09-50-37.5	WYL-10-62-87.1	WYL-09-49-36.1	WYL-10-61-190.3	WYL-10-62-93.5	WYL-09-46-31.1	WYL-09-46-32.6
Rock Type	Dioritic orthogneiss	Granitic orthogneiss	Tonalitic orthogneiss	Pelitic gneiss (Crd-Sil-Gr)	Pelitic gneiss (Grt-Crd-Sill-Spl-Gr)	Pelitic gneiss (Grt-Crd)	Pelitic gneiss (Grt-Sill)	Group A Pegmatite/ Leucogranite	Group A Pegmatite/ Leucogranite	Group B Pegmatite/ Leucogranite	Group B Pegmatite/ Leucogranite
SiO_2	51.80	74.80	62.20	63.60	59.30	51.00	58.00	85.60	71.00	62.30	56.90
TiO_2	0.98	0.25	0.85	0.74	0.94	1.58	0.86	0.42	1.20	1.00	1.22
Al_2O_3	17.20	13.50	12.90	15.50	18.80	13.60	17.80	2.83	7.89	12.60	16.20
$Fe_2O_{3\ tot}$	11.60	1.70	9.52	2.92	6.64	15.80	10.80	8.36	10.80	10.00	10.80
MnO	0.14	0.04	0.16	0.08	0.03	0.17	0.22	0.04	0.08	0.12	0.13
MgO	3.54	0.60	3.20	2.00	2.76	7.05	2.64	0.10	3.10	3.29	4.12
CaO	8.62	1.08	6.79	1.08	1.28	2.40	1.03	0.47	0.28	1.30	1.80
Na_2O	4.48	4.70	2.86	3.46	3.70	1.57	1.79	0.99	0.57	2.74	3.81
K_2O	1.72	3.80	1.11	5.08	4.78	4.64	5.49	0.27	4.12	2.84	4.21
P_2O_5	0.23	0.01	0.17	0.07	0.07	0.22	0.13	0.03	0.02	1.30	0.39
LOI	0.20	0.30	0.60	5.90	1.70	2.20	0.80	0.30	0.80	2.50	1.10
SUM	100.51	100.77	99.98	100.37	100.00	100.15	99.56	99.38	99.84	99.99	100.68
C %	0.01	0.12	0.08	3.95	0.33	6.09	0.06	0.11	0.04	0.07	0.03
S %	0.01	0.01	0.02	0.99	0.01	15.60	0.04	0.01	0.17	0.08	0.01
F %	-	-	0.16	0.12	-	0.34	-	0.09	0.42	0.20	0.34
Cl%	-	-	0.08	0.01	-	0.09	-	0.02	0.14	0.10	0.10
B	6	6	4	55	10	7	10	15	4	37	10
Br	-	-	1	16	-	1	-	14	1	5	5
Sc	24	2	28	17	21	38	28	4	14	26	20
V	192	16	244	132	134	328	133	32	91	156	201
Cr	4	7	137	80	89	264	120	16	72	49	33
Co	40	1	28	18	15	47	40	2	23	23	32
Ni	26	3	75	72	41	130	52	4	79	59	55
Cu	1	1	53	97	38	55	4	7	57	157	1
Zn	95	25	127	61	39	353	82	85	483	128	321
Cs	-	-	3	6	-	18	-	3	18	3	12
Rb	61	153	18	208	139	435	280	12	402	334	643
Sr	300	43	187	75	186	82	68	18	27	174	65
Ba	173	394	144	783	1160	660	1390	32	435	263	331
Nb	1	13	2	10	14	38	14	13	141	174	166
Zr	99	422	121	203	215	258	200	3090	2210	2700	64
Hf	2	9	1	4	5	6	3	95	76	89	1

Table 2-3 (*cont`d.*) Representative whole-rock, major- and trace-element geochemical analysis of pegmatites and gneissic host rocks.

Sample #	WYL-09-50-237	WYL-09-50-252.7	WA-08-0-0046	WYL-10-62-68.9	WYL-09-50-37.5	WYL-10-62-87.1	WYL-09-49-36.1	WYL-10-61-190.3	WYL-10-62-93.5	WYL-09-46-31.1	WYL-09-46-32.6
Y	21	30	20	28	38	47	45	149	92	1190	228
La	27	61	18	65	74	131	55	8	24	4410	1040
Ce	48	107	31	105	137	279	149	36	57	9050	2000
Pr	3	11	2	12	12	30	11	5	6	1060	238
Nd	25	39	17	44	52	126	39	14	17	3590	796
Sm	5	6	3	7	8	21	6	10	8	607	132
Eu	3	1	1	1	2	1	2	0	0	3	1
Gd	3	5	2	4	6	14	7	13	11	553	121
Tb	1	1	1	1	1	1	1	1	1	50	10
Dy	3	5	4	3	5	8	6	20	14	197	38
Ho	1	1	1	1	1	1	1	4	2	34	6
Er	2	3	2	1	4	3	3	13	9	75	13
Yb	3	3	3	1	3	3	4	15	11	33	4
Pb	13	11	22	30	11	38	24	324	709	559	153
Th	2	23	1	21	17	410	23	1190	1370	7310	1360
U	1	8	5	11	4	44	4	1260	1100	701	75
Li	15	23	9	45	74	89	34	10	66	54	53
Be	1	4	1	2	2	2	1	1	0	6	5
Ga	23	21	18	22	30	30	21	26	27	12	28
As	-	-	13	16	-	12	-	23	21	6	6
Mo	1	1	1	8	1	50	3	1	1	144	9
Ag	0	0	1	1	0	0	0	13	13	0	0
Cd	1	1	2	2	1	2	1	1	1	1	1
Ta	1	1	1	1	1	1	1	1	3	12	9
Bi	-	-	1	1	-	1	-	13	1	3	3
Sb	-	-	1	1	-	1	-	1	1	1	1
Se	-	-	39	1	-	42	-	1	27	5	44
Sn	1	12	1	1	1	1	1	9	3	13	10
W	1	1	1	10	1	1	1	1	1	1	1
Th/U	2.0	2.9	0.1	1.9	4.3	9.3	5.8	0.9	1.2	10.4	18.1
Eu/Eu*	2.7	0.4	1.4	0.7	1.1	0.1	0.8	0.0	0.1	0.0	0.0
La_n/Yb_n	7.3	13.7	4.7	31.3	14.7	27.6	10.6	0.4	1.5	89.8	184.5
∑REE	124	242	83	245	305	618	283	139	159	19662	4399
A/NK	1.86	1.14	2.18	n/a	n/a	n/a	n/a	1.47	1.46	1.66	1.50
A/CNK	0.69	0.98	0.71	n/a	n/a	n/a	n/a	1.02	1.34	1.27	1.15

Notes: - = not analyzed; n/a= not applicable

Samples of graphite-bearing pelitic gneiss contain up to 6.64 wt. % C, and some also contain up to 15.6 wt. % S (Table 3). They have varied metal concentrations. However, the highest Ni (2600 ppm in one sample: SDT), Cu (307 ppm), and Co (137 ppm) contents are in rocks with the highest S content, suggesting a relationship with sulfides; whereas the highest Cr (259 ppm) and V (566 ppm) contents occur in rocks with the highest Fe_2O_3 $_{tot}$, suggesting a relationship with iron oxide minerals. U (up to 49 ppm, av. 15 ppm) and Th (up to 557 ppm, av. 42 ppm) are enriched relative to typical values for fine-grained sedimentary rocks, as exemplified by the North American Shale Composite (NASC) of Gromet *et al.*, 1984, which has values of 2.66 ppm U and 12.30 ppm Th. Such enrichment in U and Th is expected, due to the graphitic nature of this gneiss.

Granitic pegmatites and leucogranites

Whole-rock geochemical analysis of pegmatites is fraught with difficulty because of the coarse grain size of minerals and common internal zoning. These features make determination of the bulk composition of the pegmatite-forming melt almost impossible (e.g., Stilling *et al.*, 2006) but may allow determination of the melt composition of specific zones within a pegmatite. At Fraser Lakes Zone B, samples were collected predominantly from drill core, but a few were collected from the only outcrop (Fig. 2-3b, 2-6a). However, the small volume of each sample, especially the drill core samples, means that any individual sample may not accurately reflect the modal mineralogy of the pegmatite/leucogranite at that specific location. Nevertheless, the two groups of strongly radioactive granitic pegmatites (Group A and Group B, introduced earlier) show differences in their U and Th contents and Th/U values (Fig. 2-9a); the compositions of two samples from each group are shown in Table 2-3.

Group A intrusions are enriched in U and Th and have Th/U values of ~1 (Table 2-3, Fig. 2-9a), reflecting the presence of uraninite and U-enriched thorite; they contain up to 2460 ppm U and 1100 ppm Th. In contrast, Group B intrusions are typically enriched in Th and LREE with Th/U values of >2 (commonly greater than the crustal average ratio of 4: see Fig. 2-9a); they contain up to 701 ppm U, 7310 ppm Th, 4410 ppm La, 9050 ppm Ce, 1060 ppm Pr, 3590 ppm Nd, and 607 ppm Sm (Table 2-3).

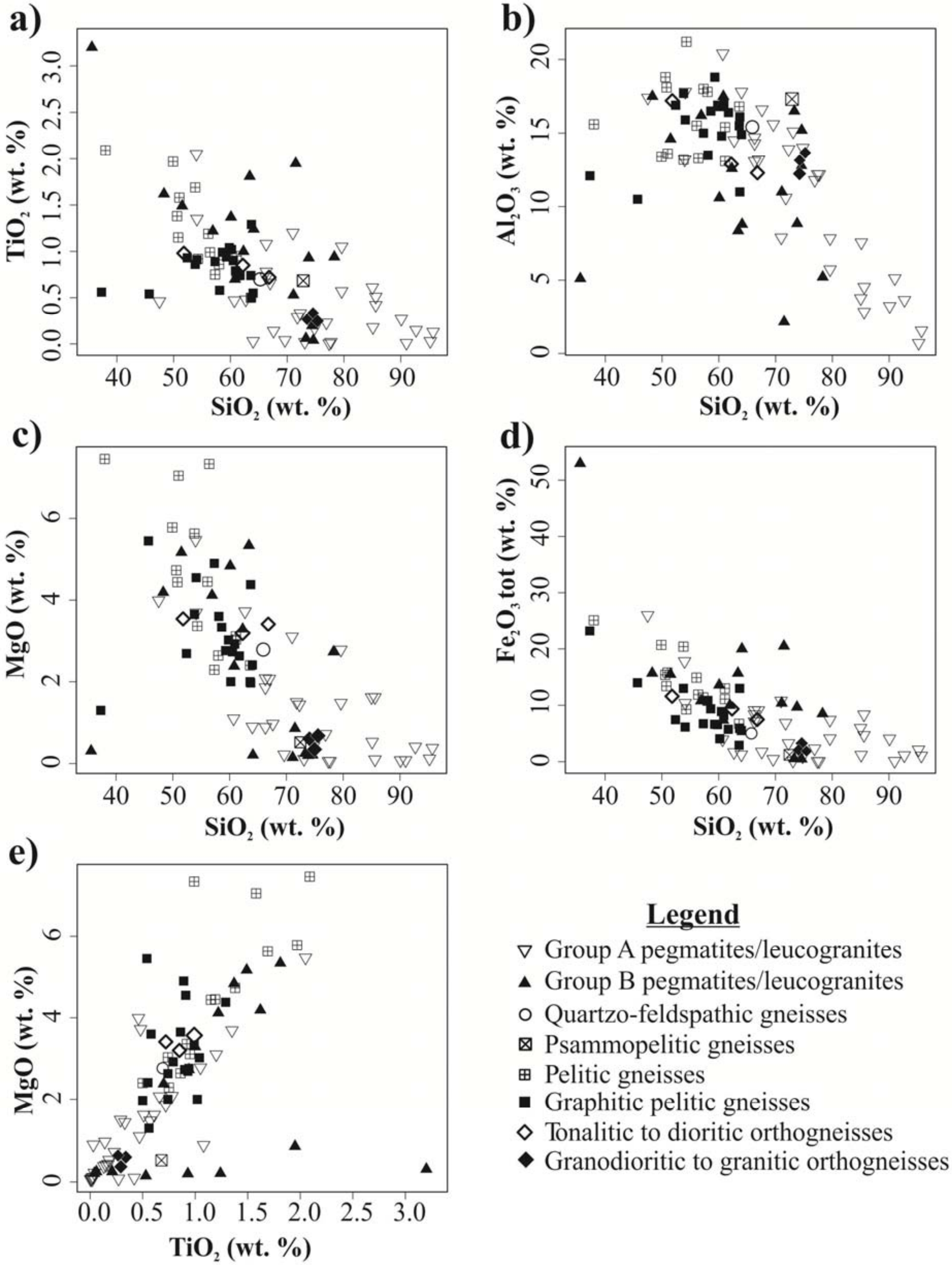

a)
TiO2 (wt. %)
SiO2 (wt. %)
b)
Al2O3 (wt. %)
SiO2 (wt. %)
c)
MgO (wt. %)
SiO2 (wt. %)
d)
Fe2O3 tot (wt. %)
SiO2 (wt. %)
e)
MgO (wt. %)
TiO2 (wt. %)
Legend
Group A pegmatites/leucogranites
Group B pegmatites/leucogranites
Quartzo-feldspathic gneisses
Psammopelitic gneisses
Pelitic gneisses
Graphitic pelitic gneisses
Tonalitic to dioritic orthogneisses
Granodioritic to granitic orthogneisses

Figure 2-8 (previous page). Major-element Harker diagrams for granitic pegmatites and leucogranites, pelitic gneiss, and orthogneiss. a) TiO_2 vs SiO_2, b) Al_2O_3 vs SiO_2, c) MgO vs SiO_2, d) $Fe_2O_{3\ tot}$ vs SiO_2, and e) MgO vs TiO_2. The major-element compositions of Group A and Group B pegmatites show some overlap with those of the pelitic gneiss and orthogneisses, suggesting a possible compositional influence (*i.e.*, the pegmatites possibly formed from melting of similar rocks and/or assimilation of host rocks). Group A pegmatites define weak trends towards higher SiO_2 contents with decreasing TiO_2, Al_2O_3, MgO, and Fe_2O_3, suggesting they formed from more evolved melts. Group B pegmatites show compositions more similar to the pelitic gneiss; they could represent more primitive melts or restitic melts, or may reflect more assimilation of the host rocks. See text for details.

Group A intrusions on average tend to be more SiO_2-rich (Fig. 2-9b) than Group B intrusions, except where the former intrusions contain magnetite and ilmenite. Group B intrusions, in contrast, have elevated P_2O_5 (Fig. 2-9c); this is related to the presence of monazite as the dominant accessory mineral, as it hosts most of the light REEs (LREEs). The Th/U vs. log Ce emphasizes the high LREE content of Group B pegmatites, especially those high in Th, which in turn reflects their monazite content (Fig. 2-9d). U-enriched thorite contains much of the U and some of the Th in Group B intrusions, with xenotime being one of the main heavy REE (HREE) hosts. Group A intrusions have elevated Pb concentrations of up to 847 ppm and Group B intrusions, up to 674 ppm (Table 2-3).

The pegmatites show variation in their major-element chemistry related to the relative amounts of quartz, plagioclase, K-feldspar, biotite, magnetite, and ilmenite in each specific sample. Group A intrusions tend to be slightly more enriched in silica and depleted in titanium relative to Group B; however, their chemistry overlaps considerably (Fig. 2-8a to e). The high-SiO_2 intrusions are quartz-rich, whereas samples with the lowest SiO_2 have the highest proportion of biotite, magnetite, and/or ilmenite. The contents of Al_2O_3, MgO, and $Fe_2O_{3\ tot}$ tend to decrease as SiO_2 increases (Fig. 2-8b to d), whereas CaO, Na_2O, and K_2O contents are more varied with respect to SiO_2 (Table 2-3, SDT).

Group A and Group B intrusions are peraluminous to weakly metaluminous and represent S-type and marginal I-type granitoids (Fig. 2-10). They overlap the pelitic gneiss and orthogneiss on major-element Harker variation diagrams (Fig. 2-8a to e), with Group A intrusions tending to be more distinct in composition from the pelitic gneisses and orthogneisses than Group B intrusions. Some of the low-MgO pegmatites define a linear trend toward higher TiO_2 with constant MgO: that is, away from the granitic orthogneiss compositions (Fig. 2-8e). These pegmatites intrude Archean granitic orthogneiss, and thus their composition may be controlled by melting or assimilation of the host rocks.

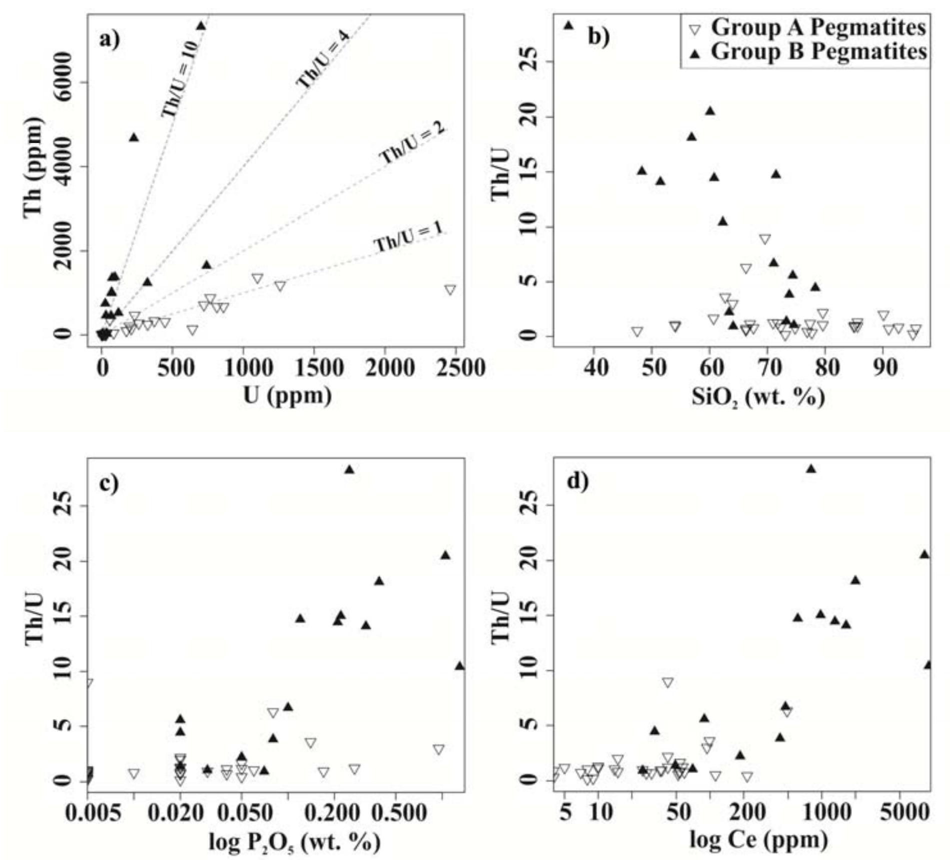

Figure 2-9. Trace element diagrams for the Fraser Lakes Zone B granitic pegmatites. (a) Th vs. U. The diagonal lines show different Th/U ratios. The Group A pegmatites have Th/U ~1, and the Group B pegmatites generally have Th/U >2. (b) Th/U vs. SiO2, which shows that the Group A pegmatites generally have higher SiO2 contents than the Group B pegmatites with some overlap between the two groups. (c) Th/U vs. P2O5 to emphasize the importance of monazite in the Group B pegmatites. (d) Th/U vs. log Ce emphasizing the high LREE content of the Group B pegmatites, especially those high in Th, which in turn reflects their monazite content.

The pegmatites contain varied amounts of F and Cl. Group A intrusions typically contain <0.20 wt. % F, but a few samples have up to 0.42 wt. % F. Chlorine is present in small amounts as well (up to 0.11 wt. % Cl). In contrast, Group B intrusions contain 0.07–0.45 wt. % F (typically >0.20 wt. % F) and up to 0.40 wt. % Cl. Zirconium ranges markedly in Group A intrusions (249–4060 ppm) and in Group B intrusions (64–11,700 ppm), depending on the modal proportion of zircon. The concentrations of Be (<6 ppm) and Li (<54 ppm) are low for both groups of intrusions (Table 2-3, SDT).

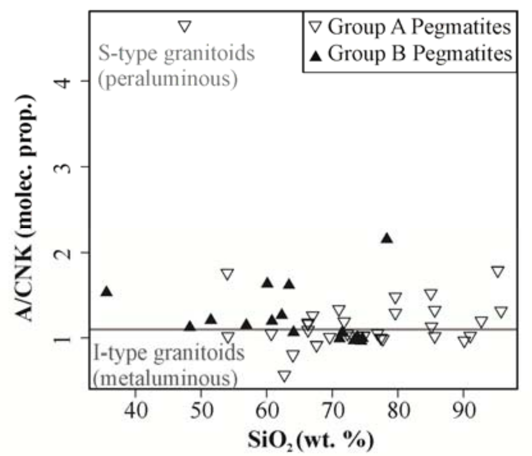

Figure 2-10. A/CNK vs SiO_2 diagram (Chappell and White, 1974), showing that the granitic pegmatites have A/CNK values similar to those of S-type granitoids with some overlap into the I-type granitoid field. A/CNK = Al_2O_3/ ($CaO + Na_2O + K_2O$).

The total REE contents in Group A intrusions tend to be lower (~35–500 ppm) than in Group B intrusions (~1000–19,000 ppm) (Fig. 2-11a, 2-11b, Table 2-3, SDT). Chondrite-normalized patterns of Group A intrusions (Fig. 2-11a) have flatter and more complex patterns than Group B intrusions (Fig. 2-11b). Group B intrusions are LREE-enriched (Fig. 2-11b), with La_n/Yb_n values up to 200 and significant negative Eu anomalies.

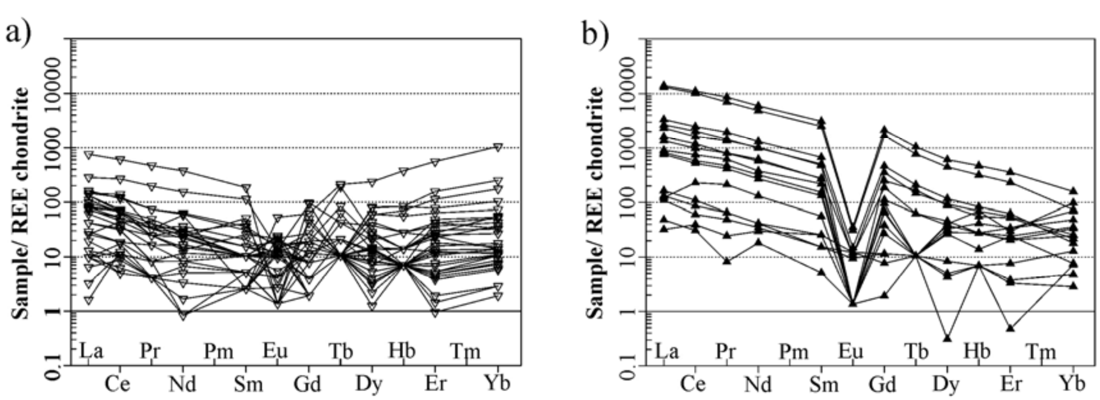

Figure 2-11. Chondrite-normalized (Boynton, 1984) REE plots for the ‘radioactive’ granitic pegmatites, showing the differences between a) Group A, and b) Group B granitic pegmatites and leucogranites.

Discussion

Classification of granitic pegmatites and leucogranites

The granitic pegmatites and leucogranites at Fraser Lakes are generally subcordant to lithological and structural contacts of their metamorphosed and locally migmatitic host rocks. These intrusions are aligned subparallel to the dominant fabric in the upper amphibolite to lower granulite facies metamorphic rocks (Fig. 2-3a, 2-3b, 2-5a). The presence of migmatite indicates that rocks in the area attained conditions suitable for melts to form and suggests that the intrusions were formed by partial melting.

On the basis of U-Th-Pb dating of uraninite (Annesley *et al.*, 2010b), Group A intrusions are interpreted to have crystallized in their present position ca. 1810–1775 Ma, a time interval similar to that interpreted for other uranium-enriched granitic pegmatites in the Wollaston Domain (Annesley *et al.*, 2000; Mercadier *et al.*, 2010). No granitic plutons of this age are known in the Wollaston Domain, especially in the vicinity of Fraser Lakes Zone B. The similarities in intrusive contacts suggests that Group B rocks were intruded at roughly the same time as Group A rocks, however, reliable primary magmatic ages for these intrusions have not yet been obtained.

The metamorphic grade of the host rocks, structural relationships (concordant to subcordant contacts), and lack of any relationship to coeval granitic rocks all suggest that the Fraser Lakes pegmatites/leucogranites can be classified as Abyssal-class pegmatites (Černý and Ercit, 2005). Group A pegmatites/leucogranites at Fraser Lakes contain abundant zircon and uraninite (Table 2-2) and have the highest U concentrations. These Group A intrusions are assigned to the U-subclass of Abyssal pegmatites of Černý and Ercit (2005), whereas the LREE-enriched pegmatites/leucogranites of Group B intrusions that contain ubiquitous monazite (Table 2-2) are assigned to the LREE subclass.

The lack of contemporaneous granitic plutons suggests that the Fraser Lakes pegmatites were derived by melting during peak thermal metamorphism along an essentially isothermal decompression path. Mechanisms driving partial melting may have included (but are not limited to) isothermal decompression, large amounts of high heat-producing elements in the crust (in particular U and Th in the Fraser Lakes area), shear heating, thinning of the mantle lithosphere, and a high crustal geothermal gradient (Nabelek and Liu, 2004).

The Fraser Lakes pegmatites are interpreted to be the same age and/or younger than the leucosomes (generated by in situ melting and crystallization) in the immediate host rocks. However, the large size of the pegmatite bodies indicates that they were generated 'off-site' at depth as anatectic melts, which migrated to and crystallized at their present location. The geochemical and mineralogical characteristics of these pegmatites are thus a function of the composition of the source rock, the nature of melt reactions, and the assimilation and fractional crystallization processes that might have operated during melt migration and/or final solidification.

Petrological and geochemical constraints

The Fraser Lakes pegmatites are peraluminous to slightly metaluminous S-type to marginally metaluminous I-type granitoids (Fig. 2-10), implying that the source area where partial melting occurred was dominated by sedimentary rocks. This was also suggested by previous studies of leucogranites and granitic pegmatites in the Wollaston Domain (Annesley *et al.*, 2000, 2005). The overlapping compositions of pelitic gneiss, orthogneiss, and pegmatite (Fig. 2-8a to e) suggest that the pegmatites are compositionally related to their host rocks, especially the pelitic gneisses, and that they may be derived by partial melting of such rocks, or that the melt may have assimilated rocks of a similar composition. The ranges in major- and trace- element compositions of the pelitic gneisses (Fig. 2-8a to e, 2-9a to d) reflect the wide range of original bulk compositions, which makes modeling of melting or assimilation processes difficult.

As the actual source rock for the granitic pegmatites is unknown, we assume that conditions during the partial melting of the Fraser Lakes pelitic gneisses and the formation of the migmatites were equivalent to those leading to the formation of the Fraser Lakes granitic pegmatites/leucogranites. Annesley *et al.* (2005) determined that partial melting of pelitic gneisses in the Wollaston Domain occurred at ca. 1815 Ma by fluid-absent melting at temperatures of up to 850ºC and pressures of up to 9 kbar. The rocks then underwent essentially isothermal decompression over the next 20–35 Ma, during which time the rocks remained within the appropriate conditions for partial melting, by biotite-dehydration reactions, until pressures decreased to ~4–5 kbar. Migmatite development was coeval with peak thermal metamorphism in the Fraser Lakes area.

The migmatites at higher levels were intruded by pegmatitic melts that were being continually generated at greater depths in the crust. The crystallization conditions of the Fraser Lakes pegmatites may be recorded by the metamorphic mineral assemblages of their host rocks, which are indicative of upper amphibolite to granulite facies metamorphism (Fig. 2-5a to f). Group A and Group B intrusions are not pure anatectic melts (e.g., Patiño Douce, 1999), because they contain varied amounts of peritectic minerals such as garnet, zircon, biotite, and monazite, some of which were entrained as xenocrysts from the source rocks. These assemblages indicate that the granitic pegmatites were emplaced at mid-crustal depths (15–20 km). After generation, the melts likely evolved due to changing pressure, temperature, or volatile content.

Weakly defined trends and clusters of analyses on Harker major-element variation diagrams (Fig. 2-8a to f) could be explained by varied degrees of partial melting and amounts of crystal fractionation, causing differences in modal mineralogy. For example, the depletion in Al_2O_3, CaO, and K_2O of the most siliceous pegmatites (Fig. 2-8b, Table 2-3) is consistent with the fractionation of plagioclase and alkali feldspar; and the decrease in Fe_2O_3, MgO, and TiO_2 with increasing SiO_2 implies fractionation of biotite. Crystal fractionation of the major minerals (Table 2-2) is important as the pegmatites are commonly zoned (Fig. 2-5a), with quartz-rich and plagioclase-rich internal zones and K-feldspar-rich margins. In addition, some zones are preferentially enriched in biotite (Fig. 2-6a, 2-7c).

The gneissic rocks in the Fraser Lakes area are enriched in U, Th, and Zr relative to the NASC, as would be expected for graphite-bearing rocks, and thus they could generate melts enriched in these elements. Bea (1996) emphasized the importance of accessory minerals as the reservoir of REE, U, and Th in metamorphic rocks but also reported that large volumes of the accessory phases occur as inclusions in biotite. Thus, the concentrations of REE, U, and Th in any melt may depend on the efficiency of the reactions that lead to the breakdown of biotite and which can release accessory minerals into the melt.

Annesley *et al.* (2005) emphasize that biotite-dehydration reactions are important in the generation of migmatites in the Wollaston Lake area (*e.g.,* Pow Peninsula, McClean Lake, among others). The U-Th-REE-bearing accessory minerals within source rock biotites would not be liberated during early melt-generating reactions that did not involve biotite dehydration. This lack of liberation would enrich the remaining source rocks in these elements and in turn would increase the likelihood that late melts would be enriched in U-Th-REE (see Nabelek and Liu, 2008; Villaros *et al.*, 2009; and Brown, 2010 and references therein).

Evidence for biotite-dehydration reactions, in the form of melt textures (Fig. 2-5e) and the metamorphic assemblages, is visible in the pelitic gneisses of the Fraser Lakes area. Accessory minerals in the granitic pegmatites, in particular zircon and monazite, are commonly found in clusters (Fig. 2-6c, 2-6e, 2-7d) rather than uniformly distributed. In addition, many zircons in the pegmatites appear to have cores (Fig. 2-6c) that are inherited.

Thus, the textural relationships suggest that some accessory minerals were entrained as xenocrysts in the melt at the source and then transported within the melt to the region of final crystallization. However, zircons are present in the pegmatites/leucogranites that have overgrowths with typical magmatic zoning, suggesting that Zr was also available in the melt. The uraninite grains in Group A intrusions also show primary igneous characteristics. Thus, it is likely that the U-Th-REE-bearing minerals formed due to a combination of inheritance (from the source rock and/or assimilation of host rocks) and igneous fractionation and crystallization processes.

The spatial association between zircon, monazite, and biotite suggests that these minerals share a common evolution during the formation of the granitic pegmatites/leucogranites. This implies that these minerals would have been incorporated into the melt to a similar extent if partial melting and entrainment processes dominated or, alternatively, that they would have been fractionated from the melt to a similar extent if crystal-liquid fractionation processes dominated.

Overall, the large-scale zoning, observed geochemical variations, and character of the U-Th-REE-Zr-bearing accessory minerals all suggest that these pegmatites represent a combination of processes: that is, partial melting of an enriched pelitic gneiss source; entrainment of accessory phases (inherited from the magma source and assimilated during transport) in the resultant peraluminous magma; fractionation of the melt with respect to U, Th, REEs, and Zr; and the growth of U, Th, REE, and Zr-bearing minerals from the melt.

Zr and REE contents in zircon and monazite have been used to calculate crystallization temperatures, under the assumption that they represent the saturation temperatures of those minerals. Petrological studies have shown that the temperature estimates are relatively close to the temperature of segregated melts, provided the accessory phases grew from the melt and were not inherited (Watson and Harrison, 1983; Montel, 1993; Miller *et al.*, 2003). Calculated temperature estimates for the Fraser Lakes granitic pegmatites range between 825ºC and 700ºC. The highest temperature of 825ºC is close to the estimate for peak thermal metamorphism in the Wollaston Domain (Annesley *et al.*, 2005), and the range indicates that the melt potentially cooled and crystallized during transport and emplacement, if the temperatures were derived from magmatic crystals.

The decrease in Zr, Th, and LREE with increasing SiO_2 (see SDT) in the granitic pegmatites probably reflects the growth and fractionation of zircon and monazite from the melt due to decreasing solubility of these phases, given that Zr and REE occur mainly in these accessory minerals; thus, not all of the zircon and monazite in these pegmatites was inherited. This also implies that some uraninite probably crystallized after zircon and monazite formation from the most fractionated melts, which would have had the highest SiO_2 contents.

Role of deformation

Annesley *et al.* (2010c) recently suggested that the identification of target areas with major structures and accumulation of peraluminous S-type granites within the basal metasedimentary rocks of the Wollaston Group can be used as an exploration tool for predicting the potential location of unconformity-type uranium deposits in the eastern Athabasca Basin. They outlined five key criteria for identifying these areas: a) structurally complex zones with a history of, and evidence for, reactivations, b) multiple sets of faults with various orientations, c) a higher than normal volume of S-type granite, d) migmatitic metasedimentary rocks (in part graphitic) near the base of the Wollaston Group, and e) an inlier of Archean rocks (antiformal core or ridge) in close proximity to the base of the Wollaston Group. All five conditions apply at Fraser Lakes Zone B, which raises the following questions.

- What is the relationship between deformation and S-type granites?
- What relationships exist between or among the mineralized granitic pegmatites and the host pelitic gneisses?
- What is the role of deformation in magma extraction, migration, differentiation, and emplacement of the granitic pegmatites and associated leucogranites?
- What is the role of the folded and sheared Archean– Paleoproterozoic contact (*i.e.*, the tectonized discontinuity or décollement)?

Opinions differ on the cause and effect of strain localization in melt-bearing continental crust, and on how magma is transferred from the source region to the sink region (Ward *et al.*, 2008; Weinberg and Mark, 2008; Brown, 2010). In the last fifteen years, however, researchers have reconciled this by considering that deformation and melts interact in a positive feedback loop (see Brown, 2010, and references therein). Still, different processes are ascribed to explain the positive feedback loop (e.g., Kisters *et al.*, 1998; Brown and Solar, 1999; Handy *et al.*, 2001; Solar and Brown, 2001; Brown, 2010). According to others including Weinberg (1999), Weinberg and Mark (2008), and Kisters *et al.* (2009), the geometry of the magma network in the source region provides the ultimate control on the transfer process.

At Fraser Lakes, we observed fertile, radioelement-enriched pelitic to psammopelitic rocks in both outcrop and drill core that have undergone syn-kinematic melting and subsequent crystal fractionation at upper amphibolite to granulite facies conditions in the presence of a volatile H_2O-F-rich phase. We also observed veinlets, dikes, and sheets of granitic pegmatites up to tens of meters wide, which are located along a folded, sheared Archean–Paleoproterozoic discontinuity that marks an inferred transfer zone of magma from deeper crustal levels.

Similarly to Weinberg and Mark (2008), we see the following important structural indicators of the sense of melt migration within the rocks (upward): 1) development of a cauliflower-shaped upper contact with host rocks, 2) preferential segregation into fold hinge zones, and 3) development of cuspate fold hinges with destruction of synformal features.

We also see on a large scale the preferential movement of high volumes of melt into antiformal structures, similar to what is observed within the area of the Rössing uranium deposit (Nex *et al.*, 2001; Basson and Greenway, 2004). It appears that folding of the rocks led to pressure gradients, causing melt to migrate preferentially along ductile, high-temperature layers and parallel to the axial plane of the folds. In addition, melt migration may have led to attenuation of the folding, in turn causing disaggregation of the rocks with a preferential destruction of synformal structures (see Weinberg and Mark, 2008, their Fig. 3, 4, 13).

Summary of model

The granitic pegmatites at Fraser Lakes Zone B are interpreted to be lower to middle crustal melts that were derived from a crustal source similar to the migmatitic metasedimentary gneiss units cropping out in the immediate Fraser Lakes area and the nearby Walker River area (Annesley *et al.*, 2009). This interpretation implies crustal thickening and associated overthrusting at Fraser Lakes along a clockwise P-T-t path with large-scale structures facilitating crustal melt transfer, as proposed by Weinberg and Mark (2008).

The peak metamorphic mineral assemblages of these metasedimentary rocks on petrogenetic grids yield P-T estimates similar to those reported from other parts of the Wollaston Domain, in which maximum P-T conditions (*i.e.*, peak thermal metamorphism) reached 6–9 kbar and 800–850ºC (Annesley *et al.*, 2005) at ca. 1815 Ma (Annesley et. al., 1997, 2005; Tran, 2001). Considering an elevated gradient of ~30–40ºC/km, partial melting may have occurred at a depth of approximately 20–30 km, which is consistent with previous estimates made by Annesley *et al.* (2005) for melting in the Wollaston Domain.

The model presented here has many similarities to models proposed for the formation and evolution of leucogranites in the Paleoproterozoic Svecofennian Orogen of Sweden, Finland, and western Russia, in particular, the uranium potential of late orogenic potassic granites (Lauri *et al.*, 2007; Cuney *et al.*, 2008; Skyttä and Mänttäri, 2008; Kukkonen and Lauri, 2009; Kurhila *et al.*, 2011).

Metasedimentary migmatites exposed in the Fraser Lakes area are cross-cut by numerous vertical to subvertical granitic pegmatite and leucogranite bodies that could represent transfer zones for melts from a deeper partial melting zone (It is assumed that accumulation of relatively low-density melts triggered vertical migration through the crust). Continuous deformation within and along major structural zones, including large-scale folds, is believed to have helped crustal melt ascent by creating alternative zones of dilation and compression within the anastomosing shear/fault zone system of the Wollaston fold-and-thrust belt. This led to the expulsion of crustal melts to upper crustal levels. At Fraser Lakes, we envisage the exposed high-grade migmatitic terrane as being the former mid-crustal melt transfer zone between the deeper crustal source region and the middle to upper crustal sink region.

An important assumption in this paper is that the sources of the granitic pegmatites and leucosomes were partially melted pelitic to psammopelitic rocks of the Wollaston Group near and below their observed emplacement depth. However, it is also possible that a different melt source (or several sources) exists below and that the similarities in composition of the granitic pegmatites/leucogranites to that of their host rocks are due to assimilation only.

Emplacement of the granitic pegmatites in the middle crust in relation to the large-, kilometer-scale folds and associated shear zones (Fig. 2-12, 2-13) demonstrates the potential role of deformation in magmatic evolution. Mineral fractionation in magmas en route to the surface is likely enhanced by regional deformation, especially in the case of highly silicic mushes that are more readily affected by stress, so that liquids (melts) may be expelled from the rigid framework once the Rigid Percolation Threshold (RPT; Vigneresse *et al.*, 1996) has been reached. This explains the extreme heterogeneity of Group A and Group B intrusions and indicates that Group B intrusions are still fairly close to their source area.

After reaching the RPT, the deformation and tectonic stress processes start to facilitate the discontinuous squeezing of residual liquids upward along the structural and metamorphic fabric toward the surface (*i.e.*, smaller amounts of melt, as proposed by Bons *et al.*, 2004). These same deformation and tectonic stress processes would also push the melt away from the limbs of the fold toward the fold nose area where they are emplaced; that is, melt migration would occur perpendicular to the fold axis and parallel to the stretching axis (see Weinberg and Mark, 2008).

Such a scenario implies that melt migration enhanced folding. Consequently, the Fraser Lakes granitic pegmatites may have crystallized from different pulses and compositions of crustal anatectic melts that experienced contrasting crystal–liquid fractionation, thus explaining their heterogeneous nature.

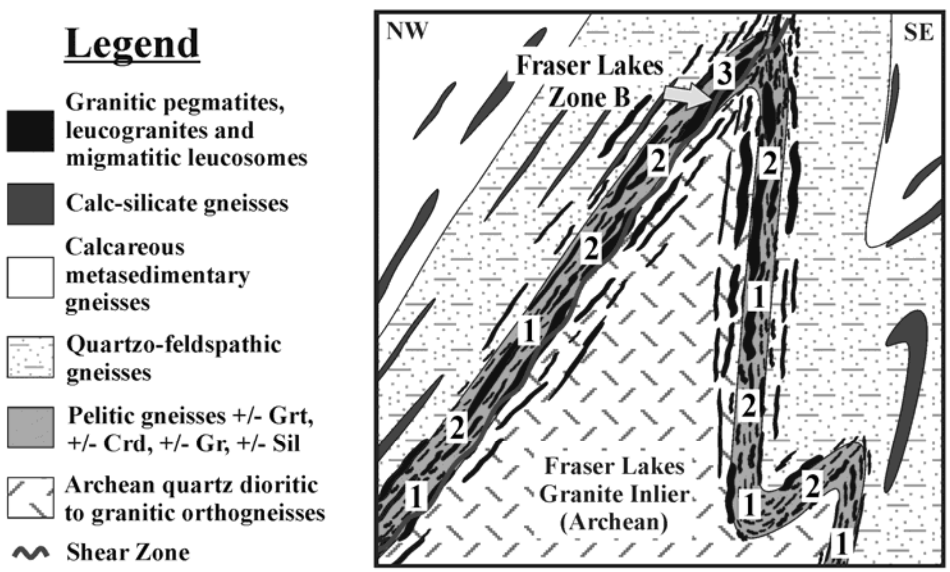

Figure 2-12. Schematic vertical cross-section (vertical scale is ~1 km) depicting the different levels of migmatization, transport, and emplacement of pegmatitic melts in the Fraser Lakes Zone B area. (See Fig. 2 for approximate location of Zone B in the report area.) Plunge of the antiformal fold noses is ~25–30ºNE. 1) Partial melting at depth/in situ of U-Th-REE-enriched metasedimentary rocks (Wollaston Group) during peak thermal metamorphism by biotite dehydration melting. 2) Transport of melt upwards and laterally along ductile shear zones and parallel to gneissosity; during transport, the melt undergoes fractionation, becoming further enriched in U-Th-REE. 3) Concentration of melt in fold noses, where it crystallizes to form pegmatites; during crystallization, the melt undergoes igneous assimilation–fractional crystallization processes.

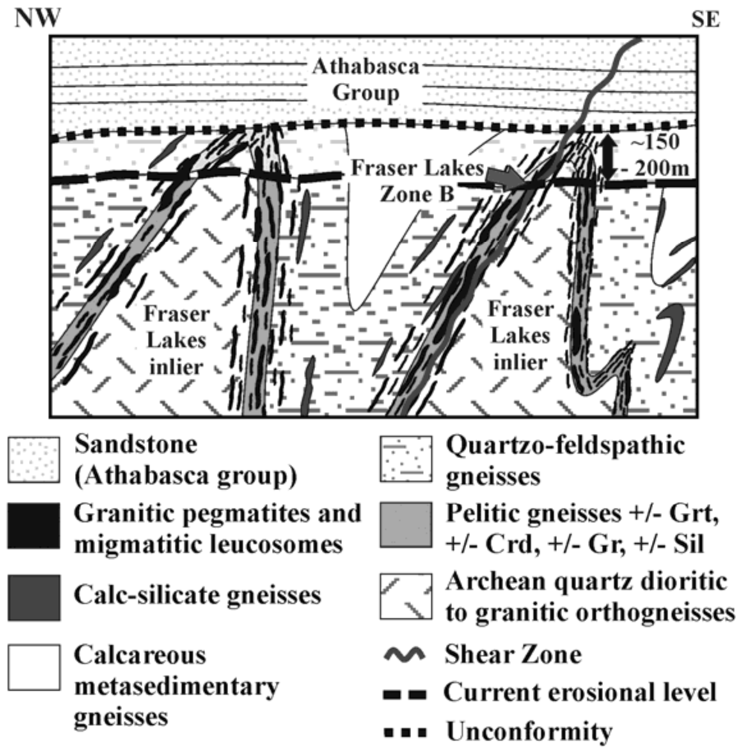

Figure 2-13. Idealized vertical cross-section of Fraser Lakes Zone B area prior to complete erosion of the overlying Athabasca group sedimentary rocks and ~150–200 m of basement rocks below the unconformity (Annesley *et al.*, 2009). The thickness of basement eroded is estimated by eastward extrapolation of the sub-Athabasca Group unconformity slope to the Fraser Lakes area. Vertical scale is ~1 km. Antiformal fold noses plunge ~25–30ºNE, as on Figure 2-12.

Link to unconformity uranium deposits

Unconformity-related uranium deposits are among the highest grade uranium deposits in the world, with grades of up to 18.3% U_3O_8 (Cigar Lake Deposit; Cameco, 2012) in the Athabasca Basin of northern Saskatchewan (Fig. 2-1). Typically, they are located along fault zones rooted in the underlying basement rocks that extend into overlying sandstones of the Athabasca Group. They result from the interaction between oxidizing fluids that transport uranium with either graphitic or 'reduced' rock types, or reduced fluids (Hoeve and Sibbald, 1978; Jefferson *et al.*, 2007).

One of the still-debated questions concerning the origin of unconformity-related uranium deposits is the source of the uranium. Kotzer and Kyser (1995), for example, consider that oxidized fluids leached the uranium from detrital minerals in the sandstone. Such fluids then interacted with basement rocks to generate mineralization and alteration (Alexandre *et al.*, 2005; Cloutier *et al.*, 2009).

In contrast, Hecht and Cuney (2000) and Madore *et al.* (2000) suggest that oxidized basinal fluids interacted with basement rocks and obtained uranium from accessory minerals, such as monazite and uraninite. Pegmatites are important in this regard, as they may 1) have interacted with fluids that led to the in situ alteration of uranium-bearing accessory minerals, 2) have been a component of the regolith underlying the basin, the uranium having been remobilized during weathering and/or by fluids moving through the regolith, and/or 3) represent the source of uranium-bearing detrital minerals in the Athabasca Basin sedimentary rocks, the uranium having been remobilized later by fluids moving through the sandstone.

Several unconformity-related uranium deposits in the Athabasca Basin, including McArthur River, P-Patch, and Moore Lakes, contain uraniferous pegmatites in the basement underlying the deposits (Annesley *et al.*, 2000, 2005). In many cases, these pegmatites have been altered to minerals similar to the alteration assemblages associated with the unconformity uranium deposits.

Annesley and Madore (1999), Hecht and Cuney (2000), and Madore *et al.* (2000), among others, suggest that monazite in the basement rocks and/or regolith were altered by hydrothermal fluids (the same fluids responsible for the unconformity-related mineralization) to different minerals including Th-silicates (thorite or huttonite?), chlorite, and poorly crystalline, hydrous, Si-bearing Ca-Th phosphates (Hecht and Cuney, 2000). This alteration would have led to uranium redistribution and leaching, with the thorium remaining in the monazite alteration products due its lower solubility (Hecht and Cuney, 2000).

Calculations by Madore *et al.* (2000) using monazite (not taking into account uraninite, which is also easily altered by oxidizing fluids) suggest that large amounts of uranium may have been remobilized from monazite within the pegmatites/leucogranites, and may have provided a large amount of the uranium necessary for unconformity-related uranium deposits of the Athabasca Basin.

In the Fraser Lakes granitic pegmatites, especially in the highly fractured Th-rich varieties, there is evidence for low-T hydrothermal alteration in the form of moderately to strongly altered feldspars, biotite, thorite, allanite, uraninite, and monazite (Fig. 2-6e, 2-6f, 2-7a to c). Monazite in particular shows alteration to chlorite, hematite, and clay minerals (Fig. 2-7a to c), an assemblage with similarities to monazite alteration products related to uranium remobilization in the Athabasca Basin (Hecht and Cuney, 2000).

Thus, hydrothermal fluids may have passed through the rocks leading to remobilization of uranium from monazite in the Group B intrusions, similar to the model proposed by Annesley and Madore (1999), Hecht and Cuney (2000), and Madore *et al.* (2000) for uranium remobilization from monazites in the sandstones of the Athabasca Group and underlying regolith and/or basement. In addition, the fluids responsible for altering the intrusions may have leached uranium from uraninite and thorite (including U-enriched thorite) from the Fraser Lakes Zone B pegmatites/leucogranites. Thus, the possibility exists that significant amounts of uranium may have been remobilized from these intrusions by the same fluids that altered the rocks.

As indicated earlier, the presence of radioelement-enriched pegmatites spatially associated with structures in this area may suggest increased potential for the discovery of unconformity-related uranium deposits in the Fraser Lakes area. This type of redox boundary is important for later geochemical reactions during reactivation of pre-existing basement structures at or near the Wollaston–Archean unconformity, ultimately leading to mineralization as the redox change at the boundary could cause a decrease in uranium solubility in the mineralizing fluids.

The most likely source of the low-T (<250ºC) fluids responsible for the alteration assemblages at Fraser Lakes Zone B are the highly oxidizing, acidic basinal brines in the Athabasca Basin (Mercadier *et al.*, 2010; Richard *et al.*, 2010, 2011, 2012). These basinal fluids may have been efficiently circulated downward in fractures, where they altered the pegmatites/leucogranites at Fraser Lakes Zone B, analogous to the process proposed recently by Mercadier *et al.* (2010).

Strongly clay-altered pelitic gneisses with a clay mineral assemblage similar to that of unconformity uranium deposits occur within an interpreted fault zone northwest of the Fraser Lakes Zone B area (Annesley *et al.*, 2010a; JNR Resources, 2012). These gneisses offer further evidence that fluids similar to those responsible for the Athabasca Basin unconformity-related uranium passed through the Fraser Lakes Zone B area. The fluids may have remobilized uranium from the Fraser Lakes Zone B granitic pegmatites/leucogranites, ultimately leading to the formation of an as yet undiscovered, basement-hosted, unconformity-related uranium deposit near Fraser Lakes Zone B.

Conclusions

The U-Th-REE mineralization at Fraser Lakes Zone B consists of primary magmatic mineralization in granitic pegmatites, which is overprinted locally by later hydrothermal alteration. The pegmatites were emplaced into the highly deformed contact zone between Archean orthogneiss and metasedimentary rocks of the Wollaston Group, specifically within a regional fold nose.

The pegmatites in the central part of the fold nose are enriched in Th and LREE, whereas those on the west side are enriched in U ± Th. The pegmatitic melts were generated by partial melting of metasedimentary rocks with slightly elevated U and Th concentrations; and with U, Th, and REE-bearing accessory minerals that were entrained in the melt as xenocrysts. Subsequently, the melts underwent assimilation and fractional crystallization processes en route to the crystallization site. Melt migration and deformation are interpreted to have formed a positive feedback loop.

The character of the mineralization and structural control is consistent with that reported in research on similarly mineralized granitic pegmatites and leucogranites in the Rössing area of

Namibia (Berning *et al.*, 1976; Basson and Greenway, 2004) and in the Grenville Province of Canada (Fowler and Doig, 1983; Lentz, 1991, 1996).

The present study will form the framework for a future metallogenetic model of U-Th-REE mineralization in the Fraser Lakes area. It will aid in exploration for similar deposits in northern Saskatchewan and will help to determine the link between these pegmatite-hosted deposits and the high-grade, unconformity-related uranium deposits in the Athabasca Basin.

CHAPTER 3
RADIOACTIVE ABYSSAL GRANITIC PEGMATITES AND LEUCOGRANITES IN THE WOLLASTON DOMAIN, NORTHERN SASKATCHEWAN (CANADA): MINERAL COMPOSITIONS AND CONDITIONS OF EMPLACEMENT IN THE FRASER LAKES AREA

Abstract

The Fraser Lakes area in the Wollaston Domain, in northern Saskatchewan, Canada, is located 25 km from the southeastern edge of the uranium-rich Athabasca Basin; it hosts a number of U- and Th–REE-bearing granitic pegmatites and leucogranites. At Fraser Lakes Zone B, the pegmatites and leucogranites intrude the deformed contact between Paleoproterozoic metasedimentary gneisses of the Wollaston Group and Archean orthogneisses, and have characteristics typical of the Abyssal pegmatite subclass. For two examples of Group-A U- and Th-enriched pegmatite and leucogranite, and two examples of Group-B Th- and LREE-enriched pegmatite and leucogranite samples that have minimal petrographic evidence of later alteration, we analyzed selected minerals by electron microprobe to provide constraints on the age and temperature of intrusion. The Group-A pegmatites contain uraninite with variable CaO and SiO_2, indicative of later recrystallization, uranoan thorite spatially associated with complexly zoned zircon (with some intermediate solid-solution between the two minerals), rare coffinite, and titaniferous magnetite and ilmenite where they intrude the Archean orthogneisses. CHIME dating of the most pristine uraninite yielded ages between 1.85 and 1.80 Ga, consistent with crystallization from the pegmatite-forming melt. The Group-B pegmatites contain monazite-(Ce) with significant Th substitution, uranoan thorite, zircon (also showing extensive solid-solution toward thorite), and rare xenotime and pyrochlore. CHIME dating of monazite from the Group-B pegmatites gave older ages of ca. 2.1 to 2.2 Ga, suggesting that they are xenocrysts from the source region of the melt. Biotite dehydration reactions have led to significant development of leucosome in the host pelitic gneisses, and likely resulted in the formation of granitic melt at depth.

Introduction

Granitic pegmatites and leucogranites are a well-known economic source of several different rare elements (including Li, B, Rb, Ta, Nb, Cs, and Be) and gemstones (Černý & Ercit 2005), but can also host significant uranium deposits, the largest being the Rössing deposit in Namibia (Berning *et al.* 1976, Basson & Greenway 2004). Canadian examples of pegmatite- and leucogranite-hosted uranium mineralization are common within the Grenville Province (Fowler & Doig 1983, Goad 1990, Lentz 1991, 1996) and in northern Saskatchewan (Canada), particularly within the Wollaston and Mudjatik domains (e.g., Mawdsley 1952, 1953, 1955, Parslow & Thomas 1982, Thomas 1983, Parslow *et al.* 1985, Annesley & Madore 1999, Annesley *et al.* 2000, and Madore *et al.* 2000). Whereas the Rössing deposit and the uraniferous pegmatites of the Grenville Province have been fairly well studied, only limited work has been carried out on pegmatite-hosted uranium deposits in northern Saskatchewan to define them as a potentially economic type of uranium deposit. Most of the recent work focused on these pegmatites and leucogranites as a potential source of uranium for unconformity-type deposits of the Athabasca Basin (Annesley & Madore 1999, Annesley *et al.* 2000, Madore *et al.* 2000, Hecht & Cuney 2000, Cuney 2009, Mercadier *et al.* 2010).

Unlike the granitic pegmatites that host significant rare-element mineralization or gemstones, uraniferous pegmatites and leucogranites only rarely show evidence of a relationship to a granite body (*i.e.*, pluton) nearby, and are typically found within upper-amphibolite- to granulite-facies host rocks (Berning *et al.* 1976, Fowler & Doig 1983, Thomas 1983, Lentz 1991, 1996, Basson & Greenway 2004), which is typical of the Abyssal pegmatite subclass of Černý & Ercit (2005). These pegmatites and leucogranites are generally acknowledged to have formed *via* partial melting or metamorphic differentiation of fertile lithologies (Berning *et al.* 1976, Parslow & Thomas 1982, Fowler & Doig 1983, Thomas 1983, Goad 1990, Lentz 1991, 1996, Basson & Greenway 2004). In the case of the Namibian examples, they are usually termed “leucogranites” or “alaskites”; however, these terms relate more to their mineralogy and color, and less so to their textures, as many of the bodies do show pegmatitic textures (*i.e.*, coarse grain-size), but lack discernible megascopic zoning (Nex *et al.* 2001). However, London (2008) has recently refined the definition for granitic pegmatites, based upon grain-size, crystal-growth habits, and other specific features. Essential to the definition of London (2008) is that pegmatites are "…essentially igneous rocks…" that are discernible from other igneous rocks by their frequently "…extremely coarse but variable grain-size…" (however, pegmatites need not be coarse, *cf*. Le Maitre 2000) "…or by an abundance of crystals showing skeletal, graphic, or other strongly directional growth-habits…" and "…occur as sharply bounded homogeneous to zoned bodies within igneous and metamorphic host rocks." We use this definition of pegmatite in this research study.

Fewer studies have been conducted on the origin of abyssal pegmatites relative to the other classes of pegmatites, owing to their lesser economic importance. However, with recent increases in the price of uranium in the last few years, there has been renewed interest in pegmatite- and leucogranite-hosted uranium mineralization, with significant exploration ongoing in several Canadian provinces (Ontario, Quebec, and Saskatchewan), as well as in Namibia, Norway, and Australia. The lack of recent studies on pegmatite- and leucogranite-hosted uranium in Saskatchewan necessitates further study of these intrusions and their host rocks in order to further understand the mineralization and the mechanisms involved in their emplacement.

This paper is part of a larger study (see McKechnie *et al.* 2012b, 2013) designed to focus on the origin of the Fraser Lakes Zone B radioactive granitic pegmatites and leucogranites and their associated U–Th–REE mineralization in the Wollaston Domain of northern Saskatchewan, Canada. The aims of the current research are to a) document the mineral assemblages found in the radioactive pegmatites and leucogranites, b) determine the composition of the U–Th–REE radioactive accessory minerals and other selected minerals from the pegmatites and leucogranites, c) determine the age of the pegmatite-hosted U–Th–REE mineralization using chemical age-dating techniques, and d) attempt to calculate the intrusion temperature of the pegmatites using biotite geothermometry and oxide geothermobarometry. This study builds upon prior geological studies of the Fraser Lakes Zone-B mineralization, first by Foster (1970) and Ko (1971), and more recently during prospecting and drilling by JNR Resources, starting in 2008 (Annesley *et al.* 2009, JNR Resources Inc. 2012). The results of this study will be used in the development of a new model for the origin of granitic pegmatite- and leucogranite-hosted uranium and thorium mineralization in northern Saskatchewan, which can then be used in exploration programs for similar uranium deposits.

Geological Setting

The Fraser Lakes area is approximately 55 km from the Key Lake uranium mine and 25 km from the southeastern edge of the Athabasca Basin in northern Saskatchewan, Canada (Fig. 3-1). Underlying the area are rocks of the Wollaston Domain, which, along with the Mudjatik, Virgin River and Peter Lake domains, make up the Cree Lake Zone (Lewry & Sibbald 1977, 1980) of the Hearne Craton (Fig. 3-1). The Wollaston Domain is comprised of Paleoproterozoic metasedimentary rocks overlying Archean felsic gneisses in a northeast-trending, highly metamorphosed fold–thrust belt. This is in contrast to the "dome and basin" structural fabric shown by the dominantly Archean orthogneisses in the adjacent Mudjatik Domain. Initially, the boundary between the Wollaston and Mudjatik domains was considered by Lewry & Sibbald (1980) to be gradational in nature, but more recent work by Annesley & Madore (1989, 1994) indicates that it may instead represent a significant crustal-scale shear zone. The Wollaston Domain is separated from the 1.865 Ga Wathaman Batholith, the tonalite–migmatite complexes of the Rottenstone Domain, and juvenile Paleoproterozoic volcanic arc and associated sedimentary rocks of the Reindeer Zone by the Needle Falls Shear Zone (Fig. 3-1). During the collisional stages of the ca. 1.8 Ga Trans- Hudson Orogen (THO), the Cree Lake and Reindeer Zones underwent significant multiphase deformation and metamorphism, ultimately leading to the development of a Himalayan-scale mountain belt that welded Archean cratons together to form the core of Laurentia during the Paleoproterozoic (Hoffman 1990, Lewry & Collerson 1990, Ansdell 2005, Corrigan *et al.* 2009).

Numerous studies of the Wollaston Domain have been done on its stratigraphy, structure, metamorphism, geochronology, and mineral potential, and the reader is referred to Tran (2001), Annesley *et al.* (2005), and Yeo & Delaney (2007) for comprehensive overviews and references. It is comprised of Archean orthogneisses (predominantly granitic gneisses) that have been unconformably overlain by Paleoproterozoic Wollaston Group metasedimentary rocks, including those deposited in rift, passive margin, and foreland basin environments. In addition, the Wollaston Domain contains subordinate Paleoproterozoic granites, amphibolites, leucogranites, migmatites, and granitic pegmatites. The area shown in Figure 3-2, which was originally mapped by Ray (1980), will be described in more detail as it contains the Fraser Lakes Zones A and B mineralization. The area is generally representative of the eastern Wollaston Domain (Annesley *et al.* 2005).

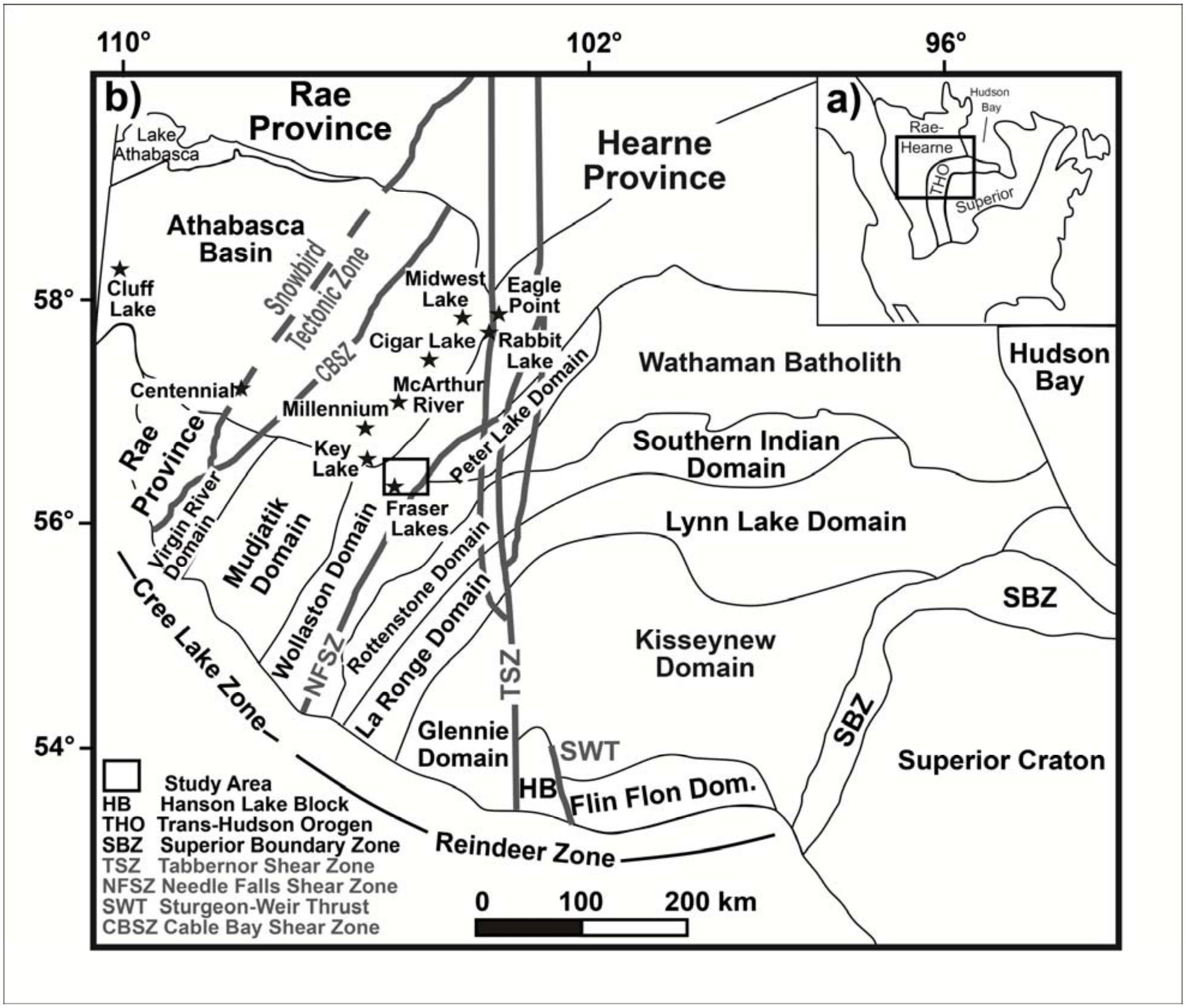

Figure 3-1. (a) Map of North America showing the location of the Archean Hearne–Rae and Superior cratons, welded by the Paleoproterozoic Trans-Hudson Orogen (THO). The box shows the location of the area in Figure 3-1b. (b) Lithotectonic domains in northern Saskatchewan and Manitoba. The position of several unconformity-related uranium deposits is shown within the Athabasca Basin. The box indicates the area shown in Figure 3-2. Dom: Domain.

Two large inliers of granitic orthogneiss basement, the Fraser Lakes and Johnson River inliers (Fig. 3-2), outcrop in the area and have been dated by U–Pb zircon geochronology to be 2593 ±

13 and 2574 ± 3 Ma, respectively (Hamilton & Delaney 2000). These are overlain by Wollaston Group metamorphosed sedimentary rocks of the eastern Wollaston Domain, which are subdivided into two main sequences, an upper calcsilicate-rich sequence, and a lower pelitic to psammitic sequence (Tran *et al.* 1998). Annesley *et al.* (2005) described the lower sequence as containing six units including, from oldest to youngest, graphitic pelitic gneisses, partly calcareous pelitic gneisses interlayered with garnetites–metaquartzites and tourmalinites, psammopelitic gneisses, metasedimentary calc-silicate gneisses, psammitic gneisses, and sillimanite-bearing metaquartzites. The lower sequence within the Fraser Lakes area consists of pelitic and quartzo-feldspathic psammitic gneisses, with graphite-bearing pelitic gneisses [delineated by electromagnetic (EM) conductors] found immediately adjacent to the Archean inliers (Figs. 3-2, 3-3). Delaney *et al.* (1996) interpreted a thick upper calc-silicate-rich sequence of calcareous and calc-silicate gneisses in the Fraser Lakes area, which has not been supported by drilling to date in the Fraser Lakes area.

The emplacement of biotite-bearing monzogranites, granodiorites, and tonalites in the Wollaston Group took place between about 1840 and 1810 Ma, with rare metagabbros and amphibolites emplaced at 1830 to 1820 Ma, and numerous granitic pegmatites and leucogranites intruded at 1820 to 1800 Ma (Annesley *et al.* 2005). Metamorphism of the Wollaston Domain to the upper amphibolite to granulite facies accompanied and postdated strong penetrative deformation during the THO (Annesley *et al.* 2005). During peak thermal metamorphism, a dominantly northeast-trending structural fabric formed, with the EM conductor around the Fraser Lakes Inlier defining NNE-plunging isoclinal folds. The area shows some offset of lithological units by north- or NNW-trending brittle faults (Fig. 3-2), which may be related to the Tabbernor Fault system (Fig. 3-1).

Mapping in the immediate vicinity of the Fraser Lakes A and B mineralized zones by Ray (1980) and Delaney & Tisdale (1996) showed that the area contains metasedimentary gneisses of the Wollaston Group overlying Archean orthogneisses of the Fraser Lakes inlier (Fig. 3-2). Defining the contact between the two packages of rocks is a 65-km-long electromagnetic (EM) conductor (*i.e.*, graphitic pelitic gneisses), which also outlines several northeast-plunging regional folds (Figs. 3-2, 3-3; Annesley *et al.* 2009). A strong aeromagnetic geophysical signature highlights the northeast-trending regional structural trend of the Fraser Lakes area, and demarcates the likely location of several younger, crosscutting E–W ductile–brittle and NNW-trending brittle structures (Fig. 3-3).

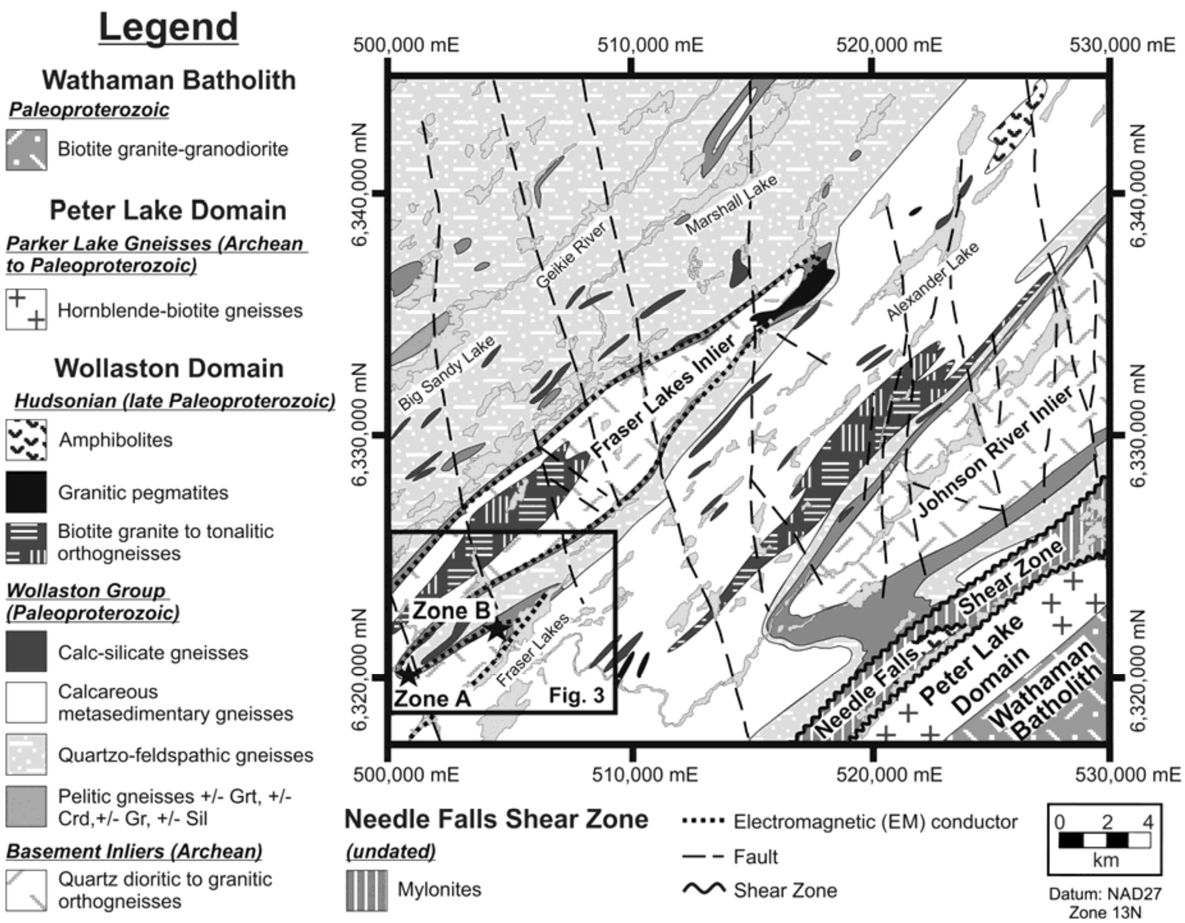

Figure 3-2. Regional geological map of the Fraser Lakes and surrounding area. Note the strong NNE structural trend and the location of the folded EM conductor 65 km long adjacent to Fraser Lakes Zones A and B. Modified from Ray (1980). The box depicts the location of Figure 3-3.

The Fraser Lakes mineralized zones (Zones A and B) are located in two northeast-plunging regional fold noses adjacent to a 5-km-long section of the EM conductor (Fig. 3-3). The two mineralized zones were found in the summer of 2008 by ground prospecting of airborne regional positive U and Th anomalies (Annesley *et al.* 2009). At Zone B, the more prospective of the two zones, the U–Th–REE mineralization is hosted by granitic pegmatites within an antiformal fold nose in a ca. 600 m x 1500 m area west of Fraser Lakes. Drilling in the Fraser Lakes Zone-B area in 2008–2011 intersected multiple intervals of moderately dipping U–Th–REE-mineralized granitic pegmatites, with up to 0.183% U_3O_8 over 1.0 m in drill core (JNR Resources Inc. 2012).

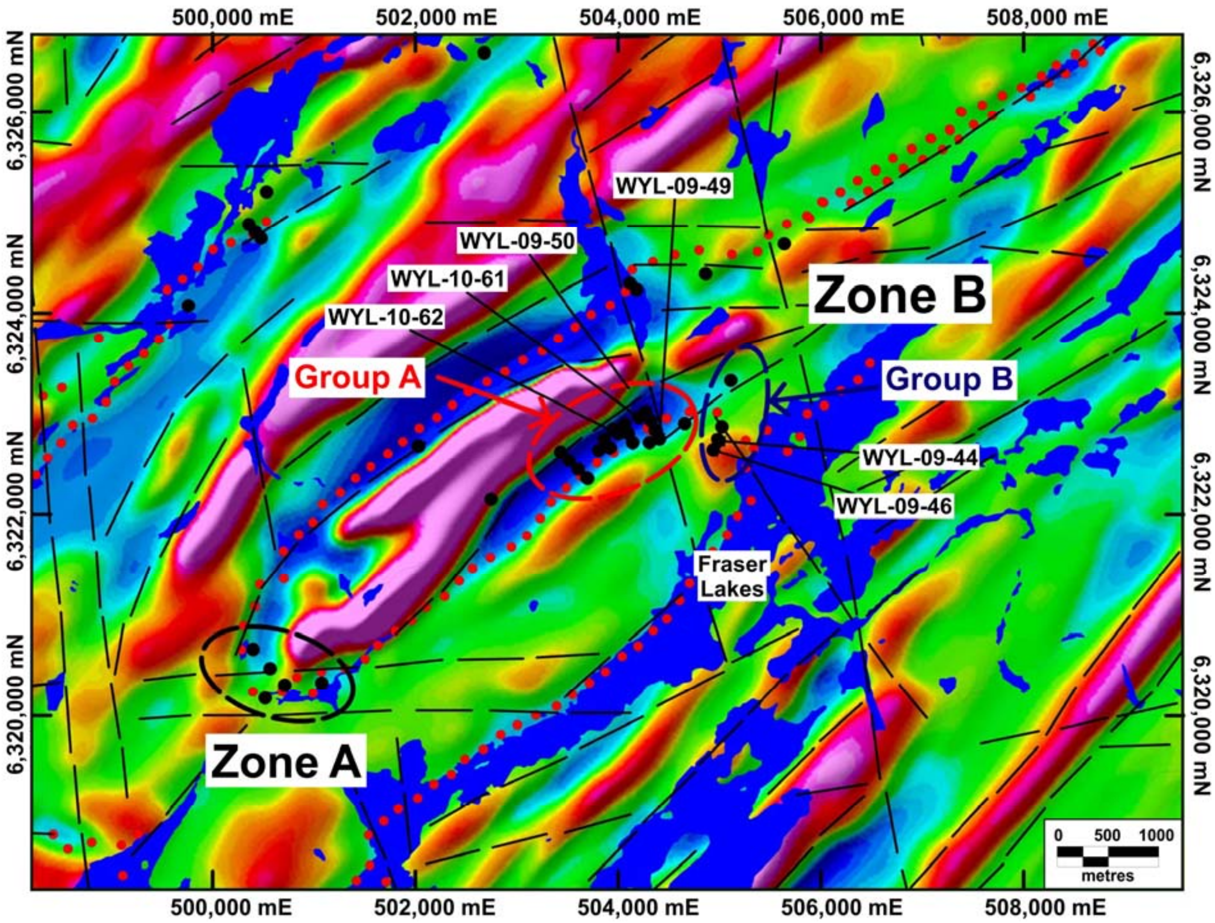

Figure 3-3. First vertical derivative total field aeromagnetic map of the Fraser Lakes area. Pink and red colors represent areas of high magnetic potential field, whereas blue and green represent areas with low magnetic potential field. Drill holes are denoted by black dots, and those that have been sampled for this study are labeled. A regional-scale electromagnetic (EM) conductor is shown by the red dots.

Observation of drill core by JNR Resources Inc. and Austman *et al.* (2010a, 2010b) and McKechnie *et al.* (2013) has indicated that there are multiple generations of granitic pegmatites, including variably mineralized (greater than 100 cps using a handheld scintillation counter, generally subcordant to gneissosity, and believed to be syntectonic) and weakly radioactive (discordant to gneissosity, and probably late-tectonic, less than 100 cps using a handheld scintillation counter) varieties. The mineralized pegmatites intrude the highly deformed, folded, northeast-plunging, unconformable contact zone between pelitic (± graphitic) gneisses of the basal Wollaston Group, and the underlying Archean granitic and tonalitic gneisses of the Fraser Lakes Inlier.

The granitic pegmatites and leucogranites are composed mainly of variable amounts of quartz, K-feldspar, plagioclase and biotite, with subordinate magnetite, ilmenite, zircon (± Th enrichment), uraninite, thorite (± U and Zr enrichment), monazite, allanite, garnet, cordierite, apatite, and fluorite. In some cases, they show zoning (see Fig. 5a of McKechnie *et al.* 2013), including K-feldspar-rich, plagioclase-rich, quartz-rich, and biotite-rich zones, thought to be the result of igneous assimilation – fractional crystallization (AFC) processes (McKechnie *et al.* 2013). Unlike the zonation patterns of typical pegmatites discussed in London (2008), both feldspar-rich and quartz-rich cores were seen in the pegmatites. Some of the pegmatites have quartz-rich margins, whereas others have biotite-rich margins (biotite being much coarser in the pegmatites than in the fine-grained host-rocks). The pegmatites and leucogranites range in size from the centimeter to the decameter scale, and show strongly variable grain-size, from fine grained to pegmatitic (*i.e.*, >5 cm) (see Figs. 5a, 6a in McKechnie *et al.* 2013), with larger bodies generally being coarser grained, especially within their core. The grain size is typically greater in the intrusive bodies than it is in the surrounding host rocks. They may exhibit a graphic texture (only found in pegmatites), skeletal and other strongly directional growth-habits, perthitic feldspar, and typically have sharp boundaries with their metamorphic and igneous host-rocks, and thus meet the definition of pegmatite of London (2008). All of the granitic pegmatites and leucogranites (hereafter referred to as pegmatites for brevity) have highly fractionated and strongly peraluminous to weakly metaluminous compositions, with major- and trace-element geochemical variation due mainly to mineralogical variation within the pegmatites (McKechnie *et al.* 2013).

The pegmatites intrusive into the western part of the fold nose and along the northwestern limb are uranium- and thorium-enriched (Group-A pegmatites), whereas those in the central part of the fold nose tend to be thorium- and LREE-enriched and U-depleted (Group-B pegmatites). McKechnie *et al.* (2013) showed that the difference in trace-element enrichment is due to mineralogical differences between the pegmatites in the two areas; the Group-A pegmatites contain uraninite, uranoan thorite, and zircon as the main U–Th–REE (with trace allanite and trace amounts of monazite), whereas the Group-B pegmatites contain predominantly monazite, uranoan thorite, zircon, and xenotime (with trace allanite) as the main U–Th–REE minerals.

Analytical Methods

Samples were collected from drill core stored at the JNR Resources Inc. exploration property. The polished thin sections were prepared in the Thin Section Laboratory in the Department of Geological Sciences at the University of Saskatchewan. Transmitted and reflected light petrography was done at the University of Saskatchewan and JNR Resources Inc. to describe the mineral assemblages, textures, and paragenesis for the three major rock-types (granitic pegmatite, granite gneiss, and pelitic gneiss; for details, see McKechnie *et al.* 2013). Samples were taken along traverses across several pegmatite dikes in several different drill-holes. From this collection of samples, four samples were selected for electron-microprobe analysis, as discussed in this paper: two Group-A and two Group-B pegmatites and leucogranites.

Automated wavelength-dispersive electron-microprobe analyses were carried out using either a Cameca SX–100 Ultra electron-microprobe analyzer (EMPA) at the Saskatchewan Research Council (SRC, see SRC 2012) or a JEOL 8600 Superprobe EMPA at the University of Saskatchewan. Prior to analysis, the phases of interest were examined and identified using SEM back-scattered electron imagery (SEM–BSE) and SEM energy-dispersive electron-microprobe spectrometry (SEM–EDS). The EMPA were operated at an accelerating voltage of 15 kV for silicate minerals, and 20 kV for U- and Th-bearing minerals, beam current of 10 nA to 50 nA, and a beam diameter of less than 5 μm to 10 μm. Standards used consisted of a suite of natural minerals and metals supplied by Structure Probe Inc. (SPI), Mt. Gore almandine garnet from the University of New Brunswick, Harvard University almandine garnet, synthetic REE phosphates from the Smithsonian Institute, University of Wisconsin synthetic phlogopite, and a high-Fe biotite standard, characterized chemically by SRC and chosen specifically for work on pelitic gneiss geothermobarometry in the Wollaston Domain, as well as a suite of synthetic oxide standards. The composition of the Smithsonian REE phosphates has been corrected for Pb. Matrix and ZAF corrections were made using the Phi–Rho–Z matrix correction algorithm (Pouchou & Pichoir 1984, Bastin & Heijligers 1991). The detection limits of the individual elements are listed in the Appendix (Appendix H). The stoichiometry of each mineral analyzed was calculated using readily available freeware spreadsheets from Tindle (2011) and the Calcmin Excel Visual Basic application (Brandelik 2009). Representative results are included in Tables 3-1 and 3-2 for the Group-A and Group-B pegmatites, respectively, with the full analytical data being available as tables of supplementary data (Supplementary Data Tables 1 and 2, respectively, Appendices C and D). Chemical age data can be found in Supplementary Data Tables 3 and 4, respectively (Appendices E and F), and geothermometry information is found in Supplementary Data Tables 1 and 2 (for biotite geothermometers) (Appendices C and D) and Supplementary Data Table 5 (for magnetite–ilmenite results) (Appendix E). This material is available from the Depository of Unpublished Data on the Mineralogical Association of Canada website [document Fraser Lakes CM50_1637].

After extensive petrography, a total of four samples of radioactive pegmatite (two of Group-A pegmatite and two of Group-B pegmatite) were selected from a larger suite of thin sections from representative samples (McKechnie *et al.* 2013) for quantitative compositional analysis by EMPA. The four samples were selected on the basis of mineral assemblages (in thin section) and not grain size. Care was taken when selecting the pegmatite samples to find the least altered, most representative samples with numerous crystals of the radioactive minerals of interest (*i.e.*, uraninite, thorite, monazite, and zircon) in order to get reliable mineral compositions. In addition, magnetite, ilmenite, and biotite were analyzed from the pegmatites in an attempt to obtain temperature constraints for the pegmatites.

The Group-A Pegmatites and Leucogranites

Sample WYL–10–62–93.5

This drill core sample is from hole WYL–10–62, drilled in a granitic (sensu lato) pegmatite body 2.3 m thick, emplaced in pelitic gneisses. The pegmatite (in core) contains visible quartz, K-feldspar, plagioclase, and biotite, with the other minerals (including radioactive minerals) being generally too small to be visible to the naked eye. Radioactivity is variable throughout the pegmatite, from 400 to up to 2000 cps locally. It is rich in smoky quartz (60–70%), and also contains white to pale grey plagioclase (10–15%), pink to red K-feldspar (~5–10%) and black biotite (5 to 10%) as the main constituents. Other minerals, including the U–Th–REE-bearing accessory minerals, are generally too small to see in drill core. The overall grain-size is highly variable (fine to coarse grained) with local patches of very coarse-grained (*i.e.*, pegmatitic) material, and an inequigranular grain-size distribution. The mineralogy of the intrusive rock is not consistent throughout the body (*i.e.*, it is zoned), with local quartz-rich and feldspar-rich patches. It has sharp contacts with its host rocks. There is some weak pigmentation of the K-feldspar by hematite, especially along fractures, and some pale green alteration of the plagioclase. This sample was taken from a quartz-rich zone in the upper portion of this pegmatite, about 20 cm away from its upper intrusive contact.

The thin section (Figs. 3-4a, b) is mostly comprised of quartz (65–70%), and also contains 25–30% biotite and trace amounts of uraninite, zircon, uranoan thorite, and allanite as the primary magmatic assemblage. The thin section shows an inequigranular grain-size distribution, with quartz grains up to 11 mm long, and randomly oriented biotite flakes up to 7.0 mm long, whereas the other minerals generally form grains less than 0.5 mm in size. The quartz and biotite are subhedral, whereas uraninite and zircon tend to form euhedral grains. Thorite and allanite form roundish grains. There is a strong association of the uraninite, thorite, zircon, and allanite with the biotite-rich portions of the sample (Figs. 3-4a, b), with zircon also forming clusters within quartz. The zircon is metamict and shows complex zoning. Radiating fractures and pleochroic halos within biotite flakes are common surrounding uraninite, thorite, and zircon.

The pegmatite experienced weak retrograde metamorphism, with biotite becoming slightly altered to chlorite, muscovite, and rutile. In addition, the quartz grains in this sample are moderately to strongly fractured owing to later brittle deformation. The rock experienced patchy, weak hydrothermal alteration resulting in the formation of carbonate, fluorite, and hematite along cleavage planes in biotite. The uraninite, thorite, and allanite show weak alteration. Pyrite occurs in trace amounts along biotite cleavage planes and is also found, along with radiogenic galena, within and surrounding uraninite and thorite.

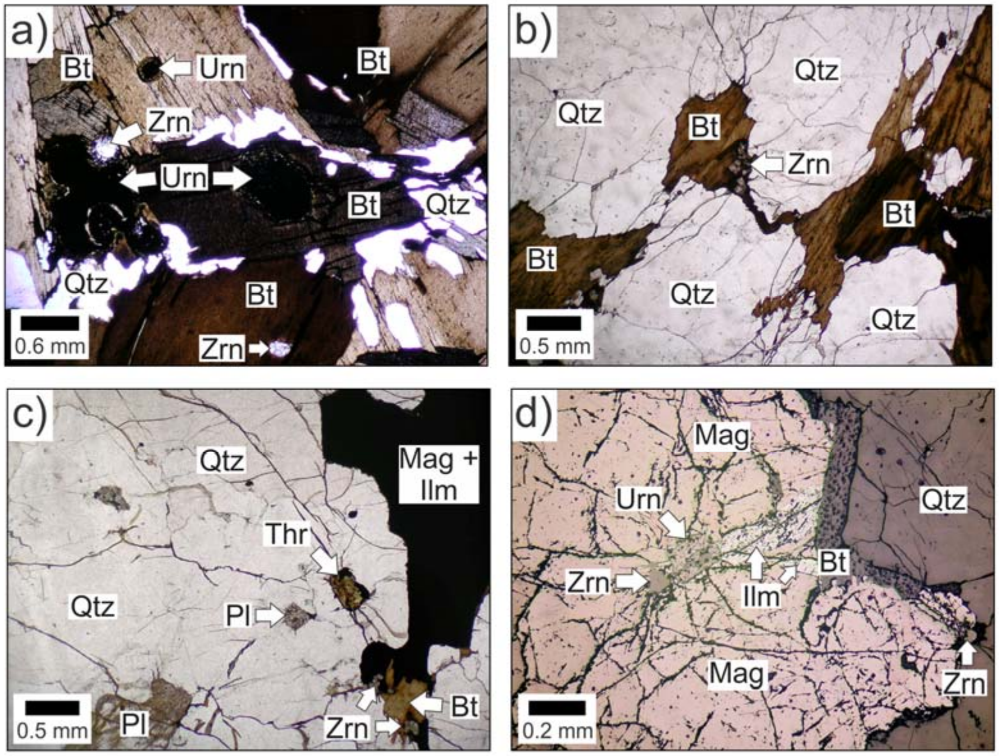

Figure 3-4. Photomicrographs of U-rich granitic pegmatites from Fraser Lakes Zone B. (a) Portion of a granitic pegmatite biotite (Bt), zircon (Zrn), and uraninite (Urn) (WYL–10–62–93.5). Note the pleochroic damage haloes surrounding the uraninite grains. (b) Quartz (Qtz)-rich portion of the same granitic pegmatite sample shown in (a). Note the strong association of the U–Th–REE phases with biotite in the pegmatite. (c) Quartz-rich, magnetite- (Mgt) and ilmenite- (Ilm) bearing granitic pegmatite (WYL–10–61–190.3) containing altered thorite (Thr) and zircon. (d) Magnetite–ilmenite intergrowth in WYL–10–61–190.3 containing zircon and uraninite (itself containing a zircon inclusion). Ilmenite forms large laths and exsolution lamellae within the magnetite grain.

Sample WYL–10–61–190.3

This sample came from drill hole WYL–10–61, and was taken at 190.3 m depth from a granitic (sensu lato) dyke 2.7 m thick. The leucogranite contains a large amount of smoky quartz (50–60%), white plagioclase (15–20%), and lesser amounts of magnetite and biotite (5 to locally 15–20%) and pinkish to greenish K-feldspar (5–10%). Other minerals, including the radioactive minerals, tend to be too fine grained to see with the naked eye. The mineralogy is not homogeneous throughout the dike, with local quartz-rich and plagioclase-rich zones. Biotite and magnetite have a patchy distribution throughout the dike. The leucogranite is moderately altered to hematite in the upper part of the dike and is weakly chloritized in the lower portion, with the feldspars generally being altered more readily than the other minerals. The minerals range in size from fine to coarse grained (locally very coarse patches) with an inequigranular grain-size distribution. The dyke has sharp contacts with migmatitic garnet–biotite gneisses above (Paleoproterozoic?) and dioritic orthogneisses below (Archean).

The rock (Figs. 3-4c, d) also is quartz-rich (60 to 70%), but is distinct from the other Group-A sample as it contains 10–15% magnetite, 5–10% plagioclase (oligoclase), 2–3% ilmenite, 2–3% K-feldspar, and 1–2% uraninite and zircon, with trace amounts of uranoan thorite, titanite, altered allanite, galena and pyrite. Magnetite is only found in granitic pegmatites at Fraser Lakes Zone B that intrude the Archean orthogneisses, in particular the more mafic varieties. The grain-size distribution is inequigranular, and the largest crystals in the thin section are those of magnetite, which are up to 15 mm long, and quartz, which are 12 mm long. The uraninite and uranoan thorite form small crystals up to 0.5 mm across, whereas zircon tends to form crystals up to 0.1 mm across. The magnetite, plagioclase, uraninite, uranoan thorite, and zircon tend to be euhedral to subhedral in shape, whereas the other minerals are subhedral to anhedral. Biotite is reddish brown to dark brown, suggesting a high Ti content. The plagioclase exhibits weak to moderate albite twinning, and the zircon grains are complexly zoned. The ilmenite forms laths within the magnetite (Fig. 3-4d), as well as exsolution lamellae within the magnetite, indicating that the magnetite initially had a high Ti content. There is one occurrence of a uraninite inclusion in magnetite that itself contains a zircon inclusion (Fig. 3-4d). Locally, pyrite and galena form tiny (<0.02 mm) grains within and surrounding altered uraninite and thorite grains. There is weak retrograde chloritization of the biotite along the cleavage, as well as alteration to fluorite and rutile. Feldspar is weakly altered to white mica, and there is locally weak patchy hematite and carbonate alteration of the feldspar. The rock is moderately fractured, and locally shows evidence for a weak foliation shown by preferential alignment of biotite flakes.

The Group-B Pegmatites and Leucogranites

Sample WYL–09–46–32.6

This sample was taken from drill hole WYL–09–46 at 32.6 m in a biotite-rich (variable, from a low of about 5–10% to locally as high as 60%) granitic (sensu lato) pegmatite. In addition to biotite, the pegmatite contains about 20–30% (locally up to 50%) weakly to moderately hematite-altered pink, orange, greenish, and white feldspar (difficult to tell composition owing to alteration), and 5–10% white to greyish quartz as well as trace monazite. The biotite has a patchy distribution, with locally biotite-rich intervals that tend to coincide with an increase in radioactivity. Overall, the grain size is very coarse (*i.e.*, pegmatitic) with the biotite forming books up to about 4 cm in size (much coarser than the biotite in the fine- to medium-grained host rocks). The upper contact with the host Archean tonalitic orthogneisses is sharp. In contrast, the lower contact is difficult to pinpoint. The pegmatite is gradational into a very biotite-rich (up to 90% biotite with local quartz ribbons), chloritized, coarse-grained unit (similar to biotite-rich pegmatite zones in other Zone-B drill holes) that separates the granitic pegmatite from the underlying tonalitic orthogneisses.

In thin section, the pegmatite sample is biotite-rich (50–55% biotite), and contains 15–20% plagioclase (albite-rich), 10–15% quartz, 5–10% K-feldspar, 1–2% monazite, and trace xenotime, altered allanite, sphalerite, and molybdenite as the primary magmatic assemblage (Figs. 3-5a, b). Secondary minerals in this sample include chlorite, white mica, carbonate, fluorite, and pyrite. The mineral assemblage has an inequigranular grain-size distribution, ranging from less than 0.2 mm (xenotime, molybdenite, and sphalerite) up to 11 mm in size (biotite, plagioclase). Monazite forms crystals up to 1.1 mm in size that are embayed and subhedral with an alteration rim (Figs. 3-5a, b). A pleochroic halo surrounds monazite inclusions within biotite. Xenotime was only discovered in this slide using the electron microprobe; it forms tiny grains adjacent to monazite. The biotite exhibits strong pleochroism, from yellow to red-brown. The shape of the crystals within this sample tends to be subhedral. There is no preferred orientation shown by the biotite or any other mineral. Allanite is metamict and shows moderate alteration and fracturing. Weak retrograde alteration of this rock is shown by the presence of chlorite alteration of biotite and white mica alteration of feldspar. There is also weak hydrothermal alteration consisting of carbonate, fluorite, and pyrite that is found along biotite cleavage planes and within fractures.

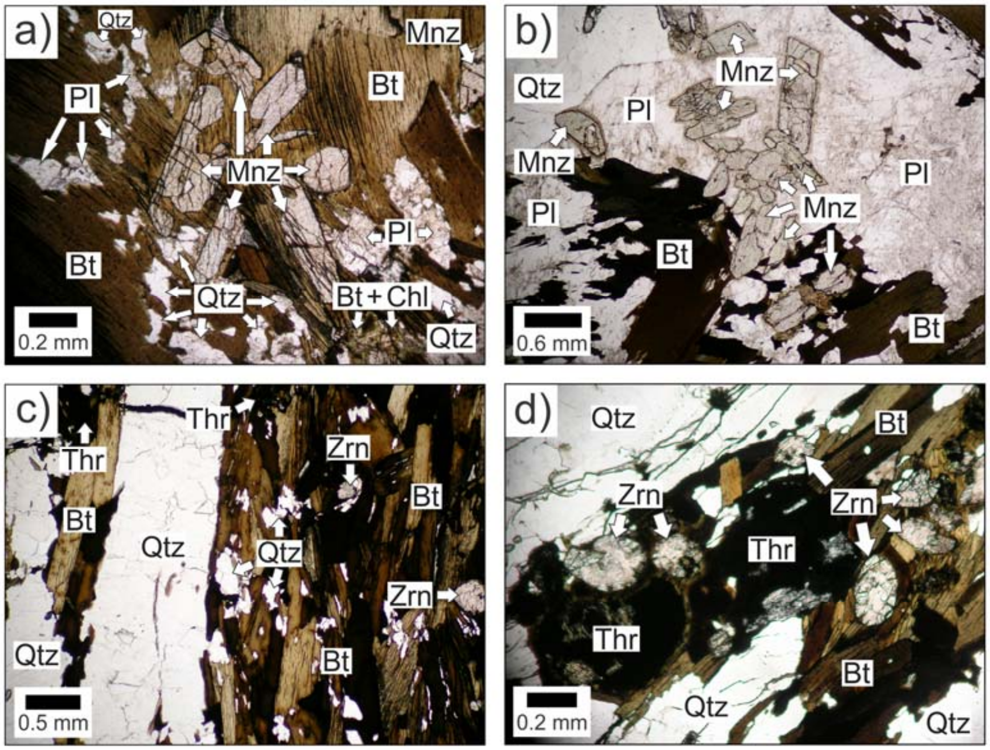

Figure 3-5. Photomicrographs of Th- and LREE-enriched granitic pegmatites from Fraser Lakes Zone B. (a) Monazite (Mnz)- and biotite-rich portion of granitic pegmatite WYL–09–46–32.6. (b) Quartz-rich portion of WYL–09–46–32.6 showing additional monazite clusters. (c) and (d) Biotite-rich granitic pegmatite (WYL–09–46–35.0) with zircon and thorite mineralization.

Sample WYL–09–46–35.0

This sample was collected from the WYL–09–46 core at a depth of 35.0 m. It was taken from the same drill hole as the previous sample, where the pegmatite previously described is gradational into a biotite-rich unit. This biotite-rich unit (part of the pegmatite?) shows more textural similarities to biotite-rich zones of pegmatites from other drill holes at Fraser Lakes Zone B than it does to the underlying tonalitic orthogneisses, namely coarser grain-size and a mottled, chaotic texture. It does not show the strong, consistent foliation or gneissosity (at about 60° to the core axis) shown by the tonalitic gneisses, instead having a much weaker foliation (where visible) at about 10° to the core axis. This biotite-rich unit is also more radioactive than the tonalitic orthogneisses and contains much higher thorium and uranium contents (*i.e.*, >100 ppm U and >200 ppm Th for the biotite-rich unit, versus <20 ppm U and <30 ppm Th in the tonalitic orthogneisses). The combination of these characteristics suggests that it is a part of the wall zone of the pegmatite body, with the high biotite content possibly due to assimilation of the tonalitic host-rock. The biotite-rich unit shows some similarities to the biotite reaction-zones at the edges of uraniferous pegmatites in the Grenville Province (Lentz 1996).

In thin section, the sample (Figs. 3-5c, d) is biotite- (40–45%) and quartz-rich (50–55%). It also contains 2–5% K-feldspar, with uranoan thorite, zircon, and altered allanite, as well as trace amounts of secondary galena, pyrite, white mica, carbonate, hematite, fluorite, and rutile. The grain size in this sample is highly variable, from <0.1 to 6.0 mm. The uranoan thorite, zircon, and allanite tend to be euhedral to subhedral, whereas quartz, biotite, and feldspar are typically subhedral to anhedral. Polysynthetic twinning is commonly shown by plagioclase. The uranoan thorite, zircon, and allanite are commonly found in clusters within biotite (Figs. 3-5c, d). The zircon in this sample is complexly zoned and metamict, and shows similarities to the igneous zircon in the other Group-B granitic pegmatite samples. Biotite shows a strong parallel alignment in thin section, but this is less visible in the core. The uranoan thorite and allanite are altered, with galena and pyrite inclusions common within the thorite. Pyrite also forms along fractures. Weak retrograde metamorphism of the biotite to chlorite and feldspar to white mica was followed by weak, patchy hydrothermal alteration that produced hematite, carbonate, and fluorite.

Mineral Compositions in the Group-A Pegmatites

Uraninite

Uraninite was analyzed in both WYL–10–61–190.3 and WYL–10–62–93.5, with analytical totals ranging from a low of 89.11 wt. % in more altered sections to 98.71 wt.% in the visually least-altered parts of the grains, but generally in the range of 94 to 96.5 wt.% (Table 3-1). The subhedral (Figs. 3-6b, c) to euhedral (Figs. 3-6a, d, h) grains show fracturing and alteration, as noted by their patchy appearance in SEM–BSE images (Figs. 3-6a, b, c, d, h). As well, some grains appear to have lost U and Pb from their structures, as suggested by the presence of secondary U-bearing minerals and galena in fractures radiating away from the uraninite (Figs. 3-6b, d). The uraninite contains 60.27 to 66.57 wt. % UO_2, with a significant amount of Th (5.51 to 8.55 wt.% ThO_2). The PbO varies in uraninite from a low of 10.79 to up to 21.06 wt. % (Table 3-1). The uraninite has a variable Y_2O_3 content of 1.44 to 5.15 wt.%, as well as variable total REE_2O_3 content, 1.49 to 4.2 wt.%. The CaO content is variable, from 0.12 to 2.84 wt.% with higher amounts in more altered areas, but is overall generally less than 1.0 wt.%. The SiO_2 contents are low (<0.30 wt. %), with the exception of one point with 1.0 wt. % SiO_2 (Table 3-1).

Thorite

Two grains of thorite were analyzed in WYL–10–62–93.5. These grains show strong signs of alteration in SEM–BSE images (Figs. 3-6e, f, g), including the formation of cubes of galena and holes (due to plucked mineral grains or possibly pore space in the grains). This is likely the result of metamictization of the thorite, which makes it more susceptible to alteration (Förster 2006). This also is reflected by the low analytical totals, ranging from 81.53 to 95.15 wt. % (Table 3-1). The thorium, uranium, and lead contents are quite variable, from 34.30 to 53.97 wt. % ThO_2, 0.20 to 5.15% UO_2, and 0.18 to 1.79% PbO. Two analyses showed high lead contents (12.59 and 16.10 wt.%, Table 3-1), likely reflecting tiny inclusions of galena in the crystals (Figs. 3-6f, g) as this is much higher than the other results on the same grain. The SiO_2 contents vary from about 15.70 to 19.44 wt. %. There is also significant and variable FeO (2.21 to 8.02 wt. %), P_2O_5 (0.19 to 4.60%), CaO (1.10 to 2.98%), Y_2O_3 (0.76 to 3.23%), and REE (1.10 to 4.57% $\sum REE_2O_3$, dominantly Ce_2O_3). Zirconium is variably enriched (from 0.89 to 18.32% ZrO_2), as well as Al (from 0.70 to 1.53% Al_2O_3). The thorite grains represent thorite-rich (X_{Thr} 43–76%) members of the thorite – xenotime – zircon – coffinite solid-solution series described by Förster (2006) (Fig. 3-7a, Table 3-1). The grains locally show enrichment in the X_{Zrn} content near the contact with zircon, with the thorite containing 0–8% $USiO_4 \bullet n\ H_2O$ (coffinite), 3–51% $ZrSiO_4$ (zircon), and 6–22% (Y, REE)PO_4 (xenotime) (Fig. 3-7a, Table 3-1).

One analysis in a bright part of a thorite grain (Fig. 3-6e) indicated a much higher amount of UO_2 (26.62%) and FeO (10.66%), and lower ThO_2 (15.98%) than the rest of the analyses; this part of the grain (in the center of an altered grain) is Th-rich (30% $ThSiO_4$) coffinite (49% $USiO_4 \bullet nH_2O$) with minor xenotime [14% (Y,REE)PO_4] and zircon (7% $ZrSiO_4$) components (Fig.3-6e, Table 3-1).

Table 3-1. Representative results of mineral analyses, Group-A pegmatites, Fraser Lakes, Zone B

Mineral	Urn	Thr	Zr-rich Thr	Cfn	Zrn	Th-rich Zrn	Th-rich Zrn
Sample	WYL-10-61-190.3 Urn1	WYL-10-62-93.5 Thr1	WYL-10-61-190.3 Thr1-Zrn1	WYL-10-62-93.5 Thr1	WYL-10-61-190.3 Urn3-Zrn2	WYL-10-61-190.3 Urn3-Zrn2	WYL-10-61-190.3 Thr1-Zrn1
Line	25	90	37	88	56	54	40
SiO_2 wt.%	0.22	19.44	20.13	15.89	31.73	23.76	24.43
TiO_2	0.01	0.09	b.d.	0.09	b.d.	b.d.	0.01
Al_2O_3	b.d.	1.19	0.75	1.49	b.d.	1.06	1.22
FeO	b.d.	2.21	4.76	10.66	0.21	4.98	8.98
MnO	0.03	0.04	0.03	0.03	b.d.	0.14	0.02
MgO	b.d.	0.12	0.04	0.05	b.d.	0.08	0.04
CaO	0.93	2.98	1.10	2.35	0.05	1.55	1.67
P_2O_5	b.d.	3.34	0.91	2.09	b.d.	b.d.	b.d.
UO_2	64.15	2.38	0.20	26.62	0.13	0.38	0.44
ThO_2	5.75	53.97	48.33	15.98	b.d.	6.47	18.38
PbO	17.31	0.30	0.23	0.44	0.12	0.20	0.16
ZrO_2	b.d.	5.05	9.15	1.67	63.64	46.01	27.09
HfO_2	-	0.05	0.14	b.d.	1.96	1.38	0.90
Y_2O_3	4.01	1.05	0.94	1.51	0.05	0.59	1.56
La_2O_3	b.d.	0.51	0.07	0.35	b.d.	0.11	0.03
Ce_2O_3	0.39	1.36	0.44	1.28	b.d.	0.09	0.24
Pr_2O_3	0.04	0.13	b.d.	0.12	b.d.	b.d.	b.d.
Nd_2O_3	0.64	0.43	0.21	0.48	0.03	0.06	0.15
Sm_2O_3	0.37	0.10	0.06	0.10	0.04	0.05	0.13
Gd_2O_3	0.47	0.11	0.15	0.14	b.d.	0.06	0.20
Dy_2O_3	0.80	0.15	0.17	0.08	b.d.	0.05	0.20
Er_2O_3	0.47	0.15	0.13	0.11	b.d.	0.08	0.19
Total	95.62	95.15	87.97	81.53	98.00	87.10	86.06
ΣREE_2O_3	3.20	2.95	1.25	2.66	0.11	0.50	1.13
O *apfu*	-	16	16	16	16	16	16
Si	-	3.59	3.96	3.44	3.99	3.61	3.99
Al	-	0.26	0.18	0.38	0.00	0.19	0.23
Ti	-	0.01	0.00	0.01	0.00	0.00	0.00
Fe	-	0.34	0.78	1.93	0.02	0.63	1.23
Mn	-	0.01	0.01	0.00	0.00	0.02	0.00
Mg	-	0.03	0.01	0.02	0.00	0.02	0.01
Ca	-	0.59	0.23	0.54	0.01	0.25	0.29
U	-	0.10	0.01	1.28	0.00	0.01	0.02
Th	-	2.27	2.16	0.79	0.00	0.22	0.68
Pb	-	0.01	0.01	0.03	0.00	0.01	0.01
Zr	-	0.46	0.88	0.18	3.90	3.41	2.16
Hf	-	0.00	0.01	0.00	0.08	0.07	0.05
P	-	0.52	0.15	0.38	0.00	0.00	0.00
Y	-	0.10	0.10	0.17	0.00	0.05	0.14
La	-	0.03	0.01	0.03	0.00	0.01	0.00
Ce	-	0.09	0.03	0.10	0.00	0.01	0.01
Pr	-	0.01	0.00	0.01	0.00	0.00	0.00
Nd	-	0.03	0.01	0.04	0.00	0.00	0.01
Sm	-	0.01	0.00	0.01	0.00	0.00	0.01
Gd	-	0.01	0.01	0.01	0.00	0.00	0.01
Dy	-	0.01	0.01	0.01	0.00	0.00	0.01
Er	-	0.01	0.01	0.01	0.00	0.00	0.01
Total	-	8.50	8.57	9.35	8.02	8.53	8.88
X $ThSiO_4$ %	-	72.7	66.7	30.0	0.0	5.9	22.0
X $USiO_4$	-	3.1	0.3	48.8	0.1	0.3	0.5
X (Zr,Hf) SiO_4	-	14.7	27.3	6.7	99.7	91.8	71.1
X (Y,REE) PO_4	-	9.6	5.7	14.5	0.2	2.0	6.4

Mineral	Ti-poor Mgt	TI-poor Mgt	Ti-rich Mgt	Ilm	Rt
Sample	WYL-10-61-190.3 Mgt3-Ilm3	WYL-10-61-190.3	WYL-10-61-190.3 Mgt3-Ilm3	WYL-10-61-190.3 Mgt3-Ilm3	WYL-10-61-190.3 Mgt-4 Ilm-4-TiO1
Line	49	35	52	41	57
SiO_2	0.08	0.22	0.09	b.d.	0.56
TiO_2	0.80	2.16	17.84	49.79	95.22
Al_2O_3	0.29	2.68	9.12	0.01	0.13
Cr_2O_3	0.00	b.d.	0.01	b.d.	b.d.
V_2O_3	0.04	0.04	0.05	0.06	0.18
FeO	92.86	89.76	70.56	44.81	0.86
MnO	0.05	0.35	2.08	4.04	0.04
ZnO	0.05	0.11	1.43	b.d.	b.d.
NiO	b.d.	0.01	0.04	b.d.	0.01
MgO	b.d.	0.05	0.08	b.d.	b.d.
CaO	b.d.	0.02	b.d.	b.d.	0.16
Total	94.19	95.39	101.30	98.71	97.15
Fe recalculation: Carmichael (1967)					
Fe_2O_3	67.48	62.23	26.17	4.59	-
FeO	32.14	33.76	47.01	40.69	-
Total	100.95	101.63	103.92	99.17	-
O *apfu*	32	32	32	3	2
Si	0.03	0.07	0.02	0.00	0.01
Ti	0.18	0.48	3.73	0.96	0.98
Al	0.10	0.94	2.99	0.00	0.00
Fe^{3+}	15.46	13.95	5.48	0.09	0.00
Fe^{2+}	8.18	8.41	10.94	0.87	0.00
ΣFe	23.65	22.36	16.41	0.96	0.01
Mn	0.01	0.09	0.49	0.09	0.00
Mg	0.00	0.02	0.04	0.00	0.00
Ca	0.00	0.01	0.00	0.00	0.00
Cr	0.00	0.00	0.00	0.00	0.00
Zn	0.01	0.02	0.29	0.00	0.00
V	0.01	0.01	0.01	0.00	0.00
Ni	0.00	0.00	0.01	0.00	0.00
Total	24.00	24.00	24.00	2.00	1.00

Mineral	Bt
Sample	WYL-10-61-190.3
Line	25
SiO_2	33.77
TiO_2	3.90
Al_2O_3	13.89
Cr_2O_3	b.d.
FeO	31.29
MgO	2.86
MnO	0.42
CaO	b.d.
Na_2O	0.13
K_2O	9.18
F	b.d.
Cl	0.52
H_2O*	3.54
Subtotal	99.51
O=F,Cl	0.12
Total	99.39
Si *apfu*	5.51
^{IV}Al	2.49
^{VI}Al	0.19
Ti	0.48
Cr	0.00
Fe	4.27
Mn	0.06
Mg	0.70
Ca	0.00
Na	0.04
K	1.91
OH*	3.86
F	0.00
Cl	0.14
Total	19.65
Σ*Y*	5.69
Σ*X*	1.95
ΣAl	2.67
Fe/(Fe+Mg)	0.86
Mg/(Mg+Fe)	0.14

-: not analyzed or determined; b.d. = below detection. The proportion of end members is quoted in mol.%. Symbols used: Bt: biotite, Cfn: coffinite, Ilm: ilmenite, Mgt: magnetite, Rt: rutile, Thr: thorite, Urn: uraninite, Zrn; zircon. Electron-microprobe data. * Calculated according to stoichiometric constraints.

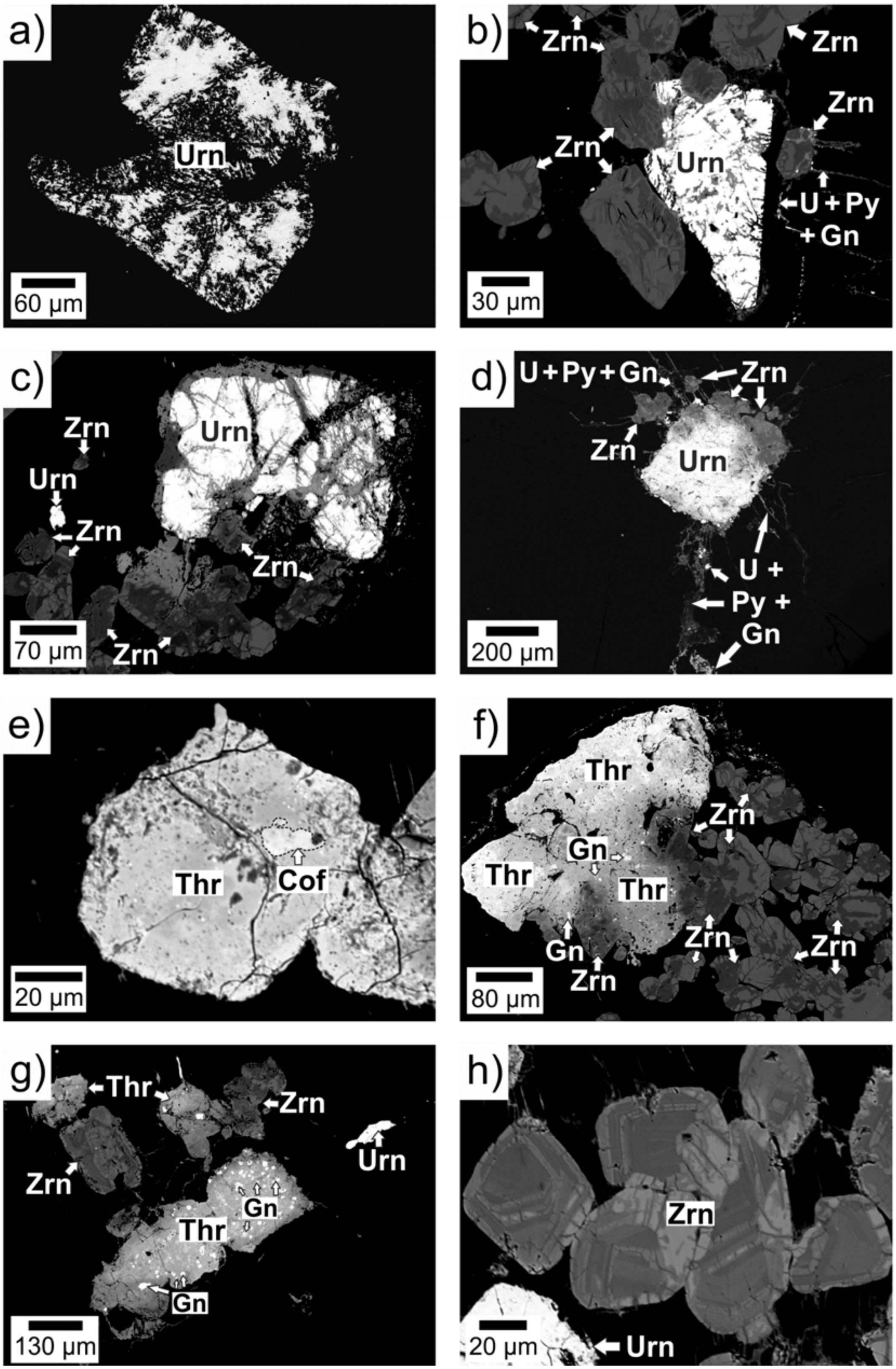

a)
Urn
60 µm
b)
Zrn
Zrn
Zrn
Zrn
Urn
U + Py
+ Gn
30 µm
c)
Zrn
Urn
Urn
Zrn
Zrn
Zrn
70 µm
d)
U + Py + Gn
Zrn
Zrn
Urn
U +
Py +
Gn
200 µm
e)
Thr
Cof
20 µm
f)
Thr
Zrn
Gn
Thr
Thr
Gn
Zrn
Zrn
Zrn
80 µm
g)
Thr
Zrn
Urn
Zrn
Gn
Thr
Gn
130 µm
h)
Zrn
20 µm
Urn

Figure 3-6. (previous page) Scanning electron microscope – back-scattered electron (SEM–BSE) imagery of U–Th–REE accessories from the U-bearing pegmatites. (a) Uraninite grain from WYL–10–61–190.3 showing alteration of the primary uraninite structure. (b) Uraninite grain from WYL–10–61–190.3 with fracturing and showing local remobilization of uranium, as witnessed by the presence of U-bearing minerals (U) + pyrite (Py) + galena (Gn) in fractures surrounding the grain. (c) Uraninite grain from WYL–10–62–93.5 showing variable amounts of fracturing and alteration. (d) Uraninite from WYL–10–61–190.3 showing alteration (to metamict phases?) and remobilization of U in fractures that also contain galena and pyrite. (e) Patchy zoned thorite (Thr) grain from WYL–10–62–93.5 with a local coffinite-rich zone (bright area with dotted outline). Grey-scale variations in the other areas of the grain reflect differences in the Th, REE, Y, and Zr components. (f) Thorite and zircon from WYL–10–62–93.5. Zircon is strongly and irregularly zoned and fractured, and locally is Th-rich where it is in contact with thorite. Thorite is also zoned and contains numerous inclusions of galena and holes in its structure due to alteration. The thorite becomes enriched in Zr near the contact with zircon due to alteration, leading to its slightly darker color. (g) Thorite from WYL–10–62–93.5 showing significant alteration, including the formation of several small cubic crystals of galena. Zircon in this sample is also fractured and zoned. (h) Zircon and thorite from WYL–10–62–93.5. These crystals are strongly and irregularly zoned, suggesting multiple stages of growth. The grains are also fractured and corroded in spots.

Zircon

The majority of the zircon from the Group-A pegmatites (Figs. 3-6b–d, f–h) shows complex patterns of internal zoning, including an anhedral core (Figs. 3-6b, f, h), euhedral (possibly magmatic) overgrowth (Figs. 3-6g, h), and anhedral (possibly hydrothermal or magmatic–hydrothermal) rim (Figs. 3-6b, f, g, h). The grains tend to be fractured and are usually metamict. The zircon crystals can be subdivided into two groups; thorium-enriched (lower analytical totals 86.06 to 88.48 wt. %) and nearly pure end-member zircon (analytical totals from 88.97 to 98.97 wt. %: Table 3-1).

The end-member zircon has from 54.11 to 64.42% ZrO_2, from 25.67 to 31.73% SiO_2, from 1.57 to 2.29% HfO_2, and up to 2.64% FeO and 2.58% CaO; Th, U, Pb, and REE are present in minor amounts (Table 3-1). This corresponds to almost 100% $(Zr,Hf)SiO_4$, with less than 3% of the $USiO_4$ and $(Y,REE)PO_4$ components (Fig. 3-7a, Table 3-1).

The thorium-enriched zircon has a much more variable composition, with significant substitution of Th for Zr (27.09–46.01 wt. % ZrO_2, 6.47–18.38 wt. % ThO_2). In addition, the zircon contains up to 9.98% FeO, 1.56% Y_2O_3 and 1.13% ∑REE_2O_3 (Table 3-1). The Th-enriched zircon grains are zirconium-rich members of the zircon–thorite solid-solution series of Förster (2006), with zircon content ranges from 71 to 92% (Zr,Hf)SiO_4, thorite from 6 to 22% $ThSiO_4$, and 2–6% (Y,REE)PO_4, with less than 1% of the $USiO_4$•nH_2O component (Fig. 3-7a).

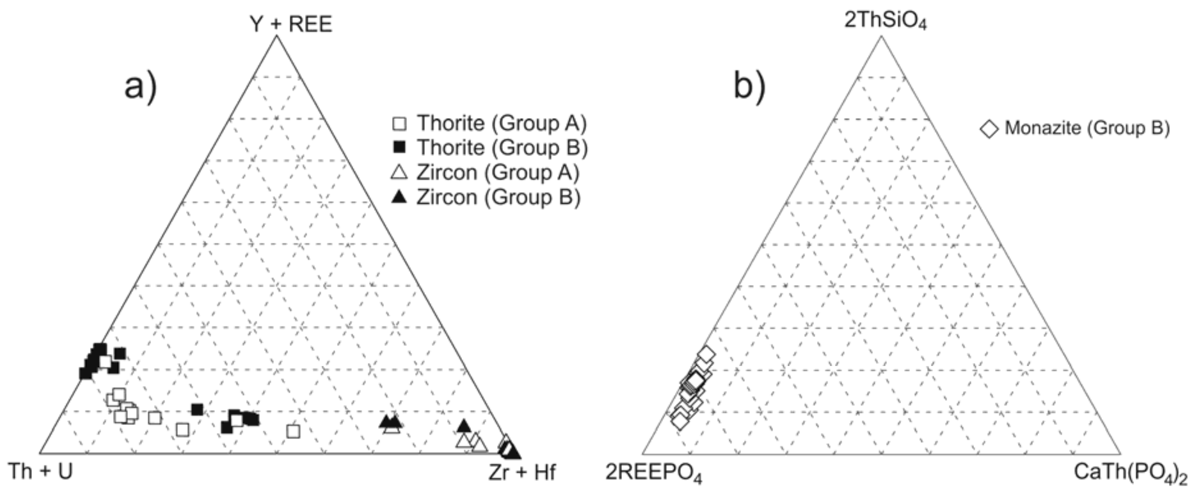

Figure 3-7. Diagrams showing the range in accessory mineral composition for (a) thorite from the Group-A pegmatites, zircon from the Group-A pegmatites, thorite from the Group-B pegmatites, zircon from the Group-B pegmatites, and (b) monazite from the Group pegmatites. These diagrams are based on Figures 2 and 4 of Förster (2006) for part a, and Figure 2 of Linthout (2007) for part b.

Magnetite

There are several large magnetite crystals in WYL–10–61–190.3 that contain various inclusions, including zircon, ilmenite, rutile, and uraninite (Fig. 3-4d). From the analytical results, we recalculated the FeO content using the method outlined by Carmichael (1967). The compositions can be broken up into compositionally distinct groups based on their Al_2O_3 and TiO_2 contents. The first comprises the bulk of the samples and includes points with 0.12 to 0.82 wt. % TiO_2 and 0.29 to 2.47% Al_2O_3. These grains contain mostly FeO (91.11 to 93.29% FeO: Table 3-1). The second group shows a slightly higher enrichment in Ti (1.28 to 2.96% TiO_2) and Al (0.76–2.68% Al_2O_3), slightly lower Fe (88.25–89.76% FeO: Table 3-1). One other analysis point (Ti-rich magnetite) had a high analytical total prior to recalculation of Fe (101.30 wt. %), and had very high Ti (17.84% TiO_2) and Al (9.12% Al_2O_3); it also had lower Fe than the other analyses (70.56% FeO). The analysis also showed high MnO (2.08%) and ZnO (1.43%) (Table 3-1).

Ilmenite

Ilmenite forms as exsolution lamellae and large, primary blebs within the magnetite grains (Fig. 3-4d). The ilmenite contains 49.16–51.17 wt. % TiO_2 and FeO (43.61 to 45.06%), and some Mn (3.41 to 4.23 wt. % MnO) (Table 3-1). The analyses lead to an approximate stoichiometry $Ti_{1.94–1.96}Fe_{1.89–1.94}Mn_{0.16–0.19}O_6$.

Rutile

Rutile forms rare inclusions within magnetite. Two grains were analyzed from WYL–10–61–190.3. The grains have >95% TiO_2, <1.25% FeO, and <1.25 MnO. This compositionally corresponds to nearly pure, end-member (>98%) rutile (TiO_2).

Biotite

Biotite was analyzed in both samples of the Group-A pegmatite in order to apply the Ti-in-biotite geothermometer of Henry *et al.* (2005), as well as the biotite geothermometer of Luhr *et al.* (1984). After analysis, the samples were recalculated to give an inferred amount of H_2O using the method in Tindle & Webb (1990). The biotite from the Group-A pegmatites has a significant but variable Ti content, 0.36 to 0.62 atoms per formula unit (*apfu*). Its X_{Fe} ranges from 0.62 to 0.89 for samples with good analytical totals (Table 3-1), and using the nomenclature of Rieder *et al.* (1998) for trioctrahedral micas of the biotite series, this biotite would be considered magnesian annite, with the biotite from WYL–10–62–93.5 having a higher proportion of the phlogopite end-member.

Mineral Compositions in the Group-B Pegmatites

Monazite

Four grains of monazite were analyzed from WYL–09–46–32.6. The grains in this sample tend to be anhedral to subhedral (Figs. 3-8a, c, d, and e) and, locally, euhedral (Fig. 3-8c), and are locally embayed and altered. Most grains show growth zoning and fracturing, but are relatively unaltered compared to the monazite found in other samples. Analytical totals range from 99.34 to 100.74 wt. %. The monazite is characterized by a high LREE content (46.37 to 57.05 wt. % $LREE_2O_3$), dominated by Ce (23.08 to 29.63%) and high Th (9.25 to 21.23% ThO_2); SiO_2 (2.25 to 6.27 wt. %), HREE (1.09 to 1.66% $HREE_2O_3$), Y_2O_3 (1.33 to 2.45%), and PbO (0.96 to 2.27%) make up most of the rest of the monazite. The uranium content is less than 1 wt. % in all grains, and CaO also is low (<0.55% CaO) (Table 3-2). The monazite is dominated by the monazite-(Ce) end-member (X_{Mnz} is 73 to 85%, with X_{Ce} equal to 35 to 42%), with a substantial amount of the huttonite [(Th,U,Pb)SiO_4] component (X_{Hut} equal to 7 to 23%) (Table 3-2, Fig. 3-7b). There is only a minor amount of cheralite [Crl; Ca(Th,U,Pb)$(PO_4)_2$] and xenotime [Xnt; YPO_4] substitution (X_{Crl} 2 to 5%, X_{Xnt} 3 to 5%) (Table 3-2, Fig. 3-7b).

Thorite

Several grains of thorite were analyzed in both WYL–09–46–32.6 and WYL–09–46–35.0. The grains in these samples typically contain numerous inclusions of galena and pyrite. They tend to have a spongy texture due to alteration and are usually fractured. The appearance of the grains suggests that at least parts of the grains are the product of the alteration of zircon (Figs. 3-8f, g). Analytical totals tend to be quite low, from 80.68 to 91.52% (Table 3-2), which is not unexpected given the altered, spongy nature of the crystals. The principal components are Th (33.60–47.47% ThO_2), Si (16.26–24.43% SiO_2), U (0.26 to 21.81% UO_2), Zr (0.08 to 13.46% ZrO_2), Fe (0.24 to 9.71% FeO), and REE (2.43 to 9.36% $\sum REE_2O_3$). Other minor components (<2.16 wt. %) include Y, P, Ca, Pb, and Al (Table 3-2). The thorite grains show large amounts of variability in their composition, with significant substitution by members of the zircon – xenotime – coffinite solid-solution series, with $X(ThSiO_4)$ ranging from 48 to 72%, $X(USiO_4)$

Table 3-2. Representative compositions of selected minerals, Group-B Pegmatites, Fraser Lakes Zone B

Mineral	Mnz	Mnz	U-rich Thr	U-rich Thr	Zr-rich Thr	Zrn	Th-rich Zrn	Xnt
Sample	WYL-09-46-32.6 Mnz1	WYL-09-46-32.6 Mnz4	WYL-09-46-35.0 Thr1	WYL-09-46-35.0 Thr5-Zrn3	WYL-09-46-35.0 Thr4-Zrn2	WYL-09-46-35.0 Thr5-Zrn3	WYL-09-46-35.0 Thr4-Zrn2	WYL-09-46-32.6 Xnt
Line	60	76	119	141	140	147	134	1
SiO_2 wt.%	5.04	2.45	20.60	21.07	24.43	31.62	25.51	4.33
TiO_2	b.d.	b.d.	0.09	0.07	0.33	0.04	0.25	-
Al_2O_3	b.d.	b.d.	0.56	0.64	0.96	b.d.	1.10	b.d.
FeO	0.04	b.d.	0.42	0.43	6.29	0.80	7.57	0.07
MnO	b.d.	b.d.	0.01	b.d.	0.10	0.11	0.11	-
MgO	b.d.	b.d.	0.00	b.d.	0.09	b.d.	0.09	-
CaO	0.38	0.42	0.89	1.45	1.67	0.50	2.55	0.04
P_2O_5	22.43	26.60	0.69	0.88	0.13	b.d.	b.d.	37.63
UO_2	0.77	0.13	13.16	20.64	2.08	0.26	2.08	b.d.
ThO_2	17.63	10.31	44.31	36.01	35.44	b.d.	15.73	0.43
PbO	1.96	1.06	0.60	0.20	0.15	0.21	0.18	-
ZrO_2	0.13	0.05	1.93	0.10	13.46	64.10	27.08	-
HfO_2	b.d.	b.d.	b.d.	b.d.	0.33	1.79	0.85	-
Y_2O_3	1.72	1.53	1.13	2.16	0.51	0.05	0.84	40.86
La_2O_3	10.32	12.23	0.23	0.19	b.d.	b.d.	b.d.	b.d.
Ce_2O_3	24.02	27.97	4.20	2.20	1.48	b.d.	1.12	0.20
Pr_2O_3	2.78	3.24	0.66	0.51	0.28	b.d.	0.26	b.d.
Nd_2O_3	9.57	11.41	2.59	2.88	1.11	b.d.	1.02	0.35
Sm_2O_3	1.31	1.76	0.17	0.44	0.06	b.d.	0.12	0.14
Gd_2O_3	0.81	1.08	0.18	0.46	0.07	b.d.	0.12	1.18
Tb_2O_3	-	-	-	-	-	-	-	b.d.
Dy_2O_3	0.37	0.32	0.17	0.30	b.d.	b.d.	b.d.	3.72
Ho_2O_3	-	-	-	-	-	-	-	b.d.
Er_2O_3	0.14	0.00	0.07	0.16	b.d.	b.d.	0.04	3.51
Yb_2O_3	-	-	-	-	-	-	-	5.05
Total	99.42	100.56	92.68	90.80	89.01	99.52	86.63	97.52
ΣREE_2O_3	49.33	58.02	8.27	7.14	3.01	0.00	2.66	14.16
O *apfu*	8	8	16	16	16	16	16	8
Si	0.42	0.20	4.20	4.30	4.29	3.94	4.09	0.27
Al	0.00	0.00	0.14	0.15	0.20	0.00	0.21	0.00
Ti	0.00	0.00	0.01	0.01	0.04	0.00	0.03	0.00
Fe	0.00	0.00	0.07	0.07	0.92	0.08	1.01	0.00
Mn	0.00	0.00	0.00	0.00	0.01	0.01	0.02	0.00
Mg	0.00	0.00	0.00	0.00	0.02	0.00	0.02	0.00
Ca	0.03	0.04	0.19	0.32	0.31	0.07	0.44	0.00
U	0.01	0.00	0.60	0.94	0.08	0.01	0.07	0.00
Th	0.34	0.19	2.05	1.67	1.42	0.00	0.57	0.01
Pb	0.04	0.02	0.03	0.01	0.01	0.01	0.01	0.00
Zr	0.01	0.00	0.19	0.01	1.15	3.89	2.12	0.00
Hf	0.00	0.00	0.00	0.00	0.02	0.07	0.05	0.00
P	1.59	1.81	0.12	0.15	0.02	0.00	0.00	1.99
Y	0.08	0.07	0.12	0.23	0.05	0.00	0.07	1.36
La	0.32	0.36	0.02	0.01	0.00	0.00	0.00	0.00
Ce	0.74	0.82	0.31	0.16	0.10	0.00	0.07	0.00
Sm	0.04	0.05	0.05	0.04	0.02	0.00	0.02	0.00
Pr	0.09	0.09	0.19	0.21	0.07	0.00	0.06	0.01
Nd	0.29	0.33	0.01	0.03	0.00	0.00	0.01	0.00
Gd	0.02	0.03	0.01	0.03	0.00	0.00	0.01	0.02
Tb	-	-	-	-	-	-	-	0.00
Dy	0.01	0.01	0.01	0.02	0.00	0.00	0.00	0.07
Ho	-	-	-	-	-	-	-	0.00
Er	0.00	0.00	0.00	0.01	0.00	0.00	0.00	0.07
Yb	-	-	-	-	-	-	-	0.10
Sum	4.04	4.02	8.34	8.39	8.75	8.09	8.86	3.91
X $LREEPO_4$	73.0	82.5	-	-	-	-	-	0.9
X $HREEPO_4$	1.8	1.9	-	-	-	-	-	16.0
X Hut	18.0	8.8	-	-	-	-	-	0.2
X Chr	3.4	3.6	-	-	-	-	-	0.3
X Xnt	3.8	3.3	-	-	-	-	-	82.5
X $ThSiO_4$	-	-	57.5	49.6	48.7	0.0	18.9	-
X $USiO_4$	-	-	16.7	27.8	2.8	0.2	2.4	-
X (Zr,HF) SiO_4	-	-	5.4	0.3	40.3	99.7	71.2	-
X (Y,REE) PO_4	-	-	20.4	22.3	8.2	0.1	7.4	-

Mineral	Bt
Sample	WYL-09-46-32.6 Bt
Line	5
SiO_2	36.42
TiO_2	2.97
Al_2O_3	14.64
Cr_2O_3	b.d.
FeO	22.35
MgO	9.48
MnO	0.33
CaO	0.04
Na_2O	0.28
K_2O	9.47
F	b.d.
Cl	0.33
H_2O*	3.80
Subtotal	100.10
O=F,Cl	0.07
Total	100.02
Si	5.62
^{IV}Al	2.38
^{VI}Al	0.28
Ti	0.34
Cr	0.00
Fe	2.88
Mn	0.04
Mg	2.18
Ca	0.01
Na	0.08
K	1.86
OH*	3.91
F	0.00
Cl	0.09
Total	19.68
Σ*Y*	5.73
Σ*X*	1.95
ΣAl	2.66
Fe/(Fe+Mg)	0.57
Mg/(Mg+Fe)	0.43

Mineral	Ilm
Sample	WYL-09-46-35.0 Ilm1
Line	66
SiO_2	0.01
TiO_2	50.46
Al_2O_3	b.d.
Cr_2O_3	0.01
V_2O_3	0.11
FeO	46.36
MnO	1.97
ZnO	0.05
NiO	b.d.
MgO	0.06
CaO	b.d.
Total	99.04
O *apfu*	6
Si	0.00
Al	0.00
Ti	1.95
Fe	1.99
Mn	0.09
Mg	0.00
Zn	0.00
Ca	0.00
Cr	0.00
Ni	0.00
V	0.00
Total	4.04

Mineral	Nb oxide
Sample	WYL-09-46-32.6 NbO
Line	5
SiO_2	4.16
TiO_2	4.16
$Al2O_3$	0.12
FeO	1.74
MgO	0.13
MnO	1.01
CaO	5.66
ZnO	b.d.
NiO	b.d.
Nb_2O_5	71.74
UO_2	1.53
ThO_2	2.31
La_2O_3	0.57
Ce_2O_3	1.87
Nd_2O_3	0.55
Gd_2O_3	0.24
Dy_2O_3	0.57
Total	96.39

-: not analyzed, b.d.: below detection limit. The proportion of end members is quoted in mol.%. Symbols used: Bt: biotite, Ilm: ilmenite, Mnz: monazite, Thr: thorite, Xnt: xenotime, Zrn; zircon. Electron-microprobe data. * Calculated according to stoichiometric constraints.

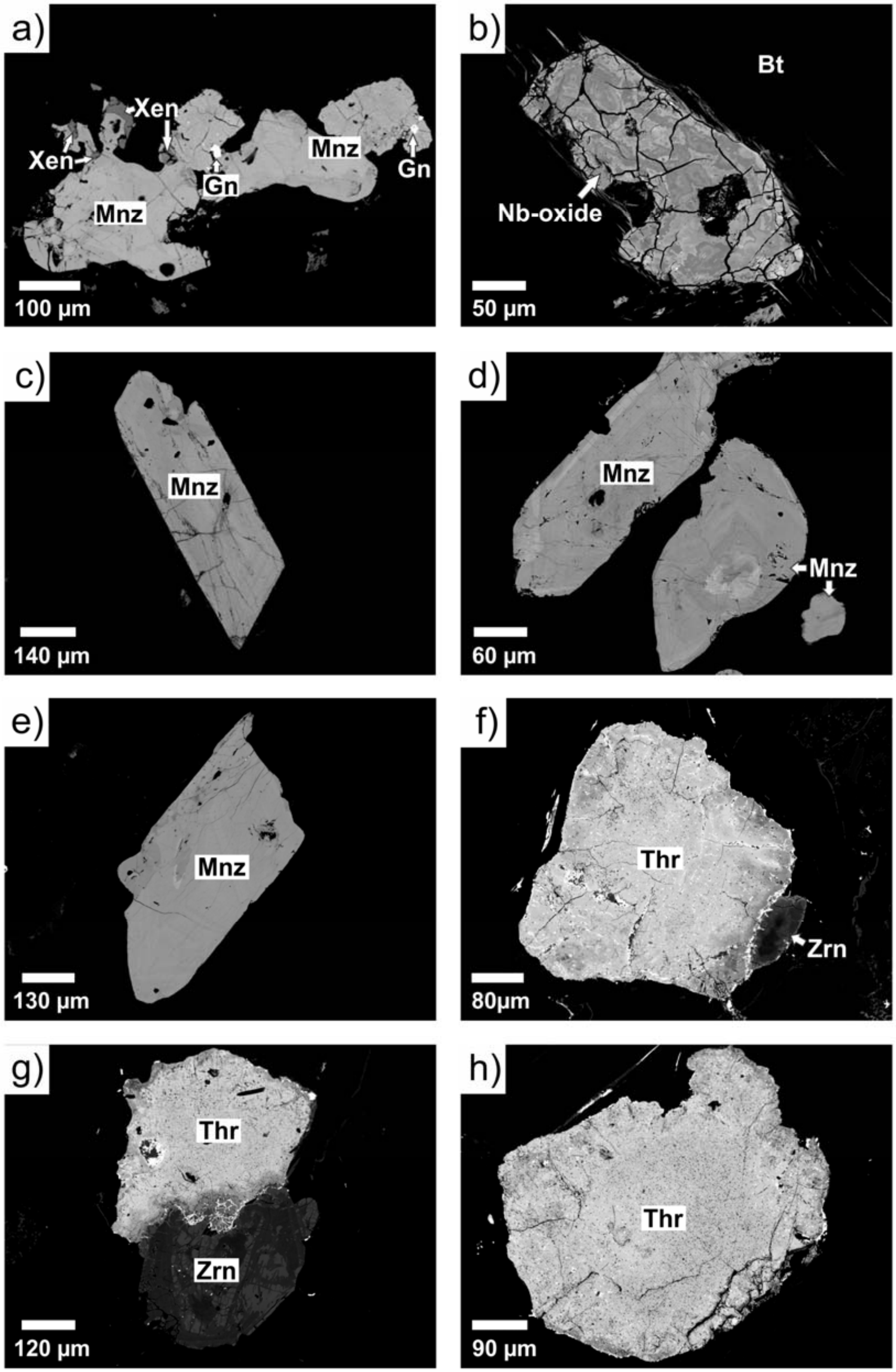
a)
Xen
Xen
Mnz
Gn
Gn
Mnz
100 µm
b)
Bt
Nb-oxide
50 µm
c)
Mnz
140 µm
d)
Mnz
Mnz
60 µm
e)
Mnz
130 µm
f)
Thr
Zrn
80µm
g)
Thr
Zrn
120 µm
h)
Thr
90 µm

Figure 3-8 (previous page). SEM–BSE imagery of U–Th–REE accessories from the Th-bearing pegmatites. (a) Monazite with xenotime growth on the rim in WYL–09–46–32.6. (b) Nb-rich oxide included in biotite from WYL–09–46–32.6. It is fractured and shows clear signs of zoning and alteration. (c) Monazite 1 from WYL–09–46–32.6. Grain is fractured and is locally embayed and contains some holes from plucked inclusions. (d) Zoned monazite grains from WYL–09–46–32.6 showing the irregular shape and growth zoning. Grains are fractured and slightly altered and embayed. (e) Irregularly shaped and zoned monazite from WYL–09–46–32.6. (f) and (g) Altered thorite in contact with altered zircon in WYL–09–46–35.0. (h) Altered thorite with numerous tiny inclusions of pyrite from WYL–09–46–35.0.

from 0 to 30%, $X[(Zr,Hf)SiO_4]$ from 0 to 39%, and $X[(Y,REE)PO_4]$ from 8 to 25% (Table 3-2, Fig. 3-7a). The thorite is enriched in Zr where it is in contact with zircon. The high FeO contents likely reflect alteration of the thorite grains or may be due to overlap by the beam on a pyrite inclusion, as they are common in the thorite grains. These grains may be a replacement of precursor U–Th–REE minerals, including zircon, in view of the high amounts of substitution of other members of the thorite – coffinite – xenotime – zircon solid-solution series.

Zircon

Zircon was analyzed from WYL–09–46–35.0. The zircon (Figs. 3-8f, g) in this sample is complexly zoned and fractured in BSE images; it is metamict (low birefringence), and shows evidence for alteration where in contact with thorite grains (*i.e.*, it has a higher Th content and lower Zr, as well as low totals, <86.7%). A few analyses show some of the zircon has a near end-member composition [$X(Zr,Hf)SiO_4 > 0.97$], whereas others show significant substitution by other members of the zircon – thorite – coffinite – xenotime solid-solution series (Table 3-2, Fig. 3-7a). There is also a significant amount of FeO (6.74 to 9.10%), which is a good indication that these do not represent compositions of pure zircon. These may instead reflect a mixture of minerals including zircon and pyrite. The end-member zircon shows a range of Zr (51.46 to 65.04% ZrO_2) and Si (25.84 to 32.21% SiO_2), and contains up to 1.56 wt. % FeO, 2.46% CaO, 1.79% HfO_2, and 1.58% Al_2O_3 (Table 3-2). The altered compositions contain significantly more Th (6.35 to 15.73% ThO_2), U (0.19 to 3.56% UO_2), and REE (including 1.08 to 1.10% Ce_2O_3), and less Si (25.51 to 26.76% SiO_2) and Zr (25.27 to 35.38% ZrO_2) (Table 3-2). The altered zircon ranges in X[(Zr,Hf) SiO_4] from 69 to 86%, whereas *X*($ThSiO_4$) varies from 7 to 19%, *X*[(Y,REE)PO_4] is around 7, and *X*($USiO_4$) is 0 to 4% (Table 3-2, Fig. 3-7a).

Ilmenite

The ilmenite from WYL–09–46–35.0 (Table 3-2) contains 50.46 to 50.68 wt. % TiO_2 and 45.97 to 46.36 wt. % FeO, with minor Mn (1.97 to 2.01 wt. % MnO). The approximate stoichiometry is $Fe_{0.94–0.97}$ $Ti_{0.97–0.98}$ $Mn_{0.07-0.09}O_3$.

Xenotime

Xenotime was observed in SEM–BSE-images of WYL–09–46–32.6 as small grains at the edge of monazite grains (Figure 3-8a), the EDS spectra confirming the Y-rich nature of these grains. Two analyses were done (Table 3-2), and show that this xenotime is mostly composed of YPO_4 [X_{YPO4} = 0.83]. There is significant incorporation of REE in the xenotime [$X_{HREEPO4}$ = 17%], but the LREE content is low [$X_{LREEPO4}$ = 1%] (Table 3-2).

Nb oxide

One roundish grain was found in WYL–09–46–32.6 of a yellow (in plane-polarized light), generally isotropic, and patchily zoned mineral (see Figure 3-7b). The EPMA analyses show that it is Nb-rich (65.96 to 74.02 wt. % Nb_2O_5; 1.85 *apfu* Nb on the basis of O = 6), with significant amounts of TiO_2 (4.16 to 8.53 wt. %), SiO_2 (1.50 to 6.95 wt. %), ThO_2 (1.16 to 4.11 wt. %), UO_2 (0 to 3.35 wt. %), FeO (1.74 to 3.18 wt. %), CaO (5.51 to 6.00 wt. %), and LREE (0.89 to 3.37 wt. % $\sum LREE_2O_3$) (Table 3-2). Other elements present in minor to trace amounts (<1 wt. %) include HREE, Al, Mg, Mn, Ni, and Zn. The analytical totals are low, in the range of 96.22 to 97.69 wt. % (Table 3-2), and it is not known whether other elements should have been sought (*i.e.*, Ta, F, Y; see Atencio *et al.* 2010 for information on the chemical formula of pyrochlore) or if the mineral may be hydrous. This mineral is one of the calciopyrochlore members of the pyrochlore group, but the full name and chemical formula cannot be deter- mined using the criteria of Atencio *et al.* (2010) due to the lack of information on the amount of F and H_2O.

Biotite

The biotite in WYL–09–46–32.6 shows weak replacement by chlorite and rutile along cleavage planes, as is common for pegmatites in this part of the fold nose. The biotite has X_{Fe} of 0.56 to 0.57 and an X_{Mg} of 0.43 to 0.44, with a Ti content ranging from 0.32 to 0.34 *apfu* (Table 3-2). No F was detected. The analytical results were recalculated using the method described by Tindle & Webb (1990) for the determination of the H_2O content. Based on these results, the biotite can be described as magnesian annite using the nomenclature of Rieder *et al.* (1998).

Chime U–Th–Pb Chemical Age Dating

The CHIME approach of U–Th–Pb chemical age dating, using the procedures of Bowles (1990), Montel *et al.* (1996), Förster (1999), Annesley *et al.* (2000), and Kempe (2003), was attempted on uraninite, thorite, zircon, and monazite from the pegmatite samples. However, owing to complex zoning, fracturing, and alteration shown by the thorite and zircon (Figures 3-6e, f, g, and h, and 3-7f, g, and h), the U–Th–Pb chemical system was strongly disturbed in both these minerals, and thus the chemical ages obtained are geologically unreasonable.

Uraninite from the Group-A pegmatites yielded CHIME results in the range of 1904 to 1102 Ma, although the most common ages obtained are between 1.85 and 1.80 Ga (Table 3-3, Figs. 3-9a, c). The error on all uraninite chemical ages is ±5 Ma. Monazite from the Group-B pegmatite (WYL–09–46–32.6) shows older ages, with a range from 2256 ± 27 Ma to 2056 ± 25 Ma (Figs. 3-9b, c), with a variable range of calculated errors.

Geothermometry

Biotite was monitored in the four samples in order to estimate their temperature of intrusion, emplacement, and crystallization. Using the method of Luhr *et al.* (1984), an average temperature of 633°C was obtained for the biotite from the Group-A pegmatite WYL–10–61–190.3, with the calculated temperatures ranging from 620°C to a high of 663°C (Table 3-3). The

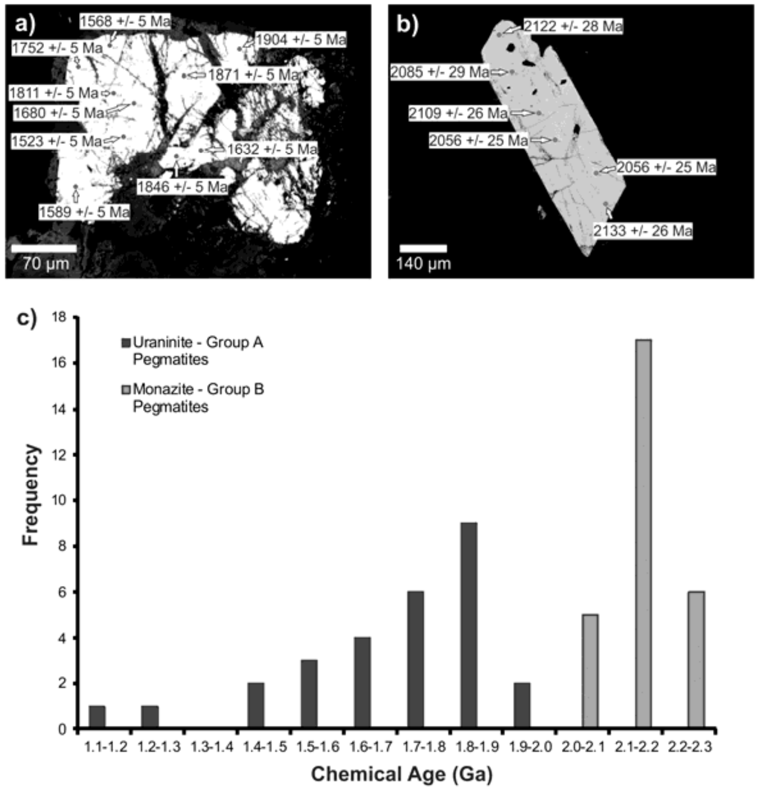

Figure 3-9. Results of CHIME chemical age dating for U–Th–REE accessory minerals from the granitic pegmatites and pelitic gneisses (see text for the methods used). (a) Uraninite from WYL–10–62–93.5 with chemical ages (in Ma) plotted for the different analysis points (all errors are ±5 Ma for this grain). The ages (and errors) are shown in millions of years (Ma) beside each analytical point. (b) Monazite from WYL–09–46–32.6 with chemical ages plotted for the different points analyzed. The ages (and associated errors) are shown beside each analytical point. (c) Histogram showing the spread of ages found for the U–Th–REE minerals at Fraser Lakes Zone B. Uraninite shows clustering of ages between 1.80 and 1.90 Ga, with a particular cluster from 1.85 to 1.80 Ga; these ages are interpreted to be the age of formation for the uraniferous pegmatites at Fraser Lakes Zone B. Monazite from the Th-bearing pegmatites show a cluster of ages at 2.1 to 2.2 Ga; these ages are much older than those determined for the U-bearing pegmatites and interpreted to be inherited from the melting region (*i.e.*, possibly the age of the source rock).

Ti-in-biotite thermometer of Henry *et al.* (2005) yielded higher temperatures between 739°C and 687°C (average 701°C; Table 3-3). The same thermometers applied to the other Group A pegmatite sample (WYL–10–62–93.5) gave average temperatures of 645°C and 682°C (Table 3-3) for the Luhr *et al.* (1985) and Henry *et al.* (2005) biotite geothermometers, respectively (ranges were from 653°C to 636°C and 688°C to 675°C, respectively). Biotite was also monitored in the Group-B pegmatites; it gave an average of 673°C using the Ti-in-biotite geothermometer and an average of 641°C (Table 3-3) using the Luhr *et al.* (1984) geothermometer (675°C to 665°C and 644°C to 636°C, respectively). Coexisting magnetite and ilmenite were also analyzed in WYL–10–61–190.3. Using the ILMAT magnetite–ilmenite geothermobarometry program by Lepage (2003), a range of temperatures was obtained (Table 3-3). The highest temperatures (average of 706°C to 811°C depending on the calibration of the magnetite–ilmenite geothermometer that was used, Table 3-3) were calculated using the single Ti-rich magnetite composition, whereas lower temperatures (ranging from 651° to 318°C depending on the calibration and grains used; Table 3-3) were calculated using the Ti-poor magnetite. Oxygen fugacities, expressed as log $f(O_2)$, were also calculated using the ILMAT program, and found to range from –15 to a low of –22.6 for the Ti-rich magnetite (average of –17.7) and from –19.0 to a low of –25.3 (average of –22.9) using the Ti-poor magnetite.

Table 3-3. Temperature and Oxygen Fugacity of Pegmatites from the Fraser Lakes Zone B Area

		Biotite geothermometry		
Sample	T (°C) average Henry *et al.* (2005)	T (°C) average Luhr *et al.* (1984)	T (°C) range Henry *et al.* (2005)	T (°C) range Luhr *et al.*(1984)
WYL-10-61-190.3 Bt	701	633	739 to 687	663 to 620
WYL-10-62-93.5 Bt	682	645	688 to 676	653 to 636
Group A Pegmatites (both samples)	692	639	739 to 676	663 to 620
WYL-09-46-32.6	673	641	675 to 665	644 to 636
All Pegmatites (Groups A and B)	685	640	739 to 665	663 to 620
		Titaniferous magnetite – ilmenite thermometer[§]: Ti-rich magnetite (WYL-10-61-190.3)		
Methods	Average T (°C)	Average log $f(O_2)$	Range T (°C)	Range log $f(O_2)$
Powell & Powell (1977)	811	-	901 to 712	-
Spencer & Lindsley (1981)	706	-18.1	822 to 582	-15.0 to -22.6
Andersen & Lindsley (1985)	730	-17.3	829 to 619	-15.2 to -20.7
All methods combined	749	-17.7	901 to 582	-15.0 to -22.6
		Titaniferous magnetite – ilmenite thermometer[§]: Ti-poor magnetite (WYL-10-61-190.3)		
Powell & Powell (1977)	440 to 372 (408)*	-	649 to 318	-
Spencer & Lindsley (1981)	532 to 493 (513)	-22.0 to -24.1 (-23.0)	626 to 450	-19.7 to -25.3
Andersen & Lindsley (1985)	538 to 491 (558)	-21.8 to -23.9 (-22.8)	651 to 443	-19.0 to -25.3
All methods combined	538 to 372 (479)	-21.8 to -24.1 (-22.9)	651 to 318	-19.0 to -25.3

[§] ILMAT program of Lepage (2003), giving an average or range of T and log $f(O_2)$.
* numbers in brackets correspond to an average for all grains combined; ranges in averages show the range in average for different grains.

Discussion

In this study, we used a multifaceted approach to understand the geological setting, age and mineral assemblages of the granitic pegmatites, the composition of the U–Th–REE accessory minerals, and emplacement and crystallization conditions of the pegmatites and leucogranites in order to constrain the origin of the radioactive granite pegmatites and leucogranites at the Fraser Lakes Zone B deposit in the Wollaston Domain of northern Saskatchewan, Canada.

Origin and alteration of U–Th–REE minerals

The results of this work show that the main U– Th–REE-bearing minerals in the Fraser Lakes area are likely a mixture of magmatic, hydrothermal, and inherited or xenocrystic minerals. The primary igneous minerals in these pegmatites include quartz, feldspar, and some of the biotite and some of the U–Th–REE accessory minerals, the determination being made on the basis of their composition and textures. Others show a more complex history, and may represent a combination of different origins, such as the zircon that shows evidence for multiple stages of growth.

The relatively high Th content of the uraninite (>5.51 wt. % ThO_2) and its euhedral habit suggest that the uraninite is a primary magmatic mineral (see Förster 1999), in marked contrast to the Th content (<1% ThO_2) of hydrothermal uraninite from unconformity-related uranium deposits in the Athabasca Basin (Fayek *et al.* 1997, 2002). In addition, chondrite-normalized REE patterns of uraninite from Fraser Lakes Zone B are consistent with a magmatic origin (see Figure 8 of Mercadier *et al.* 2013). Uraninite with the highest Ca, P, and Fe contents is typically more strongly altered. Any local increases in Pb may be due to the formation of microscopic crystals of radiogenic galena or to local remobilization of Pb in microfractures (Figures 3-6b, d, f, g, and h). The large range in PbO values in the grains, combined with the textural evidence for remobilization of Pb and U (in the form of secondary uranium oxides and galena in fractures), suggest that the uraninite was at least partially altered (with the alteration possibly causing a significant resetting of the U–Th–Pb system).

The uranoan thorite from both the Group-A and Group-B pegmatites tends to show more obvious textural and chemical signs of alteration than the other U–Th–REE minerals. The composition of the thorite seems to be strongly influenced by the minerals surrounding it. For example, thorite grains near the contact with zircon tend to be enriched in Zr, suggesting that both the zircon and thorite may have been altered by the same fluids. The high FeO content of most of the thorite from the Group-A pegmatites reflects small inclusions of secondary pyrite. Higher uranium contents (*i.e.*, increase in the coffinite end-member) in the center part of a thorite grain (which is easily distinguished by its brighter appearance in SEM–BSE: Figure 3-6e) may also be due to alteration of the thorite or be the remains of a precursor mineral; thus the thorite may represent a secondary mineral.

The zircon crystals in these samples are complexly zoned (Figures 3-6b, c, d, f, and h) and show fairly homogeneous compositions, except where they are in contact with thorite (Table 3-1). The high FeO content (Table 3-1) of some of the grains may be due to either alteration of the grains or to small pyrite inclusions (which were found within zircon from other samples). The zoned grains presumably contain inherited, rounded cores, with euhedral zoned overgrowths (possibly magmatic) and later anhedral rims (possibly magmatic–hydro- thermal). However, owing to their complex nature, in situ techniques, such as SHRIMP or LA–ICP–MS, will be needed in order to properly determine the age of the various growth and recrystallization stages. The low U and Th contents of the grains (especially U) analyzed in this study (Table 3-1) indicate that this mineral is likely not an important source of U and Th in the Group-A pegmatites.

High-Th monazite (Table 3-2) with an embayed shape (Figures 3-7a, c, d, and e), which is found in clusters within the Group-B pegmatites, are unlikely to have developed by direct crystallization from a pegmatite-forming melt. These grains also yielded chemical age dates that are older than the inferred age of the granitic pegmatites, which suggests that the monazite may be inherited from the source rock. The origin of the monazite by inheritance has been postulated for high-Th monazite found in granitoids and migmatites (Watt 1995).

The zircon and thorite in Group-B pegmatites show similar textures to those in the Group-A pegmatites, and are interpreted to have formed in a similar way. The U contents of thorite from the Group-B pegmatites are higher than in that from the Group-A pegmatites, suggesting that U was partitioned slightly differently in the two different groups of pegmatites, with uranium being preferentially partitioned into uraninite in the Group-A pegmatites over thorite. In the Group-B pegmatites, which lack uraninite, uranium partitioned into the thorite.

The high LREE, Th, and U content of the Group-B pegmatites is strongly dominated by the high proportion of monazite. Thorite, although less common, also contains significant amounts of U and Th, whereas the highest HREE contents are likely linked to the presence of rare xenotime.

P–T conditions recorded by the granitic pegmatites

The granitic pegmatites may contain garnet and rare cordierite, and lack muscovite, suggesting that the temperature of intrusion was likely quite high, above the second sillimanite isograd, in the range of 800° to 700°C at moderate pressures (Figure 3-10). The pegmatites also show evidence for subsolidus cooling (feldspar exsolution, rutile forming from biotite, and ilmenite lamellae in magnetite) and later retrograde metamorphism (chlorite forming at the expense of biotite, and white mica at the expense of plagioclase). The presence of two generations of biotite, oriented in two different directions, is suggested by their association with uraninite of two different ages (Mercadier *et al.*, pers. commun.). The older biotite is considered to be part of the primary magmatic assemblage, whereas the younger biotite is part of a high-T subsolidus assemblage postdating intrusion of the pegmatites. Later, low- to moderate-T events preserved in the granitic pegmatites led to the appearance of chlorite and rutile in biotite and white mica in the feldspars, which was stronger in the central portion of the fold nose. This was in turn followed by younger circulation of hydrothermal fluid through the rocks, which led to deposition of hematite, chlorite, white mica, clay minerals, carbonate, and quartz in the granitic pegmatites (McKechnie *et al.* 2013).

An assumption made in calculating temperatures using the two biotite geothermometers discussed in this paper is that the biotite in these samples is of magmatic origin, not xenocrystic or entrained (*i.e.*, peritectic), and not of post-crystallization origin due to resetting or growth subsolidus. In addition, the geothermometers used in this study were developed for use in other rock types with slightly different compositions: volcanic rocks for Luhr *et al.* (1994), graphitic pelites for the Henry *et al.* (2005) geothermometer. Thus, the results from these two geothermometers should be interpreted with caution.

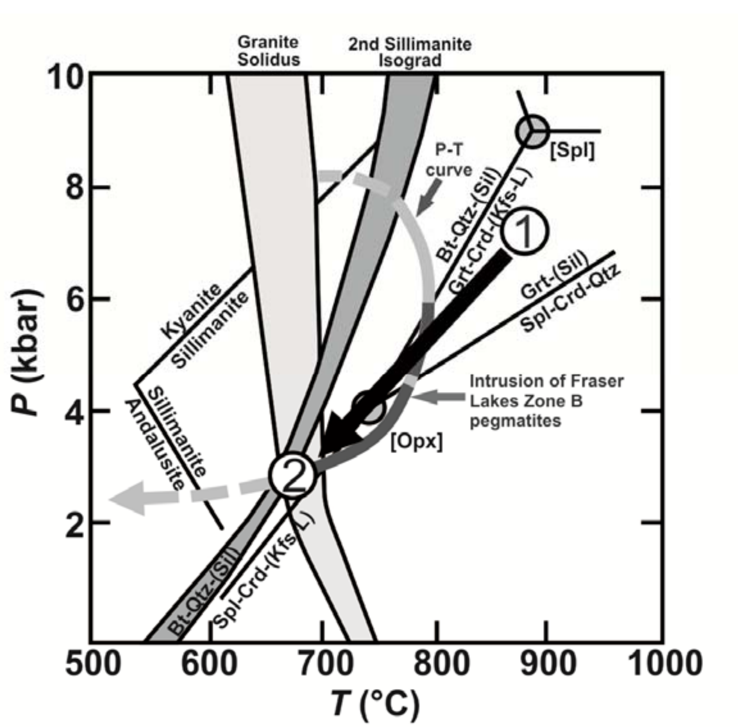

Figure 3-10. The P–T path for the Fraser Lakes pelitic gneisses showing the timing of pegmatite emplacement with respect to the clockwise P–T path for metamorphism of the eastern Wollaston Domain. This timing was determined on the basis of field relationships, thermobarometry, and mineral assemblages (modified from Annesley *et al.* 2005). In previous work, Austman *et al.* (2010a, b) and McKechnie *et al.* (2013) suggested that the pegmatites formed *via* partial melting of the pelitic gneisses by biotite-dehydration reactions (1), including the reaction Bt + Qtz + (Sil) → Grt + Crd + (Kfs + L) (among others). The bulk of partial melting (and emplacement of the pegmatites) took place as the rocks were undergoing isothermal decompression, with intrusion ongoing (though diminishing with time due to decreasing temperature) until the rocks were below the granite solidus (2). The arrow represents approximately the P–T path taken by the melts from their source (1) through the crustal melt-transfer zone to the depth of pegmatite emplacement (2).

The temperatures of the granitic pegmatites determined using the two biotite geothermometers reflect a range of temperatures (high of 739° down to 620°C, depending on the sample and the thermometer used; Table 3-3) close to those previously estimated (McKechnie *et al.* 2012b) for the peak temperatures of metamorphism in the pelitic gneisses at Fraser Lakes Zone B [up to 766°C; see Figures 8 and 9, and Table 2 of McKechnie *et al.* (2012b) for details] and elsewhere in the Wollaston Domain (see Figure 3-10, which is modified from Figure 5 of Annesley *et al.* 2005) . Thus, the results for both the Group A and Group B pegmatites could reflect either the intrusion temperature of the pegmatites, or the temperature of the second recognized generation of biotite (assumed to have grown at high T), assuming that all of the biotite in these samples is of magmatic origin (*i.e.*, not inherited or xenocrystic). The range of temperatures shown by the biotite could also be due to post-crystallization retrograde metamorphism.

There is some similarity in the temperatures calculated using the ILMAT geothermobarometry software. The highest temperatures (average of 706° to 811°C, depending on the calibration of the magnetite–ilmenite geothermometer used; Table 3-3), and calculated using the Ti-rich magnetite, are considered to represent the initial crystallization of the granitic pegmatites, whereas lower temperatures (ranging from 651° to 318°C depending on the calibration and grains used; Table 3-3) calculated using the Ti-poor magnetite are considered to be the result of subsolidus exsolution under retrograde conditions. However, these results should be treated with caution owing to the significant amounts of ilmenite lamellae in the magnetite in these pegmatites, the assumption that all of the magnetite and ilmenite is of magmatic origin, and the heterogeneity shown by the magnetite grains.

Constraints on age of metamorphism, partial melting, and pegmatite formation (McKechnie *et al.* 2013) show that the Zone-B pegmatites formed contemporaneously with metamorphism and deformation in the area, primarily on the basis of cross-cutting relationships. In addition, other uraniferous pegmatites in the Wollaston Domain have similar geological relationships with metamorphism (pegmatites intrude roughly parallel to the gneissosity shown by the high- grade assemblages), and some have yielded chemical and isotopic ages between 1.85 and 1.8 Ga (Parslow *et al.* 1985, Annesley *et al.* 1997, 1999, 2005; Hamilton & Delaney 2000, Madore *et al.*

2000, Card *et al.* 2007, Mercadier *et al.* 2010, 2011), roughly at the time that the rocks experienced high-grade regional metamorphism in the area (Annesley *et al.* 2005).

The largest cluster of chemical ages obtained for the Group-B pegmatites from Fraser Lakes Zone B is between 1.85 and 1.80 Ga (Deposited Table 3-3 (Appendix E), Figure 3-9c), which is similar to the U–Pb zircon ages (1820–1760 Ma) determined for the main pulse of leucogranite and pegmatites within the Wollaston Domain (Annesley *et al.* 2005). Thus, this cluster is considered to represent the age of crystallization of the uraninite from the pegmatite-forming melt. The ages are similar to or slightly older than the chemical ages and ion-microprobe ages obtained by Annesley *et al.* (2010b) and Mercadier *et al.* (2013) for the Fraser Lakes area, which vary from 1805 ± 11 to 1713 ± 30 Ma. Younger ages (1.7 to 1.1 Ga) are believed to represent resetting of the U–Th–Pb system during later (hydro) thermal events, particularly as they typically occur within more altered areas of the uraninite grains. Some of these younger ages overlap with known mineralizing or resetting events in the nearby Athabasca Basin (Mercadier *et al.* 2010, 2011, and references therein) and thus, these younger ages may represent times that fluids, originally from the Athabasca Basin, interacted with the Fraser Lakes granitic pegmatites. In fact, some of the later alteration-induced assemblages seen in the Fraser Lakes area (Annesley *et al.* 2010b) are similar to those found associated with unconformity-related uranium deposits. Older ages for the uraninite (>1.85 Ga) are considered to also be due to resetting of the U–Th–Pb system, possibly as a result of local intracrystalline redistribution of these elements, rather than the age of magmatic crystallization, as they do not fit with the cross-cutting relationships exhibited by the uraniferous pegmatites (which indicate intrusion during peak thermal metamorphism).

The ages of the monazite from the Group-B pegmatites (Appendix F, Figure 3-9c) are older than the known age of regional metamorphism in the area. Since the granitic pegmatites intrude during the peak of thermal metamorphism, these ages suggest that the monazite may be xenocrystic, from the source rock of the melt as initially suggested by McKechnie *et al.* (2013). They may possibly represent the age of the source rock, or at least the age of monazite growth in the source rock. The other possibility is that the older ages represent a resetting of the U–Th–Pb system (*i.e.*, U or Th loss or Pb gain). Although both processes may explain the monazite ages, the former process is preferred as textures (embayed, skeletal appearance, clustering) and a high-Th composition (Watt 1995) support a xenocrystic origin.

Figure 3-10 shows a P–T path for metamorphism of the pelitic gneiss host-rocks at Fraser Lakes Zone B, and includes the probable timing of the intrusion of the pegmatites there. The placement of the Fraser Lakes Zone B pegmatites on this curve was done on the basis of field relationships, petrography, and mineral reactions, including the work of McKechnie *et al.* (2013), as well as the chemical age dating from this study and the geothermobarometry in this paper and McKechnie *et al.* (2012b). Combining the results from the biotite and oxide geothermometers (which showed similar maximum temperatures), we can see that the Fraser Lakes Zone B pegmatites likely were emplaced at a temperature of approximately 750° to 675°C (Figure 3-10). This agrees with the initial interpretation of McKechnie *et al.* (2013) that the pegmatites were emplaced during high-T metamorphism in the Fraser Lakes area.

Model for the generation, transport and evolution of granitic pegmatites

The mineralized pegmatites at Fraser Lakes Zone B were suggested by McKechnie *et al.* (2013) to have formed by partial melting and subsequent fractional crystallization during thermal peak conditions of the Trans-Hudson Orogen (THO). The geochemical trends shown by the pegmatites and their dominantly peraluminous composition provide clear evidence that the pegmatite-forming melt probably had a source in pelitic rocks in the lower to middle crust of the Fraser Lakes area, with some contribution from Archean orthogneisses (McKechnie *et al.* 2013). Preliminary U–Th–Pb chemical dating (Annesley *et al.* 2010b) of the uraniferous pegmatites suggest that they intruded at ca.1770 ± 90 Ma, which is consistent with the results of this study. The present study provides further constraints on the model proposed earlier.

McKechnie *et al.* (2013) recognized that the Group-A pegmatites show more SiO_2-rich compositions relative to the Group-B pegmatites; however, both groups of pegmatites do not show evidence for significant fractionation (as both groups are not enriched in incompatible elements). Thus some other explanation is required to explain the difference in their compositions.

The Group-A pegmatites could represent the products of earlier melts, whereas the Group-B pegmatites may represent melts generated from the residue of this partial melting or melts that have interacted more with restitic material, as suggested by lower SiO_2 and higher MgO, FeO, and Al_2O_3 concentrations. In the pelitic gneisses, monazite generally occurs as inclusions within biotite and garnet, and thus would not have been involved in the earliest phase of partial melting. The Group-B pegmatites from Fraser Lakes Zone B show REE profiles similar to the REE profiles of the melanosomes in Nabelek & Glascock (1995). The Group-B pegmatites may thus have been formed by melting of an already depleted pelitic gneiss source. The monazite would likely have remained trapped in the biotite-rich residues of the earlier melting phase, as it has a low solubility in low-temperature peraluminous melts (Montel 1993), which explains the generally low LREE content of the Group-A pegmatites. Upon further partial melting, the restite from the first phase would begin melting. The monazite may have been entrained in the melt, and would have been partly or completely preserved, as a consequence of being quite insoluble in the pegmatite-forming melt (Watt 1995) during transport to where it cooled and crystallized. Enrichment of monazite in cumulates or restite is proposed to have caused monazite enrichment in granitoids from Finland (Lauri *et al.* 2007, Cuney & Kyser 2008, Kukkonen & Lauri 2009). The presence of abundant inherited cores in zircon is also likely due to the low solubility of this mineral in low-temperature peraluminous melts (Watson & Harrison 1983), with the cores providing nuclei for further crystallization of zircon in the melts.

The presence of uraninite only in Group-A pegmatites also is related to the amount of melting that the source rocks experienced. In order to obtain silicate melts capable of crystallizing uraninite, two conditions must be met during partial melting; a) the source must have a uranium content much higher than the Clarke abundance of continental crust, ~1 ppm according to Cuney (2010), and b) most of the uranium in the source rock must not be incorporated in the lattice of the accessory minerals (*i.e.*, it must be absorbed on the accessory mineral or present as uranium oxides) owing to the low solubility of the accessory minerals (*i.e.*, apatite, zircon, and monazite) in low-temperature (*i.e.*, <850°C) partial melts (Mercadier *et al.* 2013, and references therein).

The mineralogical and chemical differences between the two groups of pegmatites may also be related to differential incorporation of host rock and restitic material (and thus in turn related to transport distance). The presence of biotite and other peritectic and xenocrystic or inherited minerals (mainly garnet) in both groups of pegmatites indicates that they are relatively close their source areas, and incorporated significant amounts of the host-rock material. However, the Group-B pegmatites tend to contain a higher amount of biotite and garnet (possibly restitic or peritectic), including biotite schlieren, as well as important amounts of inherited monazite, and thus are more likely to be closer to their source areas and have experienced less restite unmixing (see Mercadier *et al.* 2013, and references therein for a discussion of how the composition of partial-melt-derived granitoids is related to the degree of restite unmixing). Both groups of pegmatites at Fraser Lakes Zone B experienced less unmixing when compared to the other granitoids and pegmatites found on the Way Lake property (Mercadier *et al.* 2013, and references therein).

The higher peraluminosity of the Group-A and Group-B pegmatites compared to the Rössing alaskites suggests that the Fraser Lakes Zone B pegmatites resulted from partial melting of slightly more peraluminous rocks (*i.e.*, peraluminous pelitic gneisses, versus the weakly peraluminous quartzofeldspathic metasedimentary rocks or felsic metavolcanic rocks interpreted to be the source of the Rössing alaskites). However, the rate of partial melting would have remained fairly low, as the Fraser Lakes Zone pegmatites have mineralogy similar to the granite eutectic minimum (Cuney & Kyser 2008, and references therein).

Field relationships suggest that Fraser Lakes U- and Th-bearing pegmatites were intruded into fold-nose areas, while deformation was on-going, as they both parallel and cross-cut the gneissose fabric (McKechnie *et al.* 2013), and the relationships are similar to those described by Brown (2010) and Weinberg & Mark (2008). Cuney & Kyser (2008) indicated that granitic dykes with this type of relationship to the metamorphic foliation are found only within high-grade migmatitic domains with low degrees of partial melting; this is further evidence that the Fraser Lakes Zone B pegmatites formed from low degrees of partial melting.

The relatively undeformed cores shown by the pegmatites may reflect the rheological contrasts between the granitic pegmatites and their surrounding host-rocks during intrusion and later deformation. As the pegmatite-forming melts are intruded, they localize strain until they crystallize due to the ductile nature of the melt. Strain would be localized in rheologically weak zones, such as at the margins of the granitic pegmatites after crystallization, and within biotite-rich portions of the pegmatites. In addition, the host rocks to the granitic pegmatites, in particular the basal units of the lower Wollaston Group, would also have localized more of the strain at the Archean–Paleoproterozoic contact owing to their biotite-, cordierite-, and graphite- rich mineralogy. Overall, the presence of protomylonitic to mylonitic fabrics in the area emphasize that this was a high-strain environment during syn- to late- tectonic deformation, metamorphism, and exhumation at 1820 to 1800 Ma (Annesley *et al.* 2005, Mercadier *et al.*, 2013).

The granitic pegmatites at Fraser Lakes fit the general characteristics of the Abyssal class of pegmatites of Černý & Ercit (2005), with the Group A pegmatites falling into the Abyssal-U (AB–U) subclass, and the Group-B pegmatites falling within the Abyssal- LREE (AB–LREE) subclass. The abyssal class pegmatites generally do not show any temporal or spatial connections to granitic plutons, and typically intrude into rocks metamorphosed to the upper amphibolite to granulite facies. The Fraser Lakes granitic pegmatites are interpreted to be the product of partial melting in the lower to middle crust (Figure 3-11c), as proposed by Annesley *et al.* (2009) and McKechnie *et al.* (2013).

This generation of melt at middle to lower crustal depths is supported by the lack of connection among a large granitic body (*i.e.*, pluton), the granitic pegmatites studied and leucosome in the pelitic gneisses. The amount of restite within the granitic pegmatites suggests that the currently exposed crustal level at Fraser Lakes is located in the middle part of an old crustal melt-transfer zone ~20 km thick (Figure 3-11b), a model proposed by Brown (2010) and numerically modeled by Hobbs & Ord (2010). If the rocks were in the deeper parts of this transfer zone, then we would expect more restite in the granitic melts with higher contents of peritectic garnet. Also, as there are no major plutons of similar age in the Fraser Lakes area, the authors opined that the exposed crust is not near the top of the mid-crustal melt-transfer zone. This also fits with the presence of both garnet and cordierite as stable phases within the pelitic gneisses, as cordierite is more common in the upper part of the melt-transfer zone, and garnet is more common in the lower part (Brown 2010, Brown *et al.* 2011). These constraints are consistent with the temperatures and pressures estimated from the metamorphic assemblages and thermobarometry of this study (see McKechnie *et al.* 2012b).

Complex melt-transfer processes would have led to the transfer of melt from lower in the crust to the level of emplacement (Kisters *et al.* 1998, 2009, Brown *et al.* 2011). Melt in such environments, especially those undergoing folding and ductile deformation, is preferentially concentrated within fold-nose areas and parallel to gneissosity owing to the tectonic forces acting upon the pegmatites (Brown 2010, Weinberg & Mark 2008). If the melt were derived from a deeper-seated granite body, the dykes would not converge as they do at Fraser Lakes Zone B; instead, they would be divergent from the hypothetical granitoid at depth (Cuney & Kyser 2008).

Figure 3-11 outlines schematically our proposed model for the Zone B pegmatites, whereby partial melting of fertile lithologies (*i.e.*, capable of being partially melted) occurred at depth followed by melt transport, in particular along regional foliations, shear zones, and within the fold-nose areas through the lower to middle crust to the current level of emplacement. Figure 3-11a is a seismic section of the crust covering the Wollaston– Mudjatik transition zone, Wollaston Domain, Needle Falls Shear Zone, Peter Lake Domain, and Wathaman Batholith near the Fraser Lakes area; this image shows the general structural regime of the Fraser Lakes area. Figure 3-11b shows a modified schematic section from Brown *et al.* (2011) showing the location of Fraser Lakes Zone B (rectangular box) in relationship to the biotite-dehydration and muscovite-dehydration melting zones and the potential structural regime in which this occurs (see similarities to the structures seen in a). Figure 3-11c is a schematic cross-section across the immediate Fraser Lakes Zone B area that portrays the proposed model for the Zone B pegmatites, starting with 1) partial melting (*i.e.*, biotite-dehydration melting) of U–Th–REE-enriched metasedimentary rocks during conditions of peak thermal metamorphism. The melt is then 2) transported along shear zones and parallel to the fold-nose area, where it was concentrated, and 3) crystallized to form the Fraser Lakes Zone B mineralized granitic pegmatites.

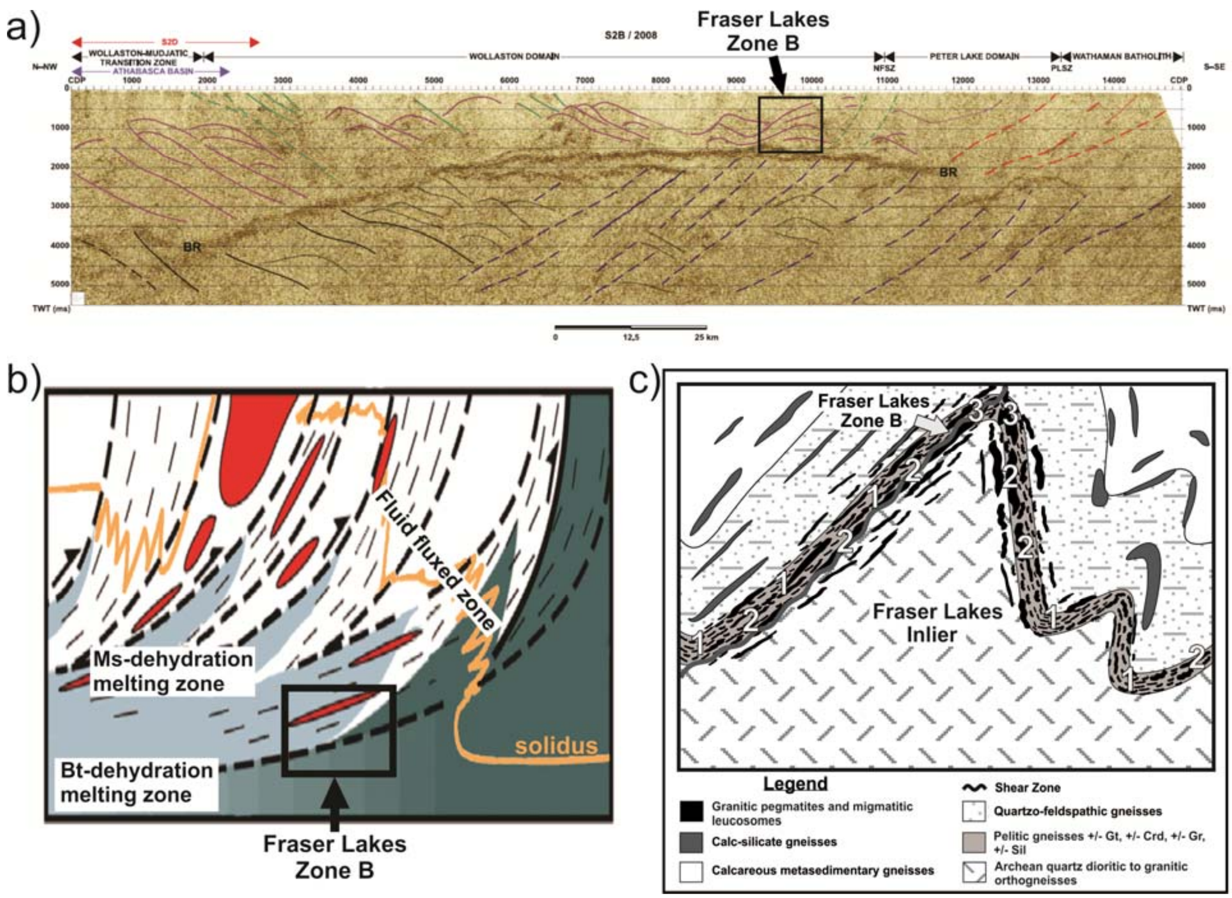

Figure 3-11. (a) The first 5.0 s (two-way travel time, TWT) of line S2B (Figure 4, Hajnal et al. 2010) of the Lithoprobe deep seismic section, Trans-Hudson Orogen (THO; Hajnal et al. 2005). Acronyms: BR: Bright reflector (Wollaston Lake reflector), NFSZ: Needle Falls Shear Zone, PLSZ: Parker Lake Shear Zone. The colored lines represent crustal structures recognized by Hajnal et al. (2005, 2010). Note the location of Fraser Lakes Zone B within a rectangular box. (b) Schematic section through the crustal-scale, dextral transpressive shear-zone system on the west side of the Fraser Lakes granite inlier. Note the location of Fraser Lakes Zone B (rectangular box) in relationship to the Bt-dehydration and Ms-dehydration melting zones. ACZ: zone of apparent constrictional strain (no pattern), which occurs within anastomosing zones of apparent flattening strain (dashed pattern). Modified from Brown et al. (2011). (c) Schematic cross-section (vertical scale is about 1 km) depicting the different levels of migmatization, melt transport, and emplacement of pegmatite-forming melts within the Fraser Lakes Zone B area. The antiformal fold noses have a plunge of approximately 25–30° to the northeast. 1) Partial

melting at depth and in situ of U–Th–REE-enriched metasedimentary rocks (Wollaston Group) during peak thermal metamorphism by biotite-dehydration melting. 2) Transport of melt upward and laterally along ductile shear-zones and parallel to gneissosity; during transport, the melts experienced different amounts of restite unmixing, leading to their variable compositions. 3) Melt was concentrated in fold noses, where it crystallized to form granitic pegmatites; during transportation and crystallization, it underwent igneous assimilation – fractional crystallization processes.

Implications for U exploration

This study is relevant to uranium exploration in Saskatchewan for two major reasons. Prior to this study, only a limited amount of published research (Mawdsley 1952, 1953, 1955, Parslow & Thomas 1982, Thomas 1983, Parslow *et al.* 1985) was carried out on pegmatite-hosted uranium mineralization as a *via*ble type of uranium deposit in Saskatchewan. This study has provided a more detailed examination of this type of mineralization in the eastern sub-Athabasca basement than previous studies, which tended to be more regional in focus (*e.g.*,, Parslow & Thomas 1982, Thomas 1983). Also, this study provides one of the first detailed descriptions of Th- and LREE-enriched pegmatites within Saskatchewan and helps to clarify how this type of uranium – thorium – rare earth-element mineralization formed with respect to regional deformation and high-grade metamorphism. This research from the western margin of the THO, in conjunction with that from other orogens, can help in modeling and targeting the location of the thickest bodies of granitic pegmatite (*i.e.*, those with the greatest tonnage). The study of the thorium mineralization could potentially prove useful in the future if the demand for thorium increases or if REE demand remains strong.

Work on similar granitic pegmatites in the Wollaston Domain, as well as in the Grenville Province (Lentz 1996) and in Namibia (Nex *et al.* 2002, Ward *et al.* 2008), has shown that the pegmatites and leucogranites formed in the areas of highest metamorphic grade and are related to upper-amphibolite- to granulite- facies metamorphism, which caused significant partial melting. The melt generated then concentrated in dilational zones, especially within fold noses, and was mobilized from depth *via* structural discontinuities (Kisters *et al.* 1998, 2009), such as major shear zones (*i.e.*,, like at Fraser Lakes Zone B). In some cases, there appears to be a compositional or textural control on the uranium grades, as biotite-rich zones tend to be higher in uranium within the Rössing deposit, as also found to be true at Fraser Lakes Zone B. Thomas (1983) and Parslow & Thomas (1982) showed that quartz-rich pegmatites in the Wollaston Domain (considered to be quartz-rich differentiates of the uranium-rich pegmatites) also contain significant amounts of uranium. As well, there seems to be a relationship between high U values and reduced lithologies, with the uranium mineralization at the Rössing deposit being located just below and within reduced lithologies of the Rössing Formation, in particular graphite–sulfide schist and marble; see Cuney & Kyser (2008) for a detailed discussion. Once a radioactive pegmatite is found, it is important that the mineralogical characteristics be determined, as certain minerals can render deposits uneconomic. For example, the SH deposit at Rössing contains a large amount of betafite, which is a refractory U-bearing mineral that is difficult to leach using the sulfuric-acid-leach process developed for the SJ open pit at Rössing (Nex *et al.* 2002, Abraham 2009). On the other hand, uraninite is an easily leachable U-rich mineral, and its presence at Fraser Lakes adds to the economic potential of the Group-A pegmatites.

This study also provides support for the proposal that uranium-enriched granitic pegmatites and leucogranites were the main U protore for unconformity-type uranium deposits of the Athabasca Basin (see Mercadier *et al.* 2012, 2013 for discussion). If this hypothesis is correct, the granitic pegmatites may have played a role in the deposition of a yet-undiscovered basement-hosted unconformity-type uranium deposit in the Fraser Lakes area.

Conclusions

On the basis of the current research, as well as what is known about uraniferous granitic pegmatites in other areas, we hereby postulate that the Fraser Lakes Zone B formed as a result of partial melting of pelitic gneisses and subordinate granitic gneisses during high-grade upper-amphibolite to granulite-facies metamorphism related to the Trans-Hudson Orogen. The melts were generated from uranium- and thorium-enriched pelitic gneisses (± graphite) *via* biotite-dehydration melting reactions in a mid-crustal melt transfer zone, with melt-transport preferentially along shear zones and the Archean–Wollaston Group unconformity, and with melts becoming concentrated owing to tectonic forces in regional fold noses, such as the one located at Fraser Lakes Zone B. The timing of the uraniferous granitic pegmatites is contemporaneous with known ages of deformation and metamorphism from regional studies of the western margin of the THO, including this research study. The uranium-bearing pegmatites are considered to represent the earlier melt phase, whereas the thorium pegmatites represent a more restitic or residual or depleted melt. The majority of the U–Th– REE phases formed as a result of primary magmatic crystallization; however, some represent xenocrysts from the melt source-rocks or products of alteration. The pressures and temperatures of the granulite-facies metamorphism in this area are consistent with the high metamorphic grade required for significant biotite- dehydration melting, and provide further support for the proposed model. This study provides useful information not only on these pegmatites as a primary source of U, Th, and the REE, but also as a possible protore for the unconformity-type uranium deposits of the Athabasca Basin.

CHAPTER 4

MEDIUM- TO LOW-PRESSURE PELITIC GNEISSES OF FRASER LAKES ZONE B, WOLLASTON DOMAIN, NORTHERN SASKATCHEWAN, CANADA: MINERAL COMPOSITIONS, METAMORPHIC P–T–T PATH, AND IMPLICATIONS FOR THE GENESIS OF RADIOACTIVE ABYSSAL GRANITIC PEGMATITES

Abstract

The Fraser Lakes Zone B is a U–Th–REE deposit hosted by granitic pegmatite and leucogranite located in the Wollaston Domain of northern Saskatchewan, Canada, in close proximity to the uranium-rich Athabasca Basin. Here, these magmatic rocks are hosted within Paleoproterozoic metasedimentary gneisses of the Wollaston Group and the underlying Archean orthogneisses. The intrusive bodies at Fraser Lakes Zone B are interpreted to have formed from crustal melts generated by upper-amphibolite to granulite-facies metamorphism during the ca. 1.8 Ga Trans-Hudson orogeny. Three pelitic gneiss host-rock samples with the least petrographic evidence of later alteration and suitable assemblages for P–T–t constraints were analyzed with an electron microprobe. Mineral assemblages in the pelitic gneisses, combined with chemical zoning in garnet, garnet–biotite and Ti-in-biotite geothermometry, and GBPQ geobarometry, suggest a peak T of about 750 to 780°C and a P of about 6 to 8 kbar, followed by isothermal decompression to a pressure of about 3 kbar. The low-P (retrograde) part of the P–T path is partially constrained by the presence of spinel in some pelitic gneiss samples. These constraints on temperature and pressure are consistent with partial melting, which would have generated significant amounts of melt *via* biotite-dehydration reactions. Evidence for this is in the form of abundant leucosome in the pelitic gneisses; however, these are generally not connected to the mineralized pegmatites. Instead, melt generated from similar rocks at slightly deeper crustal levels is believed to have crystallized within a structural trap at Fraser Lakes Zone B to form the U–Th–REE-mineralized granitic pegmatites and leucogranites.

Introduction

Uranium-bearing granitic pegmatites and leucogranites have been previously described in several places worldwide (Cuney & Kyser 2009), including in Canada (e.g., Mawdsley 1952, 1953, 1955, Parslow & Thomas 1982, Fowler & Doig 1983, Thomas 1983, Parslow *et al.* 1985, Goad 1990, Lentz 1991, 1996, Annesley & Madore 1999, Annesley *et al.* 2000, Madore *et al.* 2000). Some have been mined in the past, such as those in the Bancroft area of Ontario, whereas the only present production is at the Rössing mine in Namibia (Berning *et al.* 1976, Basson & Greenway 2004). These are generally considered to be abyssal-type pegmatites (Černý & Ercit 2005), which are arguably the least studied of all types of granitic pegmatites.

Most pegmatites described in the literature are considered to be related to large granitoid bodies located in the vicinity. However, abyssal-type pegmatites generally are unrelated in time and space to granitoid plutons, and are commonly found within upper-amphibolite- to granulite-facies host rocks. These pegmatites are interpreted to have formed by partial melting or metamorphic differentiation of fertile lithologies in the middle to lower crust (Berning *et al.* 1976, Fowler & Doig 1983, Thomas 1983, Lentz 1991, 1996, Basson & Greenway 2004, Černý & Ercit 2005). Thus, in order to fully understand the origin of these types of pegmatites, both the pegmatites and their host rocks must be studied.

This paper forms the third part of a geological study of the Fraser Lakes area undertaken to investigate the origin of U–Th–REE mineralized granitic pegmatites and leucogranites in the Fraser Lakes Zone B (McKechnie *et al.* 2012a, 2013). The aims of the current research are to: a) document the mineral assemblage found in the pelitic gneiss host-rocks, b) determine the composition of selected minerals from the pelitic gneisses, c) attempt to determine the age of metamorphism through monazite chemical age dating, d) quantify the metamorphic P–T conditions of the pelitic gneisses, and e) evaluate the relationship between pegmatite emplacement and metamorphism of the host rocks. By investigating the pelitic gneiss host-rocks, a better understanding can be obtained of the role that metamorphism and partial melting played in generating mineralization in the Fraser Lakes Zone B. This will be incorporated into an updated exploration model for granitic-pegmatite-hosted uranium and thorium mineralization in the Wollaston Domain of northern Saskatchewan.

Geological Setting

Fraser Lakes Zone B is located immediately west of Fraser Lakes, Saskatchewan, Canada, approximately 55 km southeast of the Key Lake uranium mine. The Wollaston Domain, a high-grade metamorphosed fold-and-thrust belt, underlies the area. It is part of the Cree Lake Zone (Lewry & Sibbald 1977, 1980) of the Hearne Craton (Fig. 4-1), which also includes the Mudjatik and Virgin River domains. During the collisional stages of the ca. 1.8 Ga Trans-Hudson orogen (THO), the Cree Lake Zone and the Reindeer Zone underwent significant multiphase deformation and metamorphism, ultimately leading to the development of a Himalayan-scale mountain belt (Hoffman 1990, Lewry & Collerson 1990, Portella & Annesley 2000, Ansdell 2005, Corrigan *et al.* 2009).

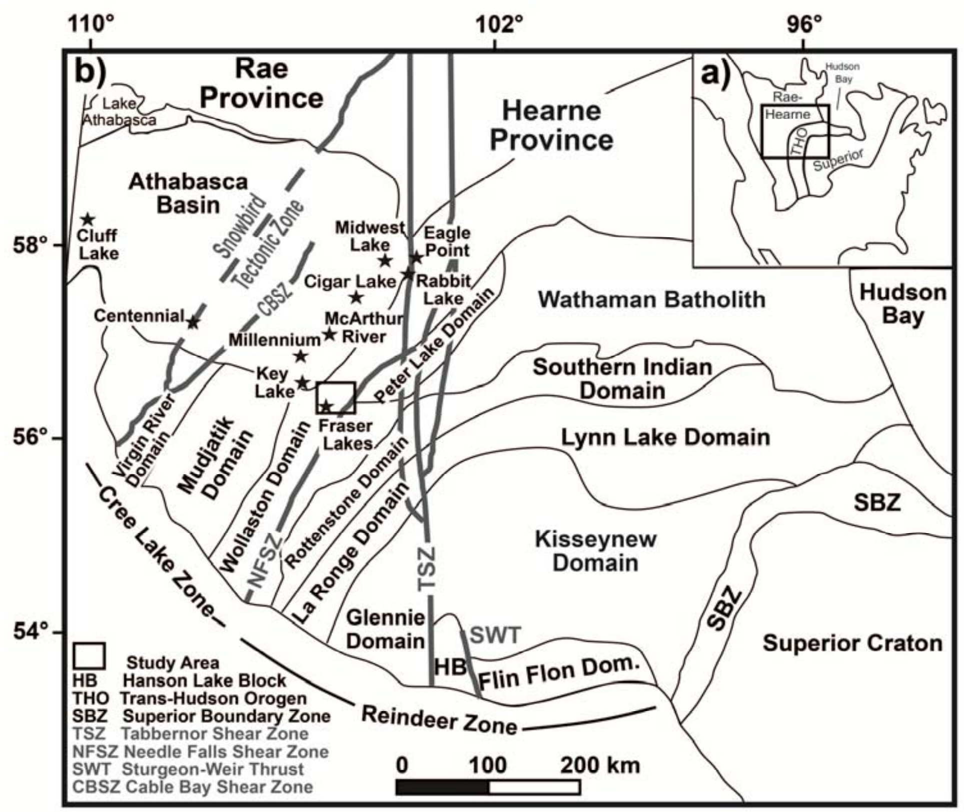

Figure 4-1. (a) Map of North America showing the location of the Archean Hearne–Rae and Superior cratons, which were welded by the Paleoproterozoic Trans-Hudson orogen (THO). The box shows the location of the area shown in Figure 4-1b. (b) Lithotectonic domains in northern Saskatchewan and Manitoba. The location of Fraser Lakes Zone B is plotted, as well as several unconformity-related uranium deposits within the Athabasca Basin. The box indicates the area shown in Figure 4-2. Dom: Domain.

In the Wollaston Domain, Paleoproterozoic metasedimentary rocks overlie unconformably (and structurally) Archean felsic gneisses, all of which were highly deformed and metamorphosed, resulting in a northeast-trending, high-grade fold-and-thrust belt intruded by felsic and mafic magmatic rocks of Hudsonian age (1840–1800 Ma: Annesley *et al.* 1997, 1999, 2005). This contrasts greatly with the "dome and basin" structural fabric illustrated by the dominantly Archean orthogneiss in the adjacent Mudjatik Domain. Details of the boundary relationship between the Wollaston and Mudjatik domains are described by Lewry & Sibbald (1980) and Annesley & Madore (1989, 1994). The Wollaston Domain is separated from the 1.865 Ga Wathaman Batholith, the tonalite–migmatite complexes of the Rottenstone Domain, and juvenile Paleoproterozoic volcanic arc and associated sedimentary rocks of the Reindeer Zone by the Needle Falls Shear Zone (Fig. 4-1). Numerous studies of the Wollaston Domain have been carried out on its stratigraphy, structure, metamorphism, geochronology, and mineral potential. The reader is referred to Tran (2001), Annesley *et al.* (2005), and Yeo & Delaney (2007) for comprehensive overviews and references.

The area shown in Figure 4-2, originally mapped by Ray (1980) and overall representative of the eastern Wollaston Domain (Annesley *et al.* 2005), comprises two large granitic orthogneiss basement inliers of Archean age, the Fraser Lakes and Johnson River inliers (Hamilton & Delaney 2000). These are overlain by strongly metamorphosed Wollaston Group sedimentary rocks of the eastern Wollaston Domain, which are subdivided into two main sequences, an upper calc-silicate-rich sequence, and a lower pelitic to psammitic sequence (Tran *et al.* 1998). Annesley *et al.* (2005) described the lower sequence as containing six units. The lower sequence within the Fraser Lakes area consists of pelitic and psammopelitic to psammitic gneisses, with graphite-bearing pelitic gneisses located immediately adjacent to the Archean inliers (Figs. 4-2, 4-3). Most important to this paper, metamorphism of these rocks to upper amphibolite to granulite facies accompanied and postdated strong deformation during the THO (Annesley *et al.* 2005). During peak metamorphism a dominantly northeasterly trending structural and migmatitic fabric formed, with the production and transport of abundant anatectic melt through this part of the ancient middle crust. Mapping in the immediate vicinity of the Fraser Lakes A and B mineralized zones by Ray (1980), Delaney & Tisdale (1996), and Delaney *et al.* (1996), showed that the area contains Wollaston Group metasedimentary gneisses overlying Archean orthogneisses of the Fraser Lakes inlier (Fig. 4-2). The geology of the Fraser Lakes area is described in greater detail by McKechnie *et al.* (2012a, 2013).

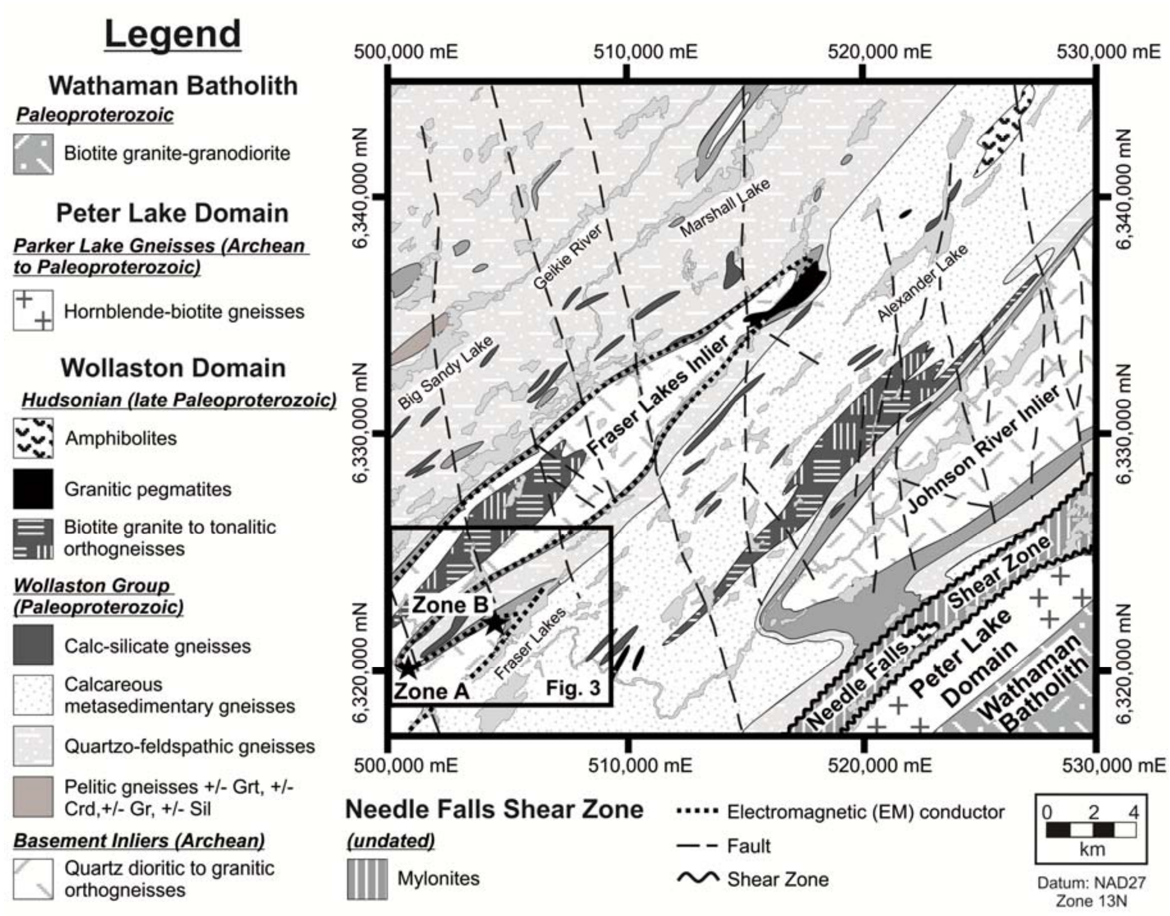

Figure 4-2. Regional geological map of the Fraser Lakes area, modified from Ray (1980). Note the strong north–northeasterly structural trend and the location of the folded 65 km long EM conductor (corresponding to graphitic or sulfidic pelitic gneisses) adjacent to Fraser Lakes Zones A and B. The box depicts the location of Figure 4-3.

The Fraser Lakes mineralized zones (Zones A and B) are located in two different northeasterly plunging regional fold noses adjacent to a section of the 65-km long EM conductor 5 km long (Fig. 4-3, see Annesley *et al.* 2009, JNR Resources Inc. 2012). At Zone B, the more prospective of the two, the multiple intervals of U–Th–REE mineralization are hosted by granitic pegmatites within an antiformal fold nose west of Fraser Lakes (McKechnie *et al.* 2012a, 2013). The mineralized pegmatites intrude the highly deformed, folded, northeasterly plunging, unconformable contact zone between pelitic (± graphitic) gneisses of the basal Wollaston Group and the underlying Archean granitic and tonalitic gneisses of the Fraser Lakes Inlier. For further details and discussion of the granitic pegmatite- and leucogranite-hosted U–Th–REE mineralization at Fraser Lakes Zone B, the reader is referred to McKechnie *et al.* (2012a, 2013).

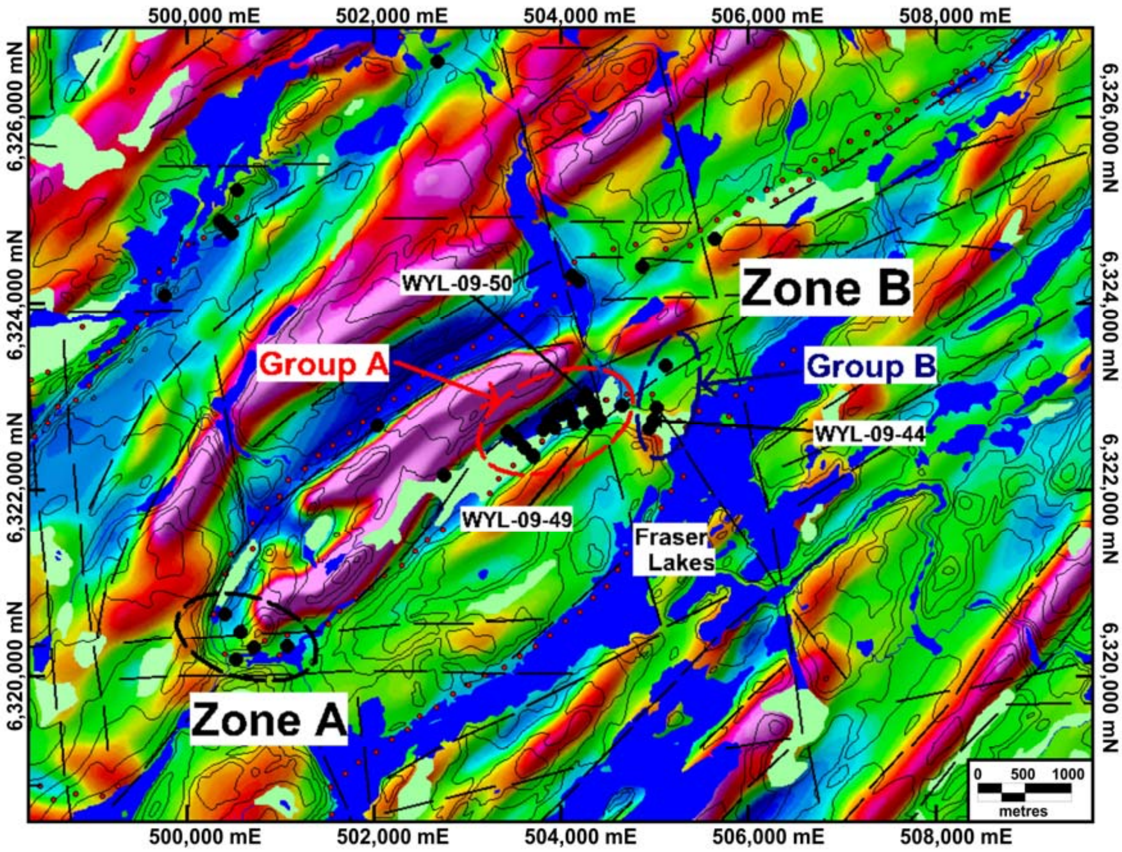

Figure 4-3. First vertical derivative total field aeromagnetic map of the Fraser Lakes area. The pink and red colors are areas of high magnetic potential field, whereas blue and green areas have a low magnetic potential field. Drill holes are denoted by black dots, with labels for the hole that have been sampled in this study. The regional scale electromagnetic (EM) conductor previously shown in Figure 4-2 is outlined by the red dots.

Analytical Methods

The samples used in the current study are part of a larger suite of drill-core samples collected from diamond-drill core stored at the Way Lake exploration property of JNR Resources Inc. Polished thin sections were prepared in the Thin Section Laboratory in the Department of Geological Sciences at the University of Saskatchewan. Transmitted and reflected light petrography was performed at the University of Saskatchewan and JNR Resources Inc. to describe the mineral assemblages, textures, and paragenesis prior to electron-microprobe analysis. From the larger subset of samples, three relatively unaltered samples of pelitic gneiss were selected for analysis on the basis of the presence of mineral assemblages useful for geothermometry and geobarometry. A Cameca SX–100 Ultra electron microprobe analyzer (EMPA) at the Saskatchewan Research Council (SRC) and a JEOL 8600 Superprobe EMPA at the University of Saskatchewan were utilized for the automated wavelength-dispersive electron-microprobe analyses of selected minerals. Back-scattered electron imagery and energy-dispersive spectrometry were used to examine and identify the phases of interest prior to chemical analysis. The reader is referred to McKechnie *et al.* (2012a) for further discussion of the EMPA techniques and standards used in the current study. An appendix (Appendix K) at the end of the paper includes the detection limits for the analyses done for this study. Representative compositions are included in Tables 4-1 to 4-4, with the full suite of analytical data available in a table of supplementary data (Supplementary Data Table 1, Appendix I). In addition, Supplementary Data Table 1 contains biotite geothermometer and chemical age dating results. Average thermobarometry data for the pelitic gneisses is included in Table 4-5, with the full results in Supplementary Data Table 2 (Appendix J). The tables of supplementary data are available from the Depository of Unpublished Data on the Mineralogical Association of Canada website [document Fraser Lakes CM50_1669].

Sample Descriptions

WYL-09-49-36.1

This sample was taken from a garnet – sillimanite – biotite pelitic gneiss at a depth of 36.1 m in drill hole WYL–09–49. This gneiss has a variable grain-size (fine to coarse grained), with 1–5% sillimanite-rich knots or lenses (*i.e.*, *faserkiesel*) and smaller wispy aggregates of fine-grained sillimanite (*i.e.*, fibrolite), 10–20% disseminated garnet, and narrow intervals with cordierite-bearing augen-like porphyroblasts. There are traces of graphite and pyrite. It has a protomylonitic texture and a strong foliation. It is variably migmatitic and contains irregular bodies of leucosome with diffuse contacts. This unit has been affected by intermittent disseminated weak chlorite alteration, and weak to moderate late fracturing containing quartz, carbonate, and a trace of pyrite.

The major components in this thin section are biotite (20–25%), garnet (20–25%), quartz (20–25%), K-feldspar (15–20%), sillimanite (10–15%), and plagioclase (5–10%), with trace amounts of graphite, monazite, and pyrite. The grain size varies from <0.1 to up to 0.8 mm. Most of the grains are anhedral to subhedral, with the exception of small cubes of pyrite and small clusters of fibrous sillimanite. Monazite forms tiny inclusions within biotite and is surrounded by a pleochroic halo. There is a strong foliation defined by biotite and sillimanite, and locally by elongate grains of garnet (Fig. 4-4a). Garnet grains tend to contain an inclusion-rich core and have a relatively inclusion-free rim (Fig. 4-5a). Quartz shows undulatory extinction, and deformation twins are common within plagioclase, with local recrystallization and sutured contacts shown by many of the grains. Locally, biotite shows a skeletal habit next to garnet and possible melt-reaction textures. There is a weak retrograde metamorphic assemblage, which includes white mica (after feldspar), and chlorite and rutile (after biotite along cleavage planes).

WYL-09-50-37.5

This sample is from a garnet – sillimanite – biotite – graphite pelitic gneiss, and was taken at a depth of 37.5 m in drill hole WYL–09–50. This unit is fine to medium grained with local coarse-grained porphyroblasts. Garnet content varies from 1 to 10% locally. Most of the garnet is fine to medium grained and disseminated, but does form porphyroblasts with, in places, a rim of quartz–feldspar or cordierite. Sillimanite is locally abundant as stretched faserkiesel and small wispy aggregates along the foliation. There are rare cordierite-rich intervals, commonly associated with fine-grained disseminated graphite and trace pyrite. The unit is variably migmatitic, with common narrow, coarse-grained felsic banding (*i.e.*, leucosome). It has a strongly foliated protomylonitic texture. The gneiss is overprinted by hematite-rich alteration bands, weak chlorite- and hematite-filled fractures, and local chlorite- and clay-filled brittle shears.

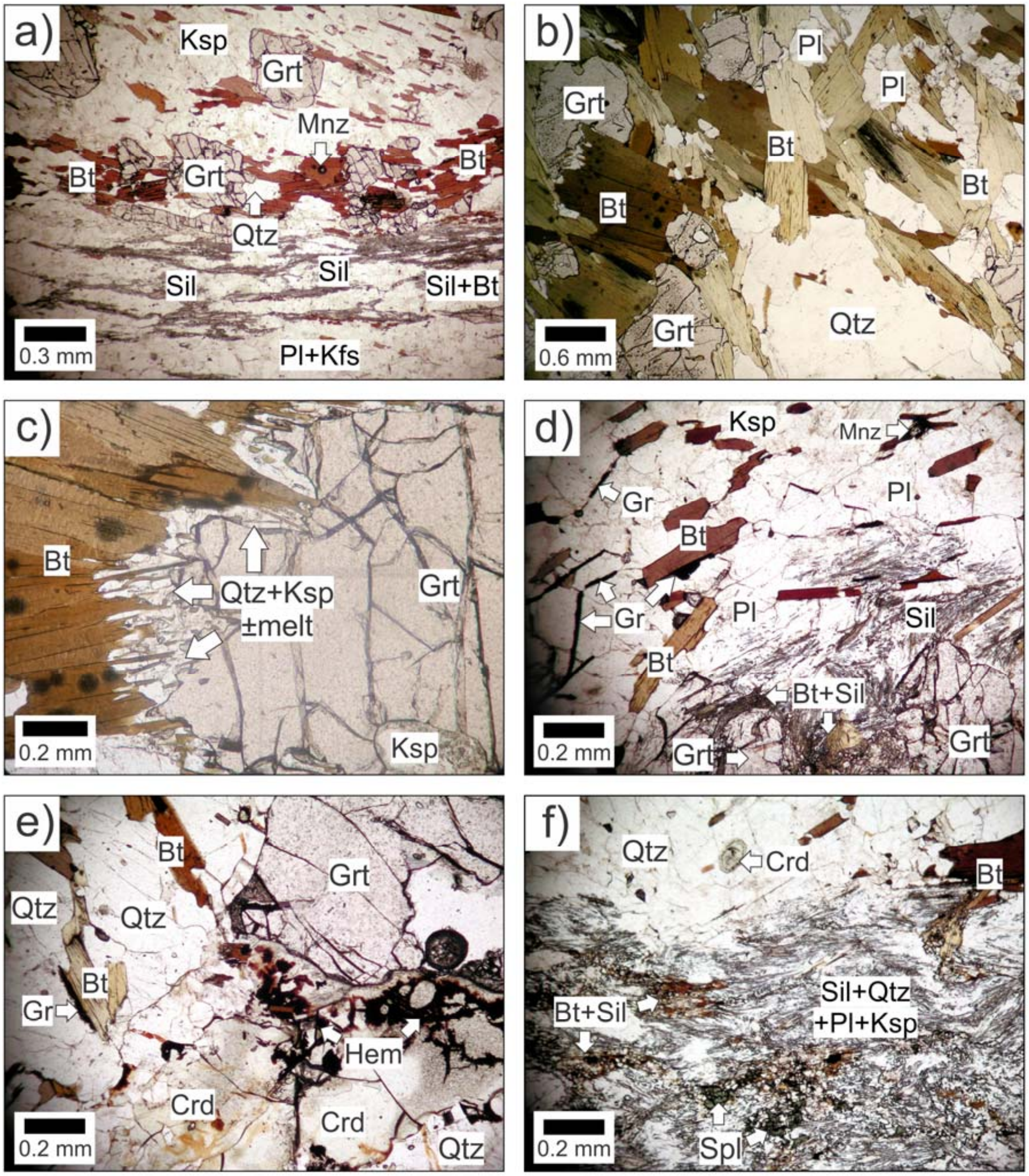

Figure 4-4. (a) Pelitic gneiss (WYL–09–49–36.1) containing biotite (Bt), garnet (Grt), sillimanite (Sil), monazite (Mnz), and feldspar (Ksp, Fsp, Pl). (b) Garnetiferous pelitic gneiss (WYL–09–44–61.4) from the eastern part of the fold nose. (c) Melt microtextures in WYL–09–44–61.4 at the contact between garnet and biotite. Biotite is being consumed in the melt-generating reaction. (d), (e) and (f) Pelitic gneiss (WYL–09–50–37.5) with a garnet – biotite – sillimanite – cordierite (Crd) – ilmenite (Ilm) – spinel (Spl) – quartz – feldspar assemblage.

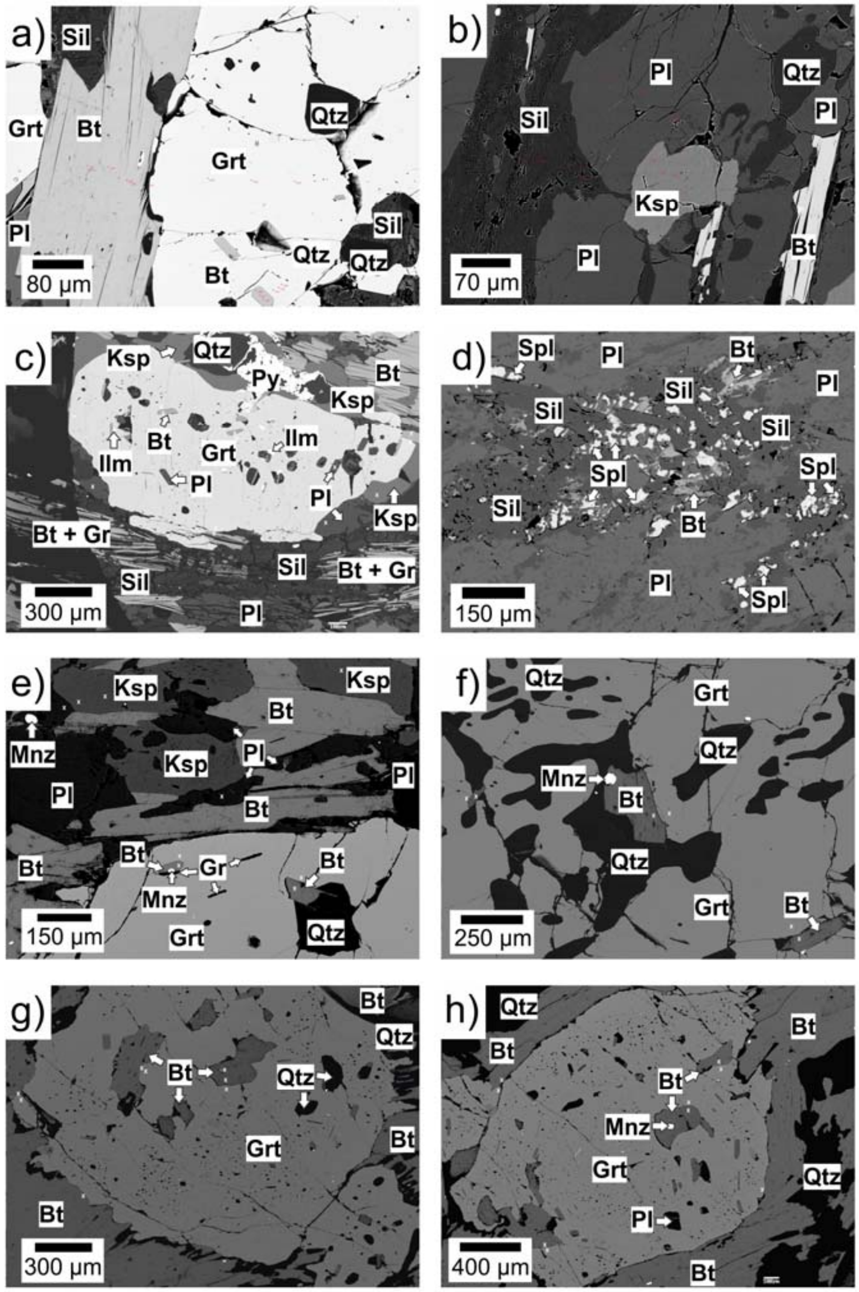

Figure 4-5. BSE images for the pelitic gneisses from Fraser Lakes Zone B. (a) Garnet – biotite – sillimanite – ilmenite – graphite – quartz – plagioclase assemblage in WYL–09–49–36.1. (b) Close-up of a sillimanite-rich area in WYL–09–49–36.1. (c) Deformed garnet with biotite, plagioclase, and ilmenite inclusions, with a deformed matrix of biotite, graphite, feldspars, and quartz. (d) Spinel – sillimanite – plagioclase – biotite assemblage in WYL–09–50–37.5. (e) Edge of the large garnet grain in WYL–09–50–37.5 with quartz – biotite – graphite – monazite inclusions. (f) Garnet – quartz – biotite symplectite texture in the large grain of garnet from WYL–09–37.5. (g) and (h) Large grain of garnet in WYL–09–50–37.5 with biotite, monazite, and ilmenite inclusions.

In thin section, the sample (Figs. 4-4d–f) contains quartz (25–30%), biotite (25–30%), cordierite (15–20%), garnet (10–15%), K-feldspar (5–10%), sillimanite (5–10%), graphite (2–3%), spinel (2–3%) and trace monazite and zircon. The grain size within this sample varies from less than 0.1 to up to 15 mm for the largest grains of garnet, but is generally less than 2.5 mm. Most of the grains are anhedral to subhedral and locally show sutured contacts, although the sillimanite tends to form small clusters of "fibrolite" (Fig. 4-4f). Biotite shows a red-brown pleochroism, indicative of high-Ti content (Figs. 4-4d, e, f). Dark green spinel (Fig. 4-4f) was found associated with cordierite, sillimanite, plagioclase, K-feldspar, and quartz within a garnet-poor area of the sample. The sillimanite grains are larger where they are associated with spinel. There is one large porphyroblast of garnet in this sample that contains sillimanite, biotite, monazite, plagioclase, and quartz inclusions with locally inclusion-poor sections; it shows a symplectitic texture with quartz and biotite locally at the rim of the grain (Fig. 4-5g). Cordierite forms large eye-shaped crystals and smaller rounded crystals; it shows moderate alteration to chlorite, "pinite", and later hematite (Figs. 4-4e, f). However, the rest of the slide shows only very weak alteration. There is a moderate to strong foliation defined by the biotite, sillimanite, graphite, and elongate porphyroblasts of cordierite. There is weak retrograde metamorphism of biotite locally to chlorite and muscovite along cleavage planes, as well as alteration of feldspars to white mica. The rock exhibits a weak development of fractures.

WYL-09-44-61.4

This sample is from garnet–biotite pelitic gneiss (Figs. 4-4b, c) in the eastern portion of the fold nose that is spatially associated with several Th-rich pegmatites. The sample was taken at a depth of 61.4 m in drill hole WYL–09–44. The pelitic gneiss is fine to medium grained, moderately foliated, and contains locally up to 30% garnet and trace graphite and pyrite. There are migmatitic bands and patches, including what are interpreted to be restite and leucosome. It contains rare weak, banded or patchy calc-silicate alteration and is weakly fractured.

In thin section, the main components are biotite (30–35%), garnet (25–30%), plagioclase (25–30%), quartz (20–25%), K-feldspar (5–10%), and trace monazite, zircon, apatite, and pyrite. It has a highly variable grain-size from less than 0.1 to up to 6.5 mm. Most of the grains are anhedral to subhedral, with biotite locally forming skeletal crystals (Fig. 4-4c) and as a symplectite with quartz and feldspar. Myrmekitic intergrowths are found in trace amounts. Monazite forms inclusions in several of the minerals, with zircon restricted to within biotite; pleochroic halos are common surrounding both minerals. Plagioclase is commonly twinned. There are trace amounts of weak alteration of feldspar to white mica, and chlorite and fluorite are present along cleavage planes in biotite. This sample exhibits a well- developed ductile deformation fabric, as shown by the undulose extinction in K-feldspar and quartz, and the strong parallel alignment of biotite (Fig. 4-4b).

Mineral Chemistry

Biotite

Several biotite grains were analyzed in each of the three pelitic gneiss samples (Table 4-1, Figs. 4-5a, b, c, f, g, and h). Analytical totals were found to be acceptable within analytical uncertainty at 97.11 to 101.97 wt. % after calculation of the Li_2O and H_2O content using the method outlined in Tindle & Webb (1990). The grains have variable Ti contents (0.18 to 0.64 atoms per formula unit, *apfu*), and variable X_{Fe} [*i.e.,* Fe/ (Fe + Mg) of 0.32 to 0.61 (Table 4-1)]. The biotite lower in TiO_2 tends to be that in the matrix adjacent to garnet. In addition, the biotite lower in TiO_2 exhibits evidence of retrograde effects, leading to chlorite and rutile along the cleavage. It occurs in a symplectitic texture involving garnet and quartz, suggesting that it likely formed during decompression. Biotite inclusions in garnet and some of the matrix biotite have higher TiO_2, suggesting that they may represent higher-temperature conditions during prograde or peak thermal metamorphism (*cf*. Cesare *et al.* 2008), which fits with textural relationships indicating that they represent prograde to peak thermal conditions of metamorphism.

Garnet

The garnet grains (Figs. 4-5a, c, f, g, and h) from these three samples show various types of chemical zonation (Fig. 4- 6). Those from WYL–09–44–61.4 show highly disrupted patterns of zoning (Figs. 4-6a, b, c). The garnet grains from WYL–09–49.36.1 and WYL–09–50–37.5 show much smoother patterns (Figs. 4-6d, e, and f). The garnet in all samples is primarily pyrope-

Table 4-1. Representative compositions of biotite in pelitic gneisses from the Fraser Lakes Zone B

Point	1 14	2 6	3 7	4 22	5 137	6 16	7 42	8 24	9 25	10 26	11 30
SiO_2 wt.%	35.95	36.50	35.35	36.38	36.20	36.52	35.59	37.56	36.75	38.96	36.83
TiO_2	1.83	3.02	1.94	3.40	5.24	3.07	4.75	3.14	5.80	3.63	3.17
Al_2O_3	16.24	15.46	15.92	18.26	17.50	19.31	17.53	17.79	16.96	18.61	18.09
FeO	23.39	21.44	24.18	19.62	16.53	15.64	17.80	15.30	15.95	15.19	17.38
MnO	0.04	0.05	0.06	b.d.	0.03	b.d.	b.d.	b.d.	b.d.	0.06	0.03
MgO	8.77	10.42	8.80	9.33	10.62	11.46	9.74	12.13	11.20	13.45	11.52
CaO	0.06	b.d.	b.d.	b.d.	b.d.	b.d.	b.d	b.d.	b.d.	b.d.	b.d.
Na_2O	0.21	0.30	0.21	0.13	0.34	0.19	0.12	0.43	0.48	0.28	0.17
K_2O	9.09	8.84	9.18	9.69	9.89	8.22	10.15	5.44	9.08	5.87	6.61
BaO	-	-	-	-	b.d.	-	b.d.	-	-	-	-
Cs_2O	-	-	-	-	b.d.	-	b.d.	-	-	-	-
F^-	b.d	b.d	b.d	b.d	1.10	b.d.	0.42	b.d.	b.d.	b.d.	b.d.
Cl^-	0.12	0.09	0.06	0.10	0.08	0.07	0.02	0.07	0.03	0.03	0.02
Cr_2O_3	b.d.	0.04	b.d.	b.d.	-	0.05	-	b.d.	0.03	b.d.	b.d.
Li_2O *	0.77	0.92	0.59	0.89	0.84	0.93	0.66	1.23	1.00	1.63	1.02
H_2O *	3.89	3.96	3.87	4.03	3.53	4.03	3.79	4.03	4.10	4.26	4.05
Subtotal	100.40	101.04	100.15	101.85	101.92	99.55	100.59	97.13	101.40	101.97	98.90
O=F,Cl	0.03	0.02	0.01	0.02	0.48	0.03	0.18	0.01	0.01	0.01	0.00
Total	100.37	101.02	100.13	101.83	101.44	99.52	100.41	97.11	101.40	101.97	98.90
O *apfu*	22	22	22	22	22	22	22	22	22	22	22
Si	5.50	5.49	5.46	5.39	5.34	5.38	5.34	5.56	5.37	5.48	5.45
Al iv	2.50	2.51	2.54	2.61	2.66	2.62	2.66	2.44	2.63	2.52	2.55
Al vi	0.43	0.23	0.36	0.57	0.38	0.73	0.44	0.67	0.29	0.57	0.61
Ti	0.21	0.34	0.22	0.38	0.58	0.34	0.54	0.35	0.64	0.38	0.35
Cr	-	0.00	-	-	-	0.01	-	-	0.00	-	-
Fe	2.99	2.70	3.12	2.43	2.04	1.93	2.23	1.90	1.95	1.79	2.15
Mn	0.01	0.01	0.01	-	0.00	-	-	-	-	0.01	0.00
Mg	2.00	2.34	2.03	2.06	2.33	2.52	2.18	2.68	2.44	2.82	2.54
Li *	0.47	0.56	0.37	0.53	0.50	0.55	0.40	0.73	0.58	0.92	0.61
Ca	0.01	-	-	-	-	-	-	-	-	-	-
Na	0.06	0.09	0.06	0.04	0.10	0.06	0.04	0.12	0.14	0.08	0.05
K	1.78	1.70	1.81	1.83	1.86	1.54	1.94	1.03	1.69	1.05	1.25
Ba	-	-	-	-	-	-	-	-	-	-	-
Cs	-	-	-	-	0.00	-	0.00	-	-	-	-
OH^- *	3.97	3.98	3.98	3.98	3.47	3.96	3.80	3.98	3.99	3.99	4.00
F^-	0.00	0.00	0.00	0.00	0.51	0.02	0.20	0.00	0.00	0.00	0.00
Cl^-	0.03	0.02	0.02	0.02	0.02	0.02	0.00	0.02	0.01	0.01	0.00
Fe/(Fe+Mg)	0.60	0.54	0.61	0.54	0.47	0.43	0.51	0.41	0.44	0.39	0.46
Mg/(Mg+Fe)	0.40	0.46	0.39	0.46	0.53	0.57	0.49	0.59	0.56	0.61	0.54

-: not analyzed or calculated, b.d.: below detection limit. The proportion of end members is expressed in mole %. The compositions were acquired with an electron microprobe. * Calculated using the formula of Tindle & Webb (1990) in the spreadsheet of Tindle (2011). Sample and photo: 1: WYL-09-44-61.4 g biot 15, location: matrix adjacent to Grt; 2: WYL-09-44-61.4 f biotite 6, location: in Grt core; 3: WYL-09-44-61.4 f biotite 7, location: in Grt rim; 4: WYL-09-49-36.1 h biotite 24, location: matrix adjacent to Grt; 5: WYL-09-49-36.1 biotite-2 img 14, location: in Grt near rim; 6: WYL-09-49-36.1 a biotite 17, location: in Grt core; 7: WYL-09-50-37.5 biotite-1 img 3, location: matrix away from Grt; 8: WYL-09-50-37.5 f biotite 26, location: in large Grt near rim, 9: WYL-09-50-37.5 f biotite 27, location: in large Grt rim; 10: WYL-09-50-37.5 g biotite 28, location: in Grt–Qtz–Bt symplectite; 11: WYL-09-50-37.5 h biotite 32, location: matrix adjacent to Grt.

bearing almandine (X_{Alm} from 0.72 to 0.83, X_{Prp} from 0.08 to 0.25), with insignificant spessartine and grossular components (Table 4-2).

The profile for WYL–09–50–37.5 represents a core-to-rim transect (*i.e.,* across half of the grain) of a garnet crystal 1.25 cm across (all compositions in this sample are from this grain). It shows a relatively smooth pattern of zoning. This grain has an inclusion-poor core, with inclusions of biotite, quartz, monazite, and sillimanite in the area between the rim or edge of the grain and the core (Fig. 4-5f). Part of the grain shows a symplectitic texture with quartz and biotite (Fig. 4-5g). The grain varies in X_{Alm} from 0.71 to 0.80, and X_{Prp} from 0.17 to 0.26, with X_{Alm} increasing and X_{Prp} decreasing as the rim of the grain is approached. Note that X_{Alm} decreases slightly immediately adjacent to the rim of the grain (Fig. 4-6f). The observed patterns of zoning shown by all analyzed grains are likely due to homogenization and retrograde exchange or to net-transfer reactions, as the zoning observed is not typical of growth zoning (*cf.* Tuccillo *et al.* 1990, and references therein).

Sillimanite

Sillimanite was abundant in both WYL–09–49–36.1 and WYL–09–50–37.5. It forms small prisms where it is found with spinel in WYL–09–50–37.5 (Fig. 4-5d), but is commonly forms bundles of needle-like to elongate, bladed crystals (*i.e.,* “fibrolite”, Figs. 4-4a, d, f, 4-5a, b, d, e). As expected, the sillimanite shows limited incorporation of Fe (0.16 to 0.31 wt. % Fe_2O_3) in its structure (Table 4-3).

Cordierite

Most of the cordierite grains in WYL–09–50–37.5 show strong alteration of the cordierite to chlorite and hematite (Figs. 4-4e, f). This was reflected in the analytical data; the low analytical totals (85.89 to 86.25 wt. %) emphasize the presence of chlorite, and thus reasonable compositions for cordierite could not be obtained.

Table 4-2. Representative compositions of garnet in pelitic gneisses from the Fraser Lakes Zone B

	1	2	3	4	5	6	7	8	9	10	11
Point	15	7	6	24	140	17	84	26	27	28	32
SiO_2 wt.%	36.58	36.82	37.96	37.89	37.83	37.29	37.70	37.99	37.47	37.57	38.28
TiO_2	b.d.	b.d.	b.d.	b.d.	0.03	b.d.	b.d.	b.d.	b.d.	b.d.	0.02
Al_2O_3	21.04	20.91	21.18	21.20	21.51	21.06	21.56	20.83	20.82	21.46	21.12
FeO	35.24	35.54	36.04	34.96	34.08	34.39	32.28	33.60	34.23	32.39	33.73
MnO	2.64	2.60	1.89	1.71	1.34	1.43	0.59	0.69	0.65	0.50	0.57
MgO	2.02	1.94	2.69	3.17	3.27	3.63	6.04	4.92	4.60	5.73	5.18
CaO	1.78	1.85	1.57	1.04	1.04	0.91	0.61	0.49	0.64	0.56	0.62
Na_2O	b.d.	0.01	b.d.	0.01	0.02	0.03	0.02	0.02	0.03	0.03	0.05
Cr_2O_3	b.d.	0.09	0.05	b.d.	0.03	0.12	b.d.	b.d.	0.07	0.09	0.03
V_2O_3	-	-	-	-	b.d.	-	b.d.	-	-	-	-
ZnO	-	-	-	-	0.02	-	b.d.	-	-	-	-
Y_2O_3	-	-	-	-	0.04	-	b.d.	-	-	-	-
Total	99.30	99.77	101.39	100.01	99.22	98.87	98.82	98.55	98.52	98.33	99.59
O *apfu*	24	24	24	24	24	24	24	24	24	24	24
Si	5.96	5.98	6.08	6.15	6.19	6.08	6.02	6.21	6.10	6.05	6.16
Ti	-	-	-	-	0.00	-	-	-	-	-	-
Al	4.04	4.00	4.00	4.06	4.15	4.05	4.06	4.02	4.00	4.07	4.01
Fe^{3+} *	0.00	0.00	0.00	0.00	0.00	0.00	0.00	0.00	0.00	0.00	0.00
Fe^{2+} *	4.80	4.83	4.83	4.75	4.67	4.69	4.31	4.60	4.66	4.36	4.54
Mn	0.36	0.36	0.26	0.24	0.19	0.20	0.08	0.10	0.09	0.07	0.08
Mg	0.49	0.47	0.64	0.77	0.80	0.88	1.44	1.20	1.12	1.38	1.24
Ca	0.31	0.32	0.27	0.18	0.18	0.16	0.10	0.09	0.11	0.10	0.11
Na	-	0.00	-	0.00	0.01	0.01	0.01	0.01	0.01	0.01	0.01
Cr	-	0.01	0.01	-	0.00	0.01	-	-	0.01	0.01	0.00
V	-	-	-	-	-	-	-	-	-	-	-
Zn	-	-	-	-	0.00	-	-	-	-	-	-
Y	-	-	-	-	0.00	-	-	-	-	-	-
grs mol.%	5	5	5	3	3	3	2	1	2	2	2
prp	8	8	11	13	14	15	24	20	19	23	21
alm	80	81	81	80	80	79	73	77	78	74	76
sps	6	6	4	4	3	3	1	2	1	1	1

-: not analyzed or calculated, b.d.: below detection limit. The proportion of end members is in mole %. The compositions were acquired with an electron microprobe. * Calculated according to stoichiometric constraints. Sample and photo: 1: WYL-09-44-61.4 g garnet 15, location: rim; 2: WYL-09-44-61.4 f garnet 7, location: near rim; 3: WYL-09-44-61.4 f garnet 6, location: intermediate between rim and core; 4: WYL-09-49-36.1 h garnet 24, location: rim; 5: WYL-09-49-36.1 garnet-2 img 14, location: near rim and Bt inclusion; 6: WYL-09-49-36.1a garnet 17, location: intermediate between rim and core; 7: WYL-09-50-37.5 big garnet, location: large Grt core; 8: WYL-09-50-37.5 f garnet 26, location: near rim; 9: WYL-09-50-37.5 f garnet 27, location: rim; 10: WYL-09-50-37.5 g garnet 28, location: Grt–Bt–Qtz symplectite; 11: WYL-09-50-37.5 h garnet 32, location: rim.

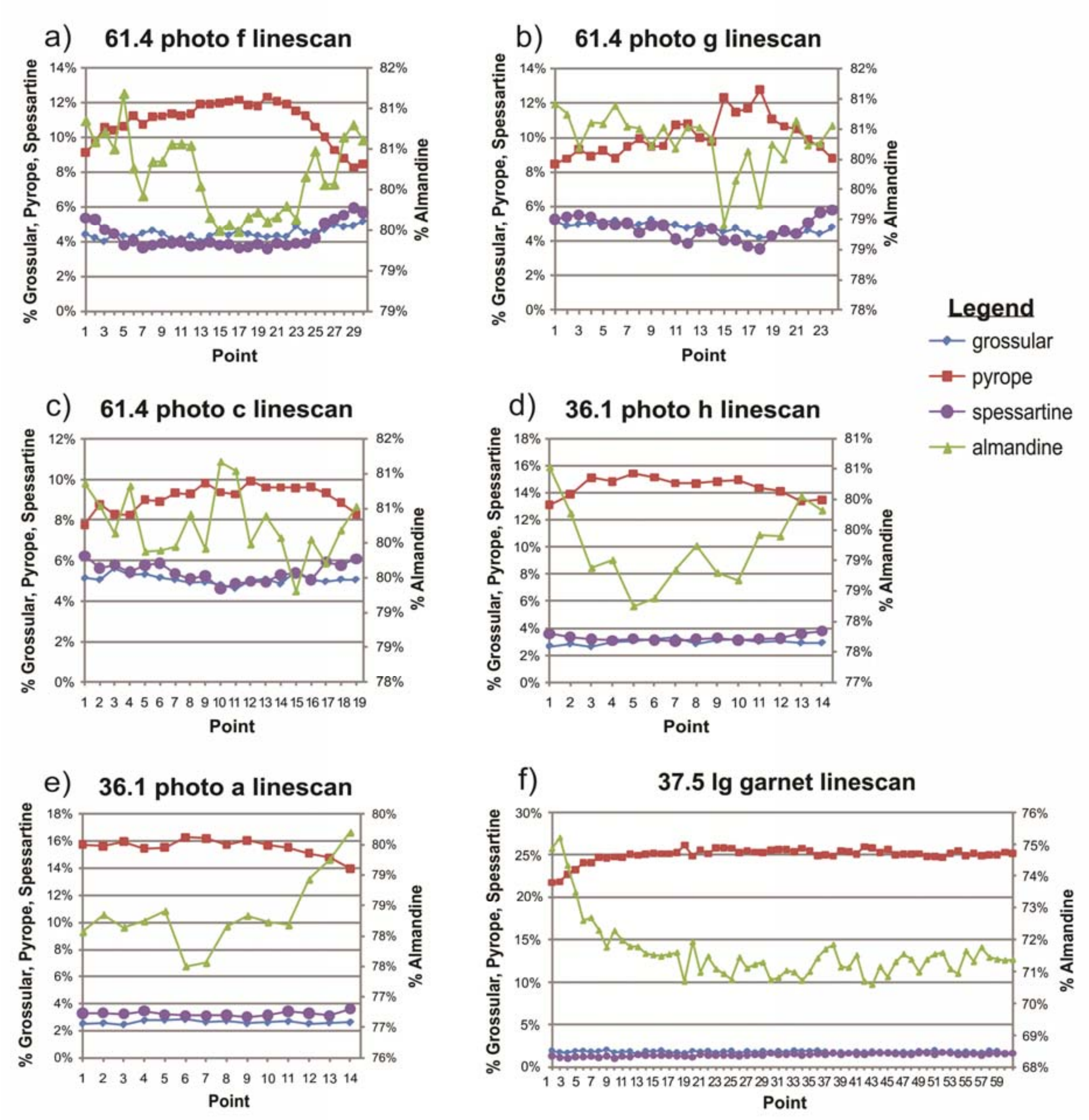

Figure 4-6. Growth profiles for garnet crystals from the pelitic gneisses in the Fraser Lakes Zone B area. (a), (b), and (c) show three grains of garnet from WYL–09–44–61.4, whereas (d) and (e) show garnet grains from WYL–09–49–36.1; (f) shows a profile for half of a large grain of garnet in WYL–09–50–37.5. The garnet profiles show prograde zoning (increasing almandine from core to rim) with variable overprinting due to retrograde diffusion processes. This is particularly evident in the garnet grains from WYL–09–44–61.4, which show highly irregular zoning.

Spinel (Hercynite)

Several irregularly shaped, dark green crystals of spinel were found associated with sillimanite and plagioclase in a sillimanite-rich zone within WYL-09-50-37.5 (Figures 4-4f, 4-5d, e). The grains were small, although several analyses with good analytical totals were made. The spinel is dominated by Al_2O_3 (57.11 to 58.18 wt. %), and FeO (31.53 to 32.99 wt. %), with lesser amounts of MgO and ZnO, and trace (<0.2 wt. %) SiO_2, TiO_2, Cr_2O_3, MnO, and NiO (Table 4-3). The spinel grains have a stoichiometry of $Al_{1.89\ to\ 2.00}\ Fe_{0.67\ to\ 0.72}\ Mg_{0.19\ to\ 0.24}\ Zn_{0.09}\ O_4$, indicating that it is spinel-rich hercynite, which is a common mineral in granulite-facies metamorphism.

Plagioclase

Plagioclase was analyzed in WYL–09–49–36.1 and WYL–09–50–37.5 (Table 4-3). The plagioclase in WYL–09–50–37.5 is oligoclase, whereas that in WYL–09–50–49–36.1 is slightly more calcic, ranging from oligoclase to andesine, with all plagioclase grains having an insignificant orthoclase component (Table 4-3).

K-feldspar

The K-feldspar in both WYL–09–49–36.1 and WYL–09–50–37.5 has a finely microperthitic texture and locally contains quartz inclusions and microcline twinning. It does not contain any appreciable Ca, and is similar in composition in the two rocks (X_{Or} of 0.82 to 0.87 and X_{Ab} of 0.13 to 0.18; Table 4-3).

Monazite

Several grains of monazite were analyzed in each of the three samples of pelitic gneiss (Table 4-4). Those in WYL–09–50–37.5 show minor compositional variation from $X(LREEPO_4)$ of 0.81 to 0.87, $X(HREEPO_4)$ of 0.02 to 0.03, X_{Hut} of 0 to 0.02, X_{Chr} of 0.06 to 0.11, and $X(YPO_4)$ of 0.02 to 0.06. Cerium is the dominant LREE (27.22 to 29.71 wt. % Ce_2O_3 out of the 55.38 to 59.71 wt. % $\sum LREE_2O_3$; Table 4-4). The four grains of monazite analyzed in this sample are

Table 4-3. Representative compositions of feldspar, spinel, sillimanite, ilmenite, and rutile in pelitic gneisses from the Fraser Lakes Zone B

	Plagioclase					K-feldspar			
	1	2	3	4	5	6	7	8	9
Point	116	1	1	20	6	121	8	25	10
SiO_2 wt.%	60.64	60.33	62.80	64.04	64.18	64.95	65.04	64.17	65.34
TiO_2	0.01	b.d.	b.d.	b.d.	0.02	b.d.	b.d.	b.d.	0.04
Al_2O_3	24.01	25.72	24.62	22.48	22.72	18.56	18.53	18.65	19.68
FeO	0.01	-	-	0.05	-	b.d.	-	0.02	-
Fe_2O_3	-	0.39	0.10	-	0.05	-	0.05	-	0.09
MgO	b.d.	b.d.	b.d.	b.d.	b.d.	b.d.	b.d.	0.005	b.d.
CaO	5.51	7.02	5.63	3.33	3.46	b.d.	0.03	b.d.	0.05
Na_2O	9.59	6.83	7.62	11.08	9.01	1.56	1.38	1.97	1.59
K_2O	0.28	0.45	0.27	0.22	0.18	14.93	14.23	14.36	12.54
BaO	b.d.	b.d.	b.d.	b.d.	b.d.	0.64	0.69	0.71	0.57
Total	100.05	100.76	101.03	101.20	99.65	100.65	99.95	99.91	99.90
O *apfu*	8	8	8	8	8	8	8	8	8
Si	2.71	2.67	2.75	2.81	2.83	2.99	3.00	2.97	2.98
Ti	0.00	-	-	-	0.00	-	-	-	0.00
Al	1.26	1.34	1.27	1.16	1.18	1.01	1.01	1.02	1.06
Fe^{3+} *1	0.00	0.01	0.00	0.00	0.00	-	0.00	0.00	0.00
Mg	-	-	-	-	-	-	0.00	0.00	-
Ca	0.26	0.33	0.26	0.16	0.16	-	0.00	-	0.00
Na	0.83	0.59	0.65	0.94	0.77	0.14	0.12	0.18	0.14
K	0.02	0.03	0.02	0.01	0.01	0.88	0.84	0.85	0.73
Ba	-	-	-	-	-	0.01	0.01	0.01	0.01
An mol.%	24	35	29	14	17	0	0	0	0
Ab	75	62	70	85	82	14	13	17	16
Or	1	3	2	1	1	86	87	83	84

	Spinel (Hercynite)
	10
Point	10
SiO_2	0.07
TiO_2	b.d.
Al_2O_3	57.40
FeO	31.65
MnO	0.06
MgO	5.27
CaO	-
Cr_2O_3	0.16
V_2O_3	-
NiO	b.d.
ZnO	4.35
Nb_2O_5	b.d.
Total	99.01
O *apfu*	4
Fe^{2+}	0.69
Mn	0.00
Mg	0.22
Ni	-
Zn	0.09
Si	0.00
Ti	-
Nb	-
Al	1.92
Cr	0.00
Fe^{3+}	0.07
V	-
Ca	-
X Spl	0.22
X Hc	0.69
X Gah	0.09

	Sillimanite	
	11	12
Point	126	64
SiO_2	36.86	37.02
TiO_2	b.d.	b.d.
Al_2O_3	63.84	64.18
Cr_2O_3	0.03	0.01
FeO	0.17	0.28
MnO	0.01	b.d.
MgO	b.d.	b.d.
CaO	0.01	0.01
Na_2O	0.01	0.02
K_2O	-	0.01
ZnO	b.d.	b.d.
BaO	-	0.005
Cs_2O	b.d.	0.01
V_2O_3	0.02	-
Y_2O_3	0.05	-
Total	101.02	101.54
O *apfu*	20	20
Si	3.95	3.94
Al	8.05	8.06
Ti	-	-
Fe	0.02	0.02
Mn	0.00	-
Mg	-	-
Zn	-	-
Ca	0.00	0.00
Na	0.00	0.00
K	-	0.00
Ba	-	0.00
Cs	-	0.00
V	0.00	-
Y	0.00	-

	Ilmenite
	13
Point	11
SiO_2	0.16
TiO_2	57.08
Al_2O_3	b.d.
Cr_2O_3	b.d.
FeO	34.06
MnO	1.81
MgO	0.04
NiO	b.d.
Total	93.20
O *apfu*	3
Si	0.00
Ti	1.17
Al	-
Cr	-
Fe^{3+} *2	0.00
Fe^{2+} *2	0.78
Mn	0.04
Mg	0.00
Ni	-

	Rutile	
	14	15
Point	12	14
SiO_2	0.57	0.23
TiO_2	94.97	96.19
Nb_2O_5	0.18	0.25
Al_2O_3	0.13	b.d.
Cr_2O_3	b.d.	b.d.
FeO	0.30	0.22
MgO	b.d.	b.d.
MnO	b.d.	b.d.
NiO	b.d.	b.d.
ZnO	b.d.	b.d.
Total	96.17	96.96
O *apfu*	2	2
Si	0.01	0.00
Ti	0.99	0.99
Nb	0.00	0.00
Al	0.00	-
Cr	-	-
Fe	0.00	0.00
Mg	-	-
Mn	-	-
Ni	-	-
Zn	-	-

-: not analyzed or calculated, b.d.: below detection limit. The proportion of end members is expressed in mol.%. The compositions were acquired with an electron microprobe. *1 All Fe is assumed to be all Fe^{3+} in feldspar. *2 Calculated according to stoichiometric constraints. Samples and photos: 1: WYL-09-49-36.1 image 10; location: matrix away from Grt; 2: WYL-09-49-36.1 a Pl 1, location: inclusion in Grt; 3: WYL-09-49-36.1 a Pl 2, location: matrix adjacent to Grt rim; 4: WYL-09-50-37.5 image 3, location: matrix away from Grt; 5: WYL-09-50-37.5 h Pl 7, location: matrix near Grt; 6: WYL-09-49-36.1 image 10, location: matrix away from Grt; 7: WYL-09-49-36.1 a Kfs 1, location: matrix adjacent to Grt; 8: WYL-09-50-37.5 image 2, location: matrix away from Grt; 9: WYL-09-50-37.5 f Kfs 3, location: matrix near Grt; 10: WYL-09-50-37.5i Spl 10, location: intergrown with Sil + Pl + Bt; 11: WYL-09-49-36.1 img 10, location: matrix in Sil band; 12: WYL-09-50-37.5 img 4, location: intergrown with Hc + Bt + Pl; 13: WYL-09-50-37.5 k ilm 1, location: in Pl; 14: WYL-09-50-37.5 m Rt 1, location: inclusion in Bt; 15: WYL-09-50-37.5 o Rt 3, location: adjacent to Bt.

inclusions in the large garnet grain (three) and in plagioclase (one), and are compositionally similar. The monazite in WYL–09–49–36.1 varies in its $X(LREEPO_4)$ from 0.81 to 0.91, $X(HREEPO_4)$ from 0.01 to 0.03, X_{Hut} from 0 to 0.02, X_{Chr} from 0.06 to 0.13, and $X(YPO_4)$ from 0.01 to 0.03 (Table 4-4), and have slightly lower UO_2 and higher ThO_2 contents. There was no significant difference in the composition of monazite included in biotite and garnet from this sample.

One monazite from within a plagioclase grain was analyzed from WYL–09–44–61.4. The UO_2 (0.35 to 0.52 wt.%), ThO_2 (5.38 to 6.70 wt.%), Y_2O_3 1.28 to 2.17 wt.%), LREE (27.85 to 29.33 wt.% Ce_2O_3, with 57.78 to 59.53 wt.% $\sum LREE_2O_3$) and HREE (1.75 to 2.58 wt.% $\sum HREE_2O_3$) contents (Table 4-4) of the monazite from this sample are broadly similar to those measured in the other two samples of pelitic gneiss.

Chime U-Th-Pb Chemical Age Dating

An attempt to determine the timing of metamorphism was carried out *via* CHIME U–Th–Pb chemical age dating, using the procedures of Montel *et al.* (1996), Annesley *et al.* (2000), and Hecht & Cuney (2000) to obtain the age of monazite included in several metamorphic minerals.

Of the monazite grains dated from the three pelitic gneiss samples, those from WYL–09–50–37.5 show the oldest chemical ages (ranging from 1813 ± 13 Ma to 1492 ± 21 Ma for monazite within a large grain of garnet, and from 1641 ± 18 Ma to 1295 ± 29 Ma for monazite within a plagioclase grain), with clusters at 1.8 to 1.75 Ga and 1.65 to 1.55 Ga (Figs. 4-7a, b, d). Three grains of monazite from WYL–09–49–36.1 generally gave younger ages (from 1776 ± 17 Ma to 1312 ± 30 Ma), with each of the grains recording multiple ages (Figs. 4-7c, e). There are three minor clusters of ages from the monazite in this sample, the oldest being from 1.8 to 1.7 Ga, with younger age clusters from 1.65 to 1.55 Ga and 1.5 to 1.45 Ga. An additional grain of monazite (within plagioclase) was analyzed from WYL–09–44–61.4, showing a range of ages from 1746 ± 18 Ma to 1532 ± 18 Ma, with a cluster from 1.65 to 1.6 Ga (Figs. 4-7f, g).

Table 4-4. Representative compositions of monazite in pelitic gneisses from the Fraser Lakes Zone B

	1	2	3	4	5
Line	70	48	52	37	46
Location	in Pl	in Grt	in Bt	in lrg Grt	in Pl
SiO_2 wt.%	0.82	0.46	0.52	0.29	0.11
TiO_2	b.d.	b.d.	b.d.	b.d.	b.d.
Al_2O_3	b.d.	b.d.	b.d.	b.d.	b.d.
FeO	b.d.	0.30	0.13	0.32	0.02
MnO	b.d.	b.d.	b.d.	b.d.	b.d.
MgO	b.d.	b.d.	b.d.	b.d.	b.d.
CaO	0.90	1.08	0.93	1.26	1.19
P_2O_5	29.09	29.81	29.43	30.29	29.81
UO_2	0.35	0.39	0.43	0.96	0.96
ThO_2	5.89	5.25	4.77	4.40	3.74
PbO	0.55	0.44	0.49	0.61	0.52
ZrO_2	0.11	0.23	0.14	0.13	0.15
HfO_2	b.d.	b.d.	b.d.	0.03	b.d.
Y_2O_3	1.57	0.30	0.65	2.22	2.80
La_2O_3	12.75	12.12	12.31	13.07	12.82
Ce_2O_3	29.14	34.93	34.87	27.92	27.32
Pr_2O_3	3.40	2.84	2.71	3.13	2.92
Nd_2O_3	11.90	10.06	9.92	10.67	11.16
Sm_2O_3	2.08	1.64	1.71	1.45	1.77
Gd_2O_3	1.47	1.22	1.49	1.05	1.19
Dy_2O_3	0.33	0.16	0.30	0.49	0.66
Er_2O_3	0.09	0.08	0.05	0.12	0.18
Total	100.44	101.31	100.86	98.39	97.33
$\Sigma LREE_2O_3$	59.28	61.59	61.52	56.23	55.99
$\Sigma HREE_2O_3$	1.88	1.45	1.84	1.66	2.03
O *apfu*	8	8	8	8	8
P	1.93	1.96	1.95	2.00	2.00
Si	0.06	0.04	0.04	0.02	0.01
Ca	0.08	0.09	0.08	0.11	0.10
U	0.01	0.01	0.01	0.02	0.02
Th	0.11	0.09	0.08	0.08	0.07
Pb	0.01	0.01	0.01	0.01	0.01
La	0.37	0.35	0.36	0.38	0.38
Ce	0.84	0.99	1.00	0.80	0.79
Sm	0.06	0.04	0.05	0.04	0.05
Pr	0.10	0.08	0.08	0.09	0.08
Nd	0.33	0.28	0.28	0.30	0.32
Gd	0.04	0.03	0.04	0.03	0.03
Dy	0.01	0.00	0.01	0.01	0.02
Er	0.00	0.00	0.00	0.00	0.00
Y	0.07	0.01	0.03	0.09	0.12
Fe	-	0.02	0.01	0.02	0.00
Mn	-	-	-	-	-
Mg	-	-	-	-	-
Zr	0.00	0.01	0.01	0.00	0.01
Hf	-	-	-	0.00	-
Ti	-	-	-	-	-
Al	-	-	-	-	-
$X(LREEPO_4)$	0.84	0.88	0.87	0.82	0.81
$X(HREEPO_4)$	0.02	0.02	0.02	0.02	0.03
X Hut	0.02	0.01	0.01	0.00	0.00
X Crl	0.08	0.09	0.08	0.11	0.10
X Xnt	0.03	0.01	0.01	0.05	0.06

-: not analyzed or calculated, b.d.: below detection limit. The proportion of end members is in mole %. The compositions were acquired with an electron microprobe. Sample and photo: 1 WYL-09-44-61.4 Mon-1, 2 WYL-09-49-36.1 Mon-1, 3 WYL-09-49-36.1 Mon-2, 4 WYL-09-50-37.5 Mon-2, 5: WYL-09-50-37.5 Mon-4. Symbols used: Crl: cheralite, Hut: huttonite, Xnt: xenotime.

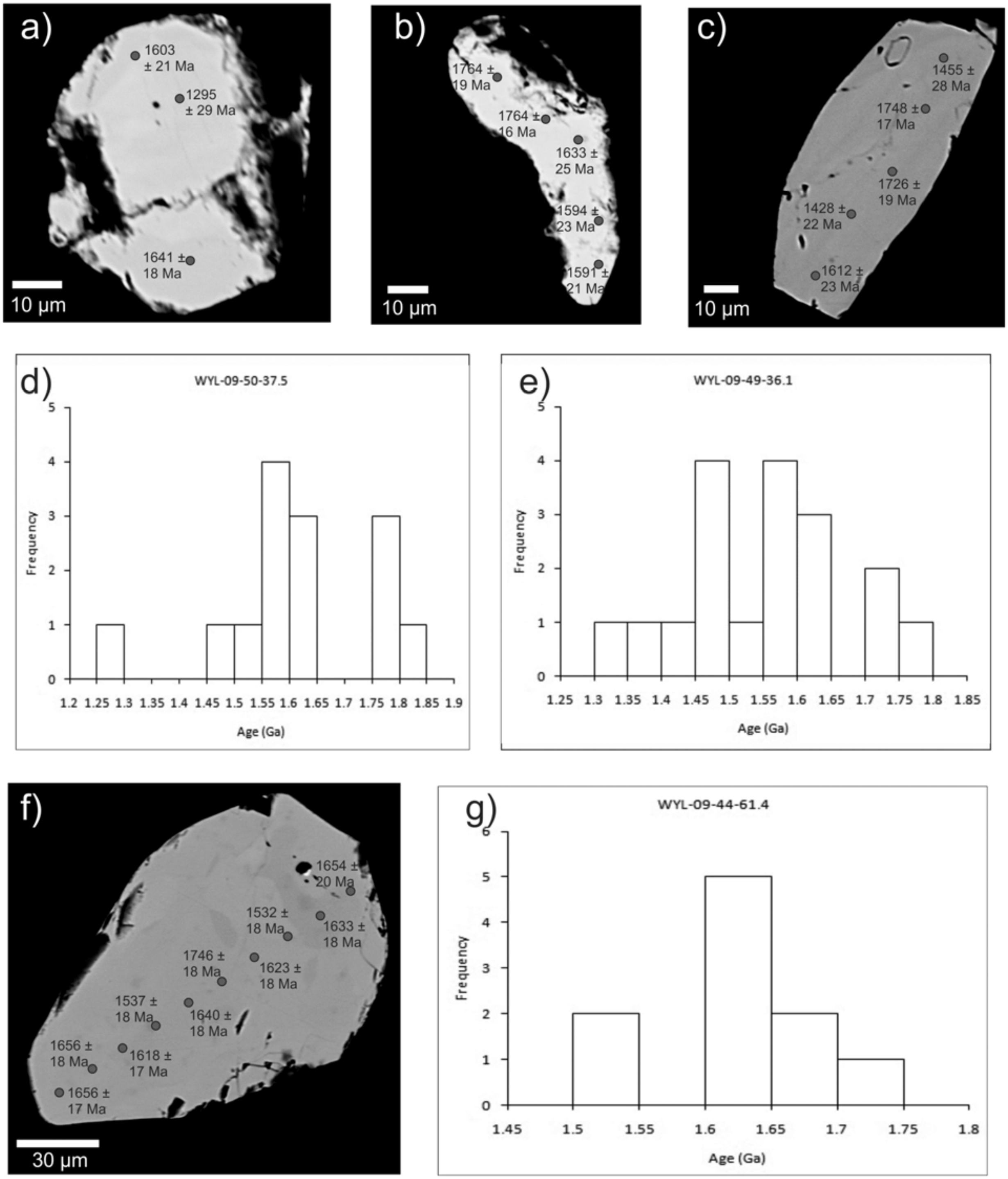
a)
1603
± 21 Ma
1295
± 29 Ma
1641 ±
18 Ma
10 μm
b)
1764 ±
19 Ma
1764 ±
16 Ma
1633 ±
25 Ma
1594 ±
23 Ma
1591 ±
21 Ma
10 μm
c)
1455 ±
28 Ma
1748 ±
17 Ma
1726 ±
19 Ma
1428 ±
22 Ma
1612 ±
23 Ma
10 μm
d)
WYL-09-50-37.5
Frequency
Age (Ga)
e)
WYL-09-49-36.1
Frequency
Age (Ga)
f)
1654 ±
20 Ma
1532 ±
18 Ma
1633 ±
18 Ma
1746 ±
18 Ma
1623 ±
18 Ma
1537 ±
18 Ma
1640 ±
18 Ma
1656 ±
18 Ma
1618 ±
17 Ma
1656 ±
17 Ma
30 μm
g)
WYL-09-44-61.4
Frequency
Age (Ga)

Figure 4-7 (previous page). Results of CHIME chemical age dating of monazite in the pelitic gneisses. (a, b) Monazite grains from WYL–09–50–37.5 show a range in U–Pb chemical ages; ages with errors are plotted in millions of years (Ma). (c) Monazite grain from WYL–09–49–36.1 with the ages (with errors) of the grain plotted in Ma. (d) Histogram showing the range in chemical ages for the monazite grains dated in WYL–09–50–37.5. Note the clusters of ages at 1.55 to 1.65 Ga and 1.75 to 1.85 Ga. The older ages are interpreted to represent the age of peak metamorphism in the Fraser Lakes area, whereas the younger ages are due to resetting of the U–Pb system. (e) Histogram showing the range in chemical ages for monazite from WYL–09–49–36.1. Note the clusters of ages at 1.45 to 1.65 Ga and 1.70 to 1.80 Ga. The older ages are interpreted to represent the age of late retrograde metamorphism in the Fraser Lakes area, whereas the younger ages are due to resetting of the U–Pb system. (f) Monazite grain (inclusion in plagioclase) in WYL–09–44–61.4 with ages (and errors) plotted in Ma. (g) Histogram showing the range in ages of monazite from WYL–09–44–61.4. The ages are interpreted to reflect postmetamorphic resetting of the U–Pb system.

Metamorphic Reactions

One of the aims of this study was to characterize the local metamorphic conditions in the Fraser Lakes area, in order to determine the relationship of metamorphism to intrusion of the Fraser Lakes Zone B granitic pegmatites. Most of the early, prograde metamorphic history of these rocks has been lost owing to re-equilibration during peak thermal metamorphism and further overprinting during retrograde metamorphism. However, parts of the prograde P–T path for the pelitic gneisses can be deduced using inclusions within the larger grains of garnet and cordierite. The garnet porphyroblasts show irregular patterns of zoning owing to variable retrograde homogenization, exchange, and net transfer (Figs. 4-6a–f). This indicates that there has been at least some re-equilibration during retrograde metamorphism.

The single large, zoned grain of garnet analyzed in WYL–09–50–37.5 contains inclusions of sillimanite, monazite, biotite, quartz, and rare plagioclase and ilmenite, reflecting the biotite dehydration-melting reactions Bt + Sil + Qtz = Grt + Kfs + melt and Bt + Sil + Qtz + Pl = Grt ± Kfs + melt. These inclusions are the remnants of the prograde mineral assemblages (Pt. 1, Fig. 4-8), and are indicative of high-T, moderate-P metamorphism of the Fraser Lakes pelitic gneisses.

This was followed by the formation of the peak thermal metamorphic assemblage of garnet, cordierite, and sillimanite (Pt. 2, Fig. 4-8), with possible reactions including Bt + Sil +Qtz = Grt + Crd + Kfs + melt, Bt + Sil + Qtz + Pl = Grt + Crd ± Kfs + melt, and Bt + Sil + Qtz + Pl = Crd

± Kfs + melt. These reactions continued during decompression, resulting in more significant partial melting and development of the abundant leucosome seen in the pelitic gneisses. Garnet – biotite – quartz symplectitic textures on the outer rim of a large grain of garnet in WYL–09–50–37.5 (Fig. 4-5f) were also formed during the decompression phase.

Spinel is observed in some pelitic gneiss (*e.g.,* WYL–09–50–37.5) and Archean orthogneiss samples, whereas the pelitic gneisses from WYL–09–49–36.1 and WYL–09–44–61.4 lack spinel. The spinel – sillimanite – biotite – quartz – plagioclase – cordierite assemblage in WYL–09–50–37.5 (Fig. 4-4f) may have formed through decompression-induced reactions such as Grt + Sil = Crd + Spl + Ilm, indicating formation under low-P – high-T retrograde metamorphic conditions (Pt. 3, Fig. 4-8). Sample WYL–09–44–66.4 shows evidence for slightly stronger retrograde re-equilibration of the high-temperature assemblage in the east-central area of the fold nose, as this sample also contains more significant transformation of biotite to muscovite than the samples from the western part of the fold nose and the northwestern fold limb. The contrast may also be compositionally controlled, as other samples of pelitic gneiss in drill core from this area of the fold nose contain significant cordierite, sillimanite, and garnet (McKechnie *et al.* 2013). Overall though, most of the samples of pelitic gneiss contain only minor to trace amounts of white mica alteration of the feldspars, and chlorite and muscovite alteration of biotite, suggesting that retrograde metamorphism only weakly affected the rocks.

The minimum temperature achieved during prograde metamorphism was at least 700°C, as the rocks lack prograde muscovite (all muscovite observed formed under retrograde conditions). The high content of biotite and plagioclase in these rocks indicates that temperatures could not have been any higher than about 825°C (Le Breton & Thompson 1988, Patiño Douce & Johnston 1991), as biotite dehydration melting did not go to completion. The rarity of orthopyroxene also suggests that the temperature for the dehydration-melting reaction Grt + Bt + H2O = Opx + Crd + melt was not achieved, which is compatible with T < 850°C, based on the petrogenetic grids of Wei *et al.* (2004) and Laberge & Pattison (2007) (Fig. 4-8), as well as work done by Spear *et al.* (1999) and references therein. This is also consistent with the presence of inclusions of sillimanite, plagioclase, biotite, and quartz within cordierite and garnet.

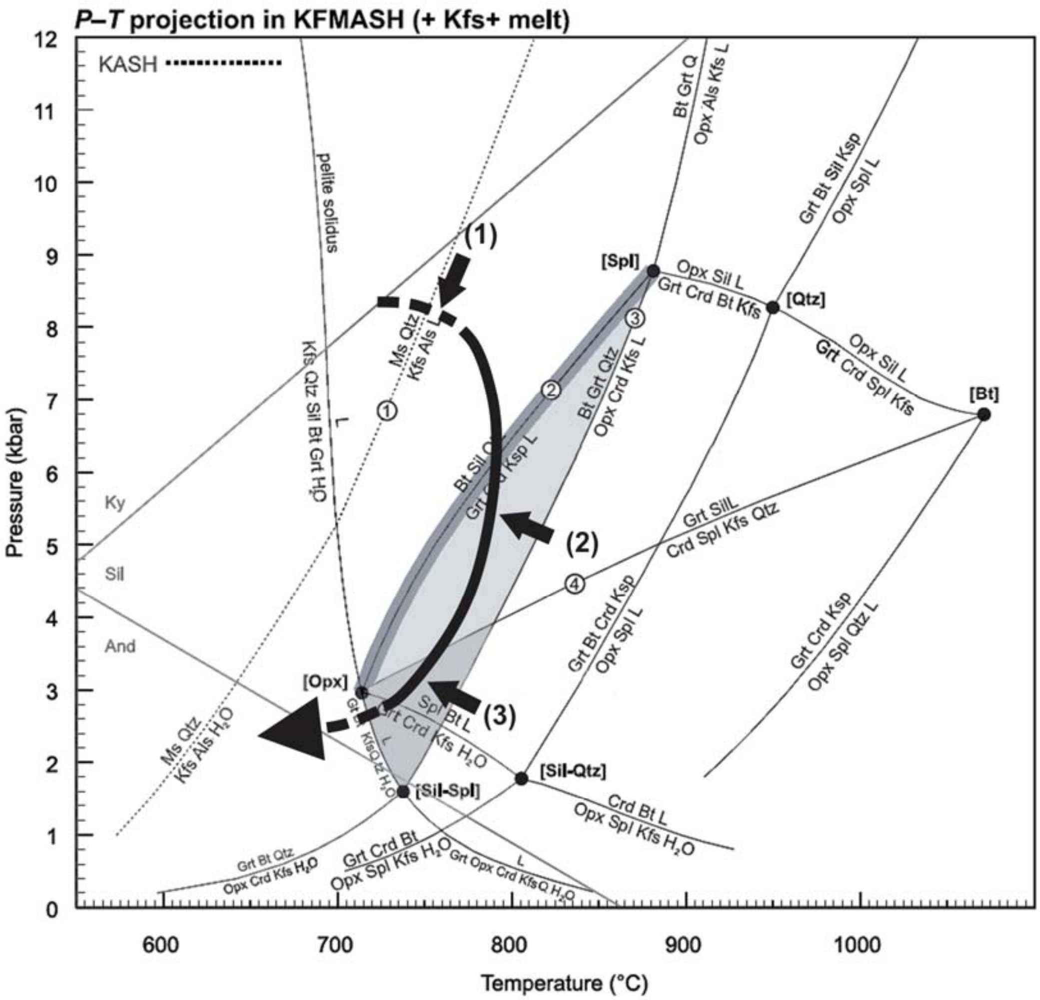

Figure 4-8. Petrogenetic grid for anatectic pelitic rocks modified from Laberge & Pattison (2007). A P–T path for the Fraser Lakes pelitic gneisses has been plotted using a combination of mineral assemblages and thermobarometry results. The absence of prograde muscovite and orthopyroxene, as well as the presence of sillimanite and the absence of kyanite and andalusite, allow us to place constraints on the maximum and minimum P–T conditions that the rocks experienced during peak thermal metamorphism. Prograde metamorphism (1) above the second sillimanite isograd is represented by garnet cores containing biotite and sillimanite inclusions (but lacking muscovite and cordierite, which would indicate lower pressure high-T metamorphism). The peak thermal metamorphism (2) is represented by garnet – biotite – sillimanite – cordierite – K-feldspar – melt assemblages found within the pelitic gneisses, and as well by abundant leucosome in the migmatitic pelitic gneisses. Retrograde metamorphism (3) during decompression is represented by the presence of spinel – sillimanite and garnet – quartz–biotite symplectites in a few samples. The absence of spinel in most of the pelitic gneisses at Fraser Lakes Zone B is likely due to a combination of their composition and the temperature during metamorphism, as spinel is found within the tonalitic orthogneiss that immediately underlies the basal pelitic gneisses.

The pressure during the latter stages of prograde metamorphism can also be estimated for the pelitic gneisses, on the basis of their mineral assemblages. The lack of kyanite in these samples indicates that the maximum pressure was less than 9 to 10 kbar (Fig. 4-8), although it is possible that it formed during prograde metamorphism and is no longer preserved owing to its transformation to sillimanite. Also, the presence of sillimanite and rutile inclusions within garnet porphyroblasts implies that pressures during prograde metamorphism were in the range of 7 to 9 kbar (Pt. 1, Fig. 4-8; *cf.* Vernon & Clarke 2008). After this, the rocks underwent isothermal decompression, which triggered significant partial melting events and led to the formation of some of the cordierite-bearing pelitic gneiss assemblages, as the pressure decreased from 7 to 3 kbar (Pt. 2, 3, Fig. 4-8). After the pressure dropped to about 3 kbar, spinel began to form in some of the rocks, preserving a record of high-T, low-P retrograde metamorphism (T up to 750°C and P from 3 to 1 kbar; *i.e.,* Pt. 3, Fig. 4-8). The presence of non-spinel-bearing pelitic gneisses and a lack of andalusite may indicate that pressures did not decrease below about 2 kbar during this part of the retrograde path (Fig. 4-8).

Geothermobarometry

Using the mineral compositions obtained with an electron microprobe, temperatures and pressures of metamorphism of the pelitic gneisses were calculated using the garnet–biotite geothermometer of Holdaway (2000), the Ti-in-biotite geothermometer of Henry *et al.* (2005), and the GBPQ geobarometer of Wu *et al.* (2004). The absolute error for the Henry *et al.* (2005) geothermometer is approximately ±12°C in the range of 700° to 800°C, whereas that of the Holdaway (2000) geothermometer is estimated to be about ±25°C, with a slight increase in the error at higher temperatures. The error of the GBPQ geobarometer [which was empirically calibrated on the basis of the garnet–biotite thermometer of Holdaway (2000) and the GASP barometer of Holdaway (2001)], is estimated to be ±1.2 kbar (Wu *et al.* 2004). The geothermometers and geobarometer were chosen on the basis of their low errors and availability of spreadsheet software used in the calculations. The rationale used in calculating the pressures and temperatures (*i.e.,* which garnet – biotite – plagioclase pairings were used) is included in Supplementary Data Table 2.

The results of Ti-in-biotite geothermometry for WYL–09–49–36.1 (garnet – sillimanite – biotite gneiss) show that the average temperature recorded by the biotite in the core of one garnet (Fig. 4-5a) is 700°C (Table 4-5), which is interpreted to reflect prograde metamorphism. Biotite inclusions further from the garnet cores record slightly higher temperatures, with biotite intermediate between the core and rim recording a temperature of 740°C, whereas those inclusions closer to the rim range from 734° to 765°C (average of 750°C) (Table 4-5). These temperatures suggest that the biotite inclusions in the rim of garnet grains formed during prograde to peak thermal metamorphism. The temperatures for biotite in the matrix adjacent to garnet preserve an average of 690°C (Table 4-5); such biotite is interpreted to be retrograde. Using these temperature constraints, the minimum pressure during peak thermal metamorphism was calculated using the GBPQ geobarometer of Wu *et al.* (2004) to be an average of 5.6 kbar, with the biotite in the garnet core calculated to have formed at a minimum pressure of 5.2 kbar (Table 4-5). The lower pressure shown by the garnet core relative to the rim (which is lower than the estimated pressure based on the mineral assemblage in the core) is interpreted to be a result of the plagioclase compositions that were used, in addition to the effects of retrograde exchange and net-transfer reactions. Biotite in the matrix in contact with garnet grew when the P was an average of ~3.8 kbar (Table 4-5). The Grt–Bt geothermometer of Holdaway (2000) yielded lower temperatures than the Ti-in-biotite geothermometer, using estimated pressures similar to those determined using the GBPQ geobarometer, with the T apparently increasing from a low of 564°C in the core of the grain to 593°C (Table 4-5) for biotite in the matrix adjacent to garnet. The garnet–biotite temperatures are lower than expected, based on the mineral assemblage (Figs. 4-8, 4-9a), and thus it is apparent that the garnet and biotite were affected by retrograde exchange reactions. Calcium in garnet has been shown to be stable in grains affected by retrograde exchange reactions (Pattison & Bégin 1994); however the GBPQ geobarometer takes into account the Fe and Mg contents of garnet and biotite; thus, the geobarometer results may have been affected by retrograde exchange reactions.

The spinel- and cordierite-bearing garnet – sillimanite – biotite gneiss (WYL–09–50–37.5) contains a record of both prograde and retrograde metamorphic temperatures and pressures. The Ti-in-biotite temperatures are an average of 732°C (Table 4-5) for biotite included in the single large grains of garnet near its rim, with a maximum temperature recorded by a grain in the rim of the garnet at 780°C. This highest temperature is interpreted to reflect the peak thermal metamorphic temperature, although it could be an underestimation due to re-equilibration processes. This metamorphism occurred at a calculated average pressure of ~5.6 kbar (Table 4-5). Biotite in the matrix away from garnet shows an average Ti-in-biotite temperature of 750°C and records a slightly higher average pressure, ~7.0 kbar, if calculated using garnet core and matrix plagioclase compositions (Table 4-5); this pressure is interpreted to be more reasonable for that during peak thermal metamorphism, but should be treated with caution in view of the low Ca contents of the garnet and plagioclase. Biotite in the garnet – quartz – biotite symplectite in this sample shows slightly lower temperatures (average of 713°C from the Ti-in-biotite geothermometer, Table 4-5). The biotite that formed in the matrix adjacent to garnet shows that it likely formed along the decompression P–T path (717°C at ~4.7 kbar, Table 4-5). Average garnet–biotite temperatures are typically about 100°C lower for the same grains (604°C for the biotite included in garnet near the rim, 596°C for both the biotite inclusion in the rim and the garnet – biotite – quartz symplectite, and 618°C for the matrix biotite), interpreted to reflect retrograde exchange and net-transfer reactions. The exception to this generalization is the garnet–biotite temperature calculated using the matrix biotite and garnet core data, which gave a temperature of 707°C; this temperature is equivalent within error limits to the results of the Ti-in-biotite geothermometer.

For the garnet–biotite gneiss in the eastern central portion of the fold nose (WYL–09–44–61.4), the average T calculated using the Ti-in-biotite geothermometer for biotite inclusions in garnet cores is 663°C (Table 4-5). Inclusions in garnet intermediate between the core and rim gave an average temperature of 603°C. Other biotite inclusions in the garnet near the rim of the grains gave an average temperature of 594°C (Table 4-5). Biotite in the matrix adjacent to garnet gives an average temperature of 580°C (Table 4-5). The garnet–biotite geothermometer reveals slightly lower temperatures (calculated using 6 kbar for inclusions in the garnet cores, 5 kbar for inclusions intermediate to near the garnet rims, and 4 kbar for the matrix biotite, the pressures being estimated in this case, as no pressure determination was made), namely 564°C for inclusions in the core, 559°C for biotite intermediate between the core and rim, 561°C for inclusions in the garnet rim, and 569°C (Table 4-5) for inclusions in the garnet rim (and corresponding garnet compositions in close proximity to the biotite, Table 4-5). Feldspar was not analyzed in this sample, and thus no P calculations could be completed for this sample using the GBPQ geobarometer. These temperatures are interpreted to reflect retrograde exchange or net-transfer reactions, or alternatively, retrograde crystallization of the garnet and biotite.

Table 4-5. Average P-T Results for Pelitic Gneisses from the Fraser Lakes Zone B area.

Sample	Location of Grt, Bt, Pl in sample	1	2	3	4
WYL-09-44-61.4	Bt inclusion in Grt core, Grt Core, no Pl	663	6000	564	n/a
WYL-09-44-61.4	Bt inclusion in Grt midway to rim, intermediate Grt, no Pl	603	5000	559	n/a
WYL-09-44-61.4	Bt inclusion in Grt rim, near rim Grt, no Pl	594	5000	561	n/a
WYL-09-44-61.4	Bt in matrix adj. to Grt rim, Grt rim, no Pl	580	4000	568	n/a
WYL-09-49-36.1	Bt inclusion in Grt core, Grt Core, core of Pl in matrix away from Grt	700	5500	564	5129
WYL-09-49-36.1	Bt inclusion in Grt midway to rim, intermediate Grt, core of Pl in matrix away from Grt	742	5500	583	5242
WYL-09-49-36.1	Bt inclusion in Grt rim, near rim Grt, core of Pl in matrix away from Grt	750	5500	576	5600
WYL-09-49-36.1	Bt in matrix adj. to Grt rim, Grt rim, rim of Pl in matrix away from Grt	690	4000	593	3826
WYL-09-50-37.5	Bt inclusion in Grt near rim, near rim Grt, Pl in matrix near Grt	732	5000	604	5070
WYL-09-50-37.5	Bt inclusion in Grt rim, Grt rim, Pl in matrix near Grt	780	5500	596	5639
WYL-09-50-37.5	Grt–Bt–Qtz symplectite	713	3500	596	n/a
WYL-09-50-37.5	Bt in matrix adj to Grt, Grt rim or near rim, Pl in matrix near Grt	717	4500	618	4720
WYL-09-50-37.5	Bt in matrix away from Grt, Grt core, Pl in matrix away from Grt	726	7000	707	6973

Results of geothermometry and geobarometry: 1 Ti-in-Biotite geothermometer (Henry *et al.* 2005), 2, 3 Grt–Bt geothermometer (Wu *et al.* 2004) (P estimated), 4 GPBQ geobarometer (Holdaway 2001) with T estimated from Henry *et al.* (2005). Temperature in °C, pressure in bars.

Discussion

In this study, we examined the pelitic gneisses that host the U–Th–REE mineralized pegmatites of the Fraser Lakes Zone B, in order to determine the temperature and pressure conditions that existed during peak thermal metamorphism as well the timing of this metamorphic event. As the Fraser Lakes Zone B pegmatites are interpreted to have resulted from partial melting during metamorphism (McKechnie *et al.* 2012a, 2013), we can provide further constraints on their origin by studying the metamorphism that occurred in the area.

P-T conditions recorded by the pelitic host rocks

The temperature and pressure constraints from mineral reactions and conventional geobarometry indicate that the pelitic gneisses achieved the granulite grade, above the second sillimanite isograd (Figs. 4-8, 4-9a) (Turner 1981, Bucher & Frey 1994). However, work by Pattison & Bégin (1994) and Pattison *et al.* (2003) indicates that the temperatures in many granulite terranes are underestimates of the peak T (by 100°C in many cases) owing to retrograde reactions, and thus the mineral assemblages in the Fraser Lakes area may not record the highest P–T conditions. Also, the absence of orthopyroxene and the abundance of sillimanite in the pelitic gneisses could be a result of inappropriate bulk-rock composition (*i.e.,* high X_{Al}, favoring the formation of sillimanite rather than orthopyroxene) and not a reflection of temperature. Therefore, the actual temperatures during prograde metamorphism could potentially be higher than those calculated, as this information was probably lost while the rocks remained at high temperatures during near-isothermal decompression (Figs. 4-8, 4-9a). The lack of cordierite and spinel in some of the analyzed samples is likely due to inappropriate bulk chemical compositions and is not a reflection of metamorphic grade, as abundant cordierite and rare spinel were found in other samples from the Fraser Lakes area.

The Grt–Bt geothermometer (Holdaway 2000) and GBPQ geobarometer (Wu *et al.* 2004) likely yielded lower temperatures and pressures than expected from the petrography because of retrograde diffusion and net-transfer reactions that affected the biotite and garnet compositions of the rocks (Pattison & Bégin 1994, Pattison *et al.* 2003), or are due to growth of garnet and biotite during retrograde metamorphism (possibly using pre-existing grains as nuclei). However, the GBPQ geobarometer results should be interpreted with additional caution in WYL–09–50–37.5 due to the low Ca contents of garnet and plagioclase, which are not quite within the calibrated composition limits. The fact that garnet does not appear to preserve its original prograde growth-induced zoning, although expected given the high temperatures of metamorphism (*cf.* Tuccillo *et al.* 1990, Caddick *et al.* 2010, and references therein), adds additional uncertainty to the accuracy of these results. The Ti-in-biotite geothermometer seems to give reasonable results for the temperatures during metamorphism (up to 780°C), as the mineral assemblages suggest a minimum temperature of about 750°C (Laberge & Pattison 2007, Vernon & Clarke 2008, Wei *et al.* 2004). The slightly lower temperatures for sample WYL–09–44–61.4 likely reflect an increase in the amount of muscovite, chlorite, and rutile because of increased retrograde alteration of high-grade metamorphic minerals in this part of the fold nose, related to late brittle faults cutting the fold nose.

The mineral assemblages and textural relationships were combined with the thermobarometry to develop the P–T paths shown in Figure 4-8, which was superimposed upon a petrogenetic grid modified from Laberge & Pattison (2007). The authors assert that the rocks first experienced high-T, high-P prograde metamorphism up to peak thermal conditions (1, Fig. 4-8) before undergoing significant biotite-dehydration melting during isothermal decompression (2, Fig. 4-8). The rocks then underwent cooling (3, Fig. 4-8), leading to the development of the high-temperature, spinel-bearing retrograde assemblage, as well as the garnet–biotite–quartz symplectites. The exact nature of the P–T path is difficult to determine, however, owing to bulk chemical differences and retrograde diffusion affecting the metamorphic assemblages, although this path is similar to that developed for pelitic gneisses within other parts of the Wollaston and Mudjatik domains (Madore *et al.* 1999, Orrell *et al.* 1999, Tran 2001, Annesley *et al.* 2005, Schneider *et al.* 2007, and references therein). Lower-temperature retrograde metamorphism is preserved in the rocks (*i.e.,* in the form of white mica alteration of feldspar and local weak conversion of biotite to chlorite), but it is not important when considering the relationship between metamorphism and pegmatite generation.

The high metamorphic temperatures would have allowed for significant amounts of melting occurring *via* biotite-dehydration reactions, especially during the isothermal decompression part of the P–T path (Le Breton & Thompson 1988, Patiño Douce & Johnston 1991, Brown 2007, Weinberg & Mark 2008) (Fig. 4-9a). The temperatures recorded by the biotite from the pelitic gneisses (up to 780°C) are well within the range for partial melting, on the basis of the work of Brown *et al.* (2011), Sawyer *et al.* (2011), and references therein. As muscovite is absent from these rocks, it appears that the muscovite-dehydration reactions have gone to completion, which places temperatures >750°C at moderate pressures of 5–8 kbar in the Fraser Lakes area. The abundance of leucosome in the pelitic gneisses at Fraser Lakes Zone B is further evidence that the rocks underwent partial melting at such temperatures.

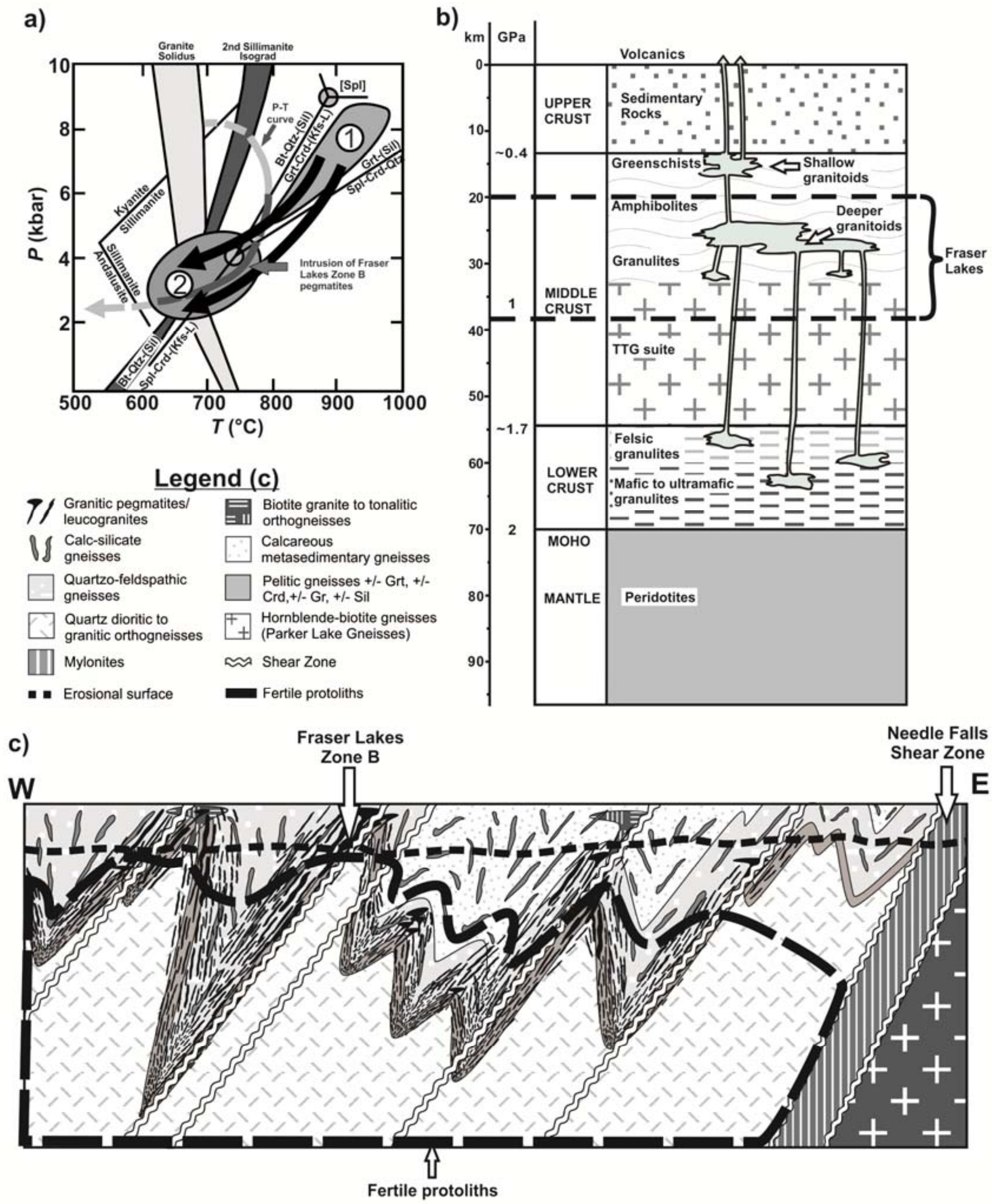

Figure 4-9. (a) P–T path for the Fraser Lakes pelitic gneisses showing the timing of pegmatite emplacement with respect to the clockwise P–T path for the pelitic gneisses. The black arrows show potential paths through P–T space that the pegmatite-forming melt took from its source area at depth (1) to where it crystallized (2) during and after isothermal decompression at peak temperatures. This timing was determined on the basis of field relationships, thermobarometry, and mineral assemblages; modified from Annesley et al. (2005). (b) Schematic crustal section (modified from Searle et al. 2011) showing the different layers of the crust and areas of magma ponding and transport. Note the location of the Fraser Lakes in the middle crust near the amphibolite-to-granulite transition. (c) Schematic cross-section depicting the geology of the

Fraser Lakes area. Melting occurred in the pelitic host-rocks and at depth within fertile protoliths (outlined in the broken black line), with melt being transported laterally and upward along structural discontinuities into areas of dilation, where it was trapped and crystallized, especially within shallowly plunging antiformal fold noses. Note the presence of overturned recumbent folds (i.e., defined by folded units) and ductile shear zones (white lines) formed during the Trans-Hudson orogeny. Shearing is particularly focused along fold limbs and within synformal fold noses. The metamorphic grade decreases to the east toward the Needle Falls Shear Zone. This section was constructed taking into account information from airborne gravity and magnetic surveys, historical geological mapping, and regional high-resolution seismic surveys.

Constraints on timing of metamorphism and partial melting, and implications for pegmatite formation

McKechnie *et al.* (2012a, 2013) recognized that the mineralized granitic pegmatites and leucogranites of Fraser Lakes Zone B intruded at roughly the same time as metamorphism and deformation in the area (similar to the timing of peak thermal metamorphism and intrusion of granitic pegmatites in the Wollaston Domain, from 1820 to 1805 Ma: Annesley *et al.* 2005). Of the two groups of mineralized granitic pegmatites described at Fraser Lakes Zone B, the primary crystallization age (between 1.85 to 1.80 Ga, McKechnie *et al.* 2012a; 1805 ± 11 Ma to 1713 ± 30 Ma, Annesley *et al.* 2010b, Mercadier *et al.* 2013) is only known for the Group-A granitic pegmatites (U- and Th-rich). Attempts were made to date the Group-B granitic pegmatites (Th- and LREE-rich), but these were unsuccessful (McKechnie *et al.* 2012a).

The significant variability in chemical age data from the pelitic gneisses (with ages from 1.8 to 1.3 Ga, even within the same grains), indicates that resetting of the monazite was common after the grains crystallized. Most of these monazite ages appear to postdate the known timing of peak thermal regional metamorphism in the Wollaston Domain (1820 to 1805 Ma, Annesley *et al.* 2005), and thus the ages cannot be used to constrain the timing of metamorphic textures or mineral growth. The oldest age of a monazite grain within the large grain of garnet in WYL–09–50–37.5, 1813 ± 13 Ma, overlaps with the timing of peak thermal regional metamorphism; thus, this grain of garnet is interpreted to have formed along the prograde P–T path slightly before and at approximately the same time as intrusion of the pegmatites at Fraser Lakes Zone B. Younger ages at *ca*. 1.75 Ga, shown by monazite inclusions in plagioclase and garnet, are interpreted to have resulted from additional growth of monazite or resetting of monazite ages as a result of thermal readjustment and relaxation from 1775 to 1720 Ma (Annesley *et al.* 2005). The youngest ages recorded by the monazite grains (*i.e.*, ages ranging from 1656 to 1295 Ma) are likely related to resetting of the monazite grains by dissolution and recrystallization processes, rather than Pb diffusion [on the basis of the experimental work of Seydoux-Guillaume *et al.* (2002) and Cherniak *et al.* (2004), and observations made by Crowley & Ghent (1999) and references therein]. The dissolution and recrystallization could have been caused by lower-temperature flow of hydrothermal fluid, which may have also modified the magmatic ages of primary uraninite in the Group-A pegmatites (these also show some evidence for resetting at various times from 1.7 to 1.1 Ga; see McKechnie *et al.* 2012a, Fig. 4-9) and led to the formation of local alteration of the pegmatites and their host rocks in brittle fractures and deformation zones in the area (*cf.* McKechnie *et al.* 2013).

Information from the current study was combined with the work of McKechnie *et al.* (2012a, 2013) at Fraser Lakes Zone B and previous descriptions of metamorphism and pegmatite emplacement within the Wollaston Domain (Annesley *et al.* 2005, and references therein) to create Figure 4-9a. This figure shows a similar P–T path to the path shown Figure 4-8, with the addition of information on the emplacement of the Fraser Lakes Zone B pegmatites on a P–T diagram modified from Annesley *et al.* (2005). A combination of field relationships, petrography, chemical age dating, and mineral reactions (this paper, and McKechnie *et al.* 2012a, 2013) was used to place the pegmatites of the Fraser Lakes Zone B on this diagram.

One key question for the origin of our U–Th–REE-mineralized pegmatites and leucogranites is the role that metamorphism and partial melting played; this is the ultimate goal of the current study. The mineralized pegmatites at Fraser Lakes Zone B were suggested by McKechnie *et al.* (2012a, 2013) to have formed by partial melting and subsequent assimilation – fractional crystallization (AFC) processes during thermal peak conditions of the THO. The melt-generating reaction Bt + Qtz + (Sil) $ Grt + Crd + (Kfs + L) provides a minimum constraint on the relative timing of pegmatite emplacement and partial melting (Fig. 4-9a). The bulk of partial melting in the pelitic gneisses (and emplacement of the pegmatites) took place on the decompression part of the original P–T curve, with emplacement (shown in the shaded region 2 in Fig. 4-9a) ongoing, though diminishing with time owing to decreasing temperature, until the rocks were at or slightly below the granite solidus (Fig. 4-9a).

The presence of numerous small bodies of leucosome (a few cm in size) in the pelitic gneisses, aligned broadly parallel to the main foliation and to the pegmatites, but not emanating from the pegmatites, suggests that while partial melting of the Wollaston Group occurred during approximately the same time interval as emplacement of the granitic pegmatites, it is likely that the pegmatite-forming melt was generated lower in the crust (at conditions similar to the shaded field 1 in Fig. 4-9a). The abundance of cordierite and garnet within the pelitic gneisses, the amount of restite in the granitic pegmatites, and the lack of similarly aged plutons in the area place the Fraser Lakes area in the middle part of an old ~20 km thick crustal melt-transfer zone (Fig. 4-9b), a melting and transport model proposed by Brown (2010) and modeled by Hobbs & Ord (2010). This model is consistent with the temperatures and pressures estimated from the metamorphic assemblages and thermobarometry in this study.

Figure 4-9c shows a schematic cross-section of the geology of the Fraser Lakes area, and visually depicts the previously proposed model (*cf.* McKechnie *et al.* 2012a, 2013) for the pegmatites of Fraser Lakes Zone B, whereby partial melting occurred in the pelitic gneisses and fertile lithologies (*i.e.,* those capable of partially melting, noted by the dashed outline) at depth within a higher P–T regime (area 1 of Fig. 4-9a), followed by melt transport, in particular along regional foliations, shear zones, and within the fold nose areas, through the lower to middle crust to the current level of emplacement (*cf.* McKechnie *et al.* 2012a, 2013). The structural interpretation of the Fraser Lakes area, based on local geological mapping and regional seismic data, suggests that overturned recumbent folds and ductile shear zones formed during the THO. Overall, the presence of protomylonitic to mylonitic fabrics in the pelitic gneiss host-rocks emphasizes that this was a high-strain environment during deformation, metamorphism, and emplacement of the pegmatites; thus it is likely that tectonic processes played a role in emplacement of the granitic pegmatites of the Fraser Lakes Zone B.

Conclusions

The current paper adds to our understanding of the geological history of the Fraser Lakes area, and in particular the relationship among partial melting, granitic pegmatite and leucogranite emplacement, and the metamorphic history of the area. The entire area underwent high-grade regional metamorphism at amphibolite to granulite facies (*i.e.*, peak temperatures of up to ~780–800°C and pressures of up to ~7–8 kbar) during the THO, at approximately 1.8 Ga. At peak thermal conditions and during post-peak isothermal decompression, widespread partial melting of the crust occurred primarily *via* biotite-dehydration reactions. Melting of uranium- and thorium-enriched pelitic gneisses (± graphite), similar to the pelitic gneisses hosting the U–Th–REE mineralized intrusive rocks of the Fraser Lakes Zone B, generated U–Th–REE-rich granitic melts. The large size (*i.e.*, thickness) of the pegmatites suggests that much of the melt was generated at depth. This melt ascended to its current structural level mainly along the contact between the pelitic gneisses and orthogneisses and in shear zones. Tectonic forces caused the melts to concentrate in regional fold noses (especially antiformal ones), including the antiformal fold nose at Fraser Lakes Zone B. The mineralized granitic pegmatites formed at the same time as deformation and metamorphism, on the basis of information from regional studies of the western margin of the THO and the current study. Thus we can conclude that mineralization at the Fraser Lakes Zone B was a consequence of partial melting of pelitic gneisses and subordinate granitic gneisses within the middle to lower crust during Hudsonian high-grade upper-amphibolite- to granulite-facies metamorphism.

CHAPTER 5
CONCLUSIONS

The Fraser Lakes Zone B U-Th-LREE-mineralized granitic pegmatites and leucogranites were examined in order to determine the controls on the mineralization – including the structural, metamorphic, and geochemical controls – that will aid in exploration in the Fraser Lakes area and elsewhere in northern Saskatchewan for pegmatite-hosted uranium ± thorium ± rare-earth element mineralization. To accomplish this overriding goal, an integrated approach using multiple datasets – *i.e.* petrography, geochemistry, electron microprobe analyses, CHIME chemical age dating, geothermobarometry, and geophysical data – was utilized in order to fully understand the Fraser Lakes Zone B U-Th-LREE-mineralized pegmatites and their host rocks.

Characteristics of the Fraser Lakes Zone B mineralized intrusives and their host rocks

The first portion of this thesis – Chapter 2 – described the macroscopic and microscopic features of the Fraser Lakes Zone B mineralization and the host Wollaston Group pelitic gneisses and Archean orthogneisses. Two groups of radioactive pegmatites were described at Fraser Lakes Zone B that are spatially, mineralogically, and geochemically distinct from one another; which were given the labels Group A (U- ±Th-rich pegmatites) and Group B (Th- and LREE-rich pegmatites). This study was one of the only studies documenting Th-LREE-rich pegmatites in northern Saskatchewan, and was the first to discuss their origin and the differences between them and the more well-known U-rich pegmatites in Northern Saskatchewan. Both groups of pegmatites are interpreted to have formed *via* partial melting of U- and Th-enriched pelitic gneisses during the Trans-Hudson Orogen; however, their mineralogical and chemical differences reflect slightly different sources, amounts of restite-unmixing, transport distances, and assimilation-fractional crystallization. Chapter 2 also discussed in detail the structural controls on the mineralization, using a combination of field observations by the author and JNR Resources Inc. staff, and by referencing the recent literature (including Handy *et al.* 2001, Kisters *et al.* 1998, 2009, Sawyer 2008, Brown 2007, 2010, Brown *et al.* 2011, and Sawyer *et al.* 2011, among others) on partial melting, melt transport, granite generation, migmatites, and uranium-enriched granitoids. Of note is the strong control that shear zones and other zones of weakness have on melt transport networks, and the abundance of granitoids in dilational areas, like the antiformal fold nose at Fraser Lakes Zone B.

Chapter 3 provides additional detail of the U-Th-REE minerals in the pegmatites, including their chemistry – this is important for metallurgy and economic reasons, as certain minerals, like uraninite, are much easier to leach uranium from than others are. This chapter also added additional constraints on the origin of the mineralization, including a discussion of the timing of pegmatite intrusion and the temperatures at which intrusion took place. The chemical age data also helped to further explain the differences between the Group A and Group B pegmatites first discussed in Chapter 2 – it was noted that the Group B pegmatites contained a large suite of inherited monazite and tended to have more mafic, lower-SiO_2 compositions due to their higher biotite contents. This study recognized that the Group A and Group B pegmatites likely did not have the same source, with the Group A pegmatites forming from more an earlier melt phase, and the Group B pegmatites forming from a more restitic, residual source which already underwent partial melting – however, both groups of pegmatites are interpreted to have formed at roughly the same time (ca. 1.85 to 1.80 Ga) during the Trans-Hudson Orogeny. The Group B pegmatites are also closer to their source rocks, and underwent less restite-unmixing during transport (see Appendix L for additional discussion of how restite-unmixing can affect the composition of the pegmatites), based on their greater amounts of xenocrystic, restitic, and peritectic minerals (biotite and monazite being two of the main minerals).

Chapter 4 discussed further the metamorphism of the pelitic gneiss host rocks at Fraser Lakes Zone. The Fraser Lakes area underwent upper-amphibolite to granulite-facies metamorphism during the THO at approximately 1.8 Ga, with peak temperatures estimated at ~780° to 800°C at a pressure of ~7-8 kbars. This was followed by isothermal decompression, which led to widespread partial melting of the crust mainly by biotite-dehydration reactions. However, there is little evidence that the pegmatites formed from melts that were generated at their emplacement level, as the pegmatites are only rarely connected to leucosomes in the pelitic gneisses. As well, large volumes of melt would have been required to form the mineralized pegmatites, and thus it is more likely that this melt would have been generated deeper down in the crust, where temperatures were even hotter. The melt source would have been enriched in uranium, thorium, and rare-earth elements, and is believed to be similar to the pelitic gneisses currently exposed at Fraser Lakes Zone B. The high grade nature of the metamorphism in the pelitic gneiss host rocks is further evidence that the Fraser Lakes pegmatites were generated by partial melting during the THO at roughly 1.8 Ga.

Implications for uranium exploration

The main goal of this study was to determine the controls on the mineralization in order to aid exploration for similar deposits in the Fraser Lakes area. A number of criteria are introduced below to help achieve this aim.

1. Area experienced high grade metamorphism of at least upper amphibolite to lower granulite-facies, enough to cause significant partial melting *via* biotite-dehydration melting reactions
2. Area contained fertile lithologies, *i.e.* those capable of partially melting. Metasedimentary rocks are particularly fertile as they contain abundant micas capable of undergoing dehydration reactions
3. Source of the partial melt was enriched in uranium, thorium, and rare-earth elements, in particular in minerals that were in contact with significant amounts of melt; allowing for greater dissolution of these minerals thus concentrating the melts in U, Th, and REE
4. There is an association with dilational areas, in particular fold noses like the antiformal fold nose at Fraser Lakes Zone B, as melt would concentrate in these areas
5. Shear zones provide good conduits for melt transport from lower in the crust, especially where there is a lithological and thus a rheological contrast in the rocks.
6. There is an association with the Wollaston Group – Archean orthogneiss unconformity – this is due to structural (this contact is often highly sheared) as well as geochemical constraints (graphitic pelitic gneisses, which are almost highly sheared and form a source of uranium and additionally can be a reducing agent for uranium, are common at this boundary and can exert a geochemical control on the mineralization- see next point)

7. In particular, there is an association with the margins of the pegmatites – this is believed to be due to redox controls and assimilation as any change in the chemistry of the melt may affect the solubility of U, Th, and REEs in the pegmatites (and thus lead to crystallization of U-Th-REE-rich minerals)
8. Late hydrothermal fluids can serve to convert the uranium into a more accessible form (*i.e.* secondary uranium oxides amenable to current leaching methods), but can also destroy the mineralization. Thus, the rocks must be looked at in detail to make sure they have not lost significant uranium to fluids.
9. The mineralogy of these pegmatites must be carefully examined to make sure it is conducive to leaching by current methods – uraninite is good, but if the uranium is locked up within Nb-Ti-oxides or other refractory minerals, then it is much harder to extract the uranium. Thus, the mineralogy can render a deposit uneconomic and should be examined shortly after discovery.
10. There is an association of these rocks with unconformity-related uranium deposits, though the exact role they play is highly debated – U-rich pegmatites have been postulated to be the source of uranium for these deposits in a number of ways (see Chapter 2 and Appendix L for further discussion).
11. The highest grades are in association with biotite- and/or quartz-rich portions of the pegmatites – the biotite association may be due to the U-Th-REE-rich minerals forming inclusions in xenocrystic biotite (this is especially true for monazite). The association with quartz-rich rocks is harder to describe, but may be due to uranium being concentrated in the residual fluid stage following the majority of crystallization of the pegmatites (Parslow and Thomas 1982).
12. The Th-rich pegmatites are interpreted to be closer to their source areas and have undergone less restite-unmixing, and are more residual in composition relative to the U-rich pegmatites – while at Fraser Lakes there is a fault separating the two areas of mineralization form each other, it is not known if this fault has juxtaposed two different levels of the crust (thus why we see the two groups of pegmatites) or if the spatial differences are just due to differences in age, melt transport paths, and source composition. Further work on the Group B pegmatites would be required to determine

their exact age and thus, their relationship to metamorphism and intrusion of the Group B pegmatites.

LIST OF REFERENCES

ABRAHAM, I.M. (2009): *Geology and Spatial Distribution of Uranium Mineralization in the SK Anomaly Area, Rössing area, Namibia.* M.Sc. thesis, Univ. Witwatersrand, Johannesburg, South Africa.

ALEXANDRE, P., KYSER, K., POLITO, P. A., SOPUCK, V., & THOMAS, D. (2005): Alteration mineralogy and stable isotope geochemistry of Paleoproterozoic basement-hosted unconformity-type uranium deposits in the Athabasca Basin, Canada. *Econ. Geol.,* **100**, 1547-1563.

ANDERSON, A.T. (1968): Oxidation of the La Blanche Lake titaniferous magnetite deposit, Québec. *J. Geol.* **76**, 528-547.

ANDERSEN, D.J. & LINDSLEY, D.H. (1985): New (and final!) models for the Ti-magnetite/ilmenite geothermometer and oxygen barometer. *Trans. Am. Geophys Union (Eos)* **66**, 416 (abstr.).

ANNESLEY, I.R., AUSTMAN, C.L., CREIGHTON, S., MERCADIER, J., ANSDELL, K.M., GITTINGS, F., BOGDAN, T.S., AND BILLARD, D. (2010a): Fraser Lakes U-Th-REE mineralization, southeastern Athabasca basement: composition and U-Th-Pb chemical/isotopic ages with consequences for U protore and U/C-type mineralization. *In* Open House 2010 Abstract Volume, Sask. Geol. Surv., Regina, Saskatchewan (8).

ANNESLEY, I. R., CREIGHTON, S., MERCADIER, J., AUSTMAN, C.L. & BONLI, T. (2010b): Composition and U–Th–Pb chemical ages of uranium and thorium mineralization at Fraser Lakes, northern Saskatchewan, Canada. *Geol. Assoc. Can. – Mineral. Assoc. Can., Program Abstr*., <http://www.cseg.ca/conventions/abstracts/2010/2010abstracts/0815_GC2010_Composition_and_U-Th-Pb_Chemical_Ages_of_Uranium.pdf>

ANNESLEY, I. R., CUTFORTH, C., BILLARD, D., KUSMIRSKI, R.T., WASYLIUK, K., BOGDAN, T., SWEET, K. & LUDWIG, C. (2009): Fraser Lakes Zones A and B, Way Lake Project, Saskatchewan: geological, geophysical, and geochemical characteristics of basement-hosted mineralization. *Proc. 24th IAGS (Fredericton), Abstr.* **1**, 409-414.

ANNESLEY, I.R. & MADORE, C. (1989): The Wollaston Group and its underlying Archean basement in Saskatchewan: 1989 fieldwork and preliminary observations. *In* Summary of Investigations 1989, Sask. Geol. Surv., Regina, Saskatchewan (54-60).

ANNESLEY, I. R. & MADORE, C. (1994): A geological study of the Wollaston–Mudjatik domain boundary in the Wollaston Lake area, Hearne Province, Saskatchewan. *Sask. Res. Council, Publ.* **R–1230–6–C–94**.

ANNESLEY, I.R. & MADORE, C. (1999): Leucogranites and pegmatites of the sub-Athabasca basement, Saskatchewan: U protore? *In* Mineral Deposits: Processes to Processing (C.J. Stanley *et al*., eds.). Balkema, Rottersdam, The Netherlands (297-300).

ANNESLEY, I.R., MADORE, C., KROGH, T.E., KWOK, Y.Y. & KAMO, S.L. (1999): New U–Pb zircon and monazite geochronological results for Archean and Paleoproterozoic basement to the southeastern part of the Athabasca Basin, Saskatchewan. *In* Summary of Investigations 1999, Vol. 2. Sask. Geol. Surv., Regina, Saskatchewan (90-99).

ANNESLEY, I.R., MADORE, C., KUSMIRSKI, R. & BONLI, T. (2000): Uraninite-bearing granitic pegmatite, Moore Lakes, Saskatchewan: petrology and U–Th–Pb chemical ages. *In* Summary of Investigations 2000, Vol. 2. Sask. Geol. Surv., Regina, Saskatchewan (201-211).

ANNESLEY, I.R., MADORE, C. & PORTELLA, P. (2005): Geology and thermotectonic evolution of the western margin of the Trans-Hudson Orogen: evidence from the eastern sub-Athabasca basement, Saskatchewan. *Can. J. Earth Sci.* **42**, 573-597.

ANNESLEY, I.R., MADORE, C., & SHI, R. (1997a): Thermotectonic evolution of the Wollaston EAGLE Project Area, in Thermotectonic and uranium metallogenic evolution of the Wollaston EAGLE Project area, in Annesley, I.R., Madore, C., Shi, R., and Quirt, D.H., eds. Saskatchewan Research Council, Publication **R-1420-2-C-97**, 1–62.

ANNESLEY, I.R., MADORE, C., SHI, R. & KROGH, T.E. (1997b): U–Pb geochronology of thermotectonic events in the Wollaston Lake area, Wollaston Domain: a summary of 1994–96 results. *In* Summary of Investigations 1997, Sask. Geol. Surv., Regina, Saskatchewan (162-173).

ANNESLEY, I. R., WHEATLEY, K., & CUNEY, M. (2010c): The Role of S-Type Granite Emplacement and Structural Control in the Genesis of the Athabasca Uranium Deposits. *GeoCanada 2010 Conference CD, Extended Abstract* **649**.

ANSDELL, K.M. (2005): Tectonic evolution of the Manitoba– Saskatchewan segment of the Paleoproterozoic Trans-Hudson Orogen, Canada. *Can. J. Earth Sci.* **42**, 741-759.

ATENCIO, D., ANDRADE, M.B., CHRISTY, A.G., GIERÉ, R. & KARTASHOV, P.M. (2010): The pyrochlore supergroup of minerals: nomenclature. *Can. Mineral.* **48**, 673-698.

AUSTMAN, C.L., ANNESLEY, I.R. & ANSDELL, K. (2010b): Mineralogy, geochemistry and economic potential of granitic pegmatite-hosted uranium, thorium, & REE mineralization adjacent to the Athabasca Basin, Saskatchewan, Canada. *In* The Challenge of Finding New Mineral Resources: Global Metallogeny, Innovative Exploration, and New Discoveries (T. Monecke, ed.). *SEG 2010 Conf. (Keystone, Colorado),* CD, Ext. Abstr. F.

AUSTMAN, C.L., ANSDELL, K.M. & ANNESLEY, I.R. (2010a): Petrography and geochemistry of granitic pegmatite- and leucogranite-hosted uranium & thorium mineralization: Fraser Lakes Zone B, northern Saskatchewan, Canada. *Geol. Assoc. Can. – Mineral. Assoc. Can., Program Abstr.,*

<http://www.cseg.ca/conventions/abstracts/2010/2010abstracts/0543_GC2010_Petrography_and_Geochemistry_Uranium_Mineralization.pdf>

BASSON, I.J. & GREENWAY, G. (2004): The Rössing uranium deposit: a product of late-kinematic localization of uraniferous granites in the Central Zone of the Damara Orogen, Namibia. *J. Afr. Earth Sci.* **38**, 413-435.

BASTIN, G.F. & HEIJLIGERS, H.J.M. (1991): Quantitative electron probe microanalysis of ultra-light elements (boron–oxygen). *In* Electron Probe Quantitation (K.J.F. Heinrich & D.E. Newbury, eds.). Plenum Press, New York, N.Y. (145-161).

BEA, F. (1996): Residence of REE, Y, Th, and U in granites and crustal protoliths; Implications for the chemistry of crustal melts: *J. Petr.* **37**, 521-552.

BERNING, J., COOK, R., HIEMSTRA, S.A. & HOFFMAN, U. (1976): The Rössing uranium deposit, South-West Africa. *Econ. Geol.* **71**, 351-368.

BOIRON, M.C., CATHELINEAU, M., & RICHARD, A. (2010): Fluid flows and metal deposition near basement ⁄cover unconformity: lessons and analogies from Pb–Zn–F–Ba systems for the understanding of Proterozoic U deposits. *Geofluids* **10**, 270–292.

BONS, P.D., ARNOLD, J., ELBURG, M.A., KALDA, J., SOESSO, A., & VAN MILLIGEN, B.P. (2004): Melt extraction and accumulation from partially molten rocks: *Lithos* **78**, 25-42.

BOWLES, J.F.W. (1990): Age dating of individual grains of uraninite in rocks from electron microprobe analyses. *Chem. Geol.* **83**, 47-53.

BOYNTON, W.V. (1984): Cosmochemistry of the rare earth elements: meteorite studies, *in*: Henderson, P. (ed.), Rare Earth Element Geochemistry: Elsevier, Amsterdam (63–114).

BRANDELIK, A. (2009): CALCMIN – an EXCEL™ Visual Basic application for calculating mineral structural formulae from electron microprobe analyses. *Comp. Geosci.* **35**, 1540-1551.

BROWN, M. (2007): Crustal melting and melt extraction, ascent and emplacement in orogens: mechanisms and consequences. *Jour. Geol. Soc. Lon.* **164**, 709-730.

BROWN, M. (2010): Melting of the continental crust during orogenesis: the thermal, rheological, and compositional consequences of melt transport from lower to upper continental crust. *Can. J. Earth Sci.* **47**, 655-694.

BROWN, M., KORHONEN, F.J. & SIDDOWAY, C.S. (2011): Organizing melt flow through the crust. *Elements* **7**, 261-266.

BROWN, M., & SOLAR, G.S. (1999): The mechanism of ascent and emplacement of granite magma during transpression: a syntectonic granite paradigm: *Tectonophys.* **312**, 1-33.

BUCHER, K., & FREY, M. (1994): Petrogenesis of Metamorphic Rocks; Springer-Verlag, Berlin, 318 p.

CADDICK, M.J., KONOPÁSEK, J. & THOMPSON, A.B. (2010): Preservation of garnet growth zoning and the duration of prograde metamorphism. *J. Petrol.* **51**, 2327-2347.

CAMECO (2012): Cameco – Mining – Cigar Lake, <http://www.cameco.com/mining/cigar_lake>

CARD, C., PANĂ, D., PORTELLA, P., THOMAS, D.J. & ANNESLEY, I.R. (2007): Basement rocks to the Athabasca Basin, Saskatchewan and Alberta. *In* EXTECH IV: Geology and Uranium Exploration Technology of the Proterozoic Athabasca Basin, Saskatchewan and Alberta (C.W. Jefferson & G. Delaney, eds.). Geol. Surv. Can., Bull. **588**, 69-88.

CARMICHAEL, I.S.E. (1967): The iron–titanium oxides of salic volcanic rocks and their associated ferromagnesian silicates. *Contrib. Mineral. Petrol.* **14**, 36-64.

ČERNÝ, P. & ERCIT, T.S. (2005): The classification of granitic pegmatites revisited. *Can. Mineral.* **43**, 2005-2026.

CESARE, B., SATISH-KUMAR, M., CRUCIANI, G., SHABEER, P. & NODARI, L. (2008): Mineral chemistry of Ti-rich biotite from pegmatite and metapelitic granulites of the Kerala Khondalite Belt (SE India): petrology and further insight into titanium substitutions. *Am. Mineral.* **93**, 327–338.

CHAPPELL, B.J., & WHITE, A.J.R. (1974): Two contrasting granite types. *Pac. Geol.* **8**, 173-174.

CHERNIAK, D. J., WATSON, E. B., GROVE, M., & HARRISON, T. M. (2004): Pb diffusion in monazite: a combined RBS/SIMS study. *Geochim. Cosmochim. Acta* **68**, 829-840.

CLARKE, D.B., HENRY, A.S., AND HAMILTON, M.A. (2005): Composition, age, and origin of granitoid rocks in the Davin Lake area, Rottenstone Domain, Trans-Hudson Orogen, northern Saskatchewan. *Can. J. Earth Sci.* **42**, 599–633.

CLOUTIER, J., KYSER, K., OLIVO, G.R., ALEXANDRE, P., & HALABURDA, J. (2009): The Millennium uranium deposit, Athabasca Basin, Saskatchewan, Canada: an atypical basement-hosted unconformity-related uranium deposit. *Econ. Geol.* **104**, 815–840.

COOMBE, W. (1994): Sediment-hosted base metal deposits of the Wollaston Domain, northern Saskatchewan. *Saskatchewan Energy and Mines Report* **213**, 108 p.

CORRIGAN, D., PEHRSSON, S., WODICKA, N. & DE KEMP, E. (2009): The Paleoproterozoic Trans-Hudson orogen: a prototype of modern accretionary processes. *Geol. Soc. London, Spec. Publ.* **327**, 457-479.

CROWLEY, J. L., & GHENT, E. D. (1999): An electron microprobe study of the U–Th–Pb systematics of metamorphosed monazite: the role of Pb diffusion versus overgrowth and recrystallization. *Chem. Geol.* **157**, 285-302.

CUNEY, M. (2009): The extreme diversity of uranium deposits. *Mineral. Deposita* **44**, 3-9.

CUNEY, M. (2010): Evolution of uranium fractionation processes through time: driving the secular variation of uranium deposit types. Econ. Geol. 105, 553-569.

CUNEY, M., BROUAND, M., LAURI, L., RÄMÖ O.T., KISTER, P., & CAILLAT, C. (2008): Accessory mineral paragenesis and U potential of late orogenic potassic granites of southern Finland. *33rd International Geological Congress, Oslo, Norway* (CD-ROM).

CUNEY, M. & KYSER, T.K. (2008): Deposits related to partial melting. *In* Recent and Not-So-Recent Developments in Uranium Deposits and Implications for Exploration (M. Cuney & K.T. Kyser, eds.) *Mineral. Assoc. Can., Short Course* **39**, 79-95.

DELANEY, G. & TISDALE, D. (1996): Bedrock geology, Fraser Lakes area (part of NTS 74H–2). *In* Summary of Investigations 1996 Vol. 2 (T.I.I. Sibbald, C.T. Harper, D.F. Paterson & P. Guliov, eds.). *Sask. Geol. Surv.,* Regina, Saskatchewan.

DELANEY, G., TISDALE, D. & DAVIES, H. (1996): Stratigraphic relationships and base metal mineralization in the Lower Proterozoic supracrustal assemblage along the Archean Johnson River Inlier, Wollaston Domain, Saskatchewan. *In* Summary of Investigations 1996 (T.I.I. Sibbald, C.T. Harper, D.F. Paterson & P. Guliov, eds.). *Sask. Geol. Surv*., Regina, Saskatchewan (3-11).

DEROME, D., CATHELINEAU, M., CUNEY, M., FABRE, C., LHOMME, T. & BANKS, D.A. (2005): Mixing of sodic and calcic brines and uranium deposition at McArthur River, Saskatchewan, Canada: a Raman and laser-induced breakdown spectroscopic study of fluid inclusions. *Econ.* Geol. **100**, 1529-1545.

FAYEK, M., JANECZEK, J. & EWING, R.C. (1997): Mineral chemistry and oxygen isotopic analyses of uraninite, pitchblende and uranium alteration minerals from the Cigar Lake deposit, Saskatchewan, Canada. *Appl. Geochem.* **12**, 549-565.

FAYEK, M., KYSER, T.K. & RICIPUTI, L.R. (2002): U and Pb isotope analysis of uranium minerals by ion microprobe and the geochronology of the McArthur river and Sue Zone uranium deposits, Saskatchewan, Canada. *Can. Mineral*. 40, 1553-1570.

FETTES, D. & DESMONS, J. (eds.). (2007). Metamorphic Rocks (A Classification and Glossary of Terms: Cambridge, Cambridge University Press, 244 p.

FÖRSTER, H.-J. (1999): The chemical composition of uraninite in Variscan granites of the Erzgebirge, Germany. *Mineral. Mag.* **63**, 239-252.

FÖRSTER, H.-J. (2006): Composition and origin of intermediate solid solutions in the system thorite–xenotime–zircon–coffinite. *Lithos* **88**, 35-55.

FOSTER, R.W. (1970): A geological report on Dynamic Petroleum Products Ltd. Permit No. 1 Geikie River area, Saskatchewan NTS 74H/3 and 74H/4. *Assessment Report* **74H02–0007**.

FOWLER, A.D. & DOIG, R. (1983): The age and origin of Grenville Province uraniferous granites and pegmatites. *Can. J. Earth Sci*. 20, 92-104.

GOAD, B.E. (1990): Granitic pegmatites of the Bancroft area, southeastern Ontario. *Ont. Geol. Surv., Open File Report* 5717.

GROMET, L. P., DYMEK, R. F., HASKIN, L. A., AND KOROTEV, R. L. (1984): The 'North American shale composite' - Its compilation, major and trace element characteristics. *Geochim. Cosmochim. Acta*, **48**, 2469-2482.

HAJNAL, Z., LEWRY, J., WHITE, D.J., ASHTON, K., CLOWES, R., STAUFFER, M., GYORFI, I. & TAKACS, E. (2005): The Sask Craton and Hearne Province margin: seismic reflection studies in the western Trans- Hudson orogen. *Can. J. Earth Sci*. **42**, 403-419.

HAJNAL, Z., WHITE, D.J., TAKACS, E., GYORFI, I., ANNESLEY, I.R., WOOD, G., O'DOWD, C. & NIMECK, G. (2010): Application of modern 2-D and 3-D seismic reflection techniques for uranium exploration in the Athabasca Basin. *Can. J. Earth Sci*. 47, 761-782.

HAMILTON, M.A. & DELANEY, G. (2000): New U–Pb geochronological constraints on the age of basement and cover in the eastern Wollaston Domain, Saskatchewan, and evolution of the SE Hearne Province. *Geol. Assoc. Can. – Mineral. Assoc. Can., Program Abstr*. **25**, 1103 (CD-ROM).

HANDY, M.R., MULCH, A., ROSENAU, N., & ROSENBERG, C.L. (2001): The role of fault zones and melts as agents of weakening, hardening, and differentiation of the continental crust: a synthesis. *In* The nature and tectonic significance of fault zone weakening. (Holdsworth, R.E., Magloughlin, J., Knipe, R.J., Strachan, R.A., and Searle, R.C. eds.) *Geol. Soc. Lon. Spec. Pub.* **186**, 305-332.

HECHT, L. & CUNEY, M. (2000): Hydrothermal alteration of monazite in the Precambrian crystalline basement of the Athabasca basin (Saskatchewan, Canada): implications for the formation of unconformity-related deposits. *Mineral. Deposita* **35**, 791-795.

HENRY, D.J., GUIDOTTI, C.V. & THOMSON, J.A. (2005): The Ti-saturation surface for low-to-medium pressure metapelitic biotites: implications for geothermometry and Ti-substitution mechanisms. *Am. Mineral.* **90**, 316-328.

HOBBS, B.E. & ORD, A. (2010): The mechanics of granitoid systems and maximum entropy production rates. *Phil. Trans. Royal Soc. A* **368**, 53-93.

HOEVE, J., & SIBBALD, T.I.I. (1978): On the genesis of Rabbit Lake and other unconformity-type uranium deposits in northern Saskatchewan, Canada: *Econ. Geol.* **73**, 1450-1473.

HOFFMAN, P.F. (1990): Subdivision of the Churchill province and extent of the Trans-Hudson Orogen. *In* The Early Proterozoic Trans-Hudson Orogen of North America (J.F. Lewry & M.R. Stauffer, eds.). *Geol. Assoc. Can., Spec. Pap*. **37**, 15-39.

HOLDAWAY, M.J. (2000): Application of new experimental and garnet Margules data to the garnet-biotite geothermometer. *Amer. Min*. **85**, 881-892.

HOLDAWAY, M.J. (2001): Recalibration of the GASP geobarometer in light of recent garnet and plagioclase activity models and versions of the garnet–biotite geothermometer. *Amer. Min.* **86**, 1117–1129.

JEFFERSON, C.W., THOMAS, D.J., GANDHI, S.S., RAMAEKERS, P., DELANEY, G., BRISBIN, D., CUTTS, C., PORTELLA, P., AND OLSON, R.A., 2007, Unconformity-associated uranium deposits of the Athabasca Basin, Saskatchewan and Alberta. *In* EXTECH IV: Geology and Uranium Exploration TECHnology of the Proterozoic Athabasca Basin, Saskatchewan and Alberta. (Jefferson C.W., and Delaney, G., eds.) *Geological Survey of Canada Bulletin* **588**, 23–67.

JNR RESOURCES INC. (2012): Home Page <http://www.jnrresources.com>

KEMPE, U. (2003): Precise electron microprobe age determination in altered uraninite: consequences on the intrusion age and the metallogenic significance of the Kirchberg granite (Erzgebirge, Germany). *Contrib. Mineral. Petrol.* **145**, 107-118.

KISTERS, A.F.M., GIBSON, R.L., CHARLESWORTH, E.G. & ANHAEUSSER, C.R. (1998): The role of strain localization in the segregation and ascent of anatectic melts, Namaqualand, South Africa. *J. Struct. Geol*. **20**, 229-242.

KISTERS, A.F.M., WARD, R. A., ANTHONISSEN, C.J. & VIETZE, M.E. (2009): Melt segregation and far-field melt transfer in the mid-crust. *J. Geol. Soc.* **166**, 905-918.

KO, C.B. (1971): Geological report on Dynamic Petroleum Products Ltd. CBS 1837, Sask. N.T.S. *Great Plains Development Company of Canada Ltd. Assessment Report* **74H–2–SW**, 1-23.

KOTZER T.G., & KYSER, T.K. (1995): Petrogenesis of the Proterozoic Athabasca Basin, northern Saskatchewan, and its relation to diagenesis, hydrothermal uranium mineralization and paleohydrology. *Chem. Geol.* **120**, 45–89.

KRETZ, R. (1983): Symbols for rock-forming minerals: *Amer. Min.* **68**, 277-279.

KUKKONEN, I.T. & LAURI, L.S. (2009): Modelling the thermal evolution of a collisional Precambrian orogen: high heat production migmatitic granites of southern Finland. *Precamb. Res.* **168**, 233-246.

KURHILA, M., MÄNTTÄRI, I., VAASJOKI, M., RÄMÖ, O.T. AND NIRONEN, M. (2011): U-Pb geochronological constraints of the late Svecofennian Leucogranites of Southern Finland: *Precamb. Res. 190*, p. 1–24.

KURHILA, M., VAASJOKI, M., MÄNTTÄRI, I., RÄMÖ, T., & NIRONEN, M. (2005): U-Pb ages and Nd isotope characteristics of the lateorogenic, migmatizing microcline granites in southwestern Finland. *Bull. Geol. Soc. Fin*. **77**, 105–128.

KYSER, T.K., & CUNEY, M. (2008): Unconformity-related uranium deposits, in Kyser, T.K., and Cuney, M., eds., Recent and Not-So-Recent Developments in Uranium Deposits and Implications for Exploration. *Min. Assoc. Can Short Course Volume* **39**, 161–219.

LABERGE, J.D. & PATTISON, D.R.M. (2007): Geology of the western margin of the Grand Forks complex, southern British Columbia: high-grade Cretaceous metamorphism followed by early Tertiary extension on the Granby fault. *Can. Journ. Earth Sci*. **44**, 199-228.

LAURI, L.S., RÄMÖ, O.T. & CUNEY, M. (2007): Source characteristics of U-enriched leucogranites of the Svecofennian orogen in southern Finland. *In* Digging Deeper (C.J. Andrew *et al*., eds.*). Proc. 9th Biennial Meeting, Soc. Geol. Applied* **2**, 1165-1168.

LE BRETON, N. & THOMPSON, A.B. (1988): Fluid-absent (dehydration) melting of biotite in metapelite in the early stages of crustal anatexis. *Contrib. Miner. Petrol.* **99**, 226–237.

LE MAITRE, R.W., ed. (2002): Igneous Rocks. A Classification and Glossary of Terms (2nd ed.). Cambridge University Press, Cambridge, U.K.

LENTZ, D. (1991): Radioelement distribution in U, Th, Mo, and rare-earth-element pegmatites, skarns, and veins in a portion of the Grenville Province, Ontario and Quebec. *Can. J. Earth Sci.* **28**, 1-12.

LENTZ, D. (1996): U, Mo, and REE mineralization in late-tectonic granitic pegmatites, southwestern Grenville Province, Canada. *Ore Geol. Rev*. **11**, 197-227.

LEPAGE, L.D. (2003): ILMAT: an Excel worksheet for ilmenite–magnetite geothermometry and geobarometry. *Comp. Geosci.* **29**, 673-678.

LEWRY, J.F. & COLLERSON, K.D. (1990): The Trans-Hudson Orogen: extent, subdivision and problems. *In* The Early Proterozoic Trans-Hudson Orogen of North America (J.F. Lewry & M.R. Stauffer, eds.). *Geol. Assoc. Can., Spec. Pap.* **37**, 1-14.

LEWRY, J.F. & SIBBALD, T.I.I. (1977): Variation in lithology and tectonometamorphic relationships in the Precambrian basement of northern Saskatchewan. *Can. J. Earth Sci.* **14**, 1453-1467.

LEWRY, J.F. & SIBBALD, T.I.I. (1980): Thermotectonic evolution of the Churchill Province in northern Saskatchewan. *Tectonophys.* **68**, 45-82.

LINDSLEY, D.H., &SPENCER, K.J. (1982): Fe-Ti oxide geothermometry: Reducing analyses of coexisting Ti-magnetite (Mt) and ilmenite (Ilm). *Eos* **63**, 471.

LINTHOUT, K. (2007): Tripartite division of the system $2REEPO_4$–$CaTh(PO4)_2$–$2ThSiO_4$, discreditation of brabantite, and recognition of cheralite as the name for members dominated by $CaTh(PO4)_2$. *Can. Mineral.* **45**, 503-508.

LONDON, D. (2008): Pegmatites. *Can. Min. Special Publication* **10**.

LUHR, J.F., CARMICHAEL, I.S.E. & VARECAMP, J.C. (1984): The 1982 eruptions of El Chichón volcano, Chiapas, Mexico: mineralogy and petrology of the anhydrite-bearing pumices. *J. Volc. Geothermal Res.* **23**, 69-108.

MADORE, C., ANNESLEY, I.R. & TRAN, H.T. (1999): Petrology and geochemistry of Paleoproterozoic Wollaston Group metasediments from the eastern Keller Lake–Siemens Lake area, Saskatchewan: a preliminary interpretation. *In* Summary of Investigations 1999, Vol. 2 (G.D. Delaney & C.T. Harper, eds.). *Sask. Geol. Surv.*, Regina, Saskatchewan (80-89).

MADORE, C., ANNESLEY, I.R. & WHEATLEY, K. (2000): Petrogenesis, age, and uranium fertility of peraluminous leucogranites and pegmatites of the McClean Lake/Sue and Key Lake deposit areas, Saskatchewan. *Geol. Assoc. Can. – Mineral. Assoc. Can., Program Abstr.* **25**, 1041(CD-ROM).

MAWDSLEY, J.B. (1952): Uraninite-bearing deposits, Charlebois Lake area, northeastern Saskatchewan. *Can. Inst. Mining Metall. Bull.* **482**, 366-375.

MAWDSLEY, J.B. (1953): Uraninite-bearing fine-grained pegmatite of the Charlebois Lake area northeastern Saskatchewan. *Geol. Soc. Am., Bull.* **64**, 1550 (abstr.).

MAWDSLEY, J.B. (1955): Radioactive pegmatites of northern Saskatchewan. *Can. Mining J.* **76**, 53-56.

MCKECHNIE, C.L., ANNESLEY, I.R., & ANSDELL, K. (2012a): Radioactive abyssal granitic pegmatites and leucogranites in the Wollaston Domain, northern Saskatchewan, Canada: mineral compositions and conditions of emplacement in the Fraser Lakes area. *Can. Mineral.* **50**, 1637-1667.

MCKECHNIE, C.L., ANNESLEY, I.R. & ANSDELL, K. (2012b): Medium- to low-pressure pelitic gneisses of Fraser Lakes Zone B, Wollaston Domain, northern Saskatchewan, Canada: mineral compositions, metamorphic P–T–t path, and implications for the genesis of radioactive abyssal granitic pegmatites. *Can. Mineral.* **50,** 1669-1694.

MCKECHNIE, C.L., ANNESLEY, I.R. & ANSDELL , K. (2013): Geological setting, petrology and geochemistry of granitic pegmatites hosting the Fraser Lakes Zone B U–Th–REE mineralization, Wollaston Domain, northern Saskatchewan, Canada. *Explor. Mining. Geol.*, **21**, 1-26.

MERCADIER, J., RICHARD, A., BOIRON, M.-C., CATHELINEAU, M. & CUNEY, M. (2010): Migration of brines in the basement rocks of the Athabasca Basin through microfracture networks (P-Patch U deposit, Canada). *Lithos* **115**, 121-136.

MERCADIER, J., CUNEY, M., LACH, P., BOIRON, M.-C., BONHOURE, J., RICHARD, A., LEISEN, M. & KISTER, P. (2011): Origin of uranium deposits revealed by their rare earth element signature. *Terra Nova* **23**, 264-269.

MERCADIER, J., ANNESLEY, I.R., MCKECHNIE, C.L., BOGDAN, T.S. & CREIGHTON, S. (2013): Magmatic and metamorphic uraninite mineralization in the western margin of the Trans-Hudson Orogen (Saskatchewan, Canada): major protores for unconformity-related uranium deposits. *Econ. Geol.* **108,** (in press).

MILLER, *C.F.*, MESCHTER MCDOWELL, S., & MAPES, R.W. (2003): Hot and cold granites? Implications of zircon saturation temperatures and preservation of inheritance. *Geology* **31**, 529-532.

MONTEL, J.-M. (1993): A model for monazite/melt equilibrium and application to the generation of granitic magmas. *Chem. Geol.* **110**, 127-146.

MONTEL, J.-M., FORET, S., VESCHAMBRE, M., NICOLLET, C. & PROVOST, A. (1996): Electron microprobe dating of monazite. Chem. Geol. 131, 37-53.

NABELEK, P.I. & GLASCOCK, M.D. (1995): REE-depleted leucogranites, Black Hills, South Dakota: a consequence of disequilibrium melting of monazite-bearing schists. *J. Petrol.* **36**, 1055-1071.

NABELEK, P.I., LIU, M. (2004): Petrologic and thermal constraints on the origin of leucogranites in collisional orogens. *Trans. Royal Soc. Edin. Earth Sci.* **95**, p. 73-85.

NEX, P., HERD, D. & KINNAIRD, J. (2002): Fluid extraction from quartz in sheeted leucogranites as a monitor to styles of uranium mineralization: an example from the Rössing area, Namibia. *Geochem. Explor. Environ., Anal.* **2**, 83-96.

NEX, P.A.M., KINNAIRD, J.A., & OLIVER, G.J.H. (2001): Petrology, geochemistry and uranium mineralization of post-collisional magmatism around Goanikontes, southern Central Zone, Damaran Orogen, Namibia. *J. Afric. Earth Sci.* **33**, 481-502.

ORRELL, S.E., BICKFORD, M.E., & LEWRY, J.F. (1999): Crustal evolution and age of thermotectonic reworking in the western hinterland of the Trans-Hudson Orogen, northern Saskatchewan. *Precamb. Resear.* **95**, 187-223.

PARSLOW, G.R. & THOMAS, D.J. (1982): Uranium occurrences in the Cree Lake Zone. *Mineral. Mag.* **46**, 163-171.

PARSLOW, G.R., BRANDSTÄTTER, F., KURAT, G. & THOMAS, D.J. (1985): Chemical ages and mobility of U and Th in anatectites of the Cree Lake Zone, Saskatchewan. *Can. Mineral.* **23**, 543-551.

PATIÑO DOUCE, A. (1999): What do experiments tell us about the relative contributions of crust and mantle to the origin of granitic magmas? *In* Understanding Granites: Integrating New and Classical Techniques (Castro, A., Fernandez, C., & Vigneresse, J.L., eds.) *Geol. Soc. Lon. Spec. Pub.* **168**, 55-75.

PATTISON, D. R. M., & BÉGIN, N. J. (2007). Zoning patterns in orthopyroxene and garnet in granulites: implications for geothermometry. *J. Meta. Geol.* **12**, 387-410.

PATTISON, D.R.M., CHACKO, T., FARQUHAR, J. & MCFARLANE, C.R.M. (2003): Temperatures of granulite-facies metamorphism: constraints from experimental phase equilibria and thermobarometry corrected for retrograde exchange. *Journ. Petr.* **44**, 867-900.

POUCHOU, J.-L. & PICHOIR, F. (1984): A new model for quantitative x-ray microanalysis. I. Application to the analysis of homogeneous samples. *Rech. Aerosp.* **3**, 13-38.

POWELL, R. & POWELL, M. (1977): Geothermometry and oxygen barometry using coexisting iron–titanium oxides: a reappraisal. *Mineral. Mag.* **41**, 257-263.

RAY, G.E. (1980): Geology of the Parker Lake–Nelson Lake Vicinity. *Sask. Geol. Surv. Rep.* **190**.

RICHARD, A., PETTKE, T., CATHELINEAU, M., BOIRON, M-C., MERCADIER, J., CUNEY, M., & DEROME, D., 2010, Brine–rock interaction in the Athabasca basement (McArthur River U deposit, Canada): consequences for fluid chemistry and uranium uptake. *Terra Nova* **22**, 303–308.

RICHARD, A., BANKS, D.A., MERCADIER, J., BOIRON, M.-C., CUNEY, M., & CATHELINEAU, M. (2011): An evaporated seawater origin for the ore-forming brines in unconformity-related uranium deposits (Athabasca Basin, Canada): Cl/Br and δ 37Cl analysis of fluid inclusions. *Geochim. Cosmo. Acta* **75**, 2792-2810.

RICHARD, A., ROZSYPAL, C., MERCADIER, J., BANKS, D.A., CUNEY, M., BOIRON, M.-C., & CATHELINEAU, M. (2012) Giant uranium deposits formed from exceptionally uranium-rich acidic brines. *Nat. Geosci.* **5**, p. 142-146.

RIEDER, M., CAVAZZINI, G., D'YAK ONOV, YU. S., FRANK- KAMENETSKII, V. A., GOTTARDI, G., GUGGENHEIM, S., KOVAL, P.V., MUELLER, G., NEIVA, A.M.R., RADOSLOVICH, E.W., ROBERT, J.-L., SASSI, F.P., TAKEDA, H., WEISS, Z. & WONES, D.R. (1998): Nomenclature of the micas. *Can. Mineral.* **36**, 905-912.

SASKATCHEWAN RESEARCH Council (2012): Uranium and Geochemistry: <http://www.src.sk.ca/html/labs_facilities/geo_labs/uranium/index.cfm>.

SAWYER, E.D. (2008): Atlas of Migmatites. *Can. Min. Special Publication* **9**, 371 p.

SAWYER, E.W., CESARE, B. & BROWN, M. (2011): When the continental crust melts. *Elements*. **7**, 229-234.

SCHNEIDER, D.A., HEIZLER, M.T., BICKFORD, M.E., WORTMAN G.L., CONDIE, K.C., & PERILLI, S. (2007): Timing constraints of orogeny to cratonization: Thermochronology of the Paleoproterozoic Trans-Hudson Orogen, Manitoba and Saskatchewan, Canada. *Precamb. Res.* **153**, 65–95.

SEARLE, M.P., ELLIOTT, J. R., PHILLIPS, R. J., & CHUNG, S.L. (2011): Crustal-lithospheric structure and continental extrusion of Tibet. *J. Geol. Soc. Lond.* **168**, 633-672.

SEYDOUX-GUILLAUME, A. M., PAQUETTE, J. L., WIEDENBECK, M., MONTEL, J. M., & HEINRICH, W. (2002): Experimental resetting of the U–Th–Pb systems in monazite. *Chem. Geol.* **191**, 165-181.

SKYTTÄ, P., & MÄNTTÄRI, I. (2008): Structural setting of late Svecofennian granites and pegmatites in Uusimaa Belt, SW Finland: Age constraints and implications for crustal evolution. *Precamb. Res.* **164**, 86–109.

SOLAR, G.S., & BROWN, M. (2001): Petrogenesis of migmatites in Maine, USA: Possible source of peraluminous leucogranite in plutons. *J. Petr.* **42**, 789-823.

SPEAR, F.S., KOHN, M.J. & CHENEY, J.T. (1999): P -T paths from anatectic pelites. *Contrib. Mineral. Petrol.* **134**, 17-32

SPENCER, K.J. & LINDSLEY, D.H. (1981): A solution model for coexisting iron–titanium oxides. *Am. Mineral.* **66**, 1189-1201.

SRC (2012): Uranium and Geochemistry: <http://www.src.sk.ca/html/labs_facilities/geo_labs/uranium/index.cfm>.

STILLING, A., CERNY, P., & VANSTONE, P.J. (2006): The Tanco Pegmatite at Bernic Lake, Manitoba: XVI. Zonal and bulk compositions and their petrogenetic significance. *Can. Min.* **44**, p. 599-623.

STORMER JR, J.C. (1983): The effects of recalculation on estimates of temperature and oxygen fugacity from analyses of multi-component iron-titanium oxides. *Amer. Mineral*. **68**, 586-594.

THOMAS, D.J. (1983): *Distribution, Geological Controls and Genesis of Uraniferous Pegmatites in the Cree Lake Zone of Northern Saskatchewan*. M.Sc. thesis, Univ. Regina, Regina, Saskatchewan.

TINDLE, A. (2011): Free Mineral Recalculation Software: <http://www.open.ac.uk/earth-research/tindle/AGTWeb-Pages/AGTSoft.html>.

TINDLE, A.G. & WEBB, P.C. (1990): Estimation of lithium contents in trioctrahedral micas using microprobe data; application to micas from granitic rocks. *Eur. J. Mineral.* **2**, 595-610.

TRAN, H.T. (2001): *Tectonic Evolution of the Paleoproterozoic Wollaston Group in the Cree Lake Zone, Northern Saskatchewan, Canada*. Ph.D. thesis, Univ. Regina, Regina, Saskatchewan.

TRAN, H.T., YEO, G.M. & BRADLEY, S. (1998): Geology of the Daly–Suttle–Middle Foster lakes area, eastern Wollaston Domain (NTS 74A–5, –11, and 12), east sheet. *In* Summary of Investigations 1998 (G.D. Delaney & C.T. Harper, eds.). *Sask. Geol. Surv.*

TRAN, H.T., ANSDELL, K., BETHUNE, K., WATTERS, B., AND ASHTON, K. (2003): Nd isotope and geochemical constraints on the depositional setting of Paleoproterozoic metasedimentary rocks along the margin of the Archean Hearne craton, Saskatchewan, Canada. *Precamb. Res.* **123**, 1–28.

TRAN, H.T., ANSDELL, K.M., BETHUNE, K.M., ASHTON, K., & HAMILTON, M.A. (2008): Provenance and tectonic setting of Paleoproterozoic metasedimentary rocks along the eastern margin of Hearne craton: Constraints from SHRIMP geochronology, Wollaston Group, Saskatchewan, Canada. *Precamb. Res.* **167**, 171-185.

TUCCILLO, M. E., ESSENE, E. J., & VAN DER PLUIJM, B. A. (1990): Growth and retrograde zoning in garnets from high-grade, metapelites: Implications for pressure-temperature paths. *Geology* **18**, 839-842.

TURNER, F.J. (1981): *Metamorphic Petrology: Mineralogical, Field, and Tectonic Aspects*. Second Edition, Hemisphere Publishing Corporation, New York.

VAN BREEMEN, O., HARPER, C.T., BERMAN, R.G., & WODICKA, N. (2007): Crustal evolution and Neoarchean assembly of the central–southern Hearne domains: Evidence from U–Pb geochronology and Sm–Nd isotopes of the Phelps Lake area, northeastern Saskatchewan. *Precamb. Res.* **159**, 33–59.

VERNON, R.H. & CLARKE, G. (2008): *Principles of Metamorphic Petrology*. Cambridge University Press, Cambridge, U.K.

VIGNERESSE, J-L., BARBEY, P., & CUNEY, M. (1996): Rheological transitions during partial melting and crystallization with application to felsic magma segregation and transfer. *J. Petr.* **37**, 1579-1600.

VILLAROS, A., STEVENS, G., MOYEN, J-F., & BUICK, I.S. (2009): The trace element compositions of S-type granites: evidence for disequilibrium melting and accessory phase entrainment in the source. *Contrib. Min. Petr.* **158**, 543-561.

WARD, R.A., STEVENS, G. & KISTERS, A. (2008): Fluid and deformation induced partial melting and melt volumes in low-temperature granulite-facies metasediments, Damara Belt, Namibia. *Lithos* **105**, 253-271.

WATSON, E.B. & HARRISON, T.M. (1983): Zircon saturation revisited: temperature and composition effects in a variety of crustal magma types. *Earth Planet. Sci. Lett.* **64**, 295-304.

WATT, G.R. (1995): High-thorium monazite-(Ce) formed during disequilibrium melting of metapelites under granulite facies conditions. *Mineral. Mag.* **59**, 735-743.

WEAVER, B., AND TARNEY, J. (1984): Empirical approach to estimating the composition of the continental crust. *Nature* **296**, 575-577.

WEI, C. J., POWELL, R. & CLARKE, G. L. (2004): Calculated phase equilibria for low- and medium-pressure metapelites in the KFMASH and KMnFMASH systems. J. Met. Geol. 22, 495-508.Weinberg, R., 1999, Mesoscale pervasive felsic magma migration: alternatives to dyking: Lithos, v. 46, p. 393–410.

WEINBERG, R.F. & MARK, G. (2008): Magma migration, folding and disaggregation of migmatites in the Karakoram Shear Zone, Ladakh, NW India. *Geol. Soc. Am., Bull.* **120**, 994-1009.

WHITNEY, D.L. & EVANS, B.W. (2010): Abbre*via*tions for names of rock-forming minerals. *Am. Mineral.* **95**, 185-187.

WILSON, S. A., 2009, Granodiorite, Silver Plume, Colorado, GSP-2, U. S. Geological Survey, Certificate of Analysis. <http://minerals.cr.usgs.gov/geo_chem_stand/granodiorite.html>

WORLD NUCLEAR ASSOCIATION (2011): World Uranium Mining. <http://www.world-nuclear.org/info/inf23.html>

WU, C-M., ZHANG, J. & REN, L-D. (2004): Empirical garnet–biotite–Empirical garnet–biotite–plagioclase–quartz (GBPQ) geobarometry in medium- to high-grade metapelites. J. Petrol. 45, 1907-1921.

YEO, G.M. & DELANEY, G. (2007): The Wollaston Supergroup, stratigraphy and metallogeny of a Paleoproterozoic Wilson cycle in the Trans-Hudson orogen, Saskatchewan. *In* EXTECH IV: Geology and Uranium Exploration TECHnology of the Proterozoic Athabasca Basin, Saskatchewan and Alberta (C.W. Jefferson & G. Delaney, eds.). *Geol. Surv. Can., Bull.* **588**, 89-117.

APPENDIX A

MODAL MINERALOGY OF THIN SECTIONS FROM FRASER LAKES ZONE B

Table A-1. Modal Mineralogy of thin sections from Fraser Lakes Zone B

Samples		Minerals																												Meta. Grade		Deformation		Lithology
DDH	Depth (m)	Qtz	Kfs	Pl	Bt	Ms	Chl	Amp	Cpx/ Opx	Grt	Crd	Sil	Gr	Clay	Cal/ Dol	Ilm	Mgt	Py/ Ccp	Hem	Fl	Ep	Rt/ Lcx	Ttn	Aln	Urn/ Thr	Ap	Mnz	Zrn	O	Peak	Retro	Ductile	Brittle	
WYL-09-50	196.6	3		3	2	tr	+	2						tr	1			+	tr							+		tr		U Amp?	Gsch/ Hydro	3-4	2	Tonalitic Orthogneiss
WA08-0-0046	n/a	3	+	4	1	tr		3								tr		tr	tr		tr					tr				U Amp?	Gsch	3-4	2-3	Tonalitic Orthogneiss
WYL-09-49	53.9	2	+	4	3	tr	+		2					tr		tr		tr	tr			tr				tr		tr		U Amp?	Gsch/ Hydro	4	2	Granodioritic to Tonalitic Orthogneiss
WYL-09-49	73.0	2	+	4	2	+	tr		2					+		tr						tr						tr		U Amp?	Gsch	3-4	3-4	Tonalitic Orthogneiss
WYL-08-525	72.0	2		3	1	tr	tr	3	2							+	+	+	tr			tr				tr				U Amp?	Gsch	4	2	Tonalitic Orthogneiss
WYL-09-49	83.4	4	1	3	2	tr	tr									+	+		tr	tr		tr		tr		tr		tr		U Amp?	Gsch	4	1-2	Tonalitic Orthogneiss
WYL-09-50	237.0	+	+	5	1	tr	tr	3	2					tr		tr	+		tr							tr		tr		U Amp?	Gsch/ Hydro	2-3	2	Quartz Dioritic Orthogneiss
WYL-09-49	88.0	4	3	3	+	tr	1							tr	+				+	+	+	tr		tr				+		U Amp?	Gsch	3	2	Granitic Orthogneiss
WYL-09-46	44.7	3	2	3	1	tr	1							tr	tr				+	+		+						tr		U Amp?	Gsch	4	2	Granodioritic Orthogneiss
WYL-08-526	37.2	2	3	4	1	tr	2	1						tr	+	+	+	tr	tr	tr		tr			tr			tr		U Amp?	Gsch/ Hydro	3	2	Granitic Orthogneiss
WYL-09-50	252.7	3	3	2	1	+	+							+	tr				tr	tr		tr				tr		tr		U Amp?	Gsch	3-4	1-2	Granitic Orthogneiss
WYL-09-44	93.1	4	3	3	1	t	t							t	t			t	t	t			t	t		t		t		U Amp?	Gsch/ Hydro	3-4	2-3	Granitic Orthogneiss
WYL-09-50	37.5	3	4	2	3	+	1			3	1	1	1			tr			+			tr					tr			L Gran	Gsch	3-4	2-3	Grt-Crd-Sill-Gr-Spl Pelitic Gneiss
WYL-09-50	174.5	3	3	1	3	+	tr				+	2	1	+					tr		1						tr			L Gran	Hydro	4	4	Crd-Sill-Gr Pelitic Gneiss
WYL-09-50	179.9	3	1	2	5	+	+			2			+	+				+	tr	+	+	tr		+			+	+		U Amp	Gsch/ Hydro	3-4	2-3	Grt-Gr-Py Pelitic Gneiss
WYL-08-525	21	2	3	3	3	+	tr			2			tr						tr	tr		tr		tr		tr	tr			U Amp	Gsch/ Hydro	3-4	2	Grt Pelitic gneiss
WYL-09-50	171.7b	3	2	3	3	tr	+			3	+		+					+	tr			tr					+			L Gran	Gsch	4	3-4	Grt-Crd-Gr-Py-Cp Pelitic Gneiss

Samples		Minerals																												Metamorphic Grade		Deformation		Lithology
DDH	Depth (m)	Qtz	Kfs	Pl	Bt	Ms	Chl	Amp	Cpx/ Opx	Grt	Crd	Sil	Gr	Clay	Cal/ Dol	Ilm	Mag	Py/ Ccp	Hem	Fl	Ep	Rt/ Lcx	Ttn	Aln	Urn/ Thr	Ap	Mnz	Zrn	O	Peak	Retro	Ductile	Brittle	
WYL-09-49	41.4	3	1	1	3	+	+			2	3		+					1	+	tr		+				tr	tr	tr		L Gran	Gsch/ Hydro	4	2-3	Grt-Crd-Gr-Py Pelitic Gneiss
WYL-09-49	36.1	3	3	2	3	tr	+			2	1	+	+					+		tr						tr	tr	tr		L Gran	Gsch	4	2	Grt-Crd-Sill-Gr Pelitic Gneiss
WYL-09-50	225	1	2	3	2	tr	+		2	2	tr		tr	tr		+						tr						tr		L Gran	Gsch	4	2	Opx-Grt Pelitic Gneiss
WYL-10-61	70.7	3	2	2	2	+	1				+		1					1	+		tr	tr	tr			tr	tr			U Amp	Gsch/ Hydro	4-5	2-3	Gr Crd Pelitic Gneiss
WYL-10-61	88.9	2	3		2	+	tr				3		1					tr	tr		tr		tr			tr		tr		U Amp	Gsch/ Hydro	4-5	3-4	Crd Gr Pelitic Gneiss
WYL-10-61	128.0	7	1	+	1	tr	+			tr	+		+	1	tr	tr		1	tr	tr		tr	tr	tr		tr	tr	tr		L Gran	Gsch/ Hydro	3-4	3-4	Gr Gneiss + Qtz vein
WYL-10-61	154.2	1	4	2	2	tr	tr			1			+	+	tr												tr	tr		U Amp	Gsch/ Hydro	3-4	2-3	Grt Gr Pelitic Gneiss
WYL-09-44	61.4	2	+	4	4	tr				1									tr			tr				tr	tr	tr		U Amp	Gsch/ Hydro	3-4	3-4	Grt Pelitic Gneiss
WYL-09-49	50.7	3	1	2	3	tr	1			3	+			+				+	tr			+	+				+	tr		L Gran	Gsch/ Hydro			Grt-Crd-Py Pelitic Gneiss
WYL-09-49	45.3	3			3	+	2			2	3		1	1		tr		3	4	+		tr					+			L Gran	Hydro	4	4-5	Grt-Crd-Gr-Py Pelitic Gneiss
WYL-09-50	67.9	3	3	1	2	+	2			1	2		tr	+	2	tr		tr	+	tr		tr					tr			L Gran	Gsch/ Hydro	3-4	4	Grt-Crd Pelitic gneiss
WYL-09-50	171.7	3	2	3	3	+	2			3	+		tr					+	tr			tr					+			L Gran	Gsch/ Hydro	3-4	3-4	Grt-Crd Pelitic gneiss
WYL-08-525	192.8	4	2	3	3	tr	+				+	3		tr		+			+			+				tr	+	+		U Amp	Gsch/ Hydro	4	2-3	Crd-Sill Pelitic Gneiss
WYL-08-525	202.9	3	2	3	4	tr	+			1	+	2							tr	+		tr					+	tr		U Amp	Gsch/ Hydro	4	3	Grt-Crd-Sill pelitic gneiss
WYL-08-525	210.1	4	3	1	2	tr				2	+	2						tr	tr	tr						tr	tr	+		U Amp	Gsch/ Hydro	4	3	Grt-Crd-Sill pelitic gneiss
WYL-10-62	44.8	5	1	3	1	tr	tr						tr	+		tr	1	tr		tr		tr			tr	tr				U Amp	Gsch/ Hydro	3-4	2-3	Pegmatite + Pelitic Gneiss
WYL-10-62	60.1	2	4	+	1	+	+						2	+		tr		2	tr	tr		tr	tr			tr	tr	tr		U Amp	Gsch/ Hydro	4-5	2-3	Gr Pelitic Gneiss
WYL-10-62	66.4	2	4		+	1	tr				3		1	+		tr		tr	+		tr		tr			tr	tr			L Gran	Gsch/ Hydro	4-5	2-3	Crd Gr Pelitic Gneiss
WYL-10-62	68.9	4	4	+	2	tr	tr				tr	tr	1	+				+					tr				tr			L Gran	Gsch	4-5	1-2	Gr Pelitic Gneiss
WYL-10-62	73.9	7			2	tr	tr			2								tr				tr	tr	tr				tr		M Amp	Gsch	3-4	3-4	Grt Migmatitic Pelitic gneiss
WYL-10-62	79.4	+	tr	1	7	tr	tr			2				tr				tr				tr	tr	tr	tr			tr		M Amp	Gsch	3-4	2-3	Grt migmatitic Pelitic Gneiss
WYL-10-62	85.7	5	+	1	3					2				tr	tr			tr								tr	tr			U Amp	Gsch/ Hydro	3-4	2-3	Grt migmatitic Pelitic Gneiss

Samples		Minerals																												Meta. Grade		Deformation		Lithology
DDH	Depth (m)	Qtz	Kfs	Pl	Bt	Ms	Chl	Amp	Cpx/ Opx	Grt	Crd	Sil	Gr	Clay	Cal/ Dol	Ilm	Mag	Py/ Ccp	Hem	Fl	Ep	Rt/ Lcx	Ttn	Aln	Urn/ Thr	Ap	Mnz	Zrn	O	Peak	Retro	Ductile	Brittle	
WYL-10-62	87.1	2	+	1	6	tr	+	tr		tr	tr				1			tr	+			tr		tr		tr		tr		U Amp	Gsch/ Hydro	3-4	4-5	Grt-Crd Pelitic gneiss
WYL-09-50	166.3	3	1?	2?	1	tr	+			6		+		+	tr?			tr	tr	tr	tr	tr	tr		tr		tr	tr		Amp	Hydro	2	4	Grt pelitic gneiss/ Qtz-rich pegmatite
WYL-09-50	225	3	1	+	3	1	1		1	2	3		tr	tr		tr		tr	tr	tr		tr				tr	tr	tr		Amp	Hydro	3-4	2	Grt-bearing pelitic gneiss
WYL-08-525	134.7	3	3	3	2	1	1							tr					2	tr		+		+	tr	tr		+		Amp	Hydro	2	4	Pegmatite
WYL-08-525	168.2	8		+	tr	1	1												+											Amp	Hydro	?	?	Pegmatite
WYL-08-525	207.2	8	1		2	tr	tr							tr	tr			+	+					tr	+	tr		+		Amp	Gsch/ Hydro	3-4	2	Qtz-rich Pegmatite
WYL-09-44	68.5	5	3	2	+	+	tr							+	tr				tr	tr					tr		tr	tr		Amp	Gsch/ Hydro	1-2	3-4	Pegmatite
WYL-09-50	14.3	3	2	2	+	1	+	2	2					tr	+				+				1	tr		+		tr		Amp	Gsch/ Hydro	2	2	Calc-silicate alt. Pegmatite w/ myrmekite (1) + perthite (1)
WYL-09-50	16.5	tr	2	7		tr	tr							tr					tr				+			tr				Amp	Gsch	2	2	Alkali Fsp-rich Pegmatite; w/ perthite (6)
WYL-09-50	18.2	+	5	5	1	tr	2	1	2					tr	tr							+	tr		tr	1			tr	Amp	Gsch/ Hydro	4	2	Fsp-rich Pegmatite; w/ myrmekite (1) + perthite (2)
WYL-09-50	64.1	2		9	tr	tr	tr											tr	tr	tr										Amp	Gsch/ Hydro	2-3	2	Fsp-rich (Perthite) Pegmatite
WYL-09-50	159	6	3	2	+	+	+							tr	tr			+	tr		tr	tr			+			+		Amp	Gsch	3	3-4	Pegmatite
WYL-09-50	160.5	4	3	4	+	1	+							tr					tr			tr						tr		Amp	Gsch	2-3	3-4	Pegmatite; w/ myrmekite & perthite
WYL-09-50	161.4	6	2	3	1	tr	tr							tr					tr	tr	tr	tr	tr	tr				+		Amp	Gsch	2-3	2	Pegmatite; w/ myrmekite & perthite
WYL-09-50	166.2	3			4		tr			2			+		+			tr	+	+	tr	tr	+	+	tr			tr	tr	Amp	Gsch	2	3	Bt-rich pegmatite?
WYL-09-50	182.5	8			2		+			1										+			+	tr	+		tr	+		Amp		2	3	Grt-bearing, Qtz-rich Pegmatite
WYL-09-50	215.8	3		3	1	+	2							tr	+			+	1	+		1		1	1			1	+	Amp	Hydro	2-3	4	Pegmatite

Samples		Minerals																												Metamorphic Grade		Deformation		Lithology
DDH	Depth (m)	Qtz	Kfs	Pl	Bt	Ms	Chl	Amp	Cpx/ Opx	Grt	Crd	Sil	Gr	Clay	Cal/ Dol	Ilm	Mgt	Py/ Ccp	Hem	Fl	Ep	Rt/ Lcx	Ttn	Aln	Urn/ Thr	Ap	Mnz	Zrn	O	Peak	Retro	Ductile	Brittle	
WYL-09-50	216.5	3		4	3	+	tr							tr	+			+		+	1				+	+		+	tr	Amp	Hydro	3	2-3	Pegmatite
WYL-09-50	171.7a	8	2		+	+	+			1			+	tr	1				+	tr								tr	tr	Amp		2	3-4	Qtz-rich Pegmatite
WA-08-0-2026	n/a	5		4	2	+	+								tr	+	1	tr	1	tr		tr		+	+			+		Amp	Hydro	2	3-4	Pegmatite (outcrop)
WYL-09-44	69.0	3	4	4	+	tr	tr							+	tr			tr									tr	tr		Amp	Hydro	1-2	3-4	Pegmatite
WYL-09-44	72.3	2	5	3	+	tr	tr							+	tr				+	tr		tr			+		+			Amp	Gsch/ Hydro	3	2-4	pegmatite
WYL-09-44	73.4	5	2	2	3	tr	tr				tr?			+	tr			tr	tr			tr					tr	tr	tr	Amp	Gsch/ Hydro	1-2	3-4	Pegmatite
WYL-09-44	76.1	6	1	2	+	tr	tr							tr	tr	+	1	tr	+			tr					tr	tr		Amp	Gsch/ Hydro	2-3	4	Pegmatite
WYL-09-44	76.4	5	+	1	+	tr	+							tr	tr	tr	4	tr	tr			tr			tr		+	tr	+	Amp	Gsch/ Hydro	2-3	4	Pegmatite
WYL-09-46	26.9	7	+	tr	3		tr								tr			tr		tr	tr	tr		tr	tr			+		Amp	Gsch/ Hydro	1-2	2-3	Qtz-rich Pegmatite
WYL-09-46	30.8	4	1	2	3	tr	1				+			+				tr	tr	tr	tr	tr		tr			tr	tr		Amp	Gsch/ Hydro	2-3	3-4	Qtz-rich Pegmatite
WYL-09-46	31.1	6	+	1	3	tr	+								tr			tr	+	tr	tr	tr		tr		tr	+	tr		Amp	Gsch/ Hydro	2-3	3-4	Qtz-rich Pegmatite
WYL-09-46	32.6	2	1	2	6	tr	tr							+	tr			tr		tr				tr			tr			Amp	Gsch/ Hydro	1-2	1-2	Bt-rich Pegmatite
WYL-09-46	34.0	2	1	3	6		tr							+	tr	tr		tr	tr	tr		tr		tr			tr			Amp	Gsch/ Hydro	1-2	3-4	Bt-rich Pegmatite
WYL-09-46	35.0	6	+		5									tr	tr			+	tr	tr		tr		tr	tr			tr		Amp	Gsch/ Hydro	4-5	3-4	Qtz-Bt Pegmatite
WYL-09-46	36.6	+	+	+	8		tr			2	tr			+	tr			+	tr	tr		tr						tr		Amp	Gsch/ Hydro	2-3	3-4	Bt-rich Pegmatite
WYL-09-46	37.0	2	+	1	4	tr	3			1				+	tr			tr	+			+	tr		tr	tr		tr		Amp	Gsch/ Hydro	1-2	1-2	Bt-rich Pegmatite
WYL-09-46	42.8	+	+	3	7						tr			+				tr	tr	tr				+			tr			Amp	Gsch/ Hydro	1-2	1-2	Bt-rich Pegmatite
WYL-09-46	44.7	5	3	2	1	tr	+							+									tr			tr	tr	tr		Amp	Gsch/ Hydro	1-2	1-2	Pegmatite
WYL-09-46	47.3	8	1	+	+		tr							+		+	1		tr	tr		tr	tr					tr		Amp	Gsch/ Hydro	1-2	1-2	Qtz-rich Pegmatite
WYL-09-46	81.6	2	5	1	2	tr	2							+	tr	tr	+	tr	tr	tr		tr	tr					tr		Amp	Gsch/ Hydro	2-3	1-2	Alkali-Fsp Pegmatite
WYL-09-46	83.0	6	2	2	tr	tr	tr							+	tr	+	+	tr	1				tr		tr	tr	tr	tr		Amp	Gsch/ Hydro	1-2	3-4	Qtz-rich Pegmatite
WYL-09-46	90.8	7	+	2	1	tr	tr			+				tr	tr		tr	tr		tr							tr	tr		Amp	Gsch/ Hydro	1-2	1-2	Qtz-rich Pegmatite

Samples		Minerals																												Metamorphic Grade		Deformation		Lithology
DDH	Depth (m)	Qtz	Kfs	Pl	Bt	Ms	Chl	Amp	Cpx/ Opx	Grt	Crd	Sil	Gr	Clay	Cal/ Dol	Ilm	Mgt	Py/ Ccp	Hem	Fl	Ep	Rt/ Lcx	Ttn	Aln	Urn/ Thr	Ap	Mnz	Zrn	O	Peak	Retro	Ductile	Brittle	
Trench 3	n/a	2	+	3	6	tr	tr							+					+			tr			tr		tr	+		Amp	Gsch/ Hydro	3	3-4	Bt-rich Pegmatite
Trench2-2	n/a	1	1	+	8	tr								tr	+	tr		+	tr	+					1			+	tr Mo	Amp	Hydro	2-3	2-3	Mo-bearing, Bt-rich Pegmatite
Trench 2-1	n/a	1	2	5	2	tr	tr							+				tr	+					+	+			tr		Amp	Hydro	2-3	3	Pl-rich Granitic Pegmatite
Trench 1	n/a	2	3	4	2	+								+		+	+	tr	+			tr		tr	+					Amp	Hydro	2-3	3-4	Pegmatite
QTPEG 0040-2	n/a	9	+	+	tr	tr								tr					tr						tr			tr		Amp	Hydro	1	2-3	Qtz-rich Pegmatite
WYL-10-61	70.7	3	2	2	2	+	1				+		tr	tr	tr			tr	tr	tr		tr	tr				tr	tr		Amp	Gsch/ Hydro	1-2	2-3	Alkali-Fsp Pegmatite
WYL-10-61	88.9	2	3		2	+	tr				3			tr	tr			tr						tr		tr		tr		Amp	Gsch/ Hydro	3-4	2-3	Bt-rich Pegmatite
WYL-10-61	135.4	5	3	3	tr	tr	tr							tr	tr			tr				tr	tr	tr				tr		Amp	Gsch/ Hydro	1-2	3-4	Pegmatite
WYL-10-61	154.2	1	4	2	2	tr	tr			1				+	tr			tr	tr	tr										Amp	Gsch/ Hydro	1-2	2-3	Pegmatite
WYL-10-61	158.2	5	5		1		tr							tr	tr			tr		tr		tr	tr		tr		tr	tr		Amp	Gsch/ Hydro	4-5	2-3	Pegmatite
WYL-10-61	162.0	3			6	tr	tr			2				tr	tr			tr				tr				tr	tr			Amp	Gsch/ Hydro	3-4	2-3	Bt-rich Pegmatite
WYL-10-61	163.5	1	+	5	3	tr	tr			2				tr	tr			tr				tr	tr					tr		Amp	Gsch/ Hydro	1-2	3-4	Pegmatite
WYL-10-61	190.3	7	+	1	+	tr	tr							+	tr			tr						tr	tr			tr		Amp	Gsch/ Hydro	1-2	2-3	Qtz-rich Pegmatite
WYL-10-61	202.8	1	+	5	5	tr		tr						tr	tr	tr	2	tr	tr	tr		tr	tr	tr	tr			+		Amp	Gsch/ Hydro	1-2	3-4	Qtz-rich Pegmatite
WYL-10-62	44.8	5	1	3	1	tr	tr						tr	+	tr	tr		1	tr		tr		tr			tr	tr			Amp	Gsch/ Hydro	3-4	2-3	Pegmatite + Pelitic Gneiss
WYL-10-62	70.7	1	1	8		tr					Tr			+				tr	tr				tr		+		tr			Amp	Gsch/ Hydro	1-2	3-4	Pl-rich Pegmatite
WYL-10-62	83.9	5	3	+	2	tr	tr			+				tr				tr		tr		tr			tr			tr		Amp	Gsch/ Hydro	1-2	3-4	Grt-bearing pegmatite
WYL-10-62	92.0	3	+	5	2	tr	tr							+				tr	+	tr		tr		tr	tr		tr	+		Amp	Gsch/ Hydro	1-2	4-5	Pegmatite
WYL-10-62	93.5	7			3	tr	tr								tr			tr	tr	tr		tr		tr	tr			tr		Amp	Gsch/ Hydro	1-2	3-4	Qtz-rich Pegmatite
WYL-10-62	107.9	3	2	5	1	tr	tr							tr				tr		tr		tr	tr	tr			tr	tr		Amp	Gsch/ Hydro	1-2	3-4	Pl-rich Pegmatite
WYL-10-62	112.2	7	+	1	+	tr	+							tr	tr	tr	1	tr		tr		tr		tr	tr			tr		Amp	Gsch/ Hydro	1-2	3-4	Qtz-rich Pegmatite

Code for modal estimate (%)			**Ductile and Brittle Deformation**						**Metamorphic Grades**		
	=	absent	1	=	very weak	Qtz	=	Quartz	L = lower	M = middle	U = upper
tr	=	trace	2	=	weak	Kfs	=	K-feldspar	Gsch	=	Greenschist
+	=	1 - 5	3	=	moderate	Pl	=	Plagioclase	Amp	=	Amphibolite
1	=	5 - 10	4	=	strong	Myr	=	Myrmektite	Granu	=	Granulite
2	=	10 - 20	5	=	very strong	Per	=	Perthite	Hydro	=	Hydrothermal alteration
3	=	20 - 30				Bt	=	Biotite	Peak	=	Peak metamorphic conditions
4	=	30 - 40				Ms/Ser	=	Muscovite/Sericite	Retro	=	Retrograde metamorphic conditions
5	=	40 - 50				Chl	=	Chlorite			or late hydrothermal alteration
6	=	50 - 60				Act/Tr	=	Actinolite/Tremolite			
7	=	60 - 70				Cpx	=	Clinopyroxene			
8	=	70 - 80				Grt	=	Garnet			
9	=	80 - 90				Crd	=	Cordierite			
10	=	90 - 100				Sil	=	Sillimanite			
						Gr	=	Graphite			
						Clay	=	Clay			
						Cal/Dol	=	Calcite/Dolomite			
						Ilm	=	Ilmenite			
						Mag	=	Magnetite			
						Py/Ccp	=	Pyrite/Chalcopyrite			
						Hem	=	Hematite			
						Fl	=	Fluorite			
						Ep/Zo	=	Epidote/Zoisite			
						Rt/Lcx	=	Rutile/Leucoxene			
						Ttn	=	Titanite			
						Aln	=	Allanite			
						Ur/Th	=	Uraninite/Thorite			
						Ap	=	Apatite			
						Mnz	=	Monazite			
						Zrn	=	Zircon			
						Oth	=	Other			

APPENDIX B

FRASER LAKES ZONE B GEOCHEMICAL DATA

Table B-1. Fraser Lakes Zone B geochemical data
Supplementary Data Table for Chapter 2 (McKechnie *et al.* 2013).

Sample Number	Lithology	Area	SiO2	SiO2 xrf	TiO2	TiO2 xrf	Al2O3	Al2O3 xrf	Fe2O3t
WYL-09-49-83.4	Granodioritic to Granitic Orthogneiss	West	74.10	-	0.32	-	12.40	-	2.77
WYL-09-49-88.0	Granodioritic to Granitic Orthogneiss	West	74.40	-	0.27	-	13.10	-	1.88
WYL-09-50-252.7	Granodioritic to Granitic Orthogneiss	West	74.80	-	0.25	-	13.50	-	1.70
WA-08-0-0046	Tonalitic to Quartz Dioritic Orthogneiss	West	62.20	59.25	0.85	0.90	12.90	12.35	9.52
WYL-09-50-196.6	Tonalitic to Quartz Dioritic Orthogneiss	West	66.80	-	0.72	-	12.30	-	7.49
WYL-09-50-237	Tonalitic to Quartz Dioritic Orthogneiss	West	51.80	-	0.98	-	17.20	-	11.60
WYL-09-49-41.4	Graphitic Pelitic Gneiss	West	58.60	-	0.99	-	16.50	-	9.38
WYL-09-49-45.3	Graphitic Pelitic Gneiss	West	58.10	-	0.58	-	13.50	-	10.80
WYL-09-50-171.7A	Graphitic Pelitic Gneiss	West	53.80	-	0.86	-	17.70	-	13.00
WYL-09-50-174.5	Graphitic Pelitic Gneiss	West	60.90	-	0.79	-	17.00	-	8.15
WYL-09-50-179.9	Graphitic Pelitic Gneiss	West	63.70	-	1.29	-	11.00	-	13.00
WYL-09-50-37.5	Graphitic Pelitic Gneiss	West	59.30	-	0.94	-	18.80	-	6.64
WYL-09-50-67.9	Graphitic Pelitic Gneiss	West	64.00	-	0.55	-	14.90	-	5.52
WYL-10-61-128.0a	Graphitic Pelitic Gneiss	West	52.40	46.30	0.93	1.07	16.90	14.37	7.46
WYL-10-61-154.2	Graphitic Pelitic Gneiss	West	61.70	58.37	0.74	0.67	16.40	16.22	5.75
WYL-10-61-70.7	Graphitic Pelitic Gneiss	West	60.50	55.12	0.90	0.67	14.80	17.37	8.90
WYL-10-61-78.1	Graphitic Pelitic Gneiss	West	59.80	56.80	1.04	0.98	16.90	18.21	6.58
WYL-10-61-88.9	Graphitic Pelitic Gneiss	West	57.30	48.80	0.89	0.61	15.00	16.07	6.74
WYL-10-61-95.4	Graphitic Pelitic Gneiss	West	54.10	45.40	0.91	0.99	15.90	15.51	6.15
WYL-10-62-44.8a	Graphitic Pelitic Gneiss	West	63.70	57.03	0.50	0.50	16.10	14.43	5.87
WYL-10-62-60.1	Graphitic Pelitic Gneiss	West	37.30	38.29	0.56	0.46	12.10	15.30	23.20
WYL-10-62-66.4	Graphitic Pelitic Gneiss	West	60.20	52.02	1.02	0.55	16.80	19.88	4.08
WYL-10-62-67.5	Graphitic Pelitic Gneiss	West	45.70	40.59	0.54	0.51	10.50	11.64	14.00
WYL-10-62-68.9	Graphitic Pelitic Gneiss	West	63.60	57.51	0.74	0.56	15.50	15.72	2.92
WA-08-0-2014	Pelitic gneiss	West	57.30	54.91	0.75	0.81	18.00	17.78	11.40
WYL-08-525-202.9	Pelitic gneiss	West	54.30	-	0.92	-	21.20	-	9.28
WYL-08-525-207.2	Pelitic gneiss	West	61.10	-	0.74	-	15.40	-	13.00
WYL-08-525-210.1	Pelitic gneiss	West	63.60	-	0.50	-	16.80	-	6.72
WYL-09-46-36.6	Pelitic gneiss	Central	38.00	-	2.09	-	15.60	-	25.10
WYL-09-49-36.1	Pelitic gneiss	West	58.00	-	0.86	-	17.80	-	10.80
WYL-09-49-50.7	Pelitic gneiss	West	50.60	-	1.38	-	18.80	-	15.40
WYL-09-49-53.9	Pelitic gneiss	West	56.40	-	0.99	-	13.30	-	11.90
WYL-10-61-162.0	Pelitic gneiss	West	49.90	44.66	1.97	2.15	13.40	11.12	20.70
WYL-10-61-163.5	Pelitic gneiss	West	56.10	50.61	1.19	1.31	15.50	13.75	14.90
WYL-10-61-166.5	Pelitic gneiss	West	50.80	46.83	1.15	1.23	18.10	16.55	13.40
WYL-10-62-73.9	Pelitic gneiss	West	53.80	45.88	1.69	1.91	13.20	9.15	20.40
WYL-10-62-85.7	Pelitic gneiss	West	61.10	55.91	0.95	0.97	13.10	12.09	11.10
WYL-10-62-87.1	Pelitic gneiss	West	51.00	42.16	1.58	1.52	13.60	10.62	15.80
WYL-08-525-192.8	Psammopelitic gneiss	West	72.60	-	0.67	-	17.20	-	1.10
WYL-09-50-24	Quartzofeldspathic gneiss	West	65.60	-	0.70	-	15.30	-	4.86
WA-08-0-2026	Group A Pegmatite	West	66.30	64.87	1.08	1.19	13.10	13.14	9.12
WYL-08-525-134.7	Group A Pegmatite	West	60.70	-	0.47	-	20.40	-	3.94
WYL-08-526-4.5	Group A Pegmatite	West	85.60	-	0.51	-	4.53	-	4.71
WYL-09-50-14.3	Group A Pegmatite	West	62.70	-	0.48	-	14.50	-	1.67
WYL-09-50-159	Group A Pegmatite	West	85.10	83.48	0.18	0.27	7.56	8.67	1.21
WYL-09-50-160.5	Group A Pegmatite	West	77.70	-	0.02	-	12.20	-	0.09
WYL-09-50-161.4	Group A Pegmatite	West	74.80	74.64	0.17	0.18	14.00	14.19	0.92
WYL-09-50-166.2	Group A Pegmatite	West	79.60	79.28	1.05	1.19	5.72	5.29	7.41
WYL-09-50-166.3	Group A Pegmatite	West	47.50	-	0.46	-	17.40	-	26.00
WYL-09-50-171.7B	Group A Pegmatite	West	95.70	-	0.13	-	1.56	-	1.06
WYL-09-50-18.2	Group A Pegmatite	West	64.00	-	0.03	-	17.80	-	1.26
WYL-09-50-182.5	Group A Pegmatite	West	85.00	85.23	0.61	0.73	3.76	3.73	5.97

Sample Number	Fe2O3 xrf	FeOt (converted)	FeO (titration)	FeO (Residual)	Fe2O3	MnO	MnO xrf	MgO	MgO xrf	CaO	CaO xrf
WYL-09-49-83.4	-	2.49	-	-	-	0.05	-	0.55	-	1.04	-
WYL-09-49-88.0	-	1.69	-	-	-	0.03	-	0.30	-	0.67	-
WYL-09-50-252.7	-	1.53	-	-	-	0.04	-	0.60	-	1.08	-
WA-08-0-0046	10.80	8.57	6.73	1.84	2.04	0.16	0.19	3.20	3.28	6.79	6.86
WYL-09-50-196.6	-	6.74	-	-	-	0.13	-	3.41	-	3.95	-
WYL-09-50-237	-	10.44	-	-	-	0.14	-	3.54	-	8.62	-
WYL-09-49-41.4	-	8.44	-	-	-	0.49	-	3.33	-	0.51	-
WYL-09-49-45.3	-	9.72	-	-	-	1.18	-	3.60	-	0.89	-
WYL-09-50-171.7A	-	11.70	-	-	-	0.34	-	3.65	-	0.91	-
WYL-09-50-174.5	-	7.33	-	-	-	0.16	-	2.92	-	0.27	-
WYL-09-50-179.9	-	11.70	-	-	-	0.27	-	4.38	-	0.37	-
WYL-09-50-37.5	-	5.97	-	-	-	0.03	-	2.76	-	1.28	-
WYL-09-50-67.9	-	4.97	-	-	-	0.06	-	2.41	-	1.57	-
WYL-10-61-128.0a	8.56	6.71	5.12	1.59	1.77	0.08	0.08	2.69	2.30	0.36	0.24
WYL-10-61-154.2	5.18	5.17	4.83	0.34	0.38	0.12	0.09	2.63	2.12	0.83	0.74
WYL-10-61-70.7	9.56	8.01	4.25	3.76	4.18	0.05	0.05	2.73	3.06	0.49	0.47
WYL-10-61-78.1	6.56	5.92	7.17	-1.25	-1.39	0.05	0.04	3.02	2.98	1.50	1.31
WYL-10-61-88.9	6.10	6.06	0.88	5.18	5.76	0.10	0.11	4.90	4.58	0.57	0.43
WYL-10-61-95.4	6.86	5.53	4.32	1.21	1.35	0.10	0.11	4.55	4.14	0.59	0.50
WYL-10-62-44.8a	5.96	5.28	3.81	1.47	1.64	0.17	0.16	1.97	1.58	2.12	1.97
WYL-10-62-60.1	19.16	20.88	3.81	17.07	18.97	0.05	0.05	1.30	1.54	0.34	0.30
WYL-10-62-66.4	3.75	3.67	1.54	2.13	2.37	0.06	0.06	2.00	2.27	0.30	0.26
WYL-10-62-67.5	18.03	12.60	4.17	8.43	9.37	0.58	0.68	5.45	5.64	4.20	4.56
WYL-10-62-68.9	2.37	2.63	1.02	1.61	1.79	0.08	0.08	2.00	1.87	1.08	0.96
WA-08-0-2014	12.17	10.26	9.00	1.26	1.40	0.20	0.15	2.29	2.33	0.86	0.68
WYL-08-525-202.9	-	8.35	-	-	-	0.10	-	3.36	-	1.20	-
WYL-08-525-207.2	-	11.70	-	-	-	0.25	-	3.03	-	0.74	-
WYL-08-525-210.1	-	6.05	-	-	-	0.08	-	2.40	-	0.53	-
WYL-09-46-36.6	-	22.58	-	-	-	0.47	-	7.46	-	0.89	-
WYL-09-49-36.1	-	9.72	-	-	-	0.22	-	2.64	-	1.03	-
WYL-09-49-50.7	-	13.86	-	-	-	0.45	-	4.73	-	2.39	-
WYL-09-49-53.9	-	10.71	-	-	-	0.17	-	7.34	-	2.43	-
WYL-10-61-162.0	23.59	18.63	17.42	1.21	1.34	0.56	0.34	5.78	5.64	0.77	0.64
WYL-10-61-163.5	16.23	13.41	12.59	0.82	0.91	0.42	0.33	4.45	4.33	1.74	1.52
WYL-10-61-166.5	14.67	12.06	11.27	0.79	0.87	0.19	0.16	4.44	4.47	1.76	1.58
WYL-10-62-73.9	21.95	18.36	15.15	3.21	3.56	0.78	0.46	5.63	4.76	0.52	0.21
WYL-10-62-85.7	10.64	`	9.22	0.77	0.85	0.15	0.11	3.11	2.69	0.62	0.50
WYL-10-62-87.1	15.57	14.22	12.08	2.14	2.37	0.17	0.17	7.05	6.26	2.40	2.19
WYL-08-525-192.8	-	0.99	-	-	-	0.01	-	0.50	-	0.37	-
WYL-09-50-24	-	4.37	-	-	-	0.05	-	2.74	-	0.62	-
WA-08-0-2026	11.83	8.21	6.15	2.06	2.29	0.04	0.04	0.89	1.13	1.20	1.16
WYL-08-525-134.7	-	3.55	-	-	-	0.06	-	1.10	-	2.28	-
WYL-08-526-4.5	-	4.24	-	-	-	0.04	-	1.62	-	0.04	-
WYL-09-50-14.3	-	1.50	-	-	-	0.05	-	3.72	-	7.62	-
WYL-09-50-159	1.27	1.09	0.81	0.28	0.31	0.03	0.04	0.53	0.93	0.64	0.76
WYL-09-50-160.5	-	0.08	-	-	-	0.01	-	0.06	-	0.17	-
WYL-09-50-161.4	0.72	0.83	0.59	0.24	0.26	0.02	0.03	0.43	0.57	1.09	0.98
WYL-09-50-166.2	7.09	6.67	5.27	1.40	1.55	0.09	0.09	2.78	3.10	0.63	1.01
WYL-09-50-166.3	-	23.39	-	-	-	0.94	-	3.99	-	0.82	-
WYL-09-50-171.7B	-	0.95	-	-	-	0.01	-	0.38	-	0.26	-
WYL-09-50-18.2	-	1.13	-	-	-	0.03	-	0.90	-	3.23	-
WYL-09-50-182.5	6.30	5.37	4.39	0.98	1.09	0.09	0.10	1.62	1.72	0.46	0.67

Sample Number	Na2O	Na2O xrf	K2O	K2O xrf	P2O5	P2O5 xrf	LOI	LOIXrf	SUM	Sum xrf	C	S	S xrf	F xrf	Cl xrf	B	Ba	Cr	Sc
WYL-09-49-83.4	5.86	-	1.80	-	0.05	-	0.50	-	99.44	0.00	0.01	0.01	-	-	-	16	394	15	5
WYL-09-49-88.0	4.79	-	4.84	-	0.05	-	0.50	-	100.83	0.00	0.03	0.01	-	-	-	12	897	12	4
WYL-09-50-252.7	4.70	-	3.80	-	0.01	-	0.30	-	100.77	0.00	0.12	0.01	-	-	-	6	394	7	2
WA-08-0-0046	2.86	2.79	1.11	0.83	0.17	0.17	0.60	-	99.98	97.41	0.08	0.02	0.00	0.16	0.08	4	144	137	28
WYL-09-50-196.6	2.86	-	1.75	-	0.04	-	1.00	-	100.45	0.00	0.23	0.08	-	-	-	9	412	119	21
WYL-09-50-237	4.48	-	1.72	-	0.23	-	0.20	-	100.51	0.00	0.01	0.01	-	-	-	6	173	4	24
WYL-09-49-41.4	1.16	-	5.61	-	0.13	-	3.30	-	100.00	0.00	0.45	0.66	-	-	-	19	1690	89	27
WYL-09-49-45.3	0.09	-	3.76	-	0.21	-	7.60	-	100.31	0.00	1.18	2.08	-	-	-	26	1830	15	17
WYL-09-50-171.7A	1.25	-	6.03	-	0.02	-	1.00	-	98.56	0.00	0.35	0.03	-	-	-	11	908	116	34
WYL-09-50-174.5	0.47	-	7.22	-	0.03	-	2.40	-	100.31	0.00	0.70	0.01	-	-	-	18	1330	101	26
WYL-09-50-179.9	0.36	-	4.27	-	0.03	-	0.90	-	99.57	0.00	0.21	0.06	-	-	-	49	581	178	27
WYL-09-50-37.5	3.70	-	4.78	-	0.07	-	1.70	-	100.00	0.00	0.33	0.01	-	-	-	10	1160	89	21
WYL-09-50-67.9	1.10	-	5.92	-	0.05	-	3.40	-	99.48	0.00	0.43	0.07	-	-	-	18	1250	39	9
WYL-10-61-128.0a	2.58	1.85	6.84	5.91	0.07	0.04	9.00	-	99.27	80.71	6.64	0.55	0.22	0.12	0.04	17	1670	83	19
WYL-10-61-154.2	1.88	1.69	8.10	7.94	0.10	0.05	1.80	-	99.98	93.08	1.03	0.01	0.00	0.72	0.04	13	1660	110	24
WYL-10-61-70.7	1.88	1.57	3.16	3.16	0.12	0.09	7.00	-	100.47	91.13	2.35	2.34	1.62	0.12	0.02	17	557	71	19
WYL-10-61-78.1	1.42	1.23	6.70	6.53	0.20	0.17	3.20	-	100.35	94.81	1.13	0.34	0.28	0.11	0.02	19	1070	86	21
WYL-10-61-88.9	0.44	0.29	6.67	5.66	0.27	0.19	8.20	-	100.73	82.83	3.66	1.89	0.99	0.12	0.01	20	1050	80	18
WYL-10-61-95.4	0.68	0.42	7.42	6.87	0.29	0.19	8.80	-	99.43	81.00	5.47	0.61	0.36	0.09	0.03	31	1100	88	23
WYL-10-62-44.8a	3.59	3.13	3.94	3.54	0.28	0.26	2.00	-	100.16	88.57	0.44	1.00	0.85	0.13	0.05	34	1770	50	15
WYL-10-62-60.1	0.61	0.59	5.51	5.56	0.13	0.07	17.70	-	98.76	81.32	6.55	15.10	10.04	0.20	0.01	12	690	70	15
WYL-10-62-66.4	0.98	0.75	7.54	7.45	0.09	0.05	7.30	-	100.31	87.04	3.70	1.13	0.87	0.10	0.02	17	1170	91	20
WYL-10-62-67.5	0.61	0.42	1.74	1.57	0.11	0.04	14.40	-	97.78	83.68	3.79	3.25	2.81	0.19	0.02	32	852	51	14
WYL-10-62-68.9	3.46	2.89	5.08	4.65	0.07	0.04	5.90	-	100.37	86.65	3.95	0.99	0.79	0.12	0.01	55	783	80	17
WA-08-0-2014	3.27	3.33	7.12	6.91	0.12	0.08	0.90	-	101.60	99.15	0.06	0.03	0.03	0.25	0.04	4	1920	98	26
WYL-08-525-202.9	4.20	-	4.21	-	0.11	-	1.20	-	100.08	0.00	0.01	0.01	-	-	-	12	447	62	15
WYL-08-525-207.2	2.17	-	3.44	-	0.11	-	0.30	-	100.28	0.00	0.01	0.28	-	-	-	10	454	55	27
WYL-08-525-210.1	2.77	-	6.89	-	0.13	-	0.40	-	100.82	0.00	0.01	0.01	-	-	-	9	688	48	6
WYL-09-46-36.6	0.70	-	6.22	-	0.20	-	3.20	-	99.93	0.00	0.08	1.30	-	-	-	6	532	166	55
WYL-09-49-36.1	1.79	-	5.49	-	0.13	-	0.80	-	99.56	0.00	0.06	0.04	-	-	-	10	1390	120	28
WYL-09-49-50.7	1.90	-	4.02	-	0.11	-	1.40	-	101.18	0.00	0.03	0.04	-	-	-	55	768	155	54
WYL-09-49-53.9	2.21	-	3.76	-	0.14	-	1.20	-	99.84	0.00	0.06	0.02	-	-	-	20	559	179	37
WYL-10-61-162.0	0.15	0.14	4.98	5.78	0.09	0.01	0.90	-	99.02	94.06	0.22	0.20	0.15	0.72	0.12	17	615	192	38
WYL-10-61-163.5	1.98	1.91	3.97	4.02	0.09	0.03	0.40	-	100.67	94.03	0.06	0.11	0.03	0.49	0.07	19	507	126	26
WYL-10-61-166.5	2.84	2.43	5.89	6.04	0.12	0.07	1.10	-	99.71	94.03	0.12	0.07	0.06	0.46	0.09	11	1060	179	29
WYL-10-62-73.9	0.20	0.17	4.14	3.92	0.11	0.06	0.80	-	101.25	88.46	0.04	0.21	0.03	0.34	0.08	18	610	259	56
WYL-10-62-85.7	0.98	0.91	7.79	7.85	0.18	0.13	0.40	-	99.41	91.80	0.28	0.02	0.00	0.31	0.05	5	617	168	29
WYL-10-62-87.1	1.57	1.09	4.64	4.00	0.22	0.14	2.20	-	100.15	83.72	6.09	15.60	0.03	0.34	0.09	7	660	264	38
WYL-08-525-192.8	2.99	-	2.94	-	0.06	-	1.20	-	99.64	0.00	0.01	0.01	-	-	-	13	361	136	6
WYL-09-50-24	4.32	-	4.38	-	0.15	-	2.40	-	101.12	0.00	0.14	0.01	-	-	-	11	721	62	15
WA-08-0-2026	3.99	4.04	2.29	2.54	0.04	0.01	0.90	-	98.91	99.95	0.49	0.13	0.04	0.17	0.10	17	270	21	7
WYL-08-525-134.7	7.32	-	2.98	-	0.05	-	0.80	-	100.10	0.00	0.02	0.01	-	-	-	13	310	25	6
WYL-08-526-4.5	0.33	-	2.59	-	0.02	-	0.50	-	100.49	0.00	0.04	0.04	-	-	-	8	255	97	10
WYL-09-50-14.3	4.08	-	4.27	-	0.14	-	1.00	-	100.23	0.00	0.20	0.01	-	-	-	30	389	51	9
WYL-09-50-159	1.54	1.40	2.74	2.66	0.01	0.03	1.00	1.00	100.53	100.49	0.10	0.03	0.01	0.04	0.01	22	543	16	5
WYL-09-50-160.5	1.91	-	8.21	-	0.01	-	0.30	-	100.66	0.00	0.04	0.01	-	-	-	6	1110	11	1
WYL-09-50-161.4	2.76	2.64	6.57	6.29	0.01	0.02	0.50	0.50	101.26	100.75	0.07	0.01	0.01	0.02	0.01	10	1240	8	3
WYL-09-50-166.2	0.07	0.17	2.40	2.28	0.01	0.02	0.80	0.80	100.55	100.32	0.18	0.04	0.01	0.25	0.01	5	422	128	14
WYL-09-50-166.3	0.38	-	1.50	-	0.01	-	0.10	-	99.09	0.00	0.05	0.02	-	-	-	20	219	152	100
WYL-09-50-171.7B	0.01	-	0.65	-	0.01	-	0.40	-	100.15	0.00	0.10	0.01	-	-	-	17	77	37	1
WYL-09-50-18.2	5.95	-	5.88	-	0.95	-	0.60	-	100.63	0.00	0.06	0.04	-	-	-	24	566	17	7
WYL-09-50-182.5	0.02	0.02	1.48	1.35	0.01	0.02	0.90	0.90	99.91	100.77	0.15	0.16	0.10	0.20	0.01	8	127	56	10

Sample Number	Sr	Y	Zr	Ag	Be	Cd	Co	Cu	Ga	Hf	Li	Mo	Nb	Ni	Pb	Rb	Sn	Ta	Th	U	Th/U	V	W	Zn	La
WYL-09-49-83.4	52	35	440	0.1	3.1	0.5	0.5	3	15	11	41	0.5	12	3	14	86.3	55	0.5	34	4	8.5	15	0.5	38	64
WYL-09-49-88.0	63	38	468	0.1	2.7	1	0.5	2	14	10	22	2	17	6	19	149	5	1	30	9	3.3	14	0.5	34	75
WYL-09-50-252.7	43	30	422	0.3	4.3	0.5	1	0.5	21	9	23	0.5	13	3	11	153	12	0.5	23	8	2.9	16	0.5	25	61
WA-08-0-0046	187	20	121	0.5	1	2	28	53	18	1	9	0.5	2	75	22	18.4	0.5	0.5	0.5	4.68	0.1	244	0.5	127	18
WYL-09-50-196.6	170	20	106	0.3	0.9	0.5	26	71	17	3	25	0.5	7	55	38	114	0.5	0.5	6	3	2.0	157	0.5	132	19
WYL-09-50-237	300	21	99	0.1	1.1	0.5	40	0.5	23	2	15	0.5	1	26	13	60.9	0.5	0.5	2	1	2.0	192	0.5	95	27
WYL-09-49-41.4	47	35	199	0.1	1.1	1	26	44	19	4	87	0.5	13	52	34	323	0.5	0.5	20	2	10.0	95	0.5	79	45
WYL-09-49-45.3	71	23	192	0.3	2.5	0.5	137	307	17	3	65	0.5	14	80	45	243	2	1	29	7	4.1	84	0.5	140	23
WYL-09-50-171.7A	63	51	147	0.1	0.6	0.5	56	23	29	4	30	0.5	13	54	63	453	0.5	0.5	20	2	10.0	138	0.5	146	60
WYL-09-50-174.5	49	32	149	0.1	1	0.5	40	2	26	4	30	0.5	10	46	67	512	0.5	0.5	28	5	5.6	116	0.5	85	67
WYL-09-50-179.9	15	616	498	0.1	0.5	0.5	83	77	37	22	45	4	169	92	31	487	0.5	6	59	37	1.6	191	0.5	236	33
WYL-09-50-37.5	186	38	215	0.1	2.1	1	15	38	30	5	74	0.5	14	41	11	139	0.5	0.5	17	4	4.3	134	0.5	39	74
WYL-09-50-67.9	90	29	196	0.4	1.7	0.5	11	34	23	6	50	0.5	8	26	22	187	0.5	0.5	16	12	1.3	78	0.5	56	152
WYL-10-61-128.0a	92	36	306	1.2	1.1	2	7	78	22	7	66	8	25	79	67	279	0.5	0.5	23	20.8	1.1	260	1	65	55
WYL-10-61-154.2	111	22	160	0.3	0.8	0.5	132	2	25	2	40	0.5	18	64	76	422	0.5	0.5	22	4.75	4.6	127	0.5	91	54
WYL-10-61-70.7	49	17	327	1.2	3.7	2	14	133	25	5	62	3	4	35	26	96.6	0.5	0.5	22	15.9	1.4	173	4	26	35
WYL-10-61-78.1	119	18	244	1	1.2	3	13	36	24	4	57	2	16	36	47	216	0.5	0.5	15	5.02	3.0	187	0.5	268	48
WYL-10-61-88.9	76	24	249	1.4	2.3	2	7	30	23	5	61	7	9	41	51	203	0.5	0.5	17	5.68	3.0	239	0.5	133	15
WYL-10-61-95.4	78	21	249	0.9	4	2	13	73	21	4	62	8	15	71	91	179	0.5	0.5	21	4.43	4.7	333	0.5	132	75
WYL-10-62-44.8a	205	26	135	1.1	2.4	2	12	36	19	3	46	3	11	37	32	119	0.5	0.5	9	5.84	1.5	187	0.5	146	51
WYL-10-62-60.1	25	36	167	2.6	1.6	2	125	133	31	4	56	65	0.5	2600	57	235	0.5	0.5	22	21	1.0	566	18	129	40
WYL-10-62-66.4	71	22	246	1.4	2.9	2	14	22	26	5	49	1	9	83	36	364	0.5	0.5	23	4.13	5.6	104	16	34	70
WYL-10-62-67.5	101	42	156	3.1	6.2	2	23	50	23	3	69	12	9	172	30	137	0.5	0.5	13	8.44	1.5	201	14	152	96
WYL-10-62-68.9	75	28	203	1.1	2.4	2	18	97	22	4	45	8	10	72	30	208	0.5	0.5	21	10.8	1.9	132	10	61	65
WA-08-0-2014	116	27	173	0.7	1.9	3	30	64	28	3	50	10	14	31	48	401	0.5	0.5	19	5.35	3.6	129	2	72	55
WYL-08-525-202.9	48	84	406	0.1	1.2	1	14	5	31	11	142	3	61	56	31	382	16	3	23	24	1.0	117	0.5	196	22
WYL-08-525-207.2	31	385	493	0.1	0.7	1	17	148	22	16	55	79	51	66	71	304	13	2	32	49	0.7	86	0.5	219	27
WYL-08-525-210.1	50	12	134	0.1	0.6	1	9	9	19	4	43	0.5	5	33	21	385	19	0.5	6	7	0.9	76	0.5	84	7
WYL-09-46-36.6	40	323	690	0.1	2.2	0.5	111	252	37	16	92	0.5	147	171	106	681	8	15	557	84	6.6	345	0.5	360	698
WYL-09-49-36.1	68	45	200	0.1	0.9	1	40	4	21	3	34	3	14	52	24	280	1	1	23	4	5.8	133	0.5	82	55
WYL-09-49-50.7	81	282	339	0.1	2.6	1	57	33	24	9	49	3	63	85	33	358	1	4	5	5	1.0	178	0.5	179	5
WYL-09-49-53.9	97	23	202	0.1	2.1	1	43	2	16	3	54	2	10	92	23	350	2	1	13	5	2.6	254	0.5	193	19
WYL-10-61-162.0	10	97	610	3.8	0.1	3	68	9	49	17	124	0.5	228	91	78	669	0.5	0.5	50	21	2.4	254	0.5	430	47
WYL-10-61-163.5	46	64	362	2.5	2.3	3	49	36	40	9	83	0.5	117	70	47	485	0.5	0.5	53	37.8	1.4	169	0.5	299	41
WYL-10-61-166.5	185	19	539	2.5	8.2	3	36	86	32	9	98	0.5	28	104	44	512	0.5	0.5	11	7.29	1.5	223	0.5	325	26
WYL-10-62-73.9	15	650	561	2.2	0.1	2	85	3	41	18	88	1	176	148	40	409	0.5	1	224	51.8	4.3	259	0.5	373	176
WYL-10-62-85.7	47	20	113	0.5	0.4	2	27	4	27	1	41	0.5	9	73	36	511	0.5	0.5	5	5.58	0.9	198	0.5	190	14
WYL-10-62-87.1	82	47	258	0.3	1.6	2	47	55	30	6	89	50	38	130	38	435	0.5	0.5	410	44.1	9.3	328	0.5	353	131
WYL-08-525-192.8	38	10	446	0.1	2.2	1	4	0.5	16	10	77	3	3	23	13	132	5	0.5	11	14	0.8	88	7	18	30
WYL-09-50-24	87	19	242	0.1	0.9	0.5	10	19	18	6	53	0.5	9	24	24	102	0.5	0.5	14	3	4.7	100	0.5	25	58
WA-08-0-2026	99	17	550	2.7	3.1	2	9	18	40	14	36	2	57	8	63	191	0.5	0.5	150	210	0.7	107	0.5	149	19
WYL-08-525-134.7	107	23	357	0.1	5.1	1	7	1	25	7	39	0.5	41	28	41	195	3	2	43	26	1.7	37	0.5	98	26
WYL-08-526-4.5	8	16	610	0.1	0.3	0.5	25	11	11	26	29	0.5	71	35	32	246	0.5	3	46	35	1.3	86	0.5	186	0.5
WYL-09-50-14.3	93	29	273	0.1	4.2	0.5	7	17	19	5	8	2	13	12	8	126	0.5	0.5	18	5	3.6	48	0.5	15	45
WYL-09-50-159	54	57	491	0.4	0.8	0.5	4	12	16	22	23	56	11	8	93	117	0.5	0.5	715	722	1.0	25	0.5	24	13
WYL-09-50-160.5	82	3	49	0.1	0.7	0.5	0.5	1	13	2	4	1	0.5	1	69	295	0.5	0.5	9	27	0.3	8	0.5	3	4
WYL-09-50-161.4	108	29	249	0.1	1	1	3	4	20	12	18	32	6	4	177	243	0.5	0.5	253	325	0.8	24	0.5	57	30
WYL-09-50-166.2	4	70	459	0.5	0.2	0.5	43	14	20	21	30	7	106	53	42	267	0.5	4	208	197	1.1	129	0.5	151	4
WYL-09-50-166.3	9	1060	333	0.1	0.3	1	67	19	21	16	32	0.5	24	31	24	167	0.5	2	45	85	0.5	124	1	143	45
WYL-09-50-171.7B	1	7	38	0.1	0.1	0.5	4	5	3	1	6	0.5	11	6	6	52.3	0.5	0.5	3	4	0.8	15	0.5	14	2
WYL-09-50-18.2	154	33	7	0.1	2.1	1	3	2	22	0.5	4	1	0.5	5	4	154	0.5	0.5	3	1	3.0	36	0.5	9	50
WYL-09-50-182.5	5	40	661	1	0.4	0.5	17	21	17	32	24	20	94	23	192	232	0.5	4	336	372	0.9	63	0.5	350	3

Sample Number	Ce	Pr	Nd	Sm	Eu	Gd	Tb	Dy	Ho	Er	Yb	Ag p	As p	Bi p	Co p	Cu p	Ge p	Hg p	Mo p	Ni p	Pb p	Sb p
WYL-09-49-83.4	145	16	55	9	1.3	9	1	4.4	0.5	1.8	1.4	0.1	0.5	4	1	3	0.5	0.5	0.5	1	1	3
WYL-09-49-88.0	148	18	62	10	1.5	10	1	4.8	0.5	2	1.4	0.1	0.5	0.5	1	2	0.5	0.5	1	1	5	0.5
WYL-09-50-252.7	107	11	39	6	0.7	5	1	4.5	1	2.9	3	0.1	0.5	0.5	1	0.5	0.5	0.5	0.5	1	3	0.5
WA-08-0-0046	31	2	17	3	1.1	2	0.5	3.8	0.5	1.7	2.6	0.1	0.5	0.5	8	48	0.5	0.5	0.5	25	3	0.5
WYL-09-50-196.6	36	2	16	3	1.9	2	0.5	2.8	1	2.2	2.6	0.1	1	0.5	13	69	0.5	0.5	0.5	36	24	0.5
WYL-09-50-237	48	3	25	5	3.4	3	1	2.8	1	2.3	2.5	0.1	0.5	0.5	8	1	0.5	0.5	0.5	6	2	0.5
WYL-09-49-41.4	110	10	35	6	1.9	6	0.5	3.6	0.5	2.1	2.4	0.1	0.5	1	24	40	0.5	0.5	0.5	50	7	2
WYL-09-49-45.3	62	5	18	3	1.4	3	0.5	2.9	0.5	1.8	2.2	0.1	0.5	0.5	1	1	0.5	0.5	0.5	2	0.5	0.5
WYL-09-50-171.7A	165	7	39	6	3	5	2	6.4	2	4.7	5.4	0.2	2	0.5	31	21	0.5	0.5	0.5	43	6	0.5
WYL-09-50-174.5	177	10	45	6	2	5	1	4.4	1	3.6	4.1	0.1	1	0.5	27	3	0.5	0.5	0.5	39	4	0.5
WYL-09-50-179.9	81	5	26	4	2	9	4	22.1	8	28.1	49.8	0.1	2	0.5	50	74	0.5	0.5	2	66	9	0.5
WYL-09-50-37.5	137	12	52	8	2.4	6	1	4.7	1	3.5	3.4	0.1	2	0.5	8	31	0.5	0.5	0.5	32	4	0.5
WYL-09-50-67.9	273	27	102	14	2	10	1	5.1	1	2.8	2.1	0.3	1	0.5	11	32	0.5	0.5	0.5	26	8	0.5
WYL-10-61-128.0a	87	10	39	6	1.7	4	0.5	4.3	1	2.6	3.7	0.1	0.5	0.5	6	76	0.5	0.5	7	68	14	2
WYL-10-61-154.2	119	10	39	6	1.7	3	0.5	3.9	0.5	1.9	2.4	0.1	0.5	0.5	82	3	0.5	0.5	1	42	4	0.5
WYL-10-61-70.7	58	6	27	4	0.8	1	0.5	2.2	0.5	1.1	2	0.5	0.5	2	12	125	0.5	0.5	2	32	16	0.5
WYL-10-61-78.1	77	8	37	6	1.8	3	0.5	2.8	0.5	1.5	2.1	0.2	0.5	0.5	10	30	0.5	0.5	2	27	9	0.5
WYL-10-61-88.9	29	3	16	3	1.7	3	0.5	3.7	0.5	1.7	2.4	0.5	0.5	0.5	5	27	0.5	0.5	7	37	7	0.5
WYL-10-61-95.4	115	13	55	8	2.2	6	0.5	4.3	0.5	1.7	2	0.3	0.5	0.5	10	71	0.5	0.5	7	59	4	0.5
WYL-10-62-44.8a	78	9	37	6	1.4	3	0.5	4	0.5	1.6	2.3	0.3	0.5	0.5	8	31	0.5	0.5	3	27	8	0.5
WYL-10-62-60.1	65	7	38	6	1	3	0.5	2.8	1	2.1	4.3	1.8	0.5	10	102	125	0.5	0.5	55	2420	34	3
WYL-10-62-66.4	116	13	51	8	1.2	5	0.5	3.7	0.5	1.8	2.1	0.1	0.5	2	10	21	0.5	0.5	1	80	8	0.5
WYL-10-62-67.5	140	16	66	11	2.4	9	1	10.7	1	3.4	4.6	1.4	0.5	6	18	48	0.5	0.5	7	150	21	0.5
WYL-10-62-68.9	105	12	44	7	1.2	4	0.5	3.4	0.5	1.3	1.4	0.3	5	0.5	15	83	0.5	0.5	7	63	9	0.5
WA-08-0-2014	118	9	40	6	1.1	3	0.5	4.2	0.5	1.8	2.8	0.1	0.5	0.5	21	59	0.5	0.5	9	27	22	0.5
WYL-08-525-202.9	67	6	21	4	0.8	4	0.5	3.9	1	3	4.1	0.1	0.5	1	6	3	0.5	0.5	3	25	4	5
WYL-08-525-207.2	86	7	27	6	0.6	10	3	28.6	11	39.1	58.9	0.1	0.5	1	10	145	0.5	0.5	64	48	38	7
WYL-08-525-210.1	26	3	10	2	0.6	2	0.5	1.9	0.5	1.1	1.2	0.1	0.5	1	5	8	0.5	0.5	1	18	0.5	4
WYL-09-46-36.6	1400	152	533	90	1.8	87	9	42.5	9	23.5	23.2	0.1	0.5	0.5	86	247	0.5	0.5	1	127	48	9
WYL-09-49-36.1	149	11	39	6	1.7	7	1	5.9	1	3.2	3.5	0.1	0.5	0.5	19	4	0.5	0.5	3	32	4	6
WYL-09-49-50.7	40	3	10	2	0.8	7	2	22.2	8	30.3	57.9	0.1	0.5	0.5	32	32	0.5	0.5	3	52	4	7
WYL-09-49-53.9	53	8	19	5	0.9	5	0.5	2.8	0.5	1.8	2.4	0.1	0.5	0.5	25	1	1	0.5	1	50	2	7
WYL-10-61-162.0	97	8	40	7	0.1	5	0.5	13.4	2	9.1	17.3	0.1	0.5	0.5	25	9	0.5	0.5	1	37	62	0.5
WYL-10-61-163.5	87	7	33	6	0.9	4	0.5	9.1	1	4.9	8.2	0.1	0.5	0.5	23	26	0.5	0.5	1	39	24	0.5
WYL-10-61-166.5	47	3	21	4	0.7	1	0.5	3.6	0.5	1.5	3.1	0.1	0.5	0.5	21	83	0.5	0.5	1	77	11	0.5
WYL-10-62-73.9	412	43	185	34	0.1	36	3	51.8	13	61.4	115	0.1	0.5	0.5	50	2	0.5	0.5	1	87	13	0.5
WYL-10-62-85.7	28	1	16	3	0.9	2	0.5	3.6	0.5	1.8	2.9	0.1	0.5	0.5	17	3	0.5	0.5	0.5	42	2	0.5
WYL-10-62-87.1	279	30	126	21	0.5	14	1	7.7	1	3.3	3.2	0.1	0.5	0.5	29	38	0.5	0.5	44	67	16	0.5
WYL-08-525-192.8	69	6	19	3	0.8	3	0.5	1.5	0.5	0.6	0.7	0.1	0.5	0.5	2	0.5	0.5	0.5	2	16	0.5	0.5
WYL-09-50-24	103	9	38	5	1.8	4	1	3	1	2.1	2	0.1	2	0.5	11	17	0.5	0.5	0.5	24	9	0.5
WA-08-0-2026	30	2	10	2	0.7	1	0.5	2.3	0.5	1.4	2.2	0.1	0.5	0.5	6	14	0.5	0.5	2	6	47	0.5
WYL-08-525-134.7	54	4	13	2	1.7	2	0.5	1.7	0.5	1	1.5	0.1	0.5	0.5	4	0.5	0.5	0.5	0.5	16	7	3
WYL-08-526-4.5	10	0.5	2	0.5	0.2	0.5	0.5	1.1	0.5	1.1	2.2	0.1	0.5	1	16	9	0.5	0.5	1	21	18	5
WYL-09-50-14.3	99	9	38	7	1.1	5	1	4.2	0.5	2.8	2.9	0.1	1	0.5	2	17	0.5	0.5	2	4	5	0.5
WYL-09-50-159	25	1	7	2	0.9	5	4	7.2	0.5	9	6.9	0.1	0.5	0.5	4	4	0.5	0.5	52	6	69	0.5
WYL-09-50-160.5	4	0.5	0.5	0.5	1.1	0.5	0.5	0.4	0.5	0.3	0.6	0.1	0.5	0.5	0.5	1	0.5	0.5	0.5	0.5	8	0.5
WYL-09-50-161.4	53	4	16	3	1.4	3	1	3.8	0.5	3.8	3.2	0.1	0.5	0.5	2	1	0.5	0.5	30	2	125	0.5
WYL-09-50-166.2	8	0.5	1	0.5	1.1	2	2	6.5	2	7.7	8.9	0.1	2	0.5	23	11	0.5	0.5	7	34	30	0.5
WYL-09-50-166.3	112	4	35	0.5	3.9	16	10	75.9	27	117	220	0.1	1	0.5	19	20	0.5	0.5	0.5	27	10	0.5
WYL-09-50-171.7B	7	0.5	2	0.5	0.1	0.5	0.5	0.7	0.5	0.8	1.2	0.1	0.5	0.5	4	4	0.5	0.5	0.5	6	1	0.5
WYL-09-50-18.2	94	9	36	6	1.2	5	0.5	4.6	0.5	2.5	2.5	0.1	0.5	0.5	1	2	0.5	0.5	0.5	2	4	0.5
WYL-09-50-182.5	4	0.5	0.5	0.5	0.8	2	3	4.3	1	5.3	5.6	0.1	2	0.5	12	20	0.5	0.5	18	18	172	0.5

Sample Number	Se p	Te p	U p	V p	Zn p	Sc xrf	V xrf	Cr xrf	Co xrf	Ni xrf	Cu xrf	Zn xrf	Ga xrf	As xrf	Se xrf	Br xrf	Rb xrf	Sr xrf
WYL-09-49-83.4	0.5	0.5	2	6	27	-	-	-	-	-	-	-	-	-	-	-	-	-
WYL-09-49-88.0	0.5	0.5	6	3	24	-	-	-	-	-	-	-	-	-	-	-	-	-
WYL-09-50-252.7	0.5	0.5	2	4	15	-	-	-	-	-	-	-	-	-	-	-	-	-
WA-08-0-0046	0.5	0.5	3.22	27	31	22.7	207.6	135.7	35.3	63.1	38.4	85.4	12.7	13	38.6	0.5	19.7	178.1
WYL-09-50-196.6	0.5	0.5	1	61	72	-	-	-	-	-	-	-	-	-	-	-	-	-
WYL-09-50-237	0.5	0.5	0.5	44	16	-	-	-	-	-	-	-	-	-	-	-	-	-
WYL-09-49-41.4	5	0.5	1	52	44	-	-	-	-	-	-	-	-	-	-	-	-	-
WYL-09-49-45.3	0.5	0.5	1	1	1	-	-	-	-	-	-	-	-	-	-	-	-	-
WYL-09-50-171.7A	0.5	0.5	0.5	90	86	-	-	-	-	-	-	-	-	-	-	-	-	-
WYL-09-50-174.5	0.5	0.5	0.5	77	59	-	-	-	-	-	-	-	-	-	-	-	-	-
WYL-09-50-179.9	0.5	0.5	30	126	126	-	-	-	-	-	-	-	-	-	-	-	-	-
WYL-09-50-37.5	0.5	0.5	0.5	85	21	-	-	-	-	-	-	-	-	-	-	-	-	-
WYL-09-50-67.9	0.5	0.5	3	54	42	-	-	-	-	-	-	-	-	-	-	-	-	-
WYL-10-61-128.0a	3	0.5	15.4	214	49	20.2	260.5	75.5	17	70.3	54.2	49.8	19.8	11	19.2	0.5	276.1	96.1
WYL-10-61-154.2	1	0.5	2.01	75	54	14.5	105.9	75.1	60.7	54.7	5.9	73.4	20.2	12	19.8	0.5	400	119.5
WYL-10-61-70.7	3	0.5	5.06	106	16	20.3	189.9	73.6	21.1	21.4	93.8	10.9	21.5	11	24.9	0.5	107.9	60.3
WYL-10-61-78.1	2	0.5	1.65	106	184	15.7	167.3	65.6	11.5	28.4	24.7	233.8	21	12	25.9	0.5	219.2	135.8
WYL-10-61-88.9	5	0.5	3.62	207	113	13.6	182	55	7.2	34.1	22	120.9	20.9	11	0.55	11.3	215	92.3
WYL-10-61-95.4	4	0.5	2.14	244	117	19.3	294	85.5	12.3	65.6	48	126.7	20.2	12	16.6	0.5	189.4	96.1
WYL-10-62-44.8a	2	0.5	4.19	152	111	12.3	164.6	38.1	7.1	18.3	27	130.8	17.5	11	23.9	0.5	125.5	246.8
WYL-10-62-60.1	39	0.5	17.5	383	76	16.4	458.6	68.5	106.3	1095.5	59.7	77.6	12.3	14	37.1	0.5	163.6	19.1
WYL-10-62-66.4	2	0.5	2.06	58	28	15.5	114.1	59.1	1.5	81	20.4	30.7	26	13	0.55	0.5	375.6	95.3
WYL-10-62-67.5	2	0.5	4.59	100	79	13.2	195.1	36.6	59.7	142.1	26.8	101.9	15.9	15	41.2	0.5	111.1	95
WYL-10-62-68.9	1	0.5	4.16	102	48	12.8	126	61	1.5	74.4	71.6	60.9	24.4	16	0.55	16	249.5	108.2
WA-08-0-2014	2	0.5	2.02	90	46	17.5	126.8	96.6	39.7	23.8	41.6	45.2	20.3	13	40.2	0.5	327.4	118.9
WYL-08-525-202.9	5	0.5	19	55	90	-	-	-	-	-	-	-	-	-	-	-	-	-
WYL-08-525-207.2	4	0.5	40	53	131	-	-	-	-	-	-	-	-	-	-	-	-	-
WYL-08-525-210.1	4	0.5	3	47	47	-	-	-	-	-	-	-	-	-	-	-	-	-
WYL-09-46-36.6	22	5	77	300	253	-	-	-	-	-	-	-	-	-	-	-	-	-
WYL-09-49-36.1	5	0.5	2	75	52	-	-	-	-	-	-	-	-	-	-	-	-	-
WYL-09-49-50.7	5	0.5	4	112	99	-	-	-	-	-	-	-	-	-	-	-	-	-
WYL-09-49-53.9	7	0.5	4	192	100	-	-	-	-	-	-	-	-	-	-	-	-	-
WYL-10-61-162.0	3	0.5	18.4	101	175	23.5	270.7	159	115.4	58	2.5	293.7	27	14	40.2	0.5	411.6	7.5
WYL-10-61-163.5	2	0.5	25.5	82	147	18.5	173.9	107.5	66.4	50.3	16.2	217.3	26.5	13	42.2	0.5	357.1	44.3
WYL-10-61-166.5	4	0.5	3.34	145	227	21.8	216.4	148.1	54.8	79.4	57.2	248.7	21.1	13	42.2	0.5	369.5	163.7
WYL-10-62-73.9	7	0.5	36.6	169	214	33.2	286.8	223.8	119	104.8	2.5	270.4	23.4	13	41.1	0.5	272.5	7.3
WYL-10-62-85.7	4	0.5	4	145	104	21	192.8	138.8	36	52.8	2.5	139.7	17	9	40.2	0.5	400.2	48.6
WYL-10-62-87.1	6	0.5	36.7	204	213	34.1	303.3	213.4	73.2	84.6	21.8	256.6	17.4	12	41.7	0.5	297.8	64.1
WYL-08-525-192.8	1	0.5	8	28	12	-	-	-	-	-	-	-	-	-	-	-	-	-
WYL-09-50-24	0.5	0.5	0.5	83	23	-	-	-	-	-	-	-	-	-	-	-	-	-
WA-08-0-2026	1	0.5	204	72	128	7.1	133.2	42.6	29.4	3.7	12.6	137.5	32.5	14	34.1	0.5	195.3	113
WYL-08-525-134.7	2	0.5	20	19	60	-	-	-	-	-	-	-	-	-	-	-	-	-
WYL-08-526-4.5	3	0.5	27	59	131	-	-	-	-	-	-	-	-	-	-	-	-	-
WYL-09-50-14.3	0.5	0.5	2	4	0.5	-	-	-	-	-	-	-	-	-	-	-	-	-
WYL-09-50-159	0.5	0.5	716	16	17	-	-	-	-	-	-	-	-	-	-	-	-	-
WYL-09-50-160.5	0.5	0.5	25	0.5	1	-	-	-	-	-	-	-	-	-	-	-	-	-
WYL-09-50-161.4	0.5	0.5	318	9	39	3.7	18.6	15.8	1.5	6.9	4.7	64.4	18.1	5.9	5	25.4	269.2	120.6
WYL-09-50-166.2	0.5	0.5	174	79	87	9.6	184.2	124.4	33.7	55.9	12.5	148.6	13.7	5.9	21	5	244.5	4.5
WYL-09-50-166.3	0.5	0.5	78	63	52	-	-	-	-	-	-	-	-	-	-	-	-	-
WYL-09-50-171.7B	0.5	0.5	2	14	10	-	-	-	-	-	-	-	-	-	-	-	-	-
WYL-09-50-18.2	0.5	0.5	0.5	7	0.5	-	-	-	-	-	-	-	-	-	-	-	-	-
WYL-09-50-182.5	0.5	0.5	365	47	302	10.3	102.9	59.4	18.9	27	21.2	394.5	13.1	5.9	5	12.8	221.3	4.2

Sample Number	Y xrf	Zr xrf	Nb xrf	Mo xrf	Sn xrf	Sb xrf	Cs xrf	Ba xrf	La xrf	Hf xrf	Ta xrf	W xrf	Pb xrf	Bi xrf	Th xrf	U xrf
WYL-09-49-83.4	-	-	-	-	-	-	-	-	-	-	-	-	-	-	-	-
WYL-09-49-88.0	-	-	-	-	-	-	-	-	-	-	-	-	-	-	-	-
WYL-09-50-252.7	-	-	-	-	-	-	-	-	-	-	-	-	-	-	-	-
WA-08-0-0046	24	112	6	5.6	4	1	2.5	158.8	18.4	0.5	11.2	0.5	16	0.5	0.53	1
WYL-09-50-196.6	-	-	-	-	-	-	-	-	-	-	-	-	-	-	-	-
WYL-09-50-237	-	-	-	-	-	-	-	-	-	-	-	-	-	-	-	-
WYL-09-49-41.4	-	-	-	-	-	-	-	-	-	-	-	-	-	-	-	-
WYL-09-49-45.3	-	-	-	-	-	-	-	-	-	-	-	-	-	-	-	-
WYL-09-50-171.7A	-	-	-	-	-	-	-	-	-	-	-	-	-	-	-	-
WYL-09-50-174.5	-	-	-	-	-	-	-	-	-	-	-	-	-	-	-	-
WYL-09-50-179.9	-	-	-	-	-	-	-	-	-	-	-	-	-	-	-	-
WYL-09-50-37.5	-	-	-	-	-	-	-	-	-	-	-	-	-	-	-	-
WYL-09-50-67.9	-	-	-	-	-	-	-	-	-	-	-	-	-	-	-	-
WYL-10-61-128.0a	34	248.1	22	13	4.8	1	2.5	1490.9	38.4	9.9	20.2	10.1	48.4	0.5	18.2	20.8
WYL-10-61-154.2	19	75.7	16	5.6	4	1	9	1532.4	27.4	0.5	18.9	0.5	60.9	0.5	14.9	2.2
WYL-10-61-70.7	16	199.3	13	5.6	3.8	1	2.5	579.3	26	0.5	18.4	0.5	18	0.5	15.4	1
WYL-10-61-78.1	18	156.3	13	5.6	3	1	9	986.1	33.1	0.5	18	0.5	25.4	0.5	0.53	1
WYL-10-61-88.9	22	185.7	13	7.5	5.4	1	5	884.5	13.7	11.8	24.4	21	33.4	0.5	14.2	11
WYL-10-61-95.4	21	157.4	12	9.4	4.8	1	7	934.9	90.2	10	20.3	0.5	79.2	0.5	13.2	1
WYL-10-62-44.8a	26	111	9	5.6	3.7	1	2.5	1711.1	38.9	0.5	19	0.5	7.5	0.5	0.53	1
WYL-10-62-60.1	38	163	13	63.5	1.5	1	5	722.8	70.2	0.5	0.5	0.5	27.4	0.5	14.6	16.3
WYL-10-62-66.4	21	215.2	16	5.6	7.7	1	9	904.1	72.7	10.8	21.6	38.5	22.1	0.5	25.9	2
WYL-10-62-67.5	45	137	15	11.8	4	1	14	898.4	115.3	0.5	9.9	0.5	25	0.5	0.53	8.1
WYL-10-62-68.9	22	201.9	14	9.5	7.2	1	6	717.7	35.8	13.3	27.1	49.5	16.9	0.5	18.2	9.4
WA-08-0-2014	26	143	17	14	3.1	1	12	1916.1	34.2	0.5	11.2	0.5	17.7	0.5	0.53	1.7
WYL-08-525-202.9	-	-	-	-	-	-	-	-	-	-	-	-	-	-	-	-
WYL-08-525-207.2	-	-	-	-	-	-	-	-	-	-	-	-	-	-	-	-
WYL-08-525-210.1	-	-	-	-	-	-	-	-	-	-	-	-	-	-	-	-
WYL-09-46-36.6	-	-	-	-	-	-	-	-	-	-	-	-	-	-	-	-
WYL-09-49-36.1	-	-	-	-	-	-	-	-	-	-	-	-	-	-	-	-
WYL-09-49-50.7	-	-	-	-	-	-	-	-	-	-	-	-	-	-	-	-
WYL-09-49-53.9	-	-	-	-	-	-	-	-	-	-	-	-	-	-	-	-
WYL-10-61-162.0	62	428	233	5.6	1.5	1	16	848.6	15.2	0.5	0.5	0.5	17.7	0.5	17.4	15
WYL-10-61-163.5	53	322	112	5.6	1.5	1	13	603.6	40.7	0.5	9.7	0.5	6.9	0.5	26.1	21.8
WYL-10-61-166.5	23	498	30	5.6	2.6	1	16	1108.6	33.1	0.5	0.5	0.5	12.6	0.5	0.53	3.3
WYL-10-62-73.9	425	444	173	5.6	1.5	1	18	754.5	103.8	0.5	0.5	0.5	27	0.5	99.4	38.4
WYL-10-62-85.7	16	101	15	5.6	5.5	1	15	587.6	23.5	0.5	11.2	0.5	4.9	0.5	0.53	2.2
WYL-10-62-87.1	34	188	41	72	4.1	1	18	681.7	143	0.5	10.3	0.5	26	0.5	220.1	38.1
WYL-08-525-192.8	-	-	-	-	-	-	-	-	-	-	-	-	-	-	-	-
WYL-09-50-24	-	-	-	-	-	-	-	-	-	-	-	-	-	-	-	-
WA-08-0-2026	18	391.1	57	10.8	9.2	1	5	386	24.8	0.5	15.4	0.5	43.8	0.5	140.2	240.6
WYL-08-525-134.7	-	-	-	-	-	-	-	-	-	-	-	-	-	-	-	-
WYL-08-526-4.5	-	-	-	-	-	-	-	-	-	-	-	-	-	-	-	-
WYL-09-50-14.3	-	-	-	-	-	-	-	-	-	-	-	-	-	-	-	-
WYL-09-50-159	-	-	-	-	-	-	-	-	-	-	-	-	-	-	-	-
WYL-09-50-160.5	-	-	-	-	-	-	-	-	-	-	-	-	-	-	-	-
WYL-09-50-161.4	41.1	190.6	17.6	58	3.1	1	9.1	1158.9	9.6	41	14.8	16.3	216	29.3	302.4	463.3
WYL-09-50-166.2	58.6	496	129.8	16.5	1.5	1	10.8	555.3	2.5	13.5	5	5	20.2	2.5	215.1	231.9
WYL-09-50-166.3	-	-	-	-	-	-	-	-	-	-	-	-	-	-	-	-
WYL-09-50-171.7B	-	-	-	-	-	-	-	-	-	-	-	-	-	-	-	-
WYL-09-50-18.2	-	-	-	-	-	-	-	-	-	-	-	-	-	-	-	-
WYL-09-50-182.5	39.4	786.3	130.6	46.6	1.5	1	10.7	184.4	2.5	38.9	5	5	180.8	2.5	367.7	480.6

Sample Number	Lithology	Area	SiO2	SiO2 xrf	TiO2	TiO2 xrf	Al2O3	Al2O3 xrf	Fe2O3t
WYL-09-50-215.8	Group A Pegmatite	West	67.60	63.90	0.14	0.18	16.60	14.66	1.76
WYL-09-50-216.5	Group A Pegmatite	West	66.30	64.41	0.78	0.98	14.70	12.43	7.12
WYL-09-50-64.1	Group A Pegmatite	West	69.60	-	0.04	-	15.60	-	0.46
WYL-10-61-128.0b	Group A Pegmatite	West	95.20	85.27	0.03	0.03	0.71	0.82	2.14
WYL-10-61-132.0	Group A Pegmatite	West	92.70	86.35	0.15	0.16	3.64	3.52	1.12
WYL-10-61-133.8	Group A Pegmatite	West	91.00	88.65	0.01	0.01	5.12	5.66	0.12
WYL-10-61-135.4	Group A Pegmatite	West	77.40	66.67	0.01	0.01	12.20	11.01	0.09
WYL-10-61-158.2	Group A Pegmatite	West	79.60	74.26	0.57	0.65	7.84	8.01	4.13
WYL-10-61-181.5	Group A Pegmatite	West	72.30	65.17	0.33	0.37	13.90	12.97	3.27
WYL-10-61-190.3	Group A Pegmatite	West	85.60	81.13	0.42	0.42	2.83	2.62	8.36
WYL-10-61-202.8	Group A Pegmatite	West	54.10	48.98	1.35	1.39	17.80	14.87	10.40
WYL-10-62-107.9	Group A Pegmatite	West	66.30	56.84	0.72	0.80	14.30	12.31	8.39
WYL-10-62-112.2	Group A Pegmatite	West	90.10	91.75	0.27	0.23	3.22	3.15	4.08
WYL-10-62-44.8b	Group A Pegmatite	West	71.80	62.28	0.29	0.30	10.60	9.53	6.86
WYL-10-62-70.7	Group A Pegmatite	West	73.10	70.74	0.02	0.01	15.10	15.96	0.16
WYL-10-62-79.4	Group A Pegmatite	West	54.00	43.44	2.05	2.06	13.20	9.59	17.80
WYL-10-62-83.9	Group A Pegmatite	West	67.00	59.49	0.66	0.67	13.20	11.97	9.10
WYL-10-62-92.0	Group A Pegmatite	West	76.90	74.11	0.23	0.23	11.80	12.31	2.33
WYL-10-62-93.5	Group A Pegmatite	West	71.00	63.15	1.20	1.28	7.89	7.41	10.80
WYL-09-44-68.5	Group B Pegmatite	Central	74.60	75.82	0.04	0.04	15.20	16.20	0.50
WYL-09-44-69.0	Group B Pegmatite	Central	73.30	72.84	0.06	0.05	16.50	17.83	0.55
WYL-09-44-73.4	Group B Pegmatite	Central	60.80	58.95	0.70	0.82	17.50	17.35	7.38
WYL-09-44-74.9	Group B Pegmatite	Central	71.50	76.56	1.95	1.83	2.16	2.47	20.50
WYL-09-44-76.1	Group B Pegmatite	Central	71.10	73.76	0.53	0.53	11.00	11.52	10.40
WYL-09-44-76.4	Group B Pegmatite	Central	35.60	47.43	3.20	3.14	5.11	5.67	53.00
WYL-09-46-26.9	Group B Pegmatite	Central	78.30	77.38	0.94	0.92	5.21	4.51	8.52
WYL-09-46-30.8	Group B Pegmatite	Central	60.10	58.42	1.37	1.62	10.60	8.72	13.60
WYL-09-46-31.1	Group B Pegmatite	Central	62.30	59.34	1.00	1.01	12.60	10.26	10.00
WYL-09-46-32.6	Group B Pegmatite	Central	56.90	53.31	1.22	1.25	16.20	12.84	10.80
WYL-09-46-34.0	Group B Pegmatite	Central	51.50	48.27	1.49	1.51	14.60	11.49	15.50
WYL-09-46-35.0	Group B Pegmatite	Central	63.40	59.02	1.81	1.86	8.36	7.54	15.70
WYL-09-46-42.8	Group B Pegmatite	Central	48.30	-	1.62	-	17.50	-	15.70
WYL-09-46-47.3	Group B Pegmatite	Central	64.10	62.93	1.24	1.05	8.80	8.28	20.00
WYL-09-46-81.6	Group B Pegmatite	Central	74.40	-	0.21	-	12.80	-	1.96
WYL-09-46-83.0	Group B Pegmatite	Central	73.80	75.55	0.93	0.70	8.85	9.30	9.69
CAR110/ASR109/BL/G2/Ma1b	Standard		69.50	-	0.50	-	15.50	-	2.67
CAR110/ASR209/BM/G2/Ma1b	Standard		69.90	-	0.48	-	15.10	-	2.60
CAR110/BL/GSP2/ASR109/MA1B	Standard		66.70	-	0.68	-	14.70	-	5.07
CAR110/BL/GSP2/ASR109/MA1B	Standard		66.60	-	0.68	-	14.90	-	5.13
CAR110/BL/GSP2/ASR109/MA1B	Standard		59.20	-	1.08	-	16.70	-	6.72
CAR110/BL/GSP2/ASR209/MA1B	Standard		59.00	-	1.08	-	16.70	-	6.75
CG515	Standard		-	-	-	-	-	-	-
CG515	Standard		-	-	-	-	-	-	-
CG515	Standard		-	-	-	-	-	-	-
CG515	Standard		-	-	-	-	-	-	-
GSP2	Standard		-	69.03	-	0.63	-	14.76	-
GSP2/CG51509/LS4/BL/Ma1b/ASR109	Standard		67.50	-	0.66	-	15.20	-	4.78
GSP2/CG51509/LS4/BL/Ma1b/ASR109	Standard		68.00	-	0.67	-	15.30	-	4.82
LLD	Standard		-	0.03	-	0.00	-	0.00	-
LLD	Standard		-	0.03	-	0.00	-	0.00	-
LLD	Standard		-	0.03	-	0.01	-	0.01	-

Sample Number	Fe2O3 xrf	FeOt (converted)	FeO (titration)	FeO (Residual)	Fe2O3	MnO	MnO xrf	MgO	MgO xrf	CaO	CaO xrf
WYL-09-50-215.8	1.74	1.58	0.81	0.77	0.86	0.05	0.07	0.97	1.31	2.42	3.27
WYL-09-50-216.5	8.08	6.41	5.20	1.21	1.34	0.05	0.07	2.08	2.21	1.43	1.57
WYL-09-50-64.1	-	0.41	-	-	-	0.01	-	0.22	-	0.26	-
WYL-10-61-128.0b	1.24	1.93	0.22	1.71	1.90	0.01	0.00	0.12	0.17	0.11	0.10
WYL-10-61-132.0	0.99	1.01	0.59	0.42	0.46	0.01	0.01	0.41	0.55	0.46	0.48
WYL-10-61-133.8	0.08	0.11	0.07	0.04	0.04	0.01	0.00	0.08	0.13	0.64	0.74
WYL-10-61-135.4	0.05	0.08	0.07	0.01	0.01	0.01	0.00	0.06	0.11	0.41	0.30
WYL-10-61-158.2	4.53	3.72	3.51	0.21	0.23	0.05	0.04	1.48	1.68	0.17	0.16
WYL-10-61-181.5	3.58	2.94	2.49	0.45	0.50	0.04	0.04	1.44	1.65	2.30	2.17
WYL-10-61-190.3	6.74	7.52	3.59	3.93	4.37	0.04	0.04	0.10	0.10	0.47	0.54
WYL-10-61-202.8	11.95	9.36	8.34	1.02	1.13	0.10	0.11	3.69	3.69	3.07	2.73
WYL-10-62-107.9	8.21	7.55	6.66	0.89	0.99	0.07	0.07	1.86	1.86	1.62	1.40
WYL-10-62-112.2	2.46	3.67	1.61	2.06	2.29	0.02	0.02	0.08	0.10	0.51	0.58
WYL-10-62-44.8b	6.10	6.17	2.78	3.39	3.77	0.08	0.07	1.50	1.14	1.15	1.02
WYL-10-62-70.7	0.12	0.14	0.07	0.07	0.08	0.01	0.00	0.11	0.14	0.50	0.42
WYL-10-62-79.4	18.47	16.02	12.81	3.21	3.56	0.34	0.20	5.47	4.23	0.48	0.29
WYL-10-62-83.9	7.88	8.19	5.27	2.92	3.24	0.26	0.20	2.07	1.95	0.59	0.46
WYL-10-62-92.0	2.16	2.10	1.10	1.00	1.11	0.02	0.02	0.72	0.78	1.73	1.62
WYL-10-62-93.5	11.57	9.72	7.54	2.18	2.42	0.08	0.08	3.10	2.99	0.28	0.23
WYL-09-44-68.5	0.45	0.45	0.15	0.30	0.33	0.02	0.02	0.21	0.37	2.95	3.01
WYL-09-44-69.0	0.45	0.49	0.37	0.12	0.14	0.01	0.01	0.25	0.40	3.28	3.26
WYL-09-44-73.4	8.94	6.64	4.90	1.74	1.93	0.09	0.10	2.38	2.60	1.66	1.57
WYL-09-44-74.9	16.65	18.45	8.86	9.59	10.65	0.09	0.08	0.86	1.25	0.48	0.59
WYL-09-44-76.1	7.16	9.36	3.88	5.48	6.09	0.04	0.04	0.15	0.24	1.90	2.06
WYL-09-44-76.4	38.75	47.69	20.72	26.97	29.97	0.27	0.20	0.31	0.49	0.70	1.10
WYL-09-46-26.9	9.36	7.67	6.15	1.52	1.69	0.11	0.11	2.73	2.49	0.12	0.10
WYL-09-46-30.8	15.73	12.24	9.81	2.43	2.70	0.14	0.18	4.84	5.16	2.04	1.77
WYL-09-46-31.1	9.17	9.00	5.34	3.66	4.07	0.12	0.13	3.29	3.23	1.30	1.14
WYL-09-46-32.6	11.26	9.72	8.27	1.45	1.61	0.13	0.16	4.12	3.91	1.80	1.65
WYL-09-46-34.0	17.78	13.95	13.25	0.70	0.77	0.16	0.18	5.17	4.76	1.43	1.51
WYL-09-46-35.0	18.78	14.13	10.03	4.10	4.55	0.13	0.13	5.34	5.25	0.24	0.11
WYL-09-46-42.8	-	14.13	-	-	-	0.19	-	4.19	-	1.49	-
WYL-09-46-47.3	14.29	18.00	6.00	12.00	13.33	0.08	0.05	0.21	0.19	0.49	0.40
WYL-09-46-81.6	-	1.76	-	-	-	0.01	-	0.25	-	0.75	-
WYL-09-46-83.0	7.18	8.72	1.17	7.55	8.39	0.04	0.03	0.20	0.22	0.58	0.52
CAR110/ASR109/BL/G2/Ma1b	-	2.40	-	-	0.00	0.03	-	0.76	-	2.04	-
CAR110/ASR209/BM/G2/Ma1b	-	2.34	-	-	0.00	0.73	-	0.03	-	1.98	-
CAR110/BL/GSP2/ASR109/MA1B	-	4.56	-	-	0.00	0.04	-	0.98	-	2.14	-
CAR110/BL/GSP2/ASR109/MA1B	-	4.62	-	-	0.00	0.04	-	0.98	-	2.15	-
CAR110/BL/GSP2/ASR109/MA1B	-	6.05	-	-	0.00	0.10	-	1.82	-	5.27	-
CAR110/BL/GSP2/ASR209/MA1B	-	6.07	-	-	0.00	0.10	-	1.86	-	5.27	-
CG515	-	-	3.81	-	-	-	-	-	-	-	-
CG515	-	-	3.81	-	-	-	-	-	-	-	-
CG515	-	-	3.81	-	-	-	-	-	-	-	-
CG515	-	-	3.81	-	-	-	-	-	-	-	-
GSP2	4.17	-	-	-	-	-	0.04	-	1.03	-	1.90
GSP2/CG51509/LS4/BL/Ma1b/ASR109	-	4.30	-	-	0.00	0.04	-	0.97	-	2.12	-
GSP2/CG51509/LS4/BL/Ma1b/ASR109	-	4.34	-	-	0.00	0.04	-	0.96	-	2.08	-
LLD	0.00	-	-	-	-	-	0.00	-	0.00	-	0.00
LLD	0.00	-	-	-	-	-	0.00	-	0.00	-	0.00
LLD	0.01	-	-	-	-	-	0.01	-	0.01	-	0.01

Sample Number	Na2O	Na2O xrf	K2O	K2O xrf	P2O5	P2O5 xrf	LOI	LOIXrf	SUM	Sum xrf	C	S	S xrf	F xrf	Cl xrf	B	Ba	Cr	Sc
WYL-09-50-215.8	7.10	6.00	1.87	1.56	0.01	0.02	2.70	2.70	101.21	95.40	0.27	0.01	0.01	0.14	0.01	27	314	4	2
WYL-09-50-216.5	4.21	3.43	2.72	2.33	0.01	0.01	1.50	1.50	100.89	97.01	0.10	0.01	0.01	0.09	0.10	15	398	5	9
WYL-09-50-64.1	2.69	-	9.72	-	0.01	-	0.60	-	99.19	0.00	0.04	0.01	-	-	-	9	687	2	1
WYL-10-61-128.0b	0.08	0.09	0.06	0.11	0.01	0.01	1.20	-	99.71	87.84	0.06	1.41	1.05	0.07	0.01	19	30	19	2
WYL-10-61-132.0	0.88	0.83	0.69	0.72	0.01	0.02	0.50	-	100.69	93.63	0.07	0.02	0.03	0.10	0.02	15	112	19	3
WYL-10-61-133.8	1.61	1.81	1.09	1.02	0.02	0.02	0.50	-	100.17	98.11	0.08	0.06	0.01	0.03	0.01	14	149	26	1
WYL-10-61-135.4	2.51	2.15	6.75	5.66	0.05	0.03	0.30	-	99.72	85.97	0.39	0.03	0.02	0.03	0.01	11	542	14	1
WYL-10-61-158.2	0.70	0.75	4.25	4.17	0.02	0.01	0.50	-	99.29	94.26	0.01	0.09	0.02	0.25	0.03	4	1120	67	6
WYL-10-61-181.5	4.05	3.62	2.22	2.11	0.02	0.00	0.80	-	100.65	91.69	0.09	0.01	0.01	0.17	0.04	18	360	23	5
WYL-10-61-190.3	0.99	0.96	0.27	0.27	0.03	0.01	0.30	-	99.38	92.83	0.11	0.01	0.01	0.09	0.02	15	32	16	4
WYL-10-61-202.8	4.76	3.75	3.73	3.96	0.17	0.14	0.80	-	99.81	91.56	0.07	0.01	0.03	0.40	0.09	13	810	18	6
WYL-10-62-107.9	4.37	3.47	2.74	2.78	0.08	0.02	0.60	-	100.97	87.74	0.02	0.08	0.02	0.34	0.07	3	237	55	10
WYL-10-62-112.2	1.22	1.25	0.36	0.36	0.02	0.00	0.20	-	100.06	99.90	0.07	0.01	0.01	0.06	0.01	9	33	14	2
WYL-10-62-44.8b	2.34	1.99	2.72	2.43	0.27	0.24	2.40	-	99.94	85.10	0.04	2.13	1.61	0.10	0.03	9	797	41	18
WYL-10-62-70.7	2.88	2.86	8.44	8.49	0.02	0.01	0.40	-	100.71	98.74	0.06	1.01	0.00	0.03	0.01	13	1320	13	1
WYL-10-62-79.4	0.77	0.57	4.95	4.57	0.06	0.01	0.80	-	99.86	83.43	0.06	0.24	0.18	0.39	0.09	6	776	221	34
WYL-10-62-83.9	1.83	1.59	5.88	5.68	0.04	0.01	0.70	-	101.29	89.90	0.02	0.10	0.12	0.27	0.11	10	905	57	19
WYL-10-62-92.0	3.51	3.79	2.10	1.91	0.05	0.03	0.80	-	100.19	96.95	0.08	0.03	0.03	0.09	0.02	25	235	22	4
WYL-10-62-93.5	0.57	0.49	4.12	4.15	0.02	0.01	0.80	-	99.84	91.35	0.04	0.17	0.19	0.42	0.14	4	435	72	14
WYL-09-44-68.5	5.28	6.29	1.12	0.79	0.03	0.01	0.60	-	100.20	103.01	0.11	0.01	0.01	0.05	0.02	5	91	15	1
WYL-09-44-69.0	5.90	6.92	1.21	0.88	0.02	0.01	0.50	-	101.26	102.65	0.28	0.00	0.00	0.05	0.03	5	104	16	2
WYL-09-44-73.4	5.44	5.24	2.44	2.35	0.21	0.15	1.60	-	100.13	98.05	0.08	0.06	0.06	0.26	0.07	10	218	56	10
WYL-09-44-74.9	0.06	0.08	0.98	1.23	0.12	0.07	0.40	-	99.07	100.81	0.14	0.61	0.50	0.34	0.05	14	106	21	12
WYL-09-44-76.1	4.11	4.76	0.81	0.65	0.10	0.06	0.30	-	100.20	100.78	0.12	0.04	0.05	0.07	0.01	6	58	15	4
WYL-09-44-76.4	0.80	1.58	0.69	0.72	0.25	0.13	0.05	-	100.79	99.20	0.14	0.02	0.05	0.29	0.03	8	56	19	20
WYL-09-46-26.9	0.08	0.08	1.91	1.73	0.02	0.01	1.00	-	99.23	96.70	0.05	0.11	0.04	0.25	0.08	5	135	160	17
WYL-09-46-30.8	0.88	0.83	1.23	0.98	1.05	0.76	3.90	3.90	99.75	98.05	0.07	0.06	0.01	0.22	0.01	29	168	51	28
WYL-09-46-31.1	2.74	2.05	2.84	2.09	1.30	0.72	2.50	2.50	99.99	91.63	0.07	0.08	0.01	0.20	0.10	37	263	49	26
WYL-09-46-32.6	3.81	2.79	4.21	3.81	0.39	0.14	1.10	1.10	100.68	92.21	0.03	0.01	0.01	0.34	0.10	10	331	33	20
WYL-09-46-34.0	2.31	1.73	5.24	4.88	0.32	0.18	1.60	1.60	99.32	93.89	0.08	0.06	0.01	0.45	0.30	13	366	47	27
WYL-09-46-35.0	0.14	0.13	4.16	4.01	0.05	0.01	1.40	-	100.68	96.83	0.06	0.34	0.51	0.33	0.40	18	519	115	32
WYL-09-46-42.8	4.17	-	5.52	-	0.22	-	0.90	-	99.80	0.00	0.03	0.01	-	-	-	12	417	29	21
WYL-09-46-47.3	2.26	2.14	3.36	2.84	0.07	0.01	0.05	-	100.54	92.17	0.09	0.01	0.01	0.10	0.02	6	222	23	5
WYL-09-46-81.6	4.11	-	4.76	-	0.02	-	0.60	-	99.87	0.00	0.03	0.01	-	-	-	15	296	10	1
WYL-09-46-83.0	3.00	3.33	2.55	2.29	0.08	0.04	0.60	-	100.25	99.16	0.09	0.16	0.11	0.07	0.02	13	185	12	4
CAR110/ASR109/BL/G2/Ma1b	4.10	-	4.46	-	0.13	-	0.00	-	99.69	0.00	2.43	1.19	-	-	-	4	1820	7	4
CAR110/ASR209/BM/G2/Ma1b	4.14	-	4.68	-	0.14	-	0.00	-	99.78	0.00	2.46	1.17	-	-	-	94	1970	8	4
CAR110/BL/GSP2/ASR109/MA1B	2.82	-	5.41	-	0.27	-	4.00	-	102.81	0.00	2.44	1.17	-	-	-	18	1330	22	8
CAR110/BL/GSP2/ASR109/MA1B	2.86	-	5.48	-	0.28	-	4.00	-	99.1	0.00	2.44	1.17	-	-	-	17	1340	22	8
CAR110/BL/GSP2/ASR109/MA1B	4.25	-	2.94	-	0.47	-	0.00	-	98.55	0.00	2.44	1.17	-	-	-	95	1110	21	14
CAR110/BL/GSP2/ASR209/MA1B	4.24	-	2.91	-	0.46	-	4.00	-	98.37	0.00	2.44	1.17	-	-	-	96	1110	19	14
CG515	-	-	-	-	-	-	-	-	-	0.00	-	-	-	-	-	-	-	-	-
CG515	-	-	-	-	-	-	-	-	-	0.00	-	-	-	-	-	-	-	-	-
CG515	-	-	-	-	-	-	-	-	-	0.00	-	-	-	-	-	-	-	-	-
CG515	-	-	-	-	-	-	-	-	-	0.00	-	-	-	-	-	-	-	-	-
GSP2	-	2.79	-	5.23	-	0.25	-	-	-	99.84	-	-	-	-	-	-	-	-	-
GSP2/CG51509/LS4/BL/Ma1b/ASR109	2.87	-	5.44	-	0.27	-	0.00	-	99.85	0.00	2.44	1.18	-	-	-	19	1370	19	6
GSP2/CG51509/LS4/BL/Ma1b/ASR109	2.81	-	5.47	-	0.26	-	0.00	-	100.41	0.00	2.44	1.17	-	-	-	91	1400	17	6
LLD	-	0.00	-	0.00	-	0.00	-	-	-	0.04	-	-	0.005	0.005	0.01	-	-	-	-
LLD	-	0.00	-	0.00	-	0.00	-	-	-	0.04	-	-	0.005	0.005	0.01	-	-	-	-
LLD	-	0.01	-	0.01	-	0.01	-	0.50	-	0.62	-	-	0.010	0.010	0.010	-	-	-	-

Sample Number	Sr	Y	Zr	Ag	Be	Cd	Co	Cu	Ga	Hf	Li	Mo	Nb	Ni	Pb	Rb	Sn	Ta	Th	U	Th/U	V	W	Zn	La
WYL-09-50-215.8	171	64	2630	2.7	3.3	0.5	1	9	27	98	29	0.5	10	5	74	89.2	1	0.5	675	860	0.8	26	0.5	10	41
WYL-09-50-216.5	153	16	259	0.4	2	0.5	16	3	33	10	55	1	50	15	96	189	1	0.5	102	175	0.6	101	0.5	148	34
WYL-09-50-64.1	59	65	62	0.1	2	1	0.5	14	22	3	6	0.5	9	3	73	394	1	0.5	9	1	9.0	17	0.5	5	25
WYL-10-61-128.0b	9	45	1480	7.7	0.4	0.5	15	181	2	61	2	43	0.5	85	297	4.2	0.5	0.5	142	641	0.2	4	0.5	176	1
WYL-10-61-132.0	22	67	487	2.1	0.8	0.5	4	6	5	19	15	151	14	3	312	65.4	0.5	0.5	673	814	0.8	14	3	23	9
WYL-10-61-133.8	35	29	479	1.7	1	0.5	0.5	2	6	15	6	63	1	0.5	105	50.3	0.5	0.5	315	447	0.7	2	2	5	13
WYL-10-61-135.4	61	26	87	0.3	1.5	1	0.5	2	15	2	6	37	7	0.5	102	276	0.5	0.5	46	38.8	1.2	8	1	5	3
WYL-10-61-158.2	43	42	308	1.5	0.4	0.5	19	15	15	11	23	19	37	40	47	235	0.5	0.5	28	12.8	2.2	82	0.5	78	22
WYL-10-61-181.5	155	2	111	0.3	4.1	1	4	7	24	2	44	1	33	11	22	160	0.5	0.5	9	10.8	0.8	45	0.5	79	41
WYL-10-61-190.3	18	149	3090	13.4	0.8	1	2	7	26	95	10	0.5	13	4	324	11.9	9	0.5	1190	1260	0.9	32	0.5	85	8
WYL-10-61-202.8	302	16	56	0.7	4.9	3	36	8	39	1	158	0.5	51	38	24	459	5	0.5	19	19.9	1.0	148	0.5	234	23
WYL-10-62-107.9	51	59	139	0.8	6.5	2	10	16	37	9	53	0.5	73	38	78	284	5	0.5	365	57.9	6.3	104	0.5	252	235
WYL-10-62-112.2	15	29	597	2.6	1	0.5	0.5	1	15	14	8	1	8	1	131	13.7	3	0.5	468	233	2.0	9	0.5	109	8
WYL-10-62-44.8b	107	37	101	1.2	1.5	1	16	59	16	2	39	0.5	5	25	21	90.5	0.5	0.5	4	3.26	1.2	113	0.5	89	25
WYL-10-62-70.7	117	2	46	0.1	1.6	1	0.5	1	18	1	10	0.5	8	3	80	279	0.5	0.5	5	30.7	0.2	12	1	19	6
WYL-10-62-79.4	21	196	1090	5.5	0.3	3	96	99	40	36	92	9	143	132	67	473	0.5	0.5	277	262	1.1	281	0.5	368	3
WYL-10-62-83.9	61	240	432	2.6	0.5	2	14	4	24	15	53	249	72	27	253	323	0.5	2	885	767	1.2	70	0.5	191	3
WYL-10-62-92.0	75	155	4060	13.6	2	0.5	4	0.5	12	155	18	10	42	11	847	120	0.5	0.5	1100	2460	0.4	25	0.5	92	88
WYL-10-62-93.5	27	92	2210	13.2	0.4	1	23	57	27	76	66	0.5	141	79	709	402	3	3	1370	1100	1.2	91	0.5	483	24
WYL-09-44-68.5	99	20	679	3.1	7.4	1	0.5	0.5	24	20	11	1	13	5	38	42.6	0.5	1	34	32.2	1.1	16	0.5	23	41
WYL-09-44-69.0	98	17	60	0.3	8.7	2	1	8	27	1	10	0.5	14	3	32	48.4	0.5	0.5	18	12.9	1.4	17	0.5	35	34
WYL-09-44-73.4	107	134	130	0.1	7.2	3	14	19	37	2	79	2	81	23	67	290	1	0.5	1020	70.6	14.4	90	0.5	183	722
WYL-09-44-74.9	19	85	11700	53.9	0.4	2	18	217	54	348	13	19	64	19	74	152	21	0.5	1380	93.8	14.7	55	0.5	165	283
WYL-09-44-76.1	67	51	3200	15.7	5.2	2	2	27	45	96	11	5	23	0.5	62	26.1	4	0.5	453	67.8	6.7	19	0.5	121	258
WYL-09-44-76.4	32	109	850	4.5	1.6	6	10	0.5	166	17	21	17	93	0.5	71	35.9	24	0.5	751	26.6	28.2	69	0.5	625	426
WYL-09-46-26.9	7	66	648	3.1	1.3	2	20	14	23	19	33	8	137	52	92	329	5	4	529	119	4.4	114	0.5	271	10
WYL-09-46-30.8	171	694	1070	0.1	3.9	0.5	31	67	19	39	93	19	182	85	220	129	16	10	4670	228	20.5	220	0.5	70	4130
WYL-09-46-31.1	174	1190	2700	0.1	5.6	0.5	23	157	12	89	54	144	174	59	559	334	13	12	7310	701	10.4	156	0.5	128	4410
WYL-09-46-32.6	65	228	64	0.1	5	1	32	0.5	28	1	53	9	166	55	153	643	10	9	1360	75	18.1	201	0.5	321	1040
WYL-09-46-34.0	53	229	103	0.1	4.3	0.5	39	64	33	5	68	3	218	92	133	784	10	13	1000	71	14.1	279	0.5	377	830
WYL-09-46-35.0	19	81	4770	24	0.7	2	41	29	26	145	56	0.5	133	75	674	457	5	1	1650	741	2.2	261	0.5	484	38
WYL-09-46-42.8	65	113	242	0.1	7.4	1	26	22	35	3	64	23	152	39	64	673	19	7	466	31	15.0	97	0.5	392	501
WYL-09-46-47.3	28	3	330	3.3	1.8	3	1	0.5	61	12	13	10	49	0.5	34	106	11	0.5	35	37.5	0.9	30	0.5	148	15
WYL-09-46-81.6	37	12	14	0.1	2.7	0.5	0.5	1	17	0.5	15	1	11	2	33	170	3	0.5	39	7	5.6	12	0.5	33	51
WYL-09-46-83.0	35	76	3170	14.3	2.8	2	3	98	27	83	11	12	28	3	101	101	7	0.5	1240	323	3.8	20	1	44	238
CAR110/ASR109/BL/G2/Ma1b	480	11	290	3.1	3.6	0.5	72	214	21	7	83	57	14	385	412	1.1	0.5	0.5	119	3370	233	5	116	440	792
CAR110/ASR209/BM/G2/Ma1b	391	12	307	2.9	3.4	0.5	68	228	21	8	82	61	15	382	419	2.8	0.5	1	107	3310	232	5	112	433	798
CAR110/BL/GSP2/ASR109/MA1B	232	27	562	4.5	3.5	1	75	222	19	7	82	68	16	416	425	1	0.5	0.5	104	3380	235	3	117	425	782
CAR110/BL/GSP2/ASR109/MA1B	239	26	563	3.4	3.7	1	72	226	21	7	85	66	17	408	424	1.2	0.5	0.5	122	3440	247	3	120	436	785
CAR110/BL/GSP2/ASR109/MA1B	634	19	234	3.2	3.5	1	76	225	22	6	84	68	16	417	424	1.1	0.5	0.5	123	3410	237	5	124	422	792
CAR110/BL/GSP2/ASR209/MA1B	634	18	235	2.7	3.5	1	65	224	20	7	86	59	17	394	403	2.9	0.5	0.5	114	3390	251	3	124	423	766
CG515	-	-	-	-	-	-	-	-	-	-	-	-	-	-	-	-	-	-	-	-	-	-	-	-	-
CG515	-	-	-	-	-	-	-	-	-	-	-	-	-	-	-	-	-	-	-	-	-	-	-	-	-
CG515	-	-	-	-	-	-	-	-	-	-	-	-	-	-	-	-	-	-	-	-	-	-	-	-	-
CG515	-	-	-	-	-	-	-	-	-	-	-	-	-	-	-	-	-	-	-	-	-	-	-	-	-
GSP2	-	-	-	-	-	-	-	-	-	-	-	-	-	-	-	-	-	-	-	-	-	-	-	-	-
GSP2/CG51509/LS4/BL/Ma1b/ASR109	245	26	548	0.2	1.8	0.5	18	4	23	4	27	0.5	8	26	19	115	3	0.5	13	1	122	0.5	82	87	152
GSP2/CG51509/LS4/BL/Ma1b/ASR109	249	26	547	0.1	1.9	0.5	18	5	24	4	27	1	9	21	19	116	2	0.5	16	4	121	0.5	82	86	153
LLD	-	-	-	-	-	-	-	-	-	-	-	-	-	-	-	-	-	-	-	-	-	-	-	-	-
LLD	-	-	-	-	-	-	-	-	-	-	-	-	-	-	-	-	-	-	-	-	-	-	-	-	-
LLD	-	-	-	-	-	-	-	-	-	-	-	-	-	-	-	-	-	-	-	-	-	-	-	-	-

Sample Number	Ce	Pr	Nd	Sm	Eu	Gd	Tb	Dy	Ho	Er	Yb	Ag p	As p	Bi p	Co p	Cu p	Ge p	Hg p	Mo p	Ni p	Pb p	Sb p
WYL-09-50-215.8	59	3	8	5	1.6	7	9	9.1	1	10.2	11.1	0.1	0.5	0.5	1	3	0.5	0.5	0.5	4	60	0.5
WYL-09-50-216.5	52	3	14	2	1.8	1	1	2.3	1	2.6	2.4	0.1	2	0.5	13	2	0.5	0.5	0.5	11	67	0.5
WYL-09-50-64.1	42	4	16	3	0.9	2	0.5	2.7	0.5	1.6	2.3	0.1	0.5	0.5	0.5	13	0.5	0.5	0.5	1	5	0.5
WYL-10-61-128.0b	9	1	0.5	1	0.3	3	0.5	4.8	1	4.7	7.8	0.9	0.5	1	14	177	0.5	0.5	33	82	268	0.5
WYL-10-61-132.0	15	2	5	2	0.3	5	0.5	8.3	1	6.5	6.8	0.1	0.5	2	2	0.5	0.5	0.5	150	1	282	0.5
WYL-10-61-133.8	27	3	9	2	0.4	3	0.5	4.4	0.5	3.3	3.7	0.1	0.5	0.5	0.5	0.5	0.5	0.5	60	0.5	82	0.5
WYL-10-61-135.4	5	0.5	1	0.5	0.9	0.5	0.5	1.3	0.5	1	1.6	0.1	0.5	0.5	0.5	0.5	0.5	0.5	36	0.5	27	0.5
WYL-10-61-158.2	42	4	16	2	1	2	0.5	4.3	1	5.7	11.7	0.1	0.5	0.5	16	13	0.5	0.5	17	31	8	0.5
WYL-10-61-181.5	54	5	17	2	0.8	1	0.5	1	0.5	0.4	0.6	0.1	0.5	0.5	4	5	0.5	0.5	1	8	8	0.5
WYL-10-61-190.3	36	5	14	10	0.1	13	0.5	19.6	4	13.4	15.2	0.1	0.5	4	1	0.5	0.5	0.5	1	1	271	0.5
WYL-10-61-202.8	37	3	18	3	0.7	1	0.5	2.3	0.5	1.1	1.8	0.1	0.5	0.5	16	3	0.5	0.5	0.5	19	6	0.5
WYL-10-62-107.9	489	57	224	36	0.1	25	2	12.1	2	5	2.9	0.1	0.5	1	5	13	0.5	0.5	0.5	20	32	0.5
WYL-10-62-112.2	15	1	5	1	0.1	2	0.5	3.4	0.5	2.2	2.9	0.4	0.5	3	0.5	0.5	0.5	0.5	1	0.5	111	0.5
WYL-10-62-44.8b	42	4	22	4	0.8	2	0.5	2.6	0.5	0.9	1.3	0.5	0.5	0.5	15	54	0.5	0.5	1	26	8	0.5
WYL-10-62-70.7	8	0.5	2	0.5	1.7	0.5	0.5	0.4	0.5	0.2	0.4	0.1	0.5	0.5	0.5	0.5	0.5	0.5	1	1	16	0.5
WYL-10-62-79.4	14	0.5	3	1	0.1	4	0.5	19	5	23.7	36.5	0.5	0.5	0.5	52	77	0.5	0.5	5	65	36	0.5
WYL-10-62-83.9	10	0.5	4	1	1	7	0.5	26	6	32.8	52.3	0.8	0.5	5	7	0.5	0.5	0.5	237	10	233	0.5
WYL-10-62-92.0	215	24	92	22	1	24	0.5	25.1	6	16.2	21.6	2.9	0.5	8	2	0.5	0.5	0.5	7	5	820	0.5
WYL-10-62-93.5	57	6	17	8	0.2	11	0.5	14	2	8.8	10.6	1.7	0.5	6	11	46	0.5	0.5	1	38	621	0.5
WYL-09-44-68.5	70	8	25	5	0.9	3	0.5	2.7	0.5	1.6	2.7	0.1	0.5	0.5	0.5	0.5	0.5	0.5	1	1	18	0.5
WYL-09-44-69.0	49	6	21	3	0.9	2	0.5	1.6	0.5	0.8	1	0.1	0.5	0.5	0.5	4	0.5	0.5	0.5	1	11	0.5
WYL-09-44-73.4	1310	169	620	94	0.1	65	8	28.2	4	11	4.6	0.1	0.5	1	10	11	0.5	0.5	1	15	31	0.5
WYL-09-44-74.9	610	76	227	43	0.1	25	0.5	13.2	5	6.3	20.7	0.1	0.5	3	17	198	0.5	0.5	17	20	34	0.5
WYL-09-44-76.1	473	58	193	30	0.1	18	0.5	9.2	2	4.4	7	0.1	0.5	1	1	19	0.5	0.5	4	0.5	22	0.5
WYL-09-44-76.4	802	99	374	53	0.1	29	3	12.4	2	4.3	5.2	0.1	0.5	2	6	0.5	0.5	0.5	15	0.5	34	0.5
WYL-09-46-26.9	32	3	18	5	0.1	7	0.5	8.6	1	5.1	7.5	0.1	0.5	0.5	15	10	0.5	0.5	8	42	78	1
WYL-09-46-30.8	8300	861	2940	489	2.3	439	37	144	23	49.1	15.5	0.1	0.5	0.5	29	62	0.5	0.5	17	75	94	0.5
WYL-09-46-31.1	9050	1060	3590	607	2.6	553	50	197	34	75.3	33.1	0.1	0.5	0.5	19	145	0.5	0.5	140	43	373	2
WYL-09-46-32.6	2000	238	796	132	1.1	121	10	37.9	6	13.2	3.8	0.1	0.5	0.5	17	0.5	0.5	0.5	7	28	59	7
WYL-09-46-34.0	1650	177	601	99	0.8	92	7	30.1	5	11.6	5.4	0.1	0.5	0.5	23	59	0.5	0.5	1	54	71	7
WYL-09-46-35.0	186	26	79	11	0.1	10	0.5	10.6	3	7.2	14.6	0.1	0.5	0.5	22	7	0.5	0.5	1	49	504	0.5
WYL-09-46-42.8	975	98	346	54	0.8	49	3	14.8	2	5.2	1.6	0.1	0.5	0.5	11	17	0.5	0.5	0.5	15	19	8
WYL-09-46-47.3	25	1	11	1	0.1	0.5	0.5	0.1	0.5	0.1	1.5	0.1	0.5	0.5	1	0.5	0.5	0.5	3	0.5	9	0.5
WYL-09-46-81.6	89	8	25	3	0.7	3	0.5	1.4	0.5	0.7	0.6	0.1	0.5	0.5	0.5	1	0.5	0.5	1	0.5	5	0.5
WYL-09-46-83.0	423	51	163	26	0.1	17	0.5	12.4	2	7.2	10.1	0.1	0.5	4	1	79	0.5	0.5	10	0.5	67	0.5
CAR110/ASR109/BL/G2/Ma1b	95	348	45	9.8	24	2	12.6	3	9	4.6	3	402	21	67	205	0.5	0.5	60	354	388	2	4
CAR110/ASR209/BM/G2/Ma1b	96	361	46	9.9	24	1	12.7	3	8.7	4.6	2.9	403	21	71	209	0.5	0.5	60	362	413	1	3
CAR110/BL/GSP2/ASR109/MA1B	91	354	46	9.8	25	2	12.2	3	8.6	4.4	4.1	399	21	63	210	0.5	0.5	59	349	398	0.5	5
CAR110/BL/GSP2/ASR109/MA1B	95	366	47	10	26	2	12.7	2	9.2	4.4	3.6	399	22	65	210	0.5	0.5	57	356	401	0.5	5
CAR110/BL/GSP2/ASR109/MA1B	96	358	46	10	26	2	13	2	8.7	4.5	3.2	391	21	69	209	0.5	0.5	54	349	395	0.5	4
CAR110/BL/GSP2/ASR209/MA1B	96	362	46	9.8	25	2	12.4	2	8.9	4.2	2.9	399	21	66	210	0.5	0.5	57	361	400	0.5	6
CG515	-	-	-	-	-	-	-	-	-	-	-	-	-	-	-	-	-	-	-	-	-	-
CG515	-	-	-	-	-	-	-	-	-	-	-	-	-	-	-	-	-	-	-	-	-	-
CG515	-	-	-	-	-	-	-	-	-	-	-	-	-	-	-	-	-	-	-	-	-	-
CG515	-	-	-	-	-	-	-	-	-	-	-	-	-	-	-	-	-	-	-	-	-	-
GSP2	-	-	-	-	-	-	-	-	-	-	-	-	-	-	-	-	-	-	-	-	-	-
GSP2/CG51509/LS4/BL/Ma1b/ASR109	15	60	8	2.9	5	1	3.2	1	2.4	1.9	0.1	11	1	38	50	0.5	0.5	14	51	25	0.5	0.5
GSP2/CG51509/LS4/BL/Ma1b/ASR109	14	57	8	2.9	5	1	3.2	1	2.6	2	0.1	14	0.5	39	52	0.5	0.5	14	53	25	0.5	0.5
LLD	-	-	-	-	-	-	-	-	-	-	-	-	-	-	-	-	-	-	-	-	-	-
LLD	-	-	-	-	-	-	-	-	-	-	-	-	-	-	-	-	-	-	-	-	-	-
LLD	-	-	-	-	-	-	-	-	-	-	-	-	-	-	-	-	-	-	-	-	-	-

Sample Number	Se p	Te p	U p	V p	Zn p	Sc xrf	V xrf	Cr xrf	Co xrf	Ni xrf	Cu xrf	Zn xrf	Ga xrf	As xrf	Se xrf	Br xrf	Rb xrf	Sr xrf
WYL-09-50-215.8	0.5	0.5	845	14	0.5	2.7	24.5	11.9	1.5	7.2	7.4	2	22.8	5.9	5	40.3	123.4	195.9
WYL-09-50-216.5	0.5	0.5	170	80	112	2.7	18.2	16.7	1.5	7.1	12.7	69.8	18.2	5.9	5	26.8	268.9	119.5
WYL-09-50-64.1	0.5	0.5	0.5	5	3	-	-	-	-	-	-	-	-	-	-	-	-	-
WYL-10-61-128.0b	1	0.5	566	3	166	2.9	0.5	13.3	1.5	65.3	170.6	278	0.5	19	0.55	33.5	28	3.2
WYL-10-61-132.0	0.5	0.5	718	11	18	5.9	13.1	23.6	1.5	1	8.3	21.4	5.5	18	0.55	42.1	102.1	29.2
WYL-10-61-133.8	0.5	0.5	356	0.5	2	2.9	0.5	12.2	1.5	1	7	2	6.8	14	0.55	37.7	91.7	59.8
WYL-10-61-135.4	0.5	0.5	28.4	0.5	2	2.9	0.5	6.7	1.5	1	4.9	2	14.8	11	0.55	37.2	338.3	89.5
WYL-10-61-158.2	1	0.5	7.47	59	58	5.7	93	67.6	8.5	36.8	15.6	82.5	12.5	14	0.55	10.5	276	57
WYL-10-61-181.5	0.5	0.5	7.94	34	61	6.5	45.3	24.3	1.5	8.4	6.6	78.8	25.7	13	0.55	16	195	183.8
WYL-10-61-190.3	0.5	0.5	1160	10	28	2.9	26.1	61.7	7.1	1	2.5	50.6	11.4	23	0.55	13.7	45.9	15.1
WYL-10-61-202.8	0.5	0.5	16.4	75	122	5.7	155.8	9.9	40	22.3	2.5	172.5	28.8	13	36.2	0.5	354.4	258.3
WYL-10-62-107.9	3	0.5	49.8	63	150	8.9	110.2	45.7	18.5	27.6	12.9	217.4	29.1	10	29.7	0.5	271.3	61
WYL-10-62-112.2	0.5	0.5	207	3	89	2.9	5.6	20.7	1.5	1	2.5	119.5	7.7	15	0.55	21	27.4	19.5
WYL-10-62-44.8b	1	0.5	1.37	98	77	14.6	100.6	35.7	9.2	9.8	46.7	83.6	11.3	11	0.55	0.5	101	137.6
WYL-10-62-70.7	0.5	0.5	23.2	0.5	13	2.9	0.5	5.3	1.5	1	2.5	12	17.8	11	0.55	19.1	349.3	164.9
WYL-10-62-79.4	7	0.5	204	140	177	20.3	301.3	172.2	109.4	90.8	44.8	272	21.4	14	40.8	0.5	335.4	16.4
WYL-10-62-83.9	3	0.5	754	26	73	12.9	65.7	37.8	20	18	2.5	142.4	17.7	16	27.3	0.5	317.4	66
WYL-10-62-92.0	3	0.5	2440	7	46	4	9.4	21.7	1.5	8.4	15.7	88.7	21.7	33	0.55	27.2	189.5	90.6
WYL-10-62-93.5	6	0.5	1030	45	278	12	116.6	50.3	36.2	55.7	39	396.9	18.8	21	26.9	0.5	348.4	15.9
WYL-09-44-68.5	0.5	0.5	21.9	5	8	4.7	0.6	15.7	1.5	1	2.5	8.1	30	13	0.55	25.5	63.9	165.3
WYL-09-44-69.0	0.5	0.5	9.6	6	16	4.1	0.5	13	1.5	1	6.7	19.1	34.9	12	0.55	24	74.3	158.4
WYL-09-44-73.4	1	0.5	49.7	50	111	12.3	99.6	52.3	21.3	18.7	13.8	158.3	35.1	9	22.4	0.5	304.7	130.9
WYL-09-44-74.9	1	0.5	33.4	15	97	11.3	101.3	6.7	59.8	9.3	150.8	100.6	22.1	17	37	0.5	118	2.2
WYL-09-44-76.1	1	0.5	25	2	45	4.1	18.5	12.6	12.4	1	19.5	78	29.8	14	15.2	0.5	34.4	77.6
WYL-09-44-76.4	1	0.5	17	8	185	18.1	150.2	30.4	223	1	2.5	226.8	42.3	16	0.55	0.5	25.1	16.2
WYL-09-46-26.9	4	0.5	101	98	242	14.3	125.8	137	25.5	44.1	12.5	278	16.8	15	18.3	0.5	310.9	6.6
WYL-09-46-30.8	18	11	210	206	66	21.5	275.5	44.9	57.2	64.8	5.1	43.9	26.3	5.9	38.9	5	95.1	86.5
WYL-09-46-31.1	6	15	675	143	98	14.4	190.3	36.4	32.3	50	29.5	95.9	23.1	5.9	5	5	251.4	82.4
WYL-09-46-32.6	14	0.5	67	126	191	16.1	234	25.3	45.1	42.1	2.2	268.7	31.9	5.9	43.5	5	473.5	47
WYL-09-46-34.0	18	2	66	194	224	21.4	300.9	35.3	71.7	63.1	32.7	270.9	29.8	5.9	50.8	5	487.8	36.4
WYL-09-46-35.0	5	0.5	600	176	351	25.8	280.8	103.5	75	52.9	10.1	374.9	19	22	41.1	0.5	345.8	5.5
WYL-09-46-42.8	9	1	22	48	173	-	-	-	-	-	-	-	-	-	-	-	-	-
WYL-09-46-47.3	1	0.5	13.6	4	66	4.2	44	6.1	34.7	1	2.5	72.1	22.5	13	33.5	0.5	89.6	27.2
WYL-09-46-81.6	0.5	0.5	5	1	25	-	-	-	-	-	-	-	-	-	-	-	-	-
WYL-09-46-83.0	1	0.5	317	2	17	2.9	27.1	25.2	9.3	1	63.6	20	19	13	0.55	11.1	119.4	35.3
CAR110/ASR109/BL/G2/Ma1b	1	3120	130	95	-	-	-	-	-	-	-	-	-	-	-	-	-	-
CAR110/ASR209/BM/G2/Ma1b	2	3230	135	100	-	-	-	-	-	-	-	-	-	-	-	-	-	-
CAR110/BL/GSP2/ASR109/MA1B	0.5	3100	136	95	-	-	-	-	-	-	-	-	-	-	-	-	-	-
CAR110/BL/GSP2/ASR109/MA1B	0.5	3280	146	93	-	-	-	-	-	-	-	-	-	-	-	-	-	-
CAR110/BL/GSP2/ASR109/MA1B	0.5	3190	146	91	-	-	-	-	-	-	-	-	-	-	-	-	-	-
CAR110/BL/GSP2/ASR209/MA1B	0.5	3210	135	95	-	-	-	-	-	-	-	-	-	-	-	-	-	-
CG515	-	-	-	-	-	-	-	-	-	-	-	-	-	-	-	-	-	-
CG515	-	-	-	-	-	-	-	-	-	-	-	-	-	-	-	-	-	-
CG515	-	-	-	-	-	-	-	-	-	-	-	-	-	-	-	-	-	-
CG515	-	-	-	-	-	-	-	-	-	-	-	-	-	-	-	-	-	-
GSP2	-	-	-	-	6	72	16	7	23	47	125	20	6	5	16	216	231	33
GSP2/CG51509/LS4/BL/Ma1b/ASR109	0.5	30	101	199	-	-	-	-	-	-	-	-	-	-	-	-	-	-
GSP2/CG51509/LS4/BL/Ma1b/ASR109	0.5	32	105	206	-	-	-	-	-	-	-	-	-	-	-	-	-	-
LLD	-	-	-	-	2	1	4	3	2	5	4	1	3	15	10	1	1	7
LLD	-	-	-	-	2	1	4	3	2	5	4	1	3	15	10	1	1	7
LLD	-	-	-	-	2	1	4	3	2	5	4	1	3	10	10	1	1	5

Sample Number	Y xrf	Zr xrf	Nb xrf	Mo xrf	Sn xrf	Sb xrf	Cs xrf	Ba xrf	La xrf	Hf xrf	Ta xrf	W xrf	Pb xrf	Bi xrf	Th xrf	U xrf
WYL-09-50-215.8	39.5	4409.2	42.1	5.8	3.4	1	10.9	292.4	45.7	267	23.8	41	91.4	50.1	834.7	1285.7
WYL-09-50-216.5	42.1	191.1	18	52.6	3	2.8	8.9	1161.9	14.4	53.5	14.8	18.3	216.4	32.3	304.1	455.8
WYL-09-50-64.1	-	-	-	-	-	-	-	-	-	-	-	-	-	-	-	-
WYL-10-61-128.0b	32	2158.3	13	35.7	7.9	2.5	2.5	17	2.5	28.2	39	67.6	308.3	66.1	161.5	828.5
WYL-10-61-132.0	46	370	20	254.6	9.7	3	5	75.9	2.5	22.2	41	74.5	328.9	77.9	674.7	930.7
WYL-10-61-133.8	28	472	6	102.3	8.8	4	5	98.6	2.5	20.8	39.1	66.9	103.8	71.3	400.4	506.2
WYL-10-61-135.4	13	50	4	46.8	9.2	4.5	8	391.2	2.5	19.1	39.3	67.3	118.9	68.2	57.4	35.9
WYL-10-61-158.2	37	297.8	35	27.4	5.9	1	7	1063.1	2.5	12	24.2	18.7	28.8	0.5	17.1	8.5
WYL-10-61-181.5	3.5	59	30	5.6	10	1.9	11	335.4	24.1	11.7	26.2	22.5	9.5	0.5	0.53	5.5
WYL-10-61-190.3	79	3530.5	38	5.6	12.7	1	2.5	15	7.2	26.7	27	31.8	211.2	13.2	1001	1273.4
WYL-10-61-202.8	17	40	49	5.6	12.9	1	17	878.1	34.3	0.5	14.4	0.5	16	0.5	0.53	5.9
WYL-10-62-107.9	43	161.9	69	5.6	12.1	1	22	259.1	92.3	0.5	16.8	0.5	44.9	0.5	189.2	51.9
WYL-10-62-112.2	19	680.4	15	5.6	11.6	1.5	2.5	30	2.5	16.2	30	36.9	112.8	26.6	427.2	250.9
WYL-10-62-44.8b	35	67	7	5.6	7.4	1	2.5	807.7	5.7	0.5	21.2	9.7	14	0.5	0.53	1
WYL-10-62-70.7	3.5	33	3	5.6	8.6	1.6	2.5	1128.9	2.5	12.4	26.8	28.5	90.8	14.8	0.53	35.8
WYL-10-62-79.4	119	696	136	5.6	2.7	1	10	945.7	2.5	0.5	12	0.5	9.2	0.5	156.6	182.2
WYL-10-62-83.9	200	452.8	74	498.8	3.9	1	6	931.6	2.5	9.7	18.1	15	236.7	0.5	750.4	816
WYL-10-62-92.0	114	7301.9	78	19.2	6.5	1	7	181.4	70.9	43.1	33.7	60.5	796.1	46.5	1152.2	2318.5
WYL-10-62-93.5	68	2038.5	147	5.6	6	1	18	473.6	24.6	15.4	16.7	0.5	500.8	0.5	924	889.7
WYL-09-44-68.5	20	832.8	11	5.6	10.5	3.5	2.5	13.8	31.1	17.9	32.3	44.5	39.3	38.1	35.7	38.9
WYL-09-44-69.0	15	52	10	5.6	6.7	3.5	6	29.8	30.5	14.5	31.1	42.8	24.4	32.1	20.2	8.1
WYL-09-44-73.4	114	103	76	5.6	9.8	1	39	258.7	689.2	0.5	19.4	0.5	37.2	0.5	773.9	64.6
WYL-09-44-74.9	54	11735.2	112	5.6	12.1	1	17	235.2	309	44.3	15.7	0.5	14	0.5	722.6	75.7
WYL-09-44-76.1	39	3743.1	33	12.3	11	1	13	41.5	238.6	22.2	21.9	11.2	22.4	0.5	308.2	44.2
WYL-09-44-76.4	80	670	133	17.7	17.3	1	27	390.5	602.4	0.5	0.5	0.5	66	0.5	306.6	11.5
WYL-09-46-26.9	55	658.6	122	6.5	9.7	1	13	160.4	10.2	12.1	22.9	11.8	67	0.5	421.9	121.9
WYL-09-46-30.8	325.6	719.4	192	31.6	9.5	1	2.5	330.2	3443.7	5	5	5	136.8	2.5	3140.4	179.1
WYL-09-46-31.1	736.9	1944.5	185.7	218.5	10.1	1	2.5	356.2	3710.4	104.7	5	5	483.9	2.5	5935.3	513.5
WYL-09-46-32.6	136.7	2.5	184.2	7.1	7.1	1	11.9	477.6	791.1	5	5	5	111.7	2.5	1033.5	62.2
WYL-09-46-34.0	125.3	49.6	202.8	5.8	6.1	1	10.5	554.8	751.6	5	5	5	82.4	2.5	781.2	59.4
WYL-09-46-35.0	61	3499.8	158	5.6	5	1	37	584.2	53.9	16.6	12.2	0.5	447.7	0.5	946.5	598.1
WYL-09-46-42.8	-	-	-	-	-	-	-	-	-	-	-	-	-	-	-	-
WYL-09-46-47.3	3.5	207	39	14.6	14.6	1	2.5	266.2	18.4	0.5	17.3	0.5	22	0.5	19.4	6.4
WYL-09-46-81.6	-	-	-	-	-	-	-	-	-	-	-	-	-	-	-	-
WYL-09-46-83.0	59	3913.3	38	12.5	12.6	1	10	199.1	219.7	25.3	26.7	26.4	69.8	0.5	950.6	343.3
CAR110/ASR109/BL/G2/Ma1b	-	-	-	-	-	-	-	-	-	-	-	-	-	-	-	-
CAR110/ASR209/BM/G2/Ma1b	-	-	-	-	-	-	-	-	-	-	-	-	-	-	-	-
CAR110/BL/GSP2/ASR109/MA1B	-	-	-	-	-	-	-	-	-	-	-	-	-	-	-	-
CAR110/BL/GSP2/ASR109/MA1B	-	-	-	-	-	-	-	-	-	-	-	-	-	-	-	-
CAR110/BL/GSP2/ASR109/MA1B	-	-	-	-	-	-	-	-	-	-	-	-	-	-	-	-
CAR110/BL/GSP2/ASR209/MA1B	-	-	-	-	-	-	-	-	-	-	-	-	-	-	-	-
CG515	-	-	-	-	-	-	-	-	-	-	-	-	-	-	-	-
CG515	-	-	-	-	-	-	-	-	-	-	-	-	-	-	-	-
CG515	-	-	-	-	-	-	-	-	-	-	-	-	-	-	-	-
CG515	-	-	-	-	-	-	-	-	-	-	-	-	-	-	-	-
GSP2	574	27	6	8	1	10	1417	187	26	5	5	33	3	102	3	-
GSP2/CG51509/LS4/BL/Ma1b/ASR109	-	-	-	-	-	-	-	-	-	-	-	-	-	-	-	-
GSP2/CG51509/LS4/BL/Ma1b/ASR109	-	-	-	-	-	-	-	-	-	-	-	-	-	-	-	-
LLD	5	1	1	3	2	5	5	5	10	10	10	1	10	13	2	-
LLD	5	1	1	3	2	5	5	5	10	10	10	1	10	13	2	-
LLD	5	1	1	3	2	5	5	5	10	10	10	1	5	10	2	-

APPENDIX C

GROUP A PEGMATITES MINERAL CHEMISTRY DATA

Supplementary Data Table 1 for Chapter 3 (McKechnie *et al.* 2012a)

Table C-1. Uraninite

Sample	WYL-10-61-190.3 Urn1	WYL-10-61-190.3 Urn1	WYL-10-61-190.3 Urn1	WYL-10-61-190.3 Urn1	WYL-10-61-190.3 Urn1	WYL-10-61-190.3 Urn1	WYL-10-61-190.3 Urn1	WYL-10-61-190.3 Urn2	WYL-10-61-190.3 Urn2	WYL-10-61-190.3 Urn2	WYL-10-61-190.3 Urn2	WYL-10-61-190.3 Urn2	WYL-10-61-190.3 Urn3-Zrn2	WYL-10-61-190.3 Urn3-Zrn2
Line	25	26	27	28	29	30	31	32	33	34	35	36	47	48
SiO2	0.22	0.41	0.19	0.33	0.11	0.10	0.23	0.07	0.10	0.07	0.09	0.03	0.10	0.25
TiO2	0.01	0.04	0.00	0.02	0.04	0.01	0.03	0.00	0.04	0.01	0.03	0.03	0.01	0.02
Al2O3	0.00	0.00	0.00	0.00	0.00	0.00	0.00	0.00	0.00	0.00	0.00	0.00	0.00	0.00
FeO	0.00	0.66	0.16	0.35	0.01	0.05	0.47	0.00	0.18	0.00	0.00	0.00	0.00	0.17
MnO	0.03	0.30	0.09	0.19	0.01	0.05	0.14	0.00	0.03	0.00	0.02	0.01	0.00	0.06
MgO	0.00	0.00	0.00	0.00	0.00	0.00	0.00	0.00	0.00	0.00	0.00	0.00	0.00	0.00
CaO	0.93	2.84	1.30	2.33	0.49	0.59	1.38	0.13	0.38	0.14	0.25	0.09	0.18	0.47
P2O5	0.00	0.00	0.00	0.01	0.03	0.02	0.01	0.00	0.02	0.03	0.01	0.00	0.00	0.03
UO2	64.15	64.00	64.39	64.40	62.41	62.42	64.32	61.31	61.03	60.27	60.57	60.30	62.88	63.62
ThO2	5.75	6.40	5.82	5.93	6.74	6.38	6.11	5.51	5.84	6.60	6.50	7.09	5.80	6.00
PbO	17.31	10.79	15.22	13.03	17.50	16.99	14.48	19.30	18.38	18.97	19.06	19.45	18.14	18.32
ZrO2	0.00	0.05	0.16	0.00	0.03	0.04	0.11	0.11	0.02	0.12	0.03	0.08	0.03	0.05
HfO2	0.00	0.00	0.00	0.00	0.00	0.00	0.00	0.00	0.00	0.03	0.00	0.00	0.00	0.00
Y2O3	4.01	4.31	4.09	4.12	4.15	4.37	4.10	5.15	4.78	4.70	4.93	4.56	4.20	2.98
La2O3	0.02	0.04	0.06	0.00	0.00	0.00	0.00	0.04	0.06	0.00	0.00	0.01	0.05	0.04
Ce2O3	0.39	0.37	0.42	0.25	0.46	0.45	0.34	0.42	0.43	0.42	0.43	0.39	0.31	0.32
Pr2O3	0.04	0.07	0.10	0.01	0.05	0.09	0.06	0.11	0.09	0.11	0.10	0.11	0.06	0.03
Nd2O3	0.64	0.67	0.60	0.57	0.69	0.73	0.54	0.65	0.78	0.71	0.65	0.59	0.54	0.47
Sm2O3	0.37	0.42	0.43	0.39	0.44	0.41	0.43	0.44	0.55	0.50	0.40	0.45	0.44	0.39
Gd2O3	0.47	0.52	0.47	0.51	0.53	0.51	0.53	0.62	0.61	0.62	0.66	0.58	0.53	0.44
Dy2O3	0.80	0.94	0.95	0.83	1.02	0.90	0.89	1.04	1.04	1.04	1.08	0.98	0.90	0.71
Er2O3	0.47	0.49	0.62	0.54	0.53	0.51	0.61	0.59	0.67	0.56	0.66	0.69	0.53	0.37
Total	95.62	93.33	95.07	93.81	95.25	94.60	94.77	95.49	95.03	94.92	95.46	95.47	94.70	94.74
REE2O3	3.20	3.51	3.64	3.11	3.72	3.58	3.39	3.90	4.24	3.96	3.98	3.81	3.36	2.77

Table C-1 (Cont`d). Uraninite

Sample	WYL-10-61-190.3 Urn3-Zrn2	WYL-10-61-190.3 Urn3-Zrn2	WYL-10-61-190.3 Urn3-Zrn2	WYL-10-61-190.3 Urn3-Zrn2	WYL-10- 62-93.5 Urn1	WYL-10- 62-93.5 Urn1	WYL-10- 62-93.5 Urn1	WYL-10- 62-93.5 Urn1	WYL-10- 62-93.5 Urn1	WYL-10- 62-93.5 Urn1	WYL-10- 62-93.5 Urn1	WYL-10- 62-93.5 Urn1	WYL-10- 62-93.5 Urn1	WYL-10- 62-93.5 Urn1
Line	49	50	51	52	108	109	110	111	112	113	114	115	116	117
SiO2	0.10	0.07	0.09	1.00	0.15	0.20	0.21	0.15	0.16	0.11	0.26	0.30	0.10	0.13
TiO2	0.02	0.03	0.02	0.05	0.06	0.01	0.03	0.03	0.07	0.06	0.03	0.02	0.05	0.08
Al2O3	0.00	0.00	0.00	0.02	0.00	0.00	0.00	0.00	0.00	0.00	0.00	0.00	0.00	0.00
FeO	0.09	0.00	0.11	0.29	0.06	0.04	0.21	0.01	0.02	0.07	0.09	0.07	0.09	0.03
MnO	0.01	0.00	0.00	0.02	0.01	0.01	0.00	0.01	0.01	0.01	0.02	0.03	0.00	0.01
MgO	0.00	0.00	0.00	0.00	0.00	0.00	0.00	0.00	0.00	0.00	0.00	0.00	0.00	0.00
CaO	0.37	0.31	0.13	0.33	0.35	0.50	0.33	0.28	0.54	0.44	0.50	0.61	0.12	0.65
P2O5	0.00	0.00	0.03	0.01	0.01	0.01	0.01	0.03	0.02	0.00	0.03	0.03	0.00	0.02
UO2	64.24	64.03	64.08	62.56	67.03	62.09	64.88	64.25	63.52	65.14	64.10	62.91	65.39	66.47
ThO2	5.70	5.90	5.76	6.20	6.92	6.21	8.71	8.55	7.40	7.84	7.39	7.25	6.57	7.96
PbO	18.97	19.51	19.70	18.22	20.78	16.53	16.05	17.87	19.29	19.00	16.58	19.89	21.06	16.94
ZrO2	0.04	0.05	0.09	1.43	0.00	0.09	0.10	0.10	0.13	0.14	0.10	0.11	0.08	0.14
HfO2	0.05	0.10	0.13	0.22	0.08	0.06	0.00	0.02	0.00	0.05	0.00	0.00	0.01	0.00
Y2O3	3.32	3.22	3.25	3.16	1.76	1.79	2.21	2.46	2.56	1.94	3.07	2.54	1.44	1.98
La2O3	0.00	0.00	0.00	0.05	0.01	0.00	0.00	0.00	0.06	0.00	0.03	0.05	0.00	0.00
Ce2O3	0.24	0.35	0.25	0.32	0.10	0.12	0.31	0.28	0.44	0.17	0.45	0.39	0.08	0.13
Pr2O3	0.02	0.08	0.12	0.03	0.00	0.00	0.07	0.00	0.04	0.00	0.04	0.12	0.03	0.00
Nd2O3	0.51	0.48	0.48	0.57	0.27	0.20	0.38	0.42	0.55	0.29	0.49	0.49	0.30	0.30
Sm2O3	0.37	0.41	0.36	0.30	0.12	0.21	0.22	0.29	0.34	0.19	0.31	0.28	0.16	0.19
Gd2O3	0.44	0.53	0.40	0.45	0.23	0.27	0.26	0.26	0.35	0.25	0.41	0.37	0.22	0.34
Dy2O3	0.78	0.68	0.79	0.77	0.46	0.53	0.57	0.57	0.54	0.47	0.74	0.61	0.40	0.43
Er2O3	0.49	0.43	0.47	0.42	0.31	0.24	0.25	0.37	0.41	0.27	0.44	0.28	0.19	0.30
Total	95.76	96.18	96.26	96.41	98.71	89.11	94.79	95.96	96.42	96.43	95.07	96.35	96.31	96.10
REE2O3	2.85	2.96	2.87	2.91	1.49	1.58	2.06	2.20	2.72	1.63	2.91	2.58	1.39	1.70

Table C-2. Thorite (Thr) + Coffinite (Cof) Chemistry

Sample	WYL-10-62-93.5 Thr1	WYL-10-62-93.5 Thr1	WYL-10-62-93.5 Thr1	WYL-10-62-93.5 Thr1	WYL-10-62-93.5 Thr1	WYL-10-62-93.5 Thr2	WYL-10-62-93.5 Thr2	WYL-10-62-93.5 Thr2	WYL-10-62-93.5 Thr2	WYL-10-62-93.5 Thr2	WYL-10-61-190.3 Thr1-Zrn1	WYL-10-61-190.3 Thr1-Zrn1	WYL-10-61-190.3 Thr1-Zrn1	WYL-10-62-93.5 Thr1 (Cof)
Line	85	86	87	89	90	103	104	105	106	107	38	37	39	88
SiO2	18.95	15.70	18.83	17.27	19.44	19.11	16.05	18.44	16.75	18.05	21.71	20.13	23.18	15.89
TiO2	0.09	0.04	0.11	0.05	0.09	0.06	0.05	0.02	0.03	0.07	0.00	0.00	0.00	0.09
Al2O3	1.05	1.00	1.14	1.53	1.19	1.11	0.95	1.10	0.70	1.12	1.14	0.75	1.05	1.49
FeO	5.45	3.07	3.57	5.57	2.21	6.11	5.56	5.16	4.51	6.73	8.02	4.76	6.53	10.66
MnO	0.06	0.00	0.04	0.04	0.04	0.01	0.04	0.03	0.04	0.12	0.05	0.03	0.02	0.03
MgO	0.06	0.07	0.09	0.08	0.12	0.04	0.04	0.03	0.02	0.03	0.04	0.04	0.04	0.05
CaO	2.57	2.78	2.69	2.37	2.98	1.77	1.83	2.01	2.17	2.20	1.41	1.10	1.44	2.35
P2O5	2.58	2.80	2.68	1.92	3.34	2.59	2.71	3.20	4.60	3.34	0.74	0.91	0.19	2.09
UO2	2.53	4.90	5.15	2.64	2.38	0.57	0.63	1.09	3.65	1.28	0.44	0.20	0.32	26.62
ThO2	48.17	44.19	45.59	40.20	53.97	46.76	43.47	48.56	46.77	45.48	38.48	48.33	34.30	15.98
PbO	0.21	0.18	0.27	16.10	0.30	0.23	12.59	1.79	0.20	1.37	0.21	0.23	0.18	0.44
ZrO2	4.04	4.10	4.04	3.74	5.05	6.18	3.34	2.69	0.89	2.80	12.28	9.15	18.32	1.67
HfO2	0.07	0.10	0.00	0.00	0.05	0.03	0.00	0.03	0.04	0.00	0.39	0.14	0.60	0.00
Y2O3	0.85	0.97	1.12	0.76	1.05	0.98	0.87	1.61	3.23	1.64	1.28	0.94	1.06	1.51
La2O3	0.39	0.44	0.49	0.38	0.51	0.31	0.23	0.33	0.34	0.34	0.17	0.07	0.08	0.35
Ce2O3	1.14	1.18	1.35	0.86	1.36	0.95	0.82	1.10	1.64	1.17	0.44	0.44	0.27	1.28
Pr2O3	0.12	0.10	0.08	0.14	0.13	0.09	0.10	0.12	0.21	0.17	0.05	0.00	0.08	0.12
Nd2O3	0.42	0.54	0.50	0.32	0.43	0.35	0.30	0.58	0.86	0.51	0.32	0.21	0.23	0.48
Sm2O3	0.08	0.10	0.07	0.05	0.10	0.10	0.08	0.14	0.31	0.16	0.16	0.06	0.08	0.10
Gd2O3	0.08	0.11	0.23	0.05	0.11	0.11	0.14	0.24	0.38	0.25	0.18	0.15	0.13	0.14
Dy2O3	0.08	0.14	0.06	0.03	0.15	0.09	0.12	0.14	0.50	0.25	0.20	0.17	0.11	0.08
Er2O3	0.08	0.16	0.07	0.00	0.15	0.11	0.03	0.12	0.34	0.23	0.18	0.13	0.12	0.11
Total	89.04	82.68	88.15	94.12	95.15	87.66	89.94	88.52	88.17	87.30	87.88	87.97	88.32	81.53
TREEO	2.37	2.78	2.83	1.83	2.95	2.10	1.82	2.76	4.57	3.08	1.70	1.25	1.10	2.66
O	16	16	16	16	16	16	16	16	16	16	16	16	16	16
Si	3.70	3.42	3.72	3.55	3.59	3.71	3.44	3.66	3.37	3.58	3.98	3.96	4.07	3.44
Al	0.24	0.26	0.26	0.37	0.26	0.25	0.24	0.26	0.17	0.26	0.25	0.18	0.22	0.38
Ti	0.01	0.01	0.02	0.01	0.01	0.01	0.01	0.00	0.00	0.01	0.00	0.00	0.00	0.01
Fe	0.89	0.56	0.59	0.96	0.34	0.99	1.00	0.86	0.76	1.12	1.23	0.78	0.96	1.93
Mn	0.01	0.00	0.01	0.01	0.01	0.00	0.01	0.01	0.01	0.02	0.01	0.01	0.00	0.00
Mg	0.02	0.02	0.03	0.02	0.03	0.01	0.01	0.01	0.01	0.01	0.01	0.01	0.01	0.02
Ca	0.54	0.65	0.57	0.52	0.59	0.37	0.42	0.43	0.47	0.47	0.28	0.23	0.27	0.54
U	0.11	0.24	0.23	0.12	0.10	0.02	0.03	0.05	0.16	0.06	0.02	0.01	0.01	1.28
Th	2.14	2.19	2.05	1.88	2.27	2.07	2.12	2.19	2.14	2.05	1.61	2.16	1.37	0.79
Pb	0.01	0.01	0.01	0.89	0.01	0.01	0.73	0.10	0.01	0.07	0.01	0.01	0.01	0.03
Zr	0.38	0.44	0.39	0.38	0.46	0.59	0.35	0.26	0.09	0.27	1.10	0.88	1.57	0.18
Hf	0.00	0.01	0.00	0.00	0.00	0.00	0.00	0.00	0.00	0.00	0.02	0.01	0.03	0.00
P	0.43	0.52	0.45	0.33	0.52	0.43	0.49	0.54	0.78	0.56	0.12	0.15	0.03	0.38
Y	0.09	0.11	0.12	0.08	0.10	0.10	0.10	0.17	0.35	0.17	0.12	0.10	0.10	0.17
La	0.03	0.04	0.04	0.03	0.03	0.02	0.02	0.02	0.03	0.02	0.01	0.01	0.00	0.03
Ce	0.08	0.09	0.10	0.06	0.09	0.07	0.06	0.08	0.12	0.08	0.03	0.03	0.02	0.10
Pr	0.01	0.01	0.01	0.01	0.01	0.01	0.01	0.01	0.02	0.01	0.00	0.00	0.00	0.01
Nd	0.03	0.04	0.04	0.02	0.03	0.02	0.02	0.04	0.06	0.04	0.02	0.01	0.01	0.04
Sm	0.01	0.01	0.00	0.00	0.01	0.01	0.01	0.01	0.02	0.01	0.01	0.00	0.00	0.01
Gd	0.01	0.01	0.01	0.00	0.01	0.01	0.01	0.02	0.03	0.02	0.01	0.01	0.01	0.01
Dy	0.01	0.01	0.00	0.00	0.01	0.01	0.01	0.01	0.03	0.02	0.01	0.01	0.01	0.01
Er	0.00	0.01	0.00	0.00	0.01	0.01	0.00	0.01	0.02	0.01	0.01	0.01	0.01	0.01
Total	8.75	8.64	8.64	9.27	8.50	8.71	9.08	8.72	8.64	8.86	8.86	8.57	8.71	9.35
∑ Th U Zr Hf Y REES	2.90	3.20	2.98	2.60	3.13	2.93	2.74	2.87	3.06	2.77	2.98	3.24	3.15	2.62
% ThSiO4	74%	68%	69%	72%	73%	71%	77%	76%	70%	74%	54%	67%	43%	30%
% SiO4	4%	7%	8%	5%	3%	1%	1%	2%	5%	2%	1%	0%	0%	49%
% Zr+ Hf	13%	14%	13%	14%	15%	20%	13%	9%	3%	10%	38%	27%	51%	7%
% Y + REE	9%	10%	11%	8%	10%	8%	9%	13%	22%	14%	8%	6%	5%	14%

Table C-3. Magnetite Chemistry

Sample	WYL-10-61-190.3 Mag1-Ilm1	WYL-10-61-190.3 Mag1-Ilm1	WYL-10-61-190.3 Mag1-Ilm1	WYL-10-61-190.3 Mag1-Ilm1	WYL-10-61-190.3 Mag1-Ilm1	WYL-10-61-190.3 Mag1-Ilm1	WYL-10-61-190.3 Mag1-Ilm1	WYL-10-61-190.3 Mag2-Ilm2	WYL-10-61-190.3 Mag2-Ilm2	WYL-10-61-190.3 Mag2-Ilm2	WYL-10-61-190.3 Mag2-Ilm2	WYL-10-61-190.3 Mag2-Ilm2	WYL-10-61-190.3 Mag2-Ilm2	WYL-10-61-190.3 Mag2-Ilm2
Line	18	19	20	24	25	26	27	32	33	34	35	36	37	38
SiO2	0.10	0.07	0.07	0.08	0.09	0.10	1.33	0.07	0.07	0.10	0.22	0.09	0.08	0.08
TiO2	0.30	0.29	0.82	0.32	0.24	2.21	6.40	1.28	0.53	0.14	2.16	0.24	0.15	0.54
Al2O3	0.40	0.41	0.41	0.32	0.43	0.76	0.94	2.37	0.89	0.40	2.68	0.44	0.33	1.28
Cr2O3	0.00	0.00	0.00	0.00	0.00	0.00	0.01	0.00	0.00	0.00	0.00	0.01	0.01	0.00
V2O3	0.03	0.04	0.02	0.04	0.05	0.04	0.04	0.03	0.04	0.01	0.04	0.04	0.05	0.05
FeO	91.48	91.11	91.16	91.49	91.44	88.65	80.55	88.25	91.73	92.61	89.76	92.36	92.99	91.63
MnO	0.03	0.01	0.03	0.03	0.03	0.34	0.16	0.26	0.10	0.04	0.35	0.04	0.02	0.06
ZnO	0.00	0.00	0.01	0.00	0.00	0.00	0.00	0.08	0.03	0.04	0.11	0.00	0.00	0.08
NiO	0.01	0.01	0.02	0.03	0.00	0.00	0.02	0.03	0.00	0.01	0.01	0.00	0.02	0.00
MgO	0.01	0.00	0.00	0.00	0.00	0.00	0.15	0.02	0.01	0.02	0.05	0.00	0.00	0.01
CaO	0.01	0.01	0.00	0.00	0.01	0.00	0.04	0.00	0.01	0.00	0.02	0.00	0.00	0.00
Total	92.37	91.95	92.54	92.31	92.29	92.09	89.65	92.40	93.39	93.37	95.39	93.23	93.65	93.73
Fe2O3 wt. %	67.02	66.77	66.13	67.06	67.06	66.75	68.13	67.73	68.37	66.46	68.02	67.48	67.16	68.48
FeO wt. %	31.17	31.02	31.65	31.15	31.11	31.67	31.31	31.42	31.47	31.83	31.93	32.14	32.03	31.66
Total	99.08	98.64	99.17	99.03	99.01	100.08	100.20	100.02	100.50	100.39	100.93	100.95	101.16	100.91
O	32	32	32	32	32	32	32	32	32	32	32	32	32	32
Si	0.03	0.02	0.02	0.02	0.03	0.02	0.03	0.03	0.03	0.02	0.03	0.03	0.03	0.03
Ti	0.07	0.07	0.19	0.08	0.06	0.12	0.03	0.06	0.03	0.12	0.11	0.18	0.09	0.05
Al	0.15	0.15	0.15	0.12	0.16	0.32	0.14	0.16	0.12	0.46	0.12	0.10	0.47	0.12
Fe+3	15.64	15.66	15.42	15.67	15.66	15.38	15.73	15.66	15.74	15.23	15.59	15.46	15.27	15.70
Fe+2	8.08	8.08	8.20	8.09	8.08	8.11	8.03	8.07	8.05	8.11	8.13	8.18	8.10	8.07
Mn	0.01	0.00	0.01	0.01	0.01	0.02	0.01	0.01	0.01	0.02	0.01	0.01	0.02	0.01
Mg	0.01	0.00	0.00	0.00	0.00	0.00	0.01	0.00	0.00	0.00	0.00	0.00	0.01	0.00
Ca	0.00	0.00	0.00	0.00	0.00	0.00	0.00	0.00	0.00	0.00	0.00	0.00	0.00	0.00
Cr	0.00	0.00	0.00	0.00	0.00	0.00	0.00	0.00	0.00	0.00	0.00	0.00	0.00	0.00
Zn	0.00	0.00	0.00	0.00	0.00	0.01	0.01	0.00	0.00	0.02	0.00	0.01	0.00	0.01
V	0.01	0.01	0.01	0.01	0.01	0.01	0.00	0.01	0.01	0.01	0.01	0.01	0.01	0.01
Ni	0.00	0.00	0.00	0.01	0.00	0.00	0.00	0.00	0.00	0.00	0.00	0.00	0.00	0.00
Total	24.00	24.00	24.00	24.00	24.00	24.00	24.00	24.00	24.00	24.00	24.00	24.00	24.00	24.00

Table C-3 (cont`d). Magnetite Chemistry

Sample	WYL-10-61-190.3 Mag3-Ilm3	WYL-10-61-190.3 Mag3-Ilm3	WYL-10-61-190.3 Mag3-Ilm3	WYL-10-61-190.3 Mag3-Ilm3	WYL-10-61-190.3 Mag3-Ilm3	WYL-10-61-190.3 Mag3-Ilm3	WYL-10-61-190.3 Mag3-Ilm3	WYL-10-61-190.3 Mag3-Ilm3	WYL-10-61-190.3 Mag4-Ilm4-TiOx1	WYL-10-61-190.3 Mag4-Ilm4-TiOx1	WYL-10-61-190.3 Mag4-Ilm4-TiOx1	WYL-10-61-190.3 Mag4-Ilm4-TiOx1	WYL-10-61-190.3 Mag4-Ilm4-TiOx1
Line	46	47	48	49	50	51	52	53	60	61	62	63	64
SiO2	3.34	0.10	0.09	0.08	0.09	0.10	0.09	0.11	0.10	0.11	0.22	0.11	0.13
TiO2	0.25	2.96	0.49	0.80	0.41	0.23	17.84	0.51	0.55	0.22	0.25	0.20	0.23
Al2O3	2.47	1.64	0.32	0.29	1.32	0.33	9.12	0.35	0.34	0.36	0.46	0.34	0.34
Cr2O3	0.00	0.00	0.01	0.00	0.01	0.01	0.01	0.01	0.02	0.00	0.00	0.00	0.00
V2O3	0.06	0.04	0.03	0.04	0.05	0.04	0.05	0.04	0.05	0.03	0.03	0.04	0.05
FeO	84.24	89.13	93.13	92.86	92.46	93.29	70.56	92.86	92.67	92.64	92.35	92.75	92.81
MnO	0.05	0.59	0.03	0.05	0.07	0.03	2.08	0.07	0.06	0.04	0.03	0.02	0.01
ZnO	0.01	0.06	0.00	0.05	0.00	0.03	1.43	0.03	0.00	0.00	0.06	0.00	0.00
NiO	0.03	0.00	0.00	0.01	0.00	0.00	0.04	0.03	0.00	0.00	0.01	0.03	0.00
MgO	0.40	0.00	0.00	0.00	0.01	0.00	0.08	0.01	0.00	0.00	0.02	0.00	0.00
CaO	0.05	0.00	0.00	0.00	0.00	0.00	0.00	0.00	0.00	0.01	0.01	0.00	0.00
Total	90.92	94.53	94.12	94.19	94.43	94.05	101.30	94.03	93.80	93.41	93.43	93.48	93.56
Fe2O3 wt. %	67.81	67.60	67.99	67.54	68.07	68.04	62.40	62.57	62.23	61.52	48.64	55.49	26.17
FeO wt. %	31.84	31.85	31.46	31.58	31.49	31.59	32.50	31.95	33.76	33.78	36.78	34.31	47.01
Total	100.82	100.57	100.22	100.20	100.30	100.38	98.34	98.67	101.63	100.69	94.52	96.48	103.92
O	32	32	32	32	32	32	32	32	32	32	32	32	32
Si	0.03	0.03	0.03	0.07	0.03	0.04	0.03	0.02	0.07	0.03	0.43	1.03	0.02
Ti	0.12	0.13	0.05	0.06	0.05	0.05	0.52	0.30	0.48	0.67	1.54	0.06	3.73
Al	0.13	0.12	0.13	0.17	0.12	0.12	0.28	0.86	0.94	0.58	0.35	0.90	2.99
Fe+3	15.56	15.55	15.69	15.58	15.70	15.68	14.62	14.49	13.95	14.00	11.70	12.90	5.48
Fe+2	8.12	8.14	8.07	8.09	8.07	8.09	8.46	8.22	8.41	8.54	9.83	8.87	10.94
Mn	0.02	0.02	0.01	0.01	0.00	0.00	0.09	0.07	0.09	0.15	0.04	0.01	0.49
Mg	0.00	0.00	0.00	0.01	0.00	0.00	0.00	0.01	0.02	0.00	0.07	0.19	0.04
Ca	0.00	0.00	0.00	0.00	0.00	0.00	0.00	0.00	0.01	0.00	0.01	0.02	0.00
Cr	0.00	0.01	0.00	0.00	0.00	0.00	0.00	0.00	0.00	0.00	0.00	0.00	0.00
Zn	0.01	0.00	0.00	0.01	0.00	0.00	0.00	0.02	0.02	0.01	0.00	0.00	0.29
V	0.01	0.01	0.01	0.01	0.01	0.01	0.01	0.01	0.01	0.01	0.01	0.01	0.01
Ni	0.01	0.00	0.00	0.00	0.01	0.00	0.00	0.01	0.00	0.00	0.01	0.01	0.01
Total	24.00	24.00	24.00	24.00	24.00	24.00	24.00	24.00	24.00	24.00	24.00	24.00	24.00

Table C-4. Ilmenite and Rutile Chemistry

Mineral	Ilmenite										Ilemenite								Rutile	
SAMPLE	WYL-10-61-190.3 Mag1-lm1	WYL-10-61-190.3 Mag1-lm1	WYL-10-61-190.3 Mag1-lm1	WYL-10-61-190.3 Mag2-Ilm2	WYL-10-61-190.3 Mag2-Ilm2	WYL-10-61-190.3 Mag2-Ilm2	WYL-10-61-190.3 Mag2-Ilm2	WYL-10-61-190.3 Mag3-Ilm3	WYL-10-61-190.3 Mag3-Ilm3	WYL-10-61-190.3 Mag3-Ilm3	WYL-10-61-190.3 Mag3-Ilm3	WYL-10-61-190.3 Mag3-Ilm3	WYL-10-61-190.3 Mag3-Ilm3	WYL-10-61-190.3 Mag3-Ilm3	WYL-10-61-190.3 Mag4-Ilm4-TiOx1	WYL-10-61-190.3 Mag4-Ilm4-TiOx1	WYL-10-61-190.3 Mag4-Ilm4-TiOx1	WYL-10-61-190.3 Mag4-Ilm4-TiOx1	WYL-10-61-190.3 Mag4-Ilm4-TiOx1	WYL-10-61-190.3 Mag4-Ilm4-TiOx1
LINE	21	22	23	28	29	30	31	39	40	41	42	43	44	45	54	55	58	59	57	56
SiO2	0.18	0.00	0.01	0.01	0.02	0.01	0.03	0.01	0.01	0.00	0.02	0.02	0.02	0.03	0.04	0.04	0.04	0.04	0.56	0.04
TiO2	49.62	49.16	49.98	50.74	50.67	50.87	50.85	49.97	50.00	49.79	49.71	50.69	51.17	50.33	50.34	50.94	50.09	50.79	95.22	95.86
Al2O3	0.01	0.01	0.00	0.01	0.00	0.00	0.00	0.02	0.00	0.01	0.00	0.00	0.00	0.00	0.01	0.00	0.01	0.01	0.13	0.01
Cr2O3	0.00	0.00	0.00	0.00	0.00	0.00	0.00	0.00	0.00	0.00	0.00	0.00	0.00	0.00	0.00	0.00	0.00	0.00	0.00	0.00
V2O3	0.05	0.05	0.07	0.07	0.05	0.06	0.04	0.05	0.06	0.06	0.06	0.03	0.07	0.04	0.05	0.05	0.07	0.06	0.18	0.18
FeO	43.61	43.97	43.93	44.88	44.66	44.79	44.59	44.84	45.06	44.81	44.88	44.68	44.81	44.82	44.32	44.04	44.94	44.28	0.86	1.25
MnO	4.23	3.92	3.97	3.56	3.41	3.52	3.75	3.86	3.78	4.04	3.91	4.04	3.69	3.97	4.15	4.08	3.82	4.21	0.04	0.00
ZnO	0.04	0.01	0.00	0.06	0.06	0.02	0.06	0.03	0.04	0.00	0.04	0.03	0.01	0.00	0.03	0.02	0.00	0.00	0.00	0.02
NiO	0.00	0.03	0.01	0.00	0.00	0.00	0.01	0.00	0.00	0.00	0.00	0.01	0.00	0.00	0.01	0.00	0.02	0.02	0.01	0.00
MgO	0.02	0.03	0.00	0.00	0.01	0.00	0.00	0.01	0.01	0.00	0.00	0.02	0.02	0.00	0.01	0.03	0.03	0.01	0.00	0.00
CaO	0.00	0.00	0.02	0.00	0.01	0.00	0.01	0.00	0.00	0.00	0.01	0.00	0.01	0.00	0.00	0.01	0.00	0.00	0.16	0.01
Total	97.77	97.18	97.99	99.33	98.90	99.27	99.34	98.79	98.97	98.71	98.63	99.52	99.80	99.20	98.96	99.21	99.02	99.43	97.15	97.37
O	3	3	3	3	3	3	3	3	3	3	3	3	3	3	3	3	3	3	2	2
Si	0.00	0.00	0.00	0.00	0.00	0.00	0.00	0.00	0.00	0.00	0.00	0.00	0.00	0.00	0.00	0.00	0.00	0.00	0.01	0.00
Al	0.00	0.00	0.00	0.00	0.00	0.00	0.00	0.00	0.00	0.00	0.00	0.00	0.00	0.00	0.00	0.00	0.00	0.00	0.00	0.00
Ti	0.97	0.97	0.98	0.98	0.98	0.98	0.98	0.97	0.97	0.97	0.97	0.98	0.98	0.97	0.97	0.98	0.97	0.98	0.98	0.99
Fe	0.95	0.97	0.95	0.96	0.96	0.96	0.95	0.97	0.97	0.97	0.97	0.96	0.95	0.96	0.95	0.94	0.97	0.95	0.01	0.01
Mn	0.09	0.09	0.09	0.08	0.07	0.08	0.08	0.08	0.08	0.09	0.09	0.09	0.08	0.09	0.09	0.09	0.08	0.09	0.00	0.00
Mg	0.00	0.00	0.00	0.00	0.00	0.00	0.00	0.00	0.00	0.00	0.00	0.00	0.00	0.00	0.00	0.00	0.00	0.00	0.00	0.00
Zn	0.00	0.00	0.00	0.00	0.00	0.00	0.00	0.00	0.00	0.00	0.00	0.00	0.00	0.00	0.00	0.00	0.00	0.00	0.00	0.00
Ca	0.00	0.00	0.00	0.00	0.00	0.00	0.00	0.00	0.00	0.00	0.00	0.00	0.00	0.00	0.00	0.00	0.00	0.00	0.00	0.00
Cr	0.00	0.00	0.00	0.00	0.00	0.00	0.00	0.00	0.00	0.00	0.00	0.00	0.00	0.00	0.00	0.00	0.00	0.00	0.00	0.00
Ni	0.00	0.00	0.00	0.00	0.00	0.00	0.00	0.00	0.00	0.00	0.00	0.00	0.00	0.00	0.00	0.00	0.00	0.00	0.00	0.00
V	0.00	0.00	0.00	0.00	0.00	0.00	0.00	0.00	0.00	0.00	0.00	0.00	0.00	0.00	0.00	0.00	0.00	0.00	0.00	0.00
Total	2.02	2.03	2.02	2.02	2.02	2.02	2.02	2.03	2.03	2.03	2.03	2.02	2.02	2.02	2.02	2.02	2.03	2.02	1.00	1.00

Table C-5. Biotite Chemistry

Sample Line	WYL-10-61-190.3 Bt 22	WYL-10-61-190.3 Bt 23	WYL-10-61-190.3 Bt 24	WYL-10-61-190.3 Bt 25	WYL-10-61-190.3 Bt 26	WYL-10-61-190.3 Bt 27	WYL-10-61-190.3 Bt 28	WYL-10-61-190.3 Bt 30	WYL-10-62-93.5 Bt 31	WYL-10-62-93.5 Bt 32	WYL-10-62-93.5 Bt 33	WYL-10-62-93.5 Bt 34	WYL-10-62-93.5 Bt 35	WYL-10-62-93.5 Bt 36	WYL-10-62-93.5 Bt 37	WYL-10-62-93.5 Bt 38	WYL-10-62-93.5 Bt 39	WYL-10-62-93.5 Bt 40
SiO2	34.13	33.55	32.39	33.77	33.09	32.14	32.48	32.99	35.92	35.94	35.91	35.84	35.53	35.45	35.86	35.79	34.88	34.59
TiO2	3.71	3.69	3.72	3.90	3.44	4.92	3.54	3.49	3.15	3.13	3.17	3.26	3.29	3.25	3.20	3.17	3.07	3.14
Al2O3	14.51	14.36	14.40	13.89	14.64	13.66	14.77	15.40	14.48	14.12	14.59	14.18	14.51	13.91	13.99	14.26	14.55	14.21
Cr2O3	0.00	0.00	0.00	0.01	0.00	0.02	0.00	0.01	0.02	0.02	0.03	0.03	0.00	0.00	0.00	0.03	0.01	0.01
FeO	30.99	31.42	31.15	31.29	32.57	31.91	31.28	30.20	24.16	23.77	23.49	23.44	22.98	23.09	23.31	22.66	24.75	24.96
MgO	3.08	2.92	3.02	2.86	2.26	2.37	2.43	2.88	7.93	7.86	7.78	7.83	7.76	7.94	7.74	7.79	8.03	7.84
MnO	0.44	0.50	0.43	0.42	0.46	0.44	0.35	0.42	0.18	0.18	0.15	0.15	0.16	0.15	0.15	0.16	0.17	0.13
CaO	0.02	0.00	0.00	0.00	0.00	0.01	0.00	0.00	0.00	0.00	0.00	0.00	0.00	0.00	0.00	0.00	0.00	0.00
Na2O	0.17	0.13	0.15	0.13	0.11	0.08	0.06	0.16	0.14	0.14	0.15	0.12	0.13	0.14	0.12	0.11	0.13	0.14
K2O	9.12	9.02	9.10	9.18	8.37	8.43	9.20	9.14	9.59	9.70	9.70	9.67	9.65	9.61	9.66	9.72	9.65	9.60
F	0.00	0.00	0.00	0.00	0.00	0.00	0.00	0.00	0.00	0.22	0.11	0.00	0.10	0.00	0.00	0.00	0.12	0.00
Cl	0.70	0.71	0.70	0.52	0.57	0.50	0.64	0.57	0.30	0.31	0.30	0.32	0.32	0.31	0.34	0.33	0.30	0.33
H2O*	3.54	3.50	3.44	3.54	3.50	3.47	3.45	3.52	3.76	3.62	3.69	3.72	3.66	3.68	3.69	3.69	3.66	3.68
Subtotal	100.41	99.81	98.50	99.51	99.02	97.95	98.19	98.78	99.62	99.01	99.08	98.57	98.09	97.53	98.07	97.70	99.32	98.63
O=F,Cl	0.16	0.16	0.16	0.12	0.13	0.11	0.14	0.13	0.07	0.16	0.11	0.07	0.11	0.07	0.08	0.07	0.12	0.07
Total	100.25	99.65	98.34	99.39	98.89	97.83	98.05	98.65	99.56	98.85	98.96	98.49	97.97	97.46	97.99	97.63	99.21	98.55
Si	5.51	5.47	5.37	5.51	5.45	5.36	5.40	5.40	5.62	5.66	5.64	5.66	5.63	5.65	5.69	5.68	5.51	5.52
Al iv	2.49	2.53	2.63	2.49	2.55	2.64	2.60	2.60	2.38	2.34	2.36	2.34	2.37	2.35	2.31	2.32	2.49	2.48
Al vi	0.26	0.23	0.18	0.19	0.29	0.05	0.29	0.37	0.29	0.28	0.34	0.29	0.34	0.27	0.30	0.35	0.22	0.19
Ti	0.45	0.45	0.46	0.48	0.43	0.62	0.44	0.43	0.37	0.37	0.37	0.39	0.39	0.39	0.38	0.38	0.36	0.38
Cr	0.00	0.00	0.00	0.00	0.00	0.00	0.00	0.00	0.00	0.00	0.00	0.00	0.00	0.00	0.00	0.00	0.00	0.00
Fe	4.18	4.28	4.32	4.27	4.48	4.45	4.35	4.14	3.16	3.13	3.08	3.09	3.04	3.08	3.09	3.01	3.27	3.33
Mn	0.06	0.07	0.06	0.06	0.06	0.06	0.05	0.06	0.02	0.02	0.02	0.02	0.02	0.02	0.02	0.02	0.02	0.02
Mg	0.74	0.71	0.75	0.70	0.56	0.59	0.60	0.70	1.85	1.85	1.82	1.84	1.83	1.89	1.83	1.84	1.89	1.86
Ca	0.00	0.00	0.00	0.00	0.00	0.00	0.00	0.00	0.00	0.00	0.00	0.00	0.00	0.00	0.00	0.00	0.00	0.00
Na	0.05	0.04	0.05	0.04	0.03	0.02	0.02	0.05	0.04	0.04	0.05	0.04	0.04	0.04	0.04	0.03	0.04	0.04
K	1.88	1.88	1.92	1.91	1.76	1.79	1.95	1.91	1.91	1.95	1.94	1.95	1.95	1.96	1.95	1.97	1.95	1.95
OH*	3.81	3.80	3.80	3.86	3.84	3.86	3.82	3.84	3.92	3.81	3.87	3.91	3.87	3.92	3.91	3.91	3.86	3.91
F	0.00	0.00	0.00	0.00	0.00	0.00	0.00	0.00	0.00	0.11	0.06	0.00	0.05	0.00	0.00	0.00	0.06	0.00
Cl	0.19	0.20	0.20	0.14	0.16	0.14	0.18	0.16	0.08	0.08	0.08	0.09	0.09	0.08	0.09	0.09	0.08	0.09
TOTAL	19.63	19.66	19.75	19.65	19.60	19.59	19.70	19.66	19.65	19.65	19.63	19.63	19.62	19.65	19.62	19.60	19.76	19.77
Y total	5.70	5.74	5.77	5.69	5.81	5.77	5.73	5.70	5.70	5.66	5.64	5.64	5.63	5.65	5.63	5.60	5.78	5.77
X total	1.93	1.92	1.97	1.95	1.79	1.82	1.97	1.96	1.96	1.99	1.99	1.98	1.99	2.00	1.99	2.00	1.98	2.00
Al total	2.76	2.76	2.81	2.67	2.84	2.69	2.89	2.97	2.67	2.62	2.70	2.64	2.71	2.62	2.62	2.67	2.71	2.67
Fe/(Fe+Mg)	0.85	0.86	0.85	0.86	0.89	0.88	0.88	0.85	0.63	0.63	0.63	0.63	0.62	0.62	0.63	0.62	0.63	0.64
Mg/(Mg+Fe)	0.15	0.14	0.15	0.14	0.11	0.12	0.12	0.15	0.37	0.37	0.37	0.37	0.38	0.38	0.37	0.38	0.37	0.36
a	-2.36	-2.36	-2.36	-2.36	-2.36	-2.36	-2.36	-2.36	-2.36	-2.36	-2.36	-2.36	-2.36	-2.36	-2.36	-2.36	-2.36	-2.36
b	0.00	0.00	0.00	0.00	0.00	0.00	0.00	0.00	0.00	0.00	0.00	0.00	0.00	0.00	0.00	0.00	0.00	0.00
c	-1.73	-1.73	-1.73	-1.73	-1.73	-1.73	-1.73	-1.73	-1.73	-1.73	-1.73	-1.73	-1.73	-1.73	-1.73	-1.73	-1.73	-1.73
Ti	0.45	0.45	0.46	0.48	0.43	0.62	0.44	0.43	0.37	0.37	0.37	0.39	0.39	0.39	0.38	0.38	0.36	0.38
X(Mg)	0.15	0.14	0.15	0.14	0.11	0.12	0.12	0.15	0.37	0.37	0.37	0.37	0.38	0.38	0.37	0.38	0.37	0.36
T(C) Cesare et al. 2008	695.98	696.56	700.33	704.87	687.09	739.46	692.99	688.97	678.77	679.06	680.55	685.88	688.12	687.78	683.63	683.23	676.04	680.16
T(K) Luhr et al. 1984	904.92	902.93	904.66	909.27	892.70	936.26	899.21	901.29	914.39	915.56	918.51	922.26	926.01	923.80	920.63	923.01	908.74	910.30
T(C) Luhr et al. 1984	631.77	629.78	631.51	636.12	619.55	663.11	626.06	628.14	641.24	642.41	645.36	649.11	652.86	650.65	647.48	649.86	635.59	637.15

APPENDIX D
GROUP B PEGMATITES MINERAL CHEMISTRY DATA

Supplementary Data Table 2 for Chapter 3 (McKechnie *et al.* 2012a)

Table D-1. Ilmenite and Pyrochlore (Nb oxide) Chemistry

Ilmenite						Nb-oxide (Pyrochlore)					
SAMPLE	WYL-09-46-35.0 Ilm1	WYL-09-46-35.0 Ilm1	WYL-09-46-35.0 Ilm1	WYL-09-46-35.0 Ilm1	WYL-09-46-35.0 Ilm1	Sample	WYL-09-46-32.6 NbO	WYL-09-46-32.6 NbO	WYL-09-46-32.6 NbO	WYL-09-46-32.6 NbO	WYL-09-46-32.6 NbO
LINE	65	66	67	68	69	Line	1	2	3	4	5
SiO2	0.00	0.01	0.00	0.01	0.01	SiO2	1.50	6.95	6.34	3.00	4.16
TiO2	50.47	50.46	50.46	50.68	50.48	TiO2	8.53	4.93	4.18	6.55	4.16
Al2O3	0.00	0.00	0.00	0.00	0.00	ThO2	1.16	4.11	2.01	1.33	2.31
Cr2O3	0.01	0.01	0.01	0.02	0.00	UO2	0.00	3.35	2.84	1.94	1.53
V2O3	0.11	0.11	0.10	0.12	0.12	Nb2O5	74.02	65.96	68.32	70.87	71.74
FeO	46.26	46.36	45.97	46.23	46.12	Al2O3	0.12	0.23	0.14	0.06	0.12
MnO	2.00	1.97	2.01	1.98	2.01	La2O3	0.07	0.45	0.65	0.26	0.57
ZnO	0.04	0.05	0.05	0.06	0.06	Ce2O3	0.37	1.21	1.99	0.76	1.87
NiO	0.00	0.00	0.00	0.00	0.00	Nd2O3	0.45	0.37	0.73	0.43	0.55
MgO	0.09	0.06	0.09	0.09	0.10	Gd2O3	0.00	0.17	0.31	0.16	0.24
CaO	0.00	0.00	0.00	0.00	0.00	Dy2O3	0.30	0.37	0.51	0.45	0.57
Total	98.98	99.04	98.69	99.18	98.90	FeO	3.18	2.20	1.80	2.85	1.74
						MgO	0.98	0.43	0.19	0.66	0.13
O	6	6	6	6	6	MnO	0.08	0.78	0.94	0.89	1.01
Si	0.00	0.00	0.00	0.00	0.00	NiO	0.00	0.00	0.00	0.00	0.00
Al	0.00	0.00	0.00	0.00	0.00	ZnO	0.00	0.38	0.00	0.02	0.03
Ti	1.95	1.95	1.96	1.95	1.95	CaO	5.87	5.83	5.51	6.00	5.66
Fe	1.99	1.99	1.98	1.98	1.98	Total	96.64	97.69	96.46	96.22	96.39
Mn	0.09	0.09	0.09	0.09	0.09	∑LREE2O4	0.89	2.03	3.37	1.45	2.99
Mg	0.01	0.00	0.01	0.01	0.01	∑HREE2O4	0.30	0.53	0.81	0.60	0.81
Zn	0.00	0.00	0.00	0.00	0.00						
Ca	0.00	0.00	0.00	0.00	0.00						
Cr	0.00	0.00	0.00	0.00	0.00						
Ni	0.00	0.00	0.00	0.00	0.00						
V	0.00	0.00	0.00	0.00	0.00						

Table D-2. Monazite Chemistry

SAMPLE	WYL-09-46-32.6 Mon1	WYL-09-46-32.6 Mon1	WYL-09-46-32.6 Mon1	WYL-09-46-32.6 Mon1	WYL-09-46-32.6 Mon1	WYL-09-46-32.6 Mon1	WYL-09-46-32.6 Mon2	WYL-09-46-32.6 Mon2	WYL-09-46-32.6 Mon2	WYL-09-46-32.6 Mon2	WYL-09-46-32.6 Mon2	WYL-09-46-32.6 Mon2	WYL-09-46-32.6 Mon3	WYL-09-46-32.6 Mon3
LINE	57	58	59	60	61	62	63	64	65	66	67	68	69	70
SiO2	4.34	4.15	4.97	5.04	5.18	4.64	5.70	6.27	3.03	4.28	4.15	3.50	3.02	3.66
TiO2	0.00	0.00	0.00	0.00	0.00	0.00	0.00	0.00	0.00	0.00	0.00	0.00	0.00	0.00
Al2O3	0.00	0.00	0.00	0.00	0.00	0.00	0.00	0.00	0.00	0.00	0.00	0.00	0.00	0.00
FeO	0.04	0.00	0.00	0.04	0.00	0.00	0.00	0.00	0.00	0.00	0.00	0.00	0.00	0.00
MnO	0.00	0.00	0.00	0.00	0.00	0.00	0.00	0.00	0.00	0.00	0.00	0.00	0.00	0.00
MgO	0.00	0.01	0.00	0.00	0.00	0.00	0.00	0.00	0.00	0.00	0.00	0.00	0.00	0.00
CaO	0.18	0.43	0.25	0.38	0.26	0.28	0.26	0.21	0.54	0.24	0.31	0.55	0.38	0.39
P2O5	24.01	23.90	22.74	22.43	22.42	23.46	21.81	20.88	25.47	24.06	24.14	25.01	25.97	24.37
UO2	0.63	0.69	0.65	0.77	0.78	0.74	0.71	0.74	0.54	0.66	0.54	0.31	0.58	0.64
ThO2	15.24	14.72	17.55	17.63	18.00	16.47	19.51	21.23	11.25	14.62	14.64	13.20	10.81	12.94
PbO	1.66	1.60	1.87	1.96	1.91	1.82	2.05	2.27	1.28	1.67	1.61	1.43	1.31	1.46
ZrO2	0.15	0.05	0.18	0.13	0.13	0.15	0.06	0.11	0.15	0.10	0.07	0.07	0.22	0.08
HfO2	0.02	0.00	0.00	0.00	0.00	0.00	0.10	0.00	0.02	0.02	0.00	0.00	0.00	0.00
Y2O3	1.78	1.82	1.69	1.72	1.64	1.65	1.48	1.33	1.92	1.56	1.69	1.69	2.45	1.93
La2O3	11.18	10.98	10.55	10.32	10.74	11.03	10.31	10.06	11.80	11.27	11.41	11.38	11.63	11.65
Ce2O3	25.40	25.54	24.30	24.02	24.19	24.81	23.31	23.08	26.88	25.95	25.91	26.55	27.20	25.99
Pr2O3	2.87	2.94	2.81	2.78	2.87	2.81	2.68	2.65	3.14	3.01	3.05	3.07	3.12	2.82
Nd2O3	9.81	10.03	9.46	9.57	9.38	9.75	9.26	9.22	10.60	10.24	10.36	10.43	10.63	10.31
Sm2O3	1.41	1.47	1.31	1.31	1.35	1.46	1.27	1.36	1.56	1.44	1.45	1.44	1.59	1.54
Gd2O3	0.78	0.92	0.69	0.81	0.75	0.88	0.93	0.81	1.11	0.87	0.87	0.95	1.04	1.05
Dy2O3	0.33	0.38	0.40	0.37	0.31	0.28	0.32	0.26	0.41	0.33	0.30	0.37	0.49	0.44
Er2O3	0.09	0.05	0.00	0.14	0.05	0.03	0.06	0.09	0.01	0.08	0.00	0.00	0.12	0.07
Total	99.91	99.68	99.43	99.42	99.97	100.26	99.82	100.57	99.70	100.39	100.51	99.95	100.55	99.34
∑LREE2O3	50.67	50.96	48.44	48.00	48.54	49.86	46.82	46.37	53.98	51.91	52.18	52.87	54.17	52.31
∑HREE2O3	1.20	1.35	1.09	1.33	1.11	1.19	1.31	1.16	1.52	1.28	1.18	1.32	1.66	1.56
∑REE2O3	51.87	52.31	49.53	49.33	49.65	51.05	48.13	47.53	55.50	53.19	53.36	54.19	55.82	53.87
O	8	8	8	8	8	8	8	8	8	8	8	8	8	8
P	1.67	1.67	1.61	1.59	1.59	1.64	1.55	1.49	1.76	1.67	1.68	1.73	1.77	1.70
Si	0.36	0.34	0.42	0.42	0.43	0.38	0.48	0.53	0.25	0.35	0.34	0.29	0.24	0.30
Ca	0.02	0.04	0.02	0.03	0.02	0.02	0.02	0.02	0.05	0.02	0.03	0.05	0.03	0.03
Th	0.29	0.28	0.33	0.34	0.34	0.31	0.37	0.41	0.21	0.27	0.27	0.25	0.20	0.24
U	0.01	0.01	0.01	0.01	0.01	0.01	0.01	0.01	0.01	0.01	0.01	0.01	0.01	0.01
Pb	0.04	0.04	0.04	0.04	0.04	0.04	0.05	0.05	0.03	0.04	0.04	0.03	0.03	0.03
La	0.34	0.33	0.33	0.32	0.33	0.34	0.32	0.31	0.35	0.34	0.35	0.34	0.34	0.36
Ce	0.77	0.77	0.74	0.74	0.74	0.75	0.72	0.71	0.80	0.78	0.78	0.79	0.80	0.79
Sm	0.04	0.04	0.04	0.04	0.04	0.04	0.04	0.04	0.04	0.04	0.04	0.04	0.04	0.04
Pr	0.09	0.09	0.09	0.09	0.09	0.08	0.08	0.08	0.09	0.09	0.09	0.09	0.09	0.08
Nd	0.29	0.30	0.28	0.29	0.28	0.29	0.28	0.28	0.31	0.30	0.30	0.30	0.31	0.30
Gd	0.02	0.03	0.02	0.02	0.02	0.02	0.03	0.02	0.03	0.02	0.02	0.03	0.03	0.03
Dy	0.01	0.01	0.01	0.01	0.01	0.01	0.01	0.01	0.01	0.01	0.01	0.01	0.01	0.01
Er	0.00	0.00	0.00	0.00	0.00	0.00	0.00	0.00	0.00	0.00	0.00	0.00	0.00	0.00
Y	0.08	0.08	0.08	0.08	0.07	0.07	0.07	0.06	0.08	0.07	0.07	0.07	0.10	0.08
Fe	0.00	0.00	0.00	0.00	0.00	0.00	0.00	0.00	0.00	0.00	0.00	0.00	0.00	0.00
Mn	0.00	0.00	0.00	0.00	0.00	0.00	0.00	0.00	0.00	0.00	0.00	0.00	0.00	0.00
Mg	0.00	0.00	0.00	0.00	0.00	0.00	0.00	0.00	0.00	0.00	0.00	0.00	0.00	0.00
Zr	0.01	0.00	0.01	0.01	0.01	0.01	0.00	0.00	0.01	0.00	0.00	0.00	0.01	0.00
Ti	0.00	0.00	0.00	0.00	0.00	0.00	0.00	0.00	0.00	0.00	0.00	0.00	0.00	0.00
Al	0.00	0.00	0.00	0.00	0.00	0.00	0.00	0.00	0.00	0.00	0.00	0.00	0.00	0.00
Xla	0.17	0.17	0.16	0.16	0.17	0.17	0.16	0.16	0.18	0.17	0.17	0.17	0.17	0.18
Xce	0.39	0.38	0.37	0.37	0.37	0.38	0.36	0.35	0.40	0.39	0.39	0.39	0.40	0.39
Xsm	0.02	0.02	0.02	0.02	0.02	0.02	0.02	0.02	0.02	0.02	0.02	0.02	0.02	0.02
Xpr	0.04	0.04	0.04	0.04	0.04	0.04	0.04	0.04	0.05	0.05	0.05	0.05	0.05	0.04
Xnd	0.15	0.15	0.14	0.14	0.14	0.14	0.14	0.14	0.15	0.15	0.15	0.15	0.15	0.15
XGd	0.01	0.01	0.01	0.01	0.01	0.01	0.01	0.01	0.01	0.01	0.01	0.01	0.01	0.01
Xdy	0.00	0.00	0.01	0.00	0.00	0.00	0.00	0.00	0.01	0.00	0.00	0.00	0.01	0.01
Xer	0.00	0.00	0.00	0.00	0.00	0.00	0.00	0.00	0.00	0.00	0.00	0.00	0.00	0.00
XLREE	0.77	0.76	0.74	0.73	0.74	0.75	0.72	0.71	0.79	0.78	0.78	0.78	0.79	0.78
XHREE	0.02	0.02	0.02	0.02	0.02	0.02	0.02	0.02	0.02	0.02	0.02	0.02	0.02	0.02
Xhut	0.16	0.14	0.18	0.18	0.19	0.17	0.21	0.23	0.10	0.15	0.14	0.12	0.10	0.12
Xchr	0.02	0.04	0.02	0.03	0.02	0.02	0.02	0.02	0.05	0.02	0.03	0.05	0.03	0.03
X YPO4	0.04	0.04	0.04	0.04	0.04	0.04	0.03	0.03	0.04	0.03	0.04	0.04	0.05	0.04

Table D-2 (cont`d). Monazite chemistry

SAMPLE	WYL-09-46-32.6 Mon3	WYL-09-46-32.6 Mon3	WYL-09-46-32.6 Mon3	WYL-09-46-32.6 Mon3	WYL-09-46-32.6 Mon4	WYL-09-46-32.6 Mon4	WYL-09-46-32.6 Mon4	WYL-09-46-32.6 Mon4	WYL-09-46-32.6 Mon4	WYL-09-46-32.6 Mon4	WYL-09-46-32.6 Mon4	WYL-09-46-32.6 Mon4	WYL-09-46-32.6 Mon4	WYL-09-46-32.6 Mon4
LINE	71	72	73	74	75	76	77	78	79	80	81	82	83	84
SiO2	4.62	4.49	4.40	4.43	2.42	2.45	3.84	2.25	4.22	4.45	4.43	4.48	4.63	4.67
TiO2	0.00	0.00	0.00	0.00	0.00	0.00	0.00	0.00	0.00	0.00	0.00	0.00	0.00	0.00
Al2O3	0.00	0.00	0.00	0.00	0.00	0.00	0.00	0.00	0.00	0.00	0.00	0.00	0.00	0.00
FeO	0.00	0.00	0.00	0.00	0.00	0.00	0.00	0.00	0.00	0.00	0.00	0.00	0.00	0.00
MnO	0.00	0.00	0.00	0.00	0.00	0.00	0.00	0.00	0.00	0.00	0.00	0.00	0.00	0.00
MgO	0.00	0.00	0.00	0.00	0.00	0.00	0.00	0.00	0.00	0.00	0.00	0.00	0.00	0.00
CaO	0.33	0.33	0.28	0.31	0.39	0.42	0.31	0.49	0.26	0.29	0.26	0.31	0.27	0.30
P2O5	23.47	23.80	23.79	23.41	26.25	26.60	24.80	26.78	24.13	23.73	23.81	23.72	23.36	23.26
UO2	0.68	0.64	0.64	0.60	0.15	0.13	0.54	0.08	0.63	0.64	0.57	0.63	0.65	0.67
ThO2	16.22	15.82	15.67	15.70	9.94	10.31	13.74	9.25	14.89	15.62	15.44	15.61	15.93	16.11
PbO	1.79	1.69	1.82	1.77	1.02	1.06	1.48	0.96	1.66	1.69	1.66	1.74	1.68	1.77
ZrO2	0.13	0.11	0.13	0.13	0.16	0.05	0.07	0.13	0.05	0.12	0.12	0.23	0.06	0.08
HfO2	0.00	0.02	0.00	0.02	0.00	0.00	0.01	0.00	0.00	0.02	0.00	0.00	0.03	0.00
Y2O3	1.80	1.83	1.84	1.55	1.48	1.53	1.66	1.57	1.60	1.68	1.55	1.61	1.75	1.82
La2O3	10.86	11.13	11.12	11.41	12.78	12.23	11.76	12.57	11.47	11.13	11.58	11.08	10.74	10.59
Ce2O3	24.96	25.06	25.24	25.46	28.63	27.97	26.23	28.42	25.60	25.49	25.78	25.48	25.03	24.86
Pr2O3	2.89	2.87	2.84	2.91	3.11	3.24	3.05	3.28	2.85	2.90	2.82	2.93	2.89	2.89
Nd2O3	9.69	9.76	10.02	9.63	11.01	11.41	10.10	11.42	9.89	9.97	9.90	9.98	9.84	9.80
Sm2O3	1.41	1.48	1.51	1.29	1.52	1.76	1.45	1.72	1.39	1.37	1.32	1.39	1.55	1.41
Gd2O3	0.95	0.92	1.01	0.91	0.95	1.08	0.85	1.06	0.98	0.98	0.90	0.90	0.95	0.96
Dy2O3	0.43	0.36	0.42	0.36	0.33	0.32	0.33	0.31	0.34	0.31	0.30	0.35	0.38	0.37
Er2O3	0.10	0.08	0.00	0.04	0.00	0.00	0.08	0.05	0.14	0.03	0.05	0.00	0.00	0.04
Total	100.32	100.40	100.74	99.92	100.14	100.56	100.31	100.33	100.10	100.40	100.50	100.43	99.74	99.60
∑LREE2O3	49.81	50.30	50.74	50.70	57.05	56.61	52.59	57.41	51.20	50.85	51.41	50.86	50.05	49.54
∑HREE2O3	1.48	1.35	1.43	1.30	1.28	1.41	1.27	1.41	1.45	1.31	1.25	1.24	1.33	1.38
∑REE2O3	51.29	51.65	52.17	52.00	58.33	58.02	53.86	58.82	52.65	52.17	52.66	52.10	51.37	50.92
O	8	8	8	8	8	8	8	8	8	8	8	8	8	8
P	1.64	1.66	1.66	1.65	1.80	1.81	1.71	1.82	1.68	1.65	1.66	1.65	1.64	1.64
Si	0.38	0.37	0.36	0.37	0.20	0.20	0.31	0.18	0.35	0.37	0.36	0.37	0.38	0.39
Ca	0.03	0.03	0.02	0.03	0.03	0.04	0.03	0.04	0.02	0.03	0.02	0.03	0.02	0.03
Th	0.30	0.30	0.29	0.30	0.18	0.19	0.25	0.17	0.28	0.29	0.29	0.29	0.30	0.30
U	0.01	0.01	0.01	0.01	0.00	0.00	0.01	0.00	0.01	0.01	0.01	0.01	0.01	0.01
Pb	0.04	0.04	0.04	0.04	0.02	0.02	0.03	0.02	0.04	0.04	0.04	0.04	0.04	0.04
La	0.33	0.34	0.34	0.35	0.38	0.36	0.35	0.37	0.35	0.34	0.35	0.34	0.33	0.32
Ce	0.75	0.75	0.76	0.77	0.85	0.82	0.78	0.84	0.77	0.77	0.78	0.77	0.76	0.76
Sm	0.04	0.04	0.04	0.04	0.04	0.05	0.04	0.05	0.04	0.04	0.04	0.04	0.04	0.04
Pr	0.09	0.09	0.09	0.09	0.09	0.09	0.09	0.10	0.09	0.09	0.08	0.09	0.09	0.09
Nd	0.29	0.29	0.29	0.29	0.32	0.33	0.29	0.33	0.29	0.29	0.29	0.29	0.29	0.29
Gd	0.03	0.02	0.03	0.02	0.03	0.03	0.02	0.03	0.03	0.03	0.02	0.02	0.03	0.03
Dy	0.01	0.01	0.01	0.01	0.01	0.01	0.01	0.01	0.01	0.01	0.01	0.01	0.01	0.01
Er	0.00	0.00	0.00	0.00	0.00	0.00	0.00	0.00	0.00	0.00	0.00	0.00	0.00	0.00
Y	0.08	0.08	0.08	0.07	0.06	0.07	0.07	0.07	0.07	0.07	0.07	0.07	0.08	0.08
Fe	0.00	0.00	0.00	0.00	0.00	0.00	0.00	0.00	0.00	0.00	0.00	0.00	0.00	0.00
Mn	0.00	0.00	0.00	0.00	0.00	0.00	0.00	0.00	0.00	0.00	0.00	0.00	0.00	0.00
Mg	0.00	0.00	0.00	0.00	0.00	0.00	0.00	0.00	0.00	0.00	0.00	0.00	0.00	0.00
Zr	0.01	0.00	0.01	0.01	0.01	0.00	0.00	0.01	0.00	0.00	0.00	0.01	0.00	0.00
Ti	0.00	0.00	0.00	0.00	0.00	0.00	0.00	0.00	0.00	0.00	0.00	0.00	0.00	0.00
Al	0.00	0.00	0.00	0.00	0.00	0.00	0.00	0.00	0.00	0.00	0.00	0.00	0.00	0.00
Xla	0.17	0.17	0.17	0.17	0.19	0.18	0.18	0.18	0.17	0.17	0.18	0.17	0.16	0.16
Xce	0.38	0.38	0.38	0.38	0.42	0.41	0.39	0.41	0.39	0.38	0.39	0.38	0.38	0.38
Xsm	0.02	0.02	0.02	0.02	0.02	0.02	0.02	0.02	0.02	0.02	0.02	0.02	0.02	0.02
Xpr	0.04	0.04	0.04	0.04	0.05	0.05	0.05	0.05	0.04	0.04	0.04	0.04	0.04	0.04
Xnd	0.14	0.14	0.15	0.14	0.16	0.16	0.15	0.16	0.15	0.15	0.15	0.15	0.15	0.15
XGd	0.01	0.01	0.01	0.01	0.01	0.01	0.01	0.01	0.01	0.01	0.01	0.01	0.01	0.01
Xdy	0.01	0.00	0.01	0.00	0.00	0.00	0.00	0.00	0.00	0.00	0.00	0.00	0.01	0.01
Xer	0.00	0.00	0.00	0.00	0.00	0.00	0.00	0.00	0.00	0.00	0.00	0.00	0.00	0.00
XLREE	0.75	0.75	0.76	0.76	0.83	0.82	0.78	0.83	0.77	0.76	0.77	0.76	0.76	0.75
XHREE	0.02	0.02	0.02	0.02	0.02	0.02	0.02	0.02	0.02	0.02	0.02	0.02	0.02	0.02
Xhut	0.16	0.16	0.16	0.16	0.09	0.09	0.14	0.07	0.15	0.16	0.16	0.16	0.16	0.16
Xchr	0.03	0.03	0.02	0.03	0.03	0.04	0.03	0.04	0.02	0.03	0.02	0.03	0.02	0.03
X YPO4	0.04	0.04	0.04	0.03	0.03	0.03	0.04	0.03	0.04	0.04	0.03	0.04	0.04	0.04

Table D-3. Thorite Chemistry

SAMPLE	WYL-09-46-35.0 Thr1	WYL-09-46-35.0 Thr1	WYL-09-46-35.0 Thr1	WYL-09-46-35.0 Thr1	WYL-09-46-35.0 Thr1	WYL-09-46-35.0 Thr2	WYL-09-46-35.0 Thr2	WYL-09-46-35.0 Thr2	WYL-09-46-35.0 Thr3-Zrn1	WYL-09-46-35.0 Thr3-Zrn1	WYL-09-46-35.0 Thr3-Zrn1	WYL-09-46-35.0 Thr3-Zrn1
LINE	118	119	120	121	122	123	124	125	126	127	128	129
SiO2	18.95	20.60	20.01	17.78	16.26	17.22	19.96	19.84	18.62	17.69	19.80	18.53
TiO2	0.06	0.09	0.13	0.09	0.13	0.03	0.06	0.03	0.03	0.08	0.00	0.11
Al2O3	0.46	0.56	0.69	0.52	0.62	0.58	0.48	0.44	0.54	0.54	0.74	0.47
FeO	0.65	0.42	1.34	5.24	1.69	4.76	0.24	0.30	0.37	0.24	0.36	0.45
MnO	0.03	0.01	0.02	0.03	0.08	0.04	0.02	0.02	0.04	0.03	0.01	0.02
MgO	0.00	0.00	0.00	0.00	0.01	0.00	0.00	0.00	0.01	0.00	0.01	0.00
CaO	0.92	0.89	0.69	0.57	0.65	1.29	1.29	1.00	0.87	1.25	1.52	1.09
P2O5	0.70	0.69	0.99	0.83	1.27	1.40	1.15	1.02	1.30	1.37	2.16	1.93
UO2	15.32	13.16	13.73	10.07	4.90	5.70	15.90	19.84	21.81	21.06	11.68	16.91
ThO2	40.67	44.31	43.24	41.04	46.45	47.47	43.85	38.98	35.05	33.60	43.63	39.00
PbO	0.24	0.60	0.46	0.96	1.67	1.88	0.24	0.28	0.27	0.23	0.20	0.31
ZrO2	0.13	1.93	0.08	0.21	0.28	0.08	0.02	0.09	0.07	0.14	0.12	0.22
HfO2	0.00	0.00	0.00	0.00	0.00	0.01	0.00	0.00	0.00	0.00	0.00	0.00
Y2O3	1.40	1.13	1.47	1.21	1.90	1.92	1.18	1.39	1.24	1.16	1.59	1.52
La2O3	0.12	0.23	0.01	0.12	0.05	0.09	0.27	0.19	0.19	0.17	0.23	0.28
Ce2O3	3.60	4.20	3.73	3.27	2.47	3.55	3.52	3.18	3.15	3.27	3.65	3.84
Pr2O3	0.74	0.66	0.91	0.67	0.66	0.82	0.73	0.64	0.72	0.75	0.85	0.92
Nd2O3	2.76	2.59	3.30	2.74	3.14	3.00	2.08	2.17	3.01	3.11	3.66	3.69
Sm2O3	0.24	0.17	0.29	0.25	0.33	0.20	0.12	0.18	0.19	0.15	0.23	0.23
Gd2O3	0.27	0.18	0.30	0.35	0.33	0.27	0.15	0.12	0.16	0.17	0.22	0.17
Dy2O3	0.16	0.17	0.22	0.03	0.20	0.13	0.14	0.08	0.13	0.14	0.22	0.22
Er2O3	0.05	0.07	0.18	0.04	0.12	0.15	0.11	0.14	0.14	0.15	0.17	0.03
Total	87.47	92.68	91.79	86.02	83.19	90.59	91.52	89.93	87.90	85.29	91.06	89.90
O	16	16	16	16	16	16	16	16	16	16	16	16
Si	4.17	4.20	4.14	3.95	3.82	3.69	4.16	4.21	4.07	3.99	4.01	3.92
Al	0.12	0.14	0.17	0.14	0.17	0.15	0.12	0.11	0.14	0.14	0.18	0.12
Ti	0.01	0.01	0.02	0.01	0.02	0.01	0.01	0.00	0.00	0.01	0.00	0.02
Fe	0.12	0.07	0.23	0.97	0.33	0.85	0.04	0.05	0.07	0.04	0.06	0.08
Mn	0.00	0.00	0.00	0.01	0.02	0.01	0.00	0.00	0.01	0.00	0.00	0.00
Mg	0.00	0.00	0.00	0.00	0.00	0.00	0.00	0.00	0.00	0.00	0.00	0.00
Ca	0.22	0.19	0.15	0.14	0.16	0.30	0.29	0.23	0.20	0.30	0.33	0.25
U	0.75	0.60	0.63	0.50	0.26	0.27	0.74	0.94	1.06	1.06	0.53	0.80
Th	2.04	2.05	2.03	2.08	2.48	2.32	2.08	1.88	1.74	1.72	2.01	1.88
Pb	0.01	0.03	0.03	0.06	0.11	0.11	0.01	0.02	0.02	0.01	0.01	0.02
Zr	0.01	0.19	0.01	0.02	0.03	0.01	0.00	0.01	0.01	0.01	0.01	0.02
Hf	0.00	0.00	0.00	0.00	0.00	0.00	0.00	0.00	0.00	0.00	0.00	0.00
P	0.13	0.12	0.17	0.16	0.25	0.25	0.20	0.18	0.24	0.26	0.37	0.35
Y	0.16	0.12	0.16	0.14	0.24	0.22	0.13	0.16	0.14	0.14	0.17	0.17
La	0.01	0.02	0.00	0.01	0.00	0.01	0.02	0.01	0.02	0.01	0.02	0.02
Ce	0.29	0.31	0.28	0.27	0.21	0.28	0.27	0.25	0.25	0.27	0.27	0.30
Pr	0.06	0.05	0.07	0.05	0.06	0.06	0.06	0.05	0.06	0.06	0.06	0.07
Nd	0.22	0.19	0.24	0.22	0.26	0.23	0.15	0.16	0.23	0.25	0.27	0.28
Sm	0.02	0.01	0.02	0.02	0.03	0.02	0.01	0.01	0.01	0.01	0.02	0.02
Gd	0.02	0.01	0.02	0.03	0.03	0.02	0.01	0.01	0.01	0.01	0.02	0.01
Dy	0.01	0.01	0.01	0.00	0.02	0.01	0.01	0.01	0.01	0.01	0.01	0.01
Er	0.00	0.00	0.01	0.00	0.01	0.01	0.01	0.01	0.01	0.01	0.01	0.00
∑ Th U Zr Hf Y REES	3.59	3.57	3.50	3.34	3.62	3.45	3.48	3.49	3.56	3.58	3.40	3.59
% ThSiO4	0.57	0.58	0.58	0.62	0.69	0.67	0.60	0.54	0.49	0.48	0.59	0.52
% USiO4	0.21	0.17	0.18	0.15	0.07	0.08	0.21	0.27	0.30	0.30	0.16	0.22
% Zr+ Hf	0.00	0.05	0.00	0.01	0.01	0.00	0.00	0.00	0.00	0.00	0.00	0.01
% Y + REE	0.22	0.20	0.24	0.22	0.23	0.25	0.19	0.19	0.21	0.22	0.25	0.25

Table D-3 (cont`d). Thorite chemistry.

WYL-09-46-35.0 Thr3-Zrn1	WYL-09-46-35.0 Thr5-Zrn3	WYL-09-46-35.0 Thr5-Zrn3	WYL-09-46-35.0 Thr5-Zrn3	WYL-09-46-35.0 Thr5-Zrn3	WYL-09-46-35.0 Thr3-Zrn1	WYL-09-46-35.0 Thr4-Zrn2	WYL-09-46-35.0 Thr4-Zrn2	WYL-09-46-35.0 Thr4-Zrn2	WYL-09-46-35.0 Thr4-Zrn2	WYL-09-46-35.0 Thr4-Zrn2	WYL-09-46-35.0 Thr5-Zrn3
130	141	142	143	144	131	136	137	138	139	140	145
17.07	21.07	19.60	19.91	17.60	20.57	23.76	21.44	17.03	22.82	24.43	21.01
0.11	0.07	0.08	0.06	0.05	0.10	0.17	0.24	0.14	0.27	0.33	0.05
0.47	0.64	0.52	0.48	0.45	0.45	0.88	0.79	0.62	0.69	0.96	0.64
2.13	0.43	1.32	0.76	3.67	3.59	6.82	8.11	9.71	4.49	6.29	4.12
0.06	0.00	0.02	0.03	0.03	0.10	0.08	0.09	0.06	0.10	0.10	0.08
0.00	0.00	0.01	0.00	0.00	0.06	0.07	0.06	0.05	0.06	0.09	0.08
1.26	1.45	1.12	1.36	0.76	0.94	1.80	1.50	1.54	1.50	1.67	1.17
1.48	0.88	1.01	1.11	1.10	0.46	0.07	0.13	0.69	0.13	0.13	0.02
15.87	20.64	20.93	15.99	7.78	0.67	1.48	1.10	2.89	0.26	2.08	1.18
38.78	36.01	35.28	40.09	43.27	46.16	35.96	34.06	43.94	42.50	35.44	41.12
0.53	0.20	0.39	0.46	0.54	0.22	0.19	0.49	0.69	0.21	0.15	0.30
0.23	0.10	0.16	0.06	1.70	9.79	12.84	12.89	4.08	12.50	13.46	13.05
0.00	0.02	0.00	0.00	0.00	0.24	0.33	0.46	0.04	0.23	0.33	0.26
1.20	2.16	1.98	2.02	1.76	0.45	0.47	0.44	0.35	0.34	0.51	0.74
0.19	0.19	0.16	0.21	0.17	0.13	0.12	0.07	0.09	0.03	0.02	0.10
2.78	2.20	2.57	2.52	3.30	2.05	1.50	1.39	1.42	1.25	1.48	1.31
0.68	0.51	0.55	0.50	0.73	0.39	0.24	0.24	0.23	0.25	0.28	0.29
2.94	2.88	2.76	2.72	2.97	1.52	1.07	0.93	0.89	0.83	1.11	1.23
0.17	0.44	0.42	0.39	0.48	0.16	0.06	0.06	0.08	0.05	0.06	0.16
0.17	0.46	0.46	0.39	0.33	0.07	0.05	0.10	0.10	0.03	0.07	0.22
0.23	0.30	0.13	0.21	0.11	0.00	0.00	0.00	0.00	0.00	0.00	0.01
0.11	0.16	0.12	0.12	0.05	0.01	0.03	0.00	0.02	0.00	0.00	0.05
86.45	90.80	89.58	89.41	86.84	88.13	87.98	84.58	84.65	88.53	89.01	87.18
16	16	16	16	16	16	16	16	16	16	16	16
3.83	4.30	4.14	4.18	3.85	4.06	4.26	4.07	3.68	4.22	4.29	4.06
0.12	0.15	0.13	0.12	0.12	0.11	0.19	0.18	0.16	0.15	0.20	0.14
0.02	0.01	0.01	0.01	0.01	0.02	0.02	0.03	0.02	0.04	0.04	0.01
0.40	0.07	0.23	0.13	0.67	0.59	1.02	1.29	1.76	0.69	0.92	0.67
0.01	0.00	0.00	0.00	0.01	0.02	0.01	0.01	0.01	0.02	0.01	0.01
0.00	0.00	0.00	0.00	0.00	0.02	0.02	0.02	0.02	0.02	0.02	0.02
0.30	0.32	0.25	0.31	0.18	0.20	0.35	0.30	0.36	0.30	0.31	0.24
0.79	0.94	0.98	0.75	0.38	0.03	0.06	0.05	0.14	0.01	0.08	0.05
1.98	1.67	1.70	1.92	2.16	2.07	1.47	1.47	2.16	1.79	1.42	1.81
0.03	0.01	0.02	0.03	0.03	0.01	0.01	0.02	0.04	0.01	0.01	0.02
0.02	0.01	0.02	0.01	0.18	0.94	1.12	1.19	0.43	1.13	1.15	1.23
0.00	0.00	0.00	0.00	0.00	0.02	0.02	0.03	0.00	0.01	0.02	0.02
0.28	0.15	0.18	0.20	0.20	0.08	0.01	0.02	0.13	0.02	0.02	0.00
0.14	0.23	0.22	0.23	0.21	0.05	0.04	0.04	0.04	0.03	0.05	0.08
0.02	0.01	0.01	0.02	0.01	0.01	0.01	0.01	0.01	0.00	0.00	0.01
0.23	0.16	0.20	0.19	0.26	0.15	0.10	0.10	0.11	0.08	0.10	0.09
0.06	0.04	0.04	0.04	0.06	0.03	0.02	0.02	0.02	0.02	0.02	0.02
0.24	0.21	0.21	0.20	0.23	0.11	0.07	0.06	0.07	0.05	0.07	0.09
0.01	0.03	0.03	0.03	0.04	0.01	0.00	0.00	0.01	0.00	0.00	0.01
0.01	0.03	0.03	0.03	0.02	0.00	0.00	0.01	0.01	0.00	0.00	0.01
0.02	0.02	0.01	0.01	0.01	0.00	0.00	0.00	0.00	0.00	0.00	0.00
0.01	0.01	0.01	0.01	0.00	0.00	0.00	0.00	0.00	0.00	0.00	0.00
3.52	3.37	3.46	3.42	3.56	3.42	2.92	2.97	3.00	3.14	2.91	3.42
0.56	0.50	0.49	0.56	0.61	0.61	0.50	0.49	0.72	0.57	0.49	0.53
0.22	0.28	0.28	0.22	0.11	0.01	0.02	0.02	0.05	0.00	0.03	0.01
0.01	0.00	0.00	0.00	0.05	0.28	0.39	0.41	0.14	0.36	0.40	0.37
0.21	0.22	0.22	0.22	0.24	0.10	0.08	0.08	0.09	0.06	0.08	0.09

Table D-4. Zircon and Xenotime Chemistry

Mineral	Zircon									Xenotime	
SAMPLE	WYL-09-46-35.0 Thr5-Zrn3	WYL-09-46-35.0 Thr5-Zrn3	WYL-09-46-35.0 Thr5-Zrn3	WYL-09-46-35.0 Thr5-Zrn3	WYL-09-46-35.0 Thr3-Zrn1	WYL-09-46-35.0 Thr3-Zrn1	WYL-09-46-35.0 Thr4-Zrn2	WYL-09-46-35.0 Thr4-Zrn2	Sample	WYL-09-46-32.6 Xen	WYL-09-46-32.6 Xen
LINE	147	148	149	150	132	133	134	135	Line	1	2
SiO2	31.62	25.84	31.79	29.07	32.21	26.76	25.51	26.21	SiO2	4.33	4.32
TiO2	0.04	0.01	0.00	0.00	0.01	0.18	0.25	0.24	ThO2	0.43	0.43
Al2O3	0.00	1.16	0.00	1.58	0.00	0.86	1.10	1.15	UO2	0.00	0.00
FeO	0.80	1.37	0.83	1.56	0.24	9.10	7.57	6.74	Al2O3	0.00	0.00
MnO	0.11	0.46	0.11	0.56	0.00	0.11	0.11	0.17	Y2O3	40.86	41.59
MgO	0.00	0.13	0.00	0.12	0.00	0.10	0.09	0.09	La2O3	0.00	0.00
CaO	0.50	2.34	0.26	2.46	0.00	2.83	2.55	2.34	Ce2O3	0.20	0.21
P2O5	0.00	0.00	0.00	0.00	0.00	0.00	0.00	0.00	Pr2O3	0.00	0.00
UO2	0.26	0.67	0.24	0.84	0.24	0.19	2.08	3.56	Nd2O3	0.35	0.35
ThO2	0.01	0.77	0.00	0.05	0.04	6.35	15.73	14.97	Sm2O3	0.14	0.13
PbO	0.21	0.12	0.19	0.12	0.22	0.09	0.18	0.15	Gd2O3	1.18	1.18
ZrO2	64.10	51.46	64.07	55.16	65.04	35.38	27.08	25.27	Tb2O3	0.00	0.00
HfO2	1.79	0.88	1.66	1.38	1.74	1.01	0.85	0.75	Dy2O3	3.72	3.67
Y2O3	0.05	0.46	0.09	0.50	0.04	0.81	0.84	0.79	Ho2O3	0.01	0.01
La2O3	0.00	0.05	0.02	0.17	0.02	0.08	0.01	0.04	Er2O3	3.51	3.56
Ce2O3	0.00	0.05	0.02	0.06	0.05	1.10	1.12	1.08	Yb2O3	5.05	5.26
Pr2O3	0.00	0.02	0.04	0.01	0.00	0.20	0.26	0.21	FeO	0.07	0.07
Nd2O3	0.00	0.08	0.00	0.00	0.00	0.95	1.02	1.00	CaO	0.04	0.04
Sm2O3	0.00	0.00	0.04	0.00	0.00	0.06	0.12	0.11	P2O5	37.63	37.57
Gd2O3	0.00	0.02	0.02	0.00	0.00	0.10	0.12	0.12	Total	97.52	98.39
Dy2O3	0.02	0.01	0.00	0.10	0.00	0.00	0.02	0.04			
Er2O3	0.00	0.11	0.00	0.04	0.00	0.00	0.04	0.02	Si	0.27	0.27
Total	99.52	86.01	99.37	93.78	99.84	86.24	86.63	85.02	Al	0.00	0.00
									Fe	0.00	0.00
O	16	16	16	16	16	16	16	16	Ca	0.00	0.00
Si	3.94	3.76	3.96	3.84	3.98	4.03	4.09	4.24	U	0.00	0.00
Al	0.00	0.20	0.00	0.25	0.00	0.15	0.21	0.22	Th	0.01	0.01
Ti	0.00	0.00	0.00	0.00	0.00	0.02	0.03	0.03	P	1.99	1.98
Fe	0.08	0.17	0.09	0.17	0.02	1.15	1.01	0.91	Y	1.36	1.38
Mn	0.01	0.06	0.01	0.06	0.00	0.01	0.02	0.02	La	0.00	0.00
Mg	0.00	0.03	0.00	0.02	0.00	0.02	0.02	0.02	Ce	0.00	0.00
Ca	0.07	0.36	0.03	0.35	0.00	0.46	0.44	0.41	Pr	0.00	0.00
U	0.01	0.02	0.01	0.02	0.01	0.01	0.07	0.13	Nd	0.01	0.01
Th	0.00	0.03	0.00	0.00	0.00	0.22	0.57	0.55	Sm	0.00	0.00
Pb	0.01	0.00	0.01	0.00	0.01	0.00	0.01	0.01	Gd	0.02	0.02
Zr	3.89	3.65	3.89	3.55	3.92	2.60	2.12	1.99	Tb	0.00	0.00
Hf	0.07	0.04	0.07	0.06	0.07	0.05	0.05	0.04	Dy	0.07	0.07
P	0.00	0.00	0.00	0.00	0.00	0.00	0.00	0.00	Ho	0.00	0.00
Y	0.00	0.04	0.01	0.04	0.00	0.06	0.07	0.07	Er	0.07	0.07
La	0.00	0.00	0.00	0.01	0.00	0.00	0.00	0.00	Yb	0.10	0.10
Ce	0.00	0.00	0.00	0.00	0.00	0.06	0.07	0.06			
Pr	0.00	0.00	0.00	0.00	0.00	0.01	0.02	0.01	Xla	0.00	0.00
Nd	0.00	0.00	0.00	0.00	0.00	0.05	0.06	0.06	Xce	0.00	0.00
Sm	0.00	0.00	0.00	0.00	0.00	0.00	0.01	0.01	Xsm	0.00	0.00
Gd	0.00	0.00	0.00	0.00	0.00	0.00	0.01	0.01	Xpr	0.00	0.00
Dy	0.00	0.00	0.00	0.00	0.00	0.00	0.00	0.00	Xnd	0.00	0.00
Er	0.00	0.00	0.00	0.00	0.00	0.00	0.00	0.00	XGd	0.01	0.01
									XTb	0.00	0.00
									Xdy	0.05	0.04
									Xho	0.00	0.00
									Xer	0.04	0.04
									Xyb	0.06	0.06
									XLREE	0.01	0.01
									XHREE	0.16	0.16
									Xhut	0.00	0.00
									Xchr	0.00	0.00
									X YPO4	0.82	0.83

Table D-5. Biotite Chemistry

Sample	WYL-09-46-32.6 Bt	WYL-09-46-32.6 Bt	WYL-09-46-32.6 Bt	WYL-09-46-32.6 Bt	WYL-09-46-32.6 Bt	WYL-09-46-32.6 Bt	WYL-09-46-32.6 Bt	WYL-09-46-32.6 Bt	WYL-09-46-32.6 Bt	WYL-09-46-32.6 Bt
Line	1	2	3	4	5	6	7	8	9	10
SiO2	36.39	36.43	36.46	36.29	36.42	35.87	36.43	36.06	36.31	36.25
TiO2	2.89	2.93	2.78	2.91	2.97	2.89	2.96	2.88	2.93	2.93
Al2O3	14.96	14.64	14.60	14.74	14.64	14.55	14.77	14.62	14.68	14.73
Cr2O3	0.02	0.02	0.01	0.00	0.00	0.03	0.01	0.00	0.00	0.02
FeO	22.47	22.37	22.45	22.10	22.35	22.58	22.12	22.23	21.93	22.09
MgO	9.71	9.47	9.49	9.36	9.48	9.58	9.58	9.61	9.55	9.52
MnO	0.30	0.31	0.33	0.34	0.33	0.37	0.33	0.30	0.31	0.32
CaO	0.00	0.00	0.03	0.00	0.04	0.00	0.00	0.00	0.00	0.00
Na2O	0.25	0.28	0.17	0.21	0.28	0.20	0.21	0.20	0.21	0.19
K2O	9.48	9.60	9.49	9.44	9.47	9.56	9.55	9.53	9.51	9.53
F	0.00	0.00	0.00	0.00	0.00	0.00	0.00	0.00	0.00	0.00
Cl	0.28	0.30	0.32	0.34	0.33	0.30	0.30	0.34	0.32	0.33
H2O*	3.84	3.81	3.80	3.78	3.80	3.78	3.82	3.78	3.79	3.79
Subtotal	100.58	100.17	99.93	99.50	100.10	99.71	100.08	99.54	99.53	99.70
O=F,Cl	0.06	0.07	0.07	0.08	0.07	0.07	0.07	0.08	0.07	0.07
Total	100.52	100.10	99.86	99.43	100.02	99.64	100.01	99.47	99.46	99.62
Si	5.58	5.62	5.63	5.62	5.62	5.57	5.61	5.60	5.62	5.61
Al iv	2.42	2.38	2.37	2.38	2.38	2.43	2.39	2.40	2.38	2.39
Al vi	0.29	0.28	0.29	0.32	0.28	0.24	0.30	0.27	0.30	0.30
Ti	0.33	0.34	0.32	0.34	0.34	0.34	0.34	0.34	0.34	0.34
Cr	0.00	0.00	0.00	0.00	0.00	0.00	0.00	0.00	0.00	0.00
Fe	2.88	2.89	2.90	2.86	2.88	2.93	2.85	2.89	2.84	2.86
Mn	0.04	0.04	0.04	0.04	0.04	0.05	0.04	0.04	0.04	0.04
Mg	2.22	2.18	2.19	2.16	2.18	2.22	2.20	2.22	2.20	2.20
Ca	0.00	0.00	0.00	0.00	0.01	0.00	0.00	0.00	0.00	0.00
Na	0.08	0.08	0.05	0.06	0.08	0.06	0.06	0.06	0.06	0.06
K	1.86	1.89	1.87	1.87	1.86	1.89	1.88	1.89	1.88	1.88
OH*	3.93	3.92	3.92	3.91	3.91	3.92	3.92	3.91	3.92	3.91
F	0.00	0.00	0.00	0.00	0.00	0.00	0.00	0.00	0.00	0.00
Cl	0.07	0.08	0.08	0.09	0.09	0.08	0.08	0.09	0.08	0.09
TOTAL	19.70	19.70	19.67	19.66	19.68	19.73	19.67	19.70	19.67	19.67
Y total	5.77	5.72	5.75	5.73	5.73	5.78	5.73	5.76	5.73	5.74
X total	1.93	1.97	1.93	1.93	1.95	1.95	1.94	1.95	1.94	1.94
Al total	2.71	2.66	2.66	2.69	2.66	2.66	2.68	2.67	2.68	2.69
Fe/Fe+Mg	0.56	0.57	0.57	0.57	0.57	0.57	0.56	0.56	0.56	0.57
Mg/Mg+Fe	0.44	0.43	0.43	0.43	0.43	0.43	0.44	0.44	0.44	0.43
a	-2.36	-2.36	-2.36	-2.36	-2.36	-2.36	-2.36	-2.36	-2.36	-2.36
b	0.00	0.00	0.00	0.00	0.00	0.00	0.00	0.00	0.00	0.00
c	-1.73	-1.73	-1.73	-1.73	-1.73	-1.73	-1.73	-1.73	-1.73	-1.73
Ti	0.33	0.34	0.32	0.34	0.34	0.34	0.34	0.34	0.34	0.34
X(Mg)	0.44	0.43	0.43	0.43	0.43	0.43	0.44	0.44	0.44	0.43
T(C) Cesare et al. (2008)	670.71	673.31	665.12	672.76	675.11	672.33	675.26	672.20	674.73	674.55
T(K) Luhr et al.(1984)	912.70	915.09	908.68	915.52	916.47	912.37	917.37	913.66	917.23	916.61
T(C) Luhr et al. (1984)	639.55	641.94	635.53	642.37	643.32	639.22	644.22	640.51	644.08	643.46

APPENDIX E

GROUP A PEGMATITES - URANINITE CHEMICAL AGE DATA

Table E-1. Uraninite Chemical Age Data

Supplementary Data Table 3 for Chapter 3 (McKechnie *et al.* 2012a)

SAMPLE	LINE	Pb CONC(PPM)	Pb REL%ERR	Pb CDL(PPM)	Th CONC(PPM)	Th REL%ERR	Th CDL(PPM)	U CONC(PPM)	U REL%ERR	U CDL(PPM)	TOTAL	BEAMCUR	Age (Ga)	+/- (Ma)
WYL-10-61-190.3 Urn1	25	160727.00	0.60	542.80	50487.90	0.75	355.40	565503.00	0.21	493.51	95.62	25.00	1.655	5
WYL-10-61-190.3 Urn1	26	100150.00	0.77	512.52	56283.00	0.70	355.58	564146.00	0.21	483.94	93.33	25.00	1.102	5
WYL-10-61-190.3 Urn1	27	141297.00	0.64	546.44	51113.20	0.74	348.91	567631.00	0.21	486.24	95.07	25.00	1.481	5
WYL-10-61-190.3 Urn1	28	121003.00	0.70	537.33	52087.60	0.73	346.83	567693.00	0.21	493.46	93.81	25.00	1.296	5
WYL-10-61-190.3 Urn1	29	162450.00	0.59	544.83	59228.40	0.68	353.11	550113.00	0.21	502.72	95.25	24.99	1.701	5
WYL-10-61-190.3 Urn1	30	157734.00	0.60	543.72	56057.20	0.71	353.96	550262.00	0.21	495.48	94.60	24.99	1.662	5
WYL-10-61-190.3 Urn1	31	134401.00	0.66	548.30	53726.60	0.72	357.23	566943.00	0.21	489.86	94.77	24.99	1.419	5
WYL-10-61-190.3 Urn2	32	179186.00	0.57	546.52	48405.50	0.78	363.59	540444.00	0.21	496.69	95.49	24.99	1.874	5
WYL-10-61-190.3 Urn2	33	170616.00	0.58	542.71	51326.80	0.75	355.48	537940.00	0.21	497.63	95.03	24.99	1.807	5
WYL-10-61-190.3 Urn2	34	176070.00	0.57	564.23	58044.80	0.70	361.10	531274.00	0.22	500.76	94.92	24.99	1.866	5
WYL-10-61-190.3 Urn2	35	176930.00	0.57	560.18	57097.20	0.70	364.41	533903.00	0.22	502.54	95.46	24.99	1.867	5
WYL-10-61-190.3 Urn2	36	180598.00	0.56	555.13	62348.80	0.67	365.66	531528.00	0.22	500.44	95.47	24.99	1.900	5
WYL-10-61-190.3 Urn3-Zrn2	47	168432.00	0.58	557.97	50990.00	0.75	358.77	554260.00	0.21	493.92	94.70	24.97	1.747	5
WYL-10-61-190.3 Urn3-Zrn2	48	170057.00	0.58	556.97	52724.30	0.73	357.18	560825.00	0.21	502.02	94.74	24.97	1.743	5
WYL-10-61-190.3 Urn3-Zrn2	49	176105.00	0.57	567.54	50059.50	0.76	366.03	566265.00	0.21	496.02	95.76	24.97	1.781	5
WYL-10-61-190.3 Urn3-Zrn2	50	181099.00	0.56	539.74	51850.20	0.74	360.80	564404.00	0.21	500.24	96.18	24.97	1.825	5
WYL-10-61-190.3 Urn3-Zrn2	51	182868.00	0.56	570.38	50662.60	0.75	362.65	564836.00	0.21	500.43	96.26	24.96	1.839	5
WYL-10-61-190.3 Urn3-Zrn2	52	169124.00	0.58	562.57	54500.70	0.72	358.06	551489.00	0.21	497.14	96.41	24.96	1.757	5
WYL-10-62-93.5 Urn1	108	192878.00	0.54	564.37	60842.40	0.68	368.00	590879.00	0.20	508.50	98.71	24.90	1.846	5
WYL-10-62-93.5 Urn1	109	153405.00	0.61	522.45	54554.90	0.71	347.56	547292.00	0.21	482.19	89.11	24.90	1.632	5
WYL-10-62-93.5 Urn1	110	148986.00	0.62	556.10	76518.90	0.59	362.92	571933.00	0.21	505.86	94.79	24.90	1.523	5
WYL-10-62-93.5 Urn1	111	165860.00	0.59	557.57	75156.70	0.60	370.17	566362.00	0.21	497.99	95.96	24.90	1.680	5
WYL-10-62-93.5 Urn1	112	179046.00	0.56	535.52	65067.90	0.65	365.41	559935.00	0.21	502.33	96.42	24.89	1.811	5
WYL-10-62-93.5 Urn1	113	176405.00	0.56	523.75	68890.90	0.63	367.27	574169.00	0.21	498.58	96.43	24.89	1.752	5
WYL-10-62-93.5 Urn1	114	153877.00	0.61	540.79	64934.40	0.65	358.75	565032.00	0.21	499.20	95.07	24.89	1.588	5
WYL-10-62-93.5 Urn1	115	184631.00	0.55	549.75	63739.90	0.66	363.59	554592.00	0.21	497.49	96.35	24.89	1.871	5
WYL-10-62-93.5 Urn1	116	195468.00	0.53	550.37	57776.40	0.70	363.43	576444.00	0.21	510.88	96.31	24.89	1.904	5
WYL-10-62-93.5 Urn1	117	157302.00	0.60	549.32	69918.50	0.62	367.27	585935.00	0.20	503.01	96.10	24.89	1.568	5

APPENDIX F

GROUP B PEGMATITE – MONAZITE CHEMICAL AGE DATA

Table F-1. Monazite Chemical Age Data
Supplementary Data Table 4 for Chapter 3 (McKechnie *et al.* 2012a)

SAMPLE	LINE	Pb CONC(PPM)	Pb REL%ERR	Pb CDL(PPM)	Th CONC(PPM)	Th REL%ERR	Th CDL(PPM)	U CONC(PPM)	U REL%ERR	U CDL(PPM)	TOTAL	BEAMCUR	Age (Ga)	+/- (Ma)
WYL-09-46-32.6 Mon1	57	15411	2.40	439.74	133891.00	0.44	313.59	5596.06	4.09	413.53	99.91	24.96	2.122	28
WYL-09-46-32.6 Mon1	58	14850.8	2.46	440.94	129375.00	0.45	316.54	6043.93	3.75	401.78	99.68	24.96	2.085	29
WYL-09-46-32.6 Mon1	59	17357.7	2.22	445.46	154268.00	0.41	316.23	5704.29	4.04	415.98	99.43	24.96	2.109	26
WYL-09-46-32.6 Mon1	60	18197.3	2.14	435.40	154973.00	0.41	317.93	6755.20	3.49	415.05	99.42	24.95	2.149	25
WYL-09-46-32.6 Mon1	61	17698	2.19	441.67	158182.00	0.40	321.47	6886.96	3.44	416.23	99.97	24.95	2.056	25
WYL-09-46-32.6 Mon1	62	16928.3	2.24	434.64	144774.00	0.42	312.41	6484.25	3.59	410.68	100.26	24.95	2.133	26
WYL-09-46-32.6 Mon2	63	19039.4	2.09	446.84	171492.00	0.39	315.16	6261.88	3.74	416.94	99.82	24.95	2.086	25
WYL-09-46-32.6 Mon2	64	21089	1.97	460.31	186593.00	0.37	326.33	6480.90	3.67	423.27	100.57	24.95	2.132	24
WYL-09-46-32.6 Mon2	65	11841.8	2.86	436.68	98850.20	0.52	314.14	4767.58	4.65	408.02	99.70	24.95	2.159	33
WYL-09-46-32.6 Mon2	66	15520.7	2.40	448.52	128463.00	0.45	317.24	5808.46	3.97	414.87	100.39	24.95	2.195	28
WYL-09-46-32.6 Mon2	67	14985	2.46	448.19	128629.00	0.45	315.82	4742.20	4.80	421.99	100.51	24.95	2.178	29
WYL-09-46-32.6 Mon2	68	13285.5	2.63	428.62	116028.00	0.48	312.67	2694.52	7.85	412.89	99.95	24.94	2.239	31
WYL-09-46-32.6 Mon3	69	12130.7	2.86	453.26	94978.40	0.53	312.04	5078.04	4.41	408.87	100.55	24.95	2.253	33
WYL-09-46-32.6 Mon3	70	13540.3	2.59	429.31	113692.00	0.48	315.08	5634.77	4.06	413.22	99.34	24.94	2.139	30
WYL-09-46-32.6 Mon3	71	16580	2.31	454.04	142512.00	0.43	324.50	5997.34	3.87	415.64	100.32	24.94	2.141	27
WYL-09-46-32.6 Mon3	72	15686.9	2.33	416.76	139009.00	0.43	313.83	5668.47	4.05	413.65	100.40	24.94	2.090	27
WYL-09-46-32.6 Mon3	73	16927.7	2.26	443.39	137733.00	0.43	311.61	5683.99	4.00	408.71	100.74	24.94	2.256	27
WYL-09-46-32.6 Mon3	74	16438.7	2.30	440.51	137964.00	0.43	313.08	5299.94	4.27	411.76	99.92	24.94	2.213	27
WYL-09-46-32.6 Mon4	75	9433.77	3.35	435.27	87346.10	0.56	308.71	1350.00	14.78	404.43	100.14	24.94	2.177	40
WYL-09-46-32.6 Mon4	76	9813	3.28	443.54	90601.10	0.54	311.16	1117.81	17.65	402.75	100.56	24.94	2.206	40
WYL-09-46-32.6 Mon4	77	13783.6	2.60	447.00	120723.00	0.47	312.59	4732.67	4.71	410.67	100.31	24.94	2.123	30
WYL-09-46-32.6 Mon4	78	8879.64	3.56	453.08	81329.40	0.58	311.19	712.08	27.94	412.31	100.33	24.94	2.250	43
WYL-09-46-32.6 Mon4	79	15438.7	2.41	447.22	130858.00	0.45	315.83	5569.86	4.05	406.17	100.10	24.93	2.165	28
WYL-09-46-32.6 Mon4	80	15707.4	2.36	437.29	137240.00	0.44	317.07	5600.98	4.10	415.29	100.40	24.93	2.117	28
WYL-09-46-32.6 Mon4	81	15391.9	2.40	443.43	135726.00	0.44	320.23	5015.54	4.51	415.43	100.50	24.93	2.124	28
WYL-09-46-32.6 Mon4	82	16125.5	2.33	439.18	137186.00	0.44	315.47	5525.81	4.13	413.39	100.43	24.93	2.173	27
WYL-09-46-32.6 Mon4	83	15596.3	2.38	441.92	139999.00	0.43	311.29	5764.88	3.98	413.25	99.74	24.93	2.063	28
WYL-09-46-32.6 Mon4	84	16465.8	2.29	435.10	141549.00	0.43	312.43	5936.11	3.91	416.83	99.60	24.93	2.141	27

APPENDIX G

MAGNETITE-ILMENITE THERMOBAROMETRY RESULTS

Supplementary Data Table 5 for Chapter 3 (McKechnie *et al.* 2012a). Results calculated using ILMAT: A Magnetite-Ilmenite Geothermobarometry Program (version 1.20).

Table G-1. Summary of Results

Grain 1 Ti-poor magnetite	Average T °C	Average log fO_2	Range T°C	Range log fO_2
Powell & Powell (1977)	440		370 to 649	
Spencer & Lindsley (1981)	532	-22.2	485 to 626	-23.8 to -19.7
Andersen & Lindsley (1985)	538	-22.0	482 to 651	-23.7 to -19.0
All methods combined	503	-22.1	370 to 651	-23.8 to -19.0
Grain 2 Ti-poor magnetite	Average T °C	Average log fO_2	Range T°C	Range log fO_2
Powell & Powell (1977)	393		318 to 494	
Spencer & Lindsley (1981)	499	-24.1	450 to 556	-25.3 to -22.5
Andersen & Lindsley (1985)	499	-23.9	443 to 567	-25.3 to -22.0
All methods combined	464	-24.0	318 to 567	-25.3 to -22.0
Grain 3 Ti-poor magnetite	Average T °C	Average log fO_2	Range T°C	Range log fO_2
Powell & Powell (1977)	426		346 to 586	
Spencer & Lindsley (1981)	531	-22.0	469 to 613	-25.0 to -19.8
Andersen & Lindsley (1985)	530	-21.8	465 to 634	-25.0 to -19.3
All methods combined	496	-21.9	346 to 634	-25.0 to -19.3
Grain 4 Ti-poor magnetite	Average T °C	Average log fO_2	Range T°C	Range log fO_2
Powell & Powell (1977)	372		339 to 426	
Spencer & Lindsley (1981)	493	-23.6	462 to 534	-25.5 to -21.6
Andersen & Lindsley (1985)	491	-23.4	456 to 539	-25.5 to -21.3
All methods combined	452	-23.5	339 to 539	-25.5 to -21.3
Grain 3 Ti-rich magnetite	Average T °C	Average log fO_2	Range T°C	Range log fO_2
Powell & Powell (1977)	811		712 to 901	
Spencer & Lindsley (1981)	706	-18.1	582 to 822	-22.6 to -15
Andersen & Lindsley (1985)	730	-17.3	619 to 829	-20.7 to -15.2
All methods combined	749	-17.7	582 to 901	-22.6 to -15

Average/Range of T and log fO_2	Ti-poor magnetite			
Methods	Average T °C	Average log fO_2	Range T°C	Range log fO_2
Powell & Powell (1977)	372 to 440 (408)		318 to 649	
Spencer & Lindsley (1981)	493 to 532 (513)	-24.1 to -22.0 (-23.0)	450 to 626	-25.3 to -19.7
Andersen & Lindsley (1985)	491 to 538 (558)	-23.9 to -21.8 (-22.8)	443 to 651	-25.3 to -19.0
All methods combined	372 to 538 (479)	-24.1 to -21.8 (-22.9)	318 to 651	-25.3 to -19.0

Average/Range of T and log fO_2	Ti-rich magnetite			
Methods	Average T °C	Average log fO_2	Range T°C	Range log fO_2
Powell & Powell (1977)	811		712 to 901	
Spencer & Lindsley (1981)	706	-18.1	582 to 822	-22.6 to -15
Andersen & Lindsley (1985)	730	-17.3	619 to 829	-20.7 to -15.2
All methods combined	749	-17.7	582 to 901	-22.6 to -15

Table G-2. Magnetite-Ilmenite Grain 1

ILMAT: A Magnetite-Ilmenite Geothermobarometry Program (version 1.20)									
	Sample #	WYL-10-61-190.3 Mag1-Ilm1	WYL-10-61-190.3 Mag1-Ilm1	WYL-10-61-190.3 Mag1-Ilm1	WYL-10-61-190.3 Mag1-Ilm1	WYL-10-61-190.3 Mag1-Ilm1	WYL-10-61-190.3 Mag1-Ilm1	WYL-10-61-190.3 Mag1-Ilm1	WYL-10-61-190.3 Mag1-Ilm1
	Line	18	21	19	21	20	21	24	21
Mol wt.	**Wt% Oxides**	**Magnetite**	**Ilmenite**	**Magnetite**	**Ilmenite**	**Magnetite**	**Ilmenite**	**Magnetite**	**Ilmenite**
60.0843	SiO2	0.10	0.18	0.07	0.18	0.07	0.18	0.08	0.18
79.8658	TiO2	0.30	49.62	0.29	49.62	0.82	49.62	0.32	49.62
101.96128	Al2O3	0.40	0.01	0.41	0.01	0.41	0.01	0.32	0.01
159.6882	Fe2O3(T)								
71.8444	FeO(T)	91.48	43.61	91.11	43.61	91.16	43.61	91.49	43.61
70.937449	MnO	0.03	4.23	0.01	4.23	0.03	4.23	0.03	4.23
40.3044	MgO	0.01	0.02	0.00	0.02	0.00	0.02	0.00	0.02
56.0774	CaO	0.01	0.00	0.01	0.00	0.00	0.00	0.00	0.00
61.97894	Na2O								
94.196	K2O								
151.9904	Cr2O3	0.00	0.00	0.00	0.00	0.00	0.00	0.00	0.00
153.3264	BaO								
81.3894	ZnO	0.00	0.04	0.00	0.04	0.01	0.04	0.00	0.04
149.8812	V2O3	0.03	0.05	0.04	0.05	0.02	0.05	0.04	0.05
74.6928	NiO	0.01	0.00	0.01	0.00	0.02	0.00	0.03	0.00
233.81096	Nb2O3								
	Sum:	92.36502	97.76543	91.948632	97.76543	92.54343	97.76543	92.312971	97.76543
	Carmichael (1967)	**Recalculated Iron and Total**		**Recalculated Iron and Total**		**Recalculated Iron and Total**		**Recalculated Iron and Total**	
	Fe2O3 wt. %	67.0	3.5	66.8	3.5	66.1	3.5	67.1	3.5
	FeO wt. %	31.2	40.5	31.0	40.5	31.7	40.5	31.2	40.5
	Total:	99.1	98.1	98.6	98.1	99.2	98.1	99.0	98.1
		Ulvöspinel	**Ilmenite**	**Ulvöspinel**	**Ilmenite**	**Ulvöspinel**	**Ilmenite**	**Ulvöspinel**	**Ilmenite**
	Sum of Atomic mol proportion:	2.3294	1.5469	2.3402	1.5469	2.3266	1.5469	2.3322	1.5469
	No. of Oxygen:	4	3	4	3	4	3	4	3
cations		**Cation prop. (Carmichael 1967)**		**Cation prop. (Carmichael 1967)**		**Cation prop. (Carmichael 1967)**		**Cation prop. (Carmichael 1967)**	
1	Si	0.0039	0.0045	0.0027	0.0045	0.0028	0.0045	0.0029	0.0045
1	Ti	0.0088	0.9611	0.0086	0.9611	0.0239	0.9611	0.0094	0.9611
2	Al	0.0182	0.0004	0.0188	0.0004	0.0187	0.0004	0.0148	0.0004
2	Fe+3	1.9554	0.0673	1.9572	0.0673	1.9271	0.0673	1.9588	0.0673
1	Fe+2	1.0106	0.8718	1.0105	0.8718	1.0250	0.8718	1.0112	0.8718
1	Mn	0.0010	0.0923	0.0004	0.0923	0.0009	0.0923	0.0009	0.0923
1	Mg	0.0007	0.0008	0.0000	0.0008	0.0000	0.0008	0.0000	0.0008
1	Ca	0.0004	0.0000	0.0003	0.0000	0.0002	0.0000	0.0000	0.0000
2	Na	0.0000	0.0000	0.0000	0.0000	0.0000	0.0000	0.0000	0.0000
2	K	0.0000	0.0000	0.0000	0.0000	0.0000	0.0000	0.0000	0.0000
2	Cr	0.0001	0.0000	0.0001	0.0000	0.0000	0.0000	0.0000	0.0000
1	Ba	0.0000	0.0000	0.0000	0.0000	0.0000	0.0000	0.0000	0.0000
1	Zn	0.0000	0.0007	0.0000	0.0007	0.0004	0.0007	0.0000	0.0007
2	V	0.0008	0.0010	0.0013	0.0010	0.0007	0.0010	0.0012	0.0010
1	Ni	0.0002	0.0001	0.0002	0.0001	0.0005	0.0001	0.0010	0.0001
2	Nb	0.0000	0.0000	0.0000	0.0000	0.0000	0.0000	0.0000	0.0000
	Total:	3.0001	2.0000	3.0000	2.0000	3.0001	2.0000	3.0002	2.0000
	Calc. Methods:	**Mol % Usp**	**Mol % Ilm**	**Mol % Usp**	**Mol % Ilm**	**Mol % Usp**	**Mol % Ilm**	**Mol % Usp**	**Mol % Ilm**
	Carmichael (1967)	1.27%	96.56%	1.13%	96.56%	2.66%	96.56%	1.23%	96.56%
	Anderson (1968)	0.84%	96.06%	0.84%	96.06%	2.36%	96.06%	0.91%	96.06%
	Lindsley & Spencer (1982)	0.89%	96.07%	0.86%	96.07%	2.41%	96.07%	0.95%	96.07%
	Stormer (1983)	0.90%	96.46%	0.87%	96.46%	2.44%	96.46%	0.96%	96.46%
	Geothermometer by:	**Powell & Powell (1977)**							
	X'Usp & X'Ilm from:	**Temp (°C)**		**Temp (°C)**		**Temp (°C)**		**Temp (°C)**	
	Carmichael (1967)	391		385		434		389	
	Anderson (1968)	376		376		436		380	
	Lindsley & Spencer (1982)	379		378		437		383	
	Stormer (1983)	374		373		431		378	
	Average:	380		378		434		383	
	Geothermobarometer by:	**Spencer & Lindsley (1981)**							
	X'Usp & X'Ilm from:	**Temp (°C)**	**log10 fO2**	**Temp (°C)**	**log10 fO2**	**Temp (°C)**	**log10 fO2**	**Temp (°C)**	**log10 fO2**
	Carmichael (1967)	505	-23.25	501	-23.34	531	-22.71	504	-23.27
	Anderson (1968)	501	-22.71	501	-22.71	538	-21.94	504	-22.65
	Lindsley & Spencer (1982)	503	-22.67	502	-22.70	539	-21.93	505	-22.62
	Stormer (1983)	496	-23.31	495	-23.34	531	-22.58	498	-23.27
	Average:	501	-23	500	-23	535	-22	503	-23
	Geothermobarometer by:	**Andersen & Lindsley (1985)**							
	X'Usp & X'Ilm from:	**Temp (°C)**	**log10 fO2**	**Temp (°C)**	**log10 fO2**	**Temp (°C)**	**log10 fO2**	**Temp (°C)**	**log10 fO2**
	Carmichael (1967)	506		501		536		505	
	Anderson (1968)	500	-22.53	500	-22.53	544	-21.64	504	-22.47
	Lindsley & Spencer (1982)	503	-22.49	501	-22.52	544	-21.63	505	-22.43
	Stormer (1983)	495	-23.16	493	-23.19	536	-22.29	497	-23.11
	Average:	501	-23	499	-23	540	-22	503	-23
Average all data for each analytical pair		461	-22.88	459	-23	503	-22	463	-23
Method Averages	Powell & Powell (1977)		440						
	Spencer & Lindsley (1981)		532	-23.79 to -19.68					
	Andersen & Lindsley (1985)		538	-23.68 to -19.04					
Average all data for all pairs for grain		503	-22.08						

Magnetite-Ilmenite Geothermobarometry								
Sample #	WYL-10-61-190.3 Mag1-Ilm1	WYL-10-61-190.3 Mag1-lm1	WYL-10-61-190.3 Mag1-Ilm1	WYL-10-61-190.3 Mag1-lm1	WYL-10-61-190.3 Mag1-Ilm1	WYL-10-61-190.3 Mag1-lm1	WYL-10-61-190.3 Mag1-Ilm1	WYL-10-61-190.3 Mag1-lm1
Line	25	21	26	21	27	21	18	22
Wt% Oxides	**Magnetite**	**Ilmenite**	**Magnetite**	**Ilmenite**	**Magnetite**	**Ilmenite**	**Magnetite**	**Ilmenite**
SiO2	0.09	0.18	0.10	0.18	1.33	0.18	0.10	0.00
TiO2	0.24	49.62	2.21	49.62	6.40	49.62	0.30	49.16
Al2O3	0.43	0.01	0.76	0.01	0.94	0.01	0.40	0.01
Fe2O3(T)								
FeO(T)	91.44	43.61	88.65	43.61	80.55	43.61	91.48	43.97
MnO	0.03	4.23	0.34	4.23	0.16	4.23	0.03	3.92
MgO	0.00	0.02	0.00	0.02	0.15	0.02	0.01	0.03
CaO	0.01	0.00	0.00	0.00	0.04	0.00	0.01	0.00
Na2O								
K2O								
Cr2O3	0.00	0.00	0.00	0.00	0.01	0.00	0.00	0.00
BaO								
ZnO	0.00	0.04	0.00	0.04	0.00	0.04	0.00	0.01
V2O3	0.05	0.05	0.04	0.05	0.04	0.05	0.03	0.05
NiO	0.00	0.00	0.00	0.00	0.02	0.00	0.01	0.03
Nb2O3								
Sum:	92.287239	97.76543	92.088705	97.76543	89.647437	97.76543	92.36502	97.178437
Carmichael (1967)	**Recalculated Iron and Total**		**Recalculated Iron and Total**		**Recalculated Iron and Total**		**Recalculated Iron and Total**	
Fe2O3 wt. %	67.1	3.5	62.4	3.5	48.6	3.5	67.0	4.2
FeO wt. %	31.1	40.5	32.5	40.5	36.8	40.5	31.2	40.2
Total:	99.0	98.1	98.3	98.1	94.5	98.1	99.1	97.6
	Ulvöspinel	**Ilmenite**	**Ulvöspinel**	**Ilmenite**	**Ulvöspinel**	**Ilmenite**	**Ulvöspinel**	**Ilmenite**
Sum of Atomic mol proportion:	2.3312	1.5469	2.3377	1.5469	2.4009	1.5469	2.3294	1.5566
No. of Oxygen:	4	3	4	3	4	3	4	3
	Cation prop. (Carmichael 1967)		**Cation prop. (Carmichael 1967)**		**Cation prop. (Carmichael 1967)**		**Cation prop. (Carmichael 1967)**	
Si	0.0034	0.0045	0.0039	0.0045	0.0533	0.0045	0.0039	0.0000
Ti	0.0071	0.9611	0.0646	0.9611	0.1924	0.9611	0.0088	0.9581
Al	0.0198	0.0004	0.0348	0.0004	0.0441	0.0004	0.0182	0.0004
Fe+3	1.9578	0.0673	1.8271	0.0673	1.4627	0.0673	1.9554	0.0821
Fe+2	1.0094	0.8718	1.0573	0.8718	1.2291	0.8718	1.0106	0.8705
Mn	0.0009	0.0923	0.0111	0.0923	0.0055	0.0923	0.0010	0.0860
Mg	0.0000	0.0008	0.0000	0.0008	0.0090	0.0008	0.0007	0.0012
Ca	0.0002	0.0000	0.0000	0.0000	0.0018	0.0000	0.0004	0.0001
Na	0.0000	0.0000	0.0000	0.0000	0.0000	0.0000	0.0000	0.0000
K	0.0000	0.0000	0.0000	0.0000	0.0000	0.0000	0.0000	0.0000
Cr	0.0000	0.0000	0.0000	0.0000	0.0002	0.0000	0.0001	0.0000
Ba	0.0000	0.0000	0.0000	0.0000	0.0000	0.0000	0.0000	0.0000
Zn	0.0000	0.0007	0.0000	0.0007	0.0000	0.0007	0.0000	0.0002
V	0.0015	0.0010	0.0012	0.0010	0.0013	0.0010	0.0008	0.0009
Ni	0.0000	0.0001	0.0000	0.0001	0.0007	0.0001	0.0002	0.0006
Nb	0.0000	0.0000	0.0000	0.0000	0.0000	0.0000	0.0000	0.0000
Total:	3.0000	2.0000	3.0000	2.0000	3.0002	2.0000	3.0001	2.0002
Calc. Methods:	**Mol % Usp**	**Mol % Ilm**	**Mol % Usp**	**Mol % Ilm**	**Mol % Usp**	**Mol % Ilm**	**Mol % Usp**	**Mol % Ilm**
Carmichael (1967)	1.05%	96.56%	6.85%	96.56%	24.56%	96.56%	1.27%	95.81%
Anderson (1968)	0.67%	96.06%	6.01%	96.06%	19.77%	96.06%	0.84%	95.52%
Lindsley & Spencer (1982)	0.71%	96.07%	6.57%	96.07%	19.95%	96.07%	0.89%	95.52%
Stormer (1983)	0.73%	96.46%	6.65%	96.46%	21.09%	96.46%	0.90%	95.70%
Geothermometer by:								
X'Usp & X'Ilm from:	**Temp (°C)**		**Temp (°C)**		**Temp (°C)**		**Temp (°C)**	
Carmichael (1967)	381		501		628		402	
Anderson (1968)	365		501		615		383	
Lindsley & Spencer (1982)	368		508		616		386	
Stormer (1983)	363		501		612		385	
Average:	369		503		618		389	
Geothermobarometer by:								
X'Usp & X'Ilm from:	**Temp (°C)**	**log10 fO2**	**Temp (°C)**	**log10 fO2**	**Temp (°C)**	**log10 fO2**	**Temp (°C)**	**log10 fO2**
Carmichael (1967)	499	-23.39	563	-22.07	597	-21.39	520	-22.01
Anderson (1968)	493	-22.88	572	-21.29	609	-20.56	510	-21.91
Lindsley & Spencer (1982)	495	-22.84	575	-21.24	610	-20.56	512	-21.87
Stormer (1983)	488	-23.48	565	-21.89	598	-21.25	510	-22.11
Average:	494	-23	569	-22	604	-21	513	-22
Geothermobarometer by:								
X'Usp & X'Ilm from:	**Temp (°C)**	**log10 fO2**	**Temp (°C)**	**log10 fO2**	**Temp (°C)**	**log10 fO2**	**Temp (°C)**	**log10 fO2**
Carmichael (1967)	498		575		623		523	
Anderson (1968)	491	-22.73	584	-20.85	633	-19.89	511	-21.70
Lindsley & Spencer (1982)	494	-22.68	588	-20.79	633	-19.89	513	-21.66
Stormer (1983)	486	-23.36	577	-21.45	622	-20.54	511	-21.90
Average:	492	-23	581	-21	628	-20	515	-22
data for each analytical pair	452	-23	551	-21	616	-21	472	-22
Powell & Powell (1977)								
Spencer & Lindsley (1981)								
Andersen & Lindsley (1985)								
data for all pairs for grain								

lagnetite-Ilmenite Geothermobarometry								
Sample #	WYL-10-61-190.3 Mag1-Ilm1	WYL-10-61-190.3 Mag1-Im1	WYL-10-61-190.3 Mag1-Ilm1	WYL-10-61-190.3 Mag1-Im1	WYL-10-61-190.3 Mag1-Ilm1	WYL-10-61-190.3 Mag1-Im1	WYL-10-61-190.3 Mag1-Ilm1	WYL-10-61-190.3 Mag1-Im1
Line	19	22	20	22	24	22	25	22
Wt% Oxides	**Magnetite**	**Ilmenite**	**Magnetite**	**Ilmenite**	**Magnetite**	**Ilmenite**	**Magnetite**	**Ilmenite**
SiO2	0.07	0.00	0.07	0.00	0.08	0.00	0.09	0.00
TiO2	0.29	49.16	0.82	49.16	0.32	49.16	0.24	49.16
Al2O3	0.41	0.01	0.41	0.01	0.32	0.01	0.43	0.01
Fe2O3(T)								
FeO(T)	91.11	43.97	91.16	43.97	91.49	43.97	91.44	43.97
MnO	0.01	3.92	0.03	3.92	0.03	3.92	0.03	3.92
MgO	0.00	0.03	0.00	0.03	0.00	0.03	0.00	0.03
CaO	0.01	0.00	0.00	0.00	0.00	0.00	0.01	0.00
Na2O								
K2O								
Cr2O3	0.00	0.00	0.00	0.00	0.00	0.00	0.00	0.00
BaO								
ZnO	0.00	0.01	0.01	0.01	0.00	0.01	0.00	0.01
V2O3	0.04	0.05	0.02	0.05	0.04	0.05	0.05	0.05
NiO	0.01	0.03	0.02	0.03	0.03	0.03	0.00	0.03
Nb2O3								
Sum:	91.948632	97.178437	92.54343	97.178437	92.312971	97.178437	92.287239	97.178437
Carmichael (1967)	**Recalculated Iron and Total**		**Recalculated Iron and Total**		**Recalculated Iron and Total**		**Recalculated Iron and Total**	
Fe2O3 wt. %	66.8	4.2	66.1	4.2	67.1	4.2	67.1	4.2
FeO wt. %	31.0	40.2	31.7	40.2	31.2	40.2	31.1	40.2
Total:	98.6	97.6	99.2	97.6	99.0	97.6	99.0	97.6
	Ulvöspinel	**Ilmenite**	**Ulvöspinel**	**Ilmenite**	**Ulvöspinel**	**Ilmenite**	**Ulvöspinel**	**Ilmenite**
Sum of Atomic mol proportion:	2.3402	1.5566	2.3266	1.5566	2.3322	1.5566	2.3312	1.5566
No. of Oxygen:	4	3	4	3	4	3	4	3
	Cation prop. (Carmichael 1967)		**Cation prop. (Carmichael 1967)**		**Cation prop. (Carmichael 1967)**		**Cation prop. (Carmichael 1967)**	
Si	0.0027	0.0000	0.0028	0.0000	0.0029	0.0000	0.0034	0.0000
Ti	0.0086	0.9581	0.0239	0.9581	0.0094	0.9581	0.0071	0.9581
Al	0.0188	0.0004	0.0187	0.0004	0.0148	0.0004	0.0198	0.0004
Fe+3	1.9572	0.0821	1.9271	0.0821	1.9588	0.0821	1.9578	0.0821
Fe+2	1.0105	0.8705	1.0250	0.8705	1.0112	0.8705	1.0094	0.8705
Mn	0.0004	0.0860	0.0009	0.0860	0.0009	0.0860	0.0009	0.0860
Mg	0.0000	0.0012	0.0000	0.0012	0.0000	0.0012	0.0000	0.0012
Ca	0.0003	0.0001	0.0002	0.0001	0.0000	0.0001	0.0002	0.0001
Na	0.0000	0.0000	0.0000	0.0000	0.0000	0.0000	0.0000	0.0000
K	0.0000	0.0000	0.0000	0.0000	0.0000	0.0000	0.0000	0.0000
Cr	0.0001	0.0000	0.0000	0.0000	0.0000	0.0000	0.0000	0.0000
Ba	0.0000	0.0000	0.0000	0.0000	0.0000	0.0000	0.0000	0.0000
Zn	0.0000	0.0002	0.0004	0.0002	0.0000	0.0002	0.0000	0.0002
V	0.0013	0.0009	0.0007	0.0009	0.0012	0.0009	0.0015	0.0009
Ni	0.0002	0.0006	0.0005	0.0006	0.0010	0.0006	0.0000	0.0006
Nb	0.0000	0.0000	0.0000	0.0000	0.0000	0.0000	0.0000	0.0000
Total:	3.0000	2.0002	3.0001	2.0002	3.0002	2.0002	3.0000	2.0002
Calc. Methods:	**Mol % Usp**	**Mol % Ilm**	**Mol % Usp**	**Mol % Ilm**	**Mol % Usp**	**Mol % Ilm**	**Mol % Usp**	**Mol % Ilm**
Carmichael (1967)	1.13%	95.81%	2.66%	95.81%	1.23%	95.81%	1.05%	95.81%
Anderson (1968)	0.84%	95.52%	2.36%	95.52%	0.91%	95.52%	0.67%	95.52%
Lindsley & Spencer (1982)	0.86%	95.52%	2.41%	95.52%	0.95%	95.52%	0.71%	95.52%
Stormer (1983)	0.87%	95.70%	2.44%	95.70%	0.96%	95.70%	0.73%	95.70%
Geothermometer by:								
X'Usp & X'Ilm from:	**Temp (°C)**		**Temp (°C)**		**Temp (°C)**		**Temp (°C)**	
Carmichael (1967)	396		447		401		392	
Anderson (1968)	383		444		388		372	
Lindsley & Spencer (1982)	385		445		390		375	
Stormer (1983)	383		443		388		373	
Average:	387		445		392		378	
Geothermobarometer by:								
X'Usp & X'Ilm from:	**Temp (°C)**	**log10 fO2**	**Temp (°C)**	**log10 fO2**	**Temp (°C)**	**log10 fO2**	**Temp (°C)**	**log10 fO2**
Carmichael (1967)	516	-22.09	548	-21.46	519	-22.03	513	-22.15
Anderson (1968)	510	-21.91	549	-21.14	513	-21.85	502	-22.08
Lindsley & Spencer (1982)	511	-21.90	549	-21.14	515	-21.82	504	-22.04
Stormer (1983)	509	-22.13	547	-21.37	512	-22.06	502	-22.27
Average:	512	-22	548	-21	515	-22	505	-22
Geothermobarometer by:								
X'Usp & X'Ilm from:	**Temp (°C)**	**log10 fO2**	**Temp (°C)**	**log10 fO2**	**Temp (°C)**	**log10 fO2**	**Temp (°C)**	**log10 fO2**
Carmichael (1967)	518		555		522		515	
Anderson (1968)	511	-21.70	556	-20.81	514	-21.63	502	-21.89
Lindsley & Spencer (1982)	512	-21.68	556	-20.81	516	-21.60	504	-21.85
Stormer (1983)	509	-21.92	553	-21.05	513	-21.84	502	-22.09
Average:	513	-22	555	-21	516	-22	506	-22
lata for each analytical pair	470	-22	516	-21	474	-22	463	-22
Powell & Powell (1977)								
Spencer & Lindsley (1981)								
Andersen & Lindsley (1985)								
lata for all pairs for grain								

lagnetite-Ilmenite Geothermobarometry								
Sample #	WYL-10-61-190.3 Mag1-Ilm1	WYL-10-61-190.3 Mag1-Im1	WYL-10-61-190.3 Mag1-Ilm1	WYL-10-61-190.3 Mag1-Im1	WYL-10-61-190.3 Mag1-Ilm1	WYL-10-61-190.3 Mag1-Im1	WYL-10-61-190.3 Mag1-Ilm1	WYL-10-61-190.3 Mag1-Im1
Line	26	22	27	22	18	23	19	23
Wt% Oxides	**Magnetite**	**Ilmenite**	**Magnetite**	**Ilmenite**	**Magnetite**	**Ilmenite**	**Magnetite**	**Ilmenite**
SiO2	0.10	0.00	1.33	0.00	0.10	0.01	0.07	0.01
TiO2	2.21	49.16	6.40	49.16	0.30	49.98	0.29	49.98
Al2O3	0.76	0.01	0.94	0.01	0.40	0.00	0.41	0.00
Fe2O3(T)								
FeO(T)	88.65	43.97	80.55	43.97	91.48	43.93	91.11	43.93
MnO	0.34	3.92	0.16	3.92	0.03	3.97	0.01	3.97
MgO	0.00	0.03	0.15	0.03	0.01	0.00	0.00	0.00
CaO	0.00	0.00	0.04	0.00	0.01	0.02	0.01	0.02
Na2O								
K2O								
Cr2O3	0.00	0.00	0.01	0.00	0.00	0.00	0.00	0.00
BaO								
ZnO	0.00	0.01	0.00	0.01	0.00	0.00	0.00	0.00
V2O3	0.04	0.05	0.04	0.05	0.03	0.07	0.04	0.07
NiO	0.00	0.03	0.02	0.03	0.01	0.01	0.01	0.01
Nb2O3								
Sum:	92.088705	97.178437	89.647437	97.178437	92.36502	97.985121	91.948632	97.985121
Carmichael (1967)	**Recalculated Iron and Total**		**Recalculated Iron and Total**		**Recalculated Iron and Total**		**Recalculated Iron and Total**	
Fe2O3 wt. %	62.4	4.2	48.6	4.2	67.0	3.3	66.8	3.3
FeO wt. %	32.5	40.2	36.8	40.2	31.2	40.9	31.0	40.9
Total:	98.3	97.6	94.5	97.6	99.1	98.3	98.6	98.3
	Ulvöspinel	**Ilmenite**	**Ulvöspinel**	**Ilmenite**	**Ulvöspinel**	**Ilmenite**	**Ulvöspinel**	**Ilmenite**
Sum of Atomic mol proportion:	2.3377	1.5566	2.4009	1.5566	2.3294	1.5448	2.3402	1.5448
No. of Oxygen:	4	3	4	3	4	3	4	3
	Cation prop. (Carmichael 1967)		**Cation prop. (Carmichael 1967)**		**Cation prop. (Carmichael 1967)**		**Cation prop. (Carmichael 1967)**	
Si	0.0039	0.0000	0.0533	0.0000	0.0039	0.0002	0.0027	0.0002
Ti	0.0646	0.9581	0.1924	0.9581	0.0088	0.9667	0.0086	0.9667
Al	0.0348	0.0004	0.0441	0.0004	0.0182	0.0000	0.0188	0.0000
Fe+3	1.8271	0.0821	1.4627	0.0821	1.9554	0.0644	1.9572	0.0644
Fe+2	1.0573	0.8705	1.2291	0.8705	1.0106	0.8801	1.0105	0.8801
Mn	0.0111	0.0860	0.0055	0.0860	0.0010	0.0864	0.0004	0.0864
Mg	0.0000	0.0012	0.0090	0.0012	0.0007	0.0000	0.0000	0.0000
Ca	0.0000	0.0001	0.0018	0.0001	0.0004	0.0005	0.0003	0.0005
Na	0.0000	0.0000	0.0000	0.0000	0.0000	0.0000	0.0000	0.0000
K	0.0000	0.0000	0.0000	0.0000	0.0000	0.0000	0.0000	0.0000
Cr	0.0000	0.0000	0.0002	0.0000	0.0001	0.0000	0.0001	0.0000
Ba	0.0000	0.0000	0.0000	0.0000	0.0000	0.0000	0.0000	0.0000
Zn	0.0000	0.0002	0.0000	0.0002	0.0000	0.0000	0.0000	0.0000
V	0.0012	0.0009	0.0013	0.0009	0.0008	0.0015	0.0013	0.0015
Ni	0.0000	0.0006	0.0007	0.0006	0.0002	0.0002	0.0002	0.0002
Nb	0.0000	0.0000	0.0000	0.0000	0.0000	0.0000	0.0000	0.0000
Total:	3.0000	2.0002	3.0002	2.0002	3.0001	2.0001	3.0000	2.0001
Calc. Methods:	**Mol % Usp**	**Mol % Ilm**	**Mol % Usp**	**Mol % Ilm**	**Mol % Usp**	**Mol % Ilm**	**Mol % Usp**	**Mol % Ilm**
Carmichael (1967)	6.85%	95.81%	24.56%	95.81%	1.27%	96.69%	1.13%	96.69%
Anderson (1968)	6.01%	95.52%	19.77%	95.52%	0.84%	96.48%	0.84%	96.48%
Lindsley & Spencer (1982)	6.57%	95.52%	19.95%	95.52%	0.89%	96.48%	0.86%	96.48%
Stormer (1983)	6.65%	95.70%	21.09%	95.70%	0.90%	96.62%	0.87%	96.62%
Geothermometer by:								
X'Usp & X'Ilm from:	**Temp (°C)**		**Temp (°C)**		**Temp (°C)**		**Temp (°C)**	
Carmichael (1967)	516		649		389		383	
Anderson (1968)	511		628		370		370	
Lindsley & Spencer (1982)	518		629		373		372	
Stormer (1983)	516		632		372		370	
Average:	515		634		376		374	
Geothermobarometer by:								
X'Usp & X'Ilm from:	**Temp (°C)**	**log10 fO2**	**Temp (°C)**	**log10 fO2**	**Temp (°C)**	**log10 fO2**	**Temp (°C)**	**log10 fO2**
Carmichael (1967)	582	-20.80	625	-19.97	503	-23.49	499	-23.58
Anderson (1968)	584	-20.48	626	-19.68	493	-23.42	493	-23.42
Lindsley & Spencer (1982)	587	-20.43	626	-19.68	495	-23.37	494	-23.40
Stormer (1983)	584	-20.66	623	-19.91	492	-23.62	491	-23.64
Average:	584	-21	625	-20	496	-23	494	-24
Geothermobarometer by:								
X'Usp & X'Ilm from:	**Temp (°C)**	**log10 fO2**	**Temp (°C)**	**log10 fO2**	**Temp (°C)**	**log10 fO2**	**Temp (°C)**	**log10 fO2**
Carmichael (1967)	596		651		503		498	
Anderson (1968)	597	-20.04	650	-19.04	491	-23.28	491	-23.28
Lindsley & Spencer (1982)	601	-19.97	650	-19.04	494	-23.23	492	-23.25
Stormer (1983)	598	-20.21	648	-19.25	491	-23.49	490	-23.51
Average:	598	-20	650	-19	495	-23	493	-23
lata for each analytical pair	566	-20	637	-19	455	-23	454	-23
Powell & Powell (1977)								
Spencer & Lindsley (1981)								
Andersen & Lindsley (1985)								
lata for all pairs for grain								

lagnetite-Ilmenite Geothermobarometry										
Sample #	WYL-10-61-190.3 Mag1-Ilm1	WYL-10-61-190.3 Mag1-Ilm1	WYL-10-61-190.3 Mag1-Ilm1	WYL-10-61-190.3 Mag1-Ilm1	WYL-10-61-190.3 Mag1-Ilm1	WYL-10-61-190.3 Mag1-Ilm1	WYL-10-61-190.3 Mag1-Ilm1	WYL-10-61-190.3 Mag1-Ilm1	WYL-10-61-190.3 Mag1-Ilm1	WYL-10-61-190.3 Mag1-Ilm1
Line	20	23	24	23	25	23	26	23	27	23
Wt% Oxides	**Magnetite**	**Ilmenite**	**Magnetite**	**Ilmenite**	**Magnetite**	**Ilmenite**	**Magnetite**	**Ilmenite**	**Magnetite**	**Ilmenite**
SiO2	0.07	0.01	0.08	0.01	0.09	0.01	0.10	0.01	1.33	0.01
TiO2	0.82	49.98	0.32	49.98	0.24	49.98	2.21	49.98	6.40	49.98
Al2O3	0.41	0.00	0.32	0.00	0.43	0.00	0.76	0.00	0.94	0.00
Fe2O3(T)										
FeO(T)	91.16	43.93	91.49	43.93	91.44	43.93	88.65	43.93	80.55	43.93
MnO	0.03	3.97	0.03	3.97	0.03	3.97	0.34	3.97	0.16	3.97
MgO	0.00	0.00	0.00	0.00	0.00	0.00	0.00	0.00	0.15	0.00
CaO	0.00	0.02	0.00	0.02	0.01	0.02	0.00	0.02	0.04	0.02
Na2O										
K2O										
Cr2O3	0.00	0.00	0.00	0.00	0.00	0.00	0.00	0.00	0.01	0.00
BaO										
ZnO	0.01	0.00	0.00	0.00	0.00	0.00	0.00	0.00	0.00	0.00
V2O3	0.02	0.07	0.04	0.07	0.05	0.07	0.04	0.07	0.04	0.07
NiO	0.02	0.01	0.03	0.01	0.00	0.01	0.00	0.01	0.02	0.01
Nb2O3										
Sum:	92.54343	97.985121	92.312971	97.985121	92.287239	97.985121	92.088705	97.985121	89.647437	97.985121
Carmichael (1967)	**Recalculated Iron and Total**		**Recalculated Iron and Total**		**Recalculated Iron and Total**		**Recalculated Iron and Total**		**Recalculated Iron and Total**	
Fe2O3 wt. %	66.1	3.3	67.1	3.3	67.1	3.3	62.4	3.3	48.6	3.3
FeO wt. %	31.7	40.9	31.2	40.9	31.1	40.9	32.5	40.9	36.8	40.9
Total:	99.2	98.3	99.0	98.3	99.0	98.3	98.3	98.3	94.5	98.3
	Ulvöspinel	**Ilmenite**	**Ulvöspinel**	**Ilmenite**	**Ulvöspinel**	**Ilmenite**	**Ulvöspinel**	**Ilmenite**	**Ulvöspinel**	**Ilmenite**
Sum of Atomic mol proportion:	2.3266	1.5448	2.3322	1.5448	2.3312	1.5448	2.3377	1.5448	2.4009	1.5448
No. of Oxygen:	4	3	4	3	4	3	4	3	4	3
	Cation prop. (Carmichael 1967)		**Cation prop. (Carmichael 1967)**		**Cation prop. (Carmichael 1967)**		**Cation prop. (Carmichael 1967)**		**Cation prop. (Carmichael 1967)**	
Si	0.0028	0.0002	0.0029	0.0002	0.0034	0.0002	0.0039	0.0002	0.0533	0.0002
Ti	0.0239	0.9667	0.0094	0.9667	0.0071	0.9667	0.0646	0.9667	0.1924	0.9667
Al	0.0187	0.0000	0.0148	0.0000	0.0198	0.0000	0.0348	0.0000	0.0441	0.0000
Fe+3	1.9271	0.0644	1.9588	0.0644	1.9578	0.0644	1.8271	0.0644	1.4627	0.0644
Fe+2	1.0250	0.8801	1.0112	0.8801	1.0094	0.8801	1.0573	0.8801	1.2291	0.8801
Mn	0.0009	0.0864	0.0009	0.0864	0.0009	0.0864	0.0111	0.0864	0.0055	0.0864
Mg	0.0000	0.0000	0.0000	0.0000	0.0000	0.0000	0.0000	0.0000	0.0090	0.0000
Ca	0.0002	0.0005	0.0000	0.0005	0.0002	0.0005	0.0000	0.0005	0.0018	0.0005
Na	0.0000	0.0000	0.0000	0.0000	0.0000	0.0000	0.0000	0.0000	0.0000	0.0000
K	0.0000	0.0000	0.0000	0.0000	0.0000	0.0000	0.0000	0.0000	0.0000	0.0000
Cr	0.0000	0.0000	0.0000	0.0000	0.0000	0.0000	0.0000	0.0000	0.0002	0.0000
Ba	0.0000	0.0000	0.0000	0.0000	0.0000	0.0000	0.0000	0.0000	0.0000	0.0000
Zn	0.0004	0.0000	0.0000	0.0000	0.0000	0.0000	0.0000	0.0000	0.0000	0.0000
V	0.0007	0.0015	0.0012	0.0015	0.0015	0.0015	0.0012	0.0015	0.0013	0.0015
Ni	0.0005	0.0002	0.0010	0.0002	0.0000	0.0002	0.0000	0.0002	0.0007	0.0002
Nb	0.0000	0.0000	0.0000	0.0000	0.0000	0.0000	0.0000	0.0000	0.0000	0.0000
Total:	3.0001	2.0001	3.0002	2.0001	3.0000	2.0001	3.0000	2.0001	3.0002	2.0001
Calc. Methods:	**Mol % Usp**	**Mol % Ilm**	**Mol % Usp**	**Mol % Ilm**	**Mol % Usp**	**Mol % Ilm**	**Mol % Usp**	**Mol % Ilm**	**Mol % Usp**	**Mol % Ilm**
Carmichael (1967)	2.66%	96.69%	1.23%	96.69%	1.05%	96.69%	6.85%	96.69%	24.56%	96.69%
Anderson (1968)	2.36%	96.48%	0.91%	96.48%	0.67%	96.48%	6.01%	96.48%	19.77%	96.48%
Lindsley & Spencer (1982)	2.41%	96.48%	0.95%	96.48%	0.71%	96.48%	6.57%	96.48%	19.95%	96.48%
Stormer (1983)	2.44%	96.62%	0.96%	96.62%	0.73%	96.62%	6.65%	96.62%	21.09%	96.62%
Geothermometer by:										
X'Usp & X'Ilm from:	**Temp (°C)**		**Temp (°C)**		**Temp (°C)**		**Temp (°C)**		**Temp (°C)**	
Carmichael (1967)	432		387		379		498		624	
Anderson (1968)	428		374		359		493		603	
Lindsley & Spencer (1982)	430		377		362		499		605	
Stormer (1983)	428		375		361		497		607	
Average:	429		378		365		497		610	
Geothermobarometer by:										
X'Usp & X'Ilm from:	**Temp (°C)**	**log10 fO2**	**Temp (°C)**	**log10 fO2**	**Temp (°C)**	**log10 fO2**	**Temp (°C)**	**log10 fO2**	**Temp (°C)**	**log10 fO2**
Carmichael (1967)	528	-22.95	502	-23.51	496	-23.63	560	-22.31	592	-21.66
Anderson (1968)	529	-22.65	495	-23.36	485	-23.59	561	-22.00	595	-21.33
Lindsley & Spencer (1982)	530	-22.63	497	-23.32	487	-23.54	564	-21.95	595	-21.33
Stormer (1983)	527	-22.88	494	-23.57	485	-23.79	561	-22.20	592	-21.59
Average:	529	-23	497	-23	488	-24	561	-22	594	-21
Geothermobarometer by:										
X'Usp & X'Ilm from:	**Temp (°C)**	**log10 fO2**	**Temp (°C)**	**log10 fO2**	**Temp (°C)**	**log10 fO2**	**Temp (°C)**	**log10 fO2**	**Temp (°C)**	**log10 fO2**
Carmichael (1967)	533		502		495		571		618	
Anderson (1968)	534	-22.37	494	-23.21	482	-23.48	572	-21.58	618	-20.65
Lindsley & Spencer (1982)	534	-22.35	496	-23.17	485	-23.42	576	-21.51	619	-20.64
Stormer (1983)	531	-22.61	493	-23.43	482	-23.68	572	-21.77	615	-20.87
Average:	533	-22	496	-23	486	-24	573	-22	617	-21
lata for each analytical pair	497	-23	457	-23	446	-24	544	-22	607	-21
Powell & Powell (1977)										
Spencer & Lindsley (1981)										
Andersen & Lindsley (1985)										
lata for all pairs for grain										

Table G-3. Magnetite-Ilmenite Grain 2

Sample #	WYL-10-61-190.3 Mag2-Ilm2	WYL-10-61-190.3 Mag2-Ilm2	WYL-10-61-190.3 Mag2-Ilm2	WYL-10-61-190.3 Mag2-Ilm2	WYL-10-61-190.3 Mag2-Ilm2	WYL-10-61-190.3 Mag2-Ilm2	WYL-10-61-190.3 Mag2-Ilm2	WYL-10-61-190.3 Mag2-Ilm2	WYL-10-61-190.3 Mag2-Ilm2	WYL-10-61-190.3 Mag2-Ilm2
Line	32	28	33	28	34	28	35	28	36	28
Wt% Oxides	**Magnetite**	**Ilmenite**	**Magnetite**	**Ilmenite**	**Magnetite**	**Ilmenite**	**Magnetite**	**Ilmenite**	**Magnetite**	**Ilmenite**
SiO2	0.07	0.01	0.07	0.01	0.10	0.01	0.22	0.01	0.09	0.01
TiO2	1.28	50.74	0.53	50.74	0.14	50.74	2.16	50.74	0.24	50.74
Al2O3	2.37	0.01	0.89	0.01	0.40	0.01	2.68	0.01	0.44	0.01
Fe2O3(T)										
FeO(T)	88.25	44.88	91.73	44.88	92.61	44.88	89.76	44.88	92.36	44.88
MnO	0.26	3.56	0.10	3.56	0.04	3.56	0.35	3.56	0.04	3.56
MgO	0.02	0.00	0.01	0.00	0.02	0.00	0.05	0.00	0.00	0.00
CaO	0.00	0.00	0.01	0.00	0.00	0.00	0.02	0.00	0.00	0.00
Na2O										
K2O										
Cr2O3	0.00	0.00	0.00	0.00	0.00	0.00	0.00	0.00	0.01	0.00
BaO										
ZnO	0.08	0.06	0.03	0.06	0.04	0.06	0.11	0.06	0.00	0.06
V2O3	0.03	0.07	0.04	0.07	0.01	0.07	0.04	0.07	0.04	0.07
NiO	0.03	0.00	0.00	0.00	0.01	0.00	0.01	0.00	0.00	0.00
Nb2O3										
Sum:	92.403168	99.330282	93.391582	99.330282	93.371427	99.330282	95.391548	99.330282	93.23201	99.330282
Carmichael (1967)	**Recalculated Iron and Total**		**Recalculated Iron and Total**		**Recalculated Iron and Total**		**Recalculated Iron and Total**		**Recalculated Iron and Total**	
Fe2O3 wt. %	62.6	3.2	66.7	3.2	68.1	3.2	62.2	3.2	67.7	3.2
FeO wt. %	31.9	42.0	31.7	42.0	31.3	42.0	33.8	42.0	31.4	42.0
Total:	98.7	99.7	100.1	99.7	100.2	99.7	101.6	99.7	100.0	99.7
	Ulvöspinel	**Ilmenite**	**Ulvöspinel**	**Ilmenite**	**Ulvöspinel**	**Ilmenite**	**Ulvöspinel**	**Ilmenite**	**Ulvöspinel**	**Ilmenite**
Sum of Atomic mol proportion:	2.3112	1.5241	2.2998	1.5241	2.3040	1.5241	2.2371	1.5241	2.3075	1.5241
No. of Oxygen:	4	3	4	3	4	3	4	3	4	3
	Cation prop. (Carmichael 1967)		**Cation prop. (Carmichael 1967)**		**Cation prop. (Carmichael 1967)**		**Cation prop. (Carmichael 1967)**		**Cation prop. (Carmichael 1967)**	
Si	0.0028	0.0003	0.0027	0.0003	0.0037	0.0003	0.0082	0.0003	0.0036	0.0003
Ti	0.0371	0.9684	0.0153	0.9684	0.0039	0.9684	0.0604	0.9684	0.0069	0.9684
Al	0.1074	0.0002	0.0400	0.0002	0.0181	0.0002	0.1177	0.0002	0.0201	0.0002
Fe+3	1.8113	0.0610	1.9226	0.0610	1.9661	0.0610	1.7437	0.0610	1.9573	0.0610
Fe+2	1.0278	0.8911	1.0137	0.8911	1.0040	0.8911	1.0511	0.8911	1.0090	0.8911
Mn	0.0086	0.0764	0.0031	0.0764	0.0012	0.0764	0.0110	0.0764	0.0014	0.0764
Mg	0.0009	0.0000	0.0003	0.0000	0.0009	0.0000	0.0027	0.0000	0.0000	0.0000
Ca	0.0000	0.0001	0.0002	0.0001	0.0002	0.0001	0.0007	0.0001	0.0001	0.0001
Na	0.0000	0.0000	0.0000	0.0000	0.0000	0.0000	0.0000	0.0000	0.0000	0.0000
K	0.0000	0.0000	0.0000	0.0000	0.0000	0.0000	0.0000	0.0000	0.0000	0.0000
Cr	0.0001	0.0000	0.0001	0.0000	0.0000	0.0000	0.0000	0.0000	0.0003	0.0000
Ba	0.0000	0.0000	0.0000	0.0000	0.0000	0.0000	0.0000	0.0000	0.0000	0.0000
Zn	0.0024	0.0011	0.0007	0.0011	0.0012	0.0011	0.0029	0.0011	0.0000	0.0011
V	0.0009	0.0015	0.0011	0.0015	0.0004	0.0015	0.0013	0.0015	0.0012	0.0015
Ni	0.0009	0.0000	0.0000	0.0000	0.0004	0.0000	0.0004	0.0000	0.0000	0.0000
Nb	0.0000	0.0000	0.0000	0.0000	0.0000	0.0000	0.0000	0.0000	0.0000	0.0000
Total:	3.0002	2.0000	3.0000	2.0000	3.0001	2.0000	3.0001	2.0000	3.0000	2.0000
Calc. Methods:	**Mol % Usp**	**Mol % Ilm**	**Mol % Usp**	**Mol % Ilm**	**Mol % Usp**	**Mol % Ilm**	**Mol % Usp**	**Mol % Ilm**	**Mol % Usp**	**Mol % Ilm**
Carmichael (1967)	3.99%	96.87%	1.81%	96.87%	0.76%	96.87%	6.86%	96.87%	1.06%	96.87%
Anderson (1968)	3.43%	96.74%	1.40%	96.74%	0.33%	96.74%	5.78%	96.74%	0.63%	96.74%
Lindsley & Spencer (1982)	3.87%	96.74%	1.56%	96.74%	0.39%	96.74%	6.34%	96.74%	0.70%	96.74%
Stormer (1983)	4.11%	96.82%	1.60%	96.82%	0.40%	96.82%	6.78%	96.82%	0.71%	96.82%
Geothermometer by:	**Powell & Powell (1977)**									
X'Usp & X'Ilm from:	**Temp (°C)**		**Temp (°C)**		**Temp (°C)**		**Temp (°C)**		**Temp (°C)**	
Carmichael (1967)	455		406		359		494		376	
Anderson (1968)	447		394		323		484		352	
Lindsley & Spencer (1982)	456		399		331		491		357	
Stormer (1983)	458		399		330		494		357	
Average:	454		400		336		491		361	
Geothermobarometer by:	**Spencer & Lindsley (1981)**									
X'Usp & X'Ilm from:	**Temp (°C)**	**log10 fO2**	**Temp (°C)**	**log10 fO2**	**Temp (°C)**	**log10 fO2**	**Temp (°C)**	**log10 fO2**	**Temp (°C)**	**log10 fO2**
Carmichael (1967)	538	-23.01	511	-23.57	481	-24.22	555	-22.66	492	-23.97
Anderson (1968)	536	-22.86	505	-23.50	456	-24.60	553	-22.51	478	-24.11
Lindsley & Spencer (1982)	540	-22.77	509	-23.42	462	-24.47	556	-22.45	481	-24.03
Stormer (1983)	540	-22.90	508	-23.57	461	-24.62	556	-22.57	480	-24.18
Average:	538	-23	508	-24	465	-24	555	-23	483	-24
Geothermobarometer by:	**Andersen & Lindsley (1985)**									
X'Usp & X'Ilm from:	**Temp (°C)**	**log10 fO2**	**Temp (°C)**	**log10 fO2**	**Temp (°C)**	**log10 fO2**	**Temp (°C)**	**log10 fO2**	**Temp (°C)**	**log10 fO2**
Carmichael (1967)	544		512		478		566		491	
Anderson (1968)	542	-22.54	506	-23.31	450	-24.61	563	-22.10	474	-24.03
Lindsley & Spencer (1982)	547	-22.44	510	-23.22	456	-24.46	567	-22.03	478	-23.94
Stormer (1983)	547	-22.56	509	-23.37	455	-24.62	567	-22.15	477	-24.10
Average:	545	-23	509	-23	460	-25	566	-22	480	-24
Average for each pair	513	-22.72	472	-23	420	-25	537	-22	441	-24
Method Averages					Ranges					
Powell & Powell (1977)		393			318 - 494					
Spencer & Lindsley (1981)		499	-24.06		450 - 556	-25.27 to -22.45				
Andersen & Lindsley (1985)		499	-23.90		443 - 567	-25.31 to -22.03				
Average for all pairs for grain	464	-24								

Sample #	WYL-10-61-190.3 Mag2-Ilm2	WYL-10-61-190.3 Mag2-Ilm2	WYL-10-61-190.3 Mag2-Ilm2	WYL-10-61-190.3 Mag2-Ilm2	WYL-10-61-190.3 Mag2-Ilm2	WYL-10-61-190.3 Mag2-Ilm2	WYL-10-61-190.3 Mag2-Ilm2	WYL-10-61-190.3 Mag2-Ilm2	WYL-10-61-190.3 Mag2-Ilm2	WYL-10-61-190.3 Mag2-Ilm2	WYL-10-61-190.3 Mag2-Ilm2	WYL-10-61-190.3 Mag2-Ilm2
Line	37	28	38	28	32	29	33	29	34	29	35	29
Wt% Oxides	**Magnetite**	**Ilmenite**	**Magnetite**	**Ilmenite**	**Magnetite**	**Ilmenite**	**Magnetite**	**Ilmenite**	**Magnetite**	**Ilmenite**	**Magnetite**	**Ilmenite**
SiO2	0.08	0.01	0.08	0.01	0.07	0.02	0.07	0.02	0.10	0.02	0.22	0.02
TiO2	0.15	50.74	0.54	50.74	1.28	50.67	0.53	50.67	0.14	50.67	2.16	50.67
Al2O3	0.33	0.01	1.28	0.01	2.37	0.00	0.89	0.00	0.40	0.00	2.68	0.00
Fe2O3(T)												
FeO(T)	92.99	44.88	91.63	44.88	88.25	44.66	91.73	44.66	92.61	44.66	89.76	44.66
MnO	0.02	3.56	0.06	3.56	0.26	3.41	0.10	3.41	0.04	3.41	0.35	3.41
MgO	0.00	0.00	0.01	0.00	0.02	0.01	0.01	0.01	0.02	0.01	0.05	0.01
CaO	0.00	0.00	0.00	0.00	0.00	0.01	0.01	0.01	0.00	0.01	0.02	0.01
Na2O												
K2O												
Cr2O3	0.01	0.00	0.00	0.00	0.00	0.00	0.00	0.00	0.00	0.00	0.00	0.00
BaO												
ZnO	0.00	0.06	0.08	0.06	0.08	0.06	0.03	0.06	0.04	0.06	0.11	0.06
V2O3	0.05	0.07	0.05	0.07	0.03	0.05	0.04	0.05	0.01	0.05	0.04	0.05
NiO	0.02	0.00	0.00	0.00	0.03	0.00	0.00	0.00	0.01	0.00	0.01	0.00
Nb2O3												
Sum:	93.649795	99.330282	93.727067	99.330282	92.403168	98.902635	93.391582	98.902635	93.371427	98.902635	95.391548	98.902635
Carmichael (1967)	**Recalculated Iron and Total**		**Recalculated Iron and Total**		**Recalculated Iron and Total**		**Recalculated Iron and Total**		**Recalculated Iron and Total**		**Recalculated Iron and Total**	
Fe2O3 wt. %	68.4	3.2	66.5	3.2	62.6	2.9	66.7	2.9	68.1	2.9	62.2	2.9
FeO wt. %	31.5	42.0	31.8	42.0	31.9	42.1	31.7	42.1	31.3	42.1	33.8	42.1
Total:	100.5	99.7	100.4	99.7	98.7	99.2	100.1	99.2	100.2	99.2	101.6	99.2
	Ulvöspinel	**Ilmenite**	**Ulvöspinel**	**Ilmenite**	**Ulvöspinel**	**Ilmenite**	**Ulvöspinel**	**Ilmenite**	**Ulvöspinel**	**Ilmenite**	**Ulvöspinel**	**Ilmenite**
Sum of Atomic mol proportion:	2.2983	1.5241	2.2879	1.5241	2.3112	1.5308	2.2998	1.5308	2.3040	1.5308	2.2371	1.5308
No. of Oxygen:	4	3	4	3	4	3	4	3	4	3	4	3
	Cation prop. (Carmichael 1967)		**Cation prop. (Carmichael 1967)**		**Cation prop. (Carmichael 1967)**		**Cation prop. (Carmichael 1967)**		**Cation prop. (Carmichael 1967)**		**Cation prop. (Carmichael 1967)**	
Si	0.0032	0.0003	0.0029	0.0003	0.0028	0.0006	0.0027	0.0006	0.0037	0.0006	0.0082	0.0006
Ti	0.0043	0.9684	0.0154	0.9684	0.0371	0.9712	0.0153	0.9712	0.0039	0.9712	0.0604	0.9712
Al	0.0151	0.0002	0.0576	0.0002	0.1074	0.0000	0.0400	0.0000	0.0181	0.0000	0.1177	0.0000
Fe+3	1.9681	0.0610	1.9043	0.0610	1.8113	0.0553	1.9226	0.0553	1.9661	0.0553	1.7437	0.0553
Fe+2	1.0066	0.8911	1.0136	0.8911	1.0278	0.8963	1.0137	0.8963	1.0040	0.8963	1.0511	0.8963
Mn	0.0007	0.0764	0.0020	0.0764	0.0086	0.0737	0.0031	0.0737	0.0012	0.0737	0.0110	0.0737
Mg	0.0000	0.0000	0.0003	0.0000	0.0009	0.0004	0.0003	0.0004	0.0009	0.0004	0.0027	0.0004
Ca	0.0000	0.0001	0.0000	0.0001	0.0000	0.0003	0.0002	0.0003	0.0002	0.0003	0.0007	0.0003
Na	0.0000	0.0000	0.0000	0.0000	0.0000	0.0000	0.0000	0.0000	0.0000	0.0000	0.0000	0.0000
K	0.0000	0.0000	0.0000	0.0000	0.0000	0.0000	0.0000	0.0000	0.0000	0.0000	0.0000	0.0000
Cr	0.0003	0.0000	0.0001	0.0000	0.0001	0.0000	0.0001	0.0000	0.0000	0.0000	0.0000	0.0000
Ba	0.0000	0.0000	0.0000	0.0000	0.0000	0.0000	0.0000	0.0000	0.0000	0.0000	0.0000	0.0000
Zn	0.0000	0.0011	0.0023	0.0011	0.0024	0.0010	0.0007	0.0010	0.0012	0.0010	0.0029	0.0010
V	0.0014	0.0015	0.0015	0.0015	0.0009	0.0011	0.0011	0.0011	0.0004	0.0011	0.0013	0.0011
Ni	0.0006	0.0000	0.0000	0.0000	0.0009	0.0000	0.0000	0.0000	0.0004	0.0000	0.0004	0.0000
Nb	0.0000	0.0000	0.0000	0.0000	0.0000	0.0000	0.0000	0.0000	0.0000	0.0000	0.0000	0.0000
Total:	3.0002	2.0000	3.0000	2.0000	3.0002	2.0000	3.0000	2.0000	3.0001	2.0000	3.0001	2.0000
Calc. Methods:	**Mol % Usp**	**Mol % Ilm**	**Mol % Usp**	**Mol % Ilm**	**Mol % Usp**	**Mol % Ilm**	**Mol % Usp**	**Mol % Ilm**	**Mol % Usp**	**Mol % Ilm**	**Mol % Usp**	**Mol % Ilm**
Carmichael (1967)	0.74%	96.87%	1.82%	96.87%	3.99%	97.18%	1.81%	97.18%	0.76%	97.18%	6.86%	97.18%
Anderson (1968)	0.40%	96.74%	1.47%	96.74%	3.43%	97.05%	1.40%	97.05%	0.33%	97.05%	5.78%	97.05%
Lindsley & Spencer (1982)	0.43%	96.74%	1.57%	96.74%	3.87%	97.06%	1.56%	97.06%	0.39%	97.06%	6.34%	97.06%
Stormer (1983)	0.43%	96.82%	1.63%	96.82%	4.11%	97.12%	1.60%	97.12%	0.40%	97.12%	6.78%	97.12%
Geothermometer by:												
X'Usp & X'Ilm from:	**Temp (°C)**		**Temp (°C)**		**Temp (°C)**		**Temp (°C)**		**Temp (°C)**		**Temp (°C)**	
Carmichael (1967)	358		406		448		399		354		486	
Anderson (1968)	331		396		441		388		318		477	
Lindsley & Spencer (1982)	334		400		449		394		326		483	
Stormer (1983)	334		400		451		394		325		487	
Average:	339		401		447		394		331		483	
Geothermobarometer by:												
X'Usp & X'Ilm from:	**Temp (°C)**	**log10 fO2**	**Temp (°C)**	**log10 fO2**	**Temp (°C)**	**log10 fO2**	**Temp (°C)**	**log10 fO2**	**Temp (°C)**	**log10 fO2**	**Temp (°C)**	**log10 fO2**
Carmichael (1967)	480	-24.24	511	-23.57	529	-23.70	503	-24.25	474	-24.90	545	-23.35
Anderson (1968)	462	-24.46	507	-23.47	528	-23.52	497	-24.16	450	-25.26	544	-23.17
Lindsley & Spencer (1982)	465	-24.40	509	-23.42	531	-23.44	501	-24.08	455	-25.13	547	-23.12
Stormer (1983)	463	-24.56	508	-23.56	531	-23.55	500	-24.21	454	-25.27	547	-23.23
Average:	468	-24	509	-24	530	-24	500	-24	458	-25	546	-23
Geothermobarometer by:												
X'Usp & X'Ilm from:	**Temp (°C)**	**log10 fO2**	**Temp (°C)**	**log10 fO2**	**Temp (°C)**	**log10 fO2**	**Temp (°C)**	**log10 fO2**	**Temp (°C)**	**log10 fO2**	**Temp (°C)**	**log10 fO2**
Carmichael (1967)	477		513		534		503		470		555	
Anderson (1968)	457	-24.45	507	-23.27	533	-23.22	497	-24.00	443	-25.31	553	-22.79
Lindsley & Spencer (1982)	460	-24.38	510	-23.22	537	-23.12	501	-23.91	449	-25.16	557	-22.72
Stormer (1983)	458	-24.54	509	-23.36	538	-23.23	500	-24.05	447	-25.31	557	-22.82
Average:	463	-24	510	-23	535	-23	500	-24	452	-25	555	-23
Average for each pair	423	-24	473	-23	504	-23	465	-24	414	-25	528	-23
Method Averages												
Powell & Powell (1977)												
Spencer & Lindsley (1981)												
Andersen & Lindsley (1985)												
Average for all pairs for grain												

Sample #	WYL-10-61-190.3 Mag2-Ilm2	WYL-10-61-190.3 Mag2-Ilm2	WYL-10-61-190.3 Mag2-Ilm2	WYL-10-61-190.3 Mag2-Ilm2	WYL-10-61-190.3 Mag2-Ilm2	WYL-10-61-190.3 Mag2-Ilm2	WYL-10-61-190.3 Mag2-Ilm2	WYL-10-61-190.3 Mag2-Ilm2	WYL-10-61-190.3 Mag2-Ilm2	WYL-10-61-190.3 Mag2-Ilm2	WYL-10-61-190.3 Mag2-Ilm2	WYL-10-61-190.3 Mag2-Ilm2
Line	36	29	37	29	38	29	32	30	33	30	34	30
Wt% Oxides	**Magnetite**	**Ilmenite**	**Magnetite**	**Ilmenite**	**Magnetite**	**Ilmenite**	**Magnetite**	**Ilmenite**	**Magnetite**	**Ilmenite**	**Magnetite**	**Ilmenite**
SiO_2	0.09	0.02	0.08	0.02	0.08	0.02	0.07	0.01	0.07	0.01	0.10	0.01
TiO_2	0.24	50.67	0.15	50.67	0.54	50.67	1.28	50.87	0.53	50.87	0.14	50.87
Al_2O_3	0.44	0.00	0.33	0.00	1.28	0.00	2.37	0.00	0.89	0.00	0.40	0.00
Fe_2O_3(T)												
FeO(T)	92.36	44.66	92.99	44.66	91.63	44.66	88.25	44.79	91.73	44.79	92.61	44.79
MnO	0.04	3.41	0.02	3.41	0.06	3.41	0.26	3.52	0.10	3.52	0.04	3.52
MgO	0.00	0.01	0.00	0.01	0.01	0.01	0.02	0.00	0.01	0.00	0.02	0.00
CaO	0.00	0.01	0.00	0.01	0.00	0.01	0.00	0.00	0.01	0.00	0.00	0.00
Na_2O												
K_2O												
Cr_2O_3	0.01	0.00	0.01	0.00	0.00	0.00	0.00	0.00	0.00	0.00	0.00	0.00
BaO												
ZnO	0.00	0.06	0.00	0.06	0.08	0.06	0.08	0.02	0.03	0.02	0.04	0.02
V_2O_3	0.04	0.05	0.05	0.05	0.05	0.05	0.03	0.06	0.04	0.06	0.01	0.06
NiO	0.00	0.00	0.02	0.00	0.00	0.00	0.03	0.00	0.00	0.00	0.01	0.00
Nb_2O_3												
Sum:	93.23201	98.902635	93.649795	98.902635	93.727067	98.902635	92.403168	99.268612	93.391582	99.268612	93.371427	99.268612
Carmichael (1967)	**Recalculated Iron and Total**		**Recalculated Iron and Total**		**Recalculated Iron and Total**		**Recalculated Iron and Total**		**Recalculated Iron and Total**		**Recalculated Iron and Total**	
Fe_2O_3 wt. %	67.7	2.9	68.4	2.9	66.5	2.9	62.6	2.9	66.7	2.9	68.1	2.9
FeO wt. %	31.4	42.1	31.5	42.1	31.8	42.1	31.9	42.2	31.7	42.2	31.3	42.2
Total:	100.0	99.2	100.5	99.2	100.4	99.2	98.7	99.6	100.1	99.6	100.2	99.6
	Ulvöspinel	**Ilmenite**	**Ulvöspinel**	**Ilmenite**	**Ulvöspinel**	**Ilmenite**	**Ulvöspinel**	**Ilmenite**	**Ulvöspinel**	**Ilmenite**	**Ulvöspinel**	**Ilmenite**
Sum of Atomic mol proportion:	2.3075	1.5308	2.2983	1.5308	2.2879	1.5308	2.3112	1.5253	2.2998	1.5253	2.3040	1.5253
No. of Oxygen:	4	3	4	3	4	3	4	3	4	3	4	3
	Cation prop. (Carmichael 1967)		**Cation prop. (Carmichael 1967)**		**Cation prop. (Carmichael 1967)**		**Cation prop. (Carmichael 1967)**		**Cation prop. (Carmichael 1967)**		**Cation prop. (Carmichael 1967)**	
Si	0.0036	0.0006	0.0032	0.0006	0.0029	0.0006	0.0028	0.0002	0.0027	0.0002	0.0037	0.0002
Ti	0.0069	0.9712	0.0043	0.9712	0.0154	0.9712	0.0371	0.9715	0.0153	0.9715	0.0039	0.9715
Al	0.0201	0.0000	0.0151	0.0000	0.0576	0.0000	0.1074	0.0000	0.0400	0.0000	0.0181	0.0000
Fe+3	1.9573	0.0553	1.9681	0.0553	1.9043	0.0553	1.8113	0.0554	1.9226	0.0554	1.9661	0.0554
Fe+2	1.0090	0.8963	1.0066	0.8963	1.0136	0.8963	1.0278	0.8956	1.0137	0.8956	1.0040	0.8956
Mn	0.0014	0.0737	0.0007	0.0737	0.0020	0.0737	0.0086	0.0757	0.0031	0.0757	0.0012	0.0757
Mg	0.0000	0.0004	0.0000	0.0004	0.0003	0.0004	0.0009	0.0000	0.0003	0.0000	0.0009	0.0000
Ca	0.0001	0.0003	0.0000	0.0003	0.0000	0.0003	0.0000	0.0000	0.0002	0.0000	0.0002	0.0000
Na	0.0000	0.0000	0.0000	0.0000	0.0000	0.0000	0.0000	0.0000	0.0000	0.0000	0.0000	0.0000
K	0.0000	0.0000	0.0000	0.0000	0.0000	0.0000	0.0000	0.0000	0.0000	0.0000	0.0000	0.0000
Cr	0.0003	0.0000	0.0003	0.0000	0.0001	0.0000	0.0001	0.0000	0.0001	0.0000	0.0000	0.0000
Ba	0.0000	0.0000	0.0000	0.0000	0.0000	0.0000	0.0000	0.0000	0.0000	0.0000	0.0000	0.0000
Zn	0.0000	0.0010	0.0000	0.0010	0.0023	0.0010	0.0024	0.0004	0.0007	0.0004	0.0012	0.0004
V	0.0012	0.0011	0.0014	0.0011	0.0015	0.0011	0.0009	0.0012	0.0011	0.0012	0.0004	0.0012
Ni	0.0000	0.0000	0.0006	0.0000	0.0000	0.0000	0.0009	0.0000	0.0000	0.0000	0.0004	0.0000
Nb	0.0000	0.0000	0.0000	0.0000	0.0000	0.0000	0.0000	0.0000	0.0000	0.0000	0.0000	0.0000
Total:	3.0000	2.0000	3.0002	2.0000	3.0000	2.0000	3.0002	2.0000	3.0000	2.0000	3.0001	2.0000
Calc. Methods:	**Mol % Usp**	**Mol % Ilm**	**Mol % Usp**	**Mol % Ilm**	**Mol % Usp**	**Mol % Ilm**	**Mol % Usp**	**Mol % Ilm**	**Mol % Usp**	**Mol % Ilm**	**Mol % Usp**	**Mol % Ilm**
Carmichael (1967)	1.06%	97.18%	0.74%	97.18%	1.82%	97.18%	3.99%	97.17%	1.81%	97.17%	0.76%	97.17%
Anderson (1968)	0.63%	97.05%	0.40%	97.05%	1.47%	97.05%	3.43%	97.01%	1.40%	97.01%	0.33%	97.01%
Lindsley & Spencer (1982)	0.70%	97.06%	0.43%	97.06%	1.57%	97.06%	3.87%	97.01%	1.56%	97.01%	0.39%	97.01%
Stormer (1983)	0.71%	97.12%	0.43%	97.12%	1.63%	97.12%	4.11%	97.12%	1.60%	97.12%	0.40%	97.12%
Geothermometer by:												
X'Usp & X'Ilm from:	**Temp (°C)**		**Temp (°C)**		**Temp (°C)**		**Temp (°C)**		**Temp (°C)**		**Temp (°C)**	
Carmichael (1967)	370		353		400		448		400		354	
Anderson (1968)	347		326		390		442		389		319	
Lindsley & Spencer (1982)	352		330		394		450		395		327	
Stormer (1983)	352		329		395		451		394		325	
Average:	355		334		395		448		394		331	
Geothermobarometer by:												
X'Usp & X'Ilm from:	**Temp (°C)**	**log10 fO2**	**Temp (°C)**	**log10 fO2**	**Temp (°C)**	**log10 fO2**	**Temp (°C)**	**log10 fO2**	**Temp (°C)**	**log10 fO2**	**Temp (°C)**	**log10 fO2**
Carmichael (1967)	485	-24.65	473	-24.92	503	-24.25	529	-23.67	503	-24.22	474	-24.87
Anderson (1968)	471	-24.76	455	-25.12	499	-24.12	529	-23.42	499	-24.06	451	-25.16
Lindsley & Spencer (1982)	474	-24.69	458	-25.06	501	-24.08	533	-23.33	502	-23.98	456	-25.03
Stormer (1983)	473	-24.82	457	-25.20	501	-24.20	532	-23.53	500	-24.20	454	-25.25
Average:	475	-25	461	-25	501	-24	531	-23	501	-24	459	-25
Geothermobarometer by:												
X'Usp & X'Ilm from:	**Temp (°C)**	**log10 fO2**	**Temp (°C)**	**log10 fO2**	**Temp (°C)**	**log10 fO2**	**Temp (°C)**	**log10 fO2**	**Temp (°C)**	**log10 fO2**	**Temp (°C)**	**log10 fO2**
Carmichael (1967)	482		469		504		535		504		470	
Anderson (1968)	466	-24.73	449	-25.15	499	-23.96	534	-23.12	498	-23.90	444	-25.21
Lindsley & Spencer (1982)	470	-24.64	452	-25.08	501	-23.91	539	-23.02	502	-23.81	450	-25.05
Stormer (1983)	469	-24.78	450	-25.23	501	-24.03	538	-23.21	500	-24.03	447	-25.29
Average:	472	-25	455	-25	501	-24	536	-23	501	-24	453	-25
Average for each pair	434	-25	417	-25	466	-24	505	-23	465	-24	414	-25
Method Averages												
Powell & Powell (1977)												
Spencer & Lindsley (1981)												
Andersen & Lindsley (1985)												
Average for all pairs for grain												

Sample #	WYL-10-61-190.3 Mag2-Ilm2	WYL-10-61-190.3 Mag2-Ilm2	WYL-10-61-190.3 Mag2-Ilm2	WYL-10-61-190.3 Mag2-Ilm2	WYL-10-61-190.3 Mag2-Ilm2	WYL-10-61-190.3 Mag2-Ilm2	WYL-10-61-190.3 Mag2-Ilm2	WYL-10-61-190.3 Mag2-Ilm2	WYL-10-61-190.3 Mag2-Ilm2	WYL-10-61-190.3 Mag2-Ilm2	WYL-10-61-190.3 Mag2-Ilm2	WYL-10-61-190.3 Mag2-Ilm2
Line	35	30	36	30	37	30	38	30	32	31	33	31
Wt% Oxides	**Magnetite**	**Ilmenite**	**Magnetite**	**Ilmenite**	**Magnetite**	**Ilmenite**	**Magnetite**	**Ilmenite**	**Magnetite**	**Ilmenite**	**Magnetite**	**Ilmenite**
SiO2	0.22	0.01	0.09	0.01	0.08	0.01	0.08	0.01	0.07	0.03	0.07	0.03
TiO2	2.16	50.87	0.24	50.87	0.15	50.87	0.54	50.87	1.28	50.85	0.53	50.85
Al2O3	2.68	0.00	0.44	0.00	0.33	0.00	1.28	0.00	2.37	0.00	0.89	0.00
Fe2O3(T)												
FeO(T)	89.76	44.79	92.36	44.79	92.99	44.79	91.63	44.79	88.25	44.59	91.73	44.59
MnO	0.35	3.52	0.04	3.52	0.02	3.52	0.06	3.52	0.26	3.75	0.10	3.75
MgO	0.05	0.00	0.00	0.00	0.00	0.00	0.01	0.00	0.02	0.00	0.01	0.00
CaO	0.02	0.00	0.00	0.00	0.00	0.00	0.00	0.00	0.00	0.01	0.01	0.01
Na2O												
K2O												
Cr2O3	0.00	0.00	0.01	0.00	0.01	0.00	0.00	0.00	0.00	0.00	0.00	0.00
BaO												
ZnO	0.11	0.02	0.00	0.02	0.00	0.02	0.08	0.02	0.08	0.06	0.03	0.06
V2O3	0.04	0.06	0.04	0.06	0.05	0.06	0.05	0.06	0.03	0.04	0.04	0.04
NiO	0.01	0.00	0.00	0.00	0.02	0.00	0.00	0.00	0.03	0.01	0.00	0.01
Nb2O3												
Sum:	95.391548	99.268612	93.23201	99.268612	93.649795	99.268612	93.727067	99.268612	92.403168	99.344674	93.391582	99.344674
Carmichael (1967)	**Recalculated Iron and Total**		**Recalculated Iron and Total**		**Recalculated Iron and Total**		**Recalculated Iron and Total**		**Recalculated Iron and Total**		**Recalculated Iron and Total**	
Fe2O3 wt. %	62.2	2.9	67.7	2.9	68.4	2.9	66.5	2.9	62.6	3.0	66.7	3.0
FeO wt. %	33.8	42.2	31.4	42.2	31.5	42.2	31.8	42.2	31.9	41.9	31.7	41.9
Total:	101.6	99.6	100.0	99.6	100.5	99.6	100.4	99.6	98.7	99.6	100.1	99.6
	Ulvöspinel	**Ilmenite**	**Ulvöspinel**	**Ilmenite**	**Ulvöspinel**	**Ilmenite**	**Ulvöspinel**	**Ilmenite**	**Ulvöspinel**	**Ilmenite**	**Ulvöspinel**	**Ilmenite**
Sum of Atomic mol proportion:	2.2371	1.5253	2.3075	1.5253	2.2983	1.5253	2.2879	1.5253	2.3112	1.5240	2.2998	1.5240
No. of Oxygen:	4	3	4	3	4	3	4	3	4	3	4	3
	Cation prop. (Carmichael 1967)		**Cation prop. (Carmichael 1967)**		**Cation prop. (Carmichael 1967)**		**Cation prop. (Carmichael 1967)**		**Cation prop. (Carmichael 1967)**		**Cation prop. (Carmichael 1967)**	
Si	0.0082	0.0002	0.0036	0.0002	0.0032	0.0002	0.0029	0.0002	0.0028	0.0008	0.0027	0.0008
Ti	0.0604	0.9715	0.0069	0.9715	0.0043	0.9715	0.0154	0.9715	0.0371	0.9703	0.0153	0.9703
Al	0.1177	0.0000	0.0201	0.0000	0.0151	0.0000	0.0576	0.0000	0.1074	0.0000	0.0400	0.0000
Fe+3	1.7437	0.0554	1.9573	0.0554	1.9681	0.0554	1.9043	0.0554	1.8113	0.0568	1.9226	0.0568
Fe+2	1.0511	0.8956	1.0090	0.8956	1.0066	0.8956	1.0136	0.8956	1.0278	0.8890	1.0137	0.8890
Mn	0.0110	0.0757	0.0014	0.0757	0.0007	0.0757	0.0020	0.0757	0.0086	0.0805	0.0031	0.0805
Mg	0.0027	0.0000	0.0000	0.0000	0.0000	0.0000	0.0003	0.0000	0.0009	0.0002	0.0003	0.0002
Ca	0.0007	0.0000	0.0001	0.0000	0.0000	0.0000	0.0000	0.0000	0.0000	0.0003	0.0002	0.0003
Na	0.0000	0.0000	0.0000	0.0000	0.0000	0.0000	0.0000	0.0000	0.0000	0.0000	0.0000	0.0000
K	0.0000	0.0000	0.0000	0.0000	0.0000	0.0000	0.0000	0.0000	0.0000	0.0000	0.0000	0.0000
Cr	0.0000	0.0000	0.0003	0.0000	0.0003	0.0000	0.0001	0.0000	0.0001	0.0000	0.0001	0.0000
Ba	0.0000	0.0000	0.0000	0.0000	0.0000	0.0000	0.0000	0.0000	0.0000	0.0000	0.0000	0.0000
Zn	0.0029	0.0004	0.0000	0.0004	0.0000	0.0004	0.0023	0.0004	0.0024	0.0012	0.0007	0.0012
V	0.0013	0.0012	0.0012	0.0012	0.0014	0.0012	0.0015	0.0012	0.0009	0.0008	0.0011	0.0008
Ni	0.0004	0.0000	0.0000	0.0000	0.0006	0.0000	0.0000	0.0000	0.0009	0.0002	0.0000	0.0002
Nb	0.0000	0.0000	0.0000	0.0000	0.0000	0.0000	0.0000	0.0000	0.0000	0.0000	0.0000	0.0000
Total:	3.0001	2.0000	3.0000	2.0000	3.0002	2.0000	3.0000	2.0000	3.0002	2.0001	3.0000	2.0001
Calc. Methods:	**Mol % Usp**	**Mol % Ilm**	**Mol % Usp**	**Mol % Ilm**	**Mol % Usp**	**Mol % Ilm**	**Mol % Usp**	**Mol % Ilm**	**Mol % Usp**	**Mol % Ilm**	**Mol % Usp**	**Mol % Ilm**
Carmichael (1967)	6.86%	97.17%	1.06%	97.17%	0.74%	97.17%	1.82%	97.17%	3.99%	97.11%	1.81%	97.11%
Anderson (1968)	5.78%	97.01%	0.63%	97.01%	0.40%	97.01%	1.47%	97.01%	3.43%	96.94%	1.40%	96.94%
Lindsley & Spencer (1982)	6.34%	97.01%	0.70%	97.01%	0.43%	97.01%	1.57%	97.01%	3.87%	96.94%	1.56%	96.94%
Stormer (1983)	6.78%	97.12%	0.71%	97.12%	0.43%	97.12%	1.63%	97.12%	4.11%	97.03%	1.60%	97.03%
Geothermometer by:												
X'Usp & X'Ilm from:	**Temp (°C)**		**Temp (°C)**		**Temp (°C)**		**Temp (°C)**		**Temp (°C)**		**Temp (°C)**	
Carmichael (1967)	487		371		353		400		449		401	
Anderson (1968)	478		348		327		391		443		390	
Lindsley & Spencer (1982)	485		353		330		395		451		396	
Stormer (1983)	487		352		329		395		453		395	
Average:	484		356		335		395		449		396	
Geothermobarometer by:												
X'Usp & X'Ilm from:	**Temp (°C)**	**log10 fO2**	**Temp (°C)**	**log10 fO2**	**Temp (°C)**	**log10 fO2**	**Temp (°C)**	**log10 fO2**	**Temp (°C)**	**log10 fO2**	**Temp (°C)**	**log10 fO2**
Carmichael (1967)	545	-23.33	485	-24.62	473	-24.89	503	-24.22	531	-23.54	505	-24.09
Anderson (1968)	545	-23.07	472	-24.66	456	-25.02	500	-24.03	531	-23.26	500	-23.91
Lindsley & Spencer (1982)	548	-23.01	475	-24.58	459	-24.96	502	-23.98	535	-23.18	504	-23.83
Stormer (1983)	547	-23.21	473	-24.81	457	-25.19	501	-24.18	534	-23.34	502	-24.01
Average:	546	-23	476	-25	461	-25	502	-24	533	-23	503	-24
Geothermobarometer by:												
X'Usp & X'Ilm from:	**Temp (°C)**	**log10 fO2**	**Temp (°C)**	**log10 fO2**	**Temp (°C)**	**log10 fO2**	**Temp (°C)**	**log10 fO2**	**Temp (°C)**	**log10 fO2**	**Temp (°C)**	**log10 fO2**
Carmichael (1967)	556		483		469		504		537		505	
Anderson (1968)	555	-22.68	467	-24.62	450	-25.05	500	-23.86	536	-22.96	500	-23.74
Lindsley & Spencer (1982)	558	-22.61	471	-24.53	453	-24.97	503	-23.80	541	-22.86	504	-23.65
Stormer (1983)	557	-22.80	469	-24.76	451	-25.21	501	-24.02	541	-23.02	503	-23.84
Average:	556	-23	472	-25	456	-25	502	-24	539	-23	503	-24
Average for each pair	529	-23	435	-25	417	-25	466	-24	507	-23	467	-24
Method Averages												
Powell & Powell (1977)												
Spencer & Lindsley (1981)												
Andersen & Lindsley (1985)												
Average for all pairs for grain												

Sample #	WYL-10-61-190.3 Mag2-Ilm2	WYL-10-61-190.3 Mag2-Ilm2	WYL-10-61-190.3 Mag2-Ilm2	WYL-10-61-190.3 Mag2-Ilm2	WYL-10-61-190.3 Mag2-Ilm2	WYL-10-61-190.3 Mag2-Ilm2	WYL-10-61-190.3 Mag2-Ilm2	WYL-10-61-190.3 Mag2-Ilm2	WYL-10-61-190.3 Mag2-Ilm2	WYL-10-61-190.3 Mag2-Ilm2
Line	34	31	35	31	36	31	37	31	38	31
Wt% Oxides	**Magnetite**	**Ilmenite**	**Magnetite**	**Ilmenite**	**Magnetite**	**Ilmenite**	**Magnetite**	**Ilmenite**	**Magnetite**	**Ilmenite**
SiO2	0.10	0.03	0.22	0.03	0.09	0.03	0.08	0.03	0.08	0.03
TiO2	0.14	50.85	2.16	50.85	0.24	50.85	0.15	50.85	0.54	50.85
Al2O3	0.40	0.00	2.68	0.00	0.44	0.00	0.33	0.00	1.28	0.00
Fe2O3(T)										
FeO(T)	92.61	44.59	89.76	44.59	92.36	44.59	92.99	44.59	91.63	44.59
MnO	0.04	3.75	0.35	3.75	0.04	3.75	0.02	3.75	0.06	3.75
MgO	0.02	0.00	0.05	0.00	0.00	0.00	0.00	0.00	0.01	0.00
CaO	0.00	0.01	0.02	0.01	0.00	0.01	0.00	0.01	0.00	0.01
Na2O										
K2O										
Cr2O3	0.00	0.00	0.00	0.00	0.01	0.00	0.01	0.00	0.00	0.00
BaO										
ZnO	0.04	0.06	0.11	0.06	0.00	0.06	0.00	0.06	0.08	0.06
V2O3	0.01	0.04	0.04	0.04	0.04	0.04	0.05	0.04	0.05	0.04
NiO	0.01	0.01	0.01	0.01	0.00	0.01	0.02	0.01	0.00	0.01
Nb2O3										
Sum:	93.371427	99.344674	95.391548	99.344674	93.23201	99.344674	93.649795	99.344674	93.727067	99.344674
Carmichael (1967)	**Recalculated Iron and Total**		**Recalculated Iron and Total**		**Recalculated Iron and Total**		**Recalculated Iron and Total**		**Recalculated Iron and Total**	
Fe2O3 wt. %	68.1	3.0	62.2	3.0	67.7	3.0	68.4	3.0	66.5	3.0
FeO wt. %	31.3	41.9	33.8	41.9	31.4	41.9	31.5	41.9	31.8	41.9
Total:	100.2	99.6	101.6	99.6	100.0	99.6	100.5	99.6	100.4	99.6
	Ulvöspinel	**Ilmenite**	**Ulvöspinel**	**Ilmenite**	**Ulvöspinel**	**Ilmenite**	**Ulvöspinel**	**Ilmenite**	**Ulvöspinel**	**Ilmenite**
Sum of Atomic mol proportion:	2.3040	1.5240	2.2371	1.5240	2.3075	1.5240	2.2983	1.5240	2.2879	1.5240
No. of Oxygen:	4	3	4	3	4	3	4	3	4	3
	Cation prop. (Carmichael 1967)		**Cation prop. (Carmichael 1967)**		**Cation prop. (Carmichael 1967)**		**Cation prop. (Carmichael 1967)**		**Cation prop. (Carmichael 1967)**	
Si	0.0037	0.0008	0.0082	0.0008	0.0036	0.0008	0.0032	0.0008	0.0029	0.0008
Ti	0.0039	0.9703	0.0604	0.9703	0.0069	0.9703	0.0043	0.9703	0.0154	0.9703
Al	0.0181	0.0000	0.1177	0.0000	0.0201	0.0000	0.0151	0.0000	0.0576	0.0000
Fe+3	1.9661	0.0568	1.7437	0.0568	1.9573	0.0568	1.9681	0.0568	1.9043	0.0568
Fe+2	1.0040	0.8890	1.0511	0.8890	1.0090	0.8890	1.0066	0.8890	1.0136	0.8890
Mn	0.0012	0.0805	0.0110	0.0805	0.0014	0.0805	0.0007	0.0805	0.0020	0.0805
Mg	0.0009	0.0002	0.0027	0.0002	0.0000	0.0002	0.0000	0.0002	0.0003	0.0002
Ca	0.0002	0.0003	0.0007	0.0003	0.0001	0.0003	0.0000	0.0003	0.0000	0.0003
Na	0.0000	0.0000	0.0000	0.0000	0.0000	0.0000	0.0000	0.0000	0.0000	0.0000
K	0.0000	0.0000	0.0000	0.0000	0.0000	0.0000	0.0000	0.0000	0.0000	0.0000
Cr	0.0000	0.0000	0.0000	0.0000	0.0003	0.0000	0.0003	0.0000	0.0001	0.0000
Ba	0.0000	0.0000	0.0000	0.0000	0.0000	0.0000	0.0000	0.0000	0.0000	0.0000
Zn	0.0012	0.0012	0.0029	0.0012	0.0000	0.0012	0.0000	0.0012	0.0023	0.0012
V	0.0004	0.0008	0.0013	0.0008	0.0012	0.0008	0.0014	0.0008	0.0015	0.0008
Ni	0.0004	0.0002	0.0004	0.0002	0.0000	0.0002	0.0006	0.0002	0.0000	0.0002
Nb	0.0000	0.0000	0.0000	0.0000	0.0000	0.0000	0.0000	0.0000	0.0000	0.0000
Total:	3.0001	2.0001	3.0001	2.0001	3.0000	2.0001	3.0002	2.0001	3.0000	2.0001
Calc. Methods:	**Mol % Usp**	**Mol % Ilm**	**Mol % Usp**	**Mol % Ilm**	**Mol % Usp**	**Mol % Ilm**	**Mol % Usp**	**Mol % Ilm**	**Mol % Usp**	**Mol % Ilm**
Carmichael (1967)	0.76%	97.11%	6.86%	97.11%	1.06%	97.11%	0.74%	97.11%	1.82%	97.11%
Anderson (1968)	0.33%	96.94%	5.78%	96.94%	0.63%	96.94%	0.40%	96.94%	1.47%	96.94%
Lindsley & Spencer (1982)	0.39%	96.94%	6.34%	96.94%	0.70%	96.94%	0.43%	96.94%	1.57%	96.94%
Stormer (1983)	0.40%	97.03%	6.78%	97.03%	0.71%	97.03%	0.43%	97.03%	1.63%	97.03%
Geothermometer by:										
X'Usp & X'Ilm from:	**Temp (°C)**		**Temp (°C)**		**Temp (°C)**		**Temp (°C)**		**Temp (°C)**	
Carmichael (1967)	355		488		372		354		401	
Anderson (1968)	320		479		349		328		392	
Lindsley & Spencer (1982)	328		486		354		331		396	
Stormer (1983)	327		489		353		330		396	
Average:	332		486		357		336		397	
Geothermobarometer by:										
X'Usp & X'Ilm from:	**Temp (°C)**	**log10 fO2**	**Temp (°C)**	**log10 fO2**	**Temp (°C)**	**log10 fO2**	**Temp (°C)**	**log10 fO2**	**Temp (°C)**	**log10 fO2**
Carmichael (1967)	475	-24.74	547	-23.19	486	-24.49	475	-24.76	505	-24.09
Anderson (1968)	452	-25.01	547	-22.92	473	-24.51	458	-24.87	502	-23.87
Lindsley & Spencer (1982)	458	-24.88	550	-22.86	477	-24.43	460	-24.81	504	-23.82
Stormer (1983)	456	-25.07	549	-23.02	475	-24.62	459	-25.00	503	-24.00
Average:	460	-25	549	-23	478	-25	463	-25	504	-24
Geothermobarometer by:										
X'Usp & X'Ilm from:	**Temp (°C)**	**log10 fO2**	**Temp (°C)**	**log10 fO2**	**Temp (°C)**	**log10 fO2**	**Temp (°C)**	**log10 fO2**	**Temp (°C)**	**log10 fO2**
Carmichael (1967)	472		558		484		471		506	
Anderson (1968)	445	-25.05	557	-22.53	469	-24.46	452	-24.88	502	-23.70
Lindsley & Spencer (1982)	452	-24.89	561	-22.45	473	-24.37	455	-24.81	505	-23.64
Stormer (1983)	450	-25.10	560	-22.61	471	-24.57	453	-25.02	504	-23.82
Average:	455	-25	559	-23	474	-24	458	-25	504	-24
Average for each pair	416	-25	531	-23	436	-24	419	-25	468	-24
Method Averages										
Powell & Powell (1977)										
Spencer & Lindsley (1981)										
Andersen & Lindsley (1985)										
Average for all pairs for grain										

Table G-4. Magnetite-Ilmenite Grain 3

Sample #	WYL-10-61-190.3 Mag3-Ilm3	WYL-10-61-190.3 Mag3-Ilm3	WYL-10-61-190.3 Mag3-Ilm3	WYL-10-61-190.3 Mag3-Ilm3	WYL-10-61-190.3 Mag3-Ilm3	WYL-10-61-190.3 Mag3-Ilm3	WYL-10-61-190.3 Mag3-Ilm3	WYL-10-61-190.3 Mag3-Ilm3	WYL-10-61-190.3 Mag3-Ilm3	WYL-10-61-190.3 Mag3-Ilm3	WYL-10-61-190.3 Mag3-Ilm3	WYL-10-61-190.3 Mag3-Ilm3	WYL-10-61-190.3 Mag3-Ilm3	WYL-10-61-190.3 Mag3-Ilm3	WYL-10-61-190.3 Mag3-Ilm3	WYL-10-61-190.3 Mag3-Ilm3
Line	46	39	47	39	48	39	49	39	50	39	51	39	53	39	46	40
Wt% Oxides	**Magnetite**	**Ilmenite**	**Magnetite**	**Ilmenite**	**Magnetite**	**Ilmenite**	**Magnetite**	**Ilmenite**	**Magnetite**	**Ilmenite**	**Magnetite**	**Ilmenite**	**Magnetite**	**Ilmenite**	**Magnetite**	**Ilmenite**
SiO2	3.34	0.01	0.10	0.01	0.09	0.01	0.08	0.01	0.09	0.01	0.10	0.01	0.11	0.01	3.34	0.01
TiO2	0.25	49.97	2.96	49.97	0.49	49.97	0.80	49.97	0.41	49.97	0.23	49.97	0.51	49.97	0.25	50.00
Al2O3	2.47	0.02	1.64	0.02	0.32	0.02	0.29	0.02	1.32	0.02	0.33	0.02	0.35	0.02	2.47	0.00
Fe2O3(T)																
FeO(T)	84.24	44.84	89.13	44.84	93.13	44.84	92.86	44.84	92.46	44.84	93.29	44.84	92.86	44.84	84.24	45.06
MnO	0.05	3.86	0.59	3.86	0.03	3.86	0.05	3.86	0.07	3.86	0.03	3.86	0.07	3.86	0.05	3.78
MgO	0.40	0.01	0.00	0.01	0.00	0.01	0.00	0.01	0.01	0.01	0.00	0.01	0.01	0.01	0.40	0.01
CaO	0.05	0.00	0.00	0.00	0.00	0.00	0.00	0.00	0.00	0.00	0.00	0.00	0.00	0.00	0.05	0.00
Na2O																
K2O																
Cr2O3	0.00	0.00	0.00	0.00	0.01	0.00	0.00	0.00	0.01	0.00	0.01	0.00	0.01	0.00	0.00	0.00
BaO																
ZnO	0.01	0.03	0.06	0.03	0.00	0.03	0.03	0.03	0.00	0.03	0.03	0.03	0.03	0.03	0.01	0.04
V2O3	0.06	0.05	0.04	0.05	0.03	0.05	0.04	0.05	0.05	0.05	0.04	0.05	0.04	0.05	0.06	0.06
NiO	0.03	0.00	0.00	0.00	0.00	0.00	0.01	0.00	0.00	0.00	0.00	0.00	0.03	0.00	0.03	0.00
Nb2O3																
Sum:	90.917893	98.78563	94.529336	98.78563	94.115266	98.78563	94.192038	98.78563	94.427703	98.78563	94.049196	98.78563	94.027638	98.78563	90.917893	98.97075
Carmichael (1967)	**Recalculated Iron and Total**		**Recalculated Iron and Total**		**Recalculated Iron and Total**		**Recalculated Iron and Total**		**Recalculated Iron and Total**		**Recalculated Iron and Total**		**Recalculated Iron and Total**		**Recalculated Iron and Total**	
Fe2O3 wt. %	55.5	4.3	61.5	4.3	68.0	4.3	67.5	4.3	67.2	4.3	68.5	4.3	67.8	4.3	55.5	4.4
FeO wt. %	34.3	41.0	33.8	41.0	31.9	41.0	32.1	41.0	32.0	41.0	31.7	41.0	31.8	41.0	34.3	41.1
Total:	96.5	99.2	100.7	99.2	100.9	99.2	101.0	99.2	101.2	99.2	100.9	99.2	100.8	99.2	96.5	99.4
	Ulvöspinel	**Ilmenite**	**Ulvöspinel**	**Ilmenite**	**Ulvöspinel**	**Ilmenite**	**Ulvöspinel**	**Ilmenite**	**Ulvöspinel**	**Ilmenite**	**Ulvöspinel**	**Ilmenite**	**Ulvöspinel**	**Ilmenite**	**Ulvöspinel**	**Ilmenite**
Sum of Atomic mol proportion:	2.3206	1.5314	2.2707	1.5314	2.2877	1.5314	2.2871	1.5314	2.2699	1.5314	2.2887	1.5314	2.2897	1.5314	2.3206	1.5286
No. of Oxygen:	4	3	4	3	4	3	4	3	4	3	4	3	4	3	4	3
	Cation prop. (Carmichael 1967)		**Cation prop. (Carmichael 1967)**		**Cation prop. (Carmichael 1967)**		**Cation prop. (Carmichael 1967)**		**Cation prop. (Carmichael 1967)**		**Cation prop. (Carmichael 1967)**		**Cation prop. (Carmichael 1967)**		**Cation prop. (Carmichael 1967)**	
Si	0.1290	0.0003	0.0039	0.0003	0.0036	0.0003	0.0032	0.0003	0.0034	0.0003	0.0038	0.0003	0.0042	0.0003	0.1290	0.0003
Ti	0.0071	0.9581	0.0843	0.9581	0.0140	0.9581	0.0230	0.9581	0.0116	0.9581	0.0066	0.9581	0.0145	0.9581	0.0071	0.9569
Al	0.1126	0.0005	0.0729	0.0005	0.0145	0.0005	0.0130	0.0005	0.0588	0.0005	0.0147	0.0005	0.0158	0.0005	0.1126	0.0000
Fe+3	1.6129	0.0818	1.7496	0.0818	1.9488	0.0818	1.9331	0.0818	1.9093	0.0818	1.9630	0.0818	1.9447	0.0818	1.6129	0.0843
Fe+2	1.1083	0.8740	1.0673	0.8740	1.0166	0.8740	1.0230	0.8740	1.0120	0.8740	1.0087	0.8740	1.0148	0.8740	1.1083	0.8744
Mn	0.0017	0.0834	0.0190	0.0834	0.0011	0.0834	0.0017	0.0834	0.0022	0.0834	0.0010	0.0834	0.0024	0.0834	0.0017	0.0816
Mg	0.0233	0.0005	0.0000	0.0005	0.0000	0.0005	0.0000	0.0005	0.0008	0.0005	0.0000	0.0005	0.0003	0.0005	0.0233	0.0004
Ca	0.0022	0.0001	0.0000	0.0001	0.0000	0.0001	0.0000	0.0001	0.0000	0.0001	0.0000	0.0001	0.0000	0.0001	0.0022	0.0000
Na	0.0000	0.0000	0.0000	0.0000	0.0000	0.0000	0.0000	0.0000	0.0000	0.0000	0.0000	0.0000	0.0000	0.0000	0.0000	0.0000
K	0.0000	0.0000	0.0000	0.0000	0.0000	0.0000	0.0000	0.0000	0.0000	0.0000	0.0000	0.0000	0.0000	0.0000	0.0000	0.0000
Cr	0.0000	0.0000	0.0001	0.0000	0.0003	0.0000	0.0001	0.0000	0.0004	0.0000	0.0003	0.0000	0.0004	0.0000	0.0000	0.0001
Ba	0.0000	0.0000	0.0000	0.0000	0.0000	0.0000	0.0000	0.0000	0.0000	0.0000	0.0000	0.0000	0.0000	0.0000	0.0000	0.0000
Zn	0.0004	0.0005	0.0016	0.0005	0.0000	0.0005	0.0014	0.0005	0.0000	0.0005	0.0008	0.0005	0.0009	0.0005	0.0004	0.0008
V	0.0018	0.0010	0.0012	0.0010	0.0011	0.0010	0.0014	0.0010	0.0015	0.0010	0.0011	0.0010	0.0012	0.0010	0.0018	0.0013
Ni	0.0010	0.0000	0.0001	0.0000	0.0000	0.0000	0.0002	0.0000	0.0000	0.0000	0.0001	0.0000	0.0010	0.0000	0.0010	0.0000
Nb	0.0000	0.0000	0.0000	0.0000	0.0000	0.0000	0.0000	0.0000	0.0000	0.0000	0.0000	0.0000	0.0000	0.0000	0.0000	0.0000
Total:	3.0003	2.0000	3.0000	2.0000	3.0000	2.0000	3.0000	2.0000	3.0000	2.0000	3.0000	2.0000	3.0002	2.0000	3.0003	2.0000
Calc. Methods:	**Mol % Usp**	**Mol % Ilm**	**Mol % Usp**	**Mol % Ilm**	**Mol % Usp**	**Mol % Ilm**	**Mol % Usp**	**Mol % Ilm**	**Mol % Usp**	**Mol % Ilm**	**Mol % Usp**	**Mol % Ilm**	**Mol % Usp**	**Mol % Ilm**	**Mol % Usp**	**Mol % Ilm**
Carmichael (1967)	13.61%	95.84%	8.81%	95.84%	1.76%	95.84%	2.62%	95.84%	1.50%	95.84%	1.05%	95.84%	1.87%	95.84%	13.61%	95.72%
Anderson (1968)	0.69%	95.55%	7.76%	95.55%	1.36%	95.55%	2.23%	95.55%	1.07%	95.55%	0.62%	95.55%	1.34%	95.55%	0.69%	95.43%
Lindsley & Spencer (1982)	0.78%	95.55%	8.71%	95.55%	1.41%	95.55%	2.32%	95.55%	1.18%	95.55%	0.67%	95.55%	1.46%	95.55%	0.78%	95.43%
Stormer (1983)	0.91%	95.72%	8.96%	95.72%	1.43%	95.72%	2.33%	95.72%	1.23%	95.72%	0.67%	95.72%	1.48%	95.72%	0.91%	95.60%
Geothermometer by:	**Powell & Powell (1977)**															
XUsp & XIlm from:	**Temp (°C)**		**Temp (°C)**		**Temp (°C)**		**Temp (°C)**		**Temp (°C)**		**Temp (°C)**		**Temp (°C)**		**Temp (°C)**	
Carmichael (1967)	579		537		421		446		412		391		425		581	
Anderson (1968)	373		532		410		440		396		367		409		374	
Lindsley & Spencer (1982)	379		542		412		442		402		371		414		380	
Stormer (1983)	385		541		410		440		402		369		412		387	
Average:	429		538		413		442		403		375		415		431	
Geothermobarometer by:	**Spencer & Lindsley (1981)**															
XUsp & XIlm from:	**Temp (°C)**	**log10 fO2**	**Temp (°C)**	**log10 fO2**	**Temp (°C)**	**log10 fO2**	**Temp (°C)**	**log10 fO2**	**Temp (°C)**	**log10 fO2**	**Temp (°C)**	**log10 fO2**	**Temp (°C)**	**log10 fO2**	**Temp (°C)**	**log10 fO2**
Carmichael (1967)	604	-20.42	590	-20.69	532	-21.81	547	-21.52	526	-21.93	513	-22.20	534	-21.77	608	-20.23
Anderson (1968)	503	-22.10	592	-20.35	528	-21.59	546	-21.22	519	-21.76	499	-22.18	527	-21.60	505	-21.94
Lindsley & Spencer (1982)	507	-22.01	596	-20.27	529	-21.56	548	-21.20	522	-21.70	501	-22.13	530	-21.54	509	-21.85
Stormer (1983)	510	-22.13	593	-20.50	526	-21.80	545	-21.44	521	-21.91	499	-22.36	527	-21.77	512	-21.95
Average:	531		593		529		546		522		503		530		533	
		-22		-20		-22		-21		-22		-22		-22		-21
Geothermobarometer by:	**Andersen & Lindsley (1985)**															
XUsp & XIlm from:	**Temp (°C)**	**log10 fO2**	**Temp (°C)**	**log10 fO2**	**Temp (°C)**	**log10 fO2**	**Temp (°C)**	**log10 fO2**	**Temp (°C)**	**log10 fO2**	**Temp (°C)**	**log10 fO2**	**Temp (°C)**	**log10 fO2**	**Temp (°C)**	**log10 fO2**
Carmichael (1967)	624		606		536		553		529		514		539		628	
Anderson (1968)	503	-21.91	608	-19.87	531	-21.33	553	-20.90	521	-21.53	498	-22.00	530	-21.34	505	-21.74
Lindsley & Spencer (1982)	507	-21.81	613	-19.78	533	-21.30	554	-20.88	525	-21.45	501	-21.94	534	-21.27	509	-21.65
Stormer (1983)	511	-21.93	610	-20.01	530	-21.54	551	-21.12	523	-21.67	498	-22.19	531	-21.51	513	-21.74
Average:	536		609		532		553		525		503		534		539	
		-22		-20		-21		-21		-22		-22		-21		-22
Average for each pair	499		380		491		514		483		460		493		501	
Average for each pair		-21.93		-20		-22		-21		-22		-22		-22		-22
Method Averages					Ranges		Ti-poor magnetite				Ranges		Ti-rich magnetite			
Powell & Powell (1977)		426			346 - 901		Powell & Powell (1977)		426		346 - 586		Powell & Powell (1977)		811	
Spencer & Lindsley (1981)		531	-22.01		469 - 822	-24.8 to -15.0	Spencer & Lindsley (1981)		531	-22.05	469 - 613	-25.0 to -19.8	Spencer & Lindsley (1981)		706	-18.10
Andersen & Lindsley (1985)		535	-21.76		465 - 829	-25.0 to -15.2	Andersen & Lindsley (1985)		530	-21.76	465 - 634	-25.0 to -19.3	Andersen & Lindsley (1985)		730	-17.30
									496	-21.91					749	-17.70
Average for all pairs	497	-22														

Sample #	WYL-10-61-190.3 Mag3-Ilm3	WYL-10-61-190.3 Mag3-Ilm3	WYL-10-61-190.3 Mag3-Ilm3	WYL-10-61-190.3 Mag3-Ilm3	WYL-10-61-190.3 Mag3-Ilm3	WYL-10-61-190.3 Mag3-Ilm3	WYL-10-61-190.3 Mag3-Ilm3	WYL-10-61-190.3 Mag3-Ilm3	WYL-10-61-190.3 Mag3-Ilm3	WYL-10-61-190.3 Mag3-Ilm3	WYL-10-61-190.3 Mag3-Ilm3	WYL-10-61-190.3 Mag3-Ilm3	WYL-10-61-190.3 Mag3-Ilm3	WYL-10-61-190.3 Mag3-Ilm3	WYL-10-61-190.3 Mag3-Ilm3	WYL-10-61-190.3 Mag3-Ilm3
Line	47	40	48	40	49	40	50	40	51	40	53	40	46	41	47	41
Wt% Oxides	**Magnetite**	**Ilmenite**	**Magnetite**	**Ilmenite**	**Magnetite**	**Ilmenite**	**Magnetite**	**Ilmenite**	**Magnetite**	**Ilmenite**	**Magnetite**	**Ilmenite**	**Magnetite**	**Ilmenite**	**Magnetite**	**Ilmenite**
SiO2	0.10	0.01	0.09	0.01	0.08	0.01	0.09	0.01	0.10	0.01	0.11	0.01	3.34	0.00	0.10	0.00
TiO2	2.96	50.00	0.49	50.00	0.80	50.00	0.41	50.00	0.23	50.00	0.51	50.00	0.25	49.79	2.96	49.79
Al2O3	1.64	0.00	0.32	0.00	0.29	0.00	1.32	0.00	0.33	0.00	0.35	0.00	2.47	0.01	1.64	0.01
Fe2O3(T)																
FeO(T)	89.13	45.06	93.13	45.06	92.86	45.06	92.46	45.06	93.29	45.06	92.86	45.06	84.24	44.81	89.13	44.81
MnO	0.59	3.78	0.03	3.78	0.05	3.78	0.07	3.78	0.03	3.78	0.07	3.78	0.05	4.04	0.59	4.04
MgO	0.00	0.01	0.00	0.01	0.00	0.01	0.01	0.01	0.00	0.01	0.01	0.01	0.40	0.00	0.00	0.00
CaO	0.00	0.00	0.00	0.00	0.00	0.00	0.00	0.00	0.00	0.00	0.00	0.00	0.05	0.00	0.00	0.00
Na2O																
K2O																
Cr2O3	0.00	0.00	0.01	0.00	0.00	0.00	0.01	0.00	0.01	0.00	0.01	0.00	0.00	0.00	0.00	0.00
BaO																
ZnO	0.06	0.04	0.00	0.04	0.03	0.04	0.00	0.04	0.03	0.04	0.03	0.04	0.01	0.00	0.06	0.00
V2O3	0.04	0.06	0.03	0.06	0.04	0.06	0.05	0.06	0.04	0.06	0.04	0.06	0.06	0.06	0.04	0.06
NiO	0.00	0.00	0.00	0.00	0.01	0.00	0.00	0.00	0.00	0.00	0.03	0.00	0.03	0.00	0.00	0.00
Nb2O3																
Sum:	94.529336	98.97075	94.115266	98.97075	94.192038	98.97075	94.427703	98.97075	94.049196	98.97075	94.027638	98.97075	90.917893	98.713918	94.529336	98.713918
Carmichael (1967)	**Recalculated Iron and Total**		**Recalculated Iron and Total**		**Recalculated Iron and Total**		**Recalculated Iron and Total**		**Recalculated Iron and Total**		**Recalculated Iron and Total**		**Recalculated Iron and Total**		**Recalculated Iron and Total**	
Fe2O3 wt. %	61.5	4.4	68.0	4.4	67.5	4.4	67.2	4.4	68.5	4.4	67.8	4.4	55.5	4.6	61.5	4.6
FeO wt. %	33.8	41.1	31.9	41.1	32.1	41.1	32.0	41.1	31.7	41.1	31.8	41.1	34.3	40.7	33.8	40.7
Total:	100.7	99.4	100.9	99.4	101.0	99.4	101.2	99.4	100.9	99.4	100.8	99.4	96.5	99.2	100.7	99.2
	Ulvöspinel	**Ilmenite**	**Ulvöspinel**	**Ilmenite**	**Ulvöspinel**	**Ilmenite**	**Ulvöspinel**	**Ilmenite**	**Ulvöspinel**	**Ilmenite**	**Ulvöspinel**	**Ilmenite**	**Ulvöspinel**	**Ilmenite**	**Ulvöspinel**	**Ilmenite**
Sum of Atomic mol proportion:	2.2707	1.5286	2.2877	1.5286	2.2871	1.5286	2.2699	1.5286	2.2887	1.5286	2.2897	1.5286	2.3206	1.5324	2.2707	1.5324
No. of Oxygen:	4	3	4	3	4	3	4	3	4	3	4	3	4	3	4	3
	Cation prop. (Carmichael 1967)		**Cation prop. (Carmichael 1967)**		**Cation prop. (Carmichael 1967)**		**Cation prop. (Carmichael 1967)**		**Cation prop. (Carmichael 1967)**		**Cation prop. (Carmichael 1967)**		**Cation prop. (Carmichael 1967)**		**Cation prop. (Carmichael 1967)**	
Si	0.0039	0.0003	0.0036	0.0003	0.0032	0.0003	0.0034	0.0003	0.0038	0.0003	0.0042	0.0003	0.1290	0.0000	0.0039	0.0000
Ti	0.0843	0.9569	0.0140	0.9569	0.0230	0.9569	0.0116	0.9569	0.0066	0.9569	0.0145	0.9569	0.0071	0.9552	0.0843	0.9552
Al	0.0729	0.0000	0.0145	0.0000	0.0130	0.0000	0.0588	0.0000	0.0147	0.0000	0.0158	0.0000	0.1126	0.0003	0.0729	0.0003
Fe+3	1.7496	0.0843	1.9488	0.0843	1.9331	0.0843	1.9093	0.0843	1.9630	0.0843	1.9447	0.0843	1.6129	0.0880	1.7496	0.0880
Fe+2	1.0675	0.8744	1.0166	0.8744	1.0230	0.8744	1.0120	0.8744	1.0087	0.8744	1.0148	0.8744	1.1083	0.8678	1.0675	0.8678
Mn	0.0190	0.0816	0.0011	0.0816	0.0017	0.0816	0.0022	0.0816	0.0010	0.0816	0.0024	0.0816	0.0017	0.0873	0.0190	0.0873
Mg	0.0000	0.0004	0.0000	0.0004	0.0000	0.0004	0.0008	0.0004	0.0000	0.0004	0.0003	0.0004	0.0233	0.0000	0.0000	0.0000
Ca	0.0000	0.0000	0.0000	0.0000	0.0000	0.0000	0.0000	0.0000	0.0000	0.0000	0.0000	0.0000	0.0022	0.0001	0.0000	0.0001
Na	0.0000	0.0000	0.0000	0.0000	0.0000	0.0000	0.0000	0.0000	0.0000	0.0000	0.0000	0.0000	0.0000	0.0000	0.0000	0.0000
K	0.0000	0.0000	0.0000	0.0000	0.0000	0.0000	0.0000	0.0000	0.0000	0.0000	0.0000	0.0000	0.0000	0.0000	0.0000	0.0000
Cr	0.0001	0.0001	0.0003	0.0001	0.0001	0.0001	0.0004	0.0001	0.0003	0.0001	0.0004	0.0001	0.0000	0.0000	0.0001	0.0000
Ba	0.0000	0.0000	0.0000	0.0000	0.0000	0.0000	0.0000	0.0000	0.0000	0.0000	0.0000	0.0000	0.0000	0.0000	0.0000	0.0000
Zn	0.0016	0.0008	0.0000	0.0008	0.0014	0.0008	0.0000	0.0008	0.0008	0.0008	0.0009	0.0008	0.0004	0.0000	0.0016	0.0000
V	0.0012	0.0013	0.0011	0.0013	0.0014	0.0013	0.0015	0.0013	0.0011	0.0013	0.0012	0.0013	0.0018	0.0012	0.0012	0.0012
Ni	0.0001	0.0000	0.0000	0.0000	0.0002	0.0000	0.0000	0.0000	0.0001	0.0000	0.0010	0.0000	0.0010	0.0000	0.0001	0.0000
Nb	0.0000	0.0000	0.0000	0.0000	0.0000	0.0000	0.0000	0.0000	0.0000	0.0000	0.0000	0.0000	0.0000	0.0000	0.0000	0.0000
Total:	3.0000	2.0000	3.0000	2.0000	3.0000	2.0000	3.0000	2.0000	3.0000	2.0000	3.0002	2.0000	3.0003	2.0000	3.0000	2.0000
Calc. Methods:	**Mol % Usp**	**Mol % Ilm**	**Mol % Usp**	**Mol % Ilm**	**Mol % Usp**	**Mol % Ilm**	**Mol % Usp**	**Mol % Ilm**	**Mol % Usp**	**Mol % Ilm**	**Mol % Usp**	**Mol % Ilm**	**Mol % Usp**	**Mol % Ilm**	**Mol % Usp**	**Mol % Ilm**
Carmichael (1967)	8.81%	95.72%	1.76%	95.72%	2.62%	95.72%	1.50%	95.72%	1.05%	95.72%	1.87%	95.72%	13.61%	95.52%	8.81%	95.52%
Anderson (1968)	7.76%	95.43%	1.36%	95.43%	2.23%	95.43%	1.07%	95.43%	0.62%	95.43%	1.34%	95.43%	0.69%	95.18%	7.76%	95.18%
Lindsley & Spencer (1982)	8.71%	95.43%	1.41%	95.43%	2.32%	95.43%	1.18%	95.43%	0.67%	95.43%	1.46%	95.43%	0.78%	95.18%	8.71%	95.18%
Stormer (1983)	8.96%	95.60%	1.43%	95.60%	2.33%	95.60%	1.23%	95.60%	0.67%	95.60%	1.48%	95.60%	0.91%	95.39%	8.96%	95.39%
Geothermometer by:																
X'Usp & X'Ilm from:	**Temp (°C)**		**Temp (°C)**		**Temp (°C)**		**Temp (°C)**		**Temp (°C)**		**Temp (°C)**		**Temp (°C)**		**Temp (°C)**	
Carmichael (1967)	540		423		448		413		393		426		385		543	
Anderson (1968)	534		411		442		398		369		411		377		538	
Lindsley & Spencer (1982)	544		414		444		403		372		416		383		549	
Stormer (1983)	544		412		442		403		371		414		390		547	
Average:	540		415		444		405		376		417		434		545	
Geothermobarometer by:																
X'Usp & X'Ilm from:	**Temp (°C)**	**log10 fO2**	**Temp (°C)**	**log10 fO2**	**Temp (°C)**	**log10 fO2**	**Temp (°C)**	**log10 fO2**	**Temp (°C)**	**log10 fO2**	**Temp (°C)**	**log10 fO2**	**Temp (°C)**	**log10 fO2**	**Temp (°C)**	**log10 fO2**
Carmichael (1967)	593	-20.50	534	-21.63	549	-21.34	528	-21.75	515	-22.02	536	-21.59	613	-19.94	597	-20.23
Anderson (1968)	595	-20.19	530	-21.43	548	-21.07	521	-21.61	501	-22.02	529	-21.44	508	-21.61	600	-19.85
Lindsley & Spencer (1982)	599	-20.11	531	-21.41	550	-21.04	524	-21.54	503	-21.97	532	-21.38	513	-21.52	605	-19.77
Stormer (1983)	596	-20.32	529	-21.62	547	-21.26	523	-21.73	501	-22.18	530	-21.59	515	-21.67	601	-20.03
Average:	596		531		548		524		505		532		537		601	
		-20		-22		-21		-22		-22		-22		-21		-20
Geothermobarometer by:																
X'Usp & X'Ilm from:	**Temp (°C)**	**log10 fO2**	**Temp (°C)**	**log10 fO2**	**Temp (°C)**	**log10 fO2**	**Temp (°C)**	**log10 fO2**	**Temp (°C)**	**log10 fO2**	**Temp (°C)**	**log10 fO2**	**Temp (°C)**	**log10 fO2**	**Temp (°C)**	**log10 fO2**
Carmichael (1967)	609		539		556		532		517		541		633		614	
Anderson (1968)	611	-19.71	533	-21.17	555	-20.74	523	-21.37	500	-21.84	533	-21.18	509	-21.40	616	-19.38
Lindsley & Spencer (1982)	616	-19.62	535	-21.14	557	-20.72	527	-21.29	503	-21.78	536	-21.11	514	-21.30	622	-19.28
Stormer (1983)	613	-19.82	532	-21.35	554	-20.93	526	-21.48	501	-22.00	534	-21.32	517	-21.45	618	-19.54
Average:	612		533		555		527		505		536		543		618	
		-20		-21		-21		-21		-22		-21		-21		-19
Average for each pair	583		493		516		485		462		495		505		588	
Average for each pair		-20		-21		-21		-22		-22		-21		-21		-20
Method Averages	Ranges															
Powell & Powell (1977)	712 - 901															
Spencer & Lindsley (1981)	582 - 822	-22.6 to -15														
Andersen & Lindsley (1985)	619 - 829	-20.7 to -15.2														
Average for all pairs																

Sample #	WYL-10-61-190.3 Mag3-Ilm3	WYL-10-61-190.3 Mag3-Ilm3	WYL-10-61-190.3 Mag3-Ilm3	WYL-10-61-190.3 Mag3-Ilm3	WYL-10-61-190.3 Mag3-Ilm3	WYL-10-61-190.3 Mag3-Ilm3	WYL-10-61-190.3 Mag3-Ilm3	WYL-10-61-190.3 Mag3-Ilm3	WYL-10-61-190.3 Mag3-Ilm3	WYL-10-61-190.3 Mag3-Ilm3
Line	48	41	49	41	50	41	51	41	53	41
Wt% Oxides	**Magnetite**	**Ilmenite**	**Magnetite**	**Ilmenite**	**Magnetite**	**Ilmenite**	**Magnetite**	**Ilmenite**	**Magnetite**	**Ilmenite**
SiO2	0.09	0.00	0.08	0.00	0.09	0.00	0.10	0.00	0.11	0.00
TiO2	0.49	49.79	0.80	49.79	0.41	49.79	0.23	49.79	0.51	49.79
Al2O3	0.32	0.01	0.29	0.01	1.32	0.01	0.33	0.01	0.35	0.01
Fe2O3(T)										
FeO(T)	93.13	44.81	92.86	44.81	92.46	44.81	93.29	44.81	92.86	44.81
MnO	0.03	4.04	0.05	4.04	0.07	4.04	0.03	4.04	0.07	4.04
MgO	0.00	0.00	0.00	0.00	0.01	0.00	0.00	0.00	0.01	0.00
CaO	0.00	0.00	0.00	0.00	0.00	0.00	0.00	0.00	0.00	0.00
Na2O										
K2O										
Cr2O3	0.01	0.00	0.00	0.00	0.01	0.00	0.01	0.00	0.01	0.00
BaO										
ZnO	0.00	0.00	0.05	0.00	0.00	0.00	0.03	0.00	0.03	0.00
V2O3	0.03	0.06	0.04	0.06	0.05	0.06	0.04	0.06	0.04	0.06
NiO	0.00	0.00	0.01	0.00	0.00	0.00	0.00	0.00	0.03	0.00
Nb2O3										
Sum:	94.115266	98.713918	94.192038	98.713918	94.427703	98.713918	94.049196	98.713918	94.027638	98.713918
Carmichael (1967)	**Recalculated Iron and Total**		**Recalculated Iron and Total**		**Recalculated Iron and Total**		**Recalculated Iron and Total**		**Recalculated Iron and Total**	
Fe2O3 wt. %	68.0	4.6	67.5	4.6	67.2	4.6	68.5	4.6	67.8	4.6
FeO wt. %	31.9	40.7	32.1	40.7	32.0	40.7	31.7	40.7	31.8	40.7
Total:	100.9	99.2	101.0	99.2	101.2	99.2	100.9	99.2	100.8	99.2
	Ulvöspinel	**Ilmenite**	**Ulvöspinel**	**Ilmenite**	**Ulvöspinel**	**Ilmenite**	**Ulvöspinel**	**Ilmenite**	**Ulvöspinel**	**Ilmenite**
Sum of Atomic mol proportion:	2.2877	1.5324	2.2871	1.5324	2.2699	1.5324	2.2887	1.5324	2.2897	1.5324
No. of Oxygen:	4	3	4	3	4	3	4	3	4	3
	Cation prop. (Carmichael 1967)		**Cation prop. (Carmichael 1967)**		**Cation prop. (Carmichael 1967)**		**Cation prop. (Carmichael 1967)**		**Cation prop. (Carmichael 1967)**	
Si	0.0036	0.0000	0.0032	0.0000	0.0034	0.0000	0.0038	0.0000	0.0042	0.0000
Ti	0.0140	0.9552	0.0230	0.9552	0.0116	0.9552	0.0066	0.9552	0.0145	0.9552
Al	0.0145	0.0003	0.0130	0.0003	0.0588	0.0003	0.0147	0.0003	0.0158	0.0003
Fe+3	1.9488	0.0880	1.9331	0.0880	1.9093	0.0880	1.9630	0.0880	1.9447	0.0880
Fe+2	1.0166	0.8678	1.0230	0.8678	1.0120	0.8678	1.0087	0.8678	1.0148	0.8678
Mn	0.0011	0.0873	0.0017	0.0873	0.0022	0.0873	0.0010	0.0873	0.0024	0.0873
Mg	0.0000	0.0000	0.0000	0.0000	0.0008	0.0000	0.0000	0.0000	0.0003	0.0000
Ca	0.0000	0.0001	0.0000	0.0001	0.0000	0.0001	0.0000	0.0001	0.0000	0.0001
Na	0.0000	0.0000	0.0000	0.0000	0.0000	0.0000	0.0000	0.0000	0.0000	0.0000
K	0.0000	0.0000	0.0000	0.0000	0.0000	0.0000	0.0000	0.0000	0.0000	0.0000
Cr	0.0003	0.0000	0.0001	0.0000	0.0004	0.0000	0.0003	0.0000	0.0004	0.0000
Ba	0.0000	0.0000	0.0000	0.0000	0.0000	0.0000	0.0000	0.0000	0.0000	0.0000
Zn	0.0000	0.0000	0.0014	0.0000	0.0000	0.0000	0.0008	0.0000	0.0009	0.0000
V	0.0011	0.0012	0.0014	0.0012	0.0015	0.0012	0.0011	0.0012	0.0012	0.0012
Ni	0.0000	0.0000	0.0002	0.0000	0.0000	0.0000	0.0001	0.0000	0.0010	0.0000
Nb	0.0000	0.0000	0.0000	0.0000	0.0000	0.0000	0.0000	0.0000	0.0000	0.0000
Total:	3.0000	2.0000	3.0000	2.0000	3.0000	2.0000	3.0000	2.0000	3.0002	2.0000
Calc. Methods:	**Mol % Usp**	**Mol % Ilm**	**Mol % Usp**	**Mol % Ilm**	**Mol % Usp**	**Mol % Ilm**	**Mol % Usp**	**Mol % Ilm**	**Mol % Usp**	**Mol % Ilm**
Carmichael (1967)	1.76%	95.52%	2.62%	95.52%	1.50%	95.52%	1.05%	95.52%	1.87%	95.52%
Anderson (1968)	1.36%	95.18%	2.23%	95.18%	1.07%	95.18%	0.62%	95.18%	1.34%	95.18%
Lindsley & Spencer (1982)	1.41%	95.18%	2.32%	95.18%	1.18%	95.18%	0.67%	95.18%	1.46%	95.18%
Stormer (1983)	1.43%	95.39%	2.33%	95.39%	1.23%	95.39%	0.67%	95.39%	1.48%	95.39%
Geothermometer by:										
X'Usp & X'Ilm from:	**Temp (°C)**		**Temp (°C)**		**Temp (°C)**		**Temp (°C)**		**Temp (°C)**	
Carmichael (1967)	426		451		416		395		429	
Anderson (1968)	415		445		401		372		414	
Lindsley & Spencer (1982)	417		448		407		375		419	
Stormer (1983)	415		445		406		373		417	
Average:	418		447		407		379		420	
Geothermobarometer by:										
X'Usp & X'Ilm from:	**Temp (°C)**	**log10 fO2**	**Temp (°C)**	**log10 fO2**	**Temp (°C)**	**log10 fO2**	**Temp (°C)**	**log10 fO2**	**Temp (°C)**	**log10 fO2**
Carmichael (1967)	538	-21.36	553	-21.07	532	-21.48	518	-21.75	540	-21.32
Anderson (1968)	534	-21.10	553	-20.74	525	-21.28	504	-21.69	533	-21.11
Lindsley & Spencer (1982)	535	-21.08	554	-20.71	528	-21.21	507	-21.64	536	-21.05
Stormer (1983)	532	-21.34	551	-20.98	527	-21.45	504	-21.90	533	-21.31
Average:	535		553		528		509		536	
		-21		-21		-21		-22		-21
Geothermobarometer by:										
X'Usp & X'Ilm from:	**Temp (°C)**	**log10 fO2**	**Temp (°C)**	**log10 fO2**	**Temp (°C)**	**log10 fO2**	**Temp (°C)**	**log10 fO2**	**Temp (°C)**	**log10 fO2**
Carmichael (1967)	543		560		536		520		545	
Anderson (1968)	538	-20.83	560	-20.41	528	-21.03	504	-21.50	537	-20.84
Lindsley & Spencer (1982)	540	-20.80	562	-20.38	532	-20.94	508	-21.43	541	-20.77
Stormer (1983)	536	-21.06	558	-20.65	530	-21.19	504	-21.71	538	-21.04
Average:	539		560		531		509		540	
		-21		-20		-21		-22		-21
Average for each pair	497		520		489		466		499	
Average for each pair		-21		-21		-21		-22		-21
Method Averages										
Powell & Powell (1977)										
Spencer & Lindsley (1981)										
Andersen & Lindsley(1985)										
Average for all pairs										

Sample #	WYL-10-61-190.3 Mag3-Ilm3	WYL-10-61-190.3 Mag3-Ilm3	WYL-10-61-190.3 Mag3-Ilm3	WYL-10-61-190.3 Mag3-Ilm3	WYL-10-61-190.3 Mag3-Ilm3	WYL-10-61-190.3 Mag3-Ilm3	WYL-10-61-190.3 Mag3-Ilm3	WYL-10-61-190.3 Mag3-Ilm3	WYL-10-61-190.3 Mag3-Ilm3	WYL-10-61-190.3 Mag3-Ilm3	WYL-10-61-190.3 Mag3-Ilm3	WYL-10-61-190.3 Mag3-Ilm3	WYL-10-61-190.3 Mag3-Ilm3	WYL-10-61-190.3 Mag3-Ilm3	WYL-10-61-190.3 Mag3-Ilm3	WYL-10-61-190.3 Mag3-Ilm3
Line	46	42	47	42	48	42	49	42	50	42	51	42	53	42	46	43
Wt% Oxides	**Magnetite**	**Ilmenite**	**Magnetite**	**Ilmenite**	**Magnetite**	**Ilmenite**	**Magnetite**	**Ilmenite**	**Magnetite**	**Ilmenite**	**Magnetite**	**Ilmenite**	**Magnetite**	**Ilmenite**	**Magnetite**	**Ilmenite**
SiO2	3.34	0.02	0.10	0.02	0.09	0.02	0.08	0.02	0.09	0.02	0.10	0.02	0.11	0.02	3.34	0.02
TiO2	0.25	49.71	2.96	49.71	0.49	49.71	0.80	49.71	0.41	49.71	0.23	49.71	0.51	49.71	0.25	50.69
Al2O3	2.47	0.00	1.64	0.00	0.32	0.00	0.29	0.00	1.32	0.00	0.33	0.00	0.35	0.00	2.47	0.00
Fe2O3(T)																
FeO(T)	84.24	44.88	89.13	44.88	93.13	44.88	92.86	44.88	92.46	44.88	93.29	44.88	92.86	44.88	84.24	44.68
MnO	0.05	3.91	0.59	3.91	0.03	3.91	0.05	3.91	0.07	3.91	0.03	3.91	0.07	3.91	0.05	4.04
MgO	0.40	0.00	0.00	0.00	0.00	0.00	0.00	0.00	0.01	0.00	0.00	0.00	0.01	0.00	0.40	0.02
CaO	0.05	0.01	0.00	0.01	0.00	0.01	0.00	0.01	0.00	0.01	0.00	0.01	0.00	0.01	0.05	0.00
Na2O																
K2O																
Cr2O3	0.00	0.00	0.00	0.00	0.01	0.00	0.00	0.00	0.01	0.00	0.01	0.00	0.01	0.00	0.00	0.00
BaO																
ZnO	0.01	0.04	0.06	0.04	0.00	0.04	0.05	0.04	0.00	0.04	0.03	0.04	0.03	0.04	0.01	0.03
V2O3	0.06	0.06	0.04	0.06	0.03	0.06	0.04	0.06	0.05	0.06	0.04	0.06	0.04	0.06	0.06	0.03
NiO	0.03	0.00	0.00	0.00	0.00	0.00	0.01	0.00	0.00	0.00	0.00	0.00	0.03	0.00	0.03	0.01
Nb2O3																
Sum:	90.917893	98.63461	94.529336	98.63461	94.115266	98.63461	94.192038	98.63461	94.427703	98.63461	94.049196	98.63461	94.027638	98.63461	90.917893	99.520994
Carmichael (1967)	**Recalculated Iron and Total**		**Recalculated Iron and Total**		**Recalculated Iron and Total**		**Recalculated Iron and Total**		**Recalculated Iron and Total**		**Recalculated Iron and Total**		**Recalculated Iron and Total**		**Recalculated Iron and Total**	
Fe2O3 wt %	55.5	4.6	61.5	4.6	68.0	4.6	67.5	4.6	67.2	4.6	68.5	4.6	67.8	4.6	55.5	3.6
FeO wt %	34.3	40.7	33.8	40.7	31.9	40.7	32.1	40.7	32.0	40.7	31.7	40.7	31.8	40.7	34.3	41.5
Total:	96.5	99.1	100.7	99.1	100.9	99.1	101.0	99.1	101.2	99.1	100.9	99.1	100.8	99.1	96.5	99.9
	Ulvöspinel	**Ilmenite**	**Ulvöspinel**	**Ilmenite**	**Ulvöspinel**	**Ilmenite**	**Ulvöspinel**	**Ilmenite**	**Ulvöspinel**	**Ilmenite**	**Ulvöspinel**	**Ilmenite**	**Ulvöspinel**	**Ilmenite**	**Ulvöspinel**	**Ilmenite**
Sum of Atomic mol proportion:	2.3206	1.5336	2.2707	1.5336	2.2877	1.5336	2.2871	1.5336	2.2699	1.5336	2.2887	1.5336	2.2897	1.5336	2.3206	1.5206
No. of Oxygen:	4	3	4	3	4	3	4	3	4	3	4	3	4	3	4	3
	Cation prop. (Carmichael 1967)		**Cation prop. (Carmichael 1967)**		**Cation prop. (Carmichael 1967)**		**Cation prop. (Carmichael 1967)**		**Cation prop. (Carmichael 1967)**		**Cation prop. (Carmichael 1967)**		**Cation prop. (Carmichael 1967)**		**Cation prop. (Carmichael 1967)**	
Si	0.1290	0.0005	0.0039	0.0005	0.0036	0.0005	0.0032	0.0005	0.0034	0.0005	0.0038	0.0005	0.0042	0.0005	0.1290	0.0005
Ti	0.0071	0.9546	0.0843	0.9546	0.0140	0.9546	0.0230	0.9546	0.0116	0.9546	0.0066	0.9546	0.0145	0.9546	0.0071	0.9652
Al	0.1126	0.0000	0.0729	0.0000	0.0145	0.0000	0.0130	0.0000	0.0588	0.0000	0.0147	0.0000	0.0158	0.0000	0.1126	0.0000
Fe+3	1.6129	0.0885	1.7496	0.0885	1.9488	0.0885	1.9331	0.0885	1.9093	0.0885	1.9630	0.0885	1.9447	0.0885	1.6129	0.0679
Fe+2	1.1083	0.8695	1.0675	0.8695	1.0166	0.8695	1.0230	0.8695	1.0120	0.8695	1.0087	0.8695	1.0148	0.8695	1.1083	0.8778
Mn	0.0017	0.0846	0.0190	0.0846	0.0011	0.0846	0.0017	0.0846	0.0022	0.0846	0.0010	0.0846	0.0024	0.0846	0.0017	0.0865
Mg	0.0233	0.0000	0.0000	0.0000	0.0000	0.0000	0.0000	0.0000	0.0008	0.0000	0.0000	0.0000	0.0003	0.0000	0.0233	0.0009
Ca	0.0022	0.0002	0.0000	0.0002	0.0000	0.0002	0.0000	0.0002	0.0000	0.0002	0.0000	0.0002	0.0000	0.0002	0.0022	0.0000
Na	0.0000	0.0000	0.0000	0.0000	0.0000	0.0000	0.0000	0.0000	0.0000	0.0000	0.0000	0.0000	0.0000	0.0000	0.0000	0.0000
K	0.0000	0.0000	0.0000	0.0000	0.0000	0.0000	0.0000	0.0000	0.0000	0.0000	0.0000	0.0000	0.0000	0.0000	0.0000	0.0000
Cr	0.0000	0.0000	0.0001	0.0000	0.0003	0.0000	0.0001	0.0000	0.0004	0.0000	0.0003	0.0000	0.0004	0.0000	0.0000	0.0000
Ba	0.0000	0.0000	0.0000	0.0000	0.0000	0.0000	0.0000	0.0000	0.0000	0.0000	0.0000	0.0000	0.0000	0.0000	0.0000	0.0000
Zn	0.0004	0.0007	0.0016	0.0007	0.0000	0.0007	0.0014	0.0007	0.0000	0.0007	0.0008	0.0007	0.0009	0.0007	0.0004	0.0005
V	0.0018	0.0013	0.0012	0.0013	0.0011	0.0013	0.0014	0.0013	0.0015	0.0013	0.0011	0.0013	0.0012	0.0013	0.0018	0.0007
Ni	0.0010	0.0000	0.0001	0.0000	0.0000	0.0000	0.0002	0.0000	0.0000	0.0000	0.0001	0.0000	0.0010	0.0000	0.0010	0.0001
Nb	0.0000	0.0000	0.0000	0.0000	0.0000	0.0000	0.0000	0.0000	0.0000	0.0000	0.0000	0.0000	0.0000	0.0000	0.0000	0.0000
Total:	3.0003	2.0000	3.0000	2.0000	3.0000	2.0000	3.0000	2.0000	3.0000	2.0000	3.0000	2.0000	3.0002	2.0000	3.0003	2.0000
Calc. Methods:	**Mol % Usp**	**Mol % Ilm**	**Mol % Usp**	**Mol % Ilm**	**Mol % Usp**	**Mol % Ilm**	**Mol % Usp**	**Mol % Ilm**	**Mol % Usp**	**Mol % Ilm**	**Mol % Usp**	**Mol % Ilm**	**Mol % Usp**	**Mol % Ilm**	**Mol % Usp**	**Mol % Ilm**
Carmichael (1967)	13.61%	95.51%	8.81%	95.51%	1.76%	95.51%	2.62%	95.51%	1.50%	95.51%	1.05%	95.51%	1.87%	95.51%	13.61%	96.37%
Anderson (1968)	0.69%	95.18%	7.76%	95.18%	1.36%	95.18%	2.23%	95.18%	1.07%	95.18%	0.62%	95.18%	1.34%	95.18%	0.69%	96.27%
Lindsley & Spencer (1982)	0.78%	95.18%	8.71%	95.18%	1.41%	95.18%	2.32%	95.18%	1.18%	95.18%	0.67%	95.18%	1.46%	95.18%	0.78%	96.28%
Stormer (1983)	0.91%	95.37%	8.96%	95.37%	1.43%	95.37%	2.33%	95.37%	1.23%	95.37%	0.67%	95.37%	1.48%	95.37%	0.91%	96.44%
Geothermometer by:																
X'Usp & X'Ilm from:	**Temp (°C)**		**Temp (°C)**		**Temp (°C)**		**Temp (°C)**		**Temp (°C)**		**Temp (°C)**		**Temp (°C)**		**Temp (°C)**	
Carmichael (1967)	386		544		426		451		416		395		429		561	
Anderson (1968)	377		538		415		445		401		371		414		364	
Lindsley & Spencer (1982)	383		549		417		448		407		375		419		369	
Stormer (1983)	390		548		415		445		406		374		417		375	
Average:	434		545		418		447		408		379		420		417	
Geothermobarometer by:																
X'Usp & X'Ilm from:	**Temp (°C)**	**log10 fO2**	**Temp (°C)**	**log10 fO2**	**Temp (°C)**	**log10 fO2**	**Temp (°C)**	**log10 fO2**	**Temp (°C)**	**log10 fO2**	**Temp (°C)**	**log10 fO2**	**Temp (°C)**	**log10 fO2**	**Temp (°C)**	**log10 fO2**
Carmichael (1967)	613	-19.92	598	-20.21	538	-21.34	553	-21.05	532	-21.46	518	-21.73	540	-21.30	583	-21.68
Anderson (1968)	508	-21.62	600	-19.86	534	-21.11	553	-20.74	525	-21.29	504	-21.70	533	-21.12	490	-23.20
Lindsley & Spencer (1982)	513	-21.53	605	-19.78	535	-21.08	554	-20.72	528	-21.21	507	-21.64	536	-21.05	494	-23.12
Stormer (1983)	516	-21.65	602	-20.01	532	-21.31	551	-20.95	527	-21.42	505	-21.88	534	-21.29	496	-23.28
Average:	537		601		535		553		528		509		536		516	
		-21		-20		-21		-21		-21		-22		-21		-23
Geothermobarometer by:																
X'Usp & X'Ilm from:	**Temp (°C)**	**log10 fO2**	**Temp (°C)**	**log10 fO2**	**Temp (°C)**	**log10 fO2**	**Temp (°C)**	**log10 fO2**	**Temp (°C)**	**log10 fO2**	**Temp (°C)**	**log10 fO2**	**Temp (°C)**	**log10 fO2**	**Temp (°C)**	**log10 fO2**
Carmichael (1967)	634		614		543		560		536		521		546		602	
Anderson (1968)	509	-21.41	616	-19.39	538	-20.83	560	-20.41	528	-21.03	504	-21.50	537	-20.84	488	-23.07
Lindsley & Spencer (1982)	514	-21.31	622	-19.29	539	-20.80	561	-20.38	532	-20.95	507	-21.44	541	-20.77	493	-22.97
Stormer (1983)	517	-21.42	619	-19.51	536	-21.04	558	-20.62	530	-21.16	505	-21.68	538	-21.01	496	-23.12
Average:	543		618		539		560		531		509		540		520	
		-21		-19		-21		-20		-21		-22		-21		-23
Average for each pair	505		588		497		520		489		466		499		484	
Average for each pair		-21		-20		-21		-21		-21		-22		-21		-23
Method Averages																
Powell & Powell (1977)																
Spencer & Lindsley (1981)																
Andersen & Lindsley(1985)																
Average for all pairs																

Sample #	WYL-10-61-190.3 Mag3-Ilm3	WYL-10-61-190.3 Mag3-Ilm3	WYL-10-61-190.3 Mag3-Ilm3	WYL-10-61-190.3 Mag3-Ilm3	WYL-10-61-190.3 Mag3-Ilm3	WYL-10-61-190.3 Mag3-Ilm3	WYL-10-61-190.3 Mag3-Ilm3	WYL-10-61-190.3 Mag3-Ilm3	WYL-10-61-190.3 Mag3-Ilm3	WYL-10-61-190.3 Mag3-Ilm3	WYL-10-61-190.3 Mag3-Ilm3	WYL-10-61-190.3 Mag3-Ilm3	WYL-10-61-190.3 Mag3-Ilm3	WYL-10-61-190.3 Mag3-Ilm3	WYL-10-61-190.3 Mag3-Ilm3	WYL-10-61-190.3 Mag3-Ilm3
Line	47	43	48	43	49	43	50	43	51	43	53	43	46	44	47	44
Wt% Oxides	**Magnetite**	**Ilmenite**	**Magnetite**	**Ilmenite**	**Magnetite**	**Ilmenite**	**Magnetite**	**Ilmenite**	**Magnetite**	**Ilmenite**	**Magnetite**	**Ilmenite**	**Magnetite**	**Ilmenite**	**Magnetite**	**Ilmenite**
SiO2	0.10	0.02	0.09	0.02	0.08	0.02	0.09	0.02	0.10	0.02	0.11	0.02	3.34	0.02	0.10	0.02
TiO2	2.96	50.69	0.49	50.69	0.80	50.69	0.41	50.69	0.23	50.69	0.51	50.69	0.25	51.17	2.96	51.17
Al2O3	1.64	0.00	0.32	0.00	0.29	0.00	1.32	0.00	0.33	0.00	0.35	0.00	2.47	0.00	1.64	0.00
Fe2O3(T)																
FeO(T)	89.13	44.68	93.13	44.68	92.86	44.68	92.46	44.68	93.29	44.68	92.86	44.68	84.24	44.81	89.13	44.81
MnO	0.59	4.04	0.03	4.04	0.05	4.04	0.07	4.04	0.03	4.04	0.07	4.04	0.05	3.69	0.59	3.69
MgO	0.00	0.02	0.00	0.02	0.00	0.02	0.01	0.02	0.00	0.02	0.01	0.02	0.40	0.02	0.00	0.02
CaO	0.00	0.00	0.00	0.00	0.00	0.00	0.00	0.00	0.00	0.00	0.00	0.00	0.05	0.01	0.00	0.01
Na2O																
K2O																
Cr2O3	0.00	0.00	0.01	0.00	0.00	0.00	0.01	0.00	0.01	0.00	0.01	0.00	0.00	0.00	0.00	0.00
BaO																
ZnO	0.06	0.03	0.00	0.03	0.05	0.03	0.00	0.03	0.03	0.03	0.03	0.03	0.01	0.01	0.06	0.01
V2O3	0.04	0.03	0.03	0.03	0.04	0.03	0.05	0.03	0.04	0.03	0.04	0.03	0.06	0.07	0.04	0.07
NiO	0.00	0.01	0.00	0.01	0.01	0.01	0.00	0.01	0.00	0.01	0.03	0.01	0.03	0.00	0.00	0.00
Nb2O3																
Sum:	94.529336	99.520994	94.115266	99.520994	94.192038	99.520994	94.427703	99.520994	94.049196	99.520994	94.027638	99.520994	90.917893	99.796086	94.529336	99.796086
Carmichael (1967)	**Recalculated Iron and Total**		**Recalculated Iron and Total**		**Recalculated Iron and Total**		**Recalculated Iron and Total**		**Recalculated Iron and Total**		**Recalculated Iron and Total**		**Recalculated Iron and Total**		**Recalculated Iron and Total**	
Fe2O3 wt. %	61.5	3.6	68.0	3.6	67.5	3.6	67.2	3.6	68.5	3.6	67.8	3.6	55.5	2.8	61.5	2.8
FeO wt. %	33.8	41.5	31.9	41.5	32.1	41.5	32.0	41.5	31.7	41.5	31.8	41.5	34.3	42.3	33.8	42.3
Total:	100.7	99.9	100.9	99.9	101.0	99.9	101.2	99.9	100.9	99.9	100.8	99.9	96.5	100.1	100.7	100.1
	Ulvöspinel	**Ilmenite**	**Ulvöspinel**	**Ilmenite**	**Ulvöspinel**	**Ilmenite**	**Ulvöspinel**	**Ilmenite**	**Ulvöspinel**	**Ilmenite**	**Ulvöspinel**	**Ilmenite**	**Ulvöspinel**	**Ilmenite**	**Ulvöspinel**	**Ilmenite**
Sum of Atomic mol proportion:	2.2707	1.5206	2.2877	1.5206	2.2871	1.5206	2.2699	1.5206	2.2887	1.5206	2.2897	1.5206	2.3206	1.5170	2.2707	1.5170
No. of Oxygen:	4	3	4	3	4	3	4	3	4	3	4	3	4	3	4	3
	Cation prop. (Carmichael 1967)		**Cation prop. (Carmichael 1967)**		**Cation prop. (Carmichael 1967)**		**Cation prop. (Carmichael 1967)**		**Cation prop. (Carmichael 1967)**		**Cation prop. (Carmichael 1967)**		**Cation prop. (Carmichael 1967)**		**Cation prop. (Carmichael 1967)**	
Si	0.0039	0.0005	0.0036	0.0005	0.0032	0.0005	0.0034	0.0005	0.0038	0.0005	0.0042	0.0005	0.1290	0.0005	0.0039	0.0005
Ti	0.0843	0.9652	0.0140	0.9652	0.0230	0.9652	0.0116	0.9652	0.0066	0.9652	0.0145	0.9652	0.0071	0.9719	0.0843	0.9719
Al	0.0729	0.0000	0.0145	0.0000	0.0130	0.0000	0.0588	0.0000	0.0147	0.0000	0.0158	0.0000	0.1126	0.0000	0.0729	0.0000
Fe+3	1.7496	0.0679	1.9488	0.0679	1.9331	0.0679	1.9093	0.0679	1.9630	0.0679	1.9447	0.0679	1.6129	0.0536	1.7496	0.0536
Fe+2	1.0675	0.8778	1.0166	0.8778	1.0230	0.8778	1.0120	0.8778	1.0087	0.8778	1.0148	0.8778	1.1083	0.8926	1.0675	0.8926
Mn	0.0190	0.0865	0.0011	0.0865	0.0017	0.0865	0.0022	0.0865	0.0010	0.0865	0.0024	0.0865	0.0017	0.0788	0.0190	0.0788
Mg	0.0000	0.0009	0.0000	0.0009	0.0000	0.0009	0.0008	0.0009	0.0000	0.0009	0.0003	0.0009	0.0233	0.0006	0.0000	0.0006
Ca	0.0000	0.0000	0.0000	0.0000	0.0000	0.0000	0.0000	0.0000	0.0000	0.0000	0.0000	0.0000	0.0022	0.0003	0.0000	0.0003
Na	0.0000	0.0000	0.0000	0.0000	0.0000	0.0000	0.0000	0.0000	0.0000	0.0000	0.0000	0.0000	0.0000	0.0000	0.0000	0.0000
K	0.0000	0.0000	0.0000	0.0000	0.0000	0.0000	0.0000	0.0000	0.0000	0.0000	0.0000	0.0000	0.0000	0.0000	0.0000	0.0000
Cr	0.0001	0.0000	0.0003	0.0000	0.0001	0.0000	0.0004	0.0000	0.0003	0.0000	0.0004	0.0000	0.0000	0.0000	0.0001	0.0000
Ba	0.0000	0.0000	0.0000	0.0000	0.0000	0.0000	0.0000	0.0000	0.0000	0.0000	0.0000	0.0000	0.0000	0.0000	0.0000	0.0000
Zn	0.0016	0.0005	0.0000	0.0005	0.0014	0.0005	0.0000	0.0005	0.0008	0.0005	0.0009	0.0005	0.0004	0.0001	0.0016	0.0001
V	0.0012	0.0007	0.0011	0.0007	0.0014	0.0007	0.0015	0.0007	0.0011	0.0007	0.0012	0.0007	0.0018	0.0015	0.0012	0.0015
Ni	0.0001	0.0001	0.0000	0.0001	0.0002	0.0001	0.0000	0.0001	0.0001	0.0001	0.0010	0.0001	0.0010	0.0001	0.0001	0.0001
Nb	0.0000	0.0000	0.0000	0.0000	0.0000	0.0000	0.0000	0.0000	0.0000	0.0000	0.0000	0.0000	0.0000	0.0000	0.0000	0.0000
Total:	3.0000	2.0000	3.0000	2.0000	3.0000	2.0000	3.0000	2.0000	3.0000	2.0000	3.0002	2.0000	3.0003	2.0000	3.0000	2.0000
Calc. Methods:	**Mol % Usp**	**Mol % Ilm**	**Mol % Usp**	**Mol % Ilm**	**Mol % Usp**	**Mol % Ilm**	**Mol % Usp**	**Mol % Ilm**	**Mol % Usp**	**Mol % Ilm**	**Mol % Usp**	**Mol % Ilm**	**Mol % Usp**	**Mol % Ilm**	**Mol % Usp**	**Mol % Ilm**
Carmichael (1967)	8.81%	96.57%	1.76%	96.57%	2.62%	96.57%	1.50%	96.57%	1.05%	96.57%	1.87%	96.57%	13.61%	97.24%	8.81%	97.24%
Anderson (1968)	7.76%	96.27%	1.36%	96.27%	2.23%	96.27%	1.07%	96.27%	0.62%	96.27%	1.34%	96.27%	0.69%	97.08%	7.76%	97.08%
Lindsley & Spencer (1982)	8.71%	96.28%	1.41%	96.28%	2.32%	96.28%	1.18%	96.28%	0.67%	96.28%	1.46%	96.28%	0.78%	97.08%	8.71%	97.08%
Stormer (1983)	8.96%	96.44%	1.43%	96.44%	2.33%	96.44%	1.23%	96.44%	0.67%	96.44%	1.48%	96.44%	0.91%	97.20%	8.96%	97.20%
Geothermometer by:																
XUsp & XIlm from:	**Temp (°C)**		**Temp (°C)**		**Temp (°C)**		**Temp (°C)**		**Temp (°C)**		**Temp (°C)**		**Temp (°C)**		**Temp (°C)**	
Carmichael (1967)	521		409		433		400		380		413		542		504	
Anderson (1968)	517		399		429		386		358		399		351		498	
Lindsley & Spencer (1982)	527		401		431		392		362		403		357		508	
Stormer (1983)	526		399		428		391		360		401		363		507	
Average:	523		402		430		392		365		404		403		504	
Geothermobarometer by:																
XUsp & XIlm from:	**Temp (°C)**	**log10 fO2**	**Temp (°C)**	**log10 fO2**	**Temp (°C)**	**log10 fO2**	**Temp (°C)**	**log10 fO2**	**Temp (°C)**	**log10 fO2**	**Temp (°C)**	**log10 fO2**	**Temp (°C)**	**log10 fO2**	**Temp (°C)**	**log10 fO2**
Carmichael (1967)	571	-21.92	517	-23.01	531	-22.72	511	-23.13	499	-23.40	519	-22.97	559	-23.16	550	-23.36
Anderson (1968)	575	-21.47	514	-22.69	532	-22.33	506	-22.87	486	-23.29	514	-22.70	473	-24.75	552	-23.06
Lindsley & Spencer (1982)	579	-21.41	515	-22.67	533	-22.30	509	-22.80	489	-23.23	517	-22.64	477	-24.67	555	-22.99
Stormer (1983)	575	-21.68	512	-22.94	530	-22.58	507	-23.05	486	-23.51	513	-22.92	479	-24.81	551	-23.26
Average:	575		515		531		508		490		516		497		552	
		-22		-23		-22		-23		-23		-23		-24		-23
Geothermobarometer by:																
XUsp & XIlm from:	**Temp (°C)**	**log10 fO2**	**Temp (°C)**	**log10 fO2**	**Temp (°C)**	**log10 fO2**	**Temp (°C)**	**log10 fO2**	**Temp (°C)**	**log10 fO2**	**Temp (°C)**	**log10 fO2**	**Temp (°C)**	**log10 fO2**	**Temp (°C)**	**log10 fO2**
Carmichael (1967)	585		519		536		513		498		522		576		562	
Anderson (1968)	589	-21.00	516	-22.47	536	-22.04	506	-22.68	484	-23.17	515	-22.48	469	-24.70	563	-22.62
Lindsley & Spencer (1982)	593	-20.91	517	-22.44	538	-22.01	510	-22.60	487	-23.10	519	-22.41	473	-24.60	567	-22.53
Stormer (1983)	590	-21.18	514	-22.73	534	-22.30	508	-22.86	484	-23.39	515	-22.70	476	-24.74	564	-22.79
Average:	589		516		536		509		488		518		499		564	
		-21		-23		-22		-23		-23		-23		-25		-23
Average for each pair	562		478		499		470		448		479		466		540	
Average for each pair		-21		-23		-22		-23		-23		-23		-25		-23
Method Averages																
Powell & Powell (1977)																
Spencer & Lindsley (1981)																
Andersen & Lindsley (1985)																
Average for all pairs																

Sample #	WYL-10-61-190.3 Mag3-Ilm3	WYL-10-61-190.3 Mag3-Ilm3	WYL-10-61-190.3 Mag3-Ilm3	WYL-10-61-190.3 Mag3-Ilm3	WYL-10-61-190.3 Mag3-Ilm3	WYL-10-61-190.3 Mag3-Ilm3	WYL-10-61-190.3 Mag3-Ilm3	WYL-10-61-190.3 Mag3-Ilm3	WYL-10-61-190.3 Mag3-Ilm3	WYL-10-61-190.3 Mag3-Ilm3	WYL-10-61-190.3 Mag3-Ilm3	WYL-10-61-190.3 Mag3-Ilm3	WYL-10-61-190.3 Mag3-Ilm3	WYL-10-61-190.3 Mag3-Ilm3
Line	48	44	49	44	50	44	51	44	53	44	46	45	47	45
Wt% Oxides	**Magnetite**	**Ilmenite**	**Magnetite**	**Ilmenite**	**Magnetite**	**Ilmenite**	**Magnetite**	**Ilmenite**	**Magnetite**	**Ilmenite**	**Magnetite**	**Ilmenite**	**Magnetite**	**Ilmenite**
SiO2	0.09	0.02	0.08	0.02	0.09	0.02	0.10	0.02	0.11	0.02	3.34	0.03	0.10	0.03
TiO2	0.49	51.17	0.80	51.17	0.41	51.17	0.23	51.17	0.51	51.17	0.25	50.33	2.96	50.33
Al2O3	0.32	0.00	0.29	0.00	1.32	0.00	0.33	0.00	0.35	0.00	2.47	0.00	1.64	0.00
Fe2O3(T)														
FeO(T)	93.13	44.81	92.86	44.81	92.46	44.81	93.29	44.81	92.86	44.81	84.24	44.82	89.13	44.82
MnO	0.03	3.69	0.05	3.69	0.07	3.69	0.03	3.69	0.07	3.69	0.05	3.97	0.59	3.97
MgO	0.00	0.02	0.00	0.02	0.01	0.02	0.00	0.02	0.01	0.02	0.40	0.00	0.00	0.00
CaO	0.00	0.01	0.00	0.01	0.00	0.01	0.00	0.01	0.00	0.01	0.05	0.00	0.00	0.00
Na2O														
K2O														
Cr2O3	0.01	0.00	0.00	0.00	0.01	0.00	0.01	0.00	0.01	0.00	0.00	0.00	0.00	0.00
BaO														
ZnO	0.00	0.01	0.05	0.01	0.00	0.01	0.03	0.01	0.03	0.01	0.01	0.00	0.06	0.00
V2O3	0.03	0.07	0.04	0.07	0.05	0.07	0.04	0.07	0.04	0.07	0.06	0.04	0.04	0.04
NiO	0.00	0.00	0.01	0.00	0.00	0.00	0.00	0.00	0.03	0.00	0.03	0.00	0.00	0.00
Nb2O3														
Sum:	94.115266	99.796086	94.192038	99.796086	94.427703	99.796086	94.049196	99.796086	94.027638	99.796086	90.917893	99.201063	94.529336	99.201063
Carmichael (1967)	**Recalculated Iron and Total**		**Recalculated Iron and Total**		**Recalculated Iron and Total**		**Recalculated Iron and Total**		**Recalculated Iron and Total**		**Recalculated Iron and Total**		**Recalculated Iron and Total**	
Fe2O3 wt. %	68.0	2.8	67.5	2.8	67.2	2.8	68.5	2.8	67.8	2.8	55.5	3.9	61.5	3.9
FeO wt. %	31.9	42.3	32.1	42.3	32.0	42.3	31.7	42.3	31.8	42.3	34.3	41.3	33.8	41.3
Total:	100.9	100.1	101.0	100.1	101.2	100.1	100.9	100.1	100.8	100.1	96.5	99.6	100.7	99.6
	Ulvöspinel	**Ilmenite**	**Ulvöspinel**	**Ilmenite**	**Ulvöspinel**	**Ilmenite**	**Ulvöspinel**	**Ilmenite**	**Ulvöspinel**	**Ilmenite**	**Ulvöspinel**	**Ilmenite**	**Ulvöspinel**	**Ilmenite**
Sum of Atomic mol proportion:	2.2877	1.5170	2.2871	1.5170	2.2699	1.5170	2.2887	1.5170	2.2897	1.5170	2.3206	1.5253	2.2707	1.5253
No. of Oxygen:	4	3	4	3	4	3	4	3	4	3	4	3	4	3
	Cation prop. (Carmichael 1967)		**Cation prop. (Carmichael 1967)**		**Cation prop. (Carmichael 1967)**		**Cation prop. (Carmichael 1967)**		**Cation prop. (Carmichael 1967)**		**Cation prop. (Carmichael 1967)**		**Cation prop. (Carmichael 1967)**	
Si	0.0036	0.0005	0.0032	0.0005	0.0034	0.0005	0.0038	0.0005	0.0042	0.0005	0.1290	0.0008	0.0039	0.0008
Ti	0.0140	0.9719	0.0230	0.9719	0.0116	0.9719	0.0066	0.9719	0.0145	0.9719	0.0071	0.9612	0.0843	0.9612
Al	0.0145	0.0000	0.0130	0.0000	0.0588	0.0000	0.0147	0.0000	0.0158	0.0000	0.1126	0.0000	0.0729	0.0000
Fe+3	1.9488	0.0536	1.9331	0.0536	1.9093	0.0536	1.9630	0.0536	1.9447	0.0536	1.6129	0.0750	1.7496	0.0750
Fe+2	1.0166	0.8926	1.0230	0.8926	1.0120	0.8926	1.0087	0.8926	1.0148	0.8926	1.1083	0.8765	1.0675	0.8765
Mn	0.0011	0.0788	0.0017	0.0788	0.0022	0.0788	0.0010	0.0788	0.0024	0.0788	0.0017	0.0854	0.0190	0.0854
Mg	0.0000	0.0006	0.0000	0.0006	0.0008	0.0006	0.0000	0.0006	0.0003	0.0006	0.0233	0.0000	0.0000	0.0000
Ca	0.0000	0.0003	0.0000	0.0003	0.0000	0.0003	0.0000	0.0003	0.0000	0.0003	0.0022	0.0001	0.0000	0.0001
Na	0.0000	0.0000	0.0000	0.0000	0.0000	0.0000	0.0000	0.0000	0.0000	0.0000	0.0000	0.0000	0.0000	0.0000
K	0.0000	0.0000	0.0000	0.0000	0.0000	0.0000	0.0000	0.0000	0.0000	0.0000	0.0000	0.0000	0.0000	0.0000
Cr	0.0003	0.0000	0.0001	0.0000	0.0004	0.0000	0.0003	0.0000	0.0004	0.0000	0.0000	0.0000	0.0001	0.0000
Ba	0.0000	0.0000	0.0000	0.0000	0.0000	0.0000	0.0000	0.0000	0.0000	0.0000	0.0000	0.0000	0.0000	0.0000
Zn	0.0000	0.0001	0.0014	0.0001	0.0000	0.0001	0.0008	0.0001	0.0009	0.0001	0.0004	0.0000	0.0016	0.0000
V	0.0011	0.0015	0.0014	0.0015	0.0015	0.0015	0.0011	0.0015	0.0012	0.0015	0.0018	0.0009	0.0012	0.0009
Ni	0.0000	0.0001	0.0002	0.0001	0.0000	0.0001	0.0001	0.0001	0.0010	0.0001	0.0010	0.0000	0.0001	0.0000
Nb	0.0000	0.0000	0.0000	0.0000	0.0000	0.0000	0.0000	0.0000	0.0000	0.0000	0.0000	0.0000	0.0000	0.0000
Total:	3.0000	2.0000	3.0000	2.0000	3.0000	2.0000	3.0000	2.0000	3.0002	2.0000	3.0003	2.0000	3.0000	2.0000
Calc. Methods:	**Mol % Usp**	**Mol % Ilm**	**Mol % Usp**	**Mol % Ilm**	**Mol % Usp**	**Mol % Ilm**	**Mol % Usp**	**Mol % Ilm**	**Mol % Usp**	**Mol % Ilm**	**Mol % Usp**	**Mol % Ilm**	**Mol % Usp**	**Mol % Ilm**
Carmichael (1967)	1.76%	97.24%	2.62%	97.24%	1.50%	97.24%	1.05%	97.24%	1.87%	97.24%	13.61%	96.20%	8.81%	96.20%
Anderson (1968)	1.36%	97.08%	2.23%	97.08%	1.07%	97.08%	0.62%	97.08%	1.34%	97.08%	0.69%	95.86%	7.76%	95.86%
Lindsley & Spencer (1982)	1.41%	97.08%	2.32%	97.08%	1.18%	97.08%	0.67%	97.08%	1.46%	97.08%	0.78%	95.86%	8.71%	95.86%
Stormer (1983)	1.43%	97.20%	2.33%	97.20%	1.23%	97.20%	0.67%	97.20%	1.48%	97.20%	0.91%	96.07%	8.96%	96.07%
Geothermometer by:														
X'Usp & X'Ilm from:	**Temp (°C)**		**Temp (°C)**		**Temp (°C)**		**Temp (°C)**		**Temp (°C)**		**Temp (°C)**		**Temp (°C)**	
Carmichael (1967)	397		420		388		369		400		570		530	
Anderson (1968)	386		414		373		346		385		369		526	
Lindsley & Spencer (1982)	388		416		378		350		390		375		536	
Stormer (1983)	386		414		378		348		388		381		534	
Average:	389		416		379		353		391		424		531	
Geothermobarometer by:														
X'Usp & X'Ilm from:	**Temp (°C)**	**log10 fO2**	**Temp (°C)**	**log10 fO2**	**Temp (°C)**	**log10 fO2**	**Temp (°C)**	**log10 fO2**	**Temp (°C)**	**log10 fO2**	**Temp (°C)**	**log10 fO2**	**Temp (°C)**	**log10 fO2**
Carmichael (1967)	500	-24.42	513	-24.13	495	-24.54	483	-24.81	502	-24.37	594	-21.01	581	-21.27
Anderson (1968)	496	-24.24	513	-23.88	488	-24.42	469	-24.84	495	-24.25	498	-22.54	585	-20.80
Lindsley & Spencer (1982)	497	-24.22	514	-23.85	491	-24.35	472	-24.78	498	-24.19	502	-22.45	589	-20.72
Stormer (1983)	494	-24.48	511	-24.12	489	-24.59	469	-25.04	495	-24.45	504	-22.66	585	-21.05
Average:	497		513		491		473		498		524		585	
		-24		-24		-24		-25		-24		-22		-21
Geothermobarometer by:														
X'Usp & X'Ilm from:	**Temp (°C)**	**log10 fO2**	**Temp (°C)**	**log10 fO2**	**Temp (°C)**	**log10 fO2**	**Temp (°C)**	**log10 fO2**	**Temp (°C)**	**log10 fO2**	**Temp (°C)**	**log10 fO2**	**Temp (°C)**	**log10 fO2**
Carmichael (1967)	500		516		494		480		503		614		596	
Anderson (1968)	495	-24.09	515	-23.65	486	-24.31	465	-24.81	494	-24.10	497	-22.37	600	-20.32
Lindsley & Spencer (1982)	496	-24.06	516	-23.63	490	-24.22	467	-24.74	498	-24.03	502	-22.27	605	-20.23
Stormer (1983)	493	-24.34	513	-23.90	488	-24.47	465	-25.02	495	-24.31	504	-22.48	600	-20.55
Average:	496		515		489		469		497		529		600	
		-24		-24		-24		-25		-24		-22		-20
Average for each pair	461		481		453		432		462		492		572	
Average for each pair		-24		-24		-24		-25		-24		-22		-21
Method Averages														
Powell & Powell (1977)														
Spencer & Lindsley(1981)														
Andersen & Lindsley(1985)														
Average for all pairs														

Sample #	WYL-10-61-190.3 Mag3-Ilm3	WYL-10-61-190.3 Mag3-Ilm3	WYL-10-61-190.3 Mag3-Ilm3	WYL-10-61-190.3 Mag3-Ilm3	WYL-10-61-190.3 Mag3-Ilm3	WYL-10-61-190.3 Mag3-Ilm3	WYL-10-61-190.3 Mag3-Ilm3	WYL-10-61-190.3 Mag3-Ilm3	WYL-10-61-190.3 Mag3-Ilm3	WYL-10-61-190.3 Mag3-Ilm3
Line	48	45	49	45	50	45	51	45	53	45
Wt% Oxides	**Magnetite**	**Ilmenite**	**Magnetite**	**Ilmenite**	**Magnetite**	**Ilmenite**	**Magnetite**	**Ilmenite**	**Magnetite**	**Ilmenite**
SiO2	0.09	0.03	0.08	0.03	0.09	0.03	0.10	0.03	0.11	0.03
TiO2	0.49	50.33	0.80	50.33	0.41	50.33	0.23	50.33	0.51	50.33
Al2O3	0.32	0.00	0.29	0.00	1.32	0.00	0.33	0.00	0.35	0.00
Fe2O3(T)										
FeO(T)	93.13	44.82	92.86	44.82	92.46	44.82	93.29	44.82	92.86	44.82
MnO	0.03	3.97	0.05	3.97	0.07	3.97	0.03	3.97	0.07	3.97
MgO	0.00	0.00	0.00	0.00	0.01	0.00	0.00	0.00	0.01	0.00
CaO	0.00	0.00	0.00	0.00	0.00	0.00	0.00	0.00	0.00	0.00
Na2O										
K2O										
Cr2O3	0.01	0.00	0.00	0.00	0.01	0.00	0.01	0.00	0.01	0.00
BaO										
ZnO	0.00	0.00	0.05	0.00	0.00	0.00	0.03	0.00	0.03	0.00
V2O3	0.03	0.04	0.04	0.04	0.05	0.04	0.04	0.04	0.04	0.04
NiO	0.00	0.00	0.01	0.00	0.00	0.00	0.00	0.00	0.03	0.00
Nb2O3										
Sum:	94.115266	99.201063	94.192038	99.201063	94.427703	99.201063	94.049196	99.201063	94.027638	99.201063
Carmichael (1967)	**Recalculated Iron and Total**		**Recalculated Iron and Total**		**Recalculated Iron and Total**		**Recalculated Iron and Total**		**Recalculated Iron and Total**	
Fe2O3 wt. %	68.0	3.9	67.5	3.9	67.2	3.9	68.5	3.9	67.8	3.9
FeO wt. %	31.9	41.3	32.1	41.3	32.0	41.3	31.7	41.3	31.8	41.3
Total:	100.9	99.6	101.0	99.6	101.2	99.6	100.9	99.6	100.8	99.6
	Ulvöspinel	**Ilmenite**	**Ulvöspinel**	**Ilmenite**	**Ulvöspinel**	**Ilmenite**	**Ulvöspinel**	**Ilmenite**	**Ulvöspinel**	**Ilmenite**
Sum of Atomic mol proportion:	2.2877	1.5253	2.2871	1.5253	2.2699	1.5253	2.2887	1.5253	2.2897	1.5253
No. of Oxygen:	4	3	4	3	4	3	4	3	4	3
	Cation prop. (Carmichael 1967)		**Cation prop. (Carmichael 1967)**		**Cation prop. (Carmichael 1967)**		**Cation prop. (Carmichael 1967)**		**Cation prop. (Carmichael 1967)**	
Si	0.0036	0.0008	0.0032	0.0008	0.0034	0.0008	0.0038	0.0008	0.0042	0.0008
Ti	0.0140	0.9612	0.0230	0.9612	0.0116	0.9612	0.0066	0.9612	0.0145	0.9612
Al	0.0145	0.0000	0.0130	0.0000	0.0588	0.0000	0.0147	0.0000	0.0158	0.0000
Fe+3	1.9488	0.0750	1.9331	0.0750	1.9093	0.0750	1.9630	0.0750	1.9447	0.0750
Fe+2	1.0166	0.8765	1.0230	0.8765	1.0120	0.8765	1.0087	0.8765	1.0148	0.8765
Mn	0.0011	0.0854	0.0017	0.0854	0.0022	0.0854	0.0010	0.0854	0.0024	0.0854
Mg	0.0000	0.0000	0.0000	0.0000	0.0008	0.0000	0.0000	0.0000	0.0003	0.0000
Ca	0.0000	0.0001	0.0000	0.0001	0.0000	0.0001	0.0000	0.0001	0.0000	0.0001
Na	0.0000	0.0000	0.0000	0.0000	0.0000	0.0000	0.0000	0.0000	0.0000	0.0000
K	0.0000	0.0000	0.0000	0.0000	0.0000	0.0000	0.0000	0.0000	0.0000	0.0000
Cr	0.0003	0.0000	0.0001	0.0000	0.0004	0.0000	0.0003	0.0000	0.0004	0.0000
Ba	0.0000	0.0000	0.0000	0.0000	0.0000	0.0000	0.0000	0.0000	0.0000	0.0000
Zn	0.0000	0.0000	0.0014	0.0000	0.0000	0.0000	0.0008	0.0000	0.0009	0.0000
V	0.0011	0.0009	0.0014	0.0009	0.0015	0.0009	0.0011	0.0009	0.0012	0.0009
Ni	0.0000	0.0000	0.0002	0.0000	0.0000	0.0000	0.0001	0.0000	0.0010	0.0000
Nb	0.0000	0.0000	0.0000	0.0000	0.0000	0.0000	0.0000	0.0000	0.0000	0.0000
Total:	3.0000	2.0000	3.0000	2.0000	3.0000	2.0000	3.0000	2.0000	3.0002	2.0000
Calc. Methods:	**Mol % Usp**	**Mol % Ilm**	**Mol % Usp**	**Mol % Ilm**	**Mol % Usp**	**Mol % Ilm**	**Mol % Usp**	**Mol % Ilm**	**Mol % Usp**	**Mol % Ilm**
Carmichael (1967)	1.76%	96.20%	2.62%	96.20%	1.50%	96.20%	1.05%	96.20%	1.87%	96.20%
Anderson (1968)	1.36%	95.86%	2.23%	95.86%	1.07%	95.86%	0.62%	95.86%	1.34%	95.86%
Lindsley & Spencer (1982)	1.41%	95.86%	2.32%	95.86%	1.18%	95.86%	0.67%	95.86%	1.46%	95.86%
Stormer (1983)	1.43%	96.07%	2.33%	96.07%	1.23%	96.07%	0.67%	96.07%	1.48%	96.07%
Geothermometer by:										
X'Usp & X'Ilm from:	**Temp (°C)**		**Temp (°C)**		**Temp (°C)**		**Temp (°C)**		**Temp (°C)**	
Carmichael (1967)	415		440		406		386		419	
Anderson (1968)	406		435		392		364		405	
Lindsley & Spencer (1982)	408		438		398		367		410	
Stormer (1983)	405		435		397		365		407	
Average:	408		437		398		370		410	
Geothermobarometer by:										
X'Usp & X'Ilm from:	**Temp (°C)**	**log10 fO2**	**Temp (°C)**	**log10 fO2**	**Temp (°C)**	**log10 fO2**	**Temp (°C)**	**log10 fO2**	**Temp (°C)**	**log10 fO2**
Carmichael (1967)	525	-22.38	539	-22.09	519	-22.50	506	-22.77	527	-22.34
Anderson (1968)	522	-22.03	540	-21.66	513	-22.20	494	-22.62	522	-22.04
Lindsley & Spencer (1982)	523	-22.00	542	-21.63	517	-22.13	496	-22.56	525	-21.97
Stormer (1983)	520	-22.33	538	-21.96	514	-22.44	493	-22.89	521	-22.30
Average:	523		540		516		497		524	
		-22		-22		-22		-23		-22
Geothermobarometer by:										
X'Usp & X'Ilm from:	**Temp (°C)**	**log10 fO2**	**Temp (°C)**	**log10 fO2**	**Temp (°C)**	**log10 fO2**	**Temp (°C)**	**log10 fO2**	**Temp (°C)**	**log10 fO2**
Carmichael (1967)	528		545		521		506		531	
Anderson (1968)	525	-21.78	546	-21.36	515	-21.99	492	-22.47	524	-21.79
Lindsley & Spencer (1982)	526	-21.75	548	-21.32	519	-21.90	495	-22.40	528	-21.72
Stormer (1983)	522	-22.09	543	-21.66	516	-22.22	491	-22.74	524	-22.06
Average:	525		545		518		496		527	
		-22		-21		-22		-23		-22
Average for each pair	485		507		477		455		487	
Average for each pair		-22		-22		-22		-23		-22
Method Averages										
Powell & Powell (1977)										
Spencer & Lindsley (1981)										
Andersen & Lindsley (1985)										
Average for all pairs										

Sample #	WYL-10-61-190.3 Mag3-Ilm3	WYL-10-61-190.3 Mag3-Ilm3	WYL-10-61-190.3 Mag3-Ilm3	WYL-10-61-190.3 Mag3-Ilm3	WYL-10-61-190.3 Mag3-Ilm3	WYL-10-61-190.3 Mag3-Ilm3	WYL-10-61-190.3 Mag3-Ilm3	WYL-10-61-190.3 Mag3-Ilm3	WYL-10-61-190.3 Mag3-Ilm3	WYL-10-61-190.3 Mag3-Ilm3	WYL-10-61-190.3 Mag3-Ilm3	WYL-10-61-190.3 Mag3-Ilm3	WYL-10-61-190.3 Mag3-Ilm3	WYL-10-61-190.3 Mag3-Ilm3
Line	52	39	52	40	52	41	52	42	52	43	52	44	52	45
Wt% Oxides	Magnetite	Ilmenite	Magnetite	Ilmenite	Magnetite	Ilmenite	Magnetite	Ilmenite	Magnetite	Ilmenite	Magnetite	Ilmenite	Magnetite	Ilmenite
SiO2	0.09	0.01	0.09	0.01	0.09	0.00	0.09	0.02	0.09	0.02	0.09	0.02	0.09	0.03
TiO2	17.84	49.97	17.84	50.00	17.84	49.79	17.84	49.71	17.84	50.69	17.84	51.17	17.84	50.33
Al2O3	9.12	0.02	9.12	0.00	9.12	0.01	9.12	0.00	9.12	0.00	9.12	0.00	9.12	0.00
Fe2O3(T)														
FeO(T)	70.56	44.84	70.56	45.06	70.56	44.81	70.56	44.88	70.56	44.68	70.56	44.81	70.56	44.82
MnO	2.08	3.86	2.08	3.78	2.08	4.04	2.08	3.91	2.08	4.04	2.08	3.69	2.08	3.97
MgO	0.08	0.01	0.08	0.01	0.08	0.00	0.08	0.00	0.08	0.02	0.08	0.02	0.08	0.00
CaO	0.00	0.00	0.00	0.00	0.00	0.00	0.00	0.01	0.00	0.00	0.00	0.01	0.00	0.00
Na2O														
K2O														
Cr2O3	0.01	0.00	0.01	0.00	0.01	0.00	0.01	0.00	0.01	0.00	0.01	0.00	0.01	0.00
BaO														
ZnO	1.43	0.03	1.43	0.04	1.43	0.00	1.43	0.04	1.43	0.03	1.43	0.01	1.43	0.00
V2O3	0.05	0.05	0.05	0.06	0.05	0.06	0.05	0.06	0.05	0.03	0.05	0.07	0.05	0.04
NiO	0.04	0.00	0.04	0.00	0.04	0.00	0.04	0.00	0.04	0.01	0.04	0.00	0.04	0.00
Nb2O3														
Sum:	101.297314	98.78563	101.297314	98.97075	101.297314	98.713918	101.297314	98.63461	101.297314	99.520994	101.297314	99.796086	101.297314	99.201063
Carmichael (1967)	**Recalculated Iron and Total**		**Recalculated Iron and Total**		**Recalculated Iron and Total**		**Recalculated Iron and Total**		**Recalculated Iron and Total**		**Recalculated Iron and Total**		**Recalculated Iron and Total**	
Fe2O3 wt. %	26.2	4.3	26.2	4.4	26.2	4.6	26.2	4.6	26.2	3.6	26.2	2.8	26.2	3.9
FeO wt. %	47.0	41.0	47.0	41.1	47.0	40.7	47.0	40.7	47.0	41.5	47.0	42.3	47.0	41.3
Total:	103.9	99.2	103.9	99.4	103.9	99.2	103.9	99.1	103.9	99.9	103.9	100.1	103.9	99.6
	Ulvöspinel	Ilmenite	Ulvöspinel	Ilmenite	Ulvöspinel	Ilmenite	Ulvöspinel	Ilmenite	Ulvöspinel	Ilmenite	Ulvöspinel	Ilmenite	Ulvöspinel	Ilmenite
Sum of Atomic mol proportion:	2.0892	1.5314	2.0892	1.5286	2.0892	1.5324	2.0892	1.5336	2.0892	1.5206	2.0892	1.5170	2.0892	1.5253
No. of Oxygen:	4	3	4	3	4	3	4	3	4	3	4	3	4	3
	Cation prop. (Carmichael 1967)		**Cation prop. (Carmichael 1967)**		**Cation prop. (Carmichael 1967)**		**Cation prop. (Carmichael 1967)**		**Cation prop. (Carmichael 1967)**		**Cation prop. (Carmichael 1967)**		**Cation prop. (Carmichael 1967)**	
Si	0.0031	0.0003	0.0031	0.0003	0.0031	0.0000	0.0031	0.0005	0.0031	0.0005	0.0031	0.0005	0.0031	0.0008
Ti	0.4667	0.9581	0.4667	0.9569	0.4667	0.9552	0.4667	0.9546	0.4667	0.9652	0.4667	0.9719	0.4667	0.9612
Al	0.3737	0.0005	0.3737	0.0000	0.3737	0.0003	0.3737	0.0000	0.3737	0.0000	0.3737	0.0000	0.3737	0.0000
Fe+3	0.6848	0.0818	0.6848	0.0843	0.6848	0.0880	0.6848	0.0885	0.6848	0.0679	0.6848	0.0536	0.6848	0.0750
Fe+2	1.3670	0.8740	1.3670	0.8744	1.3670	0.8678	1.3670	0.8695	1.3670	0.8778	1.3670	0.8926	1.3670	0.8765
Mn	0.0614	0.0834	0.0614	0.0816	0.0614	0.0873	0.0614	0.0846	0.0614	0.0865	0.0614	0.0788	0.0614	0.0854
Mg	0.0044	0.0005	0.0044	0.0004	0.0044	0.0000	0.0044	0.0000	0.0044	0.0009	0.0044	0.0006	0.0044	0.0000
Ca	0.0001	0.0001	0.0001	0.0000	0.0001	0.0001	0.0001	0.0002	0.0001	0.0000	0.0001	0.0003	0.0001	0.0001
Na	0.0000	0.0000	0.0000	0.0000	0.0000	0.0000	0.0000	0.0000	0.0000	0.0000	0.0000	0.0000	0.0000	0.0000
K	0.0000	0.0000	0.0000	0.0000	0.0000	0.0000	0.0000	0.0000	0.0000	0.0000	0.0000	0.0000	0.0000	0.0000
Cr	0.0002	0.0000	0.0002	0.0001	0.0002	0.0000	0.0002	0.0000	0.0002	0.0000	0.0002	0.0000	0.0002	0.0000
Ba	0.0000	0.0000	0.0000	0.0000	0.0000	0.0000	0.0000	0.0000	0.0000	0.0000	0.0000	0.0000	0.0000	0.0000
Zn	0.0366	0.0005	0.0366	0.0008	0.0366	0.0000	0.0366	0.0007	0.0366	0.0005	0.0366	0.0001	0.0366	0.0000
V	0.0013	0.0010	0.0013	0.0013	0.0013	0.0012	0.0013	0.0013	0.0013	0.0007	0.0013	0.0015	0.0013	0.0009
Ni	0.0012	0.0000	0.0012	0.0000	0.0012	0.0000	0.0012	0.0000	0.0012	0.0001	0.0012	0.0001	0.0012	0.0000
Nb	0.0000	0.0000	0.0000	0.0000	0.0000	0.0000	0.0000	0.0000	0.0000	0.0000	0.0000	0.0000	0.0000	0.0000
Total:	3.0003	2.0000	3.0003	2.0000	3.0003	2.0000	3.0003	2.0000	3.0003	2.0000	3.0003	2.0000	3.0003	2.0000
Calc. Methods:	Mol % Usp	Mol % Ilm	Mol % Usp	Mol % Ilm	Mol % Usp	Mol % Ilm	Mol % Usp	Mol % Ilm	Mol % Usp	Mol % Ilm	Mol % Usp	Mol % Ilm	Mol % Usp	Mol % Ilm
Carmichael (1967)	46.97%	95.84%	46.97%	95.72%	46.97%	95.52%	46.97%	95.51%	46.97%	96.57%	46.97%	97.24%	46.97%	96.20%
Anderson (1968)	52.62%	95.55%	52.62%	95.43%	52.62%	95.18%	52.62%	95.18%	52.62%	96.27%	52.62%	97.08%	52.62%	95.86%
Lindsley & Spencer (1982)	55.49%	95.55%	55.49%	95.43%	55.49%	95.18%	55.49%	95.18%	55.49%	96.28%	55.49%	97.08%	55.49%	95.86%
Stormer (1983)	66.20%	95.72%	66.20%	95.60%	66.20%	95.39%	66.20%	95.37%	66.20%	96.44%	66.20%	97.20%	66.20%	96.07%
Geothermometer by:														
X'Usp & X'Ilm from:	Temp (°C)		Temp (°C)		Temp (°C)		Temp (°C)		Temp (°C)		Temp (°C)		Temp (°C)	
Carmichael (1967)	766		770		776		777		740		712		753	
Anderson (1968)	807		811		819		819		781		748		796	
Lindsley & Spencer (1982)	823		827		836		836		797		762		813	
Stormer (1983)	888		893		901		901		857		819		873	
Average:	821		825		833		833		794		760		809	
Geothermobarometer by:														
X'Usp & X'Ilm from:	Temp (°C)	log10 fO2	Temp (°C)	log10 fO2	Temp (°C)	log10 fO2	Temp (°C)	log10 fO2	Temp (°C)	log10 fO2	Temp (°C)	log10 fO2	Temp (°C)	log10 fO2
Carmichael (1967)	671	-18.89	678	-18.63	689	-18.26	689	-18.23	628	-20.56	582	-22.55	650	-19.68
Anderson (1968)	711	-17.69	718	-17.46	733	-16.98	733	-16.99	664	-19.32	606	-21.63	692	-18.34
Lindsley & Spencer (1982)	726	-17.32	734	-17.08	750	-16.58	750	-16.59	676	-18.99	614	-21.36	706	-17.98
Stormer (1983)	791	-15.78	803	-15.48	820	-15.02	822	-14.98	726	-17.67	649	-20.24	760	-16.65
Average:	725		733		748		748		674		613		702	
		-17		-17		-17		-17		-19		-21		-18
Geothermobarometer by:														
X'Usp & X'Ilm from:	Temp (°C)	log10 fO2	Temp (°C)	log10 fO2	Temp (°C)	log10 fO2	Temp (°C)	log10 fO2	Temp (°C)	log10 fO2	Temp (°C)	log10 fO2	Temp (°C)	log10 fO2
Carmichael (1967)	700		706		715		716		662		619		682	
Anderson (1968)	735	-17.24	741	-17.05	753	-16.64	753	-16.65	695	-18.65	642	-20.70	719	-17.80
Lindsley & Spencer (1982)	748	-16.97	754	-16.76	767	-16.35	767	-16.35	705	-18.40	650	-20.49	731	-17.53
Stormer (1983)	805	-15.85	814	-15.60	828	-15.22	829	-15.18	750	-17.46	683	-19.72	779	-16.59
Average:	747		754		766		766		703		649		728	
		-17		-16		-16		-16		-18		-20		-17
Average for each pair	764		771		782		783		723		674		746	
Average for each pair		-17		-17		-16		-16		-18		-21		-18
Method Averages														
Powell & Powell (1977)														
Spencer & Lindsley (1981)														
Andersen & Lindsley (1985)														
Average for all pairs														

Table G-5. Magnetite-Ilmenite Grain 4

Sample #	WYL-10-61-190.3 Mag4-Ilm4-TiOx1	WYL-10-61-190.3 Mag4-Ilm4-TiOx1	WYL-10-61-190.3 Mag4-Ilm4-TiOx1	WYL-10-61-190.3 Mag4-Ilm4-TiOx1	WYL-10-61-190.3 Mag4-Ilm4-TiOx1	WYL-10-61-190.3 Mag4-Ilm4-TiOx1	WYL-10-61-190.3 Mag4-Ilm4-TiOx1	WYL-10-61-190.3 Mag4-Ilm4-TiOx1
Line	60	54	61	54	62	54	63	54
Wt% Oxides	**Magnetite**	**Ilmenite**	**Magnetite**	**Ilmenite**	**Magnetite**	**Ilmenite**	**Magnetite**	**Ilmenite**
SiO2	0.10	0.04	0.11	0.04	0.22	0.04	0.11	0.04
TiO2	0.55	50.34	0.22	50.34	0.25	50.34	0.20	50.34
Al2O3	0.34	0.01	0.36	0.01	0.46	0.01	0.34	0.01
Fe2O3(T)								
FeO(T)	92.67	44.32	92.64	44.32	92.35	44.32	92.75	44.32
MnO	0.06	4.15	0.04	4.15	0.03	4.15	0.02	4.15
MgO	0.00	0.01	0.00	0.01	0.02	0.01	0.00	0.01
CaO	0.00	0.00	0.01	0.00	0.01	0.00	0.00	0.00
Na2O								
K2O								
Cr2O3	0.02	0.00	0.00	0.00	0.00	0.00	0.00	0.00
BaO								
ZnO	0.00	0.03	0.00	0.03	0.06	0.03	0.00	0.03
V2O3	0.05	0.05	0.03	0.05	0.03	0.05	0.04	0.05
NiO	0.00	0.01	0.00	0.01	0.01	0.01	0.03	0.01
Nb2O3								
Sum:	93.79887	98.963294	93.409222	98.963294	93.434779	98.963294	93.48207	98.963294
Carmichael (1967)	**Recalculated Iron and Total**		**Recalculated Iron and Total**		**Recalculated Iron and Total**		**Recalculated Iron and Total**	
Fe2O3 wt. %	67.6	3.6	68.0	3.6	67.5	3.6	68.1	3.6
FeO wt. %	31.8	41.1	31.5	41.1	31.6	41.1	31.5	41.1
Total:	100.6	99.3	100.2	99.3	100.2	99.3	100.3	99.3
	Ulvöspinel	**Ilmenite**	**Ulvöspinel**	**Ilmenite**	**Ulvöspinel**	**Ilmenite**	**Ulvöspinel**	**Ilmenite**
Sum of Atomic mol proportion:	2.2953	1.5291	2.3038	1.5291	2.3016	1.5291	2.3024	1.5291
No. of Oxygen:	4	3	4	3	4	3	4	3
	Cation prop. (Carmichael 1967)		**Cation prop. (Carmichael 1967)**		**Cation prop. (Carmichael 1967)**		**Cation prop. (Carmichael 1967)**	
Si	0.0038	0.0010	0.0042	0.0010	0.0084	0.0010	0.0042	0.0010
Ti	0.0157	0.9637	0.0063	0.9637	0.0073	0.9637	0.0058	0.9637
Al	0.0155	0.0003	0.0161	0.0003	0.0208	0.0003	0.0153	0.0003
Fe+3	1.9432	0.0691	1.9618	0.0691	1.9470	0.0691	1.9630	0.0691
Fe+2	1.0175	0.8742	1.0089	0.8742	1.0116	0.8742	1.0093	0.8742
Mn	0.0020	0.0896	0.0012	0.0896	0.0010	0.0896	0.0005	0.0896
Mg	0.0000	0.0005	0.0000	0.0005	0.0010	0.0005	0.0000	0.0005
Ca	0.0000	0.0000	0.0003	0.0000	0.0003	0.0000	0.0000	0.0000
Na	0.0000	0.0000	0.0000	0.0000	0.0000	0.0000	0.0000	0.0000
K	0.0000	0.0000	0.0000	0.0000	0.0000	0.0000	0.0000	0.0000
Cr	0.0007	0.0000	0.0001	0.0000	0.0000	0.0000	0.0000	0.0000
Ba	0.0000	0.0000	0.0000	0.0000	0.0000	0.0000	0.0000	0.0000
Zn	0.0000	0.0005	0.0000	0.0005	0.0017	0.0005	0.0000	0.0005
V	0.0016	0.0010	0.0010	0.0010	0.0008	0.0010	0.0011	0.0010
Ni	0.0000	0.0003	0.0000	0.0003	0.0003	0.0003	0.0010	0.0003
Nb	0.0000	0.0000	0.0000	0.0000	0.0000	0.0000	0.0000	0.0000
Total:	3.0000	2.0001	3.0000	2.0001	3.0001	2.0001	3.0003	2.0001
Calc. Methods:	**Mol % Usp**	**Mol % Ilm**	**Mol % Usp**	**Mol % Ilm**	**Mol % Usp**	**Mol % Ilm**	**Mol % Usp**	**Mol % Ilm**
Carmichael (1967)	1.95%	96.47%	1.05%	96.47%	1.56%	96.47%	1.01%	96.47%
Anderson (1968)	1.48%	96.17%	0.57%	96.17%	0.69%	96.17%	0.56%	96.17%
Lindsley & Spencer (1982)	1.58%	96.17%	0.63%	96.17%	0.74%	96.17%	0.59%	96.17%
Stormer (1983)	1.60%	96.37%	0.64%	96.37%	0.75%	96.37%	0.59%	96.37%
Geothermometer by:	**Powell & Powell (1977)**							
X'Usp & X'Ilm from:	**Temp (°C)**		**Temp (°C)**		**Temp (°C)**		**Temp (°C)**	
Carmichael (1967)	417		382		404		380	
Anderson (1968)	406		355		365		354	
Lindsley & Spencer (1982)	410		361		368		357	
Stormer (1983)	407		358		366		355	
Average:	410		364		376		361	
Geothermobarometer by:	**Spencer & Lindsley (1981)**							
X'Usp & X'Ilm from:	**Temp (°C)**	**log10 fO2**	**Temp (°C)**	**log10 fO2**	**Temp (°C)**	**log10 fO2**	**Temp (°C)**	**log10 fO2**
Carmichael (1967)	523	-22.76	501	-23.22	515	-22.92	499	-23.25
Anderson (1968)	519	-22.45	485	-23.17	492	-23.03	485	-23.19
Lindsley & Spencer (1982)	521	-22.41	489	-23.10	494	-22.99	486	-23.16
Stormer (1983)	518	-22.74	485	-23.42	491	-23.31	483	-23.48
Average:	520	-23	490	-23	498	-23	488	-23
Geothermobarometer by:	**Andersen & Lindsley (1985)**							
X'Usp & X'Ilm from:	**Temp (°C)**	**log10 fO2**	**Temp (°C)**	**log10 fO2**	**Temp (°C)**	**log10 fO2**	**Temp (°C)**	**log10 fO2**
Carmichael (1967)	526		501		517		499	
Anderson (1968)	522	-22.22	483	-23.06	490	-22.89	482	-23.07
Lindsley & Spencer (1982)	524	-22.16	487	-22.97	493	-22.84	484	-23.04
Stormer (1983)	520	-22.50	483	-23.31	489	-23.17	480	-23.38
Average:	523	-22	488	-23	497	-23	486	-23
Average for each pair	484	-22.5	447	-23	457	-23	445	-23
Average for all pairs	452	-23.5						
Method averages					Ranges			
Powell & Powell (1977)		372			339 - 426			
Spencer & Lindsley (1981)		493	-23.6		462 - 534	-25.5 to -21.6		
Andersen & Lindsley (1985)		491	-23.4		456 - 539	-25.5 to -21.3		
		452	-23.5		339 - 539	-25.5 to -21.3		

Sample #	WYL-10-61-190.3 Mag4-Ilm4-TiOx1	WYL-10-61-190.3 Mag4-Ilm4-TiOx1	WYL-10-61-190.3 Mag4-Ilm4-TiOx1	WYL-10-61-190.3 Mag4-Ilm4-TiOx1	WYL-10-61-190.3 Mag4-Ilm4-TiOx1	WYL-10-61-190.3 Mag4-Ilm4-TiOx1	WYL-10-61-190.3 Mag4-Ilm4-TiOx1	WYL-10-61-190.3 Mag4-Ilm4-TiOx1
Line	64	54	60	55	61	55	62	55
Wt% Oxides	**Magnetite**	**Ilmenite**	**Magnetite**	**Ilmenite**	**Magnetite**	**Ilmenite**	**Magnetite**	**Ilmenite**
SiO2	0.13	0.04	0.10	0.04	0.11	0.04	0.22	0.04
TiO2	0.23	50.34	0.55	50.94	0.22	50.94	0.25	50.94
Al2O3	0.34	0.01	0.34	0.00	0.36	0.00	0.46	0.00
Fe2O3(T)								
FeO(T)	92.81	44.32	92.67	44.04	92.64	44.04	92.35	44.04
MnO	0.01	4.15	0.06	4.08	0.04	4.08	0.03	4.08
MgO	0.00	0.01	0.00	0.03	0.00	0.03	0.02	0.03
CaO	0.00	0.00	0.00	0.01	0.01	0.01	0.01	0.01
Na2O								
K2O								
Cr2O3	0.00	0.00	0.02	0.00	0.00	0.00	0.00	0.00
BaO								
ZnO	0.00	0.03	0.00	0.02	0.00	0.02	0.06	0.02
V2O3	0.05	0.05	0.05	0.05	0.03	0.05	0.03	0.05
NiO	0.00	0.01	0.00	0.00	0.00	0.00	0.01	0.00
Nb2O3								
Sum:	93.562499	98.963294	93.79887	99.212374	93.409222	99.212374	93.434779	99.212374
Carmichael (1967)	**Recalculated Iron and Total**		**Recalculated Iron and Total**		**Recalculated Iron and Total**		**Recalculated Iron and Total**	
Fe2O3 wt. %	68.0	3.6	67.6	2.7	68.0	2.7	67.5	2.7
FeO wt. %	31.6	41.1	31.8	41.6	31.5	41.6	31.6	41.6
Total:	100.4	99.3	100.6	99.5	100.2	99.5	100.2	99.5
	Ulvöspinel	**Ilmenite**	**Ulvöspinel**	**Ilmenite**	**Ulvöspinel**	**Ilmenite**	**Ulvöspinel**	**Ilmenite**
Sum of Atomic mol proportion:	2.3002	1.5291	2.2953	1.5258	2.3038	1.5258	2.3016	1.5258
No. of Oxygen:	4	3	4	3	4	3	4	3
	Cation prop. (Carmichael 1967)		**Cation prop. (Carmichael 1967)**		**Cation prop. (Carmichael 1967)**		**Cation prop. (Carmichael 1967)**	
Si	0.0049	0.0010	0.0038	0.0009	0.0042	0.0009	0.0084	0.0009
Ti	0.0067	0.9637	0.0157	0.9731	0.0063	0.9731	0.0073	0.9731
Al	0.0152	0.0003	0.0155	0.0000	0.0161	0.0000	0.0208	0.0000
Fe+3	1.9601	0.0691	1.9432	0.0509	1.9618	0.0509	1.9470	0.0509
Fe+2	1.0113	0.8742	1.0175	0.8844	1.0089	0.8844	1.0116	0.8844
Mn	0.0003	0.0896	0.0020	0.0879	0.0012	0.0879	0.0010	0.0879
Mg	0.0000	0.0005	0.0000	0.0010	0.0000	0.0010	0.0010	0.0010
Ca	0.0000	0.0000	0.0000	0.0004	0.0003	0.0004	0.0003	0.0004
Na	0.0000	0.0000	0.0000	0.0000	0.0000	0.0000	0.0000	0.0000
K	0.0000	0.0000	0.0000	0.0000	0.0000	0.0000	0.0000	0.0000
Cr	0.0000	0.0000	0.0007	0.0000	0.0001	0.0000	0.0000	0.0000
Ba	0.0000	0.0000	0.0000	0.0000	0.0000	0.0000	0.0000	0.0000
Zn	0.0000	0.0005	0.0000	0.0004	0.0000	0.0004	0.0017	0.0004
V	0.0014	0.0010	0.0016	0.0010	0.0010	0.0010	0.0008	0.0010
Ni	0.0000	0.0003	0.0000	0.0001	0.0000	0.0001	0.0003	0.0001
Nb	0.0000	0.0000	0.0000	0.0000	0.0000	0.0000	0.0000	0.0000
Total:	3.0000	2.0001	3.0000	2.0000	3.0000	2.0000	3.0001	2.0000
Calc. Methods:	**Mol % Usp**	**Mol % Ilm**	**Mol % Usp**	**Mol % Ilm**	**Mol % Usp**	**Mol % Ilm**	**Mol % Usp**	**Mol % Ilm**
Carmichael (1967)	1.16%	96.47%	1.95%	97.40%	1.05%	97.40%	1.56%	97.40%
Anderson (1968)	0.66%	96.17%	1.48%	97.20%	0.57%	97.20%	0.69%	97.20%
Lindsley & Spencer (1982)	0.68%	96.17%	1.58%	97.20%	0.63%	97.20%	0.74%	97.20%
Stormer (1983)	0.69%	96.37%	1.60%	97.33%	0.64%	97.33%	0.75%	97.33%
Geothermometer by: X'Usp & X'Ilm from:	**Temp (°C)**		**Temp (°C)**		**Temp (°C)**		**Temp (°C)**	
Carmichael (1967)	388		399		366		387	
Anderson (1968)	363		388		340		349	
Lindsley & Spencer (1982)	364		392		345		352	
Stormer (1983)	362		390		343		350	
Average:	369		392		349		360	
Geothermobarometer by: X'Usp & X'Ilm from:	**Temp (°C)**	**log10 fO2**	**Temp (°C)**	**log10 fO2**	**Temp (°C)**	**log10 fO2**	**Temp (°C)**	**log10 fO2**
Carmichael (1967)	504	-23.14	499	-24.73	479	-25.19	492	-24.89
Anderson (1968)	490	-23.06	496	-24.44	464	-25.16	470	-25.02
Lindsley & Spencer (1982)	491	-23.05	498	-24.40	467	-25.09	472	-24.97
Stormer (1983)	488	-23.37	495	-24.70	464	-25.39	469	-25.27
Average	493	-23	497	-25	468	-25	476	-25
Geothermobarometer by: X'Usp & X'Ilm from:	**Temp (°C)**	**log10 fO2**	**Temp (°C)**	**log10 fO2**	**Temp (°C)**	**log10 fO2**	**Temp (°C)**	**log10 fO2**
Carmichael (1967)	505		499		475		491	
Anderson (1968)	489	-22.92	495	-24.29	458	-25.16	465	-24.99
Lindsley & Spencer (1982)	490	-22.91	497	-24.24	462	-25.07	468	-24.94
Stormer (1983)	486	-23.25	494	-24.56	459	-25.39	465	-25.25
Average:	492	-23	496	-24	464	-25	472	-25
Average for each pair	452	-23	462	-24	427	-25	436	-25
Average for all pairs								
Method averages								
Powell & Powell (1977)								
Spencer & Lindsley (1981)								
Andersen & Lindsley (1985)								

Sample #	WYL-10-61-190.3 Mag4-Ilm4-TiOx1	WYL-10-61-190.3 Mag4-Ilm4-TiOx1	WYL-10-61-190.3 Mag4-Ilm4-TiOx1	WYL-10-61-190.3 Mag4-Ilm4-TiOx1	WYL-10-61-190.3 Mag4-Ilm4-TiOx1	WYL-10-61-190.3 Mag4-Ilm4-TiOx1	WYL-10-61-190.3 Mag4-Ilm4-TiOx1	WYL-10-61-190.3 Mag4-Ilm4-TiOx1
Line	63	55	64	55	60	58	61	58
Wt% Oxides	**Magnetite**	**Ilmenite**	**Magnetite**	**Ilmenite**	**Magnetite**	**Ilmenite**	**Magnetite**	**Ilmenite**
SiO2	0.11	0.04	0.13	0.04	0.10	0.04	0.11	0.04
TiO2	0.20	50.94	0.23	50.94	0.55	50.09	0.22	50.09
Al2O3	0.34	0.00	0.34	0.00	0.34	0.01	0.36	0.01
Fe2O3(T)								
FeO(T)	92.75	44.04	92.81	44.04	92.67	44.94	92.64	44.94
MnO	0.02	4.08	0.01	4.08	0.06	3.82	0.04	3.82
MgO	0.00	0.03	0.00	0.03	0.00	0.03	0.00	0.03
CaO	0.00	0.01	0.00	0.01	0.00	0.00	0.01	0.00
Na2O								
K2O								
Cr2O3	0.00	0.00	0.00	0.00	0.02	0.00	0.00	0.00
BaO								
ZnO	0.00	0.02	0.00	0.02	0.00	0.00	0.00	0.00
V2O3	0.04	0.05	0.05	0.05	0.05	0.07	0.03	0.07
NiO	0.03	0.00	0.00	0.00	0.00	0.02	0.00	0.02
Nb2O3								
Sum:	93.48207	99.212374	93.562499	99.212374	93.79887	99.016789	93.409222	99.016789
Carmichael (1967)	**Recalculated Iron and Total**		**Recalculated Iron and Total**		**Recalculated Iron and Total**		**Recalculated Iron and Total**	
Fe2O3 wt. %	68.1	2.7	68.0	2.7	67.6	4.2	68.0	4.2
FeO wt. %	31.5	41.6	31.6	41.6	31.8	41.2	31.5	41.2
Total:	100.3	99.5	100.4	99.5	100.6	99.4	100.2	99.4
	Ulvöspinel	**Ilmenite**	**Ulvöspinel**	**Ilmenite**	**Ulvöspinel**	**Ilmenite**	**Ulvöspinel**	**Ilmenite**
Sum of Atomic mol proportion:	2.3024	1.5258	2.3002	1.5258	2.2953	1.5277	2.3038	1.5277
No. of Oxygen:	4	3	4	3	4	3	4	3
	Cation prop. (Carmichael 1967)		**Cation prop. (Carmichael 1967)**		**Cation prop. (Carmichael 1967)**		**Cation prop. (Carmichael 1967)**	
Si	0.0042	0.0009	0.0049	0.0009	0.0038	0.0011	0.0042	0.0011
Ti	0.0058	0.9731	0.0067	0.9731	0.0157	0.9582	0.0063	0.9582
Al	0.0153	0.0000	0.0152	0.0000	0.0155	0.0002	0.0161	0.0002
Fe+3	1.9630	0.0509	1.9601	0.0509	1.9432	0.0796	1.9618	0.0796
Fe+2	1.0093	0.8844	1.0113	0.8844	1.0175	0.8760	1.0089	0.8760
Mn	0.0005	0.0879	0.0003	0.0879	0.0020	0.0823	0.0012	0.0823
Mg	0.0000	0.0010	0.0000	0.0010	0.0000	0.0010	0.0000	0.0010
Ca	0.0000	0.0004	0.0000	0.0004	0.0000	0.0000	0.0003	0.0000
Na	0.0000	0.0000	0.0000	0.0000	0.0000	0.0000	0.0000	0.0000
K	0.0000	0.0000	0.0000	0.0000	0.0000	0.0000	0.0000	0.0000
Cr	0.0000	0.0000	0.0000	0.0000	0.0007	0.0000	0.0001	0.0000
Ba	0.0000	0.0000	0.0000	0.0000	0.0000	0.0000	0.0000	0.0000
Zn	0.0000	0.0004	0.0000	0.0004	0.0000	0.0000	0.0000	0.0000
V	0.0011	0.0010	0.0014	0.0010	0.0016	0.0015	0.0010	0.0015
Ni	0.0010	0.0001	0.0000	0.0001	0.0000	0.0004	0.0000	0.0004
Nb	0.0000	0.0000	0.0000	0.0000	0.0000	0.0000	0.0000	0.0000
Total:	3.0003	2.0000	3.0000	2.0000	3.0000	2.0001	3.0000	2.0001
Calc. Methods:	**Mol % Usp**	**Mol % Ilm**	**Mol % Usp**	**Mol % Ilm**	**Mol % Usp**	**Mol % Ilm**	**Mol % Usp**	**Mol % Ilm**
Carmichael (1967)	1.01%	97.40%	1.16%	97.40%	1.95%	95.93%	1.05%	95.93%
Anderson (1968)	0.56%	97.20%	0.66%	97.20%	1.48%	95.59%	0.57%	95.59%
Lindsley & Spencer (1982)	0.59%	97.20%	0.68%	97.20%	1.58%	95.60%	0.63%	95.60%
Stormer (1983)	0.59%	97.33%	0.69%	97.33%	1.60%	95.84%	0.64%	95.84%
Geothermometer by:								
X'Usp & X'Ilm from:	**Temp (°C)**		**Temp (°C)**		**Temp (°C)**		**Temp (°C)**	
Carmichael (1967)	364		371		426		390	
Anderson (1968)	339		347		414		363	
Lindsley & Spencer (1982)	341		348		418		368	
Stormer (1983)	340		347		415		365	
Average:	346		353		418		371	
Geothermobarometer by:								
X'Usp & X'Ilm from:	**Temp (°C)**	**log10 fO2**	**Temp (°C)**	**log10 fO2**	**Temp (°C)**	**log10 fO2**	**Temp (°C)**	**log10 fO2**
Carmichael (1967)	477	-25.22	482	-25.11	534	-21.87	511	-22.33
Anderson (1968)	463	-25.18	469	-25.05	530	-21.59	495	-22.31
Lindsley & Spencer (1982)	465	-25.15	469	-25.04	532	-21.55	499	-22.23
Stormer (1983)	462	-25.45	467	-25.33	528	-21.88	495	-22.57
Average:	467	-25	472	-25	531	-22	500	-22
Geothermobarometer by:								
X'Usp & X'Ilm from:	**Temp (°C)**	**log10 fO2**	**Temp (°C)**	**log10 fO2**	**Temp (°C)**	**log10 fO2**	**Temp (°C)**	**log10 fO2**
Carmichael (1967)	474		479		539		512	
Anderson (1968)	458	-25.18	464	-25.02	534	-21.32	494	-22.14
Lindsley & Spencer (1982)	459	-25.14	465	-25.01	536	-21.27	498	-22.06
Stormer (1983)	456	-25.46	462	-25.32	532	-21.61	494	-22.41
Average:	462	-25	467	-25	535	-21	500	-22
Average for each pair	425	-25	431	-25	495	-22	457	-22
Average for all pairs								
Method averages								
Powell & Powell (1977)								
Spencer & Lindsley (1981)								
Andersen & Lindsley (1985)								

Sample #	WYL-10-61-190.3 Mag4-Ilm4-TiOx1	WYL-10-61-190.3 Mag4-Ilm4-TiOx1	WYL-10-61-190.3 Mag4-Ilm4-TiOx1	WYL-10-61-190.3 Mag4-Ilm4-TiOx1	WYL-10-61-190.3 Mag4-Ilm4-TiOx1	WYL-10-61-190.3 Mag4-Ilm4-TiOx1	WYL-10-61-190.3 Mag4-Ilm4-TiOx1	WYL-10-61-190.3 Mag4-Ilm4-TiOx1
Line	62	58	63	58	64	58	60	59
Wt% Oxides	**Magnetite**	**Ilmenite**	**Magnetite**	**Ilmenite**	**Magnetite**	**Ilmenite**	**Magnetite**	**Ilmenite**
SiO2	0.22	0.04	0.11	0.04	0.13	0.04	0.10	0.04
TiO2	0.25	50.09	0.20	50.09	0.23	50.09	0.55	50.79
Al2O3	0.46	0.01	0.34	0.01	0.34	0.01	0.34	0.01
Fe2O3(T)								
FeO(T)	92.35	44.94	92.75	44.94	92.81	44.94	92.67	44.28
MnO	0.03	3.82	0.02	3.82	0.01	3.82	0.06	4.21
MgO	0.02	0.03	0.00	0.03	0.00	0.03	0.00	0.01
CaO	0.01	0.00	0.00	0.00	0.00	0.00	0.00	0.00
Na2O								
K2O								
Cr2O3	0.00	0.00	0.00	0.00	0.00	0.00	0.02	0.00
BaO								
ZnO	0.06	0.00	0.00	0.00	0.00	0.00	0.00	0.00
V2O3	0.03	0.07	0.04	0.07	0.05	0.07	0.05	0.06
NiO	0.01	0.02	0.03	0.02	0.00	0.02	0.00	0.02
Nb2O3								
Sum:	93.434779	99.016789	93.48207	99.016789	93.562499	99.016789	93.79887	99.42729
Carmichael (1967)	**Recalculated Iron and Total**		**Recalculated Iron and Total**		**Recalculated Iron and Total**		**Recalculated Iron and Total**	
Fe2O3 wt. %	67.5	4.2	68.1	4.2	68.0	4.2	67.6	3.1
FeO wt. %	31.6	41.2	31.5	41.2	31.6	41.2	31.8	41.5
Total:	100.2	99.4	100.3	99.4	100.4	99.4	100.6	99.7
	Ulvöspinel	**Ilmenite**	**Ulvöspinel**	**Ilmenite**	**Ulvöspinel**	**Ilmenite**	**Ulvöspinel**	**Ilmenite**
Sum of Atomic mol proportion:	2.3016	1.5277	2.3024	1.5277	2.3002	1.5277	2.2953	1.5223
No. of Oxygen:	4	3	4	3	4	3	4	3
	Cation prop. (Carmichael 1967)		**Cation prop. (Carmichael 1967)**		**Cation prop. (Carmichael 1967)**		**Cation prop. (Carmichael 1967)**	
Si	0.0084	0.0011	0.0042	0.0011	0.0049	0.0011	0.0038	0.0011
Ti	0.0073	0.9582	0.0058	0.9582	0.0067	0.9582	0.0157	0.9681
Al	0.0208	0.0002	0.0153	0.0002	0.0152	0.0002	0.0155	0.0003
Fe+3	1.9470	0.0796	1.9630	0.0796	1.9601	0.0796	1.9432	0.0598
Fe+2	1.0116	0.8760	1.0093	0.8760	1.0113	0.8760	1.0175	0.8785
Mn	0.0010	0.0823	0.0005	0.0823	0.0003	0.0823	0.0020	0.0903
Mg	0.0010	0.0010	0.0000	0.0010	0.0000	0.0010	0.0000	0.0003
Ca	0.0003	0.0000	0.0000	0.0000	0.0000	0.0000	0.0000	0.0001
Na	0.0000	0.0000	0.0000	0.0000	0.0000	0.0000	0.0000	0.0000
K	0.0000	0.0000	0.0000	0.0000	0.0000	0.0000	0.0000	0.0000
Cr	0.0000	0.0000	0.0000	0.0000	0.0000	0.0000	0.0007	0.0000
Ba	0.0000	0.0000	0.0000	0.0000	0.0000	0.0000	0.0000	0.0000
Zn	0.0017	0.0000	0.0000	0.0000	0.0000	0.0000	0.0000	0.0000
V	0.0008	0.0015	0.0011	0.0015	0.0014	0.0015	0.0016	0.0013
Ni	0.0003	0.0004	0.0010	0.0004	0.0000	0.0004	0.0000	0.0004
Nb	0.0000	0.0000	0.0000	0.0000	0.0000	0.0000	0.0000	0.0000
Total:	3.0001	2.0001	3.0003	2.0001	3.0000	2.0001	3.0000	2.0001
Calc. Methods:	**Mol % Usp**	**Mol % Ilm**	**Mol % Usp**	**Mol % Ilm**	**Mol % Usp**	**Mol % Ilm**	**Mol % Usp**	**Mol % Ilm**
Carmichael (1967)	1.56%	95.93%	1.01%	95.93%	1.16%	95.93%	1.95%	96.92%
Anderson (1968)	0.69%	95.59%	0.56%	95.59%	0.66%	95.59%	1.48%	96.66%
Lindsley & Spencer (1982)	0.74%	95.60%	0.59%	95.60%	0.68%	95.60%	1.58%	96.66%
Stormer (1983)	0.75%	95.84%	0.59%	95.84%	0.69%	95.84%	1.60%	96.86%
Geothermometer by: X'Usp & X'Ilm from:	**Temp (°C)**		**Temp (°C)**		**Temp (°C)**		**Temp (°C)**	
Carmichael (1967)	413		388		396		409	
Anderson (1968)	372		362		370		398	
Lindsley & Spencer (1982)	375		364		371		402	
Stormer (1983)	373		362		369		399	
Average:	383		369		377		402	
Geothermobarometer by: X'Usp & X'Ilm from:	**Temp (°C)**	**log10 fO2**	**Temp (°C)**	**log10 fO2**	**Temp (°C)**	**log10 fO2**	**Temp (°C)**	**log10 fO2**
Carmichael (1967)	526	-22.03	510	-22.36	515	-22.25	512	-23.62
Anderson (1968)	502	-22.16	494	-22.32	500	-22.19	509	-23.31
Lindsley & Spencer (1982)	504	-22.12	496	-22.29	501	-22.18	511	-23.26
Stormer (1983)	501	-22.45	492	-22.63	498	-22.51	507	-23.66
Average	508	-22	498	-22	504	-22	510	-23
Geothermobarometer by: X'Usp & X'Ilm from:	**Temp (°C)**	**log10 fO2**	**Temp (°C)**	**log10 fO2**	**Temp (°C)**	**log10 fO2**	**Temp (°C)**	**log10 fO2**
Carmichael (1967)	529		511		517		514	
Anderson (1968)	501	-21.98	493	-22.16	500	-22.01	510	-23.11
Lindsley & Spencer (1982)	504	-21.93	495	-22.13	501	-22.00	513	-23.05
Stormer (1983)	500	-22.27	491	-22.48	497	-22.35	508	-23.46
Average:	509	-22	497	-22	504	-22	511	-23
Average for each pair	467	-22	455	-22	461	-22	474	-23
Average for all pairs								
Method averages								
Powell & Powell (1977)								
Spencer & Lindsley (1981)								
Andersen & Lindsley (1985)								

Sample #	WYL-10-61-190.3 Mag4-Ilm4-TiOx1	WYL-10-61-190.3 Mag4-Ilm4-TiOx1	WYL-10-61-190.3 Mag4-Ilm4-TiOx1	WYL-10-61-190.3 Mag4-Ilm4-TiOx1	WYL-10-61-190.3 Mag4-Ilm4-TiOx1	WYL-10-61-190.3 Mag4-Ilm4-TiOx1	WYL-10-61-190.3 Mag4-Ilm4-TiOx1	WYL-10-61-190.3 Mag4-Ilm4-TiOx1
Line	61	59	62	59	63	59	64	59
Wt% Oxides	**Magnetite**	**Ilmenite**	**Magnetite**	**Ilmenite**	**Magnetite**	**Ilmenite**	**Magnetite**	**Ilmenite**
SiO2	0.11	0.04	0.22	0.04	0.11	0.04	0.13	0.04
TiO2	0.22	50.79	0.25	50.79	0.20	50.79	0.23	50.79
Al2O3	0.36	0.01	0.46	0.01	0.34	0.01	0.34	0.01
Fe2O3(T)								
FeO(T)	92.64	44.28	92.35	44.28	92.75	44.28	92.81	44.28
MnO	0.04	4.21	0.03	4.21	0.02	4.21	0.01	4.21
MgO	0.00	0.01	0.02	0.01	0.00	0.01	0.00	0.01
CaO	0.01	0.00	0.01	0.00	0.00	0.00	0.00	0.00
Na2O								
K2O								
Cr2O3	0.00	0.00	0.00	0.00	0.00	0.00	0.00	0.00
BaO								
ZnO	0.00	0.00	0.06	0.00	0.00	0.00	0.00	0.00
V2O3	0.03	0.06	0.03	0.06	0.04	0.06	0.05	0.06
NiO	0.00	0.02	0.01	0.02	0.03	0.02	0.00	0.02
Nb2O3								
Sum:	93.409222	99.42729	93.434779	99.42729	93.48207	99.42729	93.562499	99.42729
Carmichael (1967)	**Recalculated Iron and Total**		**Recalculated Iron and Total**		**Recalculated Iron and Total**		**Recalculated Iron and Total**	
Fe2O3 wt. %	68.0	3.1	67.5	3.1	68.1	3.1	68.0	3.1
FeO wt. %	31.5	41.5	31.6	41.5	31.5	41.5	31.6	41.5
Total:	100.2	99.7	100.2	99.7	100.3	99.7	100.4	99.7
	Ulvöspinel	**Ilmenite**	**Ulvöspinel**	**Ilmenite**	**Ulvöspinel**	**Ilmenite**	**Ulvöspinel**	**Ilmenite**
Sum of Atomic mol proportion:	2.3038	1.5223	2.3016	1.5223	2.3024	1.5223	2.3002	1.5223
No. of Oxygen:	4	3	4	3	4	3	4	3
	Cation prop. (Carmichael 1967)		**Cation prop. (Carmichael 1967)**		**Cation prop. (Carmichael 1967)**		**Cation prop. (Carmichael 1967)**	
Si	0.0042	0.0011	0.0084	0.0011	0.0042	0.0011	0.0049	0.0011
Ti	0.0063	0.9681	0.0073	0.9681	0.0058	0.9681	0.0067	0.9681
Al	0.0161	0.0003	0.0208	0.0003	0.0153	0.0003	0.0152	0.0003
Fe+3	1.9618	0.0598	1.9470	0.0598	1.9630	0.0598	1.9601	0.0598
Fe+2	1.0089	0.8785	1.0116	0.8785	1.0093	0.8785	1.0113	0.8785
Mn	0.0012	0.0903	0.0010	0.0903	0.0005	0.0903	0.0003	0.0903
Mg	0.0000	0.0003	0.0010	0.0003	0.0000	0.0003	0.0000	0.0003
Ca	0.0003	0.0001	0.0003	0.0001	0.0000	0.0001	0.0000	0.0001
Na	0.0000	0.0000	0.0000	0.0000	0.0000	0.0000	0.0000	0.0000
K	0.0000	0.0000	0.0000	0.0000	0.0000	0.0000	0.0000	0.0000
Cr	0.0001	0.0000	0.0000	0.0000	0.0000	0.0000	0.0000	0.0000
Ba	0.0000	0.0000	0.0000	0.0000	0.0000	0.0000	0.0000	0.0000
Zn	0.0000	0.0000	0.0017	0.0000	0.0000	0.0000	0.0000	0.0000
V	0.0010	0.0013	0.0008	0.0013	0.0011	0.0013	0.0014	0.0013
Ni	0.0000	0.0004	0.0003	0.0004	0.0010	0.0004	0.0000	0.0004
Nb	0.0000	0.0000	0.0000	0.0000	0.0000	0.0000	0.0000	0.0000
Total:	3.0000	2.0001	3.0001	2.0001	3.0003	2.0001	3.0000	2.0001
Calc. Methods:	**Mol % Usp**	**Mol % Ilm**	**Mol % Usp**	**Mol % Ilm**	**Mol % Usp**	**Mol % Ilm**	**Mol % Usp**	**Mol % Ilm**
Carmichael (1967)	1.05%	96.92%	1.56%	96.92%	1.01%	96.92%	1.16%	96.92%
Anderson (1968)	0.57%	96.66%	0.69%	96.66%	0.56%	96.66%	0.66%	96.66%
Lindsley & Spencer (1982)	0.63%	96.66%	0.74%	96.66%	0.59%	96.66%	0.68%	96.66%
Stormer (1983)	0.64%	96.86%	0.75%	96.86%	0.59%	96.86%	0.69%	96.86%
Geothermometer by: X'Usp & X'Ilm from:	**Temp (°C)**		**Temp (°C)**		**Temp (°C)**		**Temp (°C)**	
Carmichael (1967)	375		396		373		380	
Anderson (1968)	349		358		348		356	
Lindsley & Spencer (1982)	354		361		350		357	
Stormer (1983)	351		359		347		355	
Average:	357		368		354		362	
Geothermobarometer by: X'Usp & X'Ilm from:	**Temp (°C)**	**log10 fO2**	**Temp (°C)**	**log10 fO2**	**Temp (°C)**	**log10 fO2**	**Temp (°C)**	**log10 fO2**
Carmichael (1967)	491	-24.08	505	-23.78	489	-24.12	494	-24.00
Anderson (1968)	476	-24.03	482	-23.89	475	-24.05	481	-23.92
Lindsley & Spencer (1982)	479	-23.95	484	-23.84	477	-24.01	482	-23.90
Stormer (1983)	475	-24.35	481	-24.23	473	-24.41	478	-24.29
Average	480	-24	488	-24	479	-24	484	-24
Geothermobarometer by: X'Usp & X'Ilm from:	**Temp (°C)**	**log10 fO2**	**Temp (°C)**	**log10 fO2**	**Temp (°C)**	**log10 fO2**	**Temp (°C)**	**log10 fO2**
Carmichael (1967)	489		505		488		493	
Anderson (1968)	472	-23.96	479	-23.79	471	-23.98	478	-23.83
Lindsley & Spencer (1982)	476	-23.87	482	-23.73	473	-23.94	479	-23.81
Stormer (1983)	472	-24.28	477	-24.14	469	-24.35	474	-24.22
Average:	477	-24	486	-24	475	-24	481	-24
Average for each pair	438	-24	447	-24	436	-24	442	-24
Average for all pairs								
Method averages								
Powell & Powell (1977)								
Spencer & Lindsley (1981)								
Andersen & Lindsley (1985)								

APPENDIX H

EMPA DETECTION LIMITS

Table H-1. EMPA Detection Limits
Appendix for Chapter 3 (McKechnie et al. 2012a)

Sask. Research Council Cameca SX-100				Univ. of Saskatchewan JEOL 8600 Superprobe					
Uraninite, thorite, zircon, monazite				Pyrochlore		Xenotime		Biotite	
Si	0.0023	Y	0.0125	Si	0.0125	Si	0.0120	Si	0.0115
Ti	0.0079	La	0.0233	Ti	0.0210	Th	0.2110	Ti	0.0215
Al	0.0027	Ce	0.0218	Th	0.2110	U	0.2700	Al	0.0090
Fe	0.0066	Pr	0.0188	U	0.2720	Al	0.0230	Cr	0.0325
Mn	0.0059	Nd	0.0200	Nb	0.0811	Y	0.0450	Fe	0.0314
Mg	0.0029	Sm	0.0171	Al	0.0723	La	0.0950	Mg	0.0088
Ca	0.0028	Gd	0.0187	Cr	0.0325	Ce	0.0890	Mn	0.0266
P	0.0035	Dy	0.0171	Ce	0.0862	Pr	0.1223	Ca	0.0150
U	0.0299	Er	0.0225	La	0.0972	Nd	0.0760	Na	0.0112
Th	0.0287	Cr	0.0028	Nd	0.0775	Sm	0.1240	K	0.0081
Pb	0.0268	V	0.0064	Gd	0.0712	Gd	0.0720	F	0.0448
Zr	0.0205	Zn	0.0103	Dy	0.0732	Dy	0.0736	Cl	0.0079
Hf	0.0205	Ni	0.0066	Fe	0.0375	Tb	0.0680		
				Mg	0.0142	Ho	0.0698		
				Mn	0.0270	Er	0.0740		
				Ni	0.0445	Yb	0.0819		
				Zn	0.0530	Fe	0.0360		
				Ca	0.0200	Ca	0.0150		
						P	0.0107		

Values are expressed in wt.%.

APPENDIX I

PELITIC GNEISS MINERAL CHEMISTRY

Supplementary Data Table 1 for Chapter 4 (McKechnie *et al.* 2012b)

- All mineral formulae except Bt were calculated using CALCMIN (Brandelik, 2009) with minor changes made to the calculation schemes to include additional elements not in the original subroutines of Brandelik.
- Biotite chemical formulas were calculated using Andy Tindle's spreadsheet software. Li_2O and H_2O calculations after Tindle and Webb (1990) European Journal of Mineralogy, vol. 2, pgs. 595-610.
- Monazite chemical ages calculated using the formula of Montel *et al.* (1996)
- T's given for Bt were calculated using the Ti-in-biotite geothermometer of Henry *et al.* (2005)

Table I-1. Biotite Chemistry

Sample/Photo	Point	Location	SiO2	TiO2	Al2O3	FeO	MnO	MgO	CaO	Na2O	K2O	BaO	Cs2O	F	Cl	Cr2O3	Li2O*	H2O*	Subtotal
WYL-09-44-61.4 d biot 4	4	matrix adj to Grt	35.88	1.97	16.13	23.92	0.06	8.75	0.02	0.16	9.24	-	-	0.00	0.10	0.09	0.75	3.90	100.97
WYL-09-44-61.4 e biot 5	5	matrix adj to Grt	36.02	1.97	16.20	24.45	0.06	8.90	0.00	0.16	8.91	-	-	0.00	0.11	0.00	0.79	3.92	101.49
WYL-09-44-61.4 f biot 10	10	matrix adj to Grt in embayme	35.79	1.93	16.04	23.34	0.05	8.74	0.00	0.17	9.28	-	-	0.00	0.12	0.02	0.72	3.87	100.07
WYL-09-44-61.4 f biot 6	6	in Grt core	36.50	3.02	15.46	21.44	0.05	10.42	0.00	0.30	8.84	-	-	0.00	0.09	0.04	0.92	3.96	101.04
WYL-09-44-61.4 f biot 7	7	in Grt rim	35.35	1.94	15.92	24.18	0.06	8.80	0.00	0.21	9.18	-	-	0.00	0.06	0.00	0.59	3.87	100.15
WYL-09-44-61.4 f biot 8	8	matrix adj to Grt	35.62	1.78	15.96	23.65	0.10	8.52	0.00	0.17	9.00	-	-	0.00	0.07	0.09	0.67	3.85	99.48
WYL-09-44-61.4 f biot 9	9	matrix adj to Grt	35.55	1.58	16.07	24.24	0.06	8.85	0.00	0.20	9.40	-	-	0.00	0.10	0.06	0.65	3.87	100.63
WYL-09-44-61.4 g biot 11-12	11	in Grt core, has Grt inclusion	36.83	2.80	15.27	21.31	0.03	10.36	0.00	0.21	7.88	-	-	0.00	0.16	0.07	1.02	3.93	99.87
WYL-09-44-61.4 g biot 13	12	in Grt	35.67	2.42	15.76	23.23	0.02	8.74	0.05	0.23	9.36	-	-	0.00	0.06	0.09	0.69	3.88	100.19
WYL-09-44-61.4 g biot 14	13	matrix adj to Grt	35.17	1.75	16.32	24.16	0.11	8.55	0.00	0.22	9.69	-	-	0.00	0.05	0.02	0.54	3.87	100.45
WYL-09-44-61.4 g biot 15	14	matrix adj to Grt	35.95	1.83	16.24	23.39	0.04	8.77	0.06	0.21	9.09	-	-	0.00	0.12	0.03	0.77	3.89	100.40
WYL-09-44-61.4c biot 2	2	in Grt near rim	36.95	1.93	15.97	23.07	0.08	10.06	0.00	0.19	6.55	-	-	0.00	0.10	0.08	1.05	3.95	99.98
WYL-09-44-61.4c biot 3	3	in Grt near rim	35.72	2.17	15.46	23.82	0.08	8.98	0.04	0.26	8.75	-	-	0.00	0.11	0.00	0.70	3.86	99.95
WYL-09-44-61.4c biotite #1	1	in Grt	36.13	1.97	15.95	23.92	0.08	8.80	0.00	0.22	8.78	-	-	0.00	0.08	0.02	0.82	3.91	100.68
WYL-09-49-36.1 bio-1 image 12	132	matrix adj to Grt	35.95	3.49	18.48	18.34	0.03	9.37	0.00	0.16	10.08	0.03	0.01	1.21	0.07	-	0.77	3.42	101.40
WYL-09-49-36.1 bio-1 image 12	133	matrix adj to Grt	35.80	3.49	18.42	18.23	0.04	9.29	0.00	0.17	9.98	0.07	0.00	1.16	0.07	-	0.72	3.43	100.87
WYL-09-49-36.1 bio-1 image 12	134	matrix adj to Grt	35.79	3.48	18.52	18.32	0.04	9.43	0.00	0.16	10.13	0.00	0.00	1.28	0.06	-	0.72	3.39	101.32
WYL-09-49-36.1 bio-1 image 12	135	matrix adj to Grt	35.75	3.42	18.50	18.23	0.04	9.26	0.00	0.16	10.06	0.04	0.00	1.04	0.06	-	0.71	3.48	100.77
WYL-09-49-36.1 bio-2 image 14	136	in Grt near rim	36.32	5.23	17.62	16.41	0.02	10.70	0.00	0.32	9.93	0.05	0.01	1.24	0.08	-	0.87	3.47	102.27
WYL-09-49-36.1 bio-2 image 14	137	in Grt near rim	36.20	5.24	17.50	16.53	0.03	10.62	0.00	0.34	9.89	0.00	0.02	1.10	0.08	-	0.84	3.53	101.92
WYL-09-49-36.1 bio-2 image 14	138	in Grt near rim	36.23	5.14	17.60	16.37	0.04	10.69	0.00	0.33	9.96	0.12	0.01	1.17	0.07	-	0.85	3.50	102.07
WYL-09-49-36.1 h biot 22	20	in Grt	36.33	4.88	17.37	17.89	0.00	10.03	0.00	0.24	8.29	-	-	0.00	0.03	0.01	0.87	4.02	99.97
WYL-09-49-36.1 h biot 23	21	in Grt	36.72	4.30	18.66	18.09	0.00	10.35	0.03	0.15	6.86	-	-	0.00	0.08	0.04	0.99	4.07	100.33
WYL-09-49-36.1 h biot 24	22	matrix adj to Grt	36.38	3.40	18.26	19.62	0.02	9.33	0.00	0.13	9.69	-	-	0.00	0.10	0.01	0.89	4.03	101.85
WYL-09-49-36.1 h biot 25	23	matrix adj to Grt	35.93	3.23	18.00	19.98	0.03	9.33	0.00	0.14	8.83	-	-	0.00	0.08	0.02	0.76	3.97	100.31
WYL-09-49-36.1a biot 16	15	in Grt	36.22	4.30	18.07	17.35	0.03	10.96	0.01	0.38	5.85	-	-	0.00	0.16	0.08	0.84	3.98	98.24
WYL-09-49-36.1a biot 17	16	in Grt core	36.52	3.07	19.31	15.64	0.01	11.46	0.00	0.19	8.22	-	-	0.05	0.07	0.05	0.93	4.03	99.55
WYL-09-49-36.1a biot 18	17	matrix adj to Grt	36.00	3.18	17.97	19.79	0.02	9.35	0.02	0.13	8.66	-	-	0.00	0.06	0.03	0.78	3.97	99.97
WYL-09-49-36.1a biot 21	19	matrix adj to Grt	36.72	2.89	17.64	18.34	0.00	10.59	0.00	0.10	7.44	-	-	0.00	0.02	0.03	0.99	4.00	98.75
WYL-09-50-37.5 bio-1 image 3	40	matrix away from Grt	35.57	4.77	17.74	17.09	0.03	9.64	0.00	0.14	10.02	0.00	0.00	0.60	0.02	-	0.66	3.69	99.97
WYL-09-50-37.5 bio-1 image 3	41	matrix away from Grt	35.72	4.75	17.56	17.73	0.03	9.79	0.00	0.13	10.13	0.06	0.00	0.42	0.01	-	0.70	3.81	100.83
WYL-09-50-37.5 bio-1 image 3	42	matrix away from Grt	35.59	4.75	17.53	17.80	0.02	9.74	0.00	0.12	10.15	0.00	0.00	0.42	0.02	-	0.66	3.79	100.59
WYL-09-50-37.5 bio-1 image 3	43	matrix away from Grt	35.93	4.77	17.68	17.73	0.03	9.83	0.00	0.12	10.21	0.03	0.00	0.46	0.02	-	0.76	3.81	101.39
WYL-09-50-37.5 bio-2 image 7	92	matrix adj to Grt	36.15	3.96	17.62	17.13	0.00	10.71	0.00	0.14	10.04	0.08	0.00	0.59	0.02	-	0.82	3.75	101.01
WYL-09-50-37.5 bio-2 image 7	93	matrix adj to Grt	36.23	3.88	17.82	16.96	0.00	10.78	0.00	0.13	10.15	0.00	0.00	0.51	0.01	-	0.85	3.80	101.13
WYL-09-50-37.5 bio-2 image 7	94	matrix adj to Grt	36.24	3.80	17.99	16.97	0.02	10.67	0.00	0.13	10.15	0.00	0.01	0.50	0.01	-	0.85	3.81	101.14
WYL-09-50-37.5 bio-2 image 7	95	matrix adj to Grt	36.22	3.63	18.00	16.70	0.02	10.98	0.00	0.16	10.06	0.00	0.00	0.54	0.06	-	0.84	3.77	100.99
WYL-09-50-37.5 bio2-2 image 7	100	matrix adj to Grt	35.99	4.03	17.86	17.15	0.02	10.57	0.00	0.13	10.08	0.02	0.00	0.47	0.01	-	0.78	3.80	100.90
WYL-09-50-37.5 bio2-2 image 7	101	matrix adj to Grt	35.93	3.83	17.76	17.07	0.02	10.84	0.00	0.14	10.02	0.00	0.01	0.37	0.01	-	0.76	3.84	100.60
WYL-09-50-37.5 bio2-2 image 7	102	matrix adj to Grt	36.14	3.90	17.76	16.61	0.01	10.88	0.00	0.12	10.09	0.00	0.01	0.53	0.01	-	0.82	3.78	100.64
WYL-09-50-37.5 bio2-2 image 7	103	matrix adj to Grt	36.30	3.66	18.09	16.74	0.02	10.93	0.00	0.14	10.15	0.00	0.00	0.47	0.01	-	0.86	3.83	101.19
WYL-09-50-37.5 bio3 image 9	108	matrix adj to Grt	36.16	3.66	18.05	16.68	0.03	10.92	0.00	0.18	10.12	0.03	0.00	0.61	0.02	-	0.83	3.75	101.04
WYL-09-50-37.5 bio3 image 9	109	matrix adj to Grt	36.20	3.57	18.01	16.57	0.01	10.95	0.00	0.14	9.94	0.09	0.00	0.55	0.02	-	0.84	3.77	100.65
WYL-09-50-37.5 bio3 image 9	110	matrix adj to Grt	36.23	3.59	18.16	16.75	0.00	10.99	0.00	0.18	10.08	0.00	0.00	0.52	0.02	-	0.85	3.80	101.17
WYL-09-50-37.5 bio3 image 9	111	matrix adj to Grt	36.14	3.37	18.19	16.84	0.03	11.24	0.00	0.16	9.86	0.00	0.00	0.58	0.06	-	0.82	3.76	101.05
WYL-09-50-37.5 f biot 26	24	in lrg Grt near rim	37.56	3.14	17.79	15.30	0.00	12.13	0.01	0.43	5.44	-	-	0.00	0.07	0.01	1.23	4.03	97.13
WYL-09-50-37.5 f biot 27	25	in lrg Gt rim	36.75	5.80	16.96	15.95	0.02	11.20	0.00	0.48	9.08	-	-	0.00	0.03	0.03	1.00	4.10	101.40
WYL-09-50-37.5 g biot 28	26	in Grt-Qtz-Bt symplectite	38.96	3.63	18.61	15.19	0.06	13.45	0.00	0.28	5.87	-	-	0.00	0.03	0.02	1.63	4.26	101.97
WYL-09-50-37.5 g biot 29	27	in Grt-Qtz-Bt symplectite	37.92	4.36	17.75	15.48	0.00	12.44	0.00	0.23	6.23	-	-	0.00	0.00	0.01	1.33	4.15	99.90
WYL-09-50-37.5 g biot 30	28	in Grt-Qtz-Bt symplectite	38.43	1.92	18.69	12.91	0.03	15.17	0.00	0.22	4.70	-	-	0.00	0.03	0.03	1.48	4.15	97.75
WYL-09-50-37.5 h biot 31	29	in lrg Grt near rim	37.54	4.60	17.39	15.83	0.06	11.97	0.00	0.18	7.57	-	-	0.00	0.00	0.01	1.22	4.13	100.51
WYL-09-50-37.5 h biot 32	30	matrix adj to Grt	36.83	3.17	18.09	17.38	0.03	11.52	0.00	0.17	6.61	-	-	0.00	0.02	0.02	1.02	4.05	98.90
WYL-09-50-37.5 h biot 33	31	matrix adj to Grt	36.60	3.13	18.25	17.05	0.03	11.47	0.00	0.13	6.91	-	-	0.00	0.02	0.01	0.95	4.03	98.58
WYL-09-50-37.5 h biot 34	32	matrix adj to Grt	37.62	3.01	18.75	16.86	0.00	11.09	0.00	0.13	6.15	-	-	0.00	0.00	0.06	1.24	4.09	99.01

Sample/Photo	Point	O=F,Cl	Total	O	Si	Al iv	Al vi	Ti	Cr	Fe	Mn	Mg	Li*	Ca	Na	K	Ba	Cs	OH*	F	Cl	Fe/Fe+Mg
WYL-09-44-61.4 d biot 4	4	0.02	100.95	22	5.48	2.52	0.39	0.23	0.01	3.06	0.01	1.99	0.46	0.00	0.05	1.80	-	-	3.97	0.00	0.03	0.61
WYL-09-44-61.4 e biot 5	5	0.02	101.46	22	5.47	2.53	0.37	0.23	0.00	3.11	0.01	2.02	0.48	0.00	0.05	1.73	-	-	3.97	0.00	0.03	0.61
WYL-09-44-61.4 f biot 10	10	0.03	100.04	22	5.51	2.49	0.42	0.22	0.00	3.00	0.01	2.00	0.45	0.00	0.05	1.82	-	-	3.97	0.00	0.03	0.60
WYL-09-44-61.4 f biot 6	6	0.02	101.02	22	5.49	2.51	0.23	0.34	0.00	2.70	0.01	2.34	0.56	0.00	0.09	1.70	-	-	3.98	0.00	0.02	0.54
WYL-09-44-61.4 f biot 7	7	0.01	100.13	22	5.46	2.54	0.36	0.22	0.00	3.12	0.01	2.03	0.37	0.00	0.06	1.81	-	-	3.98	0.00	0.02	0.61
WYL-09-44-61.4 f biot 8	8	0.02	99.46	22	5.52	2.48	0.43	0.21	0.01	3.06	0.01	1.97	0.42	0.00	0.05	1.78	-	-	3.98	0.00	0.02	0.61
WYL-09-44-61.4 f biot 9	9	0.02	100.61	22	5.47	2.53	0.39	0.18	0.01	3.12	0.01	2.03	0.40	0.00	0.06	1.84	-	-	3.97	0.00	0.03	0.61
WYL-09-44-61.4 g biot 11-12	11	0.04	99.83	22	5.57	2.43	0.29	0.32	0.01	2.69	0.00	2.33	0.62	0.00	0.06	1.52	-	-	3.96	0.00	0.04	0.54
WYL-09-44-61.4 g biot 13	12	0.01	100.18	22	5.49	2.51	0.34	0.28	0.01	2.99	0.00	2.00	0.42	0.01	0.07	1.84	-	-	3.98	0.00	0.02	0.60
WYL-09-44-61.4 g biot 14	13	0.01	100.44	22	5.43	2.57	0.41	0.20	0.00	3.12	0.01	1.97	0.34	0.00	0.07	1.91	-	-	3.99	0.00	0.01	0.61
WYL-09-44-61.4 g biot 15	14	0.03	100.37	22	5.50	2.50	0.43	0.21	0.00	2.99	0.01	2.00	0.47	0.01	0.06	1.78	-	-	3.97	0.00	0.03	0.60
WYL-09-44-61.4c biot 2	2	0.02	99.96	22	5.57	2.43	0.41	0.22	0.01	2.91	0.01	2.26	0.64	0.00	0.06	1.26	-	-	3.97	0.00	0.03	0.56
WYL-09-44-61.4c biot 3	3	0.02	99.92	22	5.51	2.49	0.32	0.25	0.00	3.07	0.01	2.06	0.43	0.01	0.08	1.72	-	-	3.97	0.00	0.03	0.60
WYL-09-44-61.4c biotite #1	1	0.02	100.66	22	5.52	2.48	0.39	0.23	0.00	3.05	0.01	2.00	0.50	0.00	0.07	1.71	-	-	3.98	0.00	0.02	0.60
WYL-09-49-36.1 bio-1 image 12	132	0.52	100.88	22	5.37	2.63	0.62	0.39	-	2.29	0.00	2.09	0.46	0.00	0.05	1.92	0.00	0.00	3.41	0.57	0.02	0.52
WYL-09-49-36.1 bio-1 image 12	133	0.50	100.37	22	5.37	2.63	0.63	0.39	-	2.29	0.01	2.08	0.44	0.00	0.05	1.91	0.00	0.00	3.43	0.55	0.02	0.52
WYL-09-49-36.1 bio-1 image 12	134	0.55	100.77	22	5.35	2.65	0.62	0.39	-	2.29	0.01	2.10	0.43	0.00	0.05	1.93	0.00	0.00	3.38	0.61	0.01	0.52
WYL-09-49-36.1 bio-1 image 12	135	0.45	100.32	22	5.37	2.63	0.65	0.39	-	2.29	0.00	2.07	0.43	0.00	0.05	1.93	0.00	0.00	3.49	0.50	0.02	0.52
WYL-09-49-36.1 bio-2 image 14	136	0.54	101.73	22	5.33	2.67	0.39	0.58	-	2.02	0.00	2.34	0.51	0.00	0.09	1.86	0.00	0.00	3.40	0.58	0.02	0.46
WYL-09-49-36.1 bio-2 image 14	137	0.48	101.44	22	5.34	2.66	0.38	0.58	-	2.04	0.00	2.33	0.50	0.00	0.10	1.86	0.00	0.00	3.47	0.51	0.02	0.47
WYL-09-49-36.1 bio-2 image 14	138	0.51	101.56	22	5.34	2.66	0.39	0.57	-	2.02	0.00	2.35	0.50	0.00	0.09	1.87	0.01	0.00	3.44	0.55	0.02	0.46
WYL-09-49-36.1 h biot 22	20	0.01	99.97	22	5.40	2.60	0.45	0.55	0.00	2.23	0.00	2.22	0.52	0.00	0.07	1.57	-	-	3.99	0.00	0.01	0.50
WYL-09-49-36.1 h biot 23	21	0.02	100.31	22	5.38	2.62	0.61	0.47	0.00	2.22	0.00	2.26	0.58	0.00	0.04	1.28	-	-	3.98	0.00	0.02	0.50
WYL-09-49-36.1 h biot 24	22	0.02	101.83	22	5.39	2.61	0.57	0.38	0.00	2.43	0.00	2.06	0.53	0.00	0.04	1.83	-	-	3.98	0.00	0.02	0.54
WYL-09-49-36.1 h biot 25	23	0.02	100.29	22	5.40	2.60	0.58	0.36	0.00	2.51	0.00	2.09	0.46	0.00	0.04	1.69	-	-	3.98	0.00	0.02	0.55
WYL-09-49-36.1a biot 16	15	0.04	98.20	22	5.40	2.60	0.57	0.48	0.01	2.16	0.00	2.43	0.51	0.00	0.11	1.11	-	-	3.96	0.00	0.04	0.47
WYL-09-49-36.1a biot 17	16	0.03	99.52	22	5.38	2.62	0.73	0.34	0.01	1.93	0.00	2.52	0.55	0.00	0.06	1.54	-	-	3.96	0.02	0.02	0.43
WYL-09-49-36.1a biot 18	17	0.01	99.95	22	5.41	2.59	0.60	0.36	0.00	2.49	0.00	2.10	0.47	0.00	0.04	1.66	-	-	3.98	0.00	0.02	0.54
WYL-09-49-36.1a biot 21	19	0.00	98.75	22	5.50	2.50	0.61	0.33	0.00	2.30	0.00	2.36	0.59	0.00	0.03	1.42	-	-	4.00	0.00	0.00	0.49
WYL-09-50-37.5 bio-1 image 3	40	0.26	99.71	22	5.35	2.65	0.50	0.54	-	2.15	0.00	2.16	0.40	0.00	0.04	1.92	0.00	0.00	3.71	0.29	0.00	0.50
WYL-09-50-37.5 bio-1 image 3	41	0.18	100.65	22	5.34	2.66	0.44	0.53	-	2.22	0.00	2.18	0.42	0.00	0.04	1.93	0.00	0.00	3.80	0.20	0.00	0.50
WYL-09-50-37.5 bio-1 image 3	42	0.18	100.41	22	5.34	2.66	0.44	0.54	-	2.23	0.00	2.18	0.40	0.00	0.04	1.94	0.00	0.00	3.80	0.20	0.00	0.51
WYL-09-50-37.5 bio-1 image 3	43	0.20	101.20	22	5.34	2.66	0.44	0.53	-	2.20	0.00	2.18	0.45	0.00	0.04	1.94	0.00	0.00	3.78	0.22	0.00	0.50
WYL-09-50-37.5 bio-2 image 7	92	0.25	100.76	22	5.38	2.62	0.46	0.44	-	2.13	0.00	2.38	0.49	0.00	0.04	1.90	0.00	0.00	3.72	0.28	0.00	0.47
WYL-09-50-37.5 bio-2 image 7	93	0.22	100.91	22	5.37	2.63	0.49	0.43	-	2.10	0.00	2.38	0.51	0.00	0.04	1.92	0.00	0.00	3.76	0.24	0.00	0.47
WYL-09-50-37.5 bio-2 image 7	94	0.21	100.93	22	5.37	2.63	0.51	0.42	-	2.10	0.00	2.36	0.51	0.00	0.04	1.92	0.00	0.00	3.77	0.23	0.00	0.47
WYL-09-50-37.5 bio-2 image 7	95	0.24	100.75	22	5.37	2.63	0.52	0.40	-	2.07	0.00	2.43	0.50	0.00	0.05	1.90	0.00	0.00	3.73	0.25	0.02	0.46
WYL-09-50-37.5 bio2-2 image 7	100	0.20	100.70	22	5.36	2.64	0.49	0.45	-	2.13	0.00	2.34	0.46	0.00	0.04	1.91	0.00	0.00	3.77	0.22	0.00	0.48
WYL-09-50-37.5 bio2-2 image 7	101	0.16	100.44	22	5.36	2.64	0.48	0.43	-	2.13	0.00	2.41	0.46	0.00	0.04	1.91	0.00	0.00	3.82	0.17	0.00	0.47
WYL-09-50-37.5 bio2-2 image 7	102	0.22	100.42	22	5.38	2.62	0.49	0.44	-	2.07	0.00	2.41	0.49	0.00	0.03	1.91	0.00	0.00	3.75	0.25	0.00	0.46
WYL-09-50-37.5 bio2-2 image 7	103	0.20	100.99	22	5.37	2.63	0.52	0.41	-	2.07	0.00	2.41	0.51	0.00	0.04	1.91	0.00	0.00	3.78	0.22	0.00	0.46
WYL-09-50-37.5 bio3 image 9	108	0.26	100.78	22	5.36	2.64	0.52	0.41	-	2.07	0.00	2.42	0.49	0.00	0.05	1.92	0.00	0.00	3.71	0.28	0.00	0.46
WYL-09-50-37.5 bio3 image 9	109	0.24	100.42	22	5.38	2.62	0.54	0.40	-	2.06	0.00	2.43	0.50	0.00	0.04	1.89	0.01	0.00	3.74	0.26	0.00	0.46
WYL-09-50-37.5 bio3 image 9	110	0.22	100.95	22	5.36	2.64	0.53	0.40	-	2.07	0.00	2.43	0.50	0.00	0.05	1.90	0.00	0.00	3.75	0.24	0.01	0.46
WYL-09-50-37.5 bio3 image 9	111	0.26	100.80	22	5.36	2.64	0.53	0.38	-	2.09	0.00	2.48	0.49	0.00	0.05	1.86	0.00	0.00	3.71	0.27	0.02	0.46
WYL-09-50-37.5 f biot 26	24	0.01	97.11	22	5.56	2.44	0.67	0.35	0.00	1.90	0.00	2.68	0.73	0.00	0.12	1.03	-	-	3.98	0.00	0.02	0.41
WYL-09-50-37.5 f biot 27	25	0.01	101.40	22	5.37	2.63	0.29	0.64	0.00	1.95	0.00	2.44	0.58	0.00	0.14	1.69	-	-	3.99	0.00	0.01	0.44
WYL-09-50-37.5 g biot 28	26	0.01	101.97	22	5.48	2.52	0.57	0.38	0.00	1.79	0.01	2.82	0.92	0.00	0.08	1.05	-	-	3.99	0.00	0.01	0.39
WYL-09-50-37.5 g biot 29	27	0.00	99.90	22	5.48	2.52	0.51	0.47	0.00	1.87	0.00	2.68	0.77	0.00	0.07	1.15	-	-	4.00	0.00	0.00	0.41
WYL-09-50-37.5 g biot 30	28	0.01	97.74	22	5.55	2.45	0.73	0.21	0.00	1.56	0.00	3.26	0.86	0.00	0.06	0.87	-	-	3.99	0.00	0.01	0.32
WYL-09-50-37.5 h biot 31	29	0.00	100.51	22	5.46	2.54	0.44	0.50	0.00	1.92	0.01	2.59	0.71	0.00	0.05	1.40	-	-	4.00	0.00	0.00	0.43
WYL-09-50-37.5 h biot 32	30	0.00	98.90	22	5.45	2.55	0.61	0.35	0.00	2.15	0.00	2.54	0.61	0.00	0.05	1.25	-	-	4.00	0.00	0.00	0.46
WYL-09-50-37.5 h biot 33	31	0.00	98.57	22	5.44	2.56	0.64	0.35	0.00	2.12	0.00	2.54	0.57	0.00	0.04	1.31	-	-	3.99	0.00	0.01	0.45
WYL-09-50-37.5 h biot 34	32	0.00	99.01	22	5.51	2.49	0.75	0.33	0.01	2.07	0.00	2.42	0.73	0.00	0.04	1.15	-	-	4.00	0.00	0.00	0.46

Sample/Photo	Point	Mg/(Mg+Fe)	a	b	c	Ti	X(Mg)	T(C)
WYL-09-44-61.4 d biot 4	4	0.39	-2.3594	4.6482E-09	-1.7283	0.23	0.39	595
WYL-09-44-61.4 e biot 5	5	0.39	-2.3594	4.6482E-09	-1.7283	0.23	0.39	594
WYL-09-44-61.4 f biot 10	10	0.40	-2.3594	4.6482E-09	-1.7283	0.22	0.40	594
WYL-09-44-61.4 f biot 6	6	0.46	-2.3594	4.6482E-09	-1.7283	0.34	0.46	680
WYL-09-44-61.4 f biot 7	7	0.39	-2.3594	4.6482E-09	-1.7283	0.22	0.39	594
WYL-09-44-61.4 f biot 8	8	0.39	-2.3594	4.6482E-09	-1.7283	0.21	0.39	576
WYL-09-44-61.4 f biot 9	9	0.39	-2.3594	4.6482E-09	-1.7283	0.18	0.39	548
WYL-09-44-61.4 g biot 11-12	11	0.46	-2.3594	4.6482E-09	-1.7283	0.32	0.46	668
WYL-09-44-61.4 g biot 13	12	0.40	-2.3594	4.6482E-09	-1.7283	0.28	0.40	636
WYL-09-44-61.4 g biot 14	13	0.39	-2.3594	4.6482E-09	-1.7283	0.20	0.39	571
WYL-09-44-61.4 g biot 15	14	0.40	-2.3594	4.6482E-09	-1.7283	0.21	0.40	581
WYL-09-44-61.4c biot 2	2	0.44	-2.3594	4.6482E-09	-1.7283	0.22	0.44	596
WYL-09-44-61.4c biot 3	3	0.40	-2.3594	4.6482E-09	-1.7283	0.25	0.40	617
WYL-09-44-61.4c biotite #1	1	0.40	-2.3594	4.6482E-09	-1.7283	0.23	0.40	595
WYL-09-49-36.1 bio-1 image 12	132	0.48	-2.3594	4.6482E-09	-1.7283	0.39	0.48	702
WYL-09-49-36.1 bio-1 image 12	133	0.48	-2.3594	4.6482E-09	-1.7283	0.39	0.48	703
WYL-09-49-36.1 bio-1 image 12	134	0.48	-2.3594	4.6482E-09	-1.7283	0.39	0.48	702
WYL-09-49-36.1 bio-1 image 12	135	0.48	-2.3594	4.6482E-09	-1.7283	0.39	0.48	700
WYL-09-49-36.1 bio-2 image 14	136	0.54	-2.3594	4.6482E-09	-1.7283	0.58	0.54	765
WYL-09-49-36.1 bio-2 image 14	137	0.53	-2.3594	4.6482E-09	-1.7283	0.58	0.53	765
WYL-09-49-36.1 bio-2 image 14	138	0.54	-2.3594	4.6482E-09	-1.7283	0.57	0.54	763
WYL-09-49-36.1 h biot 22	20	0.50	-2.3594	4.6482E-09	-1.7283	0.55	0.50	751
WYL-09-49-36.1 h biot 23	21	0.50	-2.3594	4.6482E-09	-1.7283	0.47	0.50	734
WYL-09-49-36.1 h biot 24	22	0.46	-2.3594	4.6482E-09	-1.7283	0.38	0.46	694
WYL-09-49-36.1 h biot 25	23	0.45	-2.3594	4.6482E-09	-1.7283	0.36	0.45	688
WYL-09-49-36.1a biot 16	15	0.53	-2.3594	4.6482E-09	-1.7283	0.48	0.53	740
WYL-09-49-36.1a biot 17	16	0.57	-2.3594	4.6482E-09	-1.7283	0.34	0.57	700
WYL-09-49-36.1a biot 18	17	0.46	-2.3594	4.6482E-09	-1.7283	0.36	0.46	686
WYL-09-49-36.1a biot 21	19	0.51	-2.3594	4.6482E-09	-1.7283	0.33	0.51	680
WYL-09-50-37.5 bio-1 image 3	40	0.50	-2.3594	4.6482E-09	-1.7283	0.54	0.50	750
WYL-09-50-37.5 bio-1 image 3	41	0.50	-2.3594	4.6482E-09	-1.7283	0.53	0.50	748
WYL-09-50-37.5 bio-1 image 3	42	0.49	-2.3594	4.6482E-09	-1.7283	0.54	0.49	748
WYL-09-50-37.5 bio-1 image 3	43	0.50	-2.3594	4.6482E-09	-1.7283	0.53	0.50	748
WYL-09-50-37.5 bio-2 image 7	92	0.53	-2.3594	4.6482E-09	-1.7283	0.44	0.53	728
WYL-09-50-37.5 bio-2 image 7	93	0.53	-2.3594	4.6482E-09	-1.7283	0.43	0.53	726
WYL-09-50-37.5 bio-2 image 7	94	0.53	-2.3594	4.6482E-09	-1.7283	0.42	0.53	723
WYL-09-50-37.5 bio-2 image 7	95	0.54	-2.3594	4.6482E-09	-1.7283	0.40	0.54	719
WYL-09-50-37.5 bio2-2 image 7	100	0.52	-2.3594	4.6482E-09	-1.7283	0.45	0.52	730
WYL-09-50-37.5 bio2-2 image 7	101	0.53	-2.3594	4.6482E-09	-1.7283	0.43	0.53	725
WYL-09-50-37.5 bio2-2 image 7	102	0.54	-2.3594	4.6482E-09	-1.7283	0.44	0.54	729
WYL-09-50-37.5 bio2-2 image 7	103	0.54	-2.3594	4.6482E-09	-1.7283	0.41	0.54	719
WYL-09-50-37.5 bio3 image 9	108	0.54	-2.3594	4.6482E-09	-1.7283	0.41	0.54	720
WYL-09-50-37.5 bio3 image 9	109	0.54	-2.3594	4.6482E-09	-1.7283	0.40	0.54	717
WYL-09-50-37.5 bio3 image 9	110	0.54	-2.3594	4.6482E-09	-1.7283	0.40	0.54	717
WYL-09-50-37.5 bio3 image 9	111	0.54	-2.3594	4.6482E-09	-1.7283	0.38	0.54	709
WYL-09-50-37.5 f biot 26	24	0.59	-2.3594	4.6482E-09	-1.7283	0.35	0.59	709
WYL-09-50-37.5 f biot 27	25	0.56	-2.3594	4.6482E-09	-1.7283	0.64	0.56	780
WYL-09-50-37.5 g biot 28	26	0.61	-2.3594	4.6482E-09	-1.7283	0.38	0.61	729
WYL-09-50-37.5 g biot 29	27	0.59	-2.3594	4.6482E-09	-1.7283	0.47	0.59	751
WYL-09-50-37.5 g biot 30	28	0.68	-2.3594	4.6482E-09	-1.7283	0.21	0.68	658
WYL-09-50-37.5 h biot 31	29	0.57	-2.3594	4.6482E-09	-1.7283	0.50	0.57	755
WYL-09-50-37.5 h biot 32	30	0.54	-2.3594	4.6482E-09	-1.7283	0.35	0.54	700
WYL-09-50-37.5 h biot 33	31	0.55	-2.3594	4.6482E-09	-1.7283	0.35	0.55	699
WYL-09-50-37.5 h biot 34	32	0.54	-2.3594	4.6482E-09	-1.7283	0.33	0.54	690

Table I-2. Garnet Point Chemistry

Sample/Photo	Point	Location	SiO2	TiO2	Al2O3	Cr2O3	V2O3	FeO	MnO	ZnO	MgO	CaO	Y2O3	Na2O	Total
WYL-09-44-61.4c garnet #1	1	intermediate b/w rim and core	37.11	0	20.9	0.0306	-	36.23	2.6482	-	2.1549	1.8206	-	0	100.9
WYL-09-44-61.4c garn 2	2	intermediate b/w rim and core	36.98	0	20.94	0.1036	-	35.65	2.4788	-	2.0635	1.9874	-	0.0277	100.22
WYL-09-44-61.4c garn 3	3	intermediate b/w rim and core	37.43	0	20.92	0.0048	-	35.03	2.6438	-	1.9171	1.9497	-	0.0411	99.94
WYL-09-44-61.4 d garn 4	4	rim	37.83	0.0066	20.87	0	-	35.47	2.6102	-	1.9147	1.7549	-	0	100.45
WYL-09-44-61.4 e grn 5	5	rim	37.12	0.024	21.12	0.0521	-	35.6	2.584	-	2.1413	1.7742	-	0.0125	100.43
WYL-09-44-61.4 f garn 6	6	intermediate b/w rim and core	37.96	0.0033	21.18	0.0544	-	36.04	1.8914	-	2.6856	1.5739	-	0	101.39
WYL-09-44-61.4 f garn 7	7	near rim	36.82	0	20.91	0.092	-	35.54	2.5994	-	1.9369	1.8531	-	0.011	99.77
WYL-09-44-61.4 f garn 8	8	rim	37.52	0.0033	20.42	0	-	35.97	2.4543	-	2.0258	1.6363	-	0.0909	100.13
WYL-09-44-61.4 f garn 9	9	rim	37.61	0.0124	20.92	0	-	35.89	2.3583	-	2.0121	1.9153	-	0	100.71
WYL-09-44-61.4 f garn 10	10	rim	37.15	0.0033	20.88	0.0472	-	35.32	2.4286	-	1.9862	1.648	-	0.0331	99.49
WYL-09-44-61.4 g garn 11	11	core	37.8	0	20.71	0.045	-	35.59	1.8481	-	2.7525	1.5972	-	0.0131	100.36
WYL-09-44-61.4 g garn 12	12	inclusion in Bt in Grt core	37.23	0	20.67	0.0236	-	35.88	1.7908	-	1.9821	1.5311	-	0	99.11
WYL-09-44-61.4 g garn 13	13	core	37.02	0.0346	20.86	0.0024	-	35.78	2.2449	-	2.1164	1.5669	-	0.0324	99.65
WYL-09-44-61.4 g garn 14	14	rim	37.33	0.0495	20.97	0.0591	-	35.94	2.5192	-	2.2389	1.4887	-	0.0313	100.63
WYL-09-44-61.4 g garn 15	15	rim	36.58	0	21.04	0	-	35.24	2.6379	-	2.0165	1.7804	-	0.0006	99.3
WYL-09-49-36.1a garn 16	16	intermediate b/w rim and core	38.08	0	21.1	0.0047	-	34.88	1.3973	-	3.7	0.9159	-	0.0306	100.11
WYL-09-49-36.1a garn 17	17	intermediate b/w rim and core	37.29	0	21.06	0.1162	-	34.39	1.4349	-	3.63	0.9146	-	0.029	98.87
WYL-09-49-36.1a garn 18	18	rim	37.93	0.0372	21.17	0	-	34.86	1.6771	-	3.2	0.8759	-	0.0121	99.76
WYL-09-49-36.1a garn 21	21	rim	36.69	0	20.61	0	-	34.85	1.5776	-	3.14	0.9126	-	0.0879	97.88
WYL-09-49-36.1 h garn 22	22	near rim	37.95	0	21.07	0	-	34.86	1.6058	-	3.42	1.0429	-	0.0229	99.97
WYL-09-49-36.1 h garn 23	23	near rim	38.05	0.0529	21.19	0.0308	-	35.26	1.5279	-	3.19	1.0775	-	0	100.37
WYL-09-49-36.1 h garn 24	24	rim	37.89	0	21.2	0.0308	-	34.96	1.7098	-	3.17	1.0411	-	0.0133	100.01
WYL-09-49-36.1 h garn 25	25	rim	37.31	0.0025	21.28	0.1091	-	35.19	1.6602	-	3.36	0.987	-	0.0536	99.96
WYL-09-49-36.1 image 12 gar-1	128	near rim	37.8765	0.002744	21.5204	0.020326	0.013405	34.0375	1.39863	0.014867	3.39232	1.03925	0.005989	0.014806	99.3367
WYL-09-49-36.1 image 12 gar-1	129	near rim	37.6923	0.017697	21.4792	0.025826	0.015321	34.1748	1.40887	0	3.30816	1.01845	0	0.011731	99.1524
WYL-09-49-36.1 image 12 gar-1	130	near rim	37.8082	0.007726	21.6103	0.022599	0	34.2751	1.46053	0.029916	3.24261	0.998205	0.061973	0.014518	99.5316
WYL-09-49-36.1 image 12 gar-1	131	rim	37.5958	0.032968	21.4919	0.030658	0.001057	34.0228	1.51759	0.011602	2.86728	0.92518	0.095981	0.015713	98.6085
WYL-09-49-36.1 image 14 gar-2	139	near rim + Bt inclusion	37.628	0.028626	21.5661	0.029617	0.029353	34.0622	1.42516	0.009847	3.29722	1.04789	0	0.013499	99.1376
WYL-09-49-36.1 image 14 gar-2	140	near rim + Bt inclusion	37.8328	0.026392	21.5096	0.029022	0.005172	34.0835	1.33947	0.018584	3.26914	1.03868	0.042001	0.021339	99.2157
WYL-09-49-36.1 image 14 gar-2	141	near rim + Bt inclusion	37.8213	0.052733	21.5142	0.015935	0.017077	34.036	1.37065	0.013173	3.20227	1.04217	0.062009	0.016193	99.1637
WYL-09-50-37.5 f garn 26	26	near rim	37.99	0	20.83	0.0167	-	33.6	0.687	-	4.92	0.4885	-	0.0179	98.55
WYL-09-50-37.5 f garn 27	27	rim	37.47	0.0124	20.82	0.0711	-	34.23	0.6452	-	4.6	0.6414	-	0.0324	98.52
WYL-09-50-37.5 g garn 28	28	Grt-Bt-Qtz symplectite	37.57	0	21.46	0.0931	-	32.39	0.4965	-	5.73	0.5604	-	0.0287	98.33
WYL-09-50-37.5 g garn 29	29	Grt-Bt-Qtz symplectite	37.5	0	21.52	0	-	32.45	0.5426	-	5.86	0.5285	-	0	98.41
WYL-09-50-37.5 g garn 30	30	Grt-Bt-Qtz symplectite	38.65	0	21.71	0.0671	-	32.35	0.5529	-	5.91	0.626	-	0.0447	99.92
WYL-09-50-37.5 h garn 31	31	near rim	38.34	0	21.17	0	-	33.53	0.5891	-	5.31	0.5884	-	0.0225	99.56
WYL-09-50-37.5 h garn 32	32	rim	38.28	0.0225	21.12	0.0334	-	33.73	0.5687	-	5.18	0.6151	-	0.0461	99.59
WYL-09-50-37.5 h garn 33	33	rim	38.28	0	21.01	0	-	33.7	0.626	-	4.86	0.5974	-	0.0055	99.08
WYL-09-50-37.5 h garn 34	34	rim	38.21	0	21.72	0	-	33.37	0.5775	-	5.16	0.5405	-	0.0571	99.62
WYL-09-50-37.5 big garnet	82	lrg Grt core	37.9954	0.003394	21.7204	0.017229	0.011527	31.8758	0.691042	0	6.11611	0.627326	0	0.022109	99.0804
WYL-09-50-37.5 big garnet	83	lrg Grt core	38.0358	0	21.7416	0.027819	0.006025	31.7327	0.648352	0.031651	6.04615	0.618573	0.115012	0.02138	99.0249
WYL-09-50-37.5 big garnet	84	lrg Grt core	37.6955	0.003052	21.5649	0.016556	0	32.2788	0.585545	0.000528	6.0439	0.61211	0	0.016227	98.8171
WYL-09-50-37.5 big garnet	85	lrg Grt core	38.183	0.010981	21.8908	0.014063	0.008745	31.9172	0.572277	0.051558	5.97211	0.631601	0.028217	0.029397	99.31
WYL-09-50-37.5 big garnet	86	lrg Grt core	37.7445	0.007182	21.6816	0.020636	0	32.1241	0.549054	0	5.91911	0.61354	0	0.024414	98.684
WYL-09-50-37.5 big garnet	87	lrg Grt core	37.201	0.017113	21.4229	0.013241	0	32.6298	0.528308	0	6.0401	0.583672	0.016131	0.019408	98.4717
WYL-09-50-37.5 big garnet	88	lrg Grt core	36.6415	0	21.0067	0.02358	0.011493	33.3543	0.506952	0.038873	5.77235	0.586977	0	0.025927	97.9685
WYL-09-50-37.5 image 7 gar-2	96	near rim of lrg Grt	38.1021	0.012193	21.7773	0.011982	0.052757	33.2669	0.511214	0.026439	4.81784	0.630598	0	0.014819	99.2241
WYL-09-50-37.5 image 7 gar-2	97	near rim of lrg Grt	38.1996	0.024837	21.6908	0.021615	0	33.3209	0.531167	0	4.66389	0.648731	0.006049	0.020965	99.1284
WYL-09-50-37.5 image 7 gar-2	98	near rim of lrg Grt	37.9934	0.005638	21.6797	0.014085	0	33.8065	0.562827	0	4.48219	0.634644	0.036265	0.019295	99.2346
WYL-09-50-37.5 image 7 gar-2	99	rim of lrg Grt	37.8902	0.032891	21.4908	0.022639	0	34.0889	0.57037	0.015533	4.0221	0.572588	0.030192	0.020201	98.7564
WYL-09-50-37.5 image 7 gar2-2	104	near rim	38.265	0.011188	21.8663	0.015422	0.022953	32.9131	0.505084	0.005778	4.8403	0.629067	0.042359	0.021858	99.1385
WYL-09-50-37.5 image 7 gar2-2	105	near rim of lrg Grt	38.1224	0.001015	21.8127	0.017608	0	33.4996	0.573994	0.004397	4.68344	0.639275	0.094721	0.014873	99.4641
WYL-09-50-37.5 image 7 gar2-2	106	near rim of lrg Grt	38.0586	0.01314	21.6721	0.030219	0.009388	33.6816	0.579511	0	4.33164	0.641205	0	0.015397	99.0329
WYL-09-50-37.5 image 7 gar2-2	107	rim of lrg Grt	38.0896	0.017354	21.6377	0.024982	0	34.1204	0.614591	0.019273	4.10457	0.612694	0	0.024202	99.2653
WYL-09-50-37.5 image 9 gar3	112	near rim of lrg Grt	38.3351	0.009664	21.8809	0.020197	0.027072	33.0017	0.47318	0	4.91789	0.620119	0	0.032635	99.3185
WYL-09-50-37.5 image 9 gar3	113	near rim of lrg Grt	38.2624	0.015483	21.7399	0.015249	0	32.9925	0.456899	0	4.83816	0.619793	0.056497	0.024214	99.0211
WYL-09-50-37.5 image 9 gar3	114	near rim of lrg Grt	38.132	0.013101	21.8029	0.018098	0.053449	33.2516	0.482348	0.013587	4.69961	0.629593	0	0.030498	99.1268
WYL-09-50-37.5 image 9 gar3	115	rim of lrg Grt	38.1881	0.025337	21.5855	0.024307	0.00864	33.557	0.539825	0	4.3306	0.638856	0	0.024076	98.9222

Sample/Photo	Point	O	Si	Ti	Al	V	Cr	Fe3	Fe2	Mg	Ca	Mn	Na	Y	Zn	grossular	pyrope	almandine	spessartine
WYL-09-44-61.4c garnet #1	1	24	5.9508	0.0000	3.9499	-	0.0039	0.0462	4.8124	0.5151	0.3128	0.3597	0.0000	-	-	5%	9%	80%	6%
WYL-09-44-61.4c garn 2	2	24	5.9709	0.0000	3.9848	-	0.0132	0.0020	4.8118	0.4967	0.3438	0.3390	0.0087	-	-	6%	8%	80%	6%
WYL-09-44-61.4c garn 3	3	24	6.1140	0.0000	4.0274	-	0.0006	0.0000	4.7852	0.4668	0.3412	0.3658	0.0130	-	-	6%	8%	80%	6%
WYL-09-44-61.4 d garn 4	4	24	6.1803	0.0008	4.0184	-	0.0000	0.0000	4.8461	0.4663	0.3072	0.3612	0.0000	-	-	5%	8%	81%	6%
WYL-09-44-61.4 e grn 5	5	24	5.9843	0.0029	4.0129	-	0.0066	0.0000	4.7997	0.5146	0.3065	0.3528	0.0039	-	-	5%	9%	80%	6%
WYL-09-44-61.4 f garn 6	6	24	6.0795	0.0004	3.9978	-	0.0069	0.0000	4.8271	0.6412	0.2701	0.2566	0.0000	-	-	5%	11%	81%	4%
WYL-09-44-61.4 f garn 7	7	24	5.9837	0.0000	4.0049	-	0.0118	0.0000	4.8301	0.4692	0.3227	0.3578	0.0035	-	-	5%	8%	81%	6%
WYL-09-44-61.4 f garn 8	8	24	6.1329	0.0004	3.9338	-	0.0000	0.0658	4.8512	0.4936	0.2866	0.3398	0.0288	-	-	5%	8%	81%	6%
WYL-09-44-61.4 f garn 9	9	24	6.0928	0.0015	3.9942	-	0.0000	0.0043	4.8580	0.4859	0.3324	0.3236	0.0000	-	-	6%	8%	81%	5%
WYL-09-44-61.4 f garn 10	10	24	6.0868	0.0004	4.0319	-	0.0061	0.0000	4.8396	0.4851	0.2893	0.3370	0.0105	-	-	5%	8%	81%	6%
WYL-09-44-61.4 g garn 11	11	24	6.1351	0.0000	3.9616	-	0.0058	0.0327	4.7981	0.6660	0.2778	0.2541	0.0041	-	-	5%	11%	80%	4%
WYL-09-44-61.4 g garn 12	12	24	6.1539	0.0000	4.0268	-	0.0031	0.0000	4.9598	0.4884	0.2712	0.2507	0.0000	-	-	5%	8%	83%	4%
WYL-09-44-61.4 g garn 13	13	24	6.0359	0.0042	4.0084	-	0.0003	0.0000	4.8786	0.5144	0.2737	0.3100	0.0102	-	-	5%	9%	81%	5%
WYL-09-44-61.4 g garn 14	14	24	6.0227	0.0060	3.9874	-	0.0075	0.0000	4.8492	0.5385	0.2573	0.3443	0.0098	-	-	4%	9%	81%	6%
WYL-09-44-61.4 g garn 15	15	24	5.9560	0.0000	4.0375	-	0.0000	0.0000	4.7985	0.4895	0.3106	0.3638	0.0002	-	-	5%	8%	80%	6%
WYL-09-49-36.1a garn 16	16	24	6.1637	0.0000	4.0251	-	0.0006	0.0000	4.7214	0.8928	0.1588	0.1916	0.0096	-	-	3%	15%	79%	3%
WYL-09-49-36.1a garn 17	17	24	6.0797	0.0000	4.0467	-	0.0150	0.0000	4.6890	0.8823	0.1598	0.1982	0.0092	-	-	3%	15%	79%	3%
WYL-09-49-36.1a garn 18	18	24	6.1892	0.0046	4.0713	-	0.0000	0.0000	4.7570	0.7784	0.1531	0.2318	0.0038	-	-	3%	13%	80%	4%
WYL-09-49-36.1a garn 21	21	24	6.0544	0.0000	4.0083	-	0.0000	0.0000	4.8093	0.7724	0.1614	0.2205	0.0281	-	-	3%	13%	80%	4%
WYL-09-49-36.1 h garn 22	22	24	6.1601	0.0000	4.0309	-	0.0000	0.0000	4.7322	0.8276	0.1814	0.2208	0.0072	-	-	3%	14%	79%	4%
WYL-09-49-36.1 h garn 23	23	24	6.1640	0.0064	4.0457	-	0.0039	0.0000	4.7769	0.7704	0.1870	0.2096	0.0000	-	-	3%	13%	80%	4%
WYL-09-49-36.1 h garn 24	24	24	6.1548	0.0000	4.0586	-	0.0040	0.0000	4.7491	0.7676	0.1812	0.2352	0.0042	-	-	3%	13%	80%	4%
WYL-09-49-36.1 h garn 25	25	24	6.0009	0.0003	4.0339	-	0.0139	0.0000	4.7333	0.8056	0.1701	0.2262	0.0167	-	-	3%	14%	80%	4%
WYL-09-49-36.1 image 12 gar-1	128	24	6.1834	0.0003	4.1406	0.0018	0.0026	0.0000	4.6470	0.8256	0.1818	0.1934	0.0047	0.0005	0.0018	3%	14%	79%	3%
WYL-09-49-36.1 image 12 gar-1	129	24	6.1609	0.0022	4.1378	0.0020	0.0033	0.0000	4.6715	0.8061	0.1784	0.1951	0.0037	0.0000	0.0000	3%	14%	80%	3%
WYL-09-49-36.1 image 12 gar-1	130	24	6.1596	0.0009	4.1494	0.0000	0.0029	0.0000	4.6699	0.7875	0.1742	0.2015	0.0046	0.0054	0.0036	3%	13%	80%	3%
WYL-09-49-36.1 image 12 gar-1	131	24	6.2169	0.0041	4.1886	0.0001	0.0040	0.0000	4.7050	0.7068	0.1639	0.2126	0.0050	0.0084	0.0014	3%	12%	81%	4%
WYL-09-49-36.1 image 14 gar-2	139	24	6.1433	0.0035	4.1497	0.0038	0.0038	0.0000	4.6507	0.8025	0.1833	0.1971	0.0043	0.0000	0.0012	3%	14%	80%	3%
WYL-09-49-36.1 image 14 gar-2	140	24	6.1920	0.0032	4.1491	0.0007	0.0038	0.0000	4.6651	0.7976	0.1821	0.1857	0.0068	0.0037	0.0022	3%	14%	80%	3%
WYL-09-49-36.1 image 14 gar-2	141	24	6.1991	0.0065	4.1559	0.0022	0.0021	0.0000	4.6653	0.7824	0.1830	0.1903	0.0051	0.0054	0.0016	3%	13%	80%	3%
WYL-09-50-37.5 f garn 26	26	24	6.2139	0.0000	4.0155	-	0.0022	0.0000	4.5961	1.1997	0.0856	0.0952	0.0057	-	-	1%	20%	77%	2%
WYL-09-50-37.5 f garn 27	27	24	6.1042	0.0015	3.9975	-	0.0092	0.0000	4.6635	1.1172	0.1120	0.0890	0.0102	-	-	2%	19%	78%	1%
WYL-09-50-37.5 g garn 28	28	24	6.0527	0.0000	4.0747	-	0.0119	0.0000	4.3639	1.3762	0.0967	0.0678	0.0090	-	-	2%	23%	74%	1%
WYL-09-50-37.5 g garn 29	29	24	6.0229	0.0000	4.0736	-	0.0000	0.0000	4.3586	1.4031	0.0909	0.0738	0.0000	-	-	2%	24%	74%	1%
WYL-09-50-37.5 g garn 30	30	24	6.1613	0.0000	4.0789	-	0.0085	0.0000	4.3128	1.4045	0.1069	0.0747	0.0138	-	-	2%	24%	73%	1%
WYL-09-50-37.5 h garn 31	31	24	6.1759	0.0000	4.0191	-	0.0000	0.0000	4.5169	1.2751	0.1016	0.0804	0.0070	-	-	2%	21%	76%	1%
WYL-09-50-37.5 h garn 32	32	24	6.1647	0.0027	4.0086	-	0.0043	0.0000	4.5427	1.2436	0.1061	0.0776	0.0144	-	-	2%	21%	76%	1%
WYL-09-50-37.5 h garn 33	33	24	6.2375	0.0000	4.0348	-	0.0000	0.0000	4.5922	1.1805	0.1043	0.0864	0.0017	-	-	2%	20%	77%	1%
WYL-09-50-37.5 h garn 34	34	24	6.1257	0.0000	4.1039	-	0.0000	0.0000	4.4739	1.2332	0.0928	0.0784	0.0177	-	-	2%	21%	76%	1%
WYL-09-50-37.5 big garnet	82	24	6.0599	0.0004	4.0828	0.0015	0.0022	0.0000	4.2516	1.4542	0.1072	0.0934	0.0068	0.0000	0.0000	2%	25%	72%	2%
WYL-09-50-37.5 big garnet	83	24	6.0818	0.0000	4.0972	0.0008	0.0035	0.0000	4.2433	1.4412	0.1060	0.0878	0.0066	0.0098	0.0037	2%	24%	72%	1%
WYL-09-50-37.5 big garnet	84	24	6.0198	0.0004	4.0588	0.0000	0.0021	0.0000	4.3109	1.4389	0.1047	0.0792	0.0050	0.0000	0.0001	2%	24%	73%	1%
WYL-09-50-37.5 big garnet	85	24	6.0905	0.0013	4.1153	0.0011	0.0018	0.0000	4.2576	1.4201	0.1079	0.0773	0.0091	0.0024	0.0061	2%	24%	72%	1%
WYL-09-50-37.5 big garnet	86	24	6.0455	0.0009	4.0929	0.0000	0.0026	0.0000	4.3030	1.4133	0.1053	0.0745	0.0076	0.0000	0.0000	2%	24%	73%	1%
WYL-09-50-37.5 big garnet	87	24	5.9348	0.0021	4.0279	0.0000	0.0017	0.0000	4.3533	1.4365	0.0998	0.0714	0.0060	0.0014	0.0000	2%	24%	73%	1%
WYL-09-50-37.5 big garnet	88	24	5.8700	0.0000	3.9662	0.0015	0.0030	0.0293	4.4393	1.3786	0.1008	0.0688	0.0081	0.0000	0.0046	2%	23%	74%	1%
WYL-09-50-37.5 image 7 gar-2	96	24	6.1567	0.0015	4.1473	0.0068	0.0015	0.0000	4.4954	1.1605	0.1092	0.0700	0.0046	0.0000	0.0032	2%	20%	77%	1%
WYL-09-50-37.5 image 7 gar-2	97	24	6.2005	0.0030	4.1495	0.0000	0.0028	0.0000	4.5231	1.1286	0.1128	0.0730	0.0066	0.0005	0.0000	2%	19%	77%	1%
WYL-09-50-37.5 image 7 gar-2	98	24	6.1544	0.0007	4.1389	0.0000	0.0018	0.0000	4.5797	1.0824	0.1101	0.0772	0.0061	0.0031	0.0000	2%	18%	78%	1%
WYL-09-50-37.5 image 7 gar-2	99	24	6.2076	0.0041	4.1496	0.0000	0.0029	0.0000	4.6705	0.9823	0.1005	0.0791	0.0064	0.0026	0.0019	2%	17%	80%	1%
WYL-09-50-37.5 image 7 gar2-2	104	24	6.1996	0.0014	4.1754	0.0030	0.0020	0.0000	4.4595	1.1691	0.1092	0.0693	0.0069	0.0037	0.0007	2%	20%	77%	1%
WYL-09-50-37.5 image 7 gar2-2	105	24	6.1514	0.0001	4.1482	0.0000	0.0022	0.0000	4.5205	1.1266	0.1105	0.0784	0.0047	0.0081	0.0005	2%	19%	77%	1%
WYL-09-50-37.5 image 7 gar2-2	106	24	6.1968	0.0016	4.1589	0.0012	0.0039	0.0000	4.5863	1.0514	0.1119	0.0799	0.0049	0.0000	0.0000	2%	18%	79%	1%
WYL-09-50-37.5 image 7 gar2-2	107	24	6.2009	0.0021	4.1516	0.0000	0.0032	0.0000	4.6453	0.9961	0.1069	0.0847	0.0076	0.0000	0.0023	2%	17%	80%	1%
WYL-09-50-37.5 image 9 gar3	112	24	6.1939	0.0012	4.1666	0.0035	0.0026	0.0000	4.4592	1.1845	0.1074	0.0648	0.0102	0.0000	0.0000	2%	20%	77%	1%
WYL-09-50-37.5 image 9 gar3	113	24	6.2137	0.0019	4.1609	0.0000	0.0020	0.0000	4.4807	1.1713	0.1078	0.0628	0.0076	0.0049	0.0000	2%	20%	77%	1%
WYL-09-50-37.5 image 9 gar3	114	24	6.1773	0.0016	4.1627	0.0069	0.0023	0.0000	4.5048	1.1350	0.1093	0.0662	0.0096	0.0000	0.0016	2%	19%	77%	1%
WYL-09-50-37.5 image 9 gar3	115	24	6.2406	0.0031	4.1574	0.0011	0.0031	0.0000	4.5860	1.0550	0.1119	0.0747	0.0076	0.0000	0.0000	2%	18%	79%	1%

Table I-3. Garnet Line Scan Chemistry

Sample/Photo	Point	SiO2	TiO2	Al2O3	Cr2O3	FeO	MgO	MnO	CaO	Na2O	Total	O	Si	Ti	Al	V	Cr	Fe3	Fe2	Mg	Ca	Mn	Na	grossular	pyrope	almandine	spessartine
WYL-09-44-61.4 photo C linesca	5	36.98	0.00	20.44	0.04	35.83	2.23	2.52	1.83	0.01	99.87	24	6.0118	0.0000	3.9163	0.0000	0.0046	0.0792	4.7921	0.5397	0.3192	0.3466	0.0025	5.3%	9.0%	79.9%	5.8%
WYL-09-44-61.4 photo C linesca	6	37.38	0.00	20.37	0.02	35.61	2.18	2.52	1.76	0.03	99.88	24	6.1138	0.0000	3.9266	0.0000	0.0026	0.0708	4.8000	0.5320	0.3078	0.3496	0.0107	5.1%	8.9%	80.0%	5.8%
WYL-09-44-61.4 photo C linesca	7	37.06	0.00	20.47	0.06	35.66	2.30	2.32	1.74	0.06	99.67	24	6.0385	0.0000	3.9309	0.0000	0.0080	0.0611	4.7980	0.5595	0.3032	0.3208	0.0185	5.1%	9.3%	80.0%	5.3%
WYL-09-44-61.4 photo C linesca	9	37.18	0.00	20.59	0.05	36.22	2.32	2.24	1.70	0.05	100.36	24	6.0087	0.0000	3.9218	0.0000	0.0068	0.0714	4.8239	0.5578	0.2949	0.3067	0.0167	4.9%	9.3%	80.4%	5.1%
WYL-09-44-61.4 photo C linesca	10	37.73	0.00	19.96	0.00	36.27	2.40	2.25	1.68	0.02	100.31	24	6.1674	0.0000	3.8453	0.0000	0.0003	0.1544	4.8037	0.5852	0.2936	0.3118	0.0057	4.9%	9.8%	80.1%	5.2%
WYL-09-44-61.4 photo C linesca	11	37.58	0.03	20.73	0.11	36.23	2.32	2.01	1.65	0.01	100.66	24	6.0845	0.0032	3.9557	0.0000	0.0136	0.0307	4.8749	0.5590	0.2864	0.2758	0.0038	4.8%	9.3%	81.2%	4.6%
WYL-09-44-61.4 photo C linesca	12	37.66	0.00	20.43	0.03	36.13	2.27	2.10	1.57	0.04	100.22	24	6.1503	0.0000	3.9322	0.0000	0.0037	0.0640	4.8705	0.5524	0.2751	0.2899	0.0121	4.6%	9.2%	81.2%	4.8%
WYL-09-44-61.4 photo C linesca	13	37.84	0.00	20.76	0.09	36.01	2.47	2.17	1.73	0.03	101.10	24	6.0960	0.0000	3.9416	0.0000	0.0113	0.0470	4.8044	0.5927	0.2980	0.2965	0.0084	5.0%	9.9%	80.1%	4.9%
WYL-09-44-61.4 photo C linesca	14	37.74	0.00	20.88	0.01	36.15	2.39	2.16	1.76	0.00	101.10	24	6.0742	0.0000	3.9607	0.0000	0.0011	0.0381	4.8276	0.5742	0.3033	0.2949	0.0000	5.1%	9.6%	80.5%	4.9%
WYL-09-44-61.4 photo C linesca	15	37.47	0.06	20.61	0.00	35.98	2.38	2.31	1.67	0.04	100.52	24	6.0690	0.0076	3.9343	0.0000	0.0000	0.0657	4.8078	0.5747	0.2896	0.3165	0.0113	4.8%	9.6%	80.1%	5.3%
WYL-09-44-61.4 photo C linesca	16	37.86	0.00	19.85	0.04	35.73	2.32	2.29	1.84	0.05	99.99	24	6.2297	0.0000	3.8495	0.0000	0.0055	0.1450	4.7717	0.5689	0.3239	0.3198	0.0158	5.4%	9.5%	79.5%	5.3%
WYL-09-44-61.4 photo C linesca	17	37.60	0.00	20.24	0.00	36.10	2.36	2.18	1.72	0.05	100.25	24	6.1290	0.0000	3.8884	0.0000	0.0000	0.1116	4.8095	0.5742	0.3007	0.3008	0.0147	5.0%	9.6%	80.2%	5.0%
WYL-09-44-61.4 photo C linesca	18	37.59	0.00	20.41	0.02	35.51	2.28	2.55	1.69	0.01	100.05	24	6.1464	0.0000	3.9332	0.0000	0.0023	0.0645	4.7913	0.5562	0.2953	0.3527	0.0045	4.9%	9.3%	79.9%	5.9%
WYL-09-44-61.4 photo C linesca	19	37.40	0.00	20.67	0.06	35.86	2.19	2.51	1.75	0.02	100.47	24	6.0595	0.0000	3.9469	0.0000	0.0083	0.0448	4.8140	0.5301	0.3031	0.3451	0.0077	5.1%	8.8%	80.2%	5.8%
WYL-09-44-61.4 photo C linesca	20	37.08	0.00	20.42	0.04	35.93	2.04	2.64	1.73	0.01	99.89	24	6.0489	0.0000	3.9260	0.0000	0.0057	0.0683	4.8334	0.4969	0.3026	0.3646	0.0026	5.0%	8.3%	80.6%	6.1%
WYL-09-44-61.4 photo F linesca	1	37.42	0.00	20.89	0.00	36.20	2.28	2.36	1.53	0.04	100.72	24	6.0347	0.0000	3.9705	0.0000	0.0000	0.0295	4.8527	0.5471	0.2651	0.3218	0.0134	4.4%	9.1%	80.9%	5.4%
WYL-09-44-61.4 photo F linesca	2	37.33	0.00	20.81	0.00	36.09	2.42	2.31	1.46	0.04	100.46	24	6.0294	0.0000	3.9613	0.0000	0.0003	0.0383	4.8365	0.5822	0.2533	0.3160	0.0121	4.2%	9.7%	80.6%	5.3%
WYL-09-44-61.4 photo F linesca	3	37.87	0.02	20.79	0.00	36.25	2.63	2.04	1.38	0.00	100.98	24	6.1133	0.0019	3.9554	0.0000	0.0000	0.0446	4.8492	0.6317	0.2392	0.2795	0.0004	4.0%	10.5%	80.8%	4.7%
WYL-09-44-61.4 photo F linesca	4	37.76	0.00	20.76	0.01	36.41	2.60	1.97	1.56	0.02	101.08	24	6.0732	0.0000	3.9352	0.0000	0.0012	0.0636	4.8338	0.6227	0.2691	0.2678	0.0067	4.5%	10.4%	80.6%	4.5%
WYL-09-44-61.4 photo F linesca	5	37.34	0.00	20.85	0.00	36.32	2.65	1.66	1.50	0.01	100.33	24	6.0293	0.0000	3.9679	0.0000	0.0000	0.0321	4.8724	0.6387	0.2589	0.2269	0.0031	4.3%	10.6%	81.2%	3.8%
WYL-09-44-61.4 photo F linesca	6	38.28	0.00	20.69	0.03	36.83	2.83	1.79	1.48	0.03	101.96	24	6.1165	0.0000	3.8962	0.0000	0.0042	0.0996	4.8218	0.6731	0.2542	0.2419	0.0090	4.2%	11.2%	80.4%	4.0%
WYL-09-44-61.4 photo F linesca	7	37.72	0.00	20.89	0.00	36.67	2.73	1.63	1.58	0.23	101.46	24	5.9989	0.0000	3.9156	0.0000	0.0000	0.0844	4.7928	0.6468	0.2700	0.2201	0.0703	4.5%	10.8%	79.9%	3.7%
WYL-09-44-61.4 photo F linesca	8	37.96	0.05	20.75	0.05	36.54	2.80	1.67	1.62	0.00	101.43	24	6.0855	0.0055	3.9205	0.0000	0.0057	0.0738	4.8251	0.6696	0.2780	0.2273	0.0000	4.6%	11.2%	80.4%	3.8%
WYL-09-44-61.4 photo F linesca	9	38.02	0.03	20.79	0.04	36.52	2.81	1.72	1.56	0.01	101.49	24	6.0927	0.0036	3.9265	0.0000	0.0051	0.0684	4.8258	0.6712	0.2671	0.2334	0.0025	4.5%	11.2%	80.4%	3.9%
WYL-09-44-61.4 photo F linesca	10	36.84	0.00	20.72	0.01	36.53	2.85	1.72	1.45	0.00	100.13	24	5.9191	0.0000	3.9236	0.0000	0.0012	0.0752	4.8332	0.6832	0.2493	0.2343	0.0000	4.2%	11.4%	80.6%	3.9%
WYL-09-44-61.4 photo F linesca	11	37.78	0.04	20.54	0.04	36.38	2.79	1.74	1.43	0.00	100.75	24	6.1092	0.0054	3.9145	0.0000	0.0054	0.0800	4.8397	0.6733	0.2482	0.2389	0.0000	4.1%	11.2%	80.7%	4.0%
WYL-09-44-61.4 photo F linesca	12	37.95	0.00	20.80	0.03	36.21	2.82	1.63	1.50	0.01	100.93	24	6.1195	0.0000	3.9530	0.0000	0.0036	0.0434	4.8397	0.6773	0.2588	0.2227	0.0016	4.3%	11.3%	80.7%	3.7%
WYL-09-44-61.4 photo F linesca	13	38.03	0.00	20.56	0.05	36.03	2.94	1.64	1.37	0.04	100.67	24	6.1602	0.0000	3.9251	0.0000	0.0060	0.0689	4.8119	0.7106	0.2382	0.2254	0.0139	4.0%	11.8%	80.2%	3.8%
WYL-09-44-61.4 photo F linesca	14	37.21	0.00	20.57	0.01	35.67	2.95	1.72	1.49	0.03	99.66	24	6.0415	0.0000	3.9362	0.0000	0.0015	0.0623	4.7811	0.7138	0.2591	0.2371	0.0089	4.3%	11.9%	79.7%	4.0%
WYL-09-44-61.4 photo F linesca	15	37.62	0.00	20.43	0.00	36.05	2.97	1.65	1.59	0.03	100.34	24	6.0869	0.0000	3.8959	0.0000	0.0000	0.1041	4.7738	0.7161	0.2753	0.2266	0.0081	4.6%	11.9%	79.6%	3.8%
WYL-09-44-61.4 photo F linesca	16	37.78	0.00	20.49	0.06	36.31	3.01	1.69	1.52	0.03	100.88	24	6.0778	0.0000	3.8850	0.0000	0.0075	0.1076	4.7775	0.7219	0.2614	0.2303	0.0090	4.4%	12.0%	79.6%	3.8%
WYL-09-44-61.4 photo F linesca	17	37.30	0.03	20.46	0.03	35.95	3.03	1.60	1.60	0.01	100.02	24	6.0349	0.0037	3.9014	0.0000	0.0042	0.0944	4.7698	0.7308	0.2781	0.2189	0.0024	4.6%	12.2%	79.5%	3.6%
WYL-09-44-61.4 photo F linesca	18	37.81	0.08	20.54	0.09	36.10	2.95	1.62	1.54	0.06	100.79	24	6.0973	0.0097	3.9038	0.0000	0.0120	0.0842	4.7843	0.7096	0.2657	0.2207	0.0196	4.4%	11.8%	79.7%	3.7%
WYL-09-44-61.4 photo F linesca	19	36.79	0.00	20.67	0.04	36.05	2.96	1.69	1.52	0.05	99.77	24	5.9243	0.0000	3.9228	0.0000	0.0048	0.0723	4.7824	0.7100	0.2614	0.2310	0.0152	4.4%	11.8%	79.7%	3.8%
WYL-09-44-61.4 photo F linesca	20	38.28	0.00	20.49	0.00	36.04	3.04	1.56	1.46	0.03	100.91	24	6.1965	0.0000	3.9090	0.0000	0.0000	0.0910	4.7878	0.7336	0.2536	0.2145	0.0105	4.2%	12.2%	79.8%	3.6%
WYL-09-44-61.4 photo F linesca	21	38.13	0.00	20.58	0.03	35.79	2.97	1.69	1.49	0.00	100.67	24	6.1838	0.0000	3.9336	0.0000	0.0036	0.0628	4.7912	0.7182	0.2584	0.2321	0.0000	4.3%	12.0%	79.9%	3.9%
WYL-09-44-61.4 photo F linesca	22	38.02	0.00	20.71	0.03	36.23	2.97	1.66	1.49	0.04	101.15	24	6.1085	0.0000	3.9216	0.0000	0.0042	0.0742	4.7937	0.7122	0.2562	0.2264	0.0114	4.3%	11.9%	79.9%	3.8%
WYL-09-44-61.4 photo F linesca	23	37.13	0.00	20.39	0.01	35.47	2.83	1.70	1.67	0.00	99.20	24	6.0718	0.0000	3.9298	0.0000	0.0012	0.0690	4.7817	0.6906	0.2929	0.2348	0.0000	4.9%	11.5%	79.7%	3.9%
WYL-09-44-61.4 photo F linesca	24	37.91	0.00	20.54	0.04	35.50	2.74	1.67	1.53	0.03	99.96	24	6.2023	0.0000	3.9605	0.0000	0.0045	0.0349	4.8222	0.6692	0.2683	0.2315	0.0088	4.5%	11.2%	80.4%	3.9%
WYL-09-44-61.4 photo F linesca	25	37.86	0.00	20.60	0.01	36.10	2.62	1.83	1.57	0.02	100.60	24	6.1414	0.0000	3.9383	0.0000	0.0012	0.0605	4.8367	0.6325	0.2729	0.2513	0.0067	4.5%	10.5%	80.6%	4.2%
WYL-09-44-61.4 photo F linesca	26	37.67	0.00	20.69	0.00	35.70	2.47	2.19	1.61	0.03	100.36	24	6.1192	0.0000	3.9611	0.0000	0.0000	0.0389	4.8110	0.5981	0.2802	0.3019	0.0089	4.7%	10.0%	80.2%	5.0%
WYL-09-44-61.4 photo F linesca	27	36.91	0.00	20.66	0.00	35.29	2.28	2.30	1.70	0.07	99.21	24	6.0342	0.0000	3.9807	0.0000	0.0000	0.0193	4.8056	0.5565	0.2979	0.3181	0.0218	5.0%	9.3%	80.1%	5.3%
WYL-09-44-61.4 photo F linesca	28	37.73	0.00	20.81	0.01	35.71	2.17	2.38	1.66	0.03	100.49	24	6.1367	0.0000	3.9891	0.0000	0.0009	0.0100	4.8473	0.5253	0.2897	0.3286	0.0091	4.8%	8.8%	80.8%	5.5%
WYL-09-44-61.4 photo F linesca	29	37.52	0.00	20.59	0.00	35.14	1.99	2.52	1.65	0.01	99.43	24	6.1962	0.0000	4.0075	0.0000	0.0000	0.0000	4.8531	0.4911	0.2920	0.3526	0.0038	4.9%	8.2%	81.0%	5.9%
WYL-09-44-61.4 photo F linesca	30	37.68	0.00	20.54	0.04	35.60	2.07	2.43	1.74	0.02	100.11	24	6.1724	0.0000	3.9655	0.0000	0.0049	0.0296	4.8473	0.5044	0.3060	0.3372	0.0051	5.1%	8.4%	80.8%	5.6%
WYL-09-50-37.5 lg garn linesca	1	39.02	0.00	21.19	0.07	32.07	5.18	0.57	0.65	0.02	98.76	24	6.4183	0.0000	4.1079	0.0000	0.0094	0.0000	4.4115	1.2702	0.1143	0.0788	0.0078	1.9%	21.6%	75.0%	1.3%
WYL-09-50-37.5 lg garn linesca	2	38.98	0.03	21.37	0.00	32.26	5.23	0.48	0.59	0.02	98.96	24	6.3864	0.0032	4.1264	0.0000	0.0000	0.0000	4.4201	1.2774	0.1028	0.0672	0.0061	1.7%	21.7%	75.3%	1.1%
WYL-09-50-37.5 lg garn linesca	3	38.93	0.00	21.11	0.02	32.20	5.45	0.44	0.56	0.04	98.77	24	6.3805	0.0003	4.0777	0.0000	0.0028	0.0000	4.4135	1.3316	0.0991	0.0615	0.0138	1.7%	22.5%	74.6%	1.0%
WYL-09-50-37.5 lg garn linesca	4	38.91	0.00	21.22	0.00	31.90	5.60	0.52	0.63	0.04	98.82	24	6.3548	0.0000	4.0845	0.0000	0.0006	0.0000	4.3570	1.3635	0.1100	0.0720	0.0123	1.9%	23.1%	73.7%	1.2%
WYL-09-50-37.5 lg garn linesca	5	39.19	0.00	21.31	0.03	31.75	5.84	0.51	0.65	0.04	99.33	24	6.3614	0.0000	4.0768	0.0000	0.0040	0.0000	4.3100	1.4132	0.1131	0.0706	0.0124	1.9%	23.9%	72.8%	1.2%
WYL-09-50-37.5 lg garn linesca	6	39.15	0.00	21.37	0.00	31.63	5.82	0.54	0.62	0.04	99.15	24	6.3660	0.0000	4.0954	0.0000	0.0000	0.0000	4.3012	1.4108	0.1075	0.0740	0.0110	1.8%	23.9%	72.8%	1.3%
WYL-09-50-37.5 lg garn linesca	7	39.17	0.00	21.30	0.05	31.55	5.99	0.48	0.63	0.00	99.17	24	6.3654	0.0000	4.0795	0.0000	0.0062	0.0000	4.2877	1.4511	0.1091	0.0663	0.0000	1.8%	24.5%	72.5%	1.1%
WYL-09-50-37.5 lg garn linesca	8	39.26	0.00	21.41	0.00	31.52	6.00	0.57	0.70	0.05	99.52	24	6.3458	0.0000	4.0786	0.0000	0.0006	0.0000	4.2607	1.4458	0.1208	0.0780	0.0155	2.0%	24.4%	72.0%	1.3%
WYL-09-50-37.5 lg garn linesca	9	38.90	0.00	21.51	0.00	31.53	6.05	0.45	0.58	0.04	99.06	24	6.2925	0.0000	4.1008	0.0000	0.0000	0.0000	4.2653	1.4589	0.1013	0.0620	0.0117	1.7%	24.7%	72.3%	1.1%
WYL-09-50-37.5 lg garn linesca	10	38.63	0.02	21.62	0.05	31.73	6.11	0.55	0.61	0.05	99.37	24	6.1919	0.0023	4.0842	0.0000	0.0068	0.0000	4.2533	1.4600	0.1055	0.0752	0.0149	1.8%	24.7%	72.0%	1.3%
WYL-09-50-37.5 lg garn linesca	11	38.14	0.00	21.15	0.03	31.00	6.07	0.52	0.63	0.01	97.55	24	6.2469	0.0000	4.0827	0.0000	0.0034	0.0000	4.2462	1.4821	0.1105	0.0720	0.0030	1.9%	25.1%	71.8%	1.2%
WYL-09-50-37.5 lg garn linesca	12	39.21	0.00	21.29	0.11	31.03	6.00	0.62	0.53	0.05	98.83	24	6.4008	0.0000	4.0961	0.0000	0.0144	0.0000	4.2362	1.4602	0.0928	0.0854	0.0150	1.6%	24.8%	71.9%	1.5%
WYL-09-50-37.5 lg garn linesca	13	38.93	0.04	21.19	0.00	31.50	6.11	0.60	0.65	0.01	99.02	24	6.3156	0.0043	4.0515	0.0000	0.0000	0.0000	4.2736	1.4777	0.1124	0.0823	0.0025	1.9%	24.8%	71.8%	1.4%
WYL-09-50-37.5 lg garn linesca	14	39.06	0.03	21.21	0.05	31.61	6.15	0.59	0.62	0.02	99.35	24	6.3153	0.0033	4.0416	0.0000	0.0068	0.0000	4.2741	1.4823	0.1077	0.0811	0.0064	1.8%	24.9%	71.8%	1.4%
WYL-09-50-37.5 lg garn linesca	15	38.82	0.00	21.08	0.00	31.66	6.13	0.61	0.67	0.01	98.98	24	6.2912	0.0000	4.0263	0.0000	0.0000	0.0000	4.2909	1.4810	0.1169	0.0832	0.0017	2.0%	24.8%	71.8%	1.4%
WYL-09-50-37.5 lg garn linesca	16	38.58	0.00	21.27	0.00	31.30	6.13	0.62	0.59	0.03	98.51	24	6.2632	0.0000	4.0697	0.0000	0.0000	0.0000	4.2495	1.4836	0.1019	0.0852	0.0102	1.7%	25.0%	71.7%	1.4%
WYL-09-50-37.5 lg garn linesca	17	38.28	0.16	21.11	0.02	31.08	6.11	0.56	0.59	0.02	97.92	24	6.2606	0.0202	4.0690	0.0000	0.0022	0.0000	4.2509	1.4897	0.1032	0.0772	0.0077	1.7%	25.1%	71.7%	1.3%

Sample/Photo	Point	SiO2	TiO2	Al2O3	Cr2O3	FeO	MgO	MnO	CaO	Na2O	Total	O	Si	Ti	Al	V	Cr	Fe3	Fe2	Mg	Ca	Mn	Na	grossular	pyrope	almandine	spessartine
WYL-09-50-37.5 lg garn linesca	18	39.03	0.00	21.16	0.04	30.89	6.32	0.56	0.55	0.04	98.60	24	6.3594	0.0000	4.0634	0.0000	0.0056	0.0000	4.2091	1.5351	0.0964	0.0768	0.0136	1.6%	25.9%	71.0%	1.3%
WYL-09-50-37.5 lg garn linesca	19	38.95	0.00	21.44	0.03	31.20	6.03	0.51	0.64	0.03	98.82	24	6.3291	0.0000	4.1060	0.0000	0.0034	0.0000	4.2398	1.4607	0.1110	0.0705	0.0086	1.9%	24.8%	72.0%	1.2%
WYL-09-50-37.5 lg garn linesca	20	39.13	0.00	21.22	0.05	31.13	6.21	0.65	0.61	0.02	99.03	24	6.3534	0.0000	4.0607	0.0000	0.0065	0.0000	4.2270	1.5031	0.1067	0.0899	0.0061	1.8%	25.3%	71.2%	1.5%
WYL-09-50-37.5 lg garn linesca	21	38.85	0.00	21.25	0.07	31.33	6.12	0.61	0.65	0.02	98.89	24	6.2993	0.0000	4.0609	0.0000	0.0096	0.0000	4.2483	1.4793	0.1129	0.0833	0.0057	1.9%	24.9%	71.6%	1.4%
WYL-09-50-37.5 lg garn linesca	22	39.06	0.00	21.25	0.05	31.25	6.28	0.60	0.57	0.01	99.07	24	6.3280	0.0000	4.0574	0.0000	0.0065	0.0000	4.2339	1.5167	0.0994	0.0830	0.0031	1.7%	25.6%	71.3%	1.4%
WYL-09-50-37.5 lg garn linesca	23	39.03	0.00	21.31	0.00	31.06	6.27	0.62	0.62	0.00	98.90	24	6.3332	0.0000	4.0754	0.0000	0.0000	0.0000	4.2149	1.5167	0.1082	0.0849	0.0000	1.8%	25.6%	71.1%	1.4%
WYL-09-50-37.5 lg garn linesca	24	39.01	0.00	21.33	0.01	31.44	6.34	0.60	0.67	0.03	99.44	24	6.2735	0.0000	4.0428	0.0000	0.0012	0.0000	4.2284	1.5200	0.1150	0.0823	0.0104	1.9%	25.5%	71.0%	1.4%
WYL-09-50-37.5 lg garn linesca	25	38.88	0.00	21.26	0.02	32.07	6.27	0.59	0.56	0.06	99.71	24	6.2252	0.0000	4.0119	0.0000	0.0021	0.0000	4.2942	1.4966	0.0965	0.0796	0.0190	1.6%	25.0%	71.7%	1.3%
WYL-09-50-37.5 lg garn linesca	26	38.46	0.00	21.52	0.01	31.77	6.38	0.62	0.66	0.03	99.43	24	6.1312	0.0000	4.0433	0.0000	0.0009	0.0000	4.2356	1.5162	0.1128	0.0831	0.0081	1.9%	25.5%	71.1%	1.4%
WYL-09-50-37.5 lg garn linesca	27	39.14	0.04	21.61	0.00	31.76	6.29	0.66	0.60	0.05	100.14	24	6.2421	0.0054	4.0618	0.0000	0.0000	0.0000	4.2359	1.4954	0.1019	0.0888	0.0161	1.7%	25.2%	71.3%	1.5%
WYL-09-50-37.5 lg garn linesca	28	38.98	0.00	21.42	0.00	32.25	6.33	0.62	0.67	0.03	100.29	24	6.1930	0.0000	4.0108	0.0000	0.0000	0.0000	4.2850	1.4992	0.1136	0.0835	0.0079	1.9%	25.0%	71.5%	1.4%
WYL-09-50-37.5 lg garn linesca	29	39.38	0.00	21.24	0.06	31.79	6.31	0.72	0.60	0.06	100.17	24	6.3065	0.0000	4.0089	0.0000	0.0080	0.0000	4.2575	1.5064	0.1036	0.0974	0.0182	1.7%	25.2%	71.2%	1.6%
WYL-09-50-37.5 lg garn linesca	30	39.28	0.00	21.33	0.00	31.82	6.35	0.63	0.66	0.04	100.10	24	6.2823	0.0000	4.0206	0.0000	0.0000	0.0000	4.2560	1.5140	0.1123	0.0853	0.0118	1.9%	25.3%	71.2%	1.4%
WYL-09-50-37.5 lg garn linesca	31	37.93	0.11	21.37	0.01	31.66	6.40	0.65	0.61	0.03	98.77	24	6.0717	0.0137	4.0317	0.0000	0.0018	0.0000	4.2383	1.5273	0.1048	0.0882	0.0079	1.8%	25.6%	71.0%	1.5%
WYL-09-50-37.5 lg garn linesca	32	39.33	0.04	21.21	0.00	32.09	6.28	0.68	0.68	0.03	100.34	24	6.2876	0.0043	3.9963	0.0000	0.0000	0.0037	4.2865	1.4967	0.1165	0.0915	0.0089	1.9%	24.9%	71.4%	1.5%
WYL-09-50-37.5 lg garn linesca	33	39.07	0.00	21.24	0.02	31.66	6.36	0.62	0.64	0.04	99.68	24	6.2704	0.0000	4.0175	0.0000	0.0031	0.0000	4.2493	1.5217	0.1106	0.0849	0.0129	1.8%	25.4%	71.1%	1.4%
WYL-09-50-37.5 lg garn linesca	34	39.01	0.00	21.32	0.02	31.95	6.33	0.65	0.65	0.04	99.97	24	6.2294	0.0000	4.0125	0.0000	0.0030	0.0000	4.2668	1.5069	0.1118	0.0881	0.0109	1.9%	25.2%	71.3%	1.5%
WYL-09-50-37.5 lg garn linesca	35	38.17	0.00	21.32	0.00	31.85	6.20	0.70	0.68	0.03	98.95	24	6.1182	0.0000	4.0276	0.0000	0.0000	0.0000	4.2694	1.4815	0.1173	0.0950	0.0092	2.0%	24.8%	71.5%	1.6%
WYL-09-50-37.5 lg garn linesca	36	38.48	0.00	21.39	0.03	32.07	6.23	0.67	0.64	0.00	99.50	24	6.1483	0.0000	4.0280	0.0000	0.0037	0.0000	4.2852	1.4839	0.1090	0.0902	0.0000	1.8%	24.9%	71.8%	1.5%
WYL-09-50-37.5 lg garn linesca	37	38.85	0.05	21.49	0.05	32.88	6.31	0.75	0.55	0.02	100.95	24	6.1153	0.0056	3.9868	0.0000	0.0063	0.0069	4.3214	1.4807	0.0922	0.1003	0.0054	1.5%	24.7%	72.0%	1.7%
WYL-09-50-37.5 lg garn linesca	38	39.19	0.00	21.23	0.00	31.92	6.29	0.66	0.61	0.02	99.91	24	6.2871	0.0000	4.0141	0.0000	0.0000	0.0000	4.2825	1.5043	0.1046	0.0897	0.0049	1.7%	25.1%	71.5%	1.5%
WYL-09-50-37.5 lg garn linesca	39	38.74	0.00	21.37	0.02	32.34	6.38	0.73	0.59	0.04	100.22	24	6.1404	0.0000	3.9920	0.0000	0.0021	0.0058	4.2810	1.5075	0.1006	0.0980	0.0129	1.7%	25.1%	71.3%	1.6%
WYL-09-50-37.5 lg garn linesca	40	38.95	0.01	21.32	0.00	32.55	6.30	0.67	0.64	0.01	100.44	24	6.1815	0.0008	3.9878	0.0000	0.0000	0.0122	4.3079	1.4905	0.1081	0.0898	0.0037	1.8%	24.8%	71.8%	1.5%
WYL-09-50-37.5 lg garn linesca	41	39.00	0.04	21.27	0.01	32.19	6.50	0.66	0.61	0.02	100.32	24	6.1951	0.0051	3.9820	0.0000	0.0018	0.0162	4.2600	1.5392	0.1040	0.0892	0.0075	1.7%	25.7%	71.0%	1.5%
WYL-09-50-37.5 lg garn linesca	42	39.52	0.00	21.09	0.00	32.55	6.46	0.73	0.65	0.01	101.01	24	6.2687	0.0000	3.9427	0.0000	0.0000	0.0573	4.2605	1.5276	0.1098	0.0980	0.0042	1.8%	25.5%	71.0%	1.6%
WYL-09-50-37.5 lg garn linesca	43	39.20	0.05	21.42	0.00	32.81	6.40	0.74	0.64	0.03	101.29	24	6.1635	0.0063	3.9693	0.0000	0.0003	0.0304	4.2838	1.5001	0.1074	0.0981	0.0106	1.8%	25.0%	71.4%	1.6%
WYL-09-50-37.5 lg garn linesca	44	39.07	0.02	21.39	0.00	32.49	6.48	0.76	0.58	0.03	100.83	24	6.1649	0.0022	3.9779	0.0000	0.0000	0.0221	4.2652	1.5243	0.0985	0.1018	0.0102	1.6%	25.4%	71.1%	1.7%
WYL-09-50-37.5 lg garn linesca	45	38.80	0.03	21.17	0.00	32.74	6.30	0.71	0.62	0.07	100.44	24	6.1471	0.0040	3.9529	0.0000	0.0000	0.0471	4.2908	1.4880	0.1049	0.0956	0.0208	1.7%	24.8%	71.5%	1.6%
WYL-09-50-37.5 lg garn linesca	46	39.02	0.00	21.46	0.04	32.62	6.33	0.67	0.63	0.02	100.78	24	6.1635	0.0000	3.9951	0.0000	0.0045	0.0004	4.3086	1.4906	0.1063	0.0899	0.0047	1.8%	24.8%	71.8%	1.5%
WYL-09-50-37.5 lg garn linesca	47	39.06	0.00	21.41	0.09	33.15	6.41	0.69	0.61	0.07	101.48	24	6.1081	0.0000	3.9459	0.0000	0.0107	0.0434	4.2918	1.4943	0.1027	0.0908	0.0204	1.7%	24.9%	71.5%	1.5%
WYL-09-50-37.5 lg garn linesca	48	39.14	0.00	21.30	0.09	32.78	6.37	0.77	0.67	0.06	101.17	24	6.1568	0.0000	3.9488	0.0000	0.0117	0.0395	4.2727	1.4938	0.1130	0.1020	0.0185	1.9%	24.9%	71.2%	1.7%
WYL-09-50-37.5 lg garn linesca	49	39.11	0.04	21.25	0.00	32.77	6.25	0.75	0.64	0.06	100.85	24	6.1886	0.0043	3.9630	0.0000	0.0000	0.0370	4.2995	1.4743	0.1084	0.0999	0.0178	1.8%	24.6%	71.7%	1.7%
WYL-09-50-37.5 lg garn linesca	50	39.08	0.00	21.25	0.00	32.97	6.26	0.68	0.71	0.03	100.98	24	6.1700	0.0000	3.9540	0.0000	0.0006	0.0454	4.3078	1.4734	0.1197	0.0905	0.0087	2.0%	24.6%	71.8%	1.5%
WYL-09-50-37.5 lg garn linesca	51	38.89	0.00	21.29	0.00	32.84	6.23	0.78	0.62	0.05	100.70	24	6.1474	0.0000	3.9663	0.0000	0.0006	0.0331	4.3081	1.4681	0.1052	0.1039	0.0148	1.8%	24.5%	71.8%	1.7%
WYL-09-50-37.5 lg garn linesca	52	38.94	0.00	21.22	0.00	33.11	6.41	0.74	0.65	0.06	101.12	24	6.1137	0.0000	3.9265	0.0000	0.0000	0.0735	4.2738	1.5003	0.1100	0.0979	0.0180	1.8%	25.0%	71.2%	1.6%
WYL-09-50-37.5 lg garn linesca	53	39.22	0.00	21.35	0.02	32.68	6.45	0.68	0.62	0.06	101.08	24	6.1792	0.0000	3.9644	0.0000	0.0021	0.0335	4.2724	1.5149	0.1050	0.0908	0.0169	1.8%	25.2%	71.2%	1.5%
WYL-09-50-37.5 lg garn linesca	54	38.46	0.00	21.16	0.03	32.80	6.28	0.68	0.65	0.03	100.08	24	6.0978	0.0000	3.9540	0.0000	0.0039	0.0421	4.3070	1.4843	0.1100	0.0907	0.0080	1.8%	24.7%	71.8%	1.5%
WYL-09-50-37.5 lg garn linesca	55	38.09	0.05	21.23	0.03	32.62	6.39	0.71	0.62	0.04	99.79	24	6.0279	0.0063	3.9597	0.0000	0.0033	0.0370	4.2801	1.5075	0.1053	0.0954	0.0116	1.8%	25.1%	71.3%	1.6%
WYL-09-50-37.5 lg garn linesca	56	38.68	0.00	21.18	0.00	33.15	6.32	0.64	0.60	0.04	100.60	24	6.1037	0.0000	3.9390	0.0000	0.0000	0.0610	4.3137	1.4867	0.1022	0.0849	0.0125	1.7%	24.8%	71.9%	1.4%
WYL-09-50-37.5 lg garn linesca	57	38.37	0.00	21.10	0.00	32.49	6.26	0.72	0.68	0.00	99.61	24	6.1177	0.0000	3.9649	0.0000	0.0000	0.0351	4.2971	1.4879	0.1168	0.0967	0.0014	1.9%	24.8%	71.6%	1.6%
WYL-09-50-37.5 lg garn linesca	58	39.18	0.00	21.11	0.04	33.04	6.30	0.70	0.67	0.03	101.06	24	6.1886	0.0000	3.9298	0.0000	0.0051	0.0651	4.2994	1.4835	0.1134	0.0933	0.0105	1.9%	24.7%	71.7%	1.6%
WYL-09-50-37.5 lg garn linesca	59	39.15	0.01	21.06	0.00	32.70	6.32	0.71	0.57	0.02	100.54	24	6.2303	0.0008	3.9499	0.0000	0.0003	0.0498	4.3021	1.4993	0.0976	0.0953	0.0056	1.6%	25.0%	71.7%	1.6%
WYL-09-50-37.5 lg garn linesca	60	39.28	0.00	21.29	0.00	33.06	6.37	0.73	0.57	0.05	101.34	24	6.1806	0.0000	3.9481	0.0000	0.0000	0.0519	4.2984	1.4942	0.0955	0.0974	0.0145	1.6%	24.9%	71.6%	1.6%

Table I-4. Feldspar Chemistry

Plagioclase													
Sample/Photo	Point	Location	SiO2	TiO2	Al2O3	FeO	Fe2O3	MgO	CaO	Na2O	K2O	BaO	Total
WYL-09-49-36.1 image 10	116	matrix away from Grt	60.636	0.009776	24.0107	0.013418	-	0	5.51026	9.58606	0.278668	0	100.045
WYL-09-49-36.1 image 10	117	matrix away from Grt	60.7836	0	24.0743	0.036871	-	0	5.58308	9.65556	0.262256	0.01317	100.409
WYL-09-49-36.1 image 10	118	matrix away from Grt	61.4686	0	24.0913	0.016316	-	0	5.51388	9.63086	0.175577	0	100.896
WYL-09-49-36.1 image 10	119	matrix away from Grt	60.9176	0	24.5224	0.004966	-	0.011501	5.95251	9.2841	0.192671	0	100.886
WYL-09-49-36.1a plag 1	1	inclusion in Grt	60.33	0	25.72	-	0.3908	0.005	7.02	6.83	0.4468	0.0235	100.76
WYL-09-49-36.1a plag 2	1	matrix adj to Grt rim	62.8	0	24.62	-	0.0972	0	5.63	7.62	0.2737	0	101.03
WYL-09-49-36.1h plag 4	3	matrix adj to Grt rim	61.47	0.0122	24.6	-	0.1377	0.0073	5.98	7.68	0.142	0	100.03
WYL-09-50-37.5 image 3	20	matrix away from Grt	64.036	0	22.4812	0.047915	-	0	3.33412	11.0753	0.223103	0	101.198
WYL-09-50-37.5 image 3	21	matrix away from Grt	64.0392	0	22.5229	0.060804	-	0	3.30938	11.1278	0.264876	0	101.325
WYL-09-50-37.5 image 3	22	matrix away from Grt	64.0584	0	22.5686	0.076554	-	0	3.36144	11.0372	0.207262	0	101.309
WYL-09-50-37.5 image 3	23	matrix away from Grt	64.8226	0	22.5822	0.022188	-	0	3.382	11.22	0.238753	0	102.268
WYL-09-50-37.5f plag 5	4	matrix near Grt	65.86	0	23.29	-	0.1092	0	3.6	9.03	0.2025	0	102.1
WYL-09-50-37.5f plag 6	5	matrix near Grt	65.51	0	23.26	-	0.175	0	3.49	9.03	0.1797	0	101.64
WYL-09-50-37.5h plag 7	6	matrix near Grt	64.18	0.0223	22.72	-	0.0513	0.0067	3.46	9.01	0.1841	0.0089	99.65
WYL-09-50-37.5h plag 8	7	matrix near Grt	65.32	0	23.37	-	0.159	0.0068	3.62	8.85	0.1788	0	101.51

Plagioclase													
Sample/Photo	Point	Si	Al	Fe3	Mg	Ti	Ba	Ca	Na	K	Anorthite	Albite	K-feldspar
WYL-09-49-36.1 image 10	116	2.7081	1.2638	0.0005	0.0000	0.0003	0.0000	0.2637	0.8301	0.0159	24%	75%	1%
WYL-09-49-36.1 image 10	117	2.7062	1.2632	0.0014	0.0000	0.0000	0.0002	0.2663	0.8335	0.0149	24%	75%	1%
WYL-09-49-36.1 image 10	118	2.7183	1.2556	0.0006	0.0000	0.0000	0.0000	0.2613	0.8258	0.0099	24%	75%	1%
WYL-09-49-36.1 image 10	119	2.6968	1.2794	0.0002	0.0000	0.0000	0.0000	0.2823	0.7969	0.0109	26%	73%	1%
WYL-09-49-36.1a plag 1	1	2.6656	1.3393	0.0144	0.0000	0.0000	0.0004	0.3323	0.5851	0.0252	35%	62%	3%
WYL-09-49-36.1a plag 2	1	2.7478	1.2696	0.0036	0.0000	0.0000	0.0000	0.2639	0.6464	0.0153	29%	70%	2%
WYL-09-49-36.1h plag 4	3	2.7233	1.2845	0.0051	0.0000	0.0004	0.0000	0.2839	0.6597	0.0080	30%	69%	1%
WYL-09-50-37.5 image 3	20	2.8097	1.1626	0.0018	0.0000	0.0000	0.0000	0.1567	0.9422	0.0125	14%	85%	1%
WYL-09-50-37.5 image 3	21	2.8076	1.1638	0.0022	0.0000	0.0000	0.0000	0.1555	0.9459	0.0148	14%	85%	1%
WYL-09-50-37.5 image 3	22	2.8074	1.1657	0.0028	0.0000	0.0000	0.0000	0.1578	0.9378	0.0116	14%	85%	1%
WYL-09-50-37.5 image 3	23	2.8146	1.1556	0.0008	0.0000	0.0000	0.0000	0.1573	0.9446	0.0132	14%	85%	1%
WYL-09-50-37.5f plag 5	4	2.8362	1.1821	0.0039	0.0000	0.0000	0.0000	0.1661	0.7540	0.0111	18%	81%	1%
WYL-09-50-37.5f plag 6	5	2.8334	1.1857	0.0063	0.0000	0.0000	0.0000	0.1617	0.7572	0.0099	17%	82%	1%
WYL-09-50-37.5h plag 7	6	2.8336	1.1822	0.0019	0.0000	0.0007	0.0002	0.1637	0.7713	0.0104	17%	82%	1%
WYL-09-50-37.5h plag 8	7	2.8287	1.1928	0.0058	0.0000	0.0000	0.0000	0.1680	0.7431	0.0099	18%	81%	1%

K-feldspar													
Sample/Photo	Point	Location	SiO2	TiO2	Al2O3	FeO	Fe2O3	MgO	CaO	Na2O	K2O	BaO	Total
WYL-09-49-36.1 image 10	120	matrix away from Grt	64.8295	0	18.5065	0.027567	-	0.012152	0.009312	1.45824	14.9652	0.735641	100.544
WYL-09-49-36.1 image 10	121	matrix away from Grt	64.9545	0.007765	18.5564	0.006364	-	0.002539	0	1.55736	14.9316	0.636808	100.653
WYL-09-49-36.1 image 10	122	matrix away from Grt	64.1419	0.010748	18.5919	0	-	0	0.00242	1.79569	14.7095	0.713201	99.9653
WYL-09-49-36.1 image 10	123	matrix away from Grt	64.6983	0.000299	18.5774	0.00707	-	0.017063	0.003911	1.62904	14.7424	0.721416	100.397
WYL-09-49-36.1a kfsp 1	8	matrix adj to Grt	65.04	0.0025	18.53	-	0.0496	0	0.0291	1.3807	14.23	0.6856	99.95
WYL-09-50-37.5 image 2	24	matrix away from Grt	64.5577	0	18.5749	0.029953	-	0	0	2.07776	14.1844	0.675699	100.1
WYL-09-50-37.5 image 2	25	matrix away from Grt	64.1732	0.018368	18.6505	0.024248	-	0.004587	0.002065	1.97041	14.3553	0.708963	99.9076
WYL-09-50-37.5 image 2	26	matrix away from Grt	64.133	0.000602	18.4946	0.007844	-	0	0.001878	1.87026	14.4764	0.671036	99.6556
WYL-09-50-37.5 image 2	27	matrix away from Grt	63.848	0.014461	18.4319	0.017116	-	0	0.006766	1.7002	14.9477	0.640033	99.6062
WYL-09-50-37.5f kfsp 2	9	matrix near Grt	66.04	0.0129	19.37	-	0.0546	0.0019	0.0094	1.3598	13.72	0.6587	101.23
WYL-09-50-37.5f kfsp 3	10	matrix near Grt	65.34	0.0421	19.68	-	0.091	0	0.0528	1.5917	12.54	0.5716	99.9
WYL-09-50-37.5f kfsp 4	11	matrix near Grt	64.5	0	19.32	-	0.0813	0	0.0236	1.7254	13.14	0.5885	99.38

K-feldspar													
Sample/Photo	Point	Si	Al	Fe3	Mg	Ti	Ba	Ca	Na	K	Anorthite	Albite	K-feldspar
WYL-09-49-36.1 image 10	120	2.9861	1.0046	0.0011	0.0000	0.0000	0.0133	0.0005	0.1302	0.8794	0%	13%	87%
WYL-09-49-36.1 image 10	121	2.9861	1.0054	0.0002	0.0000	0.0003	0.0115	0.0000	0.1388	0.8757	0%	14%	86%
WYL-09-49-36.1 image 10	122	2.9734	1.0158	0.0000	0.0000	0.0004	0.0130	0.0001	0.1614	0.8699	0%	15%	85%
WYL-09-49-36.1 image 10	123	2.9825	1.0093	0.0003	0.0000	0.0000	0.0130	0.0002	0.1456	0.8670	0%	14%	86%
WYL-09-49-36.1a kfsp 1	8	2.9969	1.0063	0.0019	0.0000	0.0001	0.0124	0.0014	0.1233	0.8365	0%	13%	87%
WYL-09-50-37.5 image 2	24	2.9799	1.0105	0.0012	0.0000	0.0000	0.0122	0.0000	0.1859	0.8353	0%	18%	82%
WYL-09-50-37.5 image 2	25	2.9722	1.0181	0.0009	0.0000	0.0006	0.0129	0.0001	0.1769	0.8482	0%	17%	83%
WYL-09-50-37.5 image 2	26	2.9780	1.0121	0.0003	0.0000	0.0000	0.0122	0.0001	0.1684	0.8576	0%	16%	84%
WYL-09-50-37.5 image 2	27	2.9737	1.0118	0.0007	0.0000	0.0005	0.0117	0.0003	0.1535	0.8882	0%	15%	85%
WYL-09-50-37.5f kfsp 2	9	2.9890	1.0333	0.0021	0.0000	0.0004	0.0117	0.0005	0.1193	0.7922	0%	13%	87%
WYL-09-50-37.5f kfsp 3	10	2.9789	1.0575	0.0035	0.0000	0.0014	0.0102	0.0026	0.1407	0.7294	0%	16%	84%
WYL-09-50-37.5f kfsp 4	11	2.9729	1.0495	0.0031	0.0000	0.0000	0.0106	0.0012	0.1542	0.7726	0%	16%	83%

Table I-5. Sillimanite and Spinel Chemistry

Sillimanite

Sample/Photo	Point	Location	SiO2	TiO2	Al2O3	Cr2O3	FeO	MnO	MgO	CaO	Na2O	K2O	ZnO	BaO	Cs2O	V2O3	Y2O3	Total
WYL-09-49-36.1 image 10	124	matrix in Sil band	38.15	0.00	60.82	0.08	0.29	0.00	0.18	0.03	0.02	-	0.00	-	-	0.09	0.00	99.65
WYL-09-49-36.1 image 10	125	matrix in Sil band	37.49	0.00	62.77	0.08	0.22	0.00	0.05	0.02	0.01	-	0.00	-	-	0.03	0.00	100.66
WYL-09-49-36.1 image 10	126	matrix in Sil band	36.86	0.00	63.84	0.03	0.17	0.01	0.00	0.01	0.01	-	0.00	-	-	0.02	0.05	101.02
WYL-09-49-36.1 image 10	127	matrix in Sil band	36.87	0.01	63.80	0.06	0.16	0.00	0.01	0.02	0.01	-	0.01	-	-	0.08	0.00	101.03
WYL-09-50-37.5 image 4	61	Intergrown w/ Hc + Bt +Pl	37.14	0.00	65.01	0.02	0.25	0.00	0.00	0.01	0.01	0.01	0.02	0.00	0.02	-	-	102.48
WYL-09-50-37.5 image 4	62	Intergrown w/ Hc + Bt +Pl	37.17	0.00	64.28	0.01	0.31	0.00	0.01	0.00	0.01	0.00	0.00	0.01	0.00	-	-	101.81
WYL-09-50-37.5 image 4	63	Intergrown w/ Hc + Bt +Pl	36.92	0.00	64.23	0.00	0.28	0.00	0.01	0.01	0.01	0.01	0.00	0.04	0.00	-	-	101.52
WYL-09-50-37.5 image 4	64	Intergrown w/ Hc + Bt +Pl	37.02	0.00	64.18	0.01	0.28	0.00	0.00	0.01	0.02	0.01	0.00	0.00	0.01	-	-	101.54
WYL-09-50-37.5 image 4	65	Intergrown w/ Hc + Bt +Pl	36.93	0.00	64.33	0.01	0.28	0.00	0.00	0.01	0.01	0.02	0.04	0.00	0.01	-	-	101.64

Spinel

Sample/Photo	Point	O	Si	Al	Ti	Fe	Mn	Mg	Zn	Ca	Na	K	Ba	Cs	V	Y
WYL-09-49-36.1 image 10	124	20	4.13	7.77	0.00	0.03	0.00	0.03	0.00	0.00	0.00	0.00	-	0.00	0.01	0.00
WYL-09-49-36.1 image 10	125	20	4.03	7.94	0.00	0.02	0.00	0.01	0.00	0.00	0.00	0.00	-	0.00	0.00	0.00
WYL-09-49-36.1 image 10	126	20	3.95	8.05	0.00	0.02	0.00	0.00	0.00	0.00	0.00	0.00	-	0.00	0.00	0.00
WYL-09-49-36.1 image 10	127	20	3.95	8.05	0.00	0.01	0.00	0.00	0.00	0.00	0.00	0.00	-	0.00	0.01	0.00
WYL-09-50-37.5 image 4	61	20	3.92	8.09	0.00	0.02	0.00	0.00	0.00	0.00	0.00	0.00	0.00	0.00	-	-
WYL-09-50-37.5 image 4	62	20	3.95	8.05	0.00	0.03	0.00	0.00	0.00	0.00	0.00	0.00	0.00	0.00	-	-
WYL-09-50-37.5 image 4	63	20	3.93	8.07	0.00	0.03	0.00	0.00	0.00	0.00	0.00	0.00	0.00	0.00	-	-
WYL-09-50-37.5 image 4	64	20	3.94	8.06	0.00	0.02	0.00	0.00	0.00	0.00	0.00	0.00	0.00	0.00	-	-
WYL-09-50-37.5 image 4	65	20	3.93	8.07	0.00	0.02	0.00	0.00	0.00	0.00	0.00	0.00	0.00	0.00	-	-

Sample/Photo	Line	Location	SiO2	TiO2	Al2O3	Cr2O3	V2O3	FeO	MnO	MgO	NiO	ZnO
WYL-09-50-37.5 image 4	56	intergrown with Sil + Pl + Bt	0.070594	0	58.5787	0.095157	0.14525	29.6047	0.036771	4.3827	0.030619	4.23692
WYL-09-50-37.5 image 4	57	intergrown with Sil + Pl + Bt	0.058548	0	58.4854	0.088152	0.129717	29.8232	0.044221	4.37989	0.030622	4.19864
WYL-09-50-37.5i spin 1	2	intergrown with Sil + Pl + Bt	0.0645	0	57.11	0.069	-	32.03	0.0707	5.41	0.0169	4.31
WYL-09-50-37.5i spin 1	1	intergrown with Sil + Pl + Bt	0.0644	0	57.14	0.0689	-	32.82	0.0706	5.42	0.0169	4.31
WYL-09-50-37.5i spin 10	10	intergrown with Sil + Pl + Bt	0.0723	0.0016	57.4	0.1555	-	31.65	0.0596	5.27	0	4.35
WYL-09-50-37.5i spin 2	2	intergrown with Sil + Pl + Bt	0.0706	0	57.72	0.1281	-	32.99	0.0274	5.74	0.0492	4.36
WYL-09-50-37.5i spin 3	3	intergrown with Sil + Pl + Bt	0.057	0	58.18	0.1079	-	32.11	0.0623	5.52	0.0243	4.42
WYL-09-50-37.5i spin 4	4	intergrown with Sil + Pl + Bt	0.0664	0.0085	57.96	0.0821	-	32.09	0.0428	5.39	0.0522	4.34
WYL-09-50-37.5i spin 5	5	intergrown with Sil + Pl + Bt	0.0871	0.0174	56.26	0.0738	-	32.09	0.036	5.55	0.0555	4.46
WYL-09-50-37.5i spin 6	6	intergrown with Sil + Pl + Bt	0.0576	0	56.31	0.1126	-	31.86	0.0722	5.12	0.0138	4.24
WYL-09-50-37.5i spin 7	7	intergrown with Sil + Pl + Bt	0.0941	0	56.96	0.1124	-	31.86	0.0899	5.52	0.0128	4.25
WYL-09-50-37.5i spin 8	8	intergrown with Sil + Pl + Bt	0.0531	0.0382	57.67	0.1006	-	31.69	0.0044	5.38	0.025	4.39
WYL-09-50-37.5i spin 9	9	intergrown with Sil + Pl + Bt	0.0592	0.0088	57.61	0.1459	-	31.53	0.0336	5.49	0.0776	4.46

Sample/Photo	Line	CaO	Nb2O5	Total	O	$Fe2^+$	Mn	Mg	Ni	Zn	Si	Ti	Nb	Al	Cr	Fe^{3+}	V	Ca	X_{Spn}	X_{Hc}	X_{Gah}
WYL-09-50-37.5 image 4	56	0.028064	-	97.20948	4	0.72	0.00	0.19	0.00	0.09	0.00	0.00	-	2.00	0.00	0.00	0.00	0.00	19%	72%	9%
WYL-09-50-37.5 image 4	57	0.020123	-	97.25851	4	0.72	0.00	0.19	0.00	0.09	0.00	0.00	-	1.99	0.00	0.00	0.00	0.00	19%	72%	9%
WYL-09-50-37.5i spin 1	2	-	0	99.07	4	0.68	0.00	0.23	0.00	0.09	0.00	0.00	0.00	1.91	0.00	0.08	-	-	23%	68%	9%
WYL-09-50-37.5i spin 1	1	-	0	99.91	4	0.68	0.00	0.23	0.00	0.09	0.00	0.00	0.00	1.90	0.00	0.09	-	-	23%	68%	9%
WYL-09-50-37.5i spin 10	10	-	0.0421	99.01	4	0.69	0.00	0.22	0.00	0.09	0.00	0.00	0.00	1.92	0.00	0.07	-	-	22%	69%	9%
WYL-09-50-37.5i spin 2	2	-	0.2199	101.3	4	0.68	0.00	0.24	0.00	0.09	0.00	0.00	0.00	1.89	0.00	0.09	-	-	24%	67%	9%
WYL-09-50-37.5i spin 3	3	-	0.0946	100.58	4	0.68	0.00	0.23	0.00	0.09	0.00	0.00	0.00	1.92	0.00	0.07	-	-	23%	68%	9%
WYL-09-50-37.5i spin 4	4	-	0	100.03	4	0.68	0.00	0.23	0.00	0.09	0.00	0.00	0.00	1.92	0.00	0.07	-	-	23%	68%	9%
WYL-09-50-37.5i spin 5	5	-	0.1331	98.77	4	0.67	0.00	0.24	0.00	0.09	0.00	0.00	0.00	1.89	0.00	0.09	-	-	24%	67%	9%
WYL-09-50-37.5i spin 6	6	-	0	97.79	4	0.69	0.00	0.22	0.00	0.09	0.00	0.00	0.00	1.91	0.00	0.08	-	-	22%	69%	9%
WYL-09-50-37.5i spin 7	7	-	0.0261	98.93	4	0.68	0.00	0.23	0.00	0.09	0.00	0.00	0.00	1.91	0.00	0.08	-	-	23%	68%	9%
WYL-09-50-37.5i spin 8	8	-	0.1655	99.52	4	0.69	0.00	0.23	0.00	0.09	0.00	0.00	0.00	1.92	0.00	0.06	-	-	23%	68%	9%
WYL-09-50-37.5i spin 9	9	-	0.1753	99.59	4	0.68	0.00	0.23	0.00	0.09	0.00	0.00	0.00	1.92	0.00	0.07	-	-	23%	68%	9%

Table I-6. Ilmenite and Rutile Chemistry

Ilmenite											
Sample/Photo	Point	Location	SiO2	TiO2	Al2O3	Cr2O3	FeO	MnO	MgO	NiO	Total
WYL-09-50-37.5 k ilmenite #1	11	in Pl	0.157	57.080	0.023	0.028	34.060	1.814	0.036	0.004	93.203

Sample/Photo	Point	O	Si	Ti	Al	Cr	Fe3	Fe2	Mn	Mg	Ni
WYL-09-50-37.5 k ilmenite #1	11	3	0.0043	1.1728	0.0007	0.0006	0.0000	0.7780	0.0420	0.0015	0.0001

Rutile													
Sample/Photo	Point	Location	SiO2	TiO2	Nb2O5	Al2O3	Cr2O3	FeO	MgO	MnO	NiO	ZnO	Total
WYL-09-50-37.5 m rutile #1	12	in inclusion in Bt	0.5675	94.97	0.179	0.1295	0.0088	0.3025	0	0.0075	0	0	96.17
WYL-09-50-37.5 m rutile #2	13	in inclusion in Bt	0.4996	93.25	0.3114	0.0898	0	0.3065	0.0143	0.0118	0.0038	0	94.49
WYL-09-50-37.5 o rutile #3	14	adj to Bt	0.2284	96.19	0.2507	0.0603	0	0.2235	0	0	0.0095	0	96.96
WYL-09-50-37.5 q rutile 4	15	adj to Bt	0.5071	94.23	0.1075	0.1393	0	0.215	0	0	0	0	95.2

Sample/Photo	Point	O	Si	Ti	Nb	Al	Cr	Fe	Mg	Mn	Ni	Zn
WYL-09-50-37.5 m rutile #1	12	2	0.008	0.987	0.001	0.002	0.000	0.003	0.000	0.000	0.000	0.000
WYL-09-50-37.5 m rutile #2	13	2	0.007	0.987	0.002	0.001	0.000	0.004	0.000	0.000	0.000	0.000
WYL-09-50-37.5 o rutile #3	14	2	0.003	0.993	0.002	0.001	0.000	0.003	0.000	0.000	0.000	0.000
WYL-09-50-37.5 q rutile 4	15	2	0.007	0.989	0.001	0.002	0.000	0.003	0.000	0.000	0.000	0.000

Table I-7. Monazite Chemistry and Chemical Ages

Sample/Photo	Line	SiO2	TiO2	Al2O3	FeO	MnO	MgO	CaO	P2O5	UO2	ThO2	PbO	ZrO2	HfO2	Y2O3	La2O3
WYL-09-44-61.4 Mon-1 (in plag)	65	0.98	0.00	0.00	0.00	0.00	0.00	0.94	29.30	0.39	6.45	0.57	0.10	0.00	1.56	12.34
WYL-09-44-61.4 Mon-1 (in plag)	66	0.93	0.00	0.00	0.00	0.00	0.00	0.88	29.12	0.39	6.08	0.54	0.04	0.00	1.51	12.53
WYL-09-44-61.4 Mon-1 (in plag)	67	0.95	0.00	0.00	0.00	0.00	0.00	0.93	29.21	0.45	6.39	0.57	0.12	0.00	1.53	12.43
WYL-09-44-61.4 Mon-1 (in plag)	68	0.98	0.00	0.00	0.00	0.00	0.00	0.95	29.16	0.46	6.23	0.53	0.12	0.00	2.17	11.81
WYL-09-44-61.4 Mon-1 (in plag)	69	0.83	0.00	0.00	0.00	0.00	0.00	0.91	29.05	0.36	5.88	0.52	0.11	0.00	1.43	12.79
WYL-09-44-61.4 Mon-1 (in plag)	70	0.82	0.00	0.00	0.00	0.00	0.00	0.90	29.09	0.35	5.89	0.55	0.11	0.00	1.57	12.75
WYL-09-44-61.4 Mon-1 (in plag)	71	0.90	0.00	0.00	0.00	0.00	0.00	0.88	29.13	0.41	6.07	0.54	0.10	0.00	1.38	12.78
WYL-09-44-61.4 Mon-1 (in plag)	72	1.10	0.00	0.00	0.00	0.00	0.00	0.91	29.07	0.40	6.70	0.54	0.13	0.00	1.28	12.42
WYL-09-44-61.4 Mon-1 (in plag)	73	0.88	0.00	0.00	0.00	0.00	0.00	0.83	29.48	0.52	5.40	0.52	0.04	0.00	3.10	11.98
WYL-09-44-61.4 Mon-1 (in plag)	74	0.75	0.00	0.00	0.01	0.00	0.00	0.94	29.75	0.35	5.38	0.48	0.18	0.00	1.59	12.96
WYL-09-49-36.1 Mon-1 (in gar)	47	0.70	0.00	0.00	0.48	0.00	0.00	1.53	29.64	0.71	7.68	0.71	0.15	0.00	0.81	10.79
WYL-09-49-36.1 Mon-1 (in gar)	48	0.46	0.00	0.00	0.30	0.00	0.00	1.08	29.81	0.39	5.25	0.44	0.23	0.01	0.30	12.12
WYL-09-49-36.1 Mon-1 (in gar)	49	0.38	0.00	0.00	0.26	0.00	0.00	0.98	29.92	0.31	4.80	0.37	0.11	0.10	0.38	12.15
WYL-09-49-36.1 Mon-1 (in gar)	50	0.45	0.00	0.00	0.93	0.00	0.00	0.81	29.74	0.35	4.13	0.38	0.11	0.01	0.65	12.05
WYL-09-49-36.1 Mon-2 (in bio)	51	0.17	0.00	0.00	0.13	0.00	0.00	0.92	30.52	0.24	3.91	0.27	0.13	0.01	1.58	12.33
WYL-09-49-36.1 Mon-2 (in bio)	52	0.52	0.00	0.00	0.13	0.00	0.00	0.93	29.43	0.43	4.77	0.49	0.14	0.00	0.65	12.31
WYL-09-49-36.1 Mon-3	53	0.40	0.00	0.00	0.02	0.00	0.00	0.94	29.70	0.14	4.66	0.33	0.13	0.05	0.60	12.26
WYL-09-49-36.1 Mon-3	54	0.51	0.00	0.00	0.01	0.00	0.00	1.02	29.94	0.54	5.16	0.56	0.18	0.00	0.59	11.98
WYL-09-49-36.1 Mon-3	55	0.48	0.00	0.00	0.03	0.00	0.00	0.93	29.81	0.49	4.58	0.48	0.21	0.02	0.51	12.47
WYL-09-49-36.1 Mon-3	56	0.51	0.00	0.00	0.00	0.00	0.00	0.93	29.36	0.49	4.76	0.40	0.17	0.00	0.57	12.31
WYL-09-49-36.1 Mon-3	57	0.42	0.00	0.00	0.04	0.00	0.00	0.82	29.64	0.39	3.98	0.38	0.07	0.05	0.52	12.45
WYL-09-49-36.1 Mon-4	58	0.44	0.00	0.00	0.05	0.00	0.00	0.98	29.87	0.14	5.06	0.34	0.11	0.02	0.25	12.55
WYL-09-49-36.1 Mon-4	59	0.36	0.00	0.00	0.04	0.00	0.00	0.76	29.87	0.35	3.58	0.31	0.16	0.00	0.55	12.43
WYL-09-49-36.1 Mon-4	60	0.41	0.00	0.00	0.00	0.00	0.00	0.89	29.49	0.46	4.17	0.39	0.18	0.00	0.54	12.30
WYL-09-49-36.1 Mon-4	61	0.45	0.00	0.00	0.00	0.00	0.00	0.99	29.37	0.52	4.95	0.47	0.17	0.01	0.52	12.23
WYL-09-49-36.1 Mon-4	62	0.41	0.00	0.00	0.00	0.00	0.00	0.88	29.55	0.29	4.52	0.36	0.14	0.03	0.31	12.72
WYL-09-49-36.1 Mon-4	63	0.35	0.00	0.00	0.01	0.00	0.00	0.95	30.23	0.29	4.58	0.39	0.18	0.02	0.36	12.14
WYL-09-49-36.1 Mon-4	64	0.31	0.00	0.00	0.06	0.00	0.00	0.68	29.79	0.30	3.20	0.31	0.15	0.00	0.46	12.65
WYL-09-50-37.5 Mon (in big garnet)	33	0.14	0.00	0.00	1.03	0.00	0.00	1.08	30.07	0.60	3.85	0.42	0.16	0.00	2.69	13.25
WYL-09-50-37.5 Mon (in big garnet)	34	0.15	0.00	0.00	0.74	0.00	0.00	1.10	30.44	0.61	4.15	0.41	0.17	0.00	0.76	13.39
WYL-09-50-37.5 Mon (in big garnet)	35	0.14	0.00	0.00	0.54	0.00	0.00	1.06	29.60	0.49	4.01	0.39	0.18	0.00	0.87	13.38
WYL-09-50-37.5 Mon-2 (in big garnet)	36	0.19	0.00	0.00	0.46	0.00	0.00	1.03	29.77	0.74	3.59	0.49	0.09	0.02	1.12	12.60
WYL-09-50-37.5 Mon-2 (in big garnet)	37	0.29	0.00	0.00	0.32	0.00	0.00	1.26	30.29	0.96	4.40	0.61	0.13	0.03	2.22	13.07
WYL-09-50-37.5 Mon-2 (in big garnet)	38	0.37	0.00	0.00	0.31	0.00	0.00	0.70	29.77	0.34	3.96	0.37	0.11	0.00	2.20	14.19
WYL-09-50-37.5 Mon-2 (in big garnet)	39	0.21	0.00	0.00	0.47	0.00	0.00	0.92	30.38	0.54	3.76	0.40	0.11	0.05	2.57	13.40
WYL-09-50-37.5 Mon-2 (in big garnet)	40	0.22	0.00	0.00	0.84	0.00	0.00	1.04	29.85	0.64	3.76	0.42	0.16	0.00	1.41	13.10
WYL-09-50-37.5 Mon-3 (in big garnet)	41	0.65	0.00	0.00	0.48	0.00	0.00	1.01	29.61	0.64	5.31	0.50	0.14	0.06	2.56	12.81
WYL-09-50-37.5 Mon-3 (in big garnet)	42	0.47	0.00	0.00	0.42	0.00	0.00	0.74	29.57	0.43	3.79	0.42	0.16	0.00	2.43	13.50
WYL-09-50-37.5 Mon-3 (in big garnet)	43	0.23	0.00	0.00	0.68	0.00	0.00	1.32	30.11	1.29	4.40	0.73	0.17	0.00	2.22	12.82
WYL-09-50-37.5 Mon-4 (in plag)	44	0.59	0.00	0.00	0.06	0.00	0.00	0.86	28.60	0.35	5.04	0.44	0.10	0.00	2.16	13.17
WYL-09-50-37.5 Mon-4 (in plag)	45	0.44	0.00	0.00	0.00	0.00	0.00	0.69	28.66	0.30	3.88	0.28	0.06	0.07	2.17	13.74
WYL-09-50-37.5 Mon-4 (in plag)	46	0.11	0.00	0.00	0.02	0.00	0.00	1.19	29.81	0.96	3.74	0.52	0.15	0.00	2.80	12.82

Sample/Photo	Line	Ce2O3	Pr2O3	Nd2O3	Sm2O3	Gd2O3	Dy2O3	Er2O3	Total	∑LREE2O3	∑HREE2O3	O	P	Si	Ca
WYL-09-44-61.4 Mon-1 (in plag)	65	28.69	3.38	11.80	2.05	1.47	0.36	0.02	100.40	58.26	1.85	8	1.94	0.08	0.08
WYL-09-44-61.4 Mon-1 (in plag)	66	28.84	3.17	11.97	2.02	1.45	0.41	0.08	99.96	58.54	1.94	8	1.94	0.07	0.07
WYL-09-44-61.4 Mon-1 (in plag)	67	28.79	3.24	11.90	2.07	1.41	0.41	0.13	100.53	58.42	1.95	8	1.94	0.07	0.08
WYL-09-44-61.4 Mon-1 (in plag)	68	28.53	3.35	12.05	2.05	1.60	0.56	0.14	100.68	57.78	2.30	8	1.93	0.08	0.08
WYL-09-44-61.4 Mon-1 (in plag)	69	29.10	3.43	11.86	2.04	1.52	0.38	0.09	100.30	59.22	1.99	8	1.94	0.07	0.08
WYL-09-44-61.4 Mon-1 (in plag)	70	29.14	3.40	11.90	2.08	1.47	0.33	0.09	100.44	59.28	1.88	8	1.93	0.06	0.08
WYL-09-44-61.4 Mon-1 (in plag)	71	28.89	3.27	11.98	2.07	1.52	0.31	0.08	100.32	58.99	1.91	8	1.94	0.07	0.07
WYL-09-44-61.4 Mon-1 (in plag)	72	28.97	3.33	11.91	2.06	1.44	0.37	0.09	100.71	58.69	1.89	8	1.93	0.09	0.08
WYL-09-44-61.4 Mon-1 (in plag)	73	27.85	3.22	11.76	2.17	1.68	0.68	0.22	100.35	56.98	2.58	8	1.94	0.07	0.07
WYL-09-44-61.4 Mon-1 (in plag)	74	29.33	3.24	11.87	2.13	1.44	0.45	0.09	100.94	59.53	1.98	8	1.95	0.06	0.08
WYL-09-49-36.1 Mon-1 (in gar)	47	31.89	2.65	9.36	1.67	1.52	0.43	0.00	100.70	56.35	1.95	8	1.95	0.05	0.13
WYL-09-49-36.1 Mon-1 (in gar)	48	34.93	2.84	10.06	1.64	1.22	0.16	0.08	101.31	61.59	1.45	8	1.96	0.04	0.09
WYL-09-49-36.1 Mon-1 (in gar)	49	35.13	2.85	10.27	1.68	1.22	0.07	0.01	100.99	62.08	1.29	8	1.97	0.03	0.08
WYL-09-49-36.1 Mon-1 (in gar)	50	35.54	2.97	10.16	1.78	1.33	0.37	0.06	101.81	62.50	1.76	8	1.95	0.03	0.07
WYL-09-49-36.1 Mon-2 (in bio)	51	34.34	2.83	9.50	1.81	1.89	0.72	0.05	101.36	60.81	2.65	8	1.99	0.01	0.08
WYL-09-49-36.1 Mon-2 (in bio)	52	34.87	2.71	9.92	1.71	1.49	0.30	0.05	100.86	61.52	1.84	8	1.95	0.04	0.08
WYL-09-49-36.1 Mon-3	53	35.49	2.86	10.13	1.62	1.20	0.15	0.02	100.70	62.36	1.38	8	1.97	0.03	0.08
WYL-09-49-36.1 Mon-3	54	34.33	2.76	9.85	1.77	1.49	0.39	0.01	101.10	60.69	1.89	8	1.97	0.04	0.09
WYL-09-49-36.1 Mon-3	55	34.80	2.86	9.98	1.65	1.43	0.26	0.05	101.04	61.76	1.74	8	1.96	0.04	0.08
WYL-09-49-36.1 Mon-3	56	34.97	2.75	9.99	1.75	1.31	0.19	0.00	100.46	61.77	1.50	8	1.95	0.04	0.08
WYL-09-49-36.1 Mon-3	57	35.52	2.82	10.12	1.64	1.45	0.36	0.03	100.71	62.56	1.84	8	1.96	0.03	0.07
WYL-09-49-36.1 Mon-4	58	36.14	2.94	10.29	1.54	1.04	0.08	0.00	101.83	63.46	1.11	8	1.96	0.03	0.08
WYL-09-49-36.1 Mon-4	59	36.27	2.86	10.36	1.65	1.14	0.23	0.04	100.95	63.57	1.41	8	1.97	0.03	0.06
WYL-09-49-36.1 Mon-4	60	35.14	2.87	10.23	1.74	1.28	0.23	0.01	100.34	62.28	1.52	8	1.96	0.03	0.08
WYL-09-49-36.1 Mon-4	61	34.49	2.83	10.20	1.74	1.38	0.26	0.00	100.57	61.48	1.63	8	1.96	0.04	0.08
WYL-09-49-36.1 Mon-4	62	35.22	2.84	10.12	1.70	1.11	0.13	0.01	100.35	62.60	1.25	8	1.97	0.03	0.07
WYL-09-49-36.1 Mon-4	63	35.75	2.95	10.36	1.69	1.13	0.10	0.00	101.48	62.89	1.24	8	1.98	0.03	0.08
WYL-09-49-36.1 Mon-4	64	36.85	2.91	10.38	1.78	1.11	0.26	0.05	101.25	64.57	1.41	8	1.97	0.02	0.06
WYL-09-50-37.5 Mon (in big garnet)	33	28.07	3.08	11.50	1.79	1.29	0.69	0.20	99.91	57.69	2.18	8	1.98	0.01	0.09
WYL-09-50-37.5 Mon (in big garnet)	34	29.41	3.25	11.83	1.84	1.05	0.16	0.08	99.55	59.71	1.30	8	2.00	0.01	0.09
WYL-09-50-37.5 Mon (in big garnet)	35	28.82	3.28	11.73	1.89	1.11	0.17	0.05	97.71	59.11	1.33	8	2.00	0.01	0.09
WYL-09-50-37.5 Mon-2 (in big garnet)	36	28.53	3.38	11.84	2.12	1.41	0.32	0.04	97.75	58.47	1.77	8	2.00	0.01	0.09
WYL-09-50-37.5 Mon-2 (in big garnet)	37	27.92	3.13	10.67	1.45	1.05	0.49	0.12	98.39	56.23	1.66	8	2.00	0.02	0.11
WYL-09-50-37.5 Mon-2 (in big garnet)	38	29.71	3.15	11.00	1.57	1.00	0.48	0.13	99.37	59.63	1.61	8	1.98	0.03	0.06
WYL-09-50-37.5 Mon-2 (in big garnet)	39	28.30	3.25	11.48	1.80	1.29	0.51	0.31	99.77	58.23	2.12	8	1.99	0.02	0.08
WYL-09-50-37.5 Mon-2 (in big garnet)	40	28.57	3.31	11.88	1.83	1.40	0.46	0.08	98.96	58.69	1.93	8	1.99	0.02	0.09
WYL-09-50-37.5 Mon-3 (in big garnet)	41	27.80	3.15	10.79	1.73	1.17	0.59	0.26	99.25	56.28	2.01	8	1.96	0.05	0.08
WYL-09-50-37.5 Mon-3 (in big garnet)	42	28.95	3.17	10.82	1.67	1.23	0.51	0.18	98.47	58.12	1.92	8	1.97	0.04	0.06
WYL-09-50-37.5 Mon-3 (in big garnet)	43	27.22	3.08	10.62	1.65	1.11	0.44	0.18	98.26	55.38	1.73	8	2.00	0.02	0.11
WYL-09-50-37.5 Mon-4 (in plag)	44	28.15	2.99	10.53	1.56	1.08	0.41	0.19	96.30	56.41	1.68	8	1.96	0.05	0.07
WYL-09-50-37.5 Mon-4 (in plag)	45	28.86	3.14	11.10	1.67	1.16	0.37	0.18	96.78	58.52	1.71	8	1.96	0.04	0.06
WYL-09-50-37.5 Mon-4 (in plag)	46	27.32	2.92	11.16	1.77	1.19	0.66	0.18	97.33	55.99	2.03	8	2.00	0.01	0.10

Sample/Photo	Line	U	Th	Pb	La	Ce	Sm	Pr	Nd	Gd	Dy	Er	Y	Fe	Mn	Mg	Zr	Ti	Al	Sum
WYL-09-44-61.4 Mon-1 (in plag)	65	0.01	0.11	0.01	0.36	0.82	0.06	0.10	0.33	0.04	0.01	0.00	0.07	0.00	0.00	0.00	0.00	0.00	0.00	4.00
WYL-09-44-61.4 Mon-1 (in plag)	66	0.01	0.11	0.01	0.36	0.83	0.05	0.09	0.34	0.04	0.01	0.00	0.06	0.00	0.00	0.00	0.00	0.00	0.00	4.01
WYL-09-44-61.4 Mon-1 (in plag)	67	0.01	0.11	0.01	0.36	0.83	0.06	0.09	0.33	0.04	0.01	0.00	0.06	0.00	0.00	0.00	0.00	0.00	0.00	4.01
WYL-09-44-61.4 Mon-1 (in plag)	68	0.01	0.11	0.01	0.34	0.82	0.06	0.10	0.34	0.04	0.01	0.00	0.09	0.00	0.00	0.00	0.00	0.00	0.00	4.01
WYL-09-44-61.4 Mon-1 (in plag)	69	0.01	0.11	0.01	0.37	0.84	0.06	0.10	0.33	0.04	0.01	0.00	0.06	0.00	0.00	0.00	0.00	0.00	0.00	4.01
WYL-09-44-61.4 Mon-1 (in plag)	70	0.01	0.11	0.01	0.37	0.84	0.06	0.10	0.33	0.04	0.01	0.00	0.07	0.00	0.00	0.00	0.00	0.00	0.00	4.01
WYL-09-44-61.4 Mon-1 (in plag)	71	0.01	0.11	0.01	0.37	0.83	0.06	0.09	0.34	0.04	0.01	0.00	0.06	0.00	0.00	0.00	0.00	0.00	0.00	4.01
WYL-09-44-61.4 Mon-1 (in plag)	72	0.01	0.12	0.01	0.36	0.83	0.06	0.09	0.33	0.04	0.01	0.00	0.05	0.00	0.00	0.00	0.01	0.00	0.00	4.01
WYL-09-44-61.4 Mon-1 (in plag)	73	0.01	0.10	0.01	0.34	0.79	0.06	0.09	0.33	0.04	0.02	0.01	0.13	0.00	0.00	0.00	0.00	0.00	0.00	4.01
WYL-09-44-61.4 Mon-1 (in plag)	74	0.01	0.10	0.01	0.37	0.83	0.06	0.09	0.33	0.04	0.01	0.00	0.07	0.00	0.00	0.00	0.01	0.00	0.00	4.01
WYL-09-49-36.1 Mon-1 (in gar)	47	0.01	0.14	0.01	0.31	0.91	0.04	0.08	0.26	0.04	0.01	0.00	0.03	0.03	0.00	0.00	0.01	0.00	0.00	4.02
WYL-09-49-36.1 Mon-1 (in gar)	48	0.01	0.09	0.01	0.35	0.99	0.04	0.08	0.28	0.03	0.00	0.00	0.01	0.02	0.00	0.00	0.01	0.00	0.00	4.02
WYL-09-49-36.1 Mon-1 (in gar)	49	0.01	0.09	0.01	0.35	1.00	0.05	0.08	0.29	0.03	0.00	0.00	0.02	0.02	0.00	0.00	0.00	0.00	0.00	4.01
WYL-09-49-36.1 Mon-1 (in gar)	50	0.01	0.07	0.01	0.34	1.01	0.05	0.08	0.28	0.03	0.01	0.00	0.03	0.06	0.00	0.00	0.00	0.00	0.00	4.04
WYL-09-49-36.1 Mon-2 (in bio)	51	0.00	0.07	0.01	0.35	0.97	0.05	0.08	0.26	0.05	0.02	0.00	0.06	0.01	0.00	0.00	0.01	0.00	0.00	4.01
WYL-09-49-36.1 Mon-2 (in bio)	52	0.01	0.08	0.01	0.36	1.00	0.05	0.08	0.28	0.04	0.01	0.00	0.03	0.01	0.00	0.00	0.01	0.00	0.00	4.02
WYL-09-49-36.1 Mon-3	53	0.00	0.08	0.01	0.35	1.02	0.04	0.08	0.28	0.03	0.00	0.00	0.03	0.00	0.00	0.00	0.00	0.00	0.00	4.01
WYL-09-49-36.1 Mon-3	54	0.01	0.09	0.01	0.34	0.98	0.05	0.08	0.27	0.04	0.01	0.00	0.02	0.00	0.00	0.00	0.01	0.00	0.00	4.00
WYL-09-49-36.1 Mon-3	55	0.01	0.08	0.01	0.36	0.99	0.04	0.08	0.28	0.04	0.01	0.00	0.02	0.00	0.00	0.00	0.01	0.00	0.00	4.01
WYL-09-49-36.1 Mon-3	56	0.01	0.09	0.01	0.36	1.01	0.05	0.08	0.28	0.03	0.00	0.00	0.02	0.00	0.00	0.00	0.01	0.00	0.00	4.01
WYL-09-49-36.1 Mon-3	57	0.01	0.07	0.01	0.36	1.02	0.04	0.08	0.28	0.04	0.01	0.00	0.02	0.00	0.00	0.00	0.00	0.00	0.00	4.01
WYL-09-49-36.1 Mon-4	58	0.00	0.09	0.01	0.36	1.03	0.04	0.08	0.28	0.03	0.00	0.00	0.01	0.00	0.00	0.00	0.00	0.00	0.00	4.01
WYL-09-49-36.1 Mon-4	59	0.01	0.06	0.01	0.36	1.03	0.04	0.08	0.29	0.03	0.01	0.00	0.02	0.00	0.00	0.00	0.01	0.00	0.00	4.01
WYL-09-49-36.1 Mon-4	60	0.01	0.07	0.01	0.36	1.01	0.05	0.08	0.29	0.03	0.01	0.00	0.02	0.00	0.00	0.00	0.01	0.00	0.00	4.01
WYL-09-49-36.1 Mon-4	61	0.01	0.09	0.01	0.35	0.99	0.05	0.08	0.29	0.04	0.01	0.00	0.02	0.00	0.00	0.00	0.01	0.00	0.00	4.01
WYL-09-49-36.1 Mon-4	62	0.01	0.08	0.01	0.37	1.01	0.05	0.08	0.28	0.03	0.00	0.00	0.01	0.00	0.00	0.00	0.01	0.00	0.00	4.01
WYL-09-49-36.1 Mon-4	63	0.00	0.08	0.01	0.35	1.01	0.05	0.08	0.29	0.03	0.00	0.00	0.01	0.00	0.00	0.00	0.01	0.00	0.00	4.00
WYL-09-49-36.1 Mon-4	64	0.01	0.06	0.01	0.36	1.05	0.05	0.08	0.29	0.03	0.01	0.00	0.02	0.00	0.00	0.00	0.01	0.00	0.00	4.01
WYL-09-50-37.5 Mon (in big garnet)	33	0.01	0.07	0.01	0.38	0.80	0.05	0.09	0.32	0.03	0.02	0.00	0.11	0.07	0.00	0.00	0.01	0.00	0.00	4.04
WYL-09-50-37.5 Mon (in big garnet)	34	0.01	0.07	0.01	0.38	0.84	0.05	0.09	0.33	0.03	0.00	0.00	0.03	0.05	0.00	0.00	0.01	0.00	0.00	4.01
WYL-09-50-37.5 Mon (in big garnet)	35	0.01	0.07	0.01	0.39	0.84	0.05	0.10	0.33	0.03	0.00	0.00	0.04	0.04	0.00	0.00	0.01	0.00	0.00	4.01
WYL-09-50-37.5 Mon-2 (in big garnet)	36	0.01	0.06	0.01	0.37	0.83	0.06	0.10	0.34	0.04	0.01	0.00	0.05	0.03	0.00	0.00	0.00	0.00	0.00	4.01
WYL-09-50-37.5 Mon-2 (in big garnet)	37	0.02	0.08	0.01	0.38	0.80	0.04	0.09	0.30	0.03	0.01	0.00	0.09	0.02	0.00	0.00	0.00	0.00	0.00	4.00
WYL-09-50-37.5 Mon-2 (in big garnet)	38	0.01	0.07	0.01	0.41	0.85	0.04	0.09	0.31	0.03	0.01	0.00	0.09	0.02	0.00	0.00	0.00	0.00	0.00	4.01
WYL-09-50-37.5 Mon-2 (in big garnet)	39	0.01	0.07	0.01	0.38	0.80	0.05	0.09	0.32	0.03	0.01	0.01	0.11	0.03	0.00	0.00	0.00	0.00	0.00	4.01
WYL-09-50-37.5 Mon-2 (in big garnet)	40	0.01	0.07	0.01	0.38	0.82	0.05	0.09	0.33	0.04	0.01	0.00	0.06	0.06	0.00	0.00	0.01	0.00	0.00	4.03
WYL-09-50-37.5 Mon-3 (in big garnet)	41	0.01	0.09	0.01	0.37	0.80	0.05	0.09	0.30	0.03	0.01	0.01	0.11	0.03	0.00	0.00	0.01	0.00	0.00	4.01
WYL-09-50-37.5 Mon-3 (in big garnet)	42	0.01	0.07	0.01	0.39	0.84	0.05	0.09	0.30	0.03	0.01	0.00	0.10	0.03	0.00	0.00	0.01	0.00	0.00	4.01
WYL-09-50-37.5 Mon-3 (in big garnet)	43	0.02	0.08	0.02	0.37	0.78	0.04	0.09	0.30	0.03	0.01	0.00	0.09	0.04	0.00	0.00	0.01	0.00	0.00	4.02
WYL-09-50-37.5 Mon-4 (in plag)	44	0.01	0.09	0.01	0.39	0.84	0.04	0.09	0.30	0.03	0.01	0.00	0.09	0.00	0.00	0.00	0.00	0.00	0.00	4.00
WYL-09-50-37.5 Mon-4 (in plag)	45	0.01	0.07	0.01	0.41	0.86	0.05	0.09	0.32	0.03	0.01	0.00	0.09	0.00	0.00	0.00	0.00	0.00	0.00	4.01
WYL-09-50-37.5 Mon-4 (in plag)	46	0.02	0.07	0.01	0.38	0.79	0.05	0.08	0.32	0.03	0.02	0.00	0.12	0.00	0.00	0.00	0.01	0.00	0.00	4.00

Sample/Photo	Line	X_{La}	X_{Ce}	X_{Sm}	X_{Pr}	X_{Nd}	X_{Gd}	X_{Dy}	X_{Er}	$X_{LREEPO4}$	$X_{HREEPO4}$	X_{Hut}	X_{Clr}	X_{Xen}	Age (Ga)	± 1s (Ma)
WYL-09-44-61.4 Mon-1 (in plag)	65	0.18	0.41	0.03	0.05	0.17	0.02	0.00	0.00	0.84	0.02	0.03	0.08	0.03	1.656	17
WYL-09-44-61.4 Mon-1 (in plag)	66	0.18	0.42	0.03	0.05	0.17	0.02	0.01	0.00	0.84	0.03	0.03	0.07	0.03	1.645	18
WYL-09-44-61.4 Mon-1 (in plag)	67	0.18	0.41	0.03	0.05	0.17	0.02	0.01	0.00	0.84	0.03	0.03	0.08	0.03	1.618	17
WYL-09-44-61.4 Mon-1 (in plag)	68	0.17	0.41	0.03	0.05	0.17	0.02	0.01	0.00	0.82	0.03	0.03	0.08	0.05	1.537	18
WYL-09-44-61.4 Mon-1 (in plag)	69	0.18	0.42	0.03	0.05	0.17	0.02	0.00	0.00	0.85	0.03	0.02	0.08	0.03	1.640	18
WYL-09-44-61.4 Mon-1 (in plag)	70	0.18	0.42	0.03	0.05	0.17	0.02	0.00	0.00	0.84	0.02	0.02	0.08	0.03	1.746	18
WYL-09-44-61.4 Mon-1 (in plag)	71	0.19	0.42	0.03	0.05	0.17	0.02	0.00	0.00	0.85	0.02	0.03	0.07	0.03	1.623	18
WYL-09-44-61.4 Mon-1 (in plag)	72	0.18	0.42	0.03	0.05	0.17	0.02	0.00	0.00	0.84	0.02	0.03	0.08	0.03	1.532	18
WYL-09-44-61.4 Mon-1 (in plag)	73	0.17	0.40	0.03	0.05	0.16	0.02	0.01	0.00	0.81	0.03	0.02	0.07	0.06	1.633	18
WYL-09-44-61.4 Mon-1 (in plag)	74	0.19	0.42	0.03	0.05	0.17	0.02	0.01	0.00	0.85	0.03	0.02	0.08	0.03	1.654	20
WYL-09-49-36.1 Mon-1 (in gar)	47	0.16	0.46	0.02	0.04	0.13	0.02	0.01	0.00	0.81	0.03	0.02	0.13	0.02	1.584	14
WYL-09-49-36.1 Mon-1 (in gar)	48	0.17	0.50	0.02	0.04	0.14	0.02	0.00	0.00	0.88	0.02	0.01	0.09	0.01	1.517	21
WYL-09-49-36.1 Mon-1 (in gar)	49	0.18	0.50	0.02	0.04	0.14	0.02	0.00	0.00	0.88	0.02	0.01	0.08	0.01	1.458	24
WYL-09-49-36.1 Mon-1 (in gar)	50	0.17	0.51	0.02	0.04	0.14	0.02	0.00	0.00	0.89	0.02	0.01	0.07	0.01	1.622	24
WYL-09-49-36.1 Mon-2 (in bio)	51	0.18	0.49	0.02	0.04	0.13	0.02	0.01	0.00	0.86	0.03	0.00	0.08	0.03	1.312	30
WYL-09-49-36.1 Mon-2 (in bio)	52	0.18	0.50	0.02	0.04	0.14	0.02	0.00	0.00	0.87	0.02	0.01	0.08	0.01	1.748	19
WYL-09-49-36.1 Mon-3	53	0.18	0.51	0.02	0.04	0.14	0.02	0.00	0.00	0.88	0.02	0.01	0.08	0.01	1.455	28
WYL-09-49-36.1 Mon-3	54	0.17	0.49	0.02	0.04	0.14	0.02	0.00	0.00	0.86	0.02	0.01	0.09	0.01	1.776	17
WYL-09-49-36.1 Mon-3	55	0.18	0.50	0.02	0.04	0.14	0.02	0.00	0.00	0.88	0.02	0.01	0.08	0.01	1.726	20
WYL-09-49-36.1 Mon-3	56	0.18	0.50	0.02	0.04	0.14	0.02	0.00	0.00	0.88	0.02	0.01	0.08	0.01	1.428	22
WYL-09-49-36.1 Mon-3	57	0.18	0.51	0.02	0.04	0.14	0.02	0.00	0.00	0.89	0.02	0.01	0.07	0.01	1.612	23
WYL-09-49-36.1 Mon-4	58	0.18	0.51	0.02	0.04	0.14	0.01	0.00	0.00	0.89	0.01	0.01	0.08	0.01	1.393	26
WYL-09-49-36.1 Mon-4	59	0.18	0.52	0.02	0.04	0.14	0.01	0.00	0.00	0.90	0.02	0.01	0.06	0.01	1.493	28
WYL-09-49-36.1 Mon-4	60	0.18	0.50	0.02	0.04	0.14	0.02	0.00	0.00	0.89	0.02	0.01	0.07	0.01	1.551	22
WYL-09-49-36.1 Mon-4	61	0.18	0.49	0.02	0.04	0.14	0.02	0.00	0.00	0.87	0.02	0.01	0.08	0.01	1.567	20
WYL-09-49-36.1 Mon-4	62	0.18	0.51	0.02	0.04	0.14	0.01	0.00	0.00	0.89	0.02	0.01	0.07	0.01	1.487	25
WYL-09-49-36.1 Mon-4	63	0.17	0.51	0.02	0.04	0.14	0.01	0.00	0.00	0.89	0.02	0.01	0.08	0.01	1.590	24
WYL-09-49-36.1 Mon-4	64	0.18	0.52	0.02	0.04	0.14	0.01	0.00	0.00	0.91	0.02	0.01	0.06	0.01	1.633	30
WYL-09-50-37.5 Mon (in big garnet)	33	0.19	0.40	0.02	0.04	0.16	0.02	0.01	0.00	0.83	0.03	0.00	0.09	0.06	1.579	21
WYL-09-50-37.5 Mon (in big garnet)	34	0.20	0.43	0.03	0.05	0.17	0.01	0.00	0.00	0.87	0.02	0.00	0.09	0.02	1.492	21
WYL-09-50-37.5 Mon (in big garnet)	35	0.20	0.43	0.03	0.05	0.17	0.01	0.00	0.00	0.87	0.02	0.00	0.09	0.02	1.554	23
WYL-09-50-37.5 Mon-2 (in big garnet)	36	0.19	0.42	0.03	0.05	0.17	0.02	0.00	0.00	0.86	0.02	0.00	0.09	0.02	1.764	19
WYL-09-50-37.5 Mon-2 (in big garnet)	37	0.19	0.41	0.02	0.05	0.15	0.01	0.01	0.00	0.82	0.02	0.00	0.11	0.05	1.764	16
WYL-09-50-37.5 Mon-2 (in big garnet)	38	0.21	0.43	0.02	0.05	0.16	0.01	0.01	0.00	0.86	0.02	0.01	0.06	0.05	1.633	25
WYL-09-50-37.5 Mon-2 (in big garnet)	39	0.20	0.41	0.02	0.05	0.16	0.02	0.01	0.00	0.84	0.03	0.00	0.08	0.05	1.594	23
WYL-09-50-37.5 Mon-2 (in big garnet)	40	0.19	0.42	0.03	0.05	0.17	0.02	0.01	0.00	0.86	0.03	0.00	0.09	0.03	1.591	21
WYL-09-50-37.5 Mon-3 (in big garnet)	41	0.19	0.41	0.02	0.05	0.15	0.02	0.01	0.00	0.82	0.03	0.02	0.09	0.05	1.513	18
WYL-09-50-37.5 Mon-3 (in big garnet)	42	0.20	0.42	0.02	0.05	0.15	0.02	0.01	0.00	0.85	0.03	0.01	0.06	0.05	1.778	22
WYL-09-50-37.5 Mon-3 (in big garnet)	43	0.19	0.40	0.02	0.05	0.15	0.01	0.01	0.00	0.81	0.02	0.00	0.11	0.05	1.813	13
WYL-09-50-37.5 Mon-4 (in plag)	44	0.20	0.42	0.02	0.04	0.15	0.01	0.01	0.00	0.84	0.02	0.02	0.08	0.05	1.603	21
WYL-09-50-37.5 Mon-4 (in plag)	45	0.20	0.43	0.02	0.05	0.16	0.02	0.00	0.00	0.86	0.02	0.01	0.06	0.05	1.295	29
WYL-09-50-37.5 Mon-4 (in plag)	46	0.19	0.40	0.02	0.04	0.16	0.02	0.01	0.00	0.81	0.03	0.00	0.10	0.06	1.641	18

APPENDIX J

GB-GBPQ RESULTS AND DATA

Supplementary Data Table 2 for Chapter 4 (McKechnie *et al.* 2012b)

Rationale:

- GBPQ geobarometer of Wu et al (2004) was chosen due to availability of spreadsheet software for calculations and for its ability to also calculate the Grt-Bt geothermometer of Holdaway (2000). The GBPQ geobarometer gives similar results to the GASP geobarometer of Holdaway (2001).
- Grain pairings are discussed in the data sheets for each sample.

Table J-1. Average Results from Ti-in-Bt and GB geothermometers, GBPQ Geobarometer

Sample/Photo	Location			Sample/Photo	Location	T (°C) Henry et al	P (bars) - estimated	Tgb(calc)	P calc
61.4 f biot 6	in Grt core	n/a	n/a	61.4 f garn 6	core	680	6000	568	n/a
61.4 g biot 11-12	in Grt core, has Grt inclusion	n/a	n/a	61.4 g garn 11	core	668	6000	577	n/a
61.4 g biot 11-12	in Grt core, has Grt inclusion	n/a	n/a	61.4 g garn 12	inclusion in Bt in Grt core	668	6000	515	n/a
61.4 g biot 13	in Grt core	n/a	n/a	61.4 g garn 13	core	636	6000	572	n/a
					Bt inclusion in Grt core, Grt core	663		558	n/a
61.4c biotite #1	in Grt (large inclusion) near rim	n/a	n/a	61.4c garnet #1	intermediate b/w rim and core	595	5000	578	n/a
61.4c biot 2	in Grt near rim	n/a	n/a	61.4c garn 2	intermediate b/w rim and core	596	5000	543	n/a
61.4c biot 3	in Grt near rim	n/a	n/a	61.4c garn 3	intermediate b/w rim and core	617	5000	556	n/a
					Bt inclusion in Grt midway to rim, intermediate Grt	603		559	n/a
61.4 f biot 7	in Grt rim	n/a	n/a	61.4 f garn 7	near rim	594	5000	561	n/a
					Bt inclusion in Grt rim, near rim Grt				
61.4 d biot 4	matrix adj to Grt	n/a	n/a	61.4 d garn 4	rim	595	4000	556	n/a
61.4 e biot 5	matrix adj to Grt	n/a	n/a	61.4 e grn 5	rim	594	4000	578	n/a
61.4 f biot 8	matrix adj to Grt	n/a	n/a	61.4 f garn 8	rim	576	4000	567	n/a
61.4 f biot 9	matrix adj to Grt	n/a	n/a	61.4 f garn 9	rim	548	4000	563	n/a
61.4 f biot 10	matrix adj to Grt in embayment	n/a	n/a	61.4 f garn 10	rim	594	4000	559	n/a
61.4 g biot 14	matrix adj to Grt	n/a	n/a	61.4 g garn 14	rim	571	4000	590	n/a
61.4 g biot 15	matrix adj to Grt	n/a	n/a	61.4 g garn 15	rim	581	4000	564	n/a
					Bt in matrix adj. to Grt rim, Grt rim	580		568	n/a

Sample/Photo	Location Bt	Sample/Photo	Location Pl	Sample/Photo	Location Grt	T (°C) Henry et al	P (bars) - estimated	Tgb(calc)	P calc
36.1a biot 17	in Grt core	49-36.1 image 10	core; matrix away from Grt	WYL-09-49-36.1a	core	700	5500	564	5129
					Bt inclusion in Grt core, Grt Core, core of Pl in matrix away from Grt	700	5500	564	5129
36.1a biot 16	in Grt intermed. To rim	49-36.1 image 10	core; matrix away from Grt	WYL-09-49-36.1a	intermediate b/w rim and core	740	5500	583	5242
					Bt inclusion in Grt midway to rim, intermediate Grt, Pl core in matrix away from Grt	740		583	5242
36.1 h biot 22	in Grt near rim	49-36.1 image 10	core; matrix away from Grt	WYL-09-49-36.1 h	near rim	751	5500	589	5394
36.1 h biot 23	in Grt near rim	49-36.1 image 10	core; matrix away from Grt	WYL-09-49-36.1 h	near rim	734	5500	575	5634
49-36.1 bio-2 image 14	in Grt near rim (core of Bt grain)	49-36.1 image 10	core; matrix away from Grt	WYL-09-49-36.1 in	near rim + Bt inclusion	765	5500	564	5772
					Bt inclusion in Grt rim, near rim Grt, Pl core in matrix away from Grt	750	5500	576	5600
36.1a biot 18	matrix adj to Grt	49-36.1 image 10	rim; matrix away from Grt	WYL-09-49-36.1a	rim	686	4000	604	3389
36.1a biot 21	matrix adj to Grt	49-36.1 image 10	rim; matrix away from Grt	WYL-09-49-36.1a	rim	680	4000	569	3668
36.1 h biot 24	matrix adj to Grt	49-36.1 image 10	rim; matrix away from Grt	WYL-09-49-36.1 h	rim	694	4000	602	4122
36.1 h biot 25	matrix adj to Grt	49-36.1 image 10	rim; matrix away from Grt	WYL-09-49-36.1 h	rim	688	4000	614	3801
49-36.1 bio-1 image 12	matrix adj to Grt (core)	49-36.1 image 10	rim; matrix away from Grt	WYL-09-49-36.1 in	rim	703	4000	578	4149
					Bt in matrix adj. to Grt rim, Grt rim, Pl rim in matrix away from Grt	690	4000	593	3826

Sample/Photo	Location Bt	Sample/Photo	Location Pl	Sample/Photo	Location Grt	T (°C) Henry et al	P (bars) - estimated	Tgb(calc)	P calc
37.5 f biot 26	in Grt near rim	WYL-09-50-37.5f plag 5	matrix near Grt	WYL-09-50-37.5 f	near rim	709	4500	593	4604
37.5 h biot 31	in Grt near rim	WYL-09-50-37.5h plag 8	matrix near Grt	WYL-09-50-37.5 h	near rim	755	5500	614	5536
					Bt inclusion in Grt near rim, near rim Grt, Pl in matrix near Grt	732	5000	604	5070
37.5 f biot 27	in lrg Gt rim	WYL-09-50-37.5f plag 5	matrix near Grt	WYL-09-50-37.5 f	rim	780	5500	596	5639
					Bt inclusion in Grt rim, Grt rim, Pl in matrix near Grt	780	5500	596	5639
37.5 g biot 28	in Grt-Qtz-Bt symplectite	n/a	n/a	WYL-09-50-37.5 g	Grt-Bt-Qtz symplectite	729	3500	603	n/a
37.5 g biot 29	in Grt-Qtz-Bt symplectite	n/a	n/a	WYL-09-50-37.5 g	Grt-Bt-Qtz symplectite	751	3500	621	n/a
37.5 g biot 30	in Grt-Qtz-Bt symplectite	n/a	n/a	WYL-09-50-37.5 g	Grt-Bt-Qtz symplectite	658	3500	566	n/a
					Grt-Bt-Qtz symplectite	713	3500	596	n/a
37.5 h biot 32	matrix adj to Grt	WYL-09-50-37.5h plag 8	matrix near Grt	WYL-09-50-37.5 h	rim	700	4500	634	4838
37.5 h biot 33	matrix adj to Grt	WYL-09-50-37.5h plag 8	matrix near Grt	WYL-09-50-37.5 h	rim	699	4500	620	4778
37.5 h biot 34	matrix adj to Grt	WYL-09-50-37.5h plag 8	matrix near Grt	WYL-09-50-37.5 h	rim	690	4500	634	4545
50-37.5 bio2-2 image 7	matrix adj to Grt	n/a	n/a	WYL-09-50-37.5 in	rim	719	4500	631	n/a
50-37.5 bio-2 image 7	matrix adj to Grt (rim)	n/a	n/a	WYL-09-50-37.5 in	rim	719	4500	622	n/a
50-37.5 bio-2 image 7	matrix adj to Grt (core)	n/a	n/a	WYL-09-50-37.5 in	near rim	728	4500	614	n/a
50-37.5 bio-2 image 7	matrix adj to Grt	n/a	n/a	WYL-09-50-37.5 in	near rim	726	4500	587	n/a
50-37.5 bio-2 image 7	matrix adj to Grt	n/a	n/a	WYL-09-50-37.5 in	near rim	723	4500	636	n/a
50-37.5 bio2-2 image 7	matrix adj to Grt	n/a	n/a	WYL-09-50-37.5 in	near rim	730	4500	622	n/a
50-37.5 bio2-2 image 7	matrix adj to Grt	n/a	n/a	WYL-09-50-37.5 in	near rim	725	4500	602	n/a
50-37.5 bio2-2 image 7	matrix adj to Grt	n/a	n/a	WYL-09-50-37.5 in	near rim	729	4500	592	n/a
50-37.5 bio3 image 9	matrix adj to Grt	n/a	n/a	WYL-09-50-37.5 in	near rim	720	4500	628	n/a
50-37.5 bio3 image 9	matrix adj to Grt	n/a	n/a	WYL-09-50-37.5 in	near rim	717	4500	624	n/a
50-37.5 bio3 image 9	matrix adj to Grt	n/a	n/a	WYL-09-50-37.5 in	near rim	717	4500	619	n/a
50-37.5 bio3 image 9	matrix adj to Grt	n/a	n/a	WYL-09-50-37.5 in	rim	709	4500	601	n/a
					Bt in matrix adj to Grt, Grt rim/near rim. Pl in matrix near Grt	717	4500	618	4720
50-37.5 bio-1 image 3	matrix away from Grt	WYL-09-50-37.5 image 3	matrix away from Grt	WYL-09-50-37.5 bi	core	750	7000	704	7140
50-37.5 bio-1 image 3	matrix away from Grt	WYL-09-50-37.5 image 3	matrix away from Grt	WYL-09-50-37.5 bi	core	748	7000	711	6806
					Bt in matrix away from Grt, Grt core, Pl in matrix away from Grt	749	7000	707	6973

Table J-2. Rationale and Data used in P-T calculations using the GB-GBPQ spreadsheet for WYL-09-44-61.4.

Biotite			11 O basis					Garnet			12 O basis			
Sample/Photo	Point	Location	Fe(tot) bio	Mg bio	Al(VI) bio	Ti bio	T(C)	Sample/Photo	Point	Location	Fe grt	Mg grt	Ca grt	Mn grt
61.4c biotite #1	1	in Grt	1.53	1.00	0.19	0.11	595	61.4c garnet #1	1	intermediate b/w rim and core	2.43	0.26	0.16	0.18
61.4c biot 2	2	in Grt near rim	1.45	1.13	0.20	0.11	596	61.4c garn 2	2	intermediate b/w rim and core	2.41	0.25	0.17	0.17
61.4c biot 3	3	in Grt near rim	1.54	1.03	0.16	0.13	617	61.4c garn 3	3	intermediate b/w rim and core	2.39	0.23	0.17	0.18
61.4 d biot 4	4	matrix adj to Grt	1.53	1.00	0.19	0.11	595	61.4 d garn 4	4	rim	2.42	0.23	0.15	0.18
61.4 e biot 5	5	matrix adj to Grt	1.55	1.01	0.19	0.11	594	61.4 e grn 5	5	rim	2.40	0.26	0.15	0.18
61.4 f biot 6	6	in Grt core	1.35	1.17	0.12	0.17	680	61.4 f garn 6	6	intermediate b/w rim and core	2.41	0.32	0.14	0.13
61.4 f biot 7	7	in Grt rim	1.56	1.01	0.18	0.11	594	61.4 f garn 7	7	near rim	2.42	0.23	0.16	0.18
61.4 f biot 8	8	matrix adj to Grt	1.53	0.98	0.21	0.10	576	61.4 f garn 8	8	rim	2.46	0.25	0.14	0.17
61.4 f biot 9	9	matrix adj to Grt	1.56	1.02	0.19	0.09	548	61.4 f garn 9	9	rim	2.43	0.24	0.17	0.16
61.4 f biot 10	10	matrix adj to Grt in embayment	1.50	1.00	0.21	0.11	594	61.4 f garn 10	10	rim	2.42	0.24	0.14	0.17
61.4 g biot 11-12	11	in Grt core, has Grt inclusion	1.35	1.17	0.14	0.16	668	61.4 g garn 11	11	core	2.42	0.33	0.14	0.13
61.4 g biot 11-12	11	in Grt core, has Grt inclusion	1.35	1.17	0.14	0.16	668	61.4 g garn 12	12	inclusion in Bt in Grt core	2.48	0.24	0.14	0.13
61.4 g biot 13	12	in Grt	1.49	1.00	0.17	0.14	636	61.4 g garn 13	13	core	2.44	0.26	0.14	0.16
61.4 g biot 14	13	matrix adj to Grt	1.56	0.98	0.20	0.10	571	61.4 g garn 14	14	rim	2.42	0.27	0.13	0.17
61.4 g biot 15	14	matrix adj to Grt	1.50	1.00	0.22	0.11	581	61.4 g garn 15	15	rim	2.40	0.24	0.16	0.18

Rationale:
Used biotite and garnet compositions that were in close proximity to each other

Table J-3. Rationale and Data used in P-T calculations using the GB-GBPQ spreadsheet for WYL-09-49-36.1.

Biotite								Garnet						
Sample/Photo	Point	Location	Fe(t) bio	Mg bio	Al(VI) bio	Ti bio	T(C)	Sample/Photo	Point	Location	Fe grt	Mg grt	Ca grt	Mn grt
36.1a biot 16	**15**	**in Grt**	**1.08**	**1.22**	**0.29**	**0.24**	**740**	**WYL-09-49-36.1a garn 16**	**16**	**intermediate b/w rim and core**	**2.36**	**0.45**	**0.08**	**0.10**
36.1a biot 17	**16**	**in Grt**	**0.96**	**1.26**	**0.37**	**0.17**	**700**	**WYL-09-49-36.1a garn 17**	**17**	**core**	**2.34**	**0.44**	**0.08**	**0.10**
36.1a biot 18	*17*	*matrix adj to Grt*	*1.24*	*1.05*	*0.30*	*0.18*	*686*	*WYL-09-49-36.1a garn 18*	*18*	*rim*	*2.38*	*0.39*	*0.08*	*0.12*
36.1a biot 21	*19*	*matrix adj to Grt*	*1.15*	*1.18*	*0.30*	*0.16*	*680*	*WYL-09-49-36.1a garn 21*	*21*	*rim*	*2.40*	*0.39*	*0.08*	*0.11*
36.1 h biot 22	**20**	**in Grt**	**1.11**	**1.11**	**0.22**	**0.27**	**751**	**WYL-09-49-36.1 h garn 22**	**22**	**near rim**	**2.37**	**0.41**	**0.09**	**0.11**
36.1 h biot 23	**21**	**in Grt**	**1.11**	**1.13**	**0.30**	**0.24**	**734**	**WYL-09-49-36.1 h garn 23**	**23**	**near rim**	**2.39**	**0.39**	**0.09**	**0.10**
36.1 h biot 24	*22*	*matrix adj to Grt*	*1.21*	*1.03*	*0.29*	*0.19*	*694*	*WYL-09-49-36.1 h garn 24*	*24*	*rim*	*2.37*	*0.38*	*0.09*	*0.12*
36.1 h biot 25	*23*	*matrix adj to Grt*	*1.25*	*1.04*	*0.29*	*0.18*	*688*	*WYL-09-49-36.1 h garn 25*	*25*	*rim*	*2.37*	*0.40*	*0.09*	*0.11*
49-36.1 bio-1 image 12	132	matrix adj to Grt	1.15	1.04	0.31	0.20	702	WYL-09-49-36.1 image 12 gar-1	128	near rim	2.32	0.41	0.09	0.10
49-36.1 bio-1 image 12	*133*	*matrix adj to Grt*	*1.14*	*1.04*	*0.32*	*0.20*	*703*	WYL-09-49-36.1 image 12 gar-1	129	near rim	2.34	0.40	0.09	0.10
49-36.1 bio-1 image 12	134	matrix adj to Grt	1.15	1.05	0.31	0.20	702	WYL-09-49-36.1 image 12 gar-1	130	near rim	2.33	0.39	0.09	0.10
49-36.1 bio-1 image 12	135	matrix adj to Grt	1.15	1.04	0.32	0.19	700	*WYL-09-49-36.1 image 12 gar-1*	*131*	*rim*	*2.35*	*0.35*	*0.08*	*0.11*
49-36.1 bio-2 image 14	136	in Grt near rim	1.01	1.17	0.19	0.29	765	WYL-09-49-36.1 image 14 gar-2	139	near rim + Bt inclusion	2.33	0.40	0.09	0.10
49-36.1 bio-2 image 14	**137**	**in Grt near rim**	**1.02**	**1.17**	**0.19**	**0.29**	**765**	**WYL-09-49-36.1 image 14 gar-2**	**140**	**near rim + Bt inclusion**	**2.33**	**0.40**	**0.09**	**0.09**
49-36.1 bio-2 image 14	138	in Grt near rim	1.01	1.17	0.20	0.28	763	WYL-09-49-36.1 image 14 gar-2	141	near rim + Bt inclusion	2.33	0.39	0.09	0.10

Plagioclase					
Sample	Line	Location	Ca	Na	K
36.1a plag 1	1	inclusion in Grt	0.33	0.59	0.03
36.1a plag 2	1	matrix adj to Grt rim	0.26	0.65	0.02
36.1h plag 4	3	matrix adj to Grt rim	0.28	0.66	0.01
49-36.1 image 10	*119*	*rim; matrix away from Grt*	*0.28*	*0.80*	*0.01*
49-36.1 image 10	**116**	**core; matrix away from Grt**	**0.26**	**0.83**	**0.02**
49-36.1 image 10	**117**	**core; matrix away from Grt**	**0.27**	**0.83**	**0.01**
49-36.1 image 10	118	core; matrix away from Grt	0.26	0.83	0.01

Rationale:
Plagioclase: core of the plagioclase grain in the matrix likely formed at higher P. Plagioclase in contact with garnet may reflect retrograde conditions due to higher Ca content. Inclusion in garnet is small, has higher Ca content, possibly lower P.
Biotite: Peak T - highest Ti in Bt temperatures, inclusions in Grt near the rim of the Grt. Use with corresponding Grt composition
Garnet - rim likely experienced RNT and RE rxn's, recorded more retrograde conditions. We have Bt inclusions in the Grt which we can use with the nearby Grt concentration to get a sense of the Grt-Bt T's.
*Plagioclase inclusion in Grt is oriented differently than the other grains included in garnet including the biotite, could reflect a different metamorphic event, as this garnet appears to be a composite grain. Also the small size of the plagioclase may have caused problems during analysis.

Thus for peak conditions, we use Bt inclusions with Grt beside it, and the core of matrix plag
For retrograde we use the Bt in the matrix adjacent to Grt and the Grt rim composition, though keeping in mind likelihood of retrograde exchange, plus the rim of matrix Pl and/or Pl adj to Grt rim

Pairings used:

Sample/Photo	Point	Location	Fe(t) bio	Mg bio	Al(VI) bio	Ti bio	T°C - Ti in Bt	P (est)	Sample/Photo	Point	Location	Fe grt	Mg grt	Ca grt	Mn grt	Sample	Line	Location	Ca	Na	K
36.1a biot 16	**15**	**in Grt (core)**	**1.08**	**1.22**	**0.29**	**0.24**	**740**	**6000**	**WYL-09-49-36.1a garn 16**	**16**	**intermediate b/w rim and core**	**2.36**	**0.45**	**0.08**	**0.10**	**49-36.1 image 10**	**117**	**core; matrix away from Grt**	**0.27**	**0.83**	**0.01**
36.1a biot 17	**16**	**in Grt**	**0.96**	**1.26**	**0.37**	**0.17**	**700**	**6000**	**WYL-09-49-36.1a garn 17**	**17**	**core**	**2.34**	**0.44**	**0.08**	**0.10**	**49-36.1 image 10**	**116**	**core; matrix away from Grt**	**0.26**	**0.83**	**0.02**
36.1 h biot 22	**20**	**in Grt**	**1.11**	**1.11**	**0.22**	**0.27**	**751**	**6000**	**WYL-09-49-36.1 h garn 22**	**22**	**near rim**	**2.37**	**0.41**	**0.09**	**0.11**	**49-36.1 image 10**	**117**	**core; matrix away from Grt**	**0.27**	**0.83**	**0.01**
36.1 h biot 23	**21**	**in Grt**	**1.11**	**1.13**	**0.30**	**0.24**	**734**	**6000**	**WYL-09-49-36.1 h garn 23**	**23**	**near rim**	**2.39**	**0.39**	**0.09**	**0.10**	**49-36.1 image 10**	**117**	**core; matrix away from Grt**	**0.27**	**0.83**	**0.01**
49-36.1 bio-2 image 14	**137**	**in Grt near rim (core)**	**1.02**	**1.17**	**0.19**	**0.29**	**765**	**6000**	**WYL-09-49-36.1 image 14 gar-2**	**140**	**near rim + Bt inclusion**	**2.33**	**0.40**	**0.09**	**0.09**	**49-36.1 image 10**	**117**	**core; matrix away from Grt**	**0.27**	**0.83**	**0.01**
36.1a biot 18	*17*	*matrix adj to Grt*	*1.24*	*1.05*	*0.30*	*0.18*	*686*	*4000*	*WYL-09-49-36.1a garn 18*	*18*	*rim*	*2.38*	*0.39*	*0.08*	*0.12*	*49-36.1 image 10*	*119*	*rim; matrix away from Grt*	*0.28*	*0.80*	*0.01*
36.1a biot 21	*19*	*matrix adj to Grt*	*1.15*	*1.18*	*0.30*	*0.16*	*680*	*4000*	*WYL-09-49-36.1a garn 21*	*21*	*rim*	*2.40*	*0.39*	*0.08*	*0.11*	*49-36.1 image 10*	*119*	*rim; matrix away from Grt*	*0.28*	*0.80*	*0.01*
36.1 h biot 24	*22*	*matrix adj to Grt*	*1.21*	*1.03*	*0.29*	*0.19*	*694*	*4000*	*WYL-09-49-36.1 h garn 24*	*24*	*rim*	*2.37*	*0.38*	*0.09*	*0.12*	*49-36.1 image 10*	*119*	*rim; matrix away from Grt*	*0.28*	*0.80*	*0.01*
36.1 h biot 25	*23*	*matrix adj to Grt*	*1.25*	*1.04*	*0.29*	*0.18*	*688*	*4000*	*WYL-09-49-36.1 h garn 25*	*25*	*rim*	*2.37*	*0.40*	*0.09*	*0.11*	*49-36.1 image 10*	*119*	*rim; matrix away from Grt*	*0.28*	*0.80*	*0.01*
49-36.1 bio-1 image 12	*133*	*matrix adj to Grt (core)*	*1.14*	*1.04*	*0.32*	*0.20*	*703*	*4000*	*WYL-09-49-36.1 image 12 gar-1*	*131*	*rim*	*2.35*	*0.35*	*0.08*	*0.11*	*49-36.1 image 10*	*119*	*rim; matrix away from Grt*	*0.28*	*0.80*	*0.01*

Table J-4. Rationale and Data used in P-T calculations using the GB-GBPQ spreadsheet for WYL-09-50-37.5.

Biotite Sample/Photo	Point	Location	Fe(tot) bio (11 O basis)	Mg bio	Al(VI) bio	Ti bio	T(C)
37.5 f biot 26	**24**	**in lrg Grt near rim**	**0.95**	**1.34**	**0.33**	**0.17**	**709**
37.5 f biot 27	**25**	**in lrg Gt rim**	**0.97**	**1.22**	**0.15**	**0.32**	**780**
37.5 g biot 28	26	in Grt-Qtz-Bt symplectite	0.89	1.41	0.28	0.19	729
37.5 g biot 29	27	in Grt-Qtz-Bt symplectite	0.94	1.34	0.25	0.24	751
37.5 g biot 30	28	in Grt-Qtz-Bt symplectite	0.78	1.63	0.36	0.10	658
37.5 h biot 31	**29**	**in lrg Grt near rim**	**0.96**	**1.30**	**0.22**	**0.25**	**755**
37.5 h biot 32	30	matrix adj to Grt	1.08	1.27	0.30	0.18	700
37.5 h biot 33	31	matrix adj to Grt	1.06	1.27	0.32	0.17	699
37.5 h biot 34	32	matrix adj to Grt	1.03	1.21	0.37	0.17	690
50-37.5 bio-2 image 7	92	matrix adj to Grt (core)	1.07	1.19	0.23	0.22	728
50-37.5 bio-2 image 7	93	matrix adj to Grt	1.05	1.19	0.24	0.22	726
50-37.5 bio-2 image 7	94	matrix adj to Grt	1.05	1.18	0.26	0.21	723
50-37.5 bio-2 image 7	95	matrix adj to Grt (rim)	1.04	1.21	0.26	0.20	719
50-37.5 bio2-2 image 7	100	matrix adj to Grt	1.07	1.17	0.24	0.23	730
50-37.5 bio2-2 image 7	101	matrix adj to Grt	1.06	1.20	0.24	0.21	725
50-37.5 bio2-2 image 7	102	matrix adj to Grt	1.03	1.21	0.25	0.22	729
50-37.5 bio2-2 image 7	103	matrix adj to Grt	1.04	1.20	0.26	0.20	719
50-37.5 bio3 image 9	108	matrix adj to Grt	1.03	1.21	0.26	0.20	720
50-37.5 bio3 image 9	109	matrix adj to Grt	1.03	1.21	0.27	0.20	717
50-37.5 bio3 image 9	110	matrix adj to Grt	1.04	1.21	0.26	0.20	717
50-37.5 bio3 image 9	111	matrix adj to Grt	1.04	1.24	0.27	0.19	709
50-37.5 bio-1 image 3	**40**	**matrix away from Grt**	**1.08**	**1.08**	**0.25**	**0.27**	**750**
50-37.5 bio-1 image 3	41	matrix away from Grt	1.11	1.09	0.22	0.27	748
50-37.5 bio-1 image 3	**42**	**matrix away from Grt**	**1.12**	**1.09**	**0.22**	**0.27**	**748**
50-37.5 bio-1 image 3	43	matrix away from Grt	1.10	1.09	0.22	0.27	748

Garnet Sample/Photo	Point	Location	Fe (12O basis)	Mg	Ca	Mn
WYL-09-50-37.5 f garn 26	**26**	**near rim**	**2.30**	**0.60**	**0.04**	**0.05**
WYL-09-50-37.5 f garn 27	**27**	**rim**	**2.33**	**0.56**	**0.06**	**0.04**
WYL-09-50-37.5 g garn 28	28	Grt-Bt-Qtz symplectite	2.18	0.69	0.05	0.03
WYL-09-50-37.5 g garn 29	29	Grt-Bt-Qtz symplectite	2.18	0.70	0.05	0.04
WYL-09-50-37.5 g garn 30	30	Grt-Bt-Qtz symplectite	2.16	0.70	0.05	0.04
WYL-09-50-37.5 h garn 31	**31**	**near rim**	**2.26**	**0.64**	**0.05**	**0.04**
WYL-09-50-37.5 h garn 32	32	rim	2.27	0.62	0.05	0.04
WYL-09-50-37.5 h garn 33	33	rim	2.30	0.59	0.05	0.04
WYL-09-50-37.5 h garn 34	34	rim	2.24	0.62	0.05	0.04
WYL-09-50-37.5 image 7 gar-2	96	near rim of lrg Grt	2.25	0.58	0.05	0.03
WYL-09-50-37.5 image 7 gar-2	97	near rim of lrg Grt	2.26	0.56	0.06	0.04
WYL-09-50-37.5 image 7 gar-2	98	near rim of lrg Grt	2.29	0.54	0.06	0.04
WYL-09-50-37.5 image 7 gar-2	99	rim of lrg Grt	2.34	0.49	0.05	0.04
WYL-09-50-37.5 image 7 gar2-:	104	near rim	2.23	0.58	0.05	0.03
WYL-09-50-37.5 image 7 gar2-:	105	near rim of lrg Grt	2.26	0.56	0.06	0.04
WYL-09-50-37.5 image 7 gar2-:	106	near rim of lrg Grt	2.29	0.53	0.06	0.04
WYL-09-50-37.5 image 7 gar2-:	107	rim of lrg Grt	2.32	0.50	0.05	0.04
WYL-09-50-37.5 image 9 gar3	112	near rim of lrg Grt	2.23	0.59	0.05	0.03
WYL-09-50-37.5 image 9 gar3	113	near rim of lrg Grt	2.24	0.59	0.05	0.03
WYL-09-50-37.5 image 9 gar3	114	near rim of lrg Grt	2.25	0.57	0.05	0.03
WYL-09-50-37.5 image 9 gar3	115	rim of lrg Grt	2.29	0.53	0.06	0.04
WYL-09-50-37.5 big garnet	82	lrg Grt core	2.13	0.73	0.05	0.05
WYL-09-50-37.5 big garnet	**83**	**lrg Grt core**	**2.12**	**0.72**	**0.05**	**0.04**
WYL-09-50-37.5 big garnet	84	lrg Grt core	2.16	0.72	0.05	0.04
WYL-09-50-37.5 big garnet	**85**	**lrg Grt core**	**2.13**	**0.71**	**0.05**	**0.04**
WYL-09-50-37.5 big garnet	86	lrg Grt core	2.15	0.71	0.05	0.04
WYL-09-50-37.5 big garnet	87	lrg Grt core	2.18	0.72	0.05	0.04
WYL-09-50-37.5 big garnet	88	lrg Grt core	2.22	0.69	0.05	0.03

Plagioclase Sample/Photo	Point	Location	Ca	Na	K
WYL-09-50-37.5 image 3	20	matrix away from Grt	0.16	0.94	0.01
WYL-09-50-37.5 image 3	21	matrix away from Grt	0.16	0.95	0.01
WYL-09-50-37.5 image 3	22	matrix away from Grt	0.16	0.94	0.01
WYL-09-50-37.5 image 3	23	matrix away from Grt	0.16	0.94	0.01
WYL-09-50-37.5f plag 5	4	matrix near Grt	0.17	0.75	0.01
WYL-09-50-37.5f plag 6	5	matrix near Grt	0.16	0.76	0.01
WYL-09-50-37.5h plag 7	6	matrix near Grt	0.16	0.77	0.01
WYL-09-50-37.5h plag 8	7	matrix near Grt	0.17	0.74	0.01

Rationale:

Plagioclase: Only the plagioclase in the matrix near garnet is in the calibration range for the GBPQ geobarometer, due to low Ca contents in the plagioclase. Thus the P results calculated using the matrix Bt and Grt core may be in error

Garnet: large garnet grain, shows zoning, had symplectite in part of the grain.
Qtz-biotite symplectite is likely a feature of decompression.
Biotite - higher T's of Ti in bt interpreted to reflect peak conditions. Matrix biotite gives T around 750. The one Bt inclusion in the rim of the large garnet has a T of 780.
Paired matrix biotite with garnet core data and with matrix plagioclase away from garnet which are all interpreted to be from the prograde path.

Other garnet-biotite pairings were from garnet and biotite analyses in close proximity to each other/interpreted to have formed contemporaneously; matrix plagioclase near the garnet was used in this case

Pairings:

Biotite Sample/Photo	Point	Location	Fe(tot) bio (11 O basis)	Mg bio	Al(VI) bio	Ti bio	T(C)	Garnet Sample/Photo	Point	Location	Fe (12O basis)	Mg	Ca	Mn	Plagioclase Sample/Photo	Point	Location	Ca	Na	K
37.5 f biot 26	**24**	**in lrg Grt near rim**	**0.95**	**1.34**	**0.33**	**0.17**	**709**	**WYL-09-50-37.5 f garn 26**	**26**	**near rim**	**2.30**	**0.60**	**0.04**	**0.05**	WYL-09-50-37.5f plag 5	4	matrix near Grt	0.17	0.75	0.01
37.5 f biot 27	**25**	**in lrg Gt rim**	**0.97**	**1.22**	**0.15**	**0.32**	**780**	**WYL-09-50-37.5 f garn 27**	**27**	**rim**	**2.33**	**0.56**	**0.06**	**0.04**	WYL-09-50-37.5f plag 5	4	matrix near Grt	0.17	0.75	0.01
37.5 g biot 28	26	in Grt-Qtz-Bt symplectite	0.89	1.41	0.28	0.19	729	WYL-09-50-37.5 g garn 28	28	Grt-Bt-Qtz symplectite	2.18	0.69	0.05	0.03						
37.5 g biot 29	27	in Grt-Qtz-Bt symplectite	0.94	1.34	0.25	0.24	751	WYL-09-50-37.5 g garn 29	29	Grt-Bt-Qtz symplectite	2.18	0.70	0.05	0.04						
37.5 g biot 30	28	in Grt-Qtz-Bt symplectite	0.78	1.63	0.36	0.10	658	WYL-09-50-37.5 g garn 30	30	Grt-Bt-Qtz symplectite	2.16	0.70	0.05	0.04						
37.5 h biot 31	**29**	**in lrg Grt near rim**	**0.96**	**1.30**	**0.22**	**0.25**	**755**	**WYL-09-50-37.5 h garn 31**	**31**	**near rim**	**2.26**	**0.64**	**0.05**	**0.04**	WYL-09-50-37.5h plag 7	6	matrix near Grt	0.16	0.77	0.01
37.5 h biot 32	30	matrix adj to Grt	1.08	1.27	0.30	0.18	700	WYL-09-50-37.5 h garn 32	32	rim	2.27	0.62	0.05	0.04	WYL-09-50-37.5h plag 8	7	matrix near Grt	0.17	0.74	0.01
37.5 h biot 33	31	matrix adj to Grt	1.06	1.27	0.32	0.17	699	WYL-09-50-37.5 h garn 33	33	rim	2.30	0.59	0.05	0.04	WYL-09-50-37.5h plag 8	7	matrix near Grt	0.17	0.74	0.01
37.5 h biot 34	32	matrix adj to Grt	1.03	1.21	0.37	0.17	690	WYL-09-50-37.5 h garn 34	34	rim	2.24	0.62	0.05	0.04	WYL-09-50-37.5h plag 8	7	matrix near Grt	0.17	0.74	0.01
50-37.5 bio-2 image 7	92	matrix adj to Grt (core)	1.07	1.19	0.23	0.22	728	WYL-09-50-37.5 image 7 gar-2	96	near rim of lrg Grt	2.25	0.58	0.05	0.03						
50-37.5 bio-2 image 7	93	matrix adj to Grt	1.05	1.19	0.24	0.22	726	WYL-09-50-37.5 image 7 gar-2	97	near rim of lrg Grt	2.26	0.56	0.06	0.04						
50-37.5 bio-2 image 7	94	matrix adj to Grt	1.05	1.18	0.26	0.21	723	WYL-09-50-37.5 image 7 gar-2	98	near rim of lrg Grt	2.29	0.54	0.06	0.04						
50-37.5 bio-2 image 7	95	matrix adj to Grt (rim)	1.04	1.21	0.26	0.20	719	WYL-09-50-37.5 image 7 gar-2	99	rim of lrg Grt	2.34	0.49	0.05	0.04						
50-37.5 bio2-2 image 7	100	matrix adj to Grt	1.07	1.17	0.24	0.23	730	WYL-09-50-37.5 image 7 gar2-:	104	near rim	2.23	0.58	0.05	0.03						
50-37.5 bio2-2 image 7	101	matrix adj to Grt	1.06	1.20	0.24	0.21	725	WYL-09-50-37.5 image 7 gar2-:	105	near rim of lrg Grt	2.26	0.56	0.06	0.04						
50-37.5 bio2-2 image 7	102	matrix adj to Grt	1.03	1.21	0.25	0.22	729	WYL-09-50-37.5 image 7 gar2-:	106	near rim of lrg Grt	2.29	0.53	0.06	0.04						
50-37.5 bio2-2 image 7	103	matrix adj to Grt	1.04	1.20	0.26	0.20	719	WYL-09-50-37.5 image 7 gar2-:	107	rim of lrg Grt	2.32	0.50	0.05	0.04						
50-37.5 bio3 image 9	108	matrix adj to Grt	1.03	1.21	0.26	0.20	720	WYL-09-50-37.5 image 9 gar3	112	near rim of lrg Grt	2.23	0.59	0.05	0.03						
50-37.5 bio3 image 9	109	matrix adj to Grt	1.03	1.21	0.27	0.20	717	WYL-09-50-37.5 image 9 gar3	113	near rim of lrg Grt	2.24	0.59	0.05	0.03						
50-37.5 bio3 image 9	110	matrix adj to Grt	1.04	1.21	0.26	0.20	717	WYL-09-50-37.5 image 9 gar3	114	near rim of lrg Grt	2.25	0.57	0.05	0.03						
50-37.5 bio3 image 9	111	matrix adj to Grt	1.04	1.24	0.27	0.19	709	WYL-09-50-37.5 image 9 gar3	115	rim of lrg Grt	2.29	0.53	0.06	0.04						
50-37.5 bio-1 image 3	**40**	**matrix away from Grt**	**1.08**	**1.08**	**0.25**	**0.27**	**750**	**WYL-09-50-37.5 big garnet**	**83**	**lrg Grt core**	**2.12**	**0.72**	**0.05**	**0.04**	WYL-09-50-37.5 image 3	22	matrix away from Grt	0.16	0.94	0.01
50-37.5 bio-1 image 3	**42**	**matrix away from Grt**	**1.12**	**1.09**	**0.22**	**0.27**	**748**	**WYL-09-50-37.5 big garnet**	**85**	**lrg Grt core**	**2.13**	**0.71**	**0.05**	**0.04**	WYL-09-50-37.5 image 3	22	matrix away from Grt	0.16	0.94	0.01

Table J-5. GB-GBPQ Spreadsheet Results

WYL-09-46-61.4

Sample/Photo	Bt Location	Sample/Photo	Location Pl	Sample/Photo	Grt Location	Input T (°C)	Input P (bars)	Computed Tgb(calc)	Computed P(1, 2) ave	Computed P(1)	Computed P(2)	Input Fe(tot) bio	Input Mg bio	Input Al(VI) bio	Input Ti bio	Input Ca pl	Input Na Pl	Input K Pl	Input Fe grt	Input Mg grt	Input Ca grt	Input Mn grt	Xalm	Xpyr
61.4c biotite #1	in Grt	N/A	N/A	61.4c garnet #1	intermediate b/w rim and core	595	5000	578	#DIV/0!	#DIV/0!	#DIV/0!	1.527	1.001	0.193	0.113				2.43	0.26	0.16	0.18	0.799	0.08730435
61.4c biot 2	in Grt near rim	N/A	N/A	61.4c garn 2	intermediate b/w rim and core	596	5000	543	#DIV/0!	#DIV/0!	#DIV/0!	1.454	1.130	0.203	0.109				2.41	0.25	0.17	0.17	0.798	0.08492032
61.4c biot 3	in Grt near rim	N/A	N/A	61.4c garn 3	intermediate b/w rim and core	617	5000	556	#DIV/0!	#DIV/0!	#DIV/0!	1.536	1.032	0.158	0.126				2.39	0.23	0.17	0.18	0.798	0.08027342
61.4 d biot 4	matrix adj to Grt	N/A	N/A	61.4 d garn 4	rim	595	4000	556	#DIV/0!	#DIV/0!	#DIV/0!	1.528	0.996	0.193	0.113				2.42	0.23	0.15	0.18	0.806	0.07991217
61.4 e biot 5	matrix adj to Grt	N/A	N/A	61.4 e grn 5	rim	594	4000	578	#DIV/0!	#DIV/0!	#DIV/0!	1.553	1.008	0.186	0.113				2.40	0.26	0.15	0.18	0.799	0.08827781
61.4 f biot 6	in Grt core	N/A	N/A	61.4 f garn 6	core	680	6000	568	#DIV/0!	#DIV/0!	#DIV/0!	1.349	1.169	0.117	0.171				2.41	0.32	0.14	0.13	0.800	0.10960456
61.4 f biot 7	in Grt rim	N/A	N/A	61.4 f garn 7	near rim	594	5000	561	#DIV/0!	#DIV/0!	#DIV/0!	1.562	1.013	0.180	0.112				2.42	0.23	0.16	0.18	0.803	0.08042006
61.4 f biot 8	matrix adj to Grt	N/A	N/A	61.4 f garn 8	rim	576	4000	567	#DIV/0!	#DIV/0!	#DIV/0!	1.532	0.983	0.215	0.104				2.46	0.25	0.14	0.17	0.810	0.08381669
61.4 f biot 9	matrix adj to Grt	N/A	N/A	61.4 f garn 9	rim	548	4000	563	#DIV/0!	#DIV/0!	#DIV/0!	1.560	1.015	0.193	0.091				2.43	0.24	0.17	0.16	0.805	0.08294529
61.4 f biot 10	matrix adj to Grt in embaymen	N/A	N/A	61.4 f garn 10	rim	594	4000	559	#DIV/0!	#DIV/0!	#DIV/0!	1.502	1.002	0.208	0.112				2.42	0.24	0.14	0.17	0.809	0.08355939
61.4 g biot 11-12	in Grt core, has Grt inclusion	N/A	N/A	61.4 g garn 11	core	668	6000	577	#DIV/0!	#DIV/0!	#DIV/0!	1.347	1.167	0.144	0.159				2.42	0.33	0.14	0.13	0.796	0.11319331
61.4 g biot 11-12	in Grt core, has Grt inclusion	N/A	N/A	61.4 g garn 12	inclusion in Bt in Grt core	668	6000	515	#DIV/0!	#DIV/0!	#DIV/0!	1.347	1.167	0.144	0.159				2.48	0.24	0.14	0.13	0.826	0.08390144
61.4 g biot 13	in Grt	N/A	N/A	61.4 g garn 13	core	636	6000	572	#DIV/0!	#DIV/0!	#DIV/0!	1.494	1.002	0.172	0.140				2.44	0.26	0.14	0.16	0.812	0.0882283
61.4 g biot 14	matrix adj to Grt	N/A	N/A	61.4 g garn 14	rim	571	4000	590	#DIV/0!	#DIV/0!	#DIV/0!	1.561	0.985	0.203	0.102				2.42	0.27	0.13	0.17	0.805	0.09214727
61.4 g biot 15	matrix adj to Grt	N/A	N/A	61.4 g garn 15	rim	581	4000	564	#DIV/0!	#DIV/0!	#DIV/0!	1.497	1.001	0.217	0.105				2.40	0.24	0.16	0.18	0.800	0.0841233

WYL-09-49-36.1

Sample/Photo	Location Bt	Sample/Photo	Location Pl	Sample/Photo	Location Grt	Input T (°C)	Input P (bars)	Computed Tgb(calc)	Computed P(1, 2) ave	Computed P(1)	Computed P(2)	Input Fe(tot) bio	Input Mg bio	Input Al(VI) bio	Input Ti bio	Input Ca pl	Input Na Pl	Input K Pl	Input Fe grt	Input Mg grt	Input Ca grt	Input Mn grt	Xalm	Xpyr
36.1a biot 16	**in Grt**	**49-36.1 image 10**	**core; matrix away from Gr**	**WYL-09-49-36.1a garn 16**	**intermediate b/w rim and cor**	**740**	**5500**	583	5242	4483	6002	**1.08**	**1.22**	**0.29**	**0.24**	**0.27**	**0.83**	**0.01**	**2.36**	**0.45**	**0.08**	**0.10**	0.787	0.15332237
36.1a biot 17	**in Grt**	**49-36.1 image 10**	**core; matrix away from Gr**	**WYL-09-49-36.1a garn 17**	**intermediate b/w rim and cor**	**700**	**5500**	564	5129	4475	5783	**0.96**	**1.26**	**0.37**	**0.17**	**0.26**	**0.83**	**0.02**	**2.34**	**0.44**	**0.08**	**0.10**	0.786	0.15241882
36.1 h biot 22	**in Grt**	**49-36.1 image 10**	**core; matrix away from Gr**	**WYL-09-49-36.1 h garn 22**	**near rim**	**751**	**5500**	589	5394	4594	6195	**1.11**	**1.11**	**0.22**	**0.27**	**0.27**	**0.83**	**0.01**	**2.37**	**0.41**	**0.09**	**0.11**	0.789	0.14219771
36.1 h biot 23	**in Grt**	**49-36.1 image 10**	**core; matrix away from Gr**	**WYL-09-49-36.1 h garn 23**	**near rim**	**734**	**5500**	575	5634	4814	6453	**1.11**	**1.13**	**0.30**	**0.24**	**0.27**	**0.83**	**0.01**	**2.39**	**0.39**	**0.09**	**0.10**	0.799	0.13280993
49-36.1 bio-2 image 14	**in Grt near rim (core)**	**49-36.1 image 10**	**core; matrix away from Gr**	**WYL-09-49-36.1 image 14 gar-2**	**near rim + Bt inclusion**	**765**	**5500**	564	5772	4767	6777	**1.02**	**1.17**	**0.19**	**0.29**	**0.27**	**0.83**	**0.01**	**2.33**	**0.40**	**0.09**	**0.09**	0.795	0.14016643
36.1a biot 18	*matrix adj to Grt*	*49-36.1 image 10*	*rim; matrix away from Grt*	*WYL-09-49-36.1a garn 18*	*rim*	*686*	*4000*	604	3389	3002	3776	*1.24*	*1.05*	*0.30*	*0.18*	*0.28*	*0.80*	*0.01*	*2.38*	*0.39*	*0.08*	*0.12*	0.799	0.13472832
36.1a biot 21	*matrix adj to Grt*	*49-36.1 image 10*	*rim; matrix away from Grt*	*WYL-09-49-36.1a garn 21*	*rim*	*680*	*4000*	569	3668	3168	4168	*1.15*	*1.18*	*0.30*	*0.16*	*0.28*	*0.80*	*0.01*	*2.40*	*0.39*	*0.08*	*0.11*	0.802	0.13273641
36.1 h biot 24	*matrix adj to Grt*	*49-36.1 image 10*	*rim; matrix away from Grt*	*WYL-09-49-36.1 h garn 24*	*rim*	*694*	*4000*	602	4122	3685	4559	*1.21*	*1.03*	*0.29*	*0.19*	*0.28*	*0.80*	*0.01*	*2.37*	*0.38*	*0.09*	*0.12*	0.796	0.1325626
36.1 h biot 25	*matrix adj to Grt*	*49-36.1 image 10*	*rim; matrix away from Grt*	*WYL-09-49-36.1 h garn 25*	*rim*	*688*	*4000*	614	3801	3454	4148	*1.25*	*1.04*	*0.29*	*0.18*	*0.28*	*0.80*	*0.01*	*2.37*	*0.40*	*0.09*	*0.11*	0.793	0.13906525
49-36.1 bio-1 image 12	*matrix adj to Grt (core)*	*49-36.1 image 10*	*rim; matrix away from Grt*	*WYL-09-49-36.1 image 12 gar-1*	*rim*	*703*	*4000*	578	4149	3529	4770	*1.14*	*1.04*	*0.32*	*0.20*	*0.28*	*0.80*	*0.01*	*2.35*	*0.35*	*0.08*	*0.11*	0.808	0.12516495

WYL-09-50-37.5

Sample/Photo	Location Bt	Sample/Photo	Location Pl	Sample/Photo	Location Grt	Input T (°C)	Input P (bars)	Computed Tgb(calc)	Computed P(1, 2) ave	Computed P(1)	Computed P(2)	Input Fe(tot) bio	Input Mg bio	Input Al(VI) bio	Input Ti bio	Input Ca pl	Input Na Pl	Input K Pl	Input Fe grt	Input Mg grt	Input Ca grt	Input Mn grt	Xalm	Xpyr
37.5 f biot 26	***in lrg Grt near rim***	WYL-09-50-37.5f plag 5	matrix near Grt	***WYL-09-50-37.5 f garn 26***	***near rim***	***709***	4500	593	4604	4143	5066	***0.95***	***1.34***	***0.33***	***0.17***	0.17	0.75	0.01	***2.30***	***0.60***	***0.04***	***0.05***	0.764	0.20547178
37.5 f biot 27	**in lrg Gt rim**	WYL-09-50-37.5f plag 5	matrix near Grt	**WYL-09-50-37.5 f garn 27**	**rim**	**780**	5500	596	5639	4798	6480	**0.97**	**1.22**	**0.15**	**0.32**	0.17	0.75	0.01	**2.33**	**0.56**	**0.06**	**0.04**	0.774	0.19123756
37.5 g biot 28	*in Grt-Qtz-Bt symplectite*			*WYL-09-50-37.5 g garn 28*	*Grt-Bt-Qtz symplectite*	*729*	3500	603	#DIV/0!	#DIV/0!	#DIV/0!	*0.89*	*1.41*	*0.28*	*0.19*				*2.18*	*0.69*	*0.05*	*0.03*	0.733	0.23835362
37.5 g biot 29	*in Grt-Qtz-Bt symplectite*			*WYL-09-50-37.5 g garn 29*	*Grt-Bt-Qtz symplectite*	*751*	3500	621	#DIV/0!	#DIV/0!	#DIV/0!	*0.94*	*1.34*	*0.25*	*0.24*				*2.18*	*0.70*	*0.05*	*0.04*	0.729	0.24209048
37.5 g biot 30	*in Grt-Qtz-Bt symplectite*			*WYL-09-50-37.5 g garn 30*	*Grt-Bt-Qtz symplectite*	*658*	3500	566	#DIV/0!	#DIV/0!	#DIV/0!	*0.78*	*1.63*	*0.36*	*0.10*				*2.16*	*0.70*	*0.05*	*0.04*	0.725	0.24343689
37.5 h biot 31	***in lrg Grt near rim***	*WYL-09-50-37.5h plag 8*	*matrix adj to Grt*	***WYL-09-50-37.5 h garn 31***	***near rim***	***755***	5500	614	5820	5250	6390	***0.96***	***1.30***	***0.22***	***0.25***	0.16	0.77	0.01	***2.26***	***0.64***	***0.05***	***0.04***	0.750	0.21840186
37.5 h biot 32	*matrix adj to Grt*	*WYL-09-50-37.5h plag 8*	*matrix adj to Grt*	*WYL-09-50-37.5 h garn 32*	*rim*	*700*	4500	634	4838	4608	5068	*1.08*	*1.27*	*0.30*	*0.18*	*0.17*	*0.74*	*0.01*	*2.27*	*0.62*	*0.05*	*0.04*	0.755	0.2131739
37.5 h biot 33	*matrix adj to Grt*	*WYL-09-50-37.5h plag 8*	*matrix adj to Grt*	*WYL-09-50-37.5 h garn 33*	*rim*	*699*	4500	620	4778	4478	5079	*1.06*	*1.27*	*0.32*	*0.17*	*0.17*	*0.74*	*0.01*	*2.30*	*0.59*	*0.05*	*0.04*	0.765	0.20264422
37.5 h biot 34	*matrix adj to Grt*	*WYL-09-50-37.5h plag 8*	*matrix adj to Grt*	*WYL-09-50-37.5 h garn 34*	*rim*	*690*	4500	634	4545	4331	4758	*1.03*	*1.21*	*0.37*	*0.17*	*0.17*	*0.74*	*0.01*	*2.24*	*0.62*	*0.05*	*0.04*	0.755	0.21468782
50-37.5 bio-2 image 7	*matrix adj to Grt (core)*			*WYL-09-50-37.5 image 7 gar-2*	*near rim of lrg Grt*	*728*	4500	631	#DIV/0!	#DIV/0!	#DIV/0!	*1.07*	*1.19*	*0.23*	*0.22*				*2.25*	*0.58*	*0.05*	*0.03*	0.765	0.20359596
50-37.5 bio-2 image 7	*matrix adj to Grt*			*WYL-09-50-37.5 image 7 gar-2*	*near rim of lrg Grt*	*726*	4500	622	#DIV/0!	#DIV/0!	#DIV/0!	*1.05*	*1.19*	*0.24*	*0.22*				*2.26*	*0.56*	*0.06*	*0.04*	0.769	0.19792829
50-37.5 bio-2 image 7	*matrix adj to Grt*			*WYL-09-50-37.5 image 7 gar-2*	*near rim of lrg Grt*	*723*	4500	614	#DIV/0!	#DIV/0!	#DIV/0!	*1.05*	*1.18*	*0.26*	*0.21*				*2.29*	*0.54*	*0.06*	*0.04*	0.778	0.18949023
50-37.5 bio-2 image 7	*matrix adj to Grt (rim)*			*WYL-09-50-37.5 image 7 gar-2*	*rim of lrg Grt*	*719*	4500	587	#DIV/0!	#DIV/0!	#DIV/0!	*1.04*	*1.21*	*0.26*	*0.20*				*2.34*	*0.49*	*0.05*	*0.04*	0.796	0.17256899
50-37.5 bio2-2 image 7	*matrix adj to Grt*			*WYL-09-50-37.5 image 7 gar2-2*	*near rim*	*730*	4500	636	#DIV/0!	#DIV/0!	#DIV/0!	*1.07*	*1.17*	*0.24*	*0.23*				*2.23*	*0.58*	*0.05*	*0.03*	0.762	0.20606591
50-37.5 bio2-2 image 7	*matrix adj to Grt*			*WYL-09-50-37.5 image 7 gar2-2*	*near rim of lrg Grt*	*725*	4500	622	#DIV/0!	#DIV/0!	#DIV/0!	*1.06*	*1.20*	*0.24*	*0.21*				*2.26*	*0.56*	*0.06*	*0.04*	0.769	0.19763134
50-37.5 bio2-2 image 7	*matrix adj to Grt*			*WYL-09-50-37.5 image 7 gar2-2*	*near rim of lrg Grt*	*729*	4500	602	#DIV/0!	#DIV/0!	#DIV/0!	*1.03*	*1.21*	*0.25*	*0.22*				*2.29*	*0.53*	*0.06*	*0.04*	0.782	0.18472113
50-37.5 bio2-2 image 7	*matrix adj to Grt*			*WYL-09-50-37.5 image 7 gar2-2*	*rim of lrg Grt*	*719*	4500	592	#DIV/0!	#DIV/0!	#DIV/0!	*1.04*	*1.20*	*0.26*	*0.20*				*2.32*	*0.50*	*0.05*	*0.04*	0.791	0.17495468
50-37.5 bio3 image 9	*matrix adj to Grt*			*WYL-09-50-37.5 image 9 gar3*	*near rim of lrg Grt*	*720*	4500	628	#DIV/0!	#DIV/0!	#DIV/0!	*1.03*	*1.21*	*0.26*	*0.20*				*2.23*	*0.59*	*0.05*	*0.03*	0.761	0.20847058
50-37.5 bio3 image 9	*matrix adj to Grt*			*WYL-09-50-37.5 image 9 gar3*	*near rim of lrg Grt*	*717*	4500	624	#DIV/0!	#DIV/0!	#DIV/0!	*1.03*	*1.21*	*0.27*	*0.20*				*2.24*	*0.59*	*0.05*	*0.03*	0.764	0.20591324
50-37.5 bio3 image 9	*matrix adj to Grt*			*WYL-09-50-37.5 image 9 gar3*	*near rim of lrg Grt*	*717*	4500	619	#DIV/0!	#DIV/0!	#DIV/0!	*1.04*	*1.21*	*0.26*	*0.20*				*2.25*	*0.57*	*0.05*	*0.03*	0.769	0.19981291
50-37.5 bio3 image 9	*matrix adj to Grt*			*WYL-09-50-37.5 image 9 gar3*	*rim of lrg Grt*	*709*	4500	601	#DIV/0!	#DIV/0!	#DIV/0!	*1.04*	*1.24*	*0.27*	*0.19*				*2.29*	*0.53*	*0.06*	*0.04*	0.782	0.18541274
50-37.5 bio-1 image 3	***matrix away from Grt***	WYL-09-50-37.5 image 3	matrix away from Grt	**WYL-09-50-37.5 big garnet**	**lrg Grt core**	***750***	7000	704	7140	6905	7375	***1.08***	***1.08***	***0.25***	***0.27***	0.16	0.94	0.01	**2.12**	**0.72**	**0.05**	**0.04**	0.716	0.25060225
50-37.5 bio-1 image 3	***matrix away from Grt***	WYL-09-50-37.5 image 3	matrix away from Grt	**WYL-09-50-37.5 big garnet**	**lrg Grt core**	***748***	7000	711	6806	6632	6980	***1.12***	***1.09***	***0.22***	***0.27***	0.16	0.94	0.01	**2.13**	**0.71**	**0.05**	**0.04**	0.720	0.24761043

Xgros	Xsps	Fea	Feb	Fec	Mga	Mgb	Mgc	Caa	Cab	Cac	Xan	Xab	Xor	Fa	Fb	Fc	X(Fe) bio	X(Mg) bio	X(Al) bio	X(Ti) bio	lnKd(Mg)	lnKd(Fe)	[1] Mg	"3(Fe+mg-Al)"	"3Ti"	Pcalc(Mg)	[2] Fe	W(MgAl)	W(Ti)	Pcalc(Fe)	Tgb numerator	Tgb denominator	Tgb(ave)
0.053	####	0.028	####	######	####	####	#######	####	####	#######	######	######	######	######	######	#DIV/0!	0.508	0.377	0.073	0.043	#DIV/0!	#DIV/0!		2.436	0.128	#DIV/0!		2.436	0.128	#DIV/0!	79457.67986	93.38766066	578
0.059	####	0.033	####	######	####	####	#######	####	####	#######	######	######	######	######	######	#DIV/0!	0.471	0.414	0.074	0.040	#DIV/0!	#DIV/0!		2.433	0.120	#DIV/0!		2.433	0.120	#DIV/0!	80944.05269	99.18602194	543
0.059	####	0.044	####	######	####	####	#######	####	####	#######	######	######	######	######	######	#DIV/0!	0.508	0.386	0.059	0.047	#DIV/0!	#DIV/0!		2.503	0.141	#DIV/0!		2.503	0.141	#DIV/0!	78213.44581	94.35052744	556
0.053	####	0.035	####	######	####	####	#######	####	####	#######	######	######	######	######	######	#DIV/0!	0.509	0.376	0.073	0.043	#DIV/0!	#DIV/0!		2.437	0.128	#DIV/0!		2.437	0.128	#DIV/0!	79395.78651	95.80194133	556
0.053	####	0.026	####	######	####	####	#######	####	####	#######	######	######	######	######	######	#DIV/0!	0.512	0.376	0.069	0.042	#DIV/0!	#DIV/0!		2.457	0.126	#DIV/0!		2.457	0.126	#DIV/0!	77997.25493	91.6059122	578
0.046	####	####	####	-4.687	####	####	#######	####	####	#######	######	######	######	######	######	#DIV/0!	0.450	0.441	0.044	0.065	#DIV/0!	#DIV/0!		2.541	0.194	#DIV/0!		2.541	0.194	#DIV/0!	80921.98769	96.15235619	568
0.055	####	0.037	####	######	####	####	#######	####	####	#######	######	######	######	######	######	#DIV/0!	0.514	0.377	0.067	0.042	#DIV/0!	#DIV/0!		2.472	0.126	#DIV/0!		2.472	0.126	#DIV/0!	78068.56601	93.54951305	561
0.049	####	0.020	####	-91.117	####	####	#######	####	####	#######	######	######	######	######	######	#DIV/0!	0.510	0.370	0.081	0.039	#DIV/0!	#DIV/0!		2.397	0.117	#DIV/0!		2.397	0.117	#DIV/0!	79840.68421	95.08732852	567
0.057	####	0.028	####	######	####	####	#######	####	####	#######	######	######	######	######	######	#DIV/0!	0.515	0.379	0.072	0.034	#DIV/0!	#DIV/0!		2.466	0.102	#DIV/0!		2.466	0.102	#DIV/0!	76311.01205	91.25823052	563
0.050	####	0.022	####	-96.741	####	####	#######	####	####	#######	######	######	######	######	######	#DIV/0!	0.501	0.378	0.078	0.042	#DIV/0!	#DIV/0!		2.403	0.127	#DIV/0!		2.403	0.127	#DIV/0!	80643.06328	96.8746347	559
0.047	####	####	####	-0.220	####	####	#######	####	####	#######	######	######	######	######	######	#DIV/0!	0.447	0.439	0.054	0.060	#DIV/0!	#DIV/0!		2.495	0.179	#DIV/0!		2.495	0.179	#DIV/0!	81775.47331	96.20045948	577
0.047	####	####	####	-47.056	####	####	#######	####	####	#######	######	######	######	######	######	#DIV/0!	0.447	0.439	0.054	0.060	#DIV/0!	#DIV/0!		2.495	0.179	#DIV/0!		2.495	0.179	#DIV/0!	82948.17577	105.2698074	515
0.047	####	0.006	####	-68.592	####	####	#######	####	####	#######	######	######	######	######	######	#DIV/0!	0.501	0.380	0.065	0.053	#DIV/0!	#DIV/0!		2.450	0.159	#DIV/0!		2.450	0.159	#DIV/0!	81072.82224	95.88521534	572
0.044	####	0.007	####	-67.635	####	####	#######	####	####	#######	######	######	######	######	######	#DIV/0!	0.517	0.369	0.076	0.038	#DIV/0!	#DIV/0!		2.429	0.114	#DIV/0!		2.429	0.114	#DIV/0!	77772.23217	90.09080975	590
0.053	####	0.034	####	######	####	####	#######	####	####	#######	######	######	######	######	######	#DIV/0!	0.500	0.378	0.082	0.040	#DIV/0!	#DIV/0!		2.388	0.119	#DIV/0!		2.388	0.119	#DIV/0!	80995.55471	96.71649934	564

Xgros	Xsps	Fea	Feb	Fec	Mga	Mgb	Mgc	Caa	Cab	Cac	Xan	Xab	Xor	Fa	Fb	Fc	X(Fe) bio	X(Mg) bio	X(Al) bio	X(Ti) bio	lnKd(Mg)	lnKd(Fe)	[1] Mg	"3(Fe+mg-Al)"	"3Ti"	Pcalc(Mg)	[2] Fe	W(MgAl)	W(Ti)	Pcalc(Fe)	Tgb numerator	Tgb denominator	Tgb(ave)
0.027	####	####	####	264.631	####	####	#######	####	####	#######	0.239	0.748	0.013	0.103	-0.010	#######	0.354	0.451	0.106	0.089	11.519	5.888		2.097	0.268	4483		2.097	0.268	6002	103551.2614	120.9114494	583
0.028	####	####	####	253.013	####	####	#######	####	####	#######	0.238	0.748	0.014	0.110	-0.011	#######	0.322	0.475	0.139	0.064	10.772	4.681		1.976	0.193	4475		1.976	0.193	5783	105195.797	125.6809722	564
0.031	####	####	####	179.420	####	####	#######	####	####	#######	0.239	0.748	0.013	0.103	-0.010	#######	0.379	0.429	0.086	0.105	11.400	5.893		2.165	0.316	4594		2.165	0.316	6195	103369.7867	119.9235902	589
0.032	####	####	####	150.412	####	####	#######	####	####	#######	0.239	0.748	0.013	0.103	-0.010	#######	0.370	0.426	0.115	0.089	10.534	4.722		2.043	0.268	4814		2.043	0.268	6453	105884.9875	124.8034284	575
0.032	####	####	####	190.648	####	####	#######	####	####	#######	0.239	0.748	0.013	0.103	-0.010	#######	0.354	0.458	0.074	0.114	11.947	5.962		2.213	0.342	4767		2.213	0.342	6777	104294.0621	124.6058241	564
0.027	####	####	####	170.210	####	####	#######	####	####	#######	0.259	0.731	0.010	0.075	-0.007	#######	0.419	0.399	0.114	0.068	12.178	6.984		2.113	0.205	3002		2.113	0.205	3776	96746.11821	110.242105	604
0.028	####	####	####	166.186	####	####	#######	####	####	#######	0.259	0.731	0.010	0.075	-0.007	#######	0.381	0.444	0.114	0.061	12.247	6.396		2.130	0.183	3168		2.130	0.183	4168	96611.09813	114.671254	569
0.031	####	####	####	136.663	####	####	#######	####	####	#######	0.259	0.731	0.010	0.075	-0.007	#######	0.416	0.399	0.111	0.073	11.299	6.049		2.113	0.220	3685		2.113	0.220	4559	97943.60853	111.9579084	602
0.029	####	####	####	174.108	####	####	#######	####	####	#######	0.259	0.731	0.010	0.075	-0.007	#######	0.422	0.398	0.111	0.069	11.539	6.498		2.128	0.208	3454		2.128	0.208	4148	96080.90989	108.310442	614
0.029	####	####	####	136.323	####	####	#######	####	####	#######	0.259	0.731	0.010	0.075	-0.007	#######	0.394	0.405	0.123	0.077	11.652	5.975		2.029	0.230	3529		2.029	0.230	4770	102808.5357	120.79977	578

Xgros	Xsps	Fea	Feb	Fec	Mga	Mgb	Mgc	Caa	Cab	Cac	Xan	Xab	Xor	Fa	Fb	Fc	X(Fe) bio	X(Mg) bio	X(Al) bio	X(Ti) bio	lnKd(Mg)	lnKd(Fe)	[1] Mg	"3(Fe+mg-Al)"	"3Ti"	Pcalc(Mg)	[2] Fe	W(MgAl)	W(Ti)	Pcalc(Fe)	Tgb numerator	Tgb denominator	Tgb(ave)
0.015	####	####	####	702.204	####	####	#######	####	####	#######	0.178	0.810	0.012	0.100	-0.011	#######	0.312	0.499	0.124	0.065	11.826	6.480		2.058	0.195	4143		2.058	0.195	5066	99600.55877	114.9365837	593
0.019	####	####	####	592.007	####	####	#######	####	####	#######	0.178	0.810	0.012	0.100	-0.011	#######	0.338	0.479	0.057	0.125	12.656	7.417		2.282	0.376	4798		2.282	0.376	6480	101607.2579	116.9049954	596
0.017	####	####	####	915.723	####	####	#######	####	####	#######	######	######	######	######	######	#DIV/0!	0.295	0.527	0.106	0.072	#DIV/0!	#DIV/0!		2.150	0.215	#DIV/0!		2.150	0.215	#DIV/0!	96699.52634	110.3652883	603
0.016	####	####	####	941.987	####	####	#######	####	####	#######	######	######	######	######	######	#DIV/0!	0.311	0.504	0.095	0.089	#DIV/0!	#DIV/0!		2.160	0.267	#DIV/0!		2.160	0.267	#DIV/0!	98543.54137	110.2387294	621
0.019	####	####	####	918.260	####	####	#######	####	####	#######	######	######	######	######	######	#DIV/0!	0.247	0.585	0.130	0.037	#DIV/0!	#DIV/0!		2.107	0.112	#DIV/0!		2.107	0.112	#DIV/0!	94363.05376	112.4982761	566
0.017	####	####	####	772.806	####	####	#######	####	####	#######	0.173	0.816	0.011	0.092	-0.010	#######	0.325	0.496	0.083	0.096	11.573	6.605		2.212	0.288	5250		2.212	0.288	6390	98629.86066	111.1902119	614
0.018	####	####	####	737.988	####	####	#######	####	####	#######	0.182	0.807	0.011	0.089	-0.010	#######	0.352	0.470	0.113	0.065	10.716	6.050		2.128	0.196	4608		2.128	0.196	5068	94977.67407	104.7077383	634
0.018	####	####	####	668.827	####	####	#######	####	####	#######	0.182	0.807	0.011	0.089	-0.010	#######	0.347	0.470	0.118	0.065	10.829	5.931		2.098	0.194	4478		2.098	0.194	5079	96625.63725	108.2418675	620
0.016	####	####	####	762.326	####	####	#######	####	####	#######	0.182	0.807	0.011	0.089	-0.010	#######	0.343	0.455	0.141	0.062	10.641	6.019		1.970	0.187	4331		1.970	0.187	4758	100598.9749	110.864818	634
0.019	####	####	####	680.754	####	####	#######	####	####	#######	######	######	######	######	######	#DIV/0!	0.365	0.460	0.090	0.086	#DIV/0!	#DIV/0!		2.203	0.257	#DIV/0!		2.203	0.257	#DIV/0!	95513.01766	105.6441965	631
0.020	####	####	####	639.755	####	####	#######	####	####	#######	######	######	######	######	######	#DIV/0!	0.360	0.461	0.094	0.084	#DIV/0!	#DIV/0!		2.182	0.252	#DIV/0!		2.182	0.252	#DIV/0!	96416.65249	107.6845283	622
0.019	####	####	####	591.686	####	####	#######	####	####	#######	######	######	######	######	######	#DIV/0!	0.361	0.457	0.100	0.082	#DIV/0!	#DIV/0!		2.155	0.247	#DIV/0!		2.155	0.247	#DIV/0!	97406.55511	109.7581203	614
0.018	####	####	####	507.469	####	####	#######	####	####	#######	######	######	######	######	######	#DIV/0!	0.353	0.469	0.100	0.078	#DIV/0!	#DIV/0!		2.167	0.234	#DIV/0!		2.167	0.234	#DIV/0!	97169.09741	112.9447295	587
0.019	####	####	####	694.686	####	####	#######	####	####	#######	######	######	######	######	######	#DIV/0!	0.365	0.453	0.094	0.087	#DIV/0!	#DIV/0!		2.173	0.262	#DIV/0!		2.173	0.262	#DIV/0!	96844.72954	106.5398	636
0.019	####	####	####	635.197	####	####	#######	####	####	#######	######	######	######	######	######	#DIV/0!	0.362	0.463	0.092	0.083	#DIV/0!	#DIV/0!		2.199	0.248	#DIV/0!		2.199	0.248	#DIV/0!	95521.4137	106.6558422	622
0.020	####	####	####	559.590	####	####	#######	####	####	#######	######	######	######	######	######	#DIV/0!	0.354	0.467	0.095	0.084	#DIV/0!	#DIV/0!		2.176	0.253	#DIV/0!		2.176	0.253	#DIV/0!	97544.26013	111.4484133	602
0.019	####	####	####	507.962	####	####	#######	####	####	#######	######	######	######	######	######	#DIV/0!	0.354	0.466	0.101	0.079	#DIV/0!	#DIV/0!		2.157	0.236	#DIV/0!		2.157	0.236	#DIV/0!	97591.31695	112.821894	592
0.019	####	####	####	717.199	####	####	#######	####	####	#######	######	######	######	######	######	#DIV/0!	0.354	0.467	0.101	0.079	#DIV/0!	#DIV/0!		2.160	0.237	#DIV/0!		2.160	0.237	#DIV/0!	96245.72	106.7721671	628
0.019	####	####	####	703.909	####	####	#######	####	####	#######	######	######	######	######	######	#DIV/0!	0.351	0.468	0.104	0.077	#DIV/0!	#DIV/0!		2.148	0.231	#DIV/0!		2.148	0.231	#DIV/0!	96527.93587	107.6147905	624
0.019	####	####	####	662.166	####	####	#######	####	####	#######	######	######	######	######	######	#DIV/0!	0.353	0.468	0.102	0.077	#DIV/0!	#DIV/0!		2.157	0.231	#DIV/0!		2.157	0.231	#DIV/0!	96366.70337	108.0634847	619
0.020	####	####	####	568.597	####	####	#######	####	####	#######	######	######	######	######	######	#DIV/0!	0.352	0.474	0.102	0.072	#DIV/0!	#DIV/0!		2.174	0.215	#DIV/0!		2.174	0.215	#DIV/0!	95396.26636	109.1332077	601
0.018	####	####	####	942.653	####	####	#######	####	####	#######	0.143	0.847	0.010	0.091	-0.011	#######	0.373	0.424	0.098	0.106	8.379	4.846		2.096	0.317	6905		2.096	0.317	7375	101968.5276	104.3414992	704
0.019	####	####	####	935.651	####	####	#######	####	####	#######	0.143	0.847	0.010	0.091	-0.011	#######	0.385	0.425	0.085	0.105	8.703	5.206		2.174	0.314	6632		2.174	0.314	6980	98330.2611	99.93193644	711

APPENDIX K
EMPA DETECTION LIMITS

Table K-1. EMPA Detection Limits

Appendix for Chapter 4 (McKechnie *et al.* 2012b)

Saskatchewan Research Council Cameca SX–100				University of Saskatchewan JEOL 8600 Superprobe							
Monazite, Sillimanite, Spinel, Feldspar, Garnet, Biotite				Biotite		Garnet		Rutile, Ilmenite, Spinel		Feldspars	
Si wt.%	0.0023	Zr	0.0205	Si	0.0115	Si	0.0114	Si	0.0125	Si	0.0126
Ti	0.0079	Hf	0.0205	Ti	0.0215	Ti	0.0212	Ti	0.021	Ti	0.0212
Al	0.0027	U	0.0299	Al	0.009	Al	0.009	Nb	0.0811	Al	0.0085
Fe	0.0066	Th	0.0287	Cr	0.0325	Cr	0.032	Al	0.0723	Ba	0.0833
Mn	0.0059	Pb	0.0268	Fe	0.0314	Fe	0.0265	Cr	0.0325	Fe	0.0265
Mg	0.0029	Y	0.0125	Mg	0.0088	Mg	0.0087	Fe	0.0375	Mg	0.008
Ca	0.0028	La	0.0233	Mn	0.0266	Mn	0.0272	Mg	0.0142	Ca	0.0153
K	0.0029	Ce	0.0218	Ca	0.015	Ca	0.015	Mn	0.027	Na	0.0108
Na	0.0021	Pr	0.0188	Na	0.0112	Na	0.011	Ni	0.0445	K	0.0081
P	0.0035	Nd	0.0200	K	0.0081			Zn	0.053		
Cr	0.0028	Sm	0.0171	F	0.0448			Ca	0.02		
V	0.0064	Gd	0.0187	Cl	0.0079						
Zn	0.0103	Dy	0.0171								
Ni	0.0066	Er	0.0225								
Ba	0.0028	F	0.0448								
Cs	0.0029	Cl	0.0079								

APPENDIX L

MAGMATIC AND METAMORPHIC URANINITE MINERALIZATION IN THE WESTERN MARGIN OF THE TRANS-HUDSON OROGEN (SASKATCHEWAN, CANADA): A URANIUM SOURCE FOR UNCONFORMITY-RELATED URANIUM DEPOSITS?

Abstract

The genetic model for the giant unconformity-related uranium (U) deposits of the Athabasca Basin is still being debated; one of the main issues being the source of the uranium concentrated by Mesoproterozoic Era (ca. 1.6-1.0 Ga) diagenetic-hydrothermal events at the interface between the Athabasca Basin and the underlying Archean/Paleoproterozoic basement rocks. Currently, accessory minerals like monazite, zircon, and/or apatite from the sedimentary basin and basement rocks are proposed as the primary uranium source for these high-grade uranium deposits. Numerous occurrences of U mineralization of Hudsonian age have been documented for decades all around the Athabasca Basin; however so far these have not been regarded as *via*ble U sources. Here, a systematic and detailed study of two areas of basement rocks near the eastern part of the Athabasca Basin is presented (*i.e.* the Way Lake property, lying outside the current margin of the basin, and the Moore Lakes property, currently covered by the basin). This study highlights the significant and widespread occurrence of Hudsonian (ca. 1.81-1.76 Ga) uranium oxide (UO_2) mineralization in these zones. Two types of mineralization are identified and documented here: magmatic uranium oxides related to granitic pegmatites and leucogranites, which are more common, and high-temperature, vein-hosted uranium oxides, which have the highest grades. The two types were formed during the peak (1.82-1.81 Ga) and/or post-thermal peak (1.81-1.72 Ga) events related to the evolution of the Trans-Hudson Orogeny. The magmatic uranium oxides formed by partial melting of Wollaston Group metasedimentary rocks. The origin of the vein-type occurrences is unclear, but their high thorium and rare earth element contents suggest a high temperature process, associated with Ca- and/or Na-metasomatism. The uranium oxides are associated with other U-, Th- and REE-bearing accessory minerals like U-rich thorite, thorite, zircon, and/or monazite, adding to the exceptional U contents (from 100 to 2,460 ppm) of these UO_2-bearing rocks (up to 200 times more primarily enriched in U than other basement or basin lithologies). A 3D model of a 1,300 m x 630 m x 200 m basement zone from the Way Lake property indicates that uraninite-bearing granitic pegmatites and leucogranites represent 7% of the total volume of crystalline rock. Within this rock volume are approximately 8,121 (assuming a mean U content of 250 ppm) to 16,242 (assuming a mean U content of 500 ppm) metric tons U. The U tonnage of this limited rock volume, contained mainly by the Hudsonian-age UO_2, corresponds between 4% (for McArthur River) to 103% (for Rabbit Lake) of the U tonnage of known unconformity-related U deposits of the basin.

Some of the studied rock samples, even macroscopically fresh and located far away from any known unconformity-related U deposit, present clear evidence of alteration, including clay minerals, alumino-phosphate-sulfate (APS) minerals, and UO_2 dissolution, indicating the percolation of the brines associated with the formation of unconformity-related uranium deposits when the basin was far more geographically extensive. Due to geological similarities between the studied zones and the basement domains from the eastern part of the Athabasca Basin, (*i.e.* the Hearne Province), it is proposed that these domains hosted widespread Hudsonian-age

uranium oxide protores. These protores provided easily leachable uranium for the metal enrichment of basinal brines during their percolation within the basement and the formation of the unconformity-related U deposits. These observations bring new insight to the debate about the genetic model of unconformity-related U deposits, and reinforce the metal source potential of the basement compared to that of the sedimentary basin.

Introduction

Uranium deposits associated with the Athabasca Basin (Saskatchewan, Canada) constitute the world's largest high-grade uranium deposits (Jefferson *et al.*, 2007), with up to 200 000 t uranium at 20% U_3O_8 for the McArthur River deposit. They are classified as unconformity-related deposits as they are located within the vicinity of an unconformity between a Proterozoic sedimentary basin (the Athabasca Basin) and subjacent Archean to Paleoproterozoic basement rocks. They are considered to have formed during several episodes of hydrothermal fluid circulation, mainly between 1.6 and 1.0 Ga (Cumming and Krstic 1992; Fayek *et al.* 2002a, b; Alexandre *et al.*, 2009 among others). In this model, documented as diagenetic-hydrothermal (Hoeve and Sibbald, 1978), the fluids responsible for the U uptake and transport are evaporated seawater-derived oxidizing brines from the basin (Richard *et al.*, 2011; Mercadier *et al.*, 2012) with a temperature ranging from 130 to 220°C (Pagel 1975; Derome *et al.* 2005). At the time of deposit formation, the basement-cover unconformity was 5-6 km below the topographic surface. The mineralizing brines percolated into the basement where they interacted with the rocks to form clay-rich (illite, Mg-chlorite and Mg-tourmaline) alteration halos by massive fluid/rock interaction (Mercadier *et al.*, 2012), and deposited U and associated metals (including Ni, Co, As, Zn, and/or rare earth elements) above/at and below the unconformity (Kyser and Cuney, 2008).

Although there have been more than thirty years of research devoted to these deposits, several uncertainties still exist concerning their formation (Cuney *et al.*, 2003; Cuney, 2005; Jefferson et al:, 2007). These include: (i) the origin of the metals, (ii) the conditions for metal transport in the brines, (iii) the reduction process for U deposition, (iv) the conditions for the massive quartz dissolution (up to 90% for some deposits, see Lorilleux *et al.*, 2003), and clay minerals formation and (v) the geodynamic conditions and structural regime favouring large, protracted fluid-flows within the basin and underlying basement. Of these questions, one of the most important is the source of the uranium. The brines in the vicinity of U deposits have been proved recently to contain the highest U contents of all crustal fluids (Richard *et al.*, 2010, 2012). These concentrations (<0.2 to 600 ppm U) are strongly related to the primary brine characteristics (acidic pH, Cl-rich composition, temperature 130-220°C), which favored efficient U extraction and transport, but also to high uranium availability in their environment. Varying hypotheses have been proposed for the U source, resulting in a contentious debate over the uranium fertility of the sedimentary basin versus the basement rocks (Jefferson *et al.*, 2007).

On the one hand, several research studies suggest that the uranium is primarily derived from altered (by brines) detrital accessory minerals within the basin sediments, such as apatite, zircon, and monazite (Kotzer and Kyser, 1995; Fayek and Kyser, 1997 among others). The widespread uranium-free alumino-phosphate-sulfate (APS) minerals in the Athabasca Basin are considered markers of detrital monazite dissolution and uranium leaching (Mwenifumbo and Bernius, 2007). Other sources of uranium in such organic matter-free clastic sediments could include uranium adsorbed on clay minerals, Ti-Fe oxides, and hematite, and/or bound to acidic volcanic ash (Cuney, 2005). The dominant clastic composition of the basin and the weak cementation of these aquifers during burial (Hiatt *et al.*, 2007) favored a high permeability for brine percolations, with abundant grain surface areas for chemical reactions and possible metal uptakes. However, the initial average U content of the sandstone before brine alteration is proposed to be below 3-5 ppm (Fayek and Kyser, 1997; Cuney *et al.*, 2003), implying a huge volume of fluid percolation required to alter the accessory minerals and extract the metals.

Other studies present clear evidence for alteration of U-bearing accessory minerals (e.g. monazite or zircon) by percolating basinal brines within the altered basement rocks around U deposits (Hecht and Cuney, 2000). In these zones, APS minerals similar to the ones described in the basin are observed, implying monazite destruction. In addition, whole-rock mass balance calculations comparing hydrothermally altered and fresh basement rocks clearly indicate U uptake from the basement rocks (Mercadier, 2008). Within the basement lithologies, Hudsonian (ca. 1.85-1.70 Ga) granites and granitic pegmatites have been proposed to be the most noteworthy primary uranium source due to their high U (estimated on average between 4 to 130 ppm; Madore *et al.*, 2000) and other metal contents. These metals, including U, are concentrated in accessory minerals, with monazite considered the main provider of uranium and rare earth elements (Hecht and Cuney, 2000). Although the permeability of the basement rocks is significantly lower than that of the overlying sedimentary basin, basin-derived brine percolations have been documented down hundreds of meters within the proximal clay-rich basement rocks surrounding the U deposits, and also in distal, macroscopically fresh samples (Mercadier *et al.*, 2010). These observations, along with mineralization and an alteration halo > 400 m below the unconformity at the Eagle Point deposit (Cloutier *et al.*, 2011; Mercadier *et al.*, 2011a), are well-documented and clearly indicate large-scale brine percolations and interactions within the basement, as demonstrated for other metal deposits (Ag, Pb-Zn, Cu) located close to basement cover interfaces (Essaraj *et al.*, 2005; Koziy *et al.*, 2009; Boiron *et al.*, 2010).

In addition to these often-described sources in both possible metal reservoirs, another potential U source mineral from the basement rocks has been proposed: uranium oxide. Magmatic uranium oxide (*i.e.* uraninite) was also suspected to be present in basement rocks (Madore *et al.*, 2000); this suggestion being reinforced by the description of Hudsonian uraninite-bearing anatectites and granitic pegmatites in the Hearne Province (Parslow and Thomas, 1982; Annesley *et al.*, 2000), which underlies the eastern Athabasca Basin (Figure L-1). However, this potential metal source has not been carefully nor extensively tested, despite this mineral i) containing over two orders of magnitude more U than other accessory minerals and ii) being far more easily leachable by brines than other accessory minerals. Thus, uraninite may have been a significant additional U source within the geological environment surrounding unconformity-related uranium deposits.

Most recent studies of the basement rocks underlying the Athabasca basin have used drill core samples located near deposits under Athabasca sandstone cover. Hydrothermally altered zones are not favorable for providing a clear understanding of the basement's initial lithology distribution, geographic distribution, and potential as a uranium source. Indeed, in the majority of the studied samples, U has been already leached *via* brine percolations, especially for such a soluble mineral as uranium oxide (Hazen *et al.*, 2009).

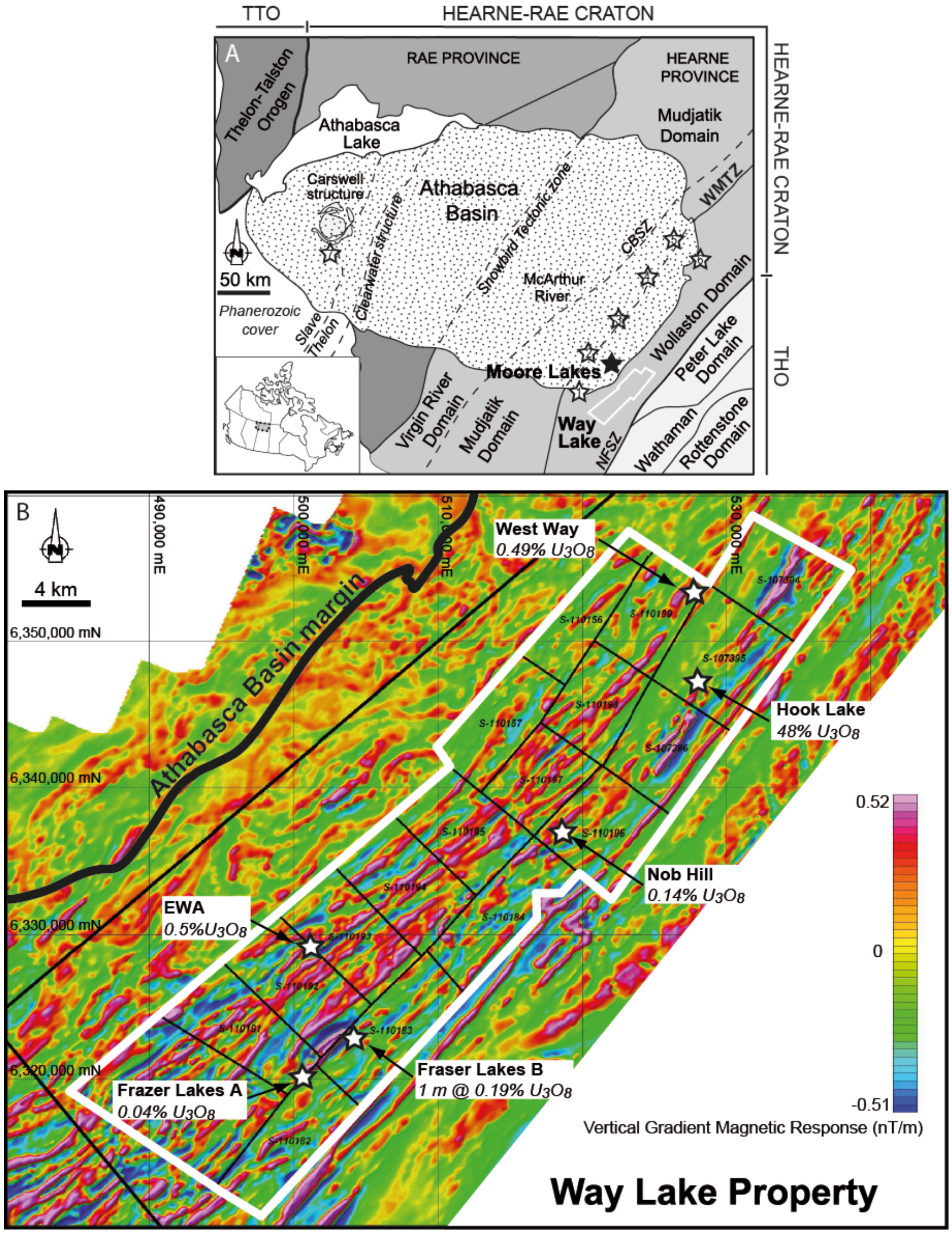

Figure L-1. (A) Simplified geological map of the Athabasca Basin (Saskatchewan, Canada) and underlying basement, showing the location of the two studied zones: Moore Lakes and Way Lake properties. (B) Aeromagnetic map of the Way Lake property (white line) with the location of the main uranium showings (stars). Maximum uranium contents (equivalent wt. % U_3O_8 in outcrop grab or core samples) are indicated for each showing. The Athabasca Basin margin is shown to the west of the property. TTO: Thelon-Taltson Orogen, THO: Trans-Hudson Orogen. Location of major unconformity-related U deposits: 1: Key Lake mine, 2: Millennium deposit, 3: McArthur River mine, 4: Cigar Lake mine, 5: Sue deposits, 6: Eagle Point mine.

In order to bring new information to the uranium source debate and to better understand the possible role of UO_2-bearing basement rocks as a potential metal source for the formation of unconformity-related uranium deposits, we carried out a study on a property hosted entirely by basement rocks near the current south-eastern margin of the Athabasca Basin: the Way Lake property (Figure L-1). This geological property lies within the eastern Wollaston Domain, and is considered analogous to the basement rocks below the eastern Athabasca Basin within the western Wollaston Domain and Wollaston-Mudjatik Transition Zone (WMTZ), an area which hosts the majority of the unconformity-related uranium deposits (Figure L-1.). The objective of this study was to examine in detail, using both outcrop and drill core, the distribution, lithologies, and mineral, chemical and isotopic characteristics of the primary uraninite-bearing basement rocks of the Wollaston Domain emplaced prior to the deposition of the basin and the formation of the unconformity-related uranium deposits. The work included petrographic and mineralogical observations, whole-rock geochemical analyses, mineral chemistry determinations (including Rare Earth Element contents of uraninite), chemical age dating, in-situ U/Pb isotopic dating of uraninite, and 3D modeling and calculation of the U contents within the main basement lithologies, including uraninite-bearing rocks. A comparison with the Moore Lakes magmatic uraninite-bearing granitic pegmatite is used to better understand i) the timing and mechanisms for the formation of uranium-rich rocks within the basement at the scale of the eastern Athabasca Basin, and ii) their diversity and distribution. Observations of the alteration features (e.g. dissolution of uraninite creating hole defined as boxwork, monazite dissolution, and clay neoformation) within UO_2-bearing rocks provide, for the first time, clear signatures of fluid-rock interactions and footprints of the brine percolations within these metal-rich basement source rocks.

Geological Settings

Geology of the Athabasca Basin

The basement of the Athabasca Basin is located within the Churchill Province of the Canadian Shield and comprises mainly Archean tonalitic to granitic domes surrounded by Paleoproterozoic (Aphebian) metasedimentary rocks, and Paleoproterozoic (Hudsonian) mafic to felsic plutons (e.g. Madore *et al.* 1999; Annesley *et al.* 2005). There are two distinct structural provinces: the Hearne Province to the east and the Rae Province to the west (Figure L-1). In the eastern part of the Athabasca Basin, where most of the known unconformity-related U deposits are located, the basement complex comprises rocks of the Mudjatik Domain, the WMTZ, and the Wollaston Domain. This complex hosts a heterogeneous assemblage of Archean plutonic rocks intercalated with Paleoproterozoic metasedimentary rocks of the Wollaston Group, initially deposited in an epicontinental setting (Yeo and Delaney, 2007). These rocks were affected by complex polyphase deformation, high-grade metamorphism, and associated partial melting and injection of plutonic rocks during the Trans-Hudson Orogen (THO) at ca. 1.86-1.72 Ga (Lewry and Sibbald, 1980; Chiarenzelli *et al.*, 1998; Annesley *et al.*, 2001; Annesley *et al.*, 2005). Peak metamorphic P-T conditions associated with the Hudsonian Orogeny, between 1.84 and 1.80 Ga, reached about 800°C and 800 MPa (Annesley *et al.*, 2005). Exhumation of the basement started at about 1.815 Ga, with metamorphic conditions following a clock-wise path down to a pressure of about 250-300 MPa and temperature of 500-550°C by about 1.78 Ga, and down to an estimated pressure of about 200 MPa and temperature of 250-400°C by about 1.72 Ga (Annesley *et al.*, 2005; Mercadier *et al.*, 2010). Isothermal decompression from peak temperatures at 1.820-

1.805 Ga was associated with decompressional melting and intrusion of the main pulse of leucogranites and granitic pegmatites (Annesley *et al.*, 2005).

The Athabasca Basin consists of Meso- to Neoproterozoic polycyclic, mature flu*via*l to marine quartz-rich sandstones and associated rocks of the Athabasca Group deposited in a near-shore shallow shelf environment (Ramaekers *et al.*, 2007), with deposition beginning at about 1.7 to 1.75 Ga (Armstrong and Ramaekers 1985; Kyser *et al.* 2000). The estimated thickness of the basin during the Mesoproterozoic was 5 to 6 km, based on fluid inclusion studies (Pagel, 1975).

Geology of the studied zones

Way Lake property

JNR Resources Inc.'s Way Lake property in northern Saskatchewan, Canada, is located ~25 km southeast of the Athabasca Basin and 55 km east of the Key Lake U mine. The property encompasses six different U showings: Fraser Lakes (Zones A and B), Hook Lake, Nob Hill, West Way, and EWA (Figure L-1). The Way Lake property, located in the eastern Wollaston Domain, is underlain by Paleoproterozoic Wollaston Group metasedimentary rocks and Archean orthogneisses that underwent complex deformation, metamorphism (upper amphibolite to granulite facies), and magmatism during the Trans-Hudson Orogen (~ 1.85-1.7 Ga). An approximately 65 km long, folded electromagnetic (EM) conductor (*i.e.* graphitic pelitic gneisses) runs across the property, with the Fraser Lakes showings hosted adjacent to a 5 km section of this conductor (Figure L-2).

The Fraser Lakes showings (Zones A and B) are located within NE-plunging regional fold noses adjacent to the EM conductor. The more prospective Zone B sits within an antiformal fold nose (McKechnie *et al.*, 2012), from which several drill holes have intersected multiple intervals of uranium and/or thorium mineralization (up to 0.183% U_3O_8 over one meter in drill core, Figures L-3 and L-4a). Zones A and B are crosscut by a number of E-W-, NNE-, and NNW-trending structures. Drill core observations reveal the existence of multiple generations of granitic pegmatites and leucogranites, including U- and Th-mineralized (generally subcordant to gneissosity and greater than 100 ppm U + Th) and non-mineralized (highly discordant to gneissosity, less than 100 ppm U + Th) varieties, with some of the pegmatites showing compositional zoning (Figure L-4c to e). The uraniferous pegmatites and leucogranites intrude the highly deformed contact (*i.e.* folded shear zone) between the basal Wollaston Group metasedimentary rocks and the underlying Archean granitoids. Drilling on Zone B has identified an extensive area approximately 1,300 m long by 650 m wide of moderately-dipping, multiple stacked mineralized horizons, open to the southwest and east-northeast, and confirmed to a minimum depth of 125 m (Figures L-2, L-3, and L-4a). The Trench 2 outcrop at Fraser Lakes Zone B represents the surface extension from depth of the same type of U mineralization observed in drill core within quartz-biotite-feldspar-rich granitic pegmatites and leucogranites (Figure L-4b).

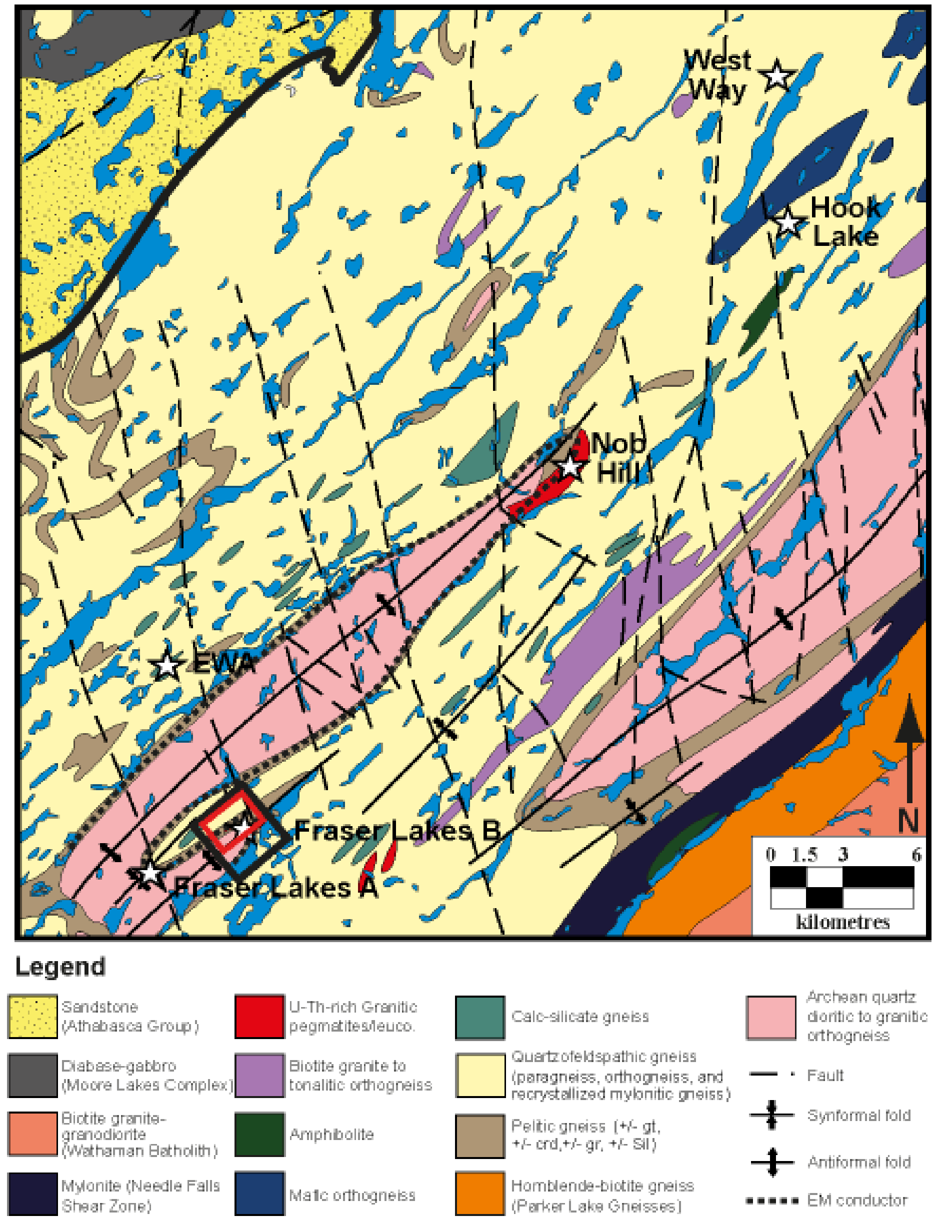

Figure L-2. Geological map of the Way Lake property with the different uranium showings studied: EWA, Hook Lake, Nob Hill, West Way, EWA and Fraser Lakes Zones A and B. All six areas occur in outcrop and have been drilled. The blue surfaces correspond to the location of lakes. The red rectangle indicates the location of the 3D modeling volume. Leuco.: leucogranite.

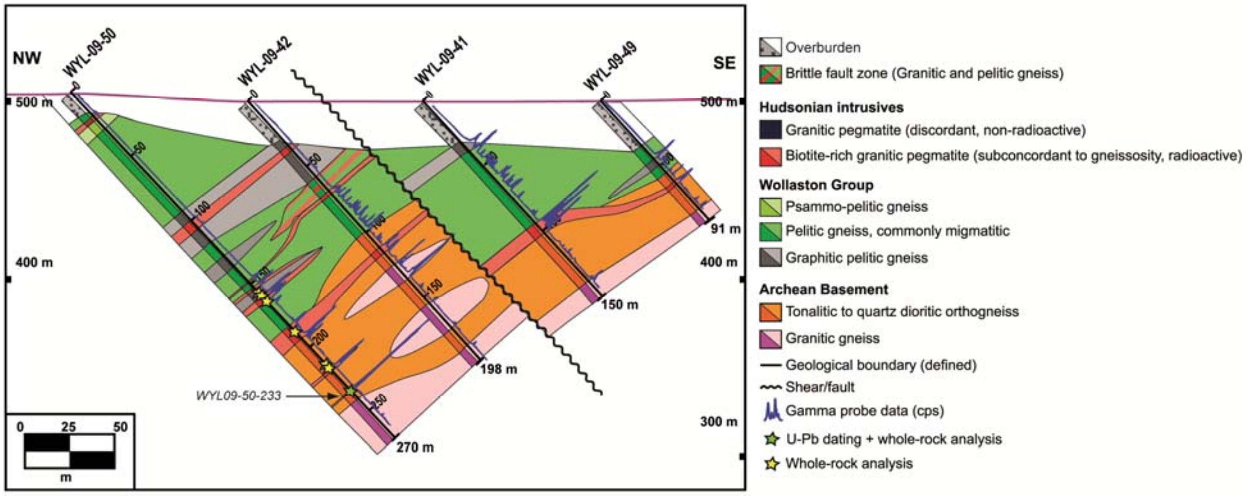

Figure L-3. Cross-section from the Fraser Lakes Zone B showing the local geology from four of the studied drill holes in this zone (WYL-09-50, WYL-09-42, WYL-09-41 and WYL-09-49). The Hudsonian U-rich intrusives (granitic pegmatites and leucogranites) represent one of the major lithological units within the basement rocks. The green star is uranium-rich samples analyzed by whole-rock chemistry and dated by in–situ U-Pb isotopic measurements on uranium oxides, yellow stars are uranium-rich samples analyzed by whole-rock geochemistry. See also Figure L-4a for location of the cross-section from the Fraser Lakes Zone B uranium showing. leuco.: leucogranite.

The EWA showing is located in the southwest corner of the property. Several grab samples of pegmatites and leucogranites returned values of 0.064 to 0.492% U_3O_8. Drill holes intersected Archean orthogneiss and granite gneiss intruded by numerous, often radioactive, granitic pegmatite dykes of variable thickness and orientation. Clay minerals, hematite and chlorite alteration is usually fracture-controlled. Anomalous uranium values of up to 0.235% U_3O_8 are scattered sporadically through the granitic pegmatite and associated with fractures and weak shearing.

The West Way showing occurs on the north end (southeast edge) of a 1 km long NE-trending ridge of discontinuous outcrops. The U mineralization is vein-type and associated with calc-silicate alteration. The West Way showing contains uranium mineralization up to 10,000 cps/s (equivalent to 0.49% U_3O_8), associated with steeply dipping east-west fractures. Drill holes confirmed the presence of well-defined and altered structures, intersecting weak alteration including calc-silicate, hematite, and bleaching.

The Hook Lake showing is a high-grade, massive uranium oxide vein (Figure L-4g) occurring in a dilational jog within a south-southwest trending ductile-brittle shear zone hosted by felsic to intermediate intrusive rocks showing evidence of high-T metasomatism. A number of NE- and NW-trending brittle faults crosscut the Hook Lake mineralization.


Fraser Lakes Zone B
Way Lake
Fraser Lakes
NE
EM conductor
Fraser Lakes
Trench 2 cross section (Fig. XX)
WYL09-X Drill hole
WYL10-X Drill hole
b
Way Lake
Fraser Lakes
Trench 2
Qtz
Pl
Bt-Zr-U
(>2.2 % U_3O_8)
20 cm
c
Way Lake
Fraser Lakes
WYL09-40
20 cm
d
Way Lake
Fraser Lakes
WYL09-50-233
Qtz
Bt
(0.11% U_3O_8)
15 cm
e
Way Lake
Fraser Lakes
WYL09-50
UO_2-bearing pegmatite
20 cm
f
Way Lake
Nob Hill
pegmatite
(< 100 ppm U_3O_8)
U-mineralized pegmatite
(0.06-0.11% U_3O_8)
20 cm
g
Way Lake
Hook Lake
(>2.2 % U_3O_8)
Secondary U-rich minerals
vein-type Urn
10 cm

Figure L-4. (previous page). Photographs of the studied uranium-rich showings on the Way Lake property. (a) Aerial photograph of the Fraser Lakes Zone B with the location of some drill holes and of Trench 2 outcrop. The location of cross-section from Figure L-3, the electromagnetic (EM) conductor, and the 3D modeling volume (red rectangle) are highlighted. (b) Photograph of the Trench 2 outcrop with U-enriched biotite (Bt)-zircon (Zrn)-quartz (Qtz)-plagioclase (Pl) zone. (c) Drill core from the WYL-09-40 drill hole in Fraser Lakes Zone B showing U-rich granitic pegmatite at 117-122 m. (d) Drill core from the WYL-09-50 drill hole in Fraser Lakes Zone B showing U-rich granitic pegmatite at 233m. (e) Drill core from the WYL-09-50 drill hole in Fraser Lakes Zone B showing U-rich granitic pegmatite at 159-162 m. (f) Photograph of one Nob Hill outcrop with a U-rich mineralization in pegmatite cross-cutting older Hudsonian pegmatite. (g) Photograph of the U-rich vein from Hook Lake showing. U grades (% U_3O_8) recalculated from cps/s measurement on the field with gamma-ray detector. 2.2% U_3O_8: upper limit of the detector.

The Nob Hill showing occurs on a large knob-like hill (oriented NNE) of discontinuous to continuous mineralized granitic pegmatite and leucogranite. The main foliation is 020/55-75 and is cut by later fractures oriented 070-080/80 and very late sub-horizontal jointing. The mineralization occurs in highly fractured granitic pegmatite and appears controlled by the intersection of these two trends (Figure L-4f). One discontinuous, mineralized pegmatite/leucogranite ranges from 1,200-22,000 cps/s (equivalent 590-10,800 ppm U_3O_8) and has up to 0.14% U_3O_8, with background radioactivity of the granitic pegmatite being 150-300 cps/s (equivalent 70-140 ppm U_3O_8). Five diamond drill holes (WYL-08-515 to WYL-08-519) intersected an often extensive and irregular mineralized pegmatite body capping a topographic high. At depth, narrow to thick, discontinuous, irregular pegmatitic masses and dykes intrude Archean granitic gneiss and orthogneiss.

Moore Lakes property

The Moore Lakes area is a site of ongoing uranium exploration in the Athabasca Basin by Denison Mines Ltd and JNR Resources Inc. Inliers of Archean/Paleoproterozoic rocks within the Athabasca Basin occur in the study area as part of the Moore Lakes Complex. This fault-bounded complex is part of the Wollaston Domain, and comprises Archean orthogneisses, Wollaston Group meta-sedimentary rocks, and extensive diabase intrusions. MacDougall and Williams (1993), mapped and documented the geological features of the Moore Lakes complex, with detailed petrographic work on the diabases carried out by MacDougall and Maxemiuk (1995). Drilling programs identified significant unconformity-related uranium mineralization near the footwall of a 125 meter-wide structural zone, called the Maverick Zone. This drilling revealed that granitic pegmatites comprise <5-10% of the basement complex, with half estimated being radioactive. Relatively fresh, radioactive granitic pegmatite was intersected in one drill hole (ML00-08, Annesley *et al.*, 2000). The pegmatite is 10 m thick, and occurs 55 m below the unconformity with the overlying Athabasca Group sandstones. More recent drilling within the Maverick Zone intersected intensely clay-altered granitic pegmatite with textures similar to the ML00-08 pegmatite. The radioactivity reaches up to 6,000 cps/s (equivalent to ~3,000 ppm U_3O_8) for the most mineralized granitic pegmatites at Moore Lakes.

Sampling and Methodology

Several uranium oxide-bearing samples from the Way Lake property were selected from outcrop (Hook Lake, Nob Hill, EWA, and Fraser Lakes Zone B (Trench 2) showings) and from drill core (Fraser Lakes Zone B, Nob Hill, and EWA showings). Three core samples were also studied from the Moore Lakes property (ML00-08 321.5m, ML00-08 322m and ML00-08 322.5m). In order to establish the mineral paragenesis, polished thin-sections were examined using a conventional transmitted and reflected light microscope, a PHILIPS XL30 scanning electron microscope (SEM) equipped with an energy dispersive spectrometer and a Si (Li) semi-conductor detector, and a HITACHI S-4800 scanning electron microscope at SCMEM (Nancy, France).

Electron microprobe analyses (EMPA) of uranium oxides were performed using a CAMECA SX-100 at SCMEM (Nancy, France), a CAMECA SX-100 at the Saskatchewan Research Council (SRC, Saskatoon, Canada), and a JEOL 8600 Superprobe at the Department of Geological Sciences of the University of Saskatchewan (Saskatoon, Canada). The calibration at SCMEM utilized natural and synthetic oxides and/or alloys (orthoclase, albite, $LaPO_4$, $CePO_4$, wollastonite, UO_2, ThO_2, $PbCrO_4$, $NdPO_4$, YPO_4, olivine, $DyRu_2Ge_2$). The analytical conditions at SCMEM were 10 nA current, accelerating voltage of 15 kV, 10 s counting time (K, Na, Ca), 20 s (Ce, U, Th, Si, Y), 40 s (Dy, Nd), 50 s for Pb and 60 s for La. The calibration at SRC used natural and synthetic minerals and metals (augite, corundum, fayalite, $REEPO_4$, YPO_4, $PbCrO_4$, Th, U, Ti, V). All elements were analyzed using high-intensity crystals for thirty seconds on peak at 20 nA beam current with 15 kV accelerating potential. The calibration at University of Saskatchewan used high purity metals as standards for U, Th, Y, and Nb. Quartz was used as a standard for Si, diopside for Ca, apatite for P, cerium phosphate for Ce, dysprosium phosphate for Dy, and crocoite for Pb. The analytical conditions at University of Saskatchewan were: 10 nA current, accelerating voltage of 20 kV, and 40 s counting time for all elements except Th (100 s).

Single-point chemical ages for UO_2 minerals were calculated using the following equation of Bowles (1990):

$$Pb = Th * (e^{\lambda_{232}t} - 1) + U * (0.99276 * (e^{\lambda_{238}t} - 1) + 0.007196 * (e^{\lambda_{235}t} - 1)),$$

where t is the age of mineral closure to U, Th and Pb exchange, λ_{232}, λ_{235} and λ_{238} are the decay constants of ^{232}Th, ^{235}U, and ^{238}U, respectively, and Pb, Th, and U are the weight percent of these elements in the analyzed U mineral. The first term of the equation is related to the decay of ^{232}Th to ^{208}Pb, the second term to the decay of ^{238}U to ^{206}Pb, and the third term to the breakdown of ^{235}U to ^{207}Pb. The decay constants (λ) for each of these terms are $\lambda_{238} = 0.00015512$ Ma^{-1}, $\lambda_{235} = 0.00098485$ Ma^{-1}, and $\lambda_{232} = 0.000049475$ Ma^{-1}, respectively. The formula is based on the assumption that no U or Th has been re-introduced into or lost from the system, and that no common Pb was present in the mineral during the initial crystallization.

U/Pb isotope compositions of U oxides were measured with a CAMECA IMS 3f ion microprobe at the CRPG (Nancy, France). The complete methodology is described in Mercadier *et al.* (2011a). Ages and error correlations were calculated using ISOPLOT (Ludwig, 1999). Uncertainties in the ages are reported at the 2σ level. Common Pb corrections were based on the measured ^{204}Pb content using the Pb isotopic composition calculated from Stacey and Kramers

(1975), at the age of uraninite. However, the high $^{206}Pb/^{204}Pb$ ratio (>10,000) obtained for all samples suggest that there is negligible common lead.

Rare earth element (REE) concentrations in uranium oxides were measured with a CAMECA IMS 3f ion microprobe at the CRPG and with a laser ablation inductively coupled plasma mass spectrometer (LA-ICP-MS) at G2R. Methodology for SIMS and LA-ICP-MS are described in Bonhoure *et al.* (2007) and Mercadier *et al.* (2011b), respectively.

All geochemical sample preparations and whole-rock analyses were performed at the SRC Geoanalytical Laboratories (Saskatoon, Canada). Whole-rock major element oxides, loss on ignition (LOI), and selected trace elements (Ba, Cr, Sc, Sr, Y, and Zr) were analyzed by a Perkin Elmer inductively coupled plasma-optical emission spectrometer (ICP-OES) following lithium metaborate fusion. Due to technical limitations, REE were not measured, except La. Detection limits are on the order of 0.01% for the major elements (except SiO_2), 0.1% for LOI and SiO_2 (when analyzed), and 2 ppm for the trace elements. The remaining trace elements (with the exception of B) were analyzed by ICP-OES or ICP-MS following acid digestion of the whole rock powder, with a detection limit of about 1 ppm. Samples for boron analysis underwent $NaO_2/NaCO_3$ fusion prior to analysis by ICP-OES, with a detection limit of 2 ppm. Carbon and sulfur concentrations of all samples were determined by combusting pulverized sample material in a LECO induction furnace supplied with oxygen. Instrument calibrations were used to determine the weight percent concentrations of both elements in the sample. The detection limits are on the order of 0.01% for both carbon and sulfur using this method. Representative samples were also analyzed by X-ray Fluorescence (XRF) to determine fluorine, chlorine and sulfur, as well as major and trace elements. Pressed pellets of homogenized rock powder were analyzed in a vacuum using a Bruker S8 TIGER XRF spectrometer. Detection limits vary depending on the element of choice, and are in the range of 0.005 to 0.01% for the major elements, 0.01% for F, S, and Cl, and from 1 to 10 ppm for the remaining elements. Analyses of samples previously measured by ICP-OES provided constraints on analytical accuracy, and the results from both techniques are very similar. Titration analyses were also carried out on the representative samples to obtain a value for FeO_{total} in the rocks. The amount of ferrous and ferric iron in the samples were calculated from the values obtained using ICP-OES/XRF and titration.

The 3D geological modeling of the Fraser Lakes Zone B (1,300 m x 630 m x 328 m) was carried out using the GOCAD software package. The Fraser Lakes Zone B was specifically selected from the Way Lake property due to its fair to good outcrop exposures of the various Archean and Paleoproterozoic lithological units, including the U mineralized granitic pegmatites and leucogranites. Most importantly, abundant drill hole data are available, which provide information on the distribution, nature, and importance of the lithological units at depth. Most of the regional to local geological structures are known from outcrops, drilling, and/or airborne geophysics. Four main types of data were used to build the 3D GOCAD model of Fraser Lakes Zone B:

1. A set of about 25 logs of drilling provided by JNR Resources Inc. The drilling pattern consists of sub-parallel, NW-SE-oriented fences of drill holes. The drill holes provide geological (e.g. descriptive logs of the different lithological units), petrological (e.g. mineral assemblages and alteration phases), and downhole logging data (e.g. whole-

rock geochemistry and radiometrics). Geochemical data (*i.e.* whole-rock geochemistry) are available along sections of all of these drill holes.

2. Outcrop data from historical and recent geological mapping and prospecting programs, on the Way Lake property, including zones A and B at Fraser Lakes.
3. Airborne geophysical surveys (*i.e.* aeromagnetics, VTEM, radiometrics) that trace conductive geophysical anomalies in the basement and trend of fault structures associated with these lithologies.
4. Eight interpreted vertical cross-sections, constructed from detailed logging and mapping of lithological units and structures within the drill cores. The eight vertical cross-sections are oriented roughly sub-parallel (see Figure L-3 for one example).

The cross-sections and drill holes served as geometrical constraints for building triangulated surfaces with the GOCAD software, representing boundaries of the geological units and structures. The building of the surface was carried out using the Discrete Smooth Interpolation method (Mallet, 1992). A volumetric model (*i.e.* voxet) was derived posteriorly from the partition of space by triangulated surfaces. Three main first-order volumes within the voxet were defined following the dominant lithology, age, and geochemical properties: Paleoproterozoic pelitic to psammopelitic gneiss (including all Paleoproterozoic lithologies, except mineralized granitic pegmatites and granites, see Figure L-2), Archean orthogneiss (including all Archean lithologies), and U-mineralized granites/pegmatites. The U-mineralized granite volume is based on lithological properties and a geochemical cutoff of 0.1% U_3O_8 (*i.e.* Paleoproterozoic rocks with U_3O_8 contents below this value are considered part of the pelitic to psammopelitic volume).

Results

Petrography and mineralogy of U-mineralized samples

Way Lake property: Fraser Lakes (Zone B and Trench 2), EWA, and West Way showings

Uranium-mineralized pegmatites and leucogranites are granitic in composition, with quartz, feldspar, and biotite the main minerals in almost every pegmatite (Figures L-5a and b). Other minerals include garnet, magnetite, ilmenite, titanite, muscovite, apatite, fluorite, sulphides, and U-Th-REE-bearing accessory minerals (mostly uraninite, thorite and zircon). The U-Th-REE mineral assemblage is dependent on the granitic pegmatite and leucogranite location within the fold nose. Granitic pegmatites and leucogranites intruded into the Archean orthogneisses contain magnetite and ilmenite intergrowths with ubiqitous fluorite. Some of the uraninite-rich samples correspond to biotitic schlierens (Figures L-5c and d) and others to quartz-rich granitic pegmatite. The uraninites are cubic to rounded, homogeneous, and generally smaller than 300 μm (Figure L-5d). They are usually associated with metamict zircons (metamictization defined by microscopic observations and electron microprobe analyses), with many of the zircons being clearly zoned. Accessory minerals are fresh, except for some monazite and uraninite crystals that have slight to moderate traces of alteration (Figures L-5a and L-6c). Chlorite, hematite, clay mineral, sericite, and carbonate alteration are present in some granitic pegmatites and leucogranites.

Way Lake property: Hook Lake

The Hook Lake mineralization, comprising a high-grade massive uranium oxide vein, exhibits a simple mineralogy. It is dominated by uraninite (Figure L-5e) with secondary uranium products (*i.e.* U-rich thorite, coffinite, gummite, and possibly uranophane). The massive uranium oxides spread outwards into highly fractured uraninite masses cut by numerous cross-cutting fracture sets possibly filled by pitchblende (UO2), which corresponds to a lower temperature mineralizing event. Minor amounts (5-10%) of hematite and quartz occur sporadically. Locally within the outer part of the vein mineralization, the uraninite grains are hosted by an albite-rich rock (*i.e.* metasomatized country rock).

Way Lake property: Nob Hill

The investigated samples from Nob Hill are representative of the main intrusion (*i.e.* approximately 80–90% of the discontinuous Nob Hill outcrop), which consists of a relatively leucocratic, overall coarse-grained to pegmatitic intrusive body of granitic composition, sometimes biotite-rich with metasedimentary enclaves or locally quartz-rich. The granitic pegmatite is massive to foliated, locally sheared, and essentially unaltered. It is composed mainly of quartz, feldspars, and biotite, with subordinate amounts of allanite, apatite, zircon, uraninite, and ilmenite. It is characterized by a highly variable content of large K-feldspar phenocrysts. The main mineralized outcrop (Figure L-4f) shows vein-type mineralization within quartz-rich portions of the granitic pegmatite. The Nob Hill mineralization exhibits an overall simple mineralogy. It is dominated by uraninite (Figure L-5f) and allanite with secondary uranium products (*i.e.* U-rich thorite, coffinite). Two generations of uranium oxides are present: fractured uraninite crystals (Figure L-5f) and small (<5 μm) hydrothermal uraninite veins which emanate from the uraninite crystals.

Moore Lakes property

The granitic pegmatite is inequigranular-pegmatitic, sheared and foliated, and essentially unaltered. It is composed mainly of quartz, feldspars, and biotite, with subordinate amounts of apatite (5-7 modal %), zircon (2-5 modal %), uraninite, and ilmenite (Figure L-5g). Other accessory minerals include pyrite, subhedral to cubic in shape, and monazite. K-feldspar grains are variably recrystallized and intergrown with the quartz grains. Biotite flakes form massive clusters along the foliation planes. Apatite grains are distributed within biotite-rich clusters. Two generations of zircon are identified: large inherited cores and younger magmatic overgrowths (Annesley *et al.*, 2000). Uraninite grains are euhedral, 0.05 to 0.50 mm in size (Figures L-5h and L-6d), and are mostly found within biotite flakes and schlierens. Some of the grains are highly fractured and variably altered compared to zircons and monazites. Trace amounts of rammelsbergite (NiAs2) are developed around uraninite grains. Late calcite veinlets are visible within sample ML00-08 322.5 m.

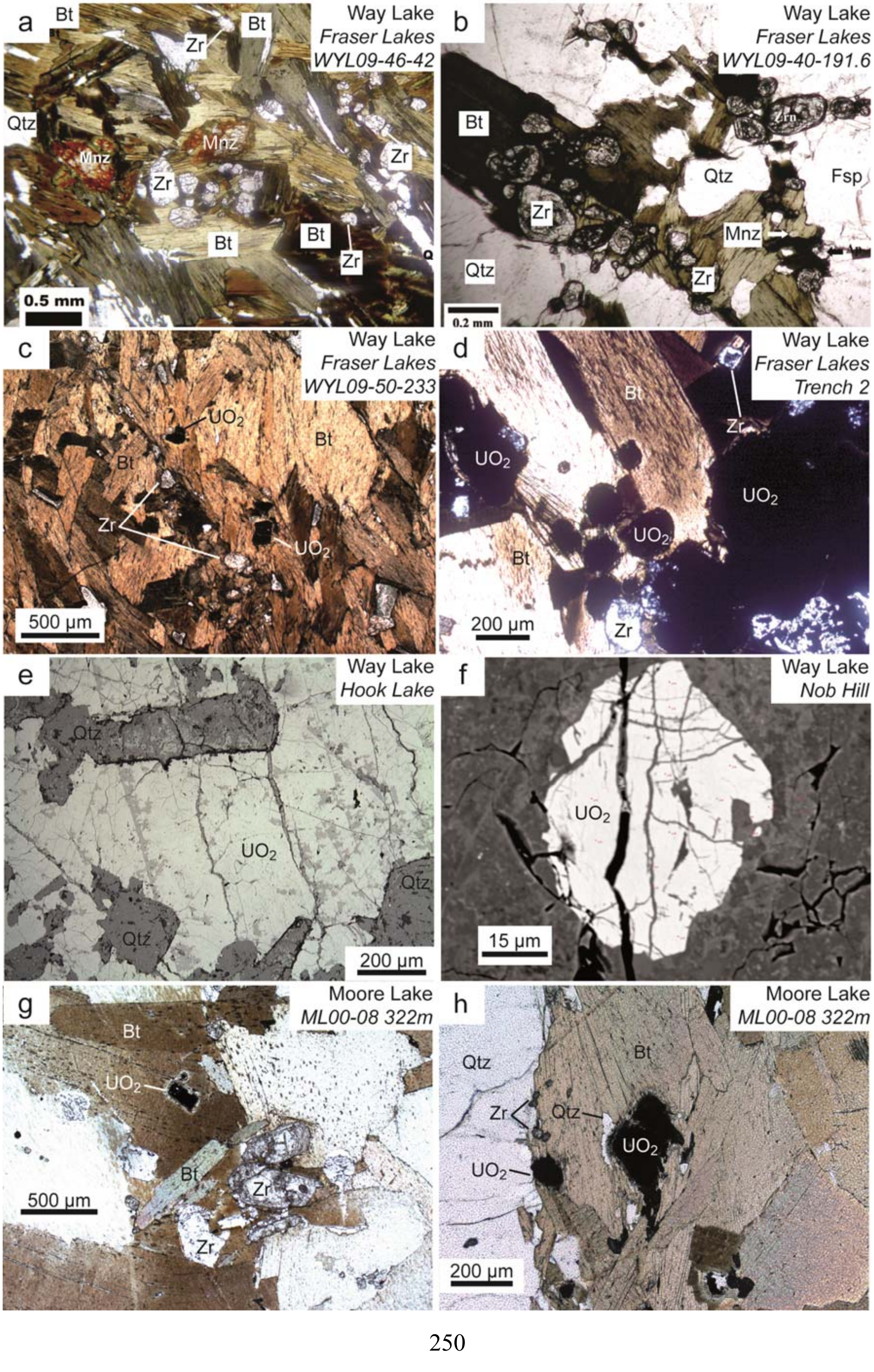
a
Way Lake
Fraser Lakes
WYL09-46-42
Bt
Zr
Bt
Qtz
Mnz
Mnz
Zr
Zr
Bt
Bt
Zr
0.5 mm
b
Way Lake
Fraser Lakes
WYL09-40-191.6
Bt
Zrn
Qtz
Fsp
Zr
Mnz
Qtz
Zr
0.2 mm
c
Way Lake
Fraser Lakes
WYL09-50-233
UO2
Bt
Bt
Zr
UO2
500 µm
d
Way Lake
Fraser Lakes
Trench 2
Bt
Zr
UO2
UO2
UO2
Bt
Zr
200 µm
e
Way Lake
Hook Lake
Qtz
UO2
Qtz
Qtz
200 µm
f
Way Lake
Nob Hill
UO2
15 µm
g
Moore Lake
ML00-08 322m
Bt
UO2
Bt
Zr
Zr
500 µm
h
Moore Lake
ML00-08 322m
Qtz
Bt
Zr
Qtz
UO2
UO2
200 µm

Figure L-5. (previous page). Photomicrograph and back scattered electron (BSE) images of typical mineral assemblages observed in U-rich samples from the Way Lake uranium showings and Moore Lakes granitic pegmatites. (a) Biotite (Bt)-rich quartz (Qtz) pegmatite with monazites (Mnz) and zircons (Zrn). (b) Biotite-feldspar (Fsp)-quartz pegmatite with a monazite-zircon-rich assemblage. (c) Biotite schlieren with disseminated zircons and uraninites (Urn). (d) Uraninite within altered granitic pegmatite. (e, f) massive uranium oxides associated with quartz in vein-type mineralization with the white (WZ) and grey (GZ) zones. (g, h) Biotite-quartz-rich granitic pegmatite with disseminated uraninite grains.

Crystal chemistry and chemical ages of uranium oxides

The pristine parts of the uraninites grains (Table L-1) in pegmatites from the Moore Lakes and Way Lake showings (Fraser Lakes Zone B, including Trench 2) are characterized by relatively high U (58-71 wt. % UO_2), Pb (14.6-20.3 wt. % PbO), Th (4.5-9.2 wt. % ThO_2) and Y (1.2-5 wt. % Y_2O_3) contents and low Ca (0-1.3 wt. % CaO) contents. The pristine parts of the vein-hosted uraninites from the Hook Lake showing are characterized by high U (64.1-70.7 wt. % UO_2), Pb (14.7-21.5 wt. % PbO) and Ca (0.6-4.4 wt. % CaO) contents and low Th (0.7-3.9 wt. % ThO_2) and Y (0.4-1.6 wt. % Y_2O_3) contents. The uraninites from fractures and veins of the Nob Hill showing have similar composition as for the Hook Lake uraninites, except they have lower U (56.7-59 wt. % UO_2) and higher Y (7.1-9 wt. % Y_2O_3) contents. Silicon, K, and Na contents, when detectable, are low (below 1.0 wt. %) for all the uranium oxides analyzed. The rare earth elements, except La, are always present at the tenths of a wt. % level. The totals of the pristine parts of the uraninite are comprised between 94 and 96 wt. % (Table L-1). The grey (GZ) and white (WZ) zones, visible in SEM back scattered electron images for Hook Lake uraninites, differ mainly chemically in their Pb and U contents (enriched in WZ), and Ca content (enriched in GZ). Several uranium oxides show significant alteration features, including boxwork formation and replacement by strongly hydrated thorite with high Th (23.4-48.4 wt. % ThO_2) and Si (6.7-23.7 wt. % SiO_2) contents and low U (2.6-15.2 wt. % UO_2) and Pb (0.4-4.9 wt. % PbO) contents.

The chondrite-normalized REE patterns of magmatic uraninites (Way Lake-Fraser Lakes and Moore Lakes) exhibit the same “flat” REE pattern with a strong negative Eu anomaly and slight negative La anomaly (Figure L-8). Vein-type uraninites (Way Lake-Hook Lake), from whatever zone (White or Grey), have weakly fractionated REE patterns with a higher global REE content, a Pr enrichment compared to the other light REE, and a small negative Eu anomaly. The REE content of vein-type uraninite is higher than magmatic-related uraninite, and the REE patterns for both types are clearly distinct (Table L-2). Notably, the REE patterns of the U-oxides are independent of the host-rock lithology. The REE patterns for magmatic and vein-types are clearly different from the bell-shaped patterns typical of unconformity-related U deposits of the Athabasca Basin (Figure L-8). The samples from EWA, Nob Hill, and Trench 2 showings (Way Lake property) were not analyzed because homogeneous uranium oxides were smaller than the analytical spot diameter of both techniques (SIMS and LA-ICPMS)

Calculated U-Th-Pb chemical ages for the pristine zones of the uranium oxides are bi-modally distributed, with a mode at 1.6-1.7 Ga (Way Lake-Hook Lake-Grey Zone, Way Lake-Fraser Lake-Trench 2 and Moore Lakes) and a second mode at 1.7-1.9 Ga (Way Lake-Hook Lake-

White zone, Way Lake-Fraser Lakes-WYL09-50-233, Way Lake-Nob Hill; Figure L-9). The calculated ages for basement uraninites of the Way Lake and Moore Lakes properties are clearly distinguishable and older than the chemical ages of unconformity-related uranium oxides (Figure L-9).

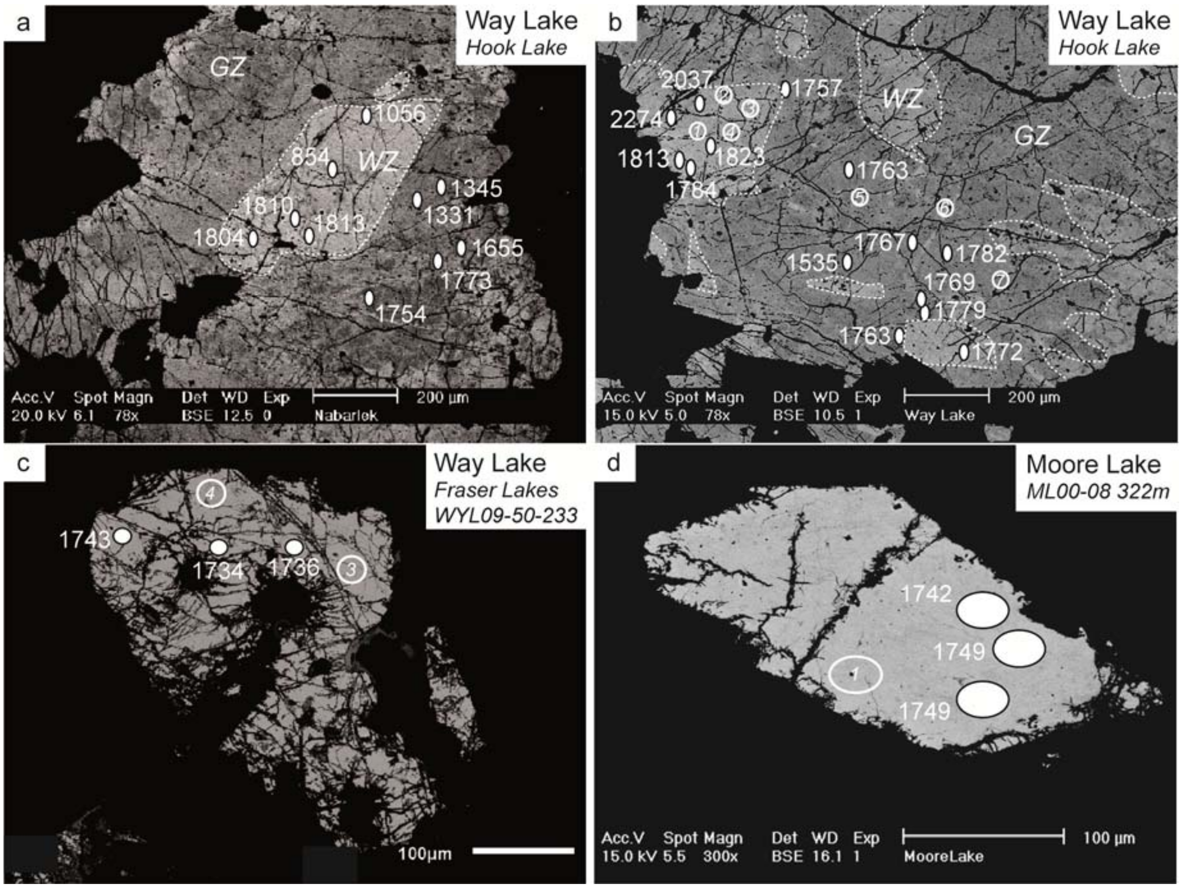

Figure L-6. BSE images of uraninites from the Way Lake and Moore Lakes properties. (a, b) Uraninites from the U-rich vein of Hook Lake showing. Two zones, a white zone (WZ) and a grey zone (GZ), are distinguishable by their grey contrast, directly related to their different chemical composition. (c) Fractured magmatic uraninite grains from the WYL-09-50 drill hole intersection of the Fraser Lakes Zone B. (d) Homogeneous magmatic uraninite from drill hole ML00-08 of the Moore Lakes uranium showing. Full circle corresponds to the location of the U-Pb isotopic analysis and the associated number at the $^{206}Pb/^{207}Pb$ age (see Figure L-10). Empty white circle correspond to the location of the REE analytical point (see Figure L-8). Different sizes of the circles are a function of the image scale.

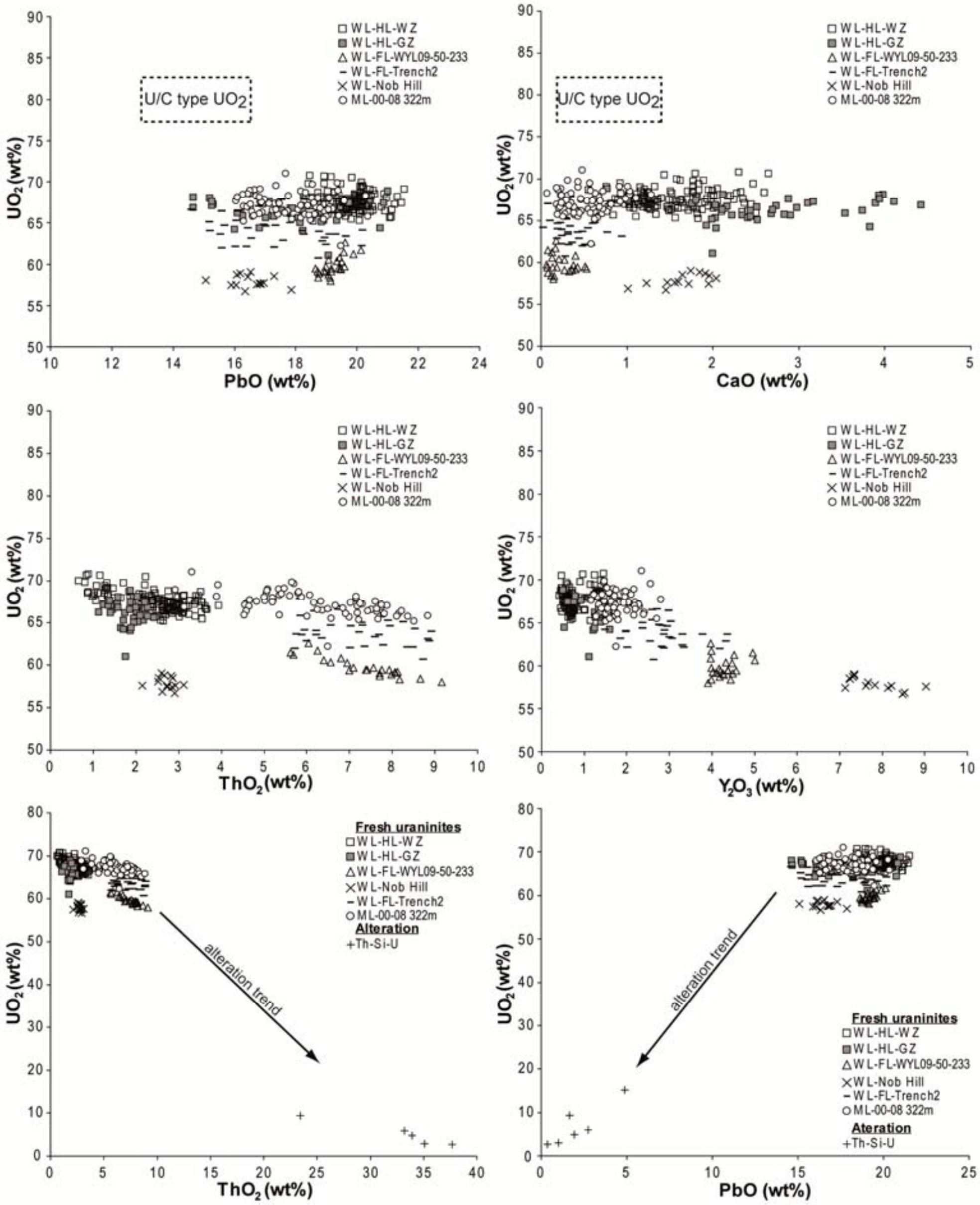

Figure L-7. Chemical composition for the studied uraninites from the Way Lake and Moore Lakes uranium properties. Significant chemical variations between uraninites are observed for Th, Ca, and Y contents. Magmatic uraninites are characterized by high Th contents (5-9 wt. % ThO2), whereas vein-type uraninites have lower Th contents (1-4 wt. % ThO2). The chemical compositions of the phases related to uraninite alteration (Th-Si-U) are shown in the lower part of the Figure. The average chemical composition of unconformity-related uranium oxides (U/C type UO2) are from Fayek and Kyser (1997) and Alexandre and Kyser (2005). WL-HL-WZ: Way Lake property, Hook Lake showing, white zone. WL-HL-GZ: Way Lake property, Hook Lake showing, grey zone. WL-FL-WYL09-50-233: Way Lake property, Fraser Lakes Zone B showing, drill hole WYL-09-50, depth: 233m. WL-FL-Trench 2: Way Lake property, Fraser Lakes Zone B showing, Trench 2 outcrop. WL-Nob Hill: Way Lake property, Nob Hill showing. ML00-08 322m: Moore Lakes property, ML00-08 drill hole, depth: 322 m.

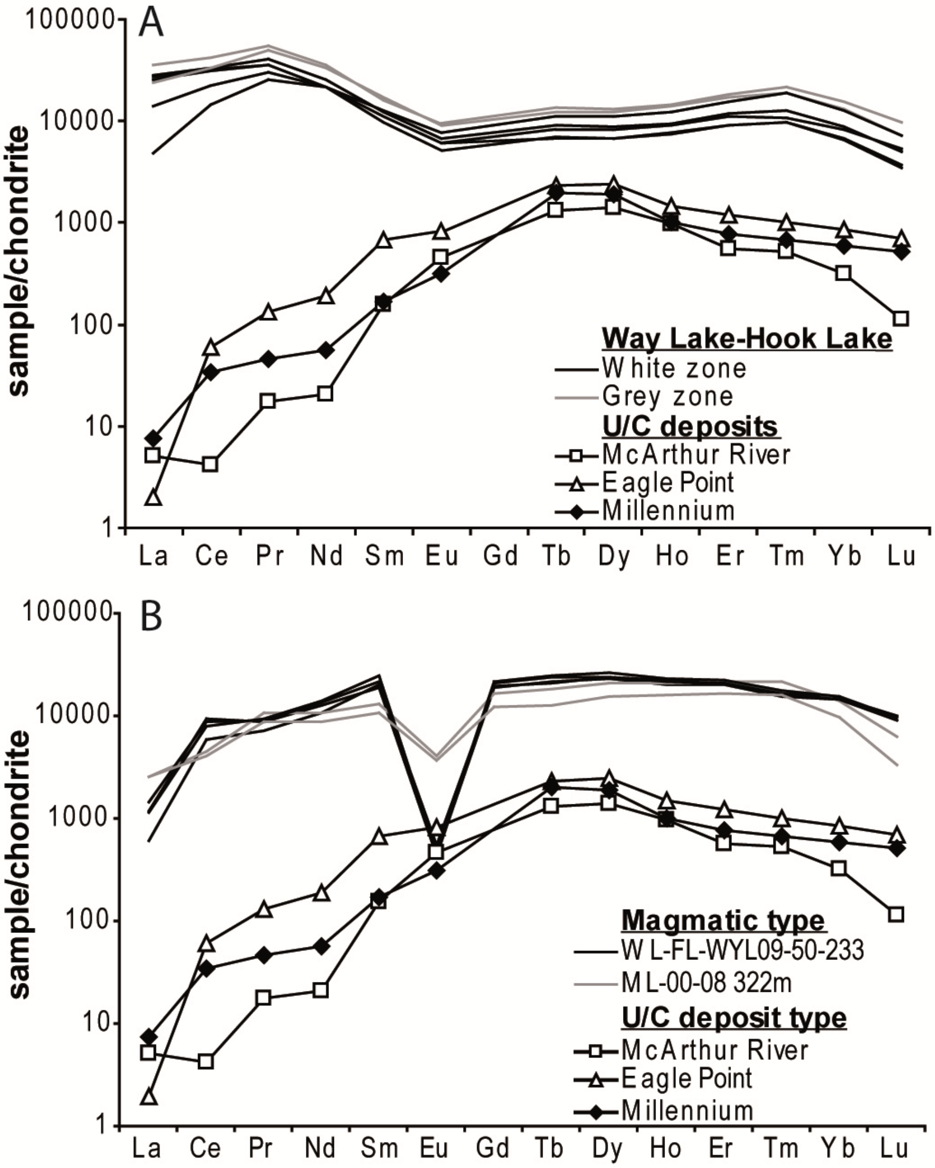

Figure L-8. (a) Chondrite-normalized rare earth element (REE) patterns for uraninites from uranium-rich vein of Hook Lake showing. The white and grey zones, despite their different U/Pb isotopic ages, have the same REE patterns. (b) Chondrite-normalized rare earth element (REE) patterns for magmatic uraninites within granitic pegmatite samples WYL-09-50-233 (Fraser Lakes Zone B) and ML00-08 322m (Moore Lakes property). REE patterns of unconformity-related hydrothermal uraninites from Millennium, Eagle Point, and McArthur River deposits (Athabasca Basin) are proposed for comparison (from Mercadier *et al.*, 2011b). Chondrite values are from Anders and Grevesse (1989). Each curve corresponds to an in-situ SIMS or LA-ICP-MS REE analysis in a selected uraninite of the studied samples.

Table L-1. Chemical composition and Th/U ratio of uranium oxides and Th-Si-U-rich alteration phases (thorium silicate) of uranium-rich samples from the Way Lake and Moore Lakes properties.
-: not analyzed; <D.L.: inferior to detection limit

	Uranium oxides												Th-Si-U phases	
Prospect	Way Lake										Moore Lake		Way Lake	
Zone	HL - WZ		HL - GZ		FL - WYL09-50-233		FL - Trench 2		Nob Hill		ML00-08 322m		Trench 2	
Analyses	133	σ	40	σ	24	σ	34	σ	14	σ	69	σ	6	σ
UO_2 (wt %)	66.23	1.42	67.43	1.72	59.77	1.15	64.06	1.64	57.90	0.72	67.20	1.37	6.82	4.76
PbO	17.72	1.66	19.79	0.70	19.24	0.38	17.36	1.54	16.51	0.67	17.83	1.11	2.1	1.58
ThO_2	1.85	0.34	2.50	0.76	7.34	0.92	7.16	1.05	2.72	0.23	6.21	1.40	35.27	8.06
SiO_2	0.38	0.70	0.21	0.13	<D.L.		<D.L.		<D.L.		<D.L.	0.09	16.09	6.12
K_2O	0.19	0.05	0.21	0.05	-	-	-	-	-	-	0.20	0.05	-	-
CaO	2.65	0.85	1.51	0.47	0.24	0.14	0.37	0.20	1.65	0.29	0.51	0.26	0.84	0.61
Na_2O	0.21	0.11	0.35	0.11	-	-	-	-	-	-	<D.L.	0.04	-	-
Y_2O_3	1.31	0.29	0.77	0.26	4.30	0.30	2.76	0.71	7.79	0.59	1.77	0.37	0.81	0.31
La_2O_3	0.19	0.07	0.11	0.06	<D.L.		<D.L.		<D.L.		<D.L.	0.01	0.06	0.04
Ce_2O_3	1.88	0.40	1.17	0.44	0.56	0.17	0.25	0.09	2.38	0.13	<D.L.	0.07	0.08	0.02
Nd_2O_3	1.04	0.27	0.53	0.22	0.75	0.22	0.39	0.11	1.03	0.09	0.34	0.18	0.07	0.05
Dy_2O_3	0.22	0.18	0.12	0.14	0.93	0.09	0.64	0.13	0.95	0.09	0.28	0.19	0.07	0.07
Total	94.09	1.03	94.91	1.65	95.35	0.47	94.81	1.05	95.25	0.66	94.75	0.93	69.5	7.2
Th/U	0.04	0.01	0.03	0.01	0.12	0.02	0.11	0.02	0.05	0.01	0.10	0.02	7.41	4.76

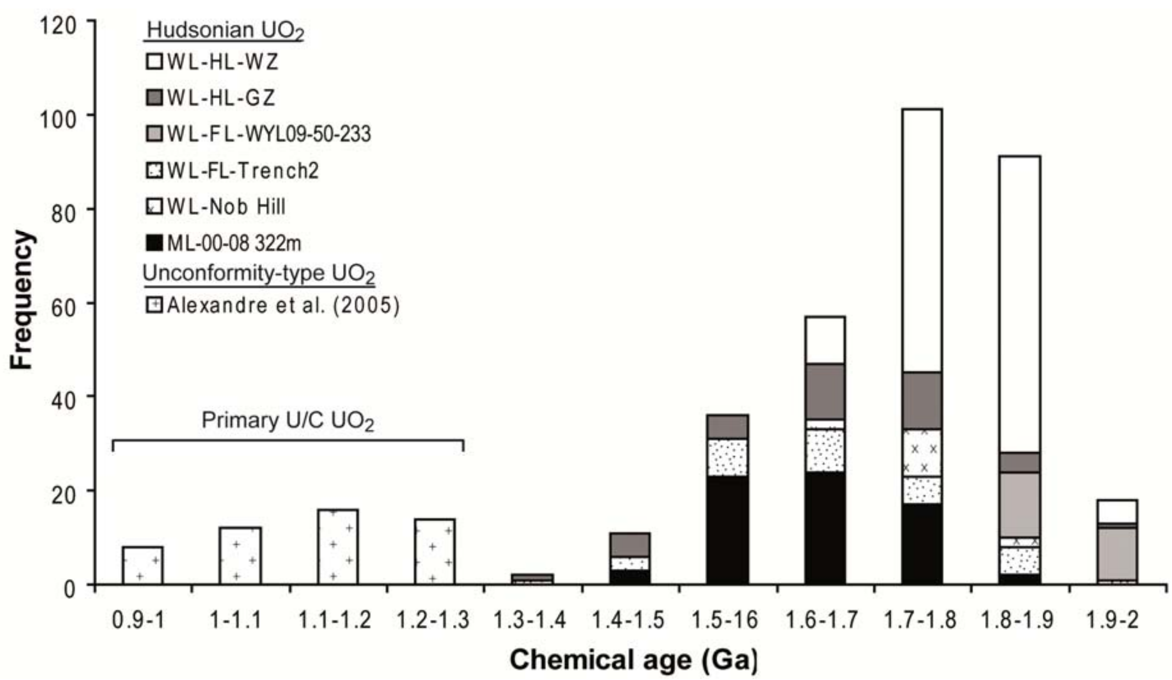

Figure L-9. Histogram of the chemical ages calculated for uraninite grains from the Way Lake uranium showings (Fraser Lakes Zone B, Hook Lake, Nob Hill) and Moore Lakes pegmatite. Chemical ages calculated from unconformity-related uranium oxides (Primary U/C UO_2) are from Alexandre and Kyser (2005). Explanation for sample naming is provided in caption from Figure L-7.

Table L-2. Analytical data for isotopic U-Pb analysis of uranium oxides from the Way Lake and Moore Lakes properties.
Analysis made by SIMS. R: rejected analysis for Discordia calculation.

Sample	Sample analytical point	207Pb/206Pb	±	204Pb/206Pb	±	208Pb/206Pb	±	207Pb/235U	±	206Pb/238U	±	Correl.err		Age 207Pb/206Pb	±	Age 206Pb/238U	±	Age 207Pb/235U	±
Way Lake - HL-WZ	1	0.1091	0.0001	0.0000	0.0000	0.0058	0.0000	5.0747	0.0896	0.3382	0.0060	1.00		1784	0	1878	29	1832	15
	2	0.1100	0.0001	0.0000	0.0000	0.0062	0.0000	5.2828	0.0931	0.3489	0.0061	1.00		1800	1	1929	29	1866	15
	3	0.1438	0.0010	0.0000	0.0000	0.0091	0.0001	5.1298	0.0969	0.2591	0.0046	0.93	*R*	2274	1	1485	23	1841	16
	4	0.1255	0.0008	0.0000	0.0000	0.0112	0.0001	4.4663	0.0842	0.2586	0.0046	0.94	*R*	2037	1	1483	23	1725	16
	5	0.1114	0.0003	0.0000	0.0000	0.0101	0.0001	5.0007	0.0892	0.3261	0.0057	0.99		1823	1	1819	28	1819	15
	6	0.1083	0.0010	0.0000	0.0000	0.0141	0.0002	5.0761	0.1002	0.3405	0.0060	0.89	*R*	1772	1	1889	29	1832	17
	7	0.1102	0.0002	0.0000	0.0000	0.0135	0.0001	5.0941	0.0900	0.3359	0.0059	1.00		1804	1	1867	28	1835	15
	8	0.1107	0.0001	0.0000	0.0000	0.0136	0.0001	5.0840	0.0897	0.3336	0.0059	1.00		1813	1	1856	28	1833	15
	9	0.1106	0.0001	0.0000	0.0000	0.0134	0.0001	4.9617	0.0875	0.3262	0.0057	1.00		1810	1	1820	28	1813	15
	10	0.0675	0.0008	0.0000	0.0000	0.0094	0.0001	2.4097	0.0510	0.2605	0.0046	0.83	*R*	854	1	1492	23	1245	15
	11	0.0745	0.0005	0.0000	0.0000	0.0086	0.0001	2.8645	0.0543	0.2802	0.0049	0.93	*R*	1056	1	1592	25	1373	14
Way Lake - HL-GZ	12	0.1078	0.0001	0.0000	0.0000	0.0062	0.0000	4.3957	0.0776	0.2964	0.0052	1.00		1763	1	1673	26	1712	14
	13	0.1087	0.0001	0.0000	0.0000	0.0067	0.0000	4.5627	0.0805	0.3050	0.0054	1.00		1779	1	1716	26	1742	15
	14	0.0953	0.0002	0.0000	0.0000	0.0071	0.0000	4.2293	0.0751	0.3226	0.0057	0.99	*R*	1535	1	1802	28	1680	14
	15	0.1080	0.0001	0.0000	0.0000	0.0079	0.0000	4.2877	0.0756	0.2886	0.0051	1.00		1767	0	1634	25	1691	14
	16	0.1089	0.0001	0.0000	0.0000	0.0089	0.0000	4.6653	0.0823	0.3114	0.0055	1.00		1782	1	1747	27	1761	15
	17	0.1081	0.0001	0.0000	0.0000	0.0065	0.0000	4.5774	0.0808	0.3077	0.0054	1.00		1769	0	1729	27	1745	15
	18	0.1079	0.0003	0.0000	0.0000	0.0062	0.0001	4.1952	0.0749	0.2826	0.0050	0.99		1765	1	1604	25	1673	15
	19	0.1074	0.0002	0.0000	0.0000	0.0088	0.0001	4.2012	0.0747	0.2842	0.0050	0.99		1757	1	1613	25	1674	14
	20	0.0863	0.0006	0.0000	0.0000	0.0065	0.0001	3.0200	0.0569	0.2553	0.0045	0.93	*R*	1345	1	1466	23	1413	14
	21	0.0856	0.0012	0.0000	0.0000	0.0065	0.0001	3.0335	0.0678	0.2584	0.0046	0.79	*R*	1331	1	1482	23	1416	17
	22	0.1017	0.0013	0.0000	0.0000	0.0063	0.0001	3.2345	0.0710	0.2321	0.0041	0.80	*R*	1655	1	1346	21	1465	17
	23	0.1084	0.0001	0.0000	0.0000	0.0074	0.0001	4.2525	0.0750	0.2857	0.0050	1.00		1773	0	1620	25	1684	14
	24	0.1073	0.0001	0.0000	0.0000	0.0079	0.0001	3.7080	0.0655	0.2519	0.0044	1.00		1754	0	1448	23	1573	14
Way Lake	1	0.1088	0.0002	0.0000	0.0000	0.0370	0.0002	8.0835	0.0561	0.5504	0.0561	1.00		1741	3	2827	##	2240	49
FL-WYL09-50-233	2	0.1084	0.0001	0.0000	0.0000	0.0402	0.0001	7.4826	0.0520	0.5113	0.0520	1.00		1734	3	2662	##	2171	46
	3	0.1085	0.0002	0.0000	0.0000	0.0397	0.0001	6.7633	0.0453	0.4617	0.0453	1.00		1736	4	2447	92	2081	39
	4	0.1087	0.0003	0.0000	0.0000	0.0309	0.0001	6.1262	0.0759	0.4175	0.0758	1.00		1739	5	2249	##	1994	64
	5	0.1094	0.0001	0.0000	0.0000	0.0379	0.0001	7.1876	0.0404	0.4869	0.0404	1.00		1750	2	2557	85	2135	35
	6	0.1082	0.0002	0.0000	0.0000	0.0393	0.0001	6.1231	0.0266	0.4195	0.0265	1.00		1729	3	2258	50	1994	23
	7	0.1085	0.0001	0.0000	0.0000	0.0405	0.0001	6.1736	0.0231	0.4218	0.0231	1.00		1734	1	2269	44	2001	20
Moore Lake	1	0.1072	0.0001	0.0000	0.0000	0.0300	0.0001	3.6845	0.0651	0.2507	0.0044	1.00		1747	2	1442	23	1568	14
ML00-08 322m	2	0.1066	0.0001	0.0000	0.0000	0.0224	0.0001	3.1742	0.0562	0.2173	0.0038	1.00		1742	3	1268	20	1451	14
	3	0.1077	0.0001	0.0000	0.0000	0.0177	0.0001	4.6656	0.0823	0.3150	0.0056	1.00		1760	1	1765	27	1761	15
	4	0.1070	0.0001	0.0000	0.0000	0.0256	0.0001	3.4347	0.0607	0.2334	0.0041	1.00		1749	2	1352	21	1512	14
	5	0.1070	0.0001	0.0000	0.0000	0.0225	0.0001	3.9219	0.0692	0.2663	0.0047	1.00		1749	1	1522	24	1618	14

U/Pb geochronology of uranium oxides

The SIMS U/Pb dating, corrected from common lead, for analyzed uraninites from the different occurrences on the Way Lake property (Hook Lake and Fraser Lakes Zone B) yields U/Pb isotopic compositions that define three distinct discordia lines and $^{207}Pb/^{206}Pb$ ages (Figure L-10 and Table L-3). For Hook Lake, the white and grey zones within the studied sample have distinct discordia with an upper intercept age of 1,805 ± 1 Ma (MSWD=13) for the WZ and of 1,774 ± 9 Ma (MSWD=2.9) for the GZ, with the difference between the two ages being over the analytical uncertainties. These ages were calculated using selected analysis, with five of the eleven analyses for the white zone and three of the thirteen analyses of the grey zone rejected due to inconsistent U/Pb ratios. The upper intercept for the sample WYL09-50-233 (Fraser Lakes Zone B) is 1,713 ± 30 Ma (MSWD=0.7). For the Moore Lakes property, the upper intercept is 1,756 ± 8 Ma (MSWD=10.5).

Table L-3. REE contents for uranium oxides from the Way Lake and Moore Lakes properties, measured by SIMS and LA-ICP-MS.
All values are expressed in ppm.

	Way Lake - FL-WYL09-50-233				Way Lake - HL - WZ			Way Lake - HL - GZ				Moore Lake - ML00-08 322m	
	1	2	3	4	1	2	3	4	5	6	7	1	2
La (ppm)	148	288	348	279	6034	6514	6671	5563	1120	3258	8321	604	607
Ce	3740	5915	5518	5022	18552	19511	20325	20439	8642	13323	25815	2725	2435
Pr	688	855	868	911	3151	3216	3663	4379	2277	2692	4939	958	781
Nd	5132	5900	6425	6680	9647	9722	11721	15238	9694	9659	15970	4904	3920
Sm	3074	2926	3343	3832	1453	1443	1795	2500	1886	1633	2357	1916	1570
Eu	32	25	26	27	293	289	376	518	437	339	529	227	209
Gd	3954	3809	4223	4385	-	-	-	-	-	-	-	-	-
Tb	789	807	878	909	257	249	328	453	398	300	491	661	464
Dy	6025	5802	5975	6699	1644	1632	2141	3006	2670	1995	3185	4974	3714
Ho	1246	1138	1238	1294	427	418	529	772	679	499	797	1142	883
Er	3507	3401	3495	3753	1464	1451	1903	2688	2497	1797	2932	3414	2624
Tm	418	392	428	449	237	239	312	463	451	264	525	530	383
Yb	2487	2396	2398	2507	-	-	-	-	-	-	-	-	-
Lu	252	230	227	246	84	91	121	176	175	130	236	150	81

The majority of the analyses are nearly concordant for the Hook Lake WZ and GZ, and do not present significant disturbance for the other samples, indicating the lack of perturbation of the isotopic systems after the crystallization of the uranium oxides. All lower intercepts are undistinguishable, at the present level of analytical uncertainty, with an age close to 0 Ma (Figure L-10), except for the GZ of Hook Lake (224 ± 120 Ma). For this sample, a possible late alteration event is suspected at approximately 220 Ma. All the ages obtained, due to their weak degree of discordance, are considered to represent the initial crystallization age of the uraninites. The samples from EWA, Nob Hill, and Trench 2 do not match the requirements for isotopic U/Pb analysis, as all of the homogeneous uraninites were smaller than the analytical spot diameter. Similar ages are obtained for both methods (electron microprobe and SIMS) for the Way Lake-Hook Lake and the Moore Lakes samples, whereas the Way Lake-Fraser Lakes-WYL09-50-233 uraninites give an isotopic age younger than the chemical ages.

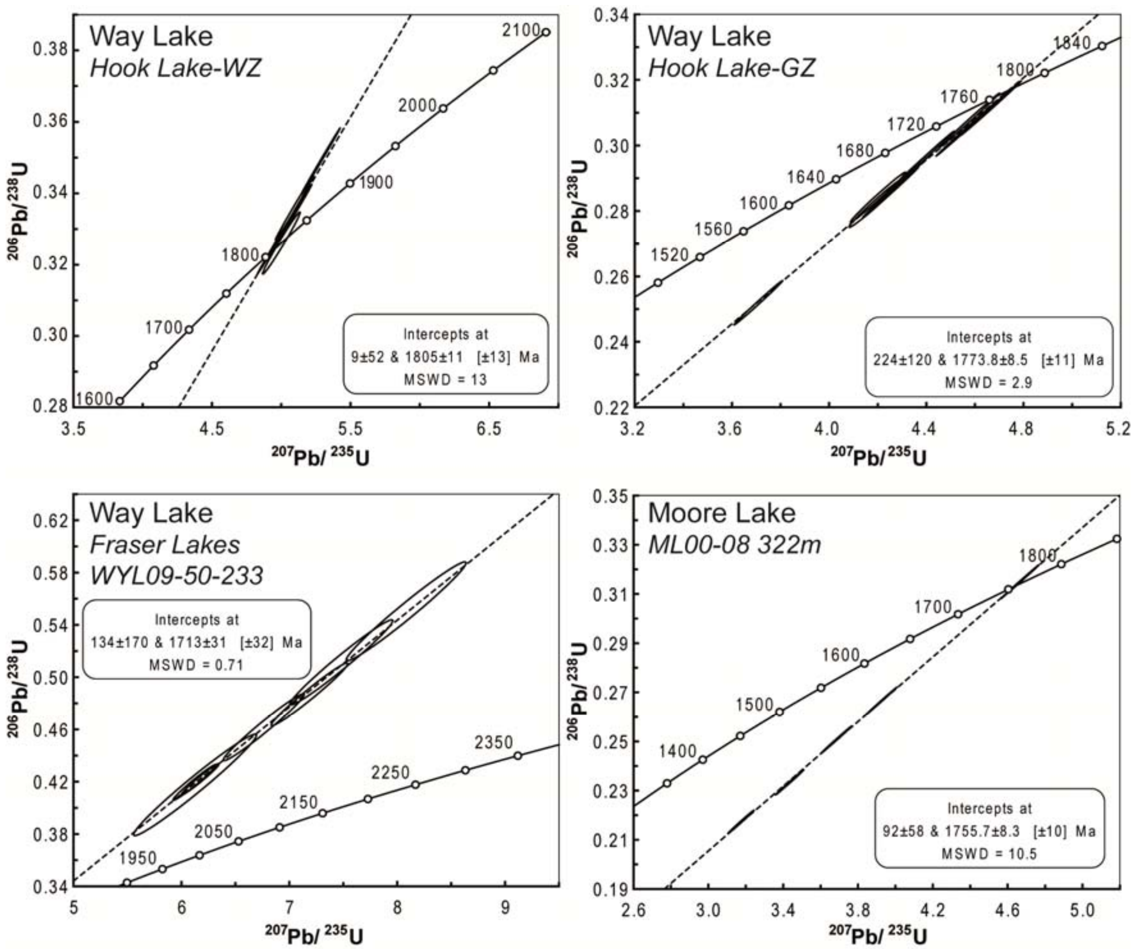

Figure L-10. Concordia diagrams showing the U/Pb isotopic analysis for uraninites from the Way Lake uranium showings and Moore Lakes pegmatite (see Figure L-7.). Explanation for sample naming is provided in caption from Figure L-7. Analysis made by SIMS, error (ellipse) given with 2σ. MSWD: Mean Square Weighted Dev*ia*tion. See Table L-2 for description of rejected data for WL-HL-WZ and WL-HL-GZ.

Whole-rock chemistry

The geochemical data are presented in Table L-4 and illustrated in Figures L-11 and L-12. The mineralized granitic pegmatites and leucogranites of the Way Lake property (Fraser Lakes Zone B, EWA and Nob Hill) have wide ranging compositions, especially for major elements (Si, Al, Fe, K, Na, and Ca), which directly reflect the strong variations in mineral proportions. Overall, they have a weakly peraluminous to slightly metaluminous composition, as shown in the A-B chemical-mineralogical diagram (Figure L-11a). These compositions represent a mixing

Table L-4. Summary of the whole-rock chemical composition, Th/La and Th/U ratios for uraninite-bearing samples from the Way Lake and Moore Lakes properties (U pegmatites/leucogranites and U vein) and from the other main basement lithologies of the Way Lake property (orthogneiss, pegmatite, pelitic gneiss).
The orthogneiss category regroups tonalitic and granitic orthogneisses, the pelitic gneiss category regroups pelitic and psammo-pelitic gneisses -: not analyzed. m: mean, σ: 1 sigma.

Location	Way Lake-FL B			Way Lake-NH			Way Lake-EWA			Moore Lake		
Lithology	U pegmatite/leucogranite			U pegmatite/leucogranite			U pegmatite/leucogranite			U pegmatite		
	Min-Max	m(16)	σ	Min-Max	m (28)	σ	Min-Max	m (32)	σ	Min-Max	m (3)	σ
Major elements (wt %)												
SiO_2	54-92.7	78.01	11.9	-	-		-	-		57.7-71.8	66.83	21.2
TiO_2	0.14-2.05	0.56	0.6	0.02-0.21	0.05	0.0	0.06-0.59	0.17	0.1	0.4-0.53	0.85	0.5
Al_2O_3	2.83-16.60	8.57	5.1	9.31-14.2	12.67	1.3	12.5-16.6	14.59	1.0	11.5-13	12.50	3.9
Fe_2O_3 tot	1.12-17.80	5.59	4.8	-	-		-	-		2.41-7.3	4.14	2.1
FeO tot	1.01-16.02	5.03	4.3	-	-		-	-		-	-	
FeO	0.59-12.81	3.50	3.5	-	-		-	-		1.2-3	1.87	0.8
Fe_2O_3	0.31-4.37	1.69	1.3	0.32-2.73	0.96	0.5	0.34-4.2	1.20	0.8	-	-	
MnO	0.01-0.34	0.07	0.1	0.01-0.05	0.01	0.0	0.01-0.06	0.02	0.0	0.04-0.15	0.08	0.0
MgO	0.08-5.47	1.34	1.5	0.04-0.53	0.13	0.1	0.18-2.74	0.70	0.5	2.59-6.78	4.07	1.9
CaO	0.26-2.42	0.82	0.6	0.29-1.35	0.88	0.3	0.36-2.62	1.31	0.7	1.63-4.43	2.92	1.2
Na_2O	0.02-7.10	1.95	1.9	1.56-7.13	4.24	1.1	2.1-4.79	3.20	0.8	0.15-2.56	1.43	0.9
K_2O	0.27-5.88	2.47	2.0	0.88-6.24	3.66	1.4	2.08-9.66	6.55	1.9	2.39-6.12	4.07	1.7
P_2O_5	0.01-0.06	0.02	0.0	0.01-0.06	0.03	0.0	0.02-0.53	0.11	0.1	0.25-2.89	1.28	1.0
LOI	0.20-2.70	0.88	0.6	-	-		-	-		1.8-2.2	2.07	0.7
Total	98.91-101.29	100.28		-	-		-	-		99.82-100.43	100.23	
C %	<0.1-0.5	0.1	0.1	-	-		-	-		-	-	
S %	<0.1-0.2	0.2	0.3	-	-		-	-		-	-	
F %	<0.1-0.4	0.2	0.1	-	-		-	-		-	-	
Cl%	<0.1-0.1	0.0	0.0	-	-		-	-		-	-	
Trace elements (ppm)												
B	4-27	13.8	7.0	5-77	15.5	20.6	21-117	42.8	18.3	-	-	
Br	1-42	19.2	15.5	-			-	-		-	-	
Sc	2-34	8	9	1-3	1	1	1-24	3	5	-	-	
V	9-281	63	71	9-25	16	4	17-107	42	21	10-38	20	12
Cr	4-221	44	57	4-15	9	3	9-72	18	12	-	-	
Co	1-96	16	24	1-2	1	0	1-51	4	9	5-14	8	4
Ni	1-132	29	39	1-9	2	2	1-39	6	9	3-5	4	1
Cu	1-99	27	48	1-25	2	5	1-30	8	7	8-38	19	12
Zn	10-483	151	139	5-31	9	5	6-33	13	6	92-285	181	82
Cs	3-18	8	4	-	-		-	-		-	-	
Rb	12-473	174	142	-	-		-	-		-	-	
Sr	4-171	55	53	10-87	64	20	88-170	116	18	59-158	110	46
Ba	32-905	376	346	69-4840	953	1226	1360-4750	3100	929	400-689	587	205
Nb	8-143	48	50	1-95	12	26	1-13	4	3	7-39	20	12
Zr	259-4060	1202	1167	4-464	122	137	1-232	40	58	1360-2810	1900	758
Hf	10-155	43	42	1-26	4	6	1-6	2	2	41-95	60	26
Li	8-92	30	25	3-19	11	4	7-114	24	18	47-105	77	29
Be	0.2-3	1	1	1-35	6	9	1-11	4	3	2	2	0
Ga	5-40	21	11	12-33	18	6	12-25	17	3	20-27	23	7
As	6-33	14	8	1-6	1	1	1	1	0	-	-	
Mo	1-249	40	68	1-12	1	2	1-510	66	108	4-10	12	7
Ag	0.4-14	4	5	<1	0	0	<1	0	0	-	-	
Cd	1-3	1	1	1	1	0	1	1	0	<1	0	0
Ta	1-4	1	1	1-17	2	4	<1	1	0	-	-	
Bi	1-78	28	28	1	1	0	<1	1	0	-	-	
Sb	1-3	2	1	1	1	0	<1	1	0	-	-	
Se	1-41	12	14	1	1	0	<1	1	1	-	-	
Sn	1-9	1	2	1-4	1	1	<1	1	0	2-5	4	1
W	0.5-3	1	1	1-3	1	0	1-2	1	0	1-2	2	1
Y	16-240	81	68	6-54	16	11	5-55	19	13	61-290	153	90
La	3-88	19	22	3-79	16	15	7-90	17	15	17-37	26	10
Pb	42-847	236	232	14-207	52	41	33-630	195	150	210-630	379	180
Th	102-1370	554	406	7-103	27	23	10-322	65	65	66-219	124	64
U	175-2460	678	583	102-434	162	94	105-2060	561	465	880-2400	1410	687
Th/U	0.4-2	0.9	0.4	0.06-1.01	0.2	0.2	0.07-0.44	0.1	0.1	0.08-0.09	0.1	0.0
Th/La	3-295	72.5	75.5	0.74-10.3	2.5	2.5	0.62-8.7	3.7	2.2	2.87-5.92	4.7	1.7

Way Lake-HL U vein	Way Lake-FL B orthogneiss Min-Max	m (6)	σ	Way Lake-FL B pegmatite Min-Max	m (16)	σ	Way Lake-FL B pelitic gneiss Min-Max	m (18)	σ
-	51.8-74.8	66.38	10.1	47.5-95.7	71.97	11.5	49.9-64	58.59	4.84
0.22	0.25-0.99	0.59	0.4	0.01-1.35	0.36	0.4	0.5-1.97	0.94	0.35
4.68	12.3-17.2	13.63	1.8	1.56-20.4	12.65	5.0	11-21.2	16.56	2.38
0.15	1.7-11.9	6.22	4.8	0.09-26	5.26	7.6	2.92-20.7	9.76	4.33
-	1.53-10.71	5.60	4.3	0.08-23.39	4.73	6.8	2.63-18.63	8.78	3.90
-	-	-		0.07-8.34	2.64	2.9	1.02-17.42	7.97	5.06
-	-	-		0.01-13.33	2.17	4.3	0.38-1.79	0.86	1.02
0.06	0.03-0.17	0.09	0.1	0.01-0.94	0.09	0.2	0.03-0.56	0.21	0.16
1.08	0.3-7.34	2.62	2.7	0.06-3.99	1.04	1.2	1.97-5.78	3.21	1.03
1.84	0.67-8.62	2.97	3.0	0.04-3.28	1.18	1.2	0.27-2.39	1.09	0.59
0.30	2.21-5.86	4.15	1.4	0.01-7.32	2.96	2.1	0.15-4.2	2.02	1.27
2.27	1.72-4.84	2.95	1.4	0.65-9.72	4.01	2.8	3.94-8.1	5.78	1.30
1.29	0.01-0.23	0.09	0.1	0.01-0.27	0.05	0.1	0.02-0.28	0.11	0.06
-	0.2-1.2	0.62	0.4	0.05-2.4	0.60	0.5	0.4-5.9	1.82	1.39
-	99.44-100-83	100.31		99.09-101.26	100.10		98.56-101.6	100.01	
-	<0.1-0.2	0.1	0.1	<0.1-0.4	0.1	0.1	<0.1-4	0.5	0.9
-	<0.1-0.1	0.0	0.0	<0-1-2.1	0.2	0.6	<0.1-1	0.2	0.3
-	-	-		<0.1-0.4	0.1	0.1	0.1-0.7	0.4	0.3
-	-	-		<0.1-0.1	0.0	0.0	<0.1-0.1	0.1	0.0
-	6-20	11.5	5.6	4-20	10.8	5.0	4-55	20.5	16.4
-		-		1-37	14.9	13.0	1-16	2.4	5.5
-	2-37	16	14	1-100	10	24	6-54	25	11
31	11-254	108	107	8-148	48	47	76-254	150	49
43	4-179	56	75	2-152	35	39	39-192	109	48
26	1-43	19	20	1-67	11	18	9-132	38	32
47	3-92	31	36	1-40	15	15	26-104	58	23
<1	1-71	13	28	1-59	10	14	2-97	34	30
2	25-193	86	67	3-234	75	71	39-430	154	106
-	-	-		3-17	7	5	3-16	11	5
-	61-350	152	103	43-459	201	122	119-669	365	150
78	43-300	121	99	1-302	82	74	10-205	87	57
418	173-897	472	242	77-1320	520	405	447-1920	1095	456
146	1-17	10	6	1-71	24	21	5-228	39	61
472	99-440	290	173	14-679	203	211	113-610	259	153
906	2-11	6	4	1-26	7	8	1-22	6	5
102	15-54	30	15	4-158	28	37	30-142	60	32
1	1-4	2	1	<1-9	3	3	<1-8	2	2
<1	14-23	18	4	3-61	22	13	19-49	27	7
-	-	-		11-14	12	1	9-16	13	2
42	1-2	1	1	1-37	5	10	1-10	2	3
< 0,2	-	0	0	<1-3	1	1	<1-4	1	1
< 0,2	1	1	0	1-3	1	1	1-3	1	1
<1	1	1	0	1-3	1	1	1-6	1	2
-	-	-		1-68	17	24	1	1	0
-	-	-		1-5	2	1	1	1	0
-	-	-		1-36	8	15	1-42	29	15
23	1-55	13	21	1-11	2	3	1-19	2	6
<1	1	1	0	1	1	0	1-10	1	2
7510	20-38	28	8	2-65	41	7	12-282	82	147
<1	19-75	44	25	1-51	23	17	5-152	49	33
123000	11-38	20	10	6-102	42	26	11-78	40	19
7340	2-34	18	13	3-46	25	17	5-59	21	14
409000	1-9	5	3	1-85	24	21	2-37	9	9
0.0	2-3.33	3.6	2.5	0.16-9	1.8	2.3	0.86-10	3.4	2.9
0.1	0.07-0.68	0.4	0.2	0.16-92	7.6	22.8	0.11-1.79	0.6	0.4

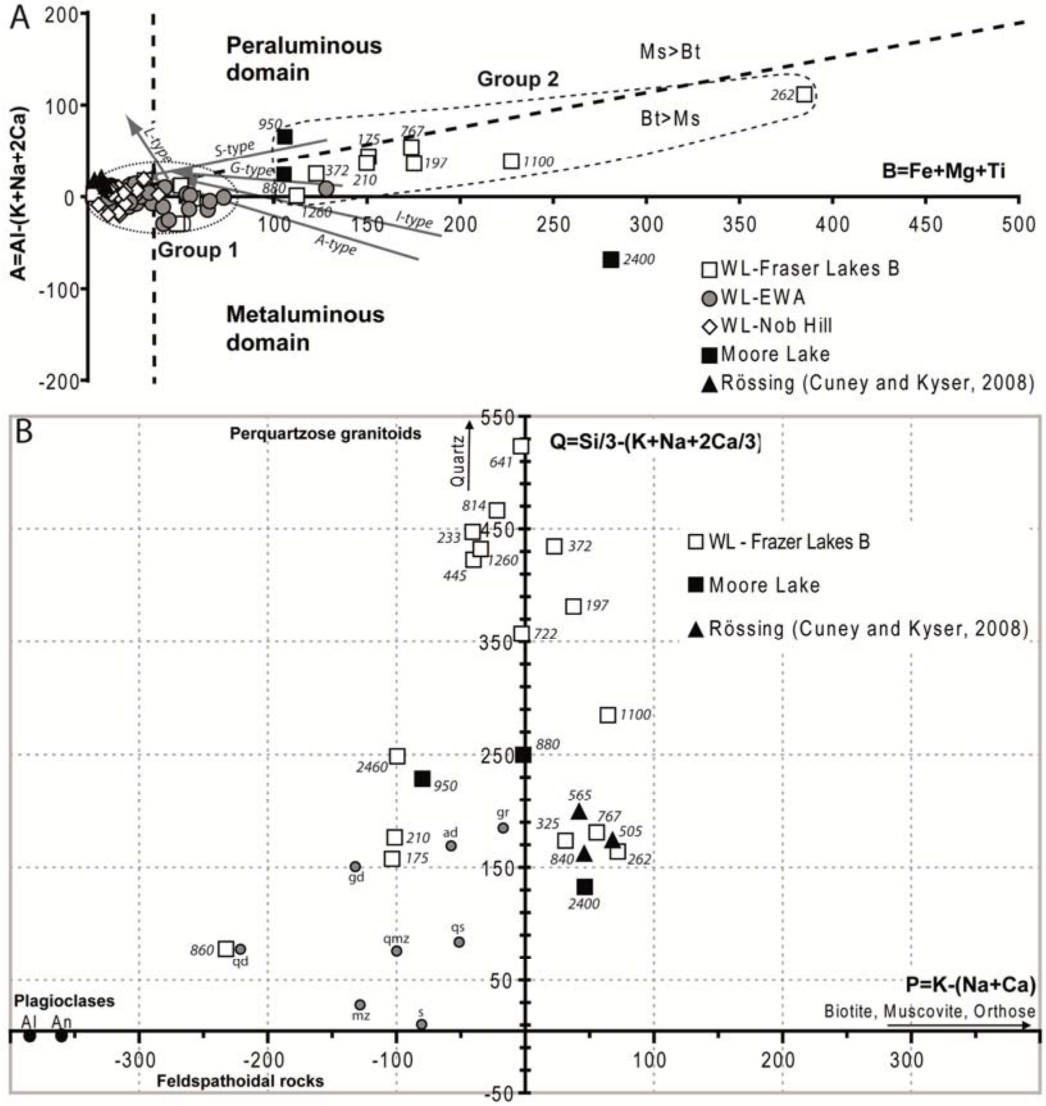

Figure L-11. (a) A-B diagram (from Debon and Le Fort, 1988) for the whole-rock analysis of uraninite-bearing granites and pegmatites from Way Lake (white square) and Moore Lakes (black square) properties. (b) Q-P diagram (from Debon and Le Fort, 1988) for the whole-rock analysis of uraninite-bearing granites and pegmatites from the Way Lake and Moore Lakes uranium showings. Uraninite-bearing alaskites from the Rössing deposit are provided for comparison. When written, the associated italic number corresponds to the U content of the sample. A-, S-, L- and I-related for granitic rocks are drawn for comparison (see White and Chapell (1977) for references). Groups 1 (<100) and 2 (>100) are function of the value of the B parameter as defined in (A). The diagonal dotted line corresponds to the domain limit for muscovite (Ms) and biotite (Bt). The two diagrams present different data sets due to the lack of SiO_2 contents for some samples. qd: quartz diorite, mz: monzonite, s: syenite, qmz: quartz monzonite, qs: syenite quartz, gd: granodiorite, ad: adamellite, gr: granite (data from Debon et Le Fort, 1988).

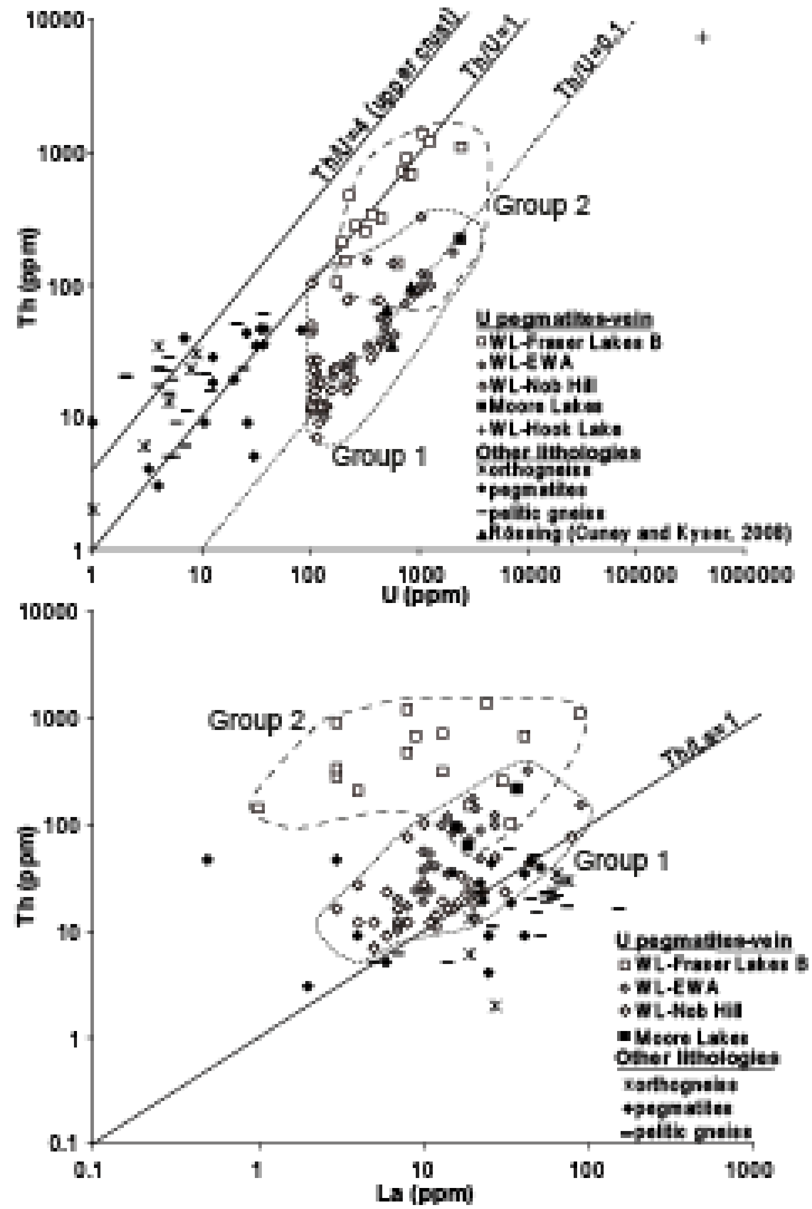

Figure L-12. (a) Th-U diagram for the whole-rock analysis of uraninite-bearing granitic pegmatites from Fraser Lakes Zone B drill holes (white square), uraninite vein of the Hook Lake showing (black square), uraninite-bearing granitic pegmatite from the Moore Lakes ML00-08 drill hole (grey square) and comparison with the other dominant basement lithologies (orthogneiss, pegmatite and pelitic gneiss). Uraninite-bearing alaskites from the Rössing deposit, from Cuney and Kyser (2008), are provided for comparison. The associated italic number corresponds to the U content of the sample. (b) Th-La diagram for the same samples. Groups 1 (small dotted contour) and 2 (big dotted contour) refer to the ones defined in Figure L-11(A).

between a eutectic granitic composition (quartz + feldspars, Group 1) and variable amounts of biotite (Group 2). The quartz-feldspar proportions, as illustrated by the Q-P chemical-mineralogical diagram (Figure L-11b), show large variations, from highly quartzose (quartz-rich) pegmatites (Q>350), to highly plagioclasic ones that are relatively poor in biotite (P<-100), and to highly potassic pegmatites, rich in quartz but very poor in biotite (P>0). Some samples are slightly metaluminous (negative A parameter) which can be related to the presence of a small amount of allanite and/or titanite and/or to late carbonate crystallization (at Moore Lakes for example). All samples have high U (100-2,460 ppm) and Pb (14-847 ppm) contents directly related to the presence of uranium oxides. The strongest U-enrichments are observed in granitic pegmatites WYL-10-62-92.0 (Table L-4), including some pegmatites significantly enriched in biotite (WYL-10-61-190.3, WYL-10-62-93.5). Th contents (102-1370 ppm) are low to moderate and mostly dependent on the thorite percentage within these rocks. Zr contents (249-3,090 ppm) are moderate to high and reflect the abundance of zircon. A clear positive correlation exists between U and Zr contents, which confirm the uranium oxide-zircon association within the samples (Figures L-5c and d). LOI is low, indicating the lack of major alteration of the silicates for these samples. Despite their very high U and Th contents, these pegmatites and leucogranites do not show significant enrichment in F and other incompatible elements such as Rb, Cs, Li, Be, Sn or W, which implies very little fractionation.

The mineralized granitic pegmatites of the Moore Lakes property have similar chemical characteristics when compared to most of the Way Lake samples. They plot in the same field in the A-B and Q-P chemical-mineralogical diagram, and also have high U (880-2,400 ppm), Pb (210-630 ppm), and Zr contents, but have lower Th concentrations. They do not differ from the Way Lake property samples in their metal and/or Zr contents. These granitic pegmatites are fresh (LOI < 2.2 wt. %), with the highest LOI observed in samples with high biotite and late calcite contents. The negative value for the A parameter is related to late calcite crystallization

The Hook Lake vein is characterized by very high U (40.9 wt. %), Pb (12.3 wt. %), and Th (7,340 ppm) concentrations and low other element contents, except the REE, and slightly anomalous B, Co, and V contents, when compared to the surrounding rocks.

All the studied samples have a Th/U below the average upper crust Th/U ratio of 4 (Cuney, 2010), indicating U enrichment and high Th/La ratio (mainly >1, Figure L-12). The granitic pegmatites and/or leucogranites from both properties are enriched in several metals including Ba (up to 4,480 ppm; Table L-4), Ni (up to 132 ppm), Zn (up to 483 ppm), Sr (up to 171 ppm), or Y (up to 240 ppm). Compared to the other major lithologies of the Way Lake property (e.g. pelitic gneiss, orthogneiss, and Th-rich pegmatite), UO2-bearing granitic pegmatites are enriched in U, and locally in other metals (Th, Ba, Sr, Zn or Y).

3D modeling of Fraser Lakes Zone B

The mineralized U-rich granitic pegmatite and leucogranite bodies (U_3O_8 cutoff of 0.1 %) represent 7.02 % of the total volume of the Fraser Lakes Zone B 3D GOCAD model;

the other Paleoproterozoic or Archean lithologies representing around 44 and 49 %, respectively (Table L-5). The U-rich granitic pegmatite and leucogranite bodies are localized at and near the highly deformed Archean-Paleoproterozoic contact. The mineralized bodies appear generally as stacked sheets around an antiformal fold nose plunging moderately to the NE. Their thicknesses vary from centimeters to 10s of meters to a maximum of about 15 m, with an average value of 5 m. Two late brittle conjugate faults (Faults 1 and 2) have crosscut the U-Th-rich granitic bodies after their emplacement.

Table L-5. Calculation of volume, volumic percentage, and U tonnages from the three main lithologies (U-rich granitic pegmatite / leucogranite, pelitic to psammopelitic gneiss, and Archean orthogneiss) within the Fraser Lakes Zone B.
(See Figure L-14 for details). The U tonnages for unconformity-related deposits of Athabasca Basin are from Jefferson *et al.* (2007). The two last columns correspond to the ratio, expressed in percent, of U tonnage from the U-rich granitic pegmatite at 500 (column 1) and 250 (column 2) ppm average U content to the U tonnage of known unconformity-related U deposits within Athabasca Basin. U-rich granitic pegmatite/leucogranite corresponds only to pegmatite and leucogranite bearing uranium oxides.

Lithological Unit	Avg. rock density	Avg. Uranium content (ppm)	Volume (m^3)	Percentage (%) of total volume	U tonnage (lbs U)	U tonnage (metric tons U)
U-rich granitic pegmatite / leucogranite	2.7	100	12,031,400	7.02	7,146,652	3,248
	2.7	250	12,031,400	7.02	17,866,629	8,121
	2.7	500	12,031,400	7.02	35,733,258	16,242
Pelitic to psammopelitic gneiss (basal Wollaston Group)	2.8	8	75,863,700	44.23	3,738,563	1,699
Archean orthogneiss	2.7	5	83,637,000	48.75	2,484,019	1,130

U deposits	U tonnage (metric tons U)	U-rich granitic pegmatite (500 ppm) / U deposit tonnage (%)	U-rich granitic pegmatite (250 ppm) / U deposit tonnage (%)
Rabbit Lake	15,769	103	52
McClean	19,327	84	42
Cluff Lake	20,608	79	40
Midwest	21,550	75	38
Collins Bay	24,400	67	34
Eagle Point	51,150	32	16
Key Lake	70,300	23	12
Cigar Lake	131,386	12	6
McArthur River	192,082	8	4

Calculations of the U tonnage for the three volumes were made (Table L-5). For the U-rich granitic pegmatites and leucogranites, three U concentration scenarios were taken into account: 100, 250, and 500 ppm (Table L-4). Uranium contents of 8 and 5 ppm were respectively used for Paleoproterozoic and Archean rock volumes. The mean U content was determined using the available geochemical data on Fraser Lakes Zone B for the three main lithologies (Table L-4 and Figure L-12). The U-rich granitic pegmatites and leucogranites contain anywhere from 3,250 (assuming a 100 ppm U concentration), to 8,120 (assuming a 250 ppm U concentration), to 16,240 (assuming a 500 ppm U concentration) metric tons U. The other volumes contain around 1,700 (Paleoproterozoic rocks) and 1,130 (Archean rocks) metric tons U. The calculated U tonnage of the U-rich granitic pegmatites and leucogranites represents between 4 and 52 % (assuming 250 ppm U concentration) to between 8 to 103 % (assuming 500 ppm U concentration) of the estimated U tonnages of the known unconformity-related U deposits in the Athabasca Basin (Table L-5).

Post-crystallization alteration features within UO_2-bearing rocks

Alteration patterns are also observed for several accessory minerals of the UO_2-bearing samples from the other drill holes or showings, especially for uraninites. Although the samples appear macroscopically fresh, clear dissolution features of monazites and uraninites are observed, with replacement by Th-Si-U-rich phases (Figures L-13a to e) similar to hydrated uranothorite (Figures L-13b to d), and are depleted in U and REE, compared to the primary minerals.

Moreover, north of the Fraser Lakes Zone B showing, two drill holes, WYL-10-53 and -55 (Figure L-4), intersected a clay-filled fault system with anomalous radioactivity and U mineralization crosscutting Wollaston Group graphitic pelitic gneisses, granitic pegmatites, and Archean orthogneisses (Figure L-13g). Samples from this clay-filled fault system yielded PIMA results with a preponderance of illite. Alumino-Phosphate-Sulfate (APS) minerals have also been observed (Figure L-13f), with a similar chemical composition to those in the alteration halos of Athabasca Basin unconformity-related uranium deposits (Gaboreau *et al.*, 2007, Mercadier *et al.*, 2011a). XRF analysis of the clay-rich mineralized zones yielded highly anomalous amounts of CaO, P_2O_5, LREE, Sr, and Pb, with U values up to 450 ppm over 0.5 meters (Annesley *et al.*, 2010).

Discussion

Nature and origin of the Hudsonian uranium oxide mineralization in the basement

Two main styles of U mineralization are found within the Way Lake and Moore Lakes properties: Th-rich magmatic uraninites in granitic pegmatites and leucogranites (e.g. Fraser Lake Zones B or EWA) and micrometric to pluri-centimetric low-Th uraninite in veins (e.g. Nob Hill and Hook Lake showings). The majority of the studied uraninites are characterized by low Si and Fe contents, which clearly indicate that they are overall fresh to slightly affected by post-crystallization alteration (Alexandre and Kyser, 2005), except for sample WYL09-50-233, and that their composition is directly related to their conditions of crystallization. The variability for Y contents corresponds to a Y-U substitution trend related to the variation of the melt composition during crystallization, and not to an alteration trend. Indeed, Y, like HREE, is weakly mobile during alteration of uraninite (Mercadier *et al.*, 2011b), contrary to Pb, Si or Fe. The high Pb and low Fe

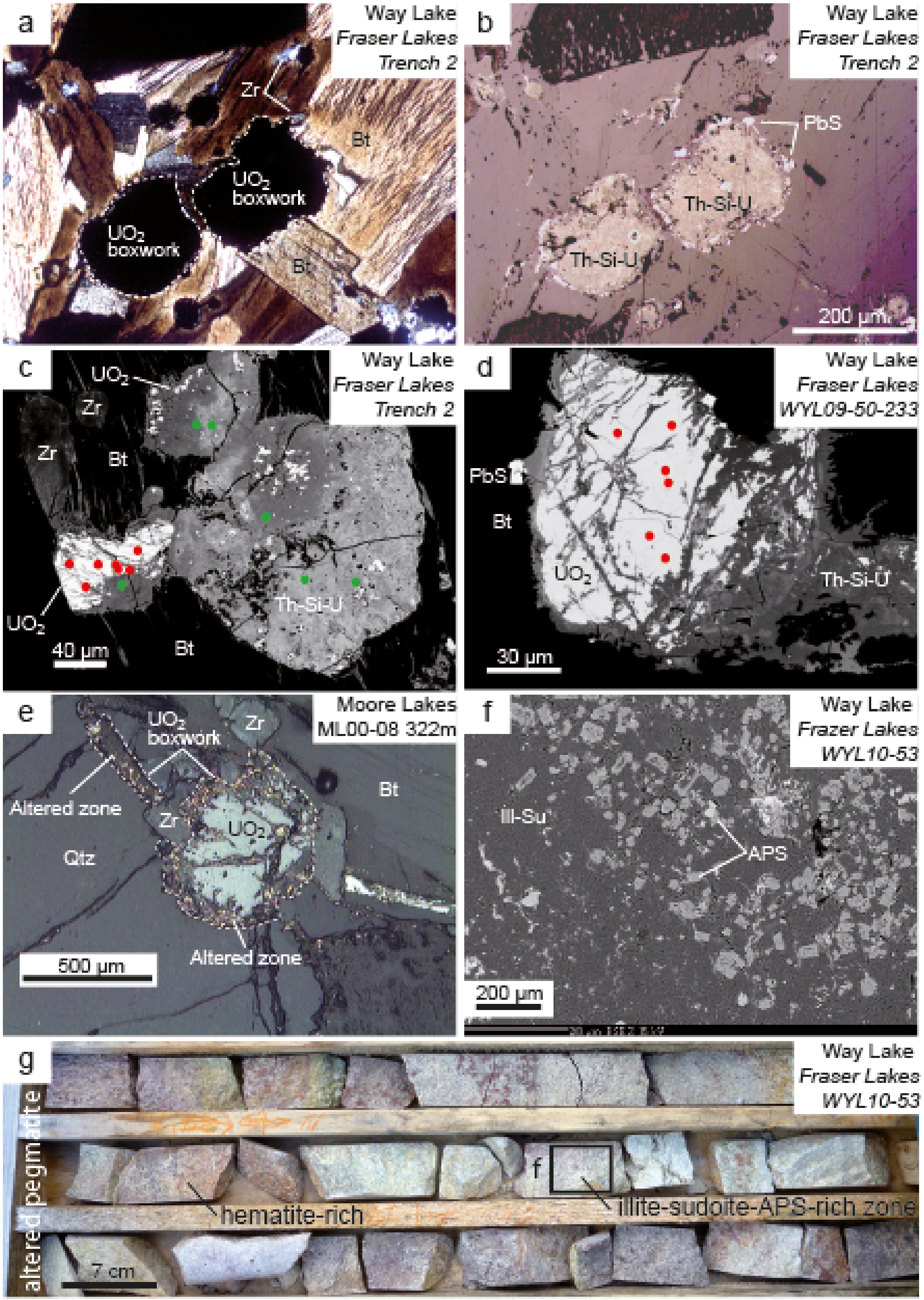
a
Way Lake
Fraser Lakes
Trench 2
Zr
Bt
UO_2 boxwork
UO_2 boxwork
Bt
b
Way Lake
Fraser Lakes
Trench 2
PbS
Th-Si-U
Th-Si-U
200 µm
c
Way Lake
Fraser Lakes
Trench 2
UO_2
Zr
Zr
Bt
UO_2
40 µm
Bt
Th-Si-U
d
Way Lake
Fraser Lakes
WYL09-50-233
PbS
Bt
UO_2
Th-Si-U
30 µm
e
Moore Lakes
ML00-08 322m
UO_2 boxwork
Zr
Bt
Altered zone
Zr
UO_2
Qtz
500 µm
Altered zone
f
Way Lake
Frazer Lakes
WYL10-53
Ill-Su
APS
200 µm
g
Way Lake
Fraser Lakes
WYL10-53
altered pegmatite
f
hematite-rich
illite-sudoite-APS-rich zone
7 cm

Figure L-13 (previous page). Macrophotographs, microphotographs and BSE images showing hydrothermal alteration features of U-rich samples from the Way Lake and Moore Lakes properties. (a, b) Uraninite boxworks in Qtz-Bt-rich granitic pegmatite showing a total replacement of uranium oxides by a Th-Si-U-rich phases plus galena (PbS). (c, d) Magmatic uraninite grains showing strong dissolution and replacement by Th-Si-U-rich phases (uranothorite) and galena crystals. (e) Uraninite boxwork with dissolution of uranium oxides and replacement by an altered zone. (f) Aluminium-Phosphate-Sulfate (APS) minerals disseminated within an illite-sudoite (Ill-Su) clay-rich matrix. (g) Strongly altered granitic pegmatite (intruding Archean orthogneiss) with illite-sudoite-APS-rich zone and hematization typical of hydrothermal alteration related to unconformity-related U deposits. BSE image in F is from the illite-sudoite-APS-rich phase zone. The red and green points correspond, respectively, to electron microprobe analysis of magmatic uraninites and Th-Si-U phases presented in Figure L-7.

and Si contents, mark the absence of post-crystallization alteration (Alexandre and Kyser, 2005), and clearly confirm the U-Y substitution trend.

Origin of magmatic uraninites

The presence of restitic biotites and garnets, lack of cordierite or Al-silicates, and low incompatible element contents for the UO2-bearing granitic pegmatites and leucogranites indicate that they are derived from partial melting of essentially quartz-feldspar-rich protoliths, within the stability field of the biotite (± garnet) mineral assemblage. A derivation from a highly fractionated, deeper-seated granitic pluton is not supported by the fact that, despite their extreme U enrichment (100-2,460 ppm), none of the pegmatites are significantly rich in fluorine (F <0.5 wt. %) and incompatible elements such as Rb, Cs, Li, Be, Sn, W (Table L-4). The latter are typically enriched in highly fractionated granitic melts (Černý *et al.*, 2005). The low to moderate peraluminosity of most pegmatites (Figure L-11) indicates that they are derived from the partial melting of a dominantly quartz-feldspar protolith like the Rössing alaskites (Cuney and Kyser, 2008). The highest A parameter values correspond to the presence of garnet in the pegmatite, whereas the negative A values (metaluminous character) of some samples correspond to the presence of Ca-bearing minerals such as allanite, titanite, and local late carbonate alteration. The increase in Ca-content in these pegmatites reflects the equilibration of some of the pegmatite melts with Ca-rich country rocks during their ascent and/or emplacement. On the diagram showing the variation in the aluminous index (A) versus the color index (B, in Figure L-11), the pegmatites define a trend interpreted to result from unmixing. This unmixing occurred between a granitic eutectic melt (which plot close to the origin of the A-B diagram) for the most felsic pegmatites (EWA, Group 1 in Figure L-11) and mafic minerals (such as biotite, garnet and Fe-Ti oxides with high B values) enriched in Fraser Lakes Zone B and Moore Lakes (Group 2 pegmatites). The mafic minerals dominantly represent restitic crystals carried by the melts, as indicated by their aggregation as schlierens (Figure L-5) together with clusters of accessory minerals (zircon, apatite, monazite and Fe-Ti oxides) that are weakly soluble in such low temperature (<850°C; Annesley *et al.*, 2005) peraluminous melts (Cuney and Friedrich, 1987; Friedrich *et al.*, 1987). The variations for the major elements between Groups 1

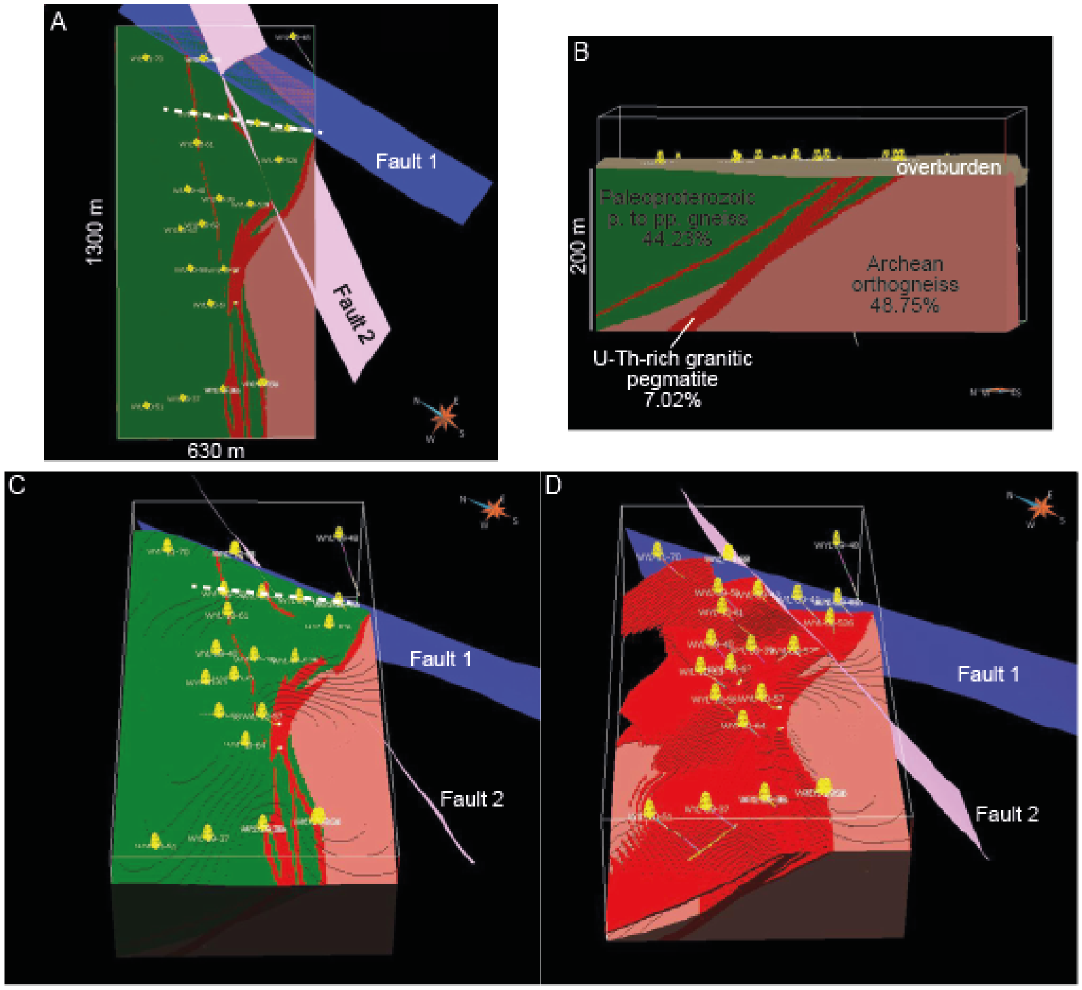

Figure L-14. 3D views of Fraser Lakes Zone B U mineralized granitic pegmatite and leucogranites. The Voxet volume used for the 3D modeling and calculation is 1,300 m long, 630 m wide, and 328 m deep, with a depth for the crystalline basement of around 200 m (around 128 m of air and overburden. (a) 3D plan view from SW to NE of whole set of drill holes (in yellow) used to build the 3D geological model with lithological surfaces (Paleoproterozoic rocks in green [mainly pelitic to psammopelitic gneiss), Archean rocks in pink [mainly orthogneiss]), tectonic contacts, and U-mineralized granitic pegmatite bodies (in red). See Figure 2 for comparison. Mineralized pegmatites are located along a highly deformed, folded Archean-Paleoproterozoic contact (*i.e.* decollement);cut by a major brittle conjugate fault system (*i.e.* N-S-trending Fault 1 and NNE-SSW-trending Fault 2), (b) 3D view of Fraser Lakes Zone B cross-section from SW to NE showing the parallel to sub-parallel nature of the sheeted granitic pegmatites at the Archean-Paleoproterozoic contact, The numbers refer to the percentage represented by each lithology within the Fraser Lakes Zone B. (c) Oblique 3D view from SW to NE of the mineralized pegmatite bodies at and above the Archean-Paleoproterozoic unconformity surface, (d) Oblique 3D view from SW to NE of the mineralized granitic pegmatite surface, without the hanging wall Wollaston Group metasediments (green in (c)). P. to pp. gneiss: pelitic to psammopelitic gneiss.

and 2 are supported by the lower Th content and Th/U of the EWA and Nob Hill felsic pegmatites (Group 1) when compared to the more mafic Fraser Lakes Zone B pegmatites (Group 2; Figure L-12). The extreme heterogeneity of the major and trace element contents (especially Zr) of Group 2 indicates that they are still close to their source area, and that the melts remained largely mixed with restitic material. In contrast, Group 1 granitic pegmatites have chemical and mineralogical compositions close to those of the Rössing alaskites, which are biotite-poor and with the same peraluminosity (Cuney and Kyser, 2008). The very low modal amount of biotite in the Rössing alaskites is explained by the fact that the melts were produced by a low degree of partial melting of dominantly quartz-feldspar-rich rocks ± biotite and have been extracted from their source with unmixing and fractionation of the biotite during the melt mobility (Cuney and Kyser, 2008). Therefore, the two groups of granitic pegmatites formed through a similar process, but the melts from Group 1 were extracted and have migrated greater distances from their source area. The difference of genetic processes between the Groups 1 and 2 pegmatites reflects their current structural setting, with a significant upwards transport of the Group 1 magmas along structural discontinuities between the basement comprised of Archean rocks and Wollaston Group metasediments, and their concentration within the noses of antiformal fold structures (e.g. Fraser Lakes Zone B, McKechnie *et al.*, 2012). However, the emplacement of the Group 2 granitic pegmatites of the Fraser Lakes Zone B at the Archean-Paleoproterozoic contact indicates a minimal distance of melt transport (Figure L-14).

The Th/U ratios of the uraniferous pegmatites and leucogranites are well below the average crustal ratio (≈4), indicating a U-rich source, or a preferential U enrichment during melting, and/or crystallization of the granitic pegmatites and leucogranites (Figure L-12). Due to the spatial association with the granitic pegmatites and leucogranites and its lithological importance within the Way Lake property, the Wollaston Group metasediments appear to be the best protolith candidates. These protoliths, Paleoproterozoic metasediments and/or metavolcanics (Parslow and Thomas, 1982; Yeo and Delaney, 2007), are initially enriched in U and/or Th (Figure L-12), and represent regionally abundant uranium-enriched source rocks (Thomas, 1983), thus explaining the current high radioelement contents of the granitic pegmatites and leucogranites. To obtain silicate melts capable of crystallizing uraninite, the partially melted original source must be enriched in uranium well over the Clarke abundance for the continental crust (about 1 ppm; Cuney, 2010) and must have a significant amount of uranium outside of accessory minerals such as apatite, zircon and monazite (Cuney and Friedrich, 1987; Friedrich *et al.*, 1987). Indeed, during the conditions of partial melting of the continental crust at low temperature (<850°C), accessory minerals like apatite, zircon or monazite have a low solubility in the silicate liquids (Watson and Harrison, 1983; Montel, 1986) and the uranium incorporated in the lattice of these minerals is not fractionated into the melt. Conversely, excess uranium not incorporated in the accessory minerals, as adsorbed on the minerals or crystallized as uranium oxide, extensively fractionates into the silicate melts, which will be able to crystallize uraninite. The Archean rocks have U contents too low (Parslow and Thomas, 1982) to represent a possible source (Figure L-12).

The geochemical variations of the uraninite-bearing granitic pegmatites and leucogranites (group 1 and 2) may result from the following:

i. the variability of protolith compositions (*i.e.* differences between the Paleoproterozoic metasediments and/or metavolcanics of the Wollaston Group), and especially their degree of U and other LILE (Th, or Zr) enrichment,
ii. the rate of partial melting of the protoliths; which however remained limited and involved mainly their quartz-feldspar fraction,
iii. the degree of unmixing of restitic material from the anatectic magmas based on their degree of extraction and transport from their source levels,
iv. the degree of fractional crystallization of the magma during its ascent, and
v. the degree of interaction of the magmas with the enclosing rocks during their ascent and emplacement, especially when encountering Ca-rich lithologies such as calcsilicates, marbles or basic rocks.

Origin of vein-type uranium oxides

The Hook Lake vein type mineralization shows a clearly distinct chemical composition when compared to magmatic uraninite, with a stronger enrichment in Ca and LREE (Table L-2), and lower Y and Th contents. Although the Th contents are low compared to those of the magmatic uraninites, such Th content (1.85 ±0.34 to 2.50 ±0.76 wt.% ThO_2) requires either a high temperature of formation, close to magmatic conditions, or the abundance of fluorine in the fluid phase to transport sufficient amounts of Th (Rand *et al.*, 2009; Cuney M., pers. commun.). The process leading to the formation of such mineralization during the peak thermal conditions of the Trans-Hudson Orogen is still unclear, but high-T metasomatism is suspected, as uraninites have high Ca contents, and the host rocks of the Hook Lake U-rich vein are characterized by highly anomalous Na- and Ca contents (Annesley *et al.*, 2010). The mineralization is clearly controlled by structure, and the relatively high temperature of formation of the uranium oxides in the vein is confirmed by their high REE content and relatively flat REE patterns (Mercadier *et al.*, 2011a). In addition, they are characterized by the absence of a significant Eu anomaly, contrary to magmatic uraninites. The relatively high Th content of this mineralization differentiates it clearly from Beaverlodge vein-type deposits to the north-west of the Athabasca Basin (Sassano, 1972), thus categorizing it as a new type of U mineralization in northern Saskatchewan.

Temporal relation between Hudsonian uranium oxide crystallization and Trans-Hudson Orogen (THO) evolution

U-Pb isotopic dates range from 1,805 ± 11 Ma (Hook Lake vein-type mineralization) to 1,713 ± 31 Ma (Fraser Lakes Zone B magmatic uraninite). However, the 1,713 ± 31 Ma date is much younger than the chemical ages calculated for the uranium oxides which give a tight 1,900-1,800 Ma interval (Figure L-9). Moreover, the uraninites of the WYL09-50-233 sample exhibit visible microfracturing associated with alteration, which would have affected the isotopic U-Th-Pb system (Figure L-6) as expressed by the excess of radiogenic lead for all measurements in the Concordia diagram (Figure L-10). Therefore, this relatively young 1,713 ± 31 Ma date probably does not correspond to the crystallization age of the uraninite, but more likely to a later resetting, and so it will not be considered further in the discussion. The chemical and isotopic ages are recording the syn- to late tectonic stages of the Trans-Hudson Orogeny (THO) (ca. 1.85-1.72 Ga; Annesley *et al.*, 2005), a period corresponding to the collision of the Superior and Rae-Hearne continental plates (Hoffman, 1988; Bickford *et al.*, 1994) during supercontinent Nuna assembly to form the current Canadian Shield (Zhao *et al.*, 2002).

The Hook Lake vein-type mineralization was formed by a primary crystallization event (1,805 ± 11 Ma), followed by a probable HT dissolution/precipitation event at 1,774 Ma, as shown by the petrographic observations, the chemical composition of the uraninite crystals, and the age dating results. A dissolution/precipitation origin is proposed for the Grey Zone (GZ) uraninite, because the GZ uraninite has lower lead contents but similar chemical and REE compositions to that of the White Zone (Figure L-7). The primary mineralizing event is related to the broad 1.82-1.79 Ga thermotectonic period of the THO associated with major terrain amalgamation (Bickford *et al.*, 1994; Schneider *et al.*, 2007). More precisely, it is related to the oblique collisional stage of the THO (described as DP_{2b} in Annesley *et al.*, 2005) at 1.820-1.805 Ga, with attainment of peak temperatures (750–825 °C) around 1.815 Ga. The dissolution/precipitation event (1,774 ± 9 Ma) can be linked to HT fluid circulation during the late oblique collisional stage of THO (D_{P3}) at 1.81-1.78 Ga and/or to the post-collisional stage (D_{P4}) at 1.775 - 1760 Ga, which is associated with an isobaric cooling P-T stage (Annesley *et al.*, 2005). This 1.77 Ga period is considered a second major peak thermal event (Schneider *et al.*, 2007) during a late stage of THO deformation (Bickford *et al.*, 1994).

The chemical ages for the magmatic uranium oxides and the U-Pb age obtained for the Moore Lakes magmatic uranium oxides are also related directly to their formation during the THO. The age interval from the present study was also determined for several pegmatites and aplite sheets (Bickford *et al.*, 2005) and post-tectonic granites (Bickford *et al.*, 1994) intruding high-grade metamorphic rocks elsewhere in the Wollaston Domain. Isotopic U-Pb dating of accessory minerals like monazites or zircons that are co-genetic with the uraninites from the Way Lake and Moore Lakes properties is deemed necessary to constrain more precisely the timing of emplacement of the different phases of uranium-bearing granitic rocks and veins during the THO.

The isotopic and chemical ages of the uranium oxides in the present study are clearly older than the chemical and isotopic ages from the uranium oxides of the unconformity-related U deposits (< 1.59 Ga; Fayek and Kyser, 1997; Fayek *et al.*, 2002 a, b; Alexandre *et al.*, 2009; Figure L-9), and pre-date initial deposition of the Athabasca Basin (< 1.75 Ga).

Importance of Hudsonian uranium oxides in the vicinity of Athabasca Basin

3D modeling of the Fraser Lakes Zone B clearly indicates that although the U-rich granitic pegmatites and leucogranites are a minor basement lithology (around 7% of the total volume), they are the main U-bearing lithologies. The U tonnages range from 3,200 (assuming 100 ppm average U content) to 16,200 (assuming 500 ppm average U content) metric tons U. Based on Figure L-12, the 500 ppm average U content is considered to be the most representative average U content. The volume of the voxet for the 3D modeling was limited by the availability of the drill holes in the area considered. However, the geophysical data (Figure L-1) and outcrops on the Way Lake property indicate that intrusive Hudsonian granitic pegmatites and leucogranites represent a significant proportion of the basement rocks within this zone, and confirm the abundance of uraninite-bearing granitoids enriched in U, Th, Pb, and REE. This property is considered to be a highly U-, Th-, and REE-enriched zone, although the current drillhole database is scattered and does not allow a global metal calculation at the scale of the Way Lake property (approximately 400 km^2). More importantly, the value of 7 % corresponding to the volume representativeness of U-rich lithologies within the 3D model can be considered a reliable representative percentage of the U-rich granitic pegmatite and leucogranite within the basement of the WMTZ.

Multiple U-rich granitic pegmatite and leucogranite occurrences similar to those of the Way Lake and Moore Lakes properties, and related to the same processes of formation, were discovered in the same area (Parslow and Thomas, 1982). They are quite extensive within the Mudjatik and Wollaston domains of the Hearne Province (Parslow *et al.*, 1985; Yeo and Delaney, 2007). At the Athabasca Basin's scale, many other uranium oxide occurrences formed in the Archean/Paleoproterozoic basement before Athabasca Basin deposition (ca. 1.75 Ga; Ramaekers, 1990). Their ages of formation are linked to the Taltson Orogeny (ca. 1.90-1.80 Ga; Card *et al.*, 2007) for the western part of the basin, and to the THO for the eastern part of the basin. The most important occurrences are: i) the numerous strata-bound uranium deposits hosted by Aphebian metasediments, such as the Karpinka Lake prospect (1.80 Ga; Williams-Jones and Sawiuk, 1985), ii) the numerous other uraninite-bearing pegmatites, such as those of Charlebois, Cup, Karin, Pipewrench Lakes, and of Pluto Bay (Thomas, 1983), (iii) the Late Hudsonian vein-type hydrothermal concentrations of the Beaverlodge U deposit (1.78 Ga; Koeppel, 1967) and mineralized episyenite of Gunnar, and iv) the high K-U-Th-REE calcalkaline plutons of the Shea Creek and Carswell U deposit area (1.92-2.00 Ga; Brouand *et al.*, 2003). Before the THO, the Paleoproterozoic sediments of the Wollaston and Mudjatik domains were deposited in shallow water epicontinental setting with a typical black shale – marl - carbonate – arkose association. They were enriched in organic matter due to stromatolite proliferation at that time, which trapped huge quantities of uranium under specific conditions created just after the great oxidation event (Cuney, 2010). During the THO, uranium disseminated in the metasediments was remobilized by hydrothermal fluids to form vein-type occurrences, such as Hook Lake, and by partial melting to form the uraninite- and/or monazite-zircon-bearing granites and granitic pegmatites. Consequently, the interpretations presented herein for the Way Lake and Moore Lakes properties are applicable to the entire Cree Lake Zone (including the Mudjatik and Wollaston domains). Stages DP_2 to DP_4 of the THO (Annesley *et al.*, 2005) are interpreted to have been very important for the production of a high volume of variably uranium-enriched peraluminous granitoid rocks.

Hudsonian uranium oxides: a uranium source for the unconformity-related uranium deposits?

The majority of unconformity-related uranium deposits within the Athabasca Basin are located within a relatively narrow corridor superimposed on the Wollaston-Mudjatik Transition Zone (Figure L-1). This zone (approximately 20x500 km^2) corresponds to a high heat production (HHP) area, due to its high radioelement (U, Th, K) contents (Madore *et al.*, 2000), similar to the Way Lake property. The Way Lake property hosts fresh to weakly altered rocks with uranium contents of 100-2,460 ppm for U-rich granitic pegmatites and leucogranites, and up to 41 wt.% for vein-type mineralization (Table L-4). Such high U contents for basement rocks near the Athabasca Basin have not been reported previously. Other fresh lithologies occurring on the Way Lake property, within the WMTZ, and/or within the Athabasca Basin are far less metal-enriched; averaging less than 20-40 ppm U for basement lithologies (Parslow and Thomas, 1982; Fayek and Kyser, 1997; and data from this study) and less than 5 ppm U for the basin formations (Fayek and Kyser, 1997; Jefferson *et al.*, 2007). The 3D modeling calculation from Fraser Lakes Zone B demonstrates that U-rich granitic pegmatites and leucogranites represent the most significant U reservoir within the basement complex (Table L-5), prior to the formation of unconformity-related U deposits.

The principal question is to define the potential of the U-rich granitic pegmatites and leucogranites as a *via*ble U source for unconformity-related U deposits. The development of massive and deep (> 400 m below the unconformity) clay-rich alteration haloes in the basement rocks near major fault systems and deposits (Alexandre *et al.*, 2005; Jefferson *et al.*, 2007) demonstrates the capability of the basinal brines to percolate into the basement rocks. This was proposed previously for the formation of some basin- and unconformity-hosted Cu and Pb-Zn deposits (Koziy *et al.*, 2009; Boiron *et al.*, 2010). Recent numerical modeling of brine flow for the Athabasca Basin at the time of unconformity-related deposit formation clearly demonstrates the possibility of downward brine percolations in basement rocks during tectonic reactivation (Cui *et al.*, 2012). This circulation is not restricted to alteration halos *sensu stricto,* since it has affected larger volumes due to the reopening of dense networks of microfractures (Mercadier *et al.*, 2010). This phenomenon is visible at the Way Lake property, where some of the studied samples show alteration features, such as clay alteration and APS mineral formation (Figure L-14), comparable to those described for hydrothermally altered basement rocks near unconformity-related uranium deposits (Fayek and Kyser, 1997; Hecht and Cuney, 2000; Hecht *et al.*, 2003).

The percolation of the brines in the basement rocks was demonstrated as the main process for the chemical modification from the initial Na-rich basinal brines to Ca-U-rich mineralizing fluids (Derome *et al.*, 2005; Richard *et al.*, 2010). Recent studies demonstrate that the Cl-dominant brines linked to the formation of unconformity-related U deposits had low pH values ($2.5 < pH < 4.5$; Richard *et al.*, 2012), and at these conditions uraninite is the most easily soluble tetravalent uranium-bearing mineral (Hazen *et al.*, 2009). This is confirmed by observations made of some samples from the Way Lake and Moore Lakes properties, for which UO_2 minerals (*i.e.* uraninite and monazite) show alteration features similar to those described for monazites in the alteration halo surrounding unconformity-related U deposits (Hecht and Cuney, 2000; Hecht *et al.*, 2003), even in a zone macroscopically free of clay alteration. Consequently, pervasive brine percolations in basement rocks having a high proportion of different types of granitic rocks enriched in uraninite, could be a key parameter to explain the unique and exceptional U contents of the brines (<0.2 to 600 ppm U) trapped in quartz from unconformity-related uranium deposits comparatively to other basinal fluids worldwide (Richard *et al.*, 2012). Their uranium concentrations, far higher than classical sedimentary basin brines, and the correlation between uranium and metal contents in the brines, indicate that these mineralizing fluids acquired their uranium content through fluid-rock interaction, with the basement being the best candidate (Richard *et al.*, 2010; 2012). Despite the small volume of basement modeled (1,300 m x 630 m x 200 m), the U tonnage of the Fraser Lakes Zone B (*i.e.* mostly from uraninite within the U-rich granitic pegmatites and leucogranites) represents from 8% (McArthur River) to 103 % (Rabbit Lake) of the U tonnage of unconformity-related uranium deposits of the Athabasca Basin (Table L-5, assuming a 500 ppm average U concentration). This conservative estimation does not take into account any possible U provided by other U-bearing minerals (*i.e.* monazite, zircon, apatite) within the other lithological units of the model.

Considering the major U reservoir formed by U-rich lithologies), the capability of the basinal brines to percolate within the basement rocks and leach U-bearing minerals, and the volumetric importance of the U-rich lithologies within the WMTZ, the Hudsonian U-rich granitic pegmatites and leucogranites are thought to have been a major uranium source for the formation of unconformity-related U deposits. The present study provides additional evidence for the initial proposal of Annesley *et al.* (2005) and Pana (2008), which suggested that these shear–fault zones (full of uranium-enriched crustal melts) must be considered a *via*ble uranium source for the unconformity-type uranium deposits due to their significant metal contents. This detailed study of uraninite-bearing basement lithologies in the vicinity of Athabasca Basin, both distal and intermediate to major hydrothermal alteration and/or unconformity-related U deposits, clearly reinforces their metal source potential, as proposed by previous studies that mainly took into account accessory minerals (which have lower U contents) like monazite (Hecht and Cuney, 2000; Madore *et al.*, 2000) or zircon and apatite (Fayek and Kyser, 1997).

Implications for uranium exploration

Exploration companies in the Athabasca Basin area target two types of U deposits: (i) pre-Athabasca Basin Hudsonian mineralization related to the THO (ca. 1.8-1.7 Ga), and (ii) hydrothermal unconformity-related uranium deposits (dated at ca. 1.6 to 1 Ga for the primary events); the economic potential and exploration effort being much higher for the latter. Due to the presence of unconformity-related U deposits, the different types of Hudsonian uranium mineralization have not been prospected at the level of potential offered by the Cree Lake Zone. However, the magmatic uranium oxides from the Way Lake and Moore Lakes properties have similar chemical composition (*i.e.* especially high REE and Th and low Ca). Also, they formed under comparable conditions (*i.e.* derived from the partial melting of U-rich sedimentary rocks) to magmatic uraninites from granitic pegmatites and strongly peraluminous granites in Germany (Forster, 1999), France (Cuney and Friedrich, 1987; Friedrich *et al.*, 1987), Finland (Raisanen, 1989;

Mercadier *et al.*, 2011b), Russia (Savitskii *et al.*, 1995), Canada (Lentz, 1996; Duhamel, 2010), and Namibia (Cuney and Kyser, 2008). Moreover, their average U concentration is similar to that of the Rössing alaskites (Figure L-9), which are currently mined for uranium. Following this study, reconsideration of the potential of this uranium province to host sub-economic to economic magmatic U deposits, like the Rössing deposit, is necessary.

A spatial distinction can explain the potential locations of the two distinct types of uranium occurrences. In the vicinity of unconformity-related U deposits, the massive brine percolations and associated source leaching have probably strongly decreased the U content (and so the economic potential) of Hudsonian U occurrences by reworking the U into the hydrothermal systems. On the other hand, areas proposed to be non-prospective for unconformity-related U deposits (*i.e.* covered and/or lying outside of basin current margin and/or unaffected by diagenetic alteration) need to be reconsidered for their Hudsonian U mineralization potential.

Finally, zones i) rich in Hudsonian U occurrences, such as granitic bodies, ii) structurally reworked during late THO and later at 1.6-1.0 Ga to facilitate fluid circulation, and iii) showing evidence of brine percolations, are of outmost importance for discovering basement-hosted unconformity-related uranium deposits outside the current limits of the Athabasca Basin; for example, the Eagle Point uranium deposit. These basement-hosted deposits, outside of the current aerial extent of the Athabasca Basin, are favorable exploration targets when compared to the location of economic Australian unconformity-related uranium deposits (e.g. Ranger, Jabiluka, Koongarra), which are all currently outside of the McArthur Basin margin.

Conclusions

This study is the first exhaustive and systematic description (petrography, mineralogy, mineral chemistry, chemical age dating, ion microprobe dating, whole-rock geochemistry and 3D modeling) of basement-hosted uraninite mineralization of different speciation, predating deposition of the Athabasca Basin (Saskatchewan, Canada) for areas in the eastern part of this basin far away from any known hydrothermal U deposits and significant alteration halos. Two types of mineralized occurrences related to the THO (ca. 1.8-1.7 Ga) are described: granitic pegmatite-related and vein-type. The most common is the uranium oxide-bearing granitic rocks formed by partial melting of mostly Wollaston Group metasedimentary rocks during the peak thermal events of the THO. Similar results obtained for the Way Lake (outside the basin margin) and Moore Lakes (currently within the basin margin under Athabasca cover) properties, and comparison with previous published data, clearly demonstrate that the western margin of the THO (e.g. Wollaston Domain) hosts abundant, widely disseminated uraninite-bearing lithologies (up to 7% of the total rock volume). Several of the studied rocks show clear evidence of incipient hydrothermal alteration similar to that linked to brine percolation during the formation of unconformity-related deposits, especially dissolution features of the uranium oxides. Such observations have been made on samples occurring away from any known unconformity-related deposits (*i.e.* outside the basin) demonstrating that the Hudsonian basement uranium occurrences, highly enriched in metals when compared to other basement or basin lithologies, can be altered by the mineralizing brines. Applying this conclusion to the strongly hydrothermally-altered basement rock surrounding the U deposits (e.g. at Moore Lakes), the Hudsonian basement uranium occurrences should be reconsidered as major metal sources for the formation of giant unconformity-related uranium deposits. This study does not allow a total reconsideration of the current hypotheses of the basement rocks versus the sedimentary basin as the main uranium source, but highlights the role of some specific basement lithologies in the formation of unconformity-related uranium deposits. Following this first step, additional studies are required to quantify precisely the input of UO_2-bearing lithologies in the formation of such high-grade U deposits.

References deposits. This study does not allow a total reconsideration of the current hypotheses of the basement rocks versus the sedimentary basin as the main uranium source, but highlights the role of some specific basement lithologies in the formation of unconformity-related uranium deposits. Following this first step, additional studies are required to quantify precisely the input of UO_2-bearing lithologies in the formation of such high-grade U deposits.

References

Alexandre, P., and Kyser, K., 2005, effects of cationic substitutions and alteration in uraninite, and implications for the dating of uranium deposits: Canadian Mineralogist, v. 43, p. 1005-1017.

Alexandre, P., Kyser, K., Thomas, D., Polito, P., and Marlatt, J., 2009, Geochronology of unconformity-related uranium deposits in the Athabasca Basin, Saskatchewan, Canada and their integration in the evolution of the basin: Mineralium Deposita, v. 44, p. 41-59.

Anders, E., and Grevesse, N., 1989, Abundances of the elements: Meteoritic and solar: Geochimica et Cosmochimica Acta, v. 53, p. 197-214.

Annesley, I. R., Austman, C. L., Creighton, S., Mercadier, J., Ansdell, K., Gittings, F., Bogdan, T., and Billard, D., 2010, Fraser Lakes U-Th-REE mineralization, southeastern Athabasca basement: composition and U-Th-Pb chemical/isotopic ages, with implications for U protore and U/C-type mineralization: SGS Open House Conference 2010, Saskatoon (Canada), 20-30 November 2010.

Annesley, I. R., Madore, C., Kusmirski, R. T., and Bonli, T., 2000, Uraninite-bearing granitic pegmatite, Moore Lakes, Saskatchewan: petrology and U-Th-Pb chemical ages. Summary of Investigations, Saskatchewan Energy and Mines, Saskatchewan Geological Survey miscellaneous report 2000-4.2, p. 201-211.

Annesley, I. R., Madore, C., and Portella, P., 2001, Paleoproterozoic structural, metamorphic, and magmatic evolution of the eastern sub-Athabasca basement: Controls on unconformity-type uranium deposits: A hydrothermal odyssey, Townsville (Australia), 17-19 May 2001, p. 3-4.

Annesley, I. R., Madore, C., and Portella, P., 2005, Geology and thermotectonic evolution of the western margin of the Trans-Hudson Orogen: evidence from the eastern sub-Athabasca basement, Saskatchewan: Canadian Journal of Earth Sciences, v. 42, p. 573-597.

Armstrong, R. L., and Ramaekers, P., 1985, Sr isotopic study of Helikian sediment and diabase dikes in the Athabasca Basin, northern Saskatchewan: Canadian Journal of Earth Sciences, v. 22, p. 399-407.

Bickford, M. E., Collerson, K. D., and Lewry, J. F., 1994, Crustal history of the Rae and Hearne provinces, southwestern Canadian Shield, Saskatchewan: constraints from geochronologic and isotopic data: Precambrian Research, v. 68, p. 1-21.

Bickford, M. E., Mock, T. D., Steinhart, W. E., Collerson, K. D., and Lewry, J. F., 2005, Origin of the Archean Sask craton and its extent within the Trans-Hudson orogen: Evidence from Pb and Nd isotopic compositions of basement rocks and post-orogenic intrusions: Canadian Journal of Earth Sciences, v. 42, p. 659-684.

Boiron, M.C., Cathelineau, M. and Richard, A. (2010) Fluid flows and metal deposition near basement/cover unconformity: lessons and analogies from Pb-Zn-F-Ba systems for the understanding of Proterozoic U deposits. *Geofluids*, 10, 270–292.

Bonhoure, J., Kister, P., Cuney, M., and Deloule, E., 2007, Methodology for rare earth element determinations of uranium oxides by ion microprobe: Geostandards and Geoanalytical Research, v. 31, p. 209-225.

Bowles, J. F. W., 1990, Age dating of individual grains of uraninite in rocks from electron microprobe analyses: Chemical Geology, v. 83, p. 47-53.

Brouand, M., Cuney, M., and Deloule, E., 2003, Eastern extension of the Taltson orogenic belt and eastern provenance of Athabasca sandstone: IMS 1270 ion microprobe U/Pb dating of zircon form concealed basement plutonic rocks and from overlying sandstone (northern Saskatchewan, Canada): Uranium geochemistry, Nancy (France), 13-16 April 2003, p. 91-94.

Card, C. D., Pana. D., Portella. P., Thomas, D. J., and Annesley, I. R., 2007, Basement rocks to the Athabasca Basin, Saskatchewan and Alberta, *in* Jefferson, C. W., and Delauney.G., eds., EXTECH IV: Geology and Uranium EXploration TECHnology of the Proterozoic Athabasca Basin, Saskatchewan and Alberta. Geological Survey of Canada. Bulletin 588, p. 69-87.

Černý, P., P.L., B., Cuney, M., and London, D., 2005, Granite-related ore deposits: Economic Geology, v. 100, p. 337-370.

Chiarenzelli, J., Aspler, L., Villeneuve, M., and Lewry, J., 1998, Early Proterozoic evolution of the Saskatchewan craton and its allochthonous cover, Trans-Hudson Orogen: Journal of Geology, v. 106, p. 247-267.

Cloutier, J., Kyser, K., Olivio, G. R., and Brisbin, D., 2011, Geochemical, isotopic, and geochronological constraints on the formation of the Eagle Point basement-hosted uranium deposit, Athabasca Basin, Saskatchewan, Canada and recent remobilization of primary uraninite in secondary structures: Mineralium Deposita, v. 46, p. 35-56.

Cui, T., Yang, J. and Samson, I.M., 2012, Tectonic deformation and fluid flow: implications for the formation of unconformity-related uranium deposits: Economic geology, v. 107, 147-163.

Cumming, G. L., and Krstic, D., 1992, The age of unconformity-related uranium mineralization in the Athabasca Basin, northern Saskatchewan: Canadian Journal of Earth Sciences, v. 29, p. 1623-1639.

Cuney, M., 2005, World-class unconformity-related uranium deposits: key factors for their genesis: 8th Society of Applied Geology biennial meeting, Beijing (China), p. 245-246.

Cuney, M., 2010, Evolution of uranium fractionation processes through time: driving the secular variation of uranium deposit types: Economic Geology, v. 105, 553-569

Cuney, M., Brouand, M., Cathelineau, M., Derome, D., Freiberger, R., Hecht, L., Kister, P., Lobaev, G., Lorilleux, G., Peiffert, C., and Bastoul, A. M., 2003, What parameters control the high grade-large tonnage of the Proterozoic unconformity related uranium deposit?: Uranium Geochemistry, International Conference Proceeding, Nancy (France), p. 123-126.

Cuney, M., and Friedrich, M. H., 1987, Physico-chemical and crystal-chemical controls on accessory mineral paragenesis in granitoids: implications for uranium metallogenesis: Bulletin de Mineralogie, v. 110, p. 235-247.

Debon, F., and Le Fort, P., 1988, A cationic classification of common plutonic rocks and their magmatic associations: principles, method and applications: Bulletin de Mineralogie, v. 111, p. 493-510.

Derome, D., Cathelineau, M., Cuney, M., Fabre, C., Lhomme, T., and Banks, D. A., 2005, Mixing of sodic and calcic brines and uranium deposition at McArthur River, Saskatchewan, Canada: A Raman and laser-induced breakdown spectroscopic study of fluid inclusions: Economic Geology, v. 100, p. 1529-1545.

Duhamel, I., 2010, Caractérisation des sources d'uranium à l'Archéen. Mécanismes de genèse des gisements d'uranium les plus anciens (3,0 à 2,2 Ga) et des préconcentrations uranifères paleoprotérozoïques: Unpub. Ph.D thesis, Université Henri Poincaré, France, 439 p.

Essaraj, S., Boiron, M. C., Cathelineau, M., Banks, D. A., and Benahareff, M., 2005, Penetration of surface-evaporated brines into the Proterozoic basement and deposition of Co and Ag at Bou Azzer (Morocco): evidence from fluid inclusions: Journal of African Earth Sciences, v. 41, p. 25-39.

Fayek, M., Harrison, T. M., Ewing, R. C., Grove, M., and Coath, C. D., 2002a, O and Pb isotopic analyses of uranium minerals by ion microprobe and U-Pb ages from the Cigar Lake deposit: Chemical Geology, v. 185, p. 205-225.

Fayek, M., and Kyser, T. K., 1997, Characterization of multiple fluid-flow events and rare-earth-element mobility associated with formation of unconformity-type uranium deposits in the Athabasca Basin, Saskatchewan: Canadian Mineralogist, v. 35, p. 627-658.

Fayek, M., Kyser, T. K., and Riciputi, L. R., 2002b, U and Pb isotope analysis of uranium minerals by ion microprobe and the geochronology of McArthur River and Sue zone uranium deposits, Saskatchewan, Canada: Canadian Mineralogist, v. 40, p. 1553-1569.

Forster, B. J., 1999, the chemical composition of uraninite in Variscan granites of the Erzgebirge, Germany: Mineralogical Magazine, v. 63, p. 239-252.

Friedrich, M. H., Cuney, M., and Poty, B., 1987, Uranium geochemistry in peraluminous leucogranites: Uranium, v. 3, p. 353-385.

Gaboreau, S., Cuney, M., Quirt, D., Beaufort, D., Patrier, P. and Mathieu R., 2007, Significance of aluminium phosphate-sulfate minerals associated with U unconformity-type deposits: The Athabasca Basin, Canada: American Mineralogist, v. 92, p. 267-280.

Hazen, R. M., Ewing, R. C., and Sverjensky, D. A., 2009, Evolution of uranium and thorium minerals: American Mineralogist, v. 94, p. 1293-1311.

Hecht, L., and Cuney, M., 2000, Hydrothermal alternation of monazite in the Precambrian crystalline basement of the Athabasca Basin (Saskatchewan, Canada): Implications for the formation of unconformity-related uranium deposits: Mineralium Deposita, v. 35, p. 791-795.

Hecht, L., Cuney, M., Brouand, M., and Deloule, E., 2003, Tracing the sources of unconformity-type uranium deposits: Uranium Geochemistry, International Conference Proceeding, Nancy, France, 2003, p. 37-40.

Hiatt, E. E., Kyser, T. K., Fayek, M., Polito, P., Holk, G. J., and Riciputi L. R., 2007, Early quartz cements and evolution of paleohydraulic properties of basal sandstones in three Paleoproterozoic continental basins: evidence from in-situ $\delta^{18}O$ of quartz cements: Chemical Geology, v. 238, p. 19-37.

Hoeve, J., and Sibbald, T. I. I., 1978, On the genesis of Rabbit Lake and other unconformity-types uranium ores in the Athabasca basin: Economic Geology, v. 73, p. 1450-1473.

Hoffman, P. F., 1988, United plates of America, the birth of a craton: Early Proterozoic assembly and growth of Laurentia: Annual Review of Earth and Planetary Sciences. Vol. 16, p. 543-603.

Jefferson, C. W., Thomas, D., Gandhi, S. S., Ramaekers, P., Delauney.G., Brisbin, D., Cutts, C., Portella, P., and Olson, R. A., 2007, Unconformity-associated uranium deposits of the Athabasca Basin, Saskatchewan and Alberta, *in* Jefferson, C. W., and Delaney, G., eds., EXTECH IV: Geology and Uranium EXploration TECHnology of the Proterozoic Athabasca Basin, Saskatchewan and Alberta., Geological Survey of Canada, p. 23-67.

Koeppel, V., 1967, Age and history of uranium mineralization of the Beaverlodge area, Saskatchewan: Geological Survey of Canada report 67-31, 111 p.

Koziy, L., Bull S., Large, R., and Selley, D., 2009, Salt as a fluid driver, and basement as a metal source, for stratiform sediment-hosted copper deposits: Geology, v. 37, p. 1107-1110.

Kotzer, T. G., and Kyser, T. K., 1995, Petrogenesis of the Proterozoic Athabasca Basin, northern Saskatchewan, Canada, and its relation to diagenesis, hydrothermal uranium mineralization and paleohydrogeology: Chemical Geology, v. 120, p. 45-89.

Kyser, K., Hiatt, E., Renac, C., Durocher, K., Holk, G., and Deckart, K., 2000, Diagenetic fluids in paleo- and meso-proterozoic sedimentary basins and their implications for long protracted fluid histories, *in* Kyser, T., ed., Fluids and basin evolution: Mineralogical Association of Canada Short Course series 28, p. 225-262.

Kyser, T. K., and Cuney, M., 2008, Unconformity-related uranium deposits, *in* Cuney, M., and Kyser, T. K., eds., Recent and not-so-recent developments in uranium deposits and implications for exploration: Mineralogical Association of Canada Short Course series 39, p. 161-219.

Lentz, D., 1996, U, Mo, and REE mineralization in late-tectonic granitic pegmatites, southwestern Grenville Province, Canada: Ore Geology Reviews, v. 11, p. 197-227.

Lewry, J. F., and Sibbald, T. I. I., 1980, Thermotectonic evolution of the Churchill Province in Northern Saskatchewan: Tectonophysics, v. 68, p. 45-82.

Lorilleux, G., Cuney, M., Jébrak, M., Rippert, J. C., and Portella, P., 2003, Chemical brecciation in the Sue unconformity-type uranium deposits, Eastern Athabasca Basin (Canada): Journal of Geochemical Exploration, v. 80, p. 241-258.

Ludwig, K. R., 1999, Isoplot/ex version 2.1.0. A geochronological toolkit for Microsoft Excel. Special Publication n°1a, Berkeley Geochronological Center.

MacDougall, D. G., and Maxemiuk, L. M. T., 1995, Moore Lakes revisited-Gold and palladium concentrations in altered diabase from the Moore Lake Complex (part of NTS 74H-6 and-7). Summary of Investigations, Saskatchewan Energy and Mines, Saskatchewan Geological Survey miscellaneous report 95-4, p. 68-76.

MacDougall, D. G., and Williams, D. H., 1993, The Moore Lakes Complex, Neohelikian olivine diabase lopoliths in the Athabasca Group (Part of NTS 74H-6 and -7). Summary of Investigations, Saskatchewan Energy and Mines, Saskatchewan Geological Survey miscellaneous report 93-4, p. 201-211.

Madore, C., Annesley, I. R., and Tran, H. T., 1999, Petrology and geochemistry of Paleoproterozoic Wollaston Group metasediments from the eastern Keller Lake-Siemens Lake area, Saskatchewan; A preliminary interpretation. Summary of Investigations, Saskatchewan Energy and Mines, Saskatchewan Geological Survey miscellaneous report 99-4.2, v.2, p. 80-89.

Madore, C., Annesley, I. R., and Wheatley, K., 2000, Petrogenesis, age, and uranium fertility of peraluminous leucogranites and pegmatites of the McClean Lake / Sue and Key Lake / P-Patch deposit areas, Saskatchewan: GeoCanada: the Millennium Geoscience Summit, Calgary (Canada), 29 May-2 June 2000.

Mallet, J.L., 1992, A computer aided design program for geological application, in Turner, A.K., ed., Three-dimensional modeling with geoscientific information systems: Dordrecht (Netherlands), Kluwer Academic Publishers, NATO ASI 354, p. 123-142.

McKechnie , C. L., Annesley, I. R., and Ansdell, K. M., 2012, Anatexis and uranium protore in the Wollaston Domain, Saskatchewan: Goldschmidt 2012 Conference, Montréal (Canada), 24-29 June 2012.

Mercadier, J., 2008, Conditions de genèse des gisements d'uranium associés aux discordances protérozoïques et localisés dans les socles. Exemple du socle du bassin d'Athabasca (Saskatchewan, Canada): Unpub. Ph.D thesis, INPL, 325 p.

Mercadier, J., Cuney, M., Cathelineau, M., and Lacorde, M., 2011a, U redox fronts and kaolinisation in basement-hosted unconformity-related U ores of the Athabasca

Basin (Canada): Late U remobilization by meteoric fluids: Mineralium Deposita, v. 46, p. 105-135.

Mercadier, J., Cuney, M., Lach, P., Boiron, M.-C., Bonhoure, J., Richard, A., Leisen, M., and Kister, P., 2011b, Origin of uranium deposits revealed by their rare earth element signature: Terra Nova, v. 23, 264-269.

Mercadier, J., Richard, A., Boiron, M.-C., Cathelineau, M., and Cuney, M., 2010, Migration of brines in the basement rocks of the Athabasca Basin through microfracture networks (P-Patch U deposit, Canada): Lithos, v. 115, p. 121-136.

Mercadier J., Richard A., Cathelineau, M., 2012, Boron and magnesium-rich marine brines at the origin of giant unconformity-related uranium deposits: $\delta^{11}B$ evidence from Mg-tourmalines: Geology, v. 40, 231–234.

Montel, J.M., 1986, Experimental determination of the solubility of Ce-monazite in SiO2-Al2O3-K2O-Na2O melts at 800°C, 2 kbar, under H2O- saturated conditions: Geology, v. 14, 659-662.

Mwenifumbo, C. J., and Bernius, G. R., 2007, Crandallite-group minerals: hosts of thorium enrichment in the eastern Athabasca basin, Saskatchewan, *in* Jefferson, C. W., and Delaney, G., eds., EXTECH IV: Geology and Uranium EXploration TECHnology of the Proterozoic Athabasca Basin, Saskatchewan and Alberta. Geological Survey of Canada, p. 521-538.

Pagel, M., 1975, Détermination des conditions physico-chimiques de la silicification diagénétique des grès Athabasca (Canada) au moyen des inclusions fluides: Comptes Rendus Académie Sciences Paris, v. 280, p. 2301-2304.

Pana, D.I., 2008, Basement shear zones and uranium enrichment in and around the Athabasca Basin: GAC-MAC 2008 Conference, Québec (Canada), 26-28 May 2008, p. 128

Parslow, G. R., Brandstatter, F., Kurat, G., and Thomas, D., 1985, Chemical ages and mobility of U and Th in anatectites of the Cree Lake zone, Saskatchewan: Canadian Mineralogist, v. 23, p. 543-552.

Parslow, G. R., and Thomas, D. J., 1982, Uranium occurrences in the Cree Lake zone, Saskatchewan, Canada: Mineralogical Magazine, v. 46, p. 165-173.

Raisanen, E., 1989, Uraniferous granitic veins in the Svecofennian schist belt in Nummi-Pusula, southern Finland: Uranium Deposits in Magmatic and Metamorphic Rocks Proceedings. IAEA Technical Commitee Meeting, Salamanca, Spain, 1989.

Ramaekers, P., 1990, Geology of the Athabasca Group (Helikian) in northern Saskatchewan. Technical Report, Saskatchewan Geological Survey, Saskatchewan Mineral Resources, no. 1950, 49p.

Ramaekers, P., Jefferson, C. W., Yeo, G., Collier, B., Long, D. G. F., Catueanu, O., Bernier, S., Kupsch, B., Post, R., Drever, G., McHardy, S., Jiricka, D., Cutts, C., and Wheatley, K., 2007, Revised geological map and stratigraphy of the Athabasca Group, Saskatchewan and Alberta, *in* Jefferson, C. W., and Delauney.G., eds., EXTECH IV: Geology and Uranium EXploration TECHnology of the Proterozoic Athabasca Basin, Saskatchewan and Alberta. Geological Survey of Canada. Bulletin 588, Geological Survey of Canada.

Rand, M. H., Mompean, F. J., Perrone, J., and Illemassène, M., 2009, Chemical thermodynamics of thorium: Paris, Organization for Economic Co-operation and Development (OECD), 900 p.

Richard, A., Rozsypal, C., Mercadier, J., Banks, DA, Cuney, M., Boiron, M.-C., and Cathelineau, M., 2012, Giant uranium deposits formed from exceptionally uranium-rich acidic brines. *Nature Geoscience*, 5, 142–146.

Richard, A., Banks, D. A., Mercadier, J., Boiron, M.-C., Cuney, M., and Cathelineau, M., 2011, An evaporated seawater origin for the ore-forming brines in unconformity-related uranium deposits (Athabasca Basin, Canada): Cl/Br and δ^{37}Cl analysis of fluid inclusions: Geochimica et Cosmochimica Acta, v. 75, p. 2792-2810.

Richard, A., Pettke, T., Cathelineau, M., Boiron, M.-C., Mercadier, J., Cuney, M., and Derome, D., 2010, Brine-rock interaction in the Athabasca basement (McArthur River U deposit, Canada): consequences for fluid chemistry and uranium uptake: Terra Nova, v. 22, p. 303-308.

Sassano, G., 1972, The nature and origin of the uranium mineralization at the Eldorado Fay Mine, Saskatchewan: Unpub. PhD thesis, University of Alberta, Canada, 248 p.

Savitskii, A. V., Gromov, A. Y., Mel'nikov, E. K., and Sharikov, P. I., 1995, Uranium ore mineralization of the Litsk District in the Kola Peninsula (Russia): Geology of ore deposits, v. 37, p. 351-362.

Schneider, D. A., Heizler, M. T., Bickford, M. E., Wortman, G. L., Condie, K. C., and Perilli, S., 2007, Timing constraints of orogeny to cratonization: Thermochronology of the Paleoproterozoic Trans-Hudson orogen, Manitoba and Saskatchewan, Canada: Precambrian Research, v. 153, p. 65-95.

Stacey, J. S., and Kramers, J. D., 1975, Approximation of terrestrial lead isotope evolution by a two-model: Earth and Planetary Science Letters, v. 26, p. 207-221.

Thomas, D., 1983, Distribution, geological controls and genesis of uraniferous pegmatites in the Cree lake zone of Northern Saskatchewan: Unpub. Master thesis, University of Regina, Canada, 212 p.

Watson, E.B., and Harrison, T.M., 1983, Zircon saturation revisited: temperature and composition effects in a variety of crustal magma types: Earth and Planetary Science Letters, v. 64, p. 295-304.

White, A. J. R., and Chapell B. W., 1977, Ultrametamorphism and granitoid genesis: Tectonophysics, v. 43, p. 7-22.

Williams-Jones, A. E., and Sawiuk, M. J., 1985, The Karpinka Lake uranium prospect, Saskatchewan: a possible metamorphosed middle Precambrian sandstone-type uranium deposit: Economic Geology, v. 80, p. 1927-1941.

Yeo, G. M., and Delaney, G., 2007, The Wollaston Supergroup, stratigraphy and metallogeny of a Paleoproterozoic Wilson cycle in the Trans-Hudson Orogen, Saskatchewan, *in* Jefferson, C. W., and Delaney, G., eds., EXTECH IV: Geology and Uranium EXploration TECHnology of the Proterozoic Athabasca Basin, Saskatchewan and Alberta. Geological Survey of Canada. Bulletin 588, Geological Survey of Canada, p. 89-117.

Zhao, G., Cawood, P. A., Wilde, S. A., and Sun, M., 2002, Reviews of global 2.1-1.8 Ga orogens: implications for a pre-Rodinia supercontinent: Earth Science Reviews, v. 59, p. 125-162.